

Department Chemie, Lehrstuhl für Anorganische Chemie
der Technischen Universität München und
Department of Chemistry, University of Bergen

Rare-Earth Metal Alkyls

Melanie Zimmermann

Vollständiger Abdruck der von den Fakultäten für Chemie der Technischen Universität
München und der Universität Bergen zur Erlangung des akademischen Grades eines

Doktors der Naturwissenschaften

genehmigten Dissertation.

Vorsitzender: Univ.-Prof. Dr. Klaus Köhler

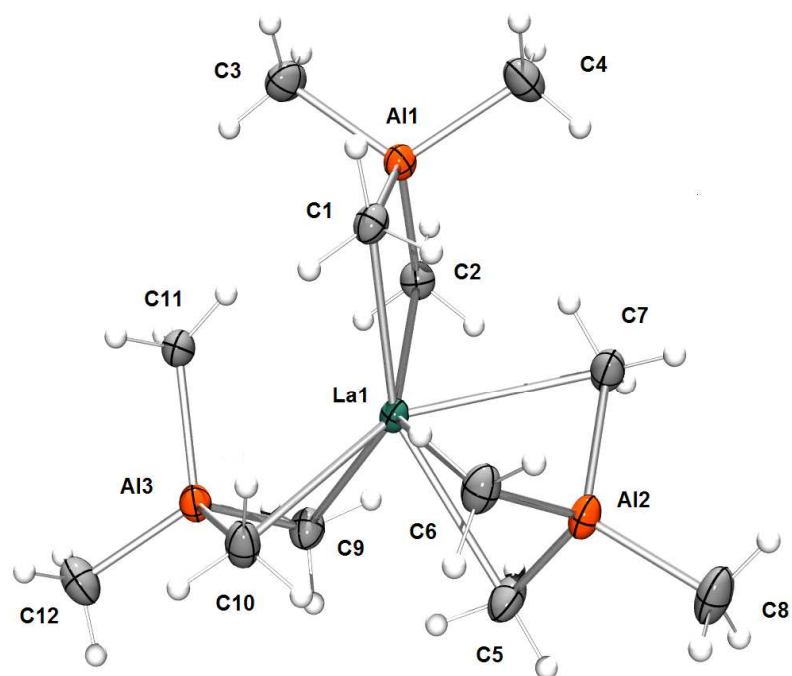
Prüfer der Dissertation:

1. Univ.-Prof. Dr. Reiner Anwander
University of Bergen / Norwegen
2. Univ.-Prof. Dr. Oskar Nuyken, i. R.
3. Univ.-Prof. Dr. Peter Härter
4. Prof. Leif Saethre
University of Bergen / Norwegen

Die Dissertation wurde am 8. Oktober 2007 bei der Technischen Universität München
eingereicht und durch die Fakultät für Chemie am 29. Oktober 2007 angenommen.

Melanie Zimmermann

Rare-Earth Metal Alkyls



*"I want to know God's thoughts ...
...the rest are details."*

Albert Einstein
(1879-1955)

*To my family
and good friends*

Preface

This thesis, submitted for the joint degree of Doktor der Naturwissenschaften (Dr. rer. nat.) at the Technische Universität München, Germany, and at the University of Bergen, Norway, consists of a review on homoleptic rare-earth metal alkyl complexes, a summary, concluding remarks, and eight scientific papers. The work was carried out at the Departments of Chemistry of the Technische Universität München and the University in Bergen over the period February 2004 to October 2007. Prof. Dr. Reiner Anwander has been my advisor in München and Bergen.

From January to March 2005, I was fortunate to work with Prof. Robert M. Waymouth at the Stanford University, Stanford, California, on a joined project, learning about instrumentation for the polymerization of gaseous monomers.

Parts of this thesis have been presented at several international and national conferences and meetings as oral and poster contributions.

Acknowledgements

First of all, my sincere thanks go to my advisor **Prof. Reiner Anwander**. Without any doubt, your contribution to this thesis is indispensable. I thank you for your encouragement throughout the last years, for your understanding and motivation. I appreciated your subtle way of leading and directing, and your never-ending assurance. Your wide knowledge and enthusiasm has been a great inspiration and made research an excitement to me.

I wish to thank **Prof. Peter Härter** for co-supervising this thesis and stimulating research discussions.

I want to thank all my former and present colleagues in the Anwander group in München and Bergen for providing a supportive and cheerful atmosphere in the lab.

Special thanks go to **Andreas Fischbach**. Your ability to teach and fascinate significantly influenced my decision to work with rare-earth elements. I had the pleasure of sharing my glovebox with **Rannveig Litlabø**. You had to compromise a lot during the last months and I thank you for your never-ending patience and reliability. Further thanks go to **Erwan Le Roux** and “The little Viking” **Hanne-Marthe Sommerfeldt** for freshening up my mind with their unconventional way of thinking. I thank **Laura Gerber** for proof-reading. I will also use the opportunity to thank the colleagues in the “heterogeneous lab”. **Thomas Deschner**, for his friendship and helpfulness, **Yucang Liang** for providing inspiring insight into the Chinese culture, **Alan Crozier** for his subtle humour, and our Master Students **Bjørn-Tore Longstad** and **Hjørdis Skår**. I thank **Martin Dietrich** for pushing my limits and **Malaika Schnitzlbaumer** for sunny moments.

I wish to thank all colleagues at the Department of Chemistry in Bergen, for their support and help, particularly during my first months in Bergen. Especially, **Prof. Leif Saethre**, **Prof. Vidar R. Jensen**, **Maria G. Zahl**, **Elaine Olsson**, **Giovanni Occhipinti**, **Alf Holme**, **Jarle Harnes**, and **Mathias Winkler** for cheering me up countless times.

I am indebted to **Prof. Karl W. Törnroos** for many successful and attempted X-ray structure determinations. Your commitment and interest was crucial for the outcome of this thesis. Further thanks go to the crystallographers in München **Eberhardt Herdtweck** and **Peter Sirsch**.

I thank **Inger Johanne Fjellanger** for careful elemental analysis measurements and several non-scientific discussions. Further thanks go to **Prof. Nils Åge Frøystein**, for all the time he has spent explaining me various aspects of NMR spectroscopy.

I also want to thank the administrative staff at the Departments of Chemistry in Bergen and München for all help and support through these years. Especially, **Nina Berg-Johannesen** and **Irmgard Grötsch**.

My special thanks go to **Christian Meermann**. Your encouragement, commitment, and patience have been invaluable.

I deeply thank **my family** for their love and endless support in many ways. I thank my good friends **Markus Armbruster**, **Sören Randoll**, **Manuel Sparta**, **Rüdiger Schulz**, **Elke Moser**, and **Jeanny S. Samuelsen** for many compassionate talks and simply their friendship.

I acknowledge a scholarship from the Bayerische Forschungstiftung.

Contents

| | |
|--|-----------|
| List of Papers | xi |
| Objectives of this Thesis | xvii |
| Chapter A: Rare-Earth Metal Alkyls | 1 |
| 1 Rare-Earth Metal Alkyls | 2 |
| 2 Homoleptic Bis(trimethylsilyl)methyl Complexes Ln(II)[CH(SiMe₃)₂]₂(solv)_x and Ln(III)[CH(SiMe₃)₂]₃ | 8 |
| 2.1 Synthesis, Structure, and Properties of Ln(II)[CH(SiMe ₃) ₂] ₂ (solv) _x | 8 |
| 2.2 Synthesis, Structure, and Properties of Ln(III)[CH(SiMe ₃) ₂] ₃ | 11 |
| 2.3 Ln(III)[CH(SiMe ₃) ₂] ₃ as Synthesis Precursors | 14 |
| 3 Ln(II)[C(SiMe₃)₃]₂ and Ln(II)[C(SiMe₃)₂(SiMe₂R)]₂ | 19 |
| 3.1 Related Ln(II) Silylmethyl Complexes | 23 |
| 4 Homoleptic Tris(trimethylsilyl)methyl Complexes Ln(III)(CH₂SiMe₃)₃(thf)_x | 25 |
| 4.1 Synthesis, Structure, and Properties | 25 |
| 4.2 Ln(CH ₂ SiMe ₃) ₃ (thf) _x as Synthesis Precursors | 29 |
| 4.2.1 Cationic Complexes [Ln(CH ₂ SiMe ₃) _{3-n} (solv) _x] ⁿ⁺ [anion] ⁿ⁻ | 29 |
| 4.2.2 Half-Sandwich Complexes | 30 |
| 4.2.3 Complexes with Functionalized Cp ^R Ligands | 33 |
| 4.2.4 Complexes with Neutral Nitrogen- and Oxygen-based Ligands | 35 |
| 4.2.5 Complexes with Monoanionic Nitrogen-, Oxygen-, and Phosphorus-based Ligands | 37 |
| 4.2.6 Complexes with Dianionic Nitrogen- and Oxygen-based Ligands | 43 |
| 5 Ln(CH₂SiMe₂Ph)₃(thf)₂ | 47 |
| 5.1 Synthesis, Structure, and Properties | 47 |
| 5.2 Ln(CH ₂ SiMe ₂ Ph) ₃ (thf) ₂ as Synthesis Precursors | 48 |
| 6 Heteroleptic Alkyl, Alkyl/Aryloxo and Alkyl/Alkoxo Compounds | 50 |
| 6.1 Lu(CH ₂ SiMe ₃) ₂ (CHPh ₂)(thf) ₂ | 50 |
| 6.2 Alkyl/Aryloxo | 51 |
| 6.3 Alkyl/Alkoxo | 54 |
| 7 [Li(solv)_x][Ln^tBu₄] | 56 |
| 8 Ln(CH₂^tBu)₃(thf)₂ | 58 |

Contents

| | | |
|--------------------------------------|--|------------|
| 9 | Lanthanide Benzyl Complexes | 60 |
| 9.1 | La(CH ₂ Ph) ₃ (thf) ₃ and La(CH ₂ C ₆ H ₄ -4-Me) ₃ (thf) ₃ | 60 |
| 9.2 | Ln(CH ₂ C ₆ H ₄ -o-NMe ₂) ₃ and Ln(CH ₂ C ₆ H ₄ -o-SiMe ₃) ₃ | 62 |
| 10 | Ln(o-C₆H₄CH₂NMe₂)₃ | 64 |
| 11 | Lanthanide Alkynides | 67 |
| 11.1 | Ln(II) Alkynides | 67 |
| 11.2 | Ln(III) Alkynides | 71 |
| 12 | [Li(donor)]₃[LnMe₆] and [LnMe₃]_n | 74 |
| 13 | Mixed Methyl/Chloride Rare-Earth Metal Compounds | 79 |
| 14 | Homoleptic Rare-Earth Metal Tetraalkylaluminates | 81 |
| 14.1 | Synthesis, Structure, and Properties of Ln(II)(AlR ₄) ₂ | 81 |
| 14.2 | Synthesis, Structure, and Properties of Ln(III)(AlR ₄) ₃ | 85 |
| 14.3 | Ln(III)(AlMe ₄) ₃ as Synthesis Precursors | 90 |
| 15 | Homoleptic Ln(III) Tris(tetramethylgallates) Ln(GaMe₄)₃ | 95 |
| Chapter B: Summary | | 97 |
| 1 | Homoleptic Rare-Earth Metal(III) Tetramethylaluminates | 99 |
| 2 | Ln(AlMe₄)₃ as Synthesis Precursors for Post-Lanthanidocene Chemistry | 100 |
| 3 | Reactivity of Post-Lanthanidocene Tetramethylaluminate Complexes | 103 |
| 4 | Pre-Catalyst/Co-Catalyst Interactions of Cp^RLn(AlMe₄)₂ | 106 |
| 5 | Structure-Reactivity Relationships of Amido-Pyridine Supported Rare-Earth Metal Alkyl Complexes | 108 |
| Chapter C: Concluding Remarks | | 111 |
| Chapter D: Bibliography | | 115 |

List of Papers

This thesis is based on the following scientific papers. In the text, they will be referred to by their Roman numerals.

- Paper I** Homoleptic Rare-Earth Metal(III) Tetramethylaluminates: Structural Chemistry, Reactivity, and Performance in Isoprene Polymerization.
M. Zimmermann, N. Å. Frøystein, A. Fischbach, P. Sirsch, H. M. Dietrich, K. W. Törnroos, E. Herdtweck, R. Anwander.
Chemistry-A European Journal **2007**, *13*, 8784-8800.
- Paper II** Implementation of Ln(AlMe₄)₃ as Precursors in Postlanthanidocene Chemistry.
M. Zimmermann, K. W. Törnroos, R. Anwander.
Organometallics **2006**, *25*, 3593-3598.
- Paper III** Alkyl Migration and an Unusual Tetramethylaluminate Coordination Mode: Unexpected Reactivity of Organolanthanide Imino-Amido-Pyridine Complexes.
M. Zimmermann, K. W. Törnroos, R. Anwander.
Angewandte Chemie International Edition **2007**, *46*, 3126-3130.
Angewandte Chemie **2007**, *119*, 3187-3191.
- Paper IV** Distinct C–H Bond Activation Pathways in Diamido-Pyridine-Supported Rare-Earth Metal Hydrocarbyl Complexes.
M. Zimmermann, F. Estler, E. Herdtweck, K. W. Törnroos, R. Anwander.
Organometallics **2007**, *26*, 6029-6041.

List of Papers

- Paper V** Ln(III) methyl and methyldene complexes stabilized by a bulky hydrotris(pyrazolyl)borate ligand.
M. Zimmermann, J. Takats, G. Kiel, K. W. Törnroos, R. Anwander.
Chemical Communications **2008**, 612-614.
- Paper VI** Cationic Rare-Earth-Metal Half-Sandwich Complexes for the Living *trans*-1,4 Isoprene Polymerization.
M. Zimmermann, K. W. Törnroos, R. Anwander.
Angewandte Chemie International Edition **2008**, 47, 775-778.
Angewandte Chemie **2008**, 120, 787-790.
- Paper VII** Half-Sandwich Bis(tetramethylaluminate) Complexes of the Rare-Earth Metals: Synthesis, Structural Chemistry, and Performance in Isoprene Polymerization.
M. Zimmermann, K. W. Törnroos, H. Sitzmann, R. Anwander.
Chemistry-A European Journal **2008**, 14, 7266-7277.
- Paper VIII** Structure-Reactivity Relationships of Amido-Pyridine Supported Rare-Earth-Metal Alkyl Complexes
M. Zimmermann, K. W. Törnroos, R. M. Waymouth, R. Anwander.
Organometallics **2008**, 27, 4310-4317.

Abbreviations

| | | | |
|-----------------------|---|----------------------|---|
| Ar | Aryl | M | Metal |
| tBu | Tertbutyl | <i>M</i> | Molecular weight |
| Cp | Cyclopentadienyl | <i>M_n</i> | Number average molar mass |
| Cp* | 1,2,3,4,5-Pentamethyl- cyclopentadienyl | <i>M_w</i> | Weight average molar mass |
| Cp ^R | Substituted cyclopentadienyl | MAO | Methylaluminoxane |
| CPMAS | Cross-polarization magic angle spinning | MAS | Magic angle spinning |
| δ | Chemical shift | Me | Methyl |
| DFT | Density functional theory | MHz | Megahertz |
| diglyme | Bis(2-methoxyethyl) ether | min | Minute(s) |
| dme | 1,2-Dimethoxyethane | MMA | Methyl methacrylate |
| dmpe | 1,2-Bis(dimethyl- phosphino)ethane | NMR | Nuclear magnetic resonance spectroscopy |
| DMSO | Dimethylsulfoxide | PBD | Poly(butadiene) |
| eq. | Equivalent(s) | PDI | Polydispersity index |
| Et | Ethyl | Ph | Phenyl |
| exc. | Excess | PIP | Poly(isoprene) |
| FTIR | Fourier-transformation infrared spectroscopy | PMMA | Poly(methyl methacrylate) |
| h | Hour(s) | <i>i</i> Pr | <i>Isopropyl</i> |
| HMQC | Heteronuclear multiple quantum coherence | ppm | Parts per million |
| Hz | Hertz | R | Organic substituent |
| IP | Isoprene | Ref. | Reference |
| IR | Infrared | ROP | Ring-opening polymerization |
| ⁿ <i>J</i> | Coupling constant over <i>n</i> bonds | rt | Ambient temperature |
| Ln | Rare-earth metal (Sc, Y, La- Lu) | SEC | Size exclusion chromatography |
| | | teed | Tetraethylethylenediamine |
| | | thf | Tetrahydrofuran |
| | | TiBAO | Tris(<i>isobutyl</i>)aluminoxane |
| | | tmeda | <i>N,N,N',N'</i> -Tetramethyl- ethylenediamine |
| | | X | Halide |

Definitions

The term **rare-earth metal** is used for the group 3b elements scandium, yttrium, and the fourteen **lanthanides** (lanthanum - lutetium) excluding promethium. The elements will be abbreviated by **Ln**.

A **homoleptic rare-earth metal hydrocarbyl** is a species of the formula $\text{Ln(III)R}_3(\text{solv})_x$ or $\text{Ln(II)R}_2(\text{solv})_x$ in which R is a monohapto (σ -bond) hydrocarbyl group, including an alkyl, aralkyl, or alkynyl group or a substituted derivative thereof. Compounds containing donor solvent molecules (solv) as the only additional ligands are also referred to as homoleptic (e.g., $\text{Ln}(\text{CH}_2\text{SiMe}_3)_3(\text{thf})_x$).

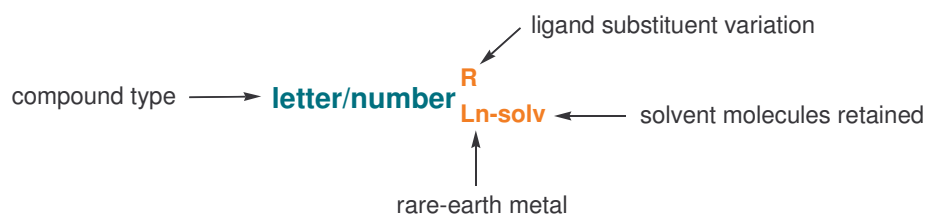
Stability is clearly a relative term and refers to thermal robustness under vacuum or in an anhydrous, anaerobic, inert atmosphere (exceptions mentioned in the text).

According to the IUPAC definition, a **metallocene** contains a transition metal and two cyclopentadienyl ligands (Cp) coordinated in a sandwich structure (bis(η^5 -cyclopentadienyl) metal complex). In contrast to the more strict definition proposed by IUPAC, this term will further be used for complexes containing two η^5 -coordinated cyclopentadienyl derivatives (Cp^R).

In the special case of rare-earth metal derivatives containing two η^5 -coordinated cyclopentadienyl derivatives (Cp^R) the term **lanthanidocene** will be used.

Nomenclature

Compounds will be labelled according to the system:



Chapter A: Rare-Earth Metal Alkyls

Homoleptic rare-earth metal hydrocarbyl complexes will be named **A - Z** (see list).

Heteroleptic rare-earth metal complexes will be numbered **1 - 156**.

Chapter B: Summary of the Main Results

Rare-earth metal complexes will be numbered **a-u**.

Nomenclature

- A** $\text{Ln(II)[CH(SiMe}_3)_2]_2(\text{solv})_x$
- B** $\text{Ln(II)[CH(SiMe}_3)_2]_3\text{M(solv)}_x$
- C** $\text{Ln(III)[CH(SiMe}_3)_2]_3$
- D** $\text{Ln(III)[CH(SiMe}_3)(\text{SiMe}_2\text{OMe})]_3$
- E** $\{\text{Ln[CH(SiMe}_3)_2]_3\text{X}\}\{\text{M(solv)}_x\}$
- F** $\{\text{Ln[CH(SiMe}_3)_2]_3\text{Me}\}\{\text{M(solv)}_x\}$
- G** $\text{Ln(II)[C(SiMe}_3)_3]_2$
- H** $\text{Ln(II)[C(SiMe}_3)_2(\text{SiMe}_2\text{R})]_2$
- J** $\{\text{Ln(II)[C(SiMe}_3)_2(\text{SiMe}_2\text{R})](\text{Et}_2\text{O})_2\}_2$
- K** $\text{Ln(III)(CH}_2\text{SiMe}_3)_3(\text{thf})_x$
- L** $[\text{Li(solv)}_x][\text{Ln(CH}_2\text{SiMe}_3)_4]$
- M** $\text{Ln(III)(CH}_2\text{SiMe}_2\text{Ph})_3(\text{thf})_2$
- N** $[\text{Li(solv)}_x][\text{Ln}^t\text{Bu}_4]$
- O** $\text{Ln(CH}_2^t\text{Bu})_3(\text{thf})_2$
- P** $\text{Ln(CH}_2\text{Ph})_3(\text{thf})_3$, $\text{Ln(CH}_2\text{C}_6\text{H}_4\text{-4-Me})_3(\text{thf})_3$, $\text{Ln(CH}_2\text{C}_6\text{H}_4\text{-o-NMe}_2)_3$,
and $\text{Ln(CH}_2\text{C}_6\text{H}_4\text{-o-SiMe}_3)_3$
- Q** $\text{Ln(o-C}_6\text{H}_4\text{CH}_2\text{NMe}_2)_3$
- R** $\text{Ln(II)(C}\equiv\text{CR)}_2(\text{solv})_x$
- S** $\{[(\text{PhC}\equiv\text{C})_3\text{Cu}][\text{Ln(solv)}_x]\}_2$
- T** $\text{Ln(III)(C}\equiv\text{CR)}_3(\text{solv})_x$
- U** $[\text{Li(donor)}]_3[\text{LnMe}_6]$
- V** $[\text{LnMe}_3]_n$
- W** $[\text{Ln}_a\text{Al}_b\text{Me}_c\text{Cl}_d]_n$
- X** $\text{Ln(II)(AIR}_4)_2$
- Y** $\text{Ln(III)(AIR}_4)_3$
- Z** $\text{Ln(III)(GaMe}_4)_3$

Objectives of this Thesis

Homoleptic rare-earth metal hydrocarbyl compounds and particularly rare-earth metal alkyl compounds constitute a prolific field of rare-earth metal chemistry. Such compounds are routinely used as precursor compounds for the synthesis of heteroleptic derivatives providing an efficient entry into organo-rare-earth metal based catalysis as well as unique model systems for studying elementary processes in olefin polymerization.

However, their implementation is hampered by several factors like formation of anionic or ate complexes, donor/solvent complexation, and the formation of polymeric networks. One major challenge remains the Ln cation size dependent availability and stability of rare-earth metal alkyl precursors. **Chapter A** of this thesis gives a detailed summary of all known homoleptic rare-earth metal hydrocarbyl compounds. Main aspects addressed are synthesis protocols, availability, (thermal) stability, and the suitability as rare-earth metal alkyl precursors.

Besides the right choice of the rare-earth metal alkyl precursor, ancillary ligand design is an important strategy to improve complex stability and the overall catalytic performance of homogeneous catalysts. Optimization, however, often turns into a tightrope walk between ultimate complex stability and catalytic inactivity/activity.

Based on these considerations, this thesis is devoted to the investigation of structure-reactivity relationships of heteroleptic rare-earth metal alkyl complexes (**Chapter B** and **Chapter C**). The suitability of rare-earth metal alkyl precursors is addressed as well as the ancillary ligand design. Particularly emphasized are the following aspects:

- Intrinsic properties of homoleptic tris(tetramethylaluminate) complexes $\text{Ln}(\text{AlMe}_4)_3$
- Application of $\text{Ln}(\text{AlMe}_4)_3$ as homoleptic rare-earth metal alkyl precursors in the synthesis of non-cyclopentadienyl (post-lanthanidocene) and cyclopentadienyl rare-earth metal alkyl complexes
- Heterobimetallic Ln/Al complexes as model systems for post-lanthanidocene based ZIEGLER-NATTA catalysis
- Heterobimetallic Ln/Al complexes as pre-catalysts
- Pre-catalyst/co-catalyst interactions and the implications for the catalytic performance

A

Rare-Earth Metal Alkyls

1 Rare-Earth Metal Alkyls

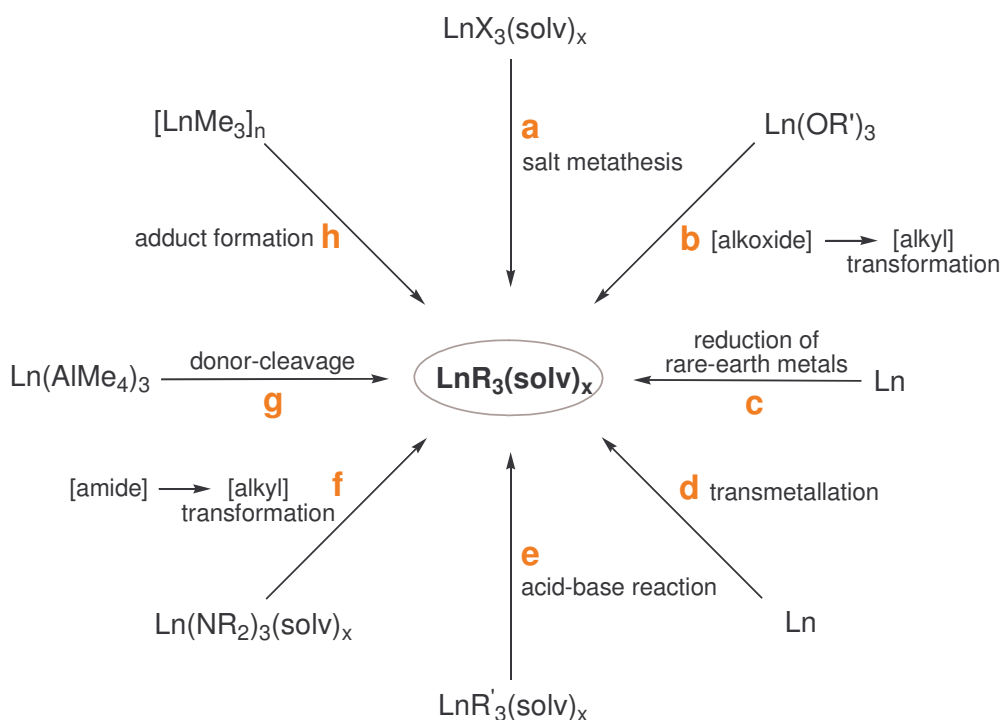
Since FRANKLAND'S discovery of the spontaneously inflammable ZnEt_2 in 1849,¹ metal alkyls have been of considerably growing interest. Until the 1960s homoleptic metal σ -hydrocarbyls were described for most of the main group elements, albeit only in the higher oxidation states for elements such as Hg, Tl, Sn, or Pb.² Unsuccessful attempts to prepare simple transition metal alkyl derivatives were generally attributed to the low stability of such compounds³ – a result of weak transition metal carbon bonds.⁴ The following decade was marked by significant progress in the transition metal chemistry of σ -hydrocarbyl ligands.⁵ However, homoleptic transition metal compounds were unusual and the known compounds highly unstable (TiMe_4 , ZrMe_4).⁶⁻⁸ A breakthrough in organo-transition metal alkyl chemistry was independently achieved by LAPPERT and WILKINSON. With the introduction of bulky alkyl groups like $[\text{CH}_2\text{SiMe}_3]$, $[\text{CH}(\text{SiMe}_3)_2]$, $[\text{CH}_2\text{CMe}_3]$, or $[\text{CH}_2\text{Ph}]$, stable transition metal alkyl complexes became accessible, suggesting that transition metal carbon bonds are not inherently weak.⁹⁻¹² The synthesis of kinetically stable complexes rather depends on the choice of a suitable ligand.

The first preparation of an organo-rare-earth metal compound, the synthesis of LnEt_3 ($\text{Ln} = \text{Sc}, \text{Y}$), had been claimed as early as 1938.¹³ The synthesis, however, could never be repeated. In connection with the Manhattan-project GILMAN and JONES attempted the preparation of organo-lanthanide compounds. Reacting LaCl_3 with phenyllithium in ether or lanthanum metal with diphenylmercury at 135°C in a sealed tube for 100 days, rather yielded biphenyl than an organometallic compound.¹⁴ In 1968 HART and SARAN reported the synthesis of $\text{Sc}(\text{C}_6\text{H}_5)_3$ as the first genuine σ -bonded organometallic compound of a rare-earth element.¹⁵ Attempts to obtain permethylated rare-earth metal complexes " LnMe_3 " as the simplest organometallic derivative are strongly related to SCHUMANN.¹⁶⁻¹⁸ In the early 1980s SCHUMANN and MÜLLER succeeded in the synthesis of thermally stable ate complexes $[\text{Li}(\text{donor})]_3[\text{LnMe}_6]$,¹⁹ but it took another 20 years until the elusive neutral rare-earth metal methyl complexes $[\text{LnMe}_3]_n$ were isolated and characterized by ANWANDER.²⁰

In accordance with *d*-transition metal chemistry, the introduction of "neopentyl"-type ligands $[\text{CH}_2\text{CMe}_3]$, and particularly the silyl-substituted variants $[\text{CH}_2\text{SiMe}_3]$, $[\text{CH}(\text{SiMe}_3)_2]$, and $[\text{C}(\text{SiMe}_3)_3]$ by LAPPERT and EABORN opened up for prolific organo-rare-

earth metal chemistry.²¹⁻²³ Until today, such (trimethylsilyl)-methane derivatives are the most widely applied alkyl ligands in rare-earth metal chemistry.

Associated with the exceptional progression in the field of rare-earth metal hydrocarbyls several synthesis routes to homoleptic rare-earth metal alkyl, aralkyl, and alkynyl complexes have been developed. Scheme 1 indicates common synthesis pathways toward the formation of Ln–C(hydrocarbyl) bonds. Important compound-specific details and differing synthesis protocols are mentioned in the following chapters.



Scheme 1: Synthesis routes to homoleptic rare-earth metal hydrocarbyls.

Rare-earth metal halides are suitable precursors for a variety of rare-earth metal hydrocarbyl compounds. Traditional salt metathesis reaction of $\text{LnX}_3(\text{solv})_x$ and an organo-alkali metal compound therefore remains by far the predominant synthesis route (Scheme 1 a). However, incorporation of alkali metal salts and ate complex formation are often observed (*vide infra*). As this is usually an undesired feature and particularly pronounced in rare-earth metal alkyl chemistry, alternative synthesis routes involving well-defined metalorganic precursors have been developed.

The transformation of lanthanide alkoxide bonds to lanthanide alkyl bonds in some cases is an attractive alternative to the traditional salt metathesis reaction (Scheme 1 b). The outcome of this kinetically controlled metathesis reaction is very sensitive toward slight changes of reaction conditions and the properties of the reactants, though.

Reduction of rare-earth metals (Scheme 1 c) and transmetallation reactions (Scheme 1 d) as synthesis protocols are so far limited to the few lanthanide elements with readily available divalent oxidation states (Sm, Eu, Yb).

Due to the comparatively low acidity of hydrocarbon acids (*vide infra*), an [alkyl] → [alkyl] exchange as a synthesis route toward homoleptic rare-earth metal hydrocarbyl complexes could only be utilized for relatively acidic alkynes (Scheme 1 e).

Peralkylation of rare-earth metal amide complexes ([amide] → [alkyl] transformation) using LEWIS acidic group 3a alkyls (AlR₃, GaMe₃) offers an elegant route to heterobimetallic Ln/M alkyl compounds (Scheme 1 f). Strongly connected to the intrinsic properties of such heterobimetallic compounds the donor-cleavage of a tetraalkylaluminato moiety was found to be a unique route to highly reactive rare-earth metal methyl compounds (Scheme 1 g). The reverse adduct formation displays an economic pathway toward several other bimetallic compounds (Scheme 1 h).

Rare-earth metals are characterized by high electrophilicity, coordinative unsaturation and the ability to support high coordination numbers (8 to 12).²⁴ The 4f valence orbitals of the lanthanides are embedded in the interior of the ion, well shielded by the 5s² and 5p⁶ orbitals.²⁵ Consequently, their poor overlap with ligand orbitals contributes to the predominant ionic character of organo-lanthanide complexes. Thus, the chemistry of the rare-earth metal complexes is rather governed by electrostatic and steric requirements than by filled orbital considerations. The gradual decrease in ionic radius (lanthanide contraction) and the limited radial extension of the valence orbitals are manifested in subtle reactivity changes of complexes with analogous ligand environments but different rare-earth metal centers.²⁶⁻²⁹

The given general characterization of rare-earth metals imply challenges inherent to the accessibility and stability of homoleptic rare-earth metal hydrocarbyl complexes. Besides extreme sensitivity toward air and moisture, the large size of the rare-earth metal cation and its preference for high coordination numbers are the main challenges to be met by the hydrocarbyl ligand. Potential ligands have to provide enough steric bulk and/or additionally coordinating groups to achieve steric and electronic saturation of the rare-earth metal center. In the absence of such bulky ligands, steric and electronic saturation is achieved by various methods severely influencing the complex stability and reactivity:

- **Formation of anionic or ate complexes**

The formation of anionic rare-earth metal ligand moieties or ate complexation are commonly observed features of salt metathesis reactions when alkali metal hydrocarbyl derivatives are employed (*vide infra*). Ate complexation, as main product or as contamination, occurs via coordination of additional counter ligands or alkali metal halide incorporation. Due to the additional electronic and steric saturation of the metal environment, the reactivity of ate complexes is significantly decreased.

- **Donor-interactions/Solvent complexation**

Solvent complexation usually results from salt metathesis reactions carried out in ethereal solvents such as Et₂O or thf (*vide infra*). Solvent coordination usually decreases the reactivity of Ln–R bonds by depolarization, steric saturation, and competitive reactions. As the majority of organic transformations mediated/catalyzed by lanthanide centers depends on the pre-coordination of a neutral, functionalized substrate, solvent coordination possibly suppresses substrate coordination by stereoelectronic saturation of the rare-earth metal center. However, donor-coordination in many cases allows for the isolation of otherwise labile homoleptic rare-earth metal hydrocarbyl complexes. It can further enforce crystallization and brake up polymeric networks.

- **Formation of polymeric networks**

Steric and electronic factors often force the stabilization of monometallic species via agglomeration (*vide infra*). Formation of di- and multinuclear species is achieved by intermolecular bridging of the smallest, most reactive and labile Ln–R bond and, hence leads to decreased reactivity. Formation of polymeric networks can further result in low solubility of the respective compounds, frustrating characterization and further reactions.

Despite the requirements for a suitable ligand system a variety of hydrocarbyl ligands has been successfully applied to organo-rare-earth metal chemistry.

One of the concepts applied includes hydrocarbyl ligands containing “built in” chelating donor functionalities. Intramolecular ring formation via dative bonds stabilizes mononuclear complexes by the chelate- and entropy-effect. Ligand-bonded donor groups successfully compete with donor solvent molecules for coordination sites, implying improved thermal stability. The interaction of strong donor-groups significantly decreases the reactivity of an adjacent Ln–R bond, but enhances the complex stability.

Introduction of bulky neopentyl-type ligands and particularly the use of silyl-substituted derivatives $[\text{CH}_2\text{SiMe}_3]$, $[\text{CH}(\text{SiMe}_3)_2]$, and $[\text{C}(\text{SiMe}_3)_3]$ resulted in very high stability of the respective rare-earth metal complexes. As the β -elimination pathway is an important decomposition route in early transition metal chemistry, ligand degradation reactions are impeded by the absence of β -hydrogen atoms. The remarkable stabilizing effect of the silyl substituents is further attributed to the stabilization of the respective carbanion by $(p \rightarrow d)_\pi$ or $(p \rightarrow \sigma^*)$ interaction with the silicon atom.³⁰⁻³²

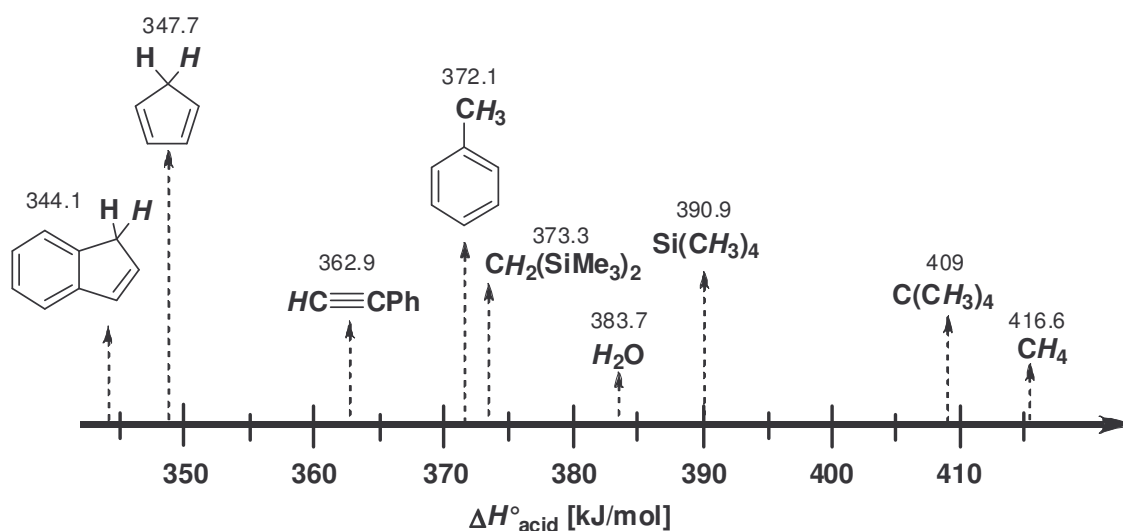


Figure 1: Gas-phase acidities of several CH acidic compounds relevant for rare-earth metal hydrocarbyl chemistry.³²⁻³⁴

Measurement of the gas-phase acidity^[*] of the corresponding carbon acids indeed revealed a significant stabilization of the α -silyl substituted carbanions. The acidity, relative to neopentane, increases by about 20 kcal/mol and 36 kcal/mol for the addition of one or two silyl-groups.^{32,33}

Rare-earth metal alkyl compounds are important alkyl transfer reagents and initiate a variety of catalytic reactions. The $\text{Ln}-\text{C}(\text{hydrocarbyl})$ bond is significantly weaker than $\text{Ln}-\text{O}(\text{alkoxide})$ bonds and even weaker as $\text{Ln}-\text{N}(\text{amide})$ bonds (except $\text{Ln}-\text{C}\equiv\text{CPh}$), which strongly affects the synthesis chemistry and derivatization of rare-earth metal hydrocarbyl complexes.

[*] The gas-phase proton affinity (gas-phase acidity) is defined as the enthalpy change for the heterolytic $\text{H}-\text{R}$ bond dissociation, $\Delta H^\circ_{\text{acid}}(\text{HR}) = D^\circ(\text{H}-\text{R}) - \text{EA}(\text{R}) + \text{IP}(\text{H})$. The smaller the $\Delta H^\circ_{\text{acid}}$ value, the more acidic the compound.

This has been confirmed by the determination of absolute bond disruption enthalpies D by means of calorimetric titrations for the representative systems $\text{Cp}^+\text{Sm}-\text{X}$ ($\text{X} = \text{OtBu}$, $D = 82.4$ kcal/mol; $\text{NMe}_2 = 48.2$ kcal/mol; $\text{CH}(\text{SiMe}_3)_2 = 47.0$ kcal/mol).³⁵ In addition to the comparably low thermodynamic stability the $\text{Ln}-\text{C}(\text{hydrocarbyl})$ bond displays kinetic lability due to its high ligand exchange ability, chelating, and solvent effects. Acid-base exchange reactions are fundamental for the derivatization of rare-earth metal hydrocarbyl complexes and the formation of catalytically active species. Therefore, the most common hydrocarbyl ligands are depicted in Figure 2 according to their increasing $\text{p}K_{\text{a}}$ values in $\text{H}_2\text{O}/\text{DMSO}$.^{36,37} Under certain restrictions this scale might be used as a measure of reactivity.

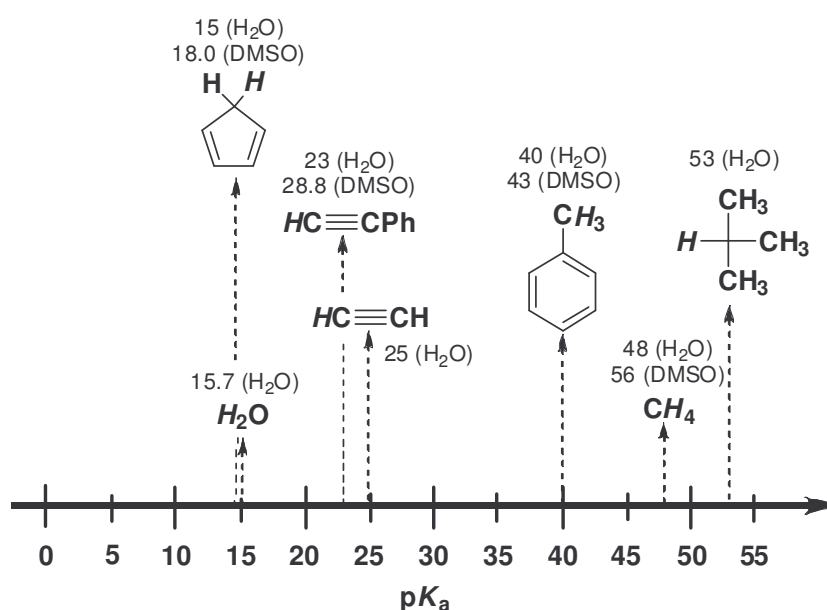


Figure 2: $\text{p}K_{\text{a}}$ values of several C–H acidic compounds relevant for rare-earth metal hydrocarbyl chemistry.^{36,37}

Due to the weak acidity of organosilanes and competitive nucleophilic displacement reactions, $\text{p}K_{\text{a}}$ values of the organosilicon compounds could so far not be measured by the usual proton-transfer equilibria studies.³⁸ A good estimation of relative acidities can, however, be obtained from the respective gas-phase acidities as depicted in Figure 1.³²⁻³⁴ Hydrocarbyl ligands show (with some exceptions) relatively high $\text{p}K_{\text{a}}$ values. In an acid-base type reaction a hydrocarbyl ligand and particularly alkyl ligands can therefore be displaced by a ligand with lower $\text{p}K_{\text{a}}$. This applies for almost all known classes of ligands, be it hydrides, amides, and alkoxides. Even though the reactivity of a $\text{Ln}-\text{C}$ bond is critically dependent upon several additional kinetic/steric and thermodynamic factors, shown characteristics give an impression of the high synthetic potential of rare-earth hydrocarbyl complexes.

2 Homoleptic Bis(trimethylsilyl)methyl Complexes

Ln(II)[CH(SiMe₃)₂]₂(solv)_x and Ln(III)[CH(SiMe₃)₂]₃

The stabilization of organorare-earth metal species has predominantly relied on π -donating ligands, especially cyclopentadienyl ligands. In the absence of these bulky ancillaries, complex stability has primarily been achieved by the use of chelates or neutral donors to increase the coordination number at the large rare-earth metal cation. In 1969 trimethylsilyl-substituted methyls were recognized as valuable ligands for main group and transition metal organometallic chemistry.³⁹ Useful properties like thermal stability, solubility, and chemical reactivity are conferred to their metal complexes. Steric bulk, the stabilizing effect of the silyl group, and the absence of β -hydrogen or β -alkyl substituents characterize this important class of alkyl ligands.⁹

The introduction of the [CH(SiMe₃)₂] ligand to group 3 metal chemistry by LAPPERT in 1974 marked the beginning of a new era of organolanthanide chemistry.²² With Y[CH(SiMe₃)₂]₃ the first neutral homoleptic solvent-free lanthanide alkyl species had been isolated and the synthesis protocol could successfully be extended to the whole series of rare-earth metals. Further, steric shielding and the stabilizing effect of trimethylsilyl methyls contributed significantly to the development of low-valent organolanthanide chemistry.

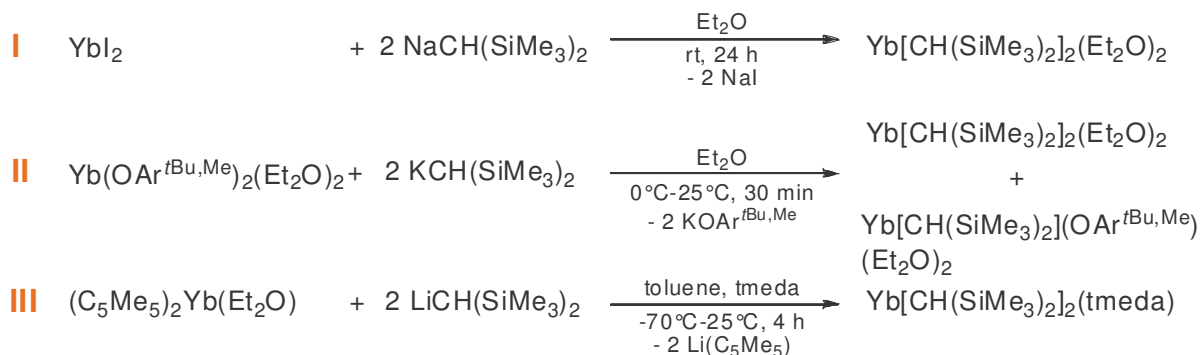
2.1 Synthesis, Structure, and Properties of Ln(II)[CH(SiMe₃)₂]₂(solv)_x

Due to their high reactivity and their potential as one-electron reducing agents, complexes of the divalent ytterbium, europium, and samarium are valuable compounds not only in organic syntheses but also as polymerization catalysts.

As shown by LAPPERT and coworkers bis(trimethylsilyl)methyl ligands provide enough steric bulk to stabilize bis(alkyl) complexes of divalent ytterbium.⁴⁰ Several synthesis approaches have been developed to produce neutral homoleptic complexes Yb[CH(SiMe₃)₂]₂(solv)_x (**A_{Yb}**) and ionic Yb[CH(SiMe₃)₂]₃M(solv)_x (**B_{Yb}**) (Scheme 2 and Scheme 3). YbI₂ and Yb(OAr^{tBu,Me})₂(Et₂O)₂ (Ar^{tBu,Me} = C₆H₂-4-Me-2,6-tBu) proved to be convenient synthesis precursors to obtain Yb[CH(SiMe₃)₂]₂(Et₂O)₂ via salt metathesis reaction with the respective sodium or potassium salts (Scheme 2, I and II).^{40,41} The bis(alkyl) products are stabilized by two molecules of weakly bound Et₂O donors. The reaction of (C₅Me₅)₂Yb(Et₂O) with two equivalents of LiCH(SiMe₃)₂ in diethyl ether

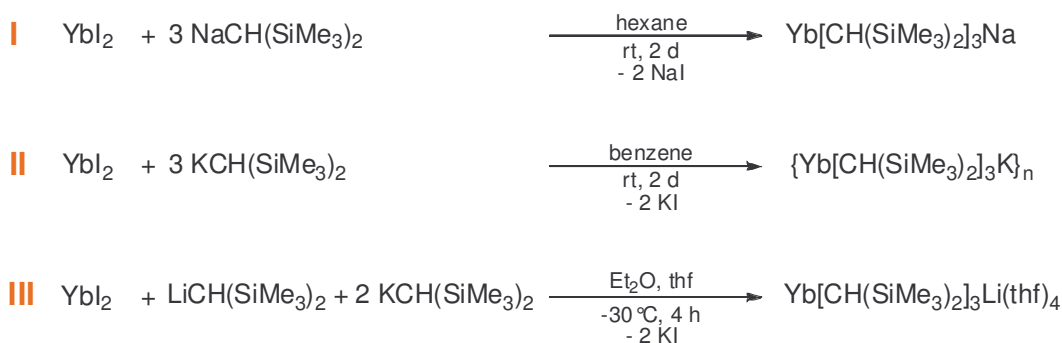
afforded a red oil, which upon dissolving in toluene and an excess of tmeda yielded the tmeda adduct Yb[CH(SiMe₃)₂]₂(tmeda) (Scheme 2, III).⁴¹

The neutral solvates have been characterized by means of ¹H, ¹³C, ²⁹Si{H}, and ¹⁷¹Yb{H} NMR spectroscopy but final structural proof is frustrated by the unavailability of suitable single crystals.



Scheme 2: Synthesis of Yb[CH(SiMe₃)₂]₂(solV)_x (**A_{Yb}**).

The lanthanide cation's desire for higher coordination numbers is impressively reflected by the reactions depicted in Scheme 3. The formation of ate complexes with lithium, sodium, and potassium cations has been reported irrespective of the stoichiometry. High yields and the formation of crystalline material substantiate higher stability of such ionic compounds Yb[CH(SiMe₃)₂]₃M(solV)_x (**B_{Yb}**) (M = Li, Na, K) compared to their neutral analogues.⁴¹



Scheme 3: Synthesis of ionic compounds Yb[CH(SiMe₃)₂]₃M(solV)_x (**B_{Yb}**).

The solid state structure of potassium salt {Yb[CH(SiMe₃)₂]₃K}_n revealed double chains of {Yb[CH(SiMe₃)₂]₃} anions linked by potassium cations along one axis (Figure 4).⁴² Each potassium has four additional close contacts to methyl carbon atoms.

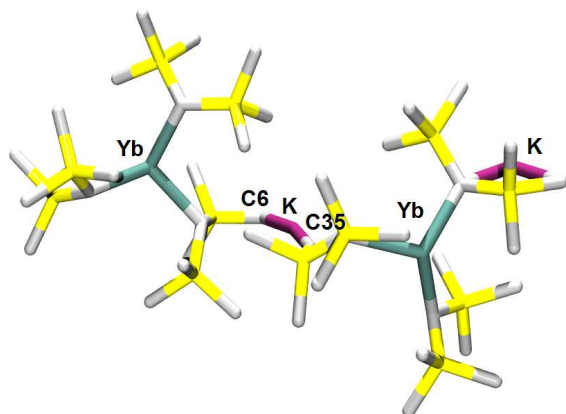


Figure 4: Solid-state structure of $\{\text{Yb}[\text{CH}(\text{SiMe}_3)_2]_3\text{K}\}_n$.

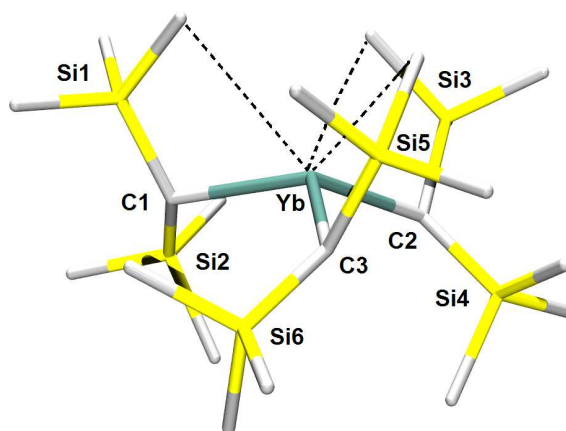
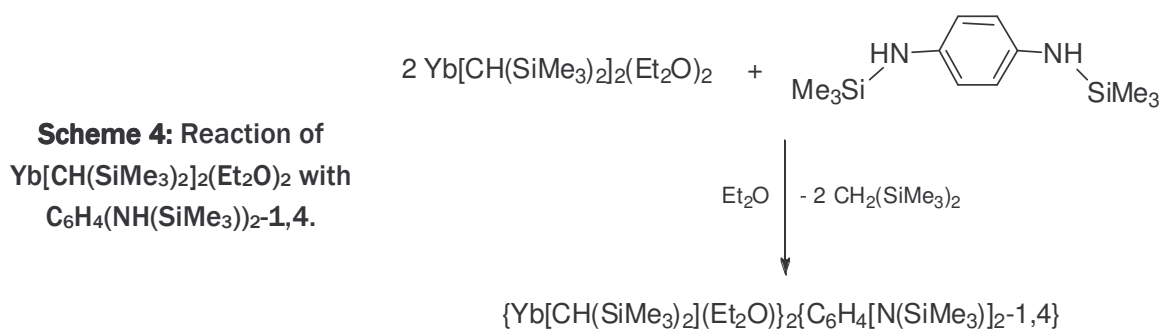


Figure 3: Solid-state structure of the $\{\text{Yb}[\text{CH}(\text{SiMe}_3)_2]_3\}$ anion in $\text{Yb}[\text{CH}(\text{SiMe}_3)_2]_3\text{Li}(\text{thf})_4$.

Stabilization by metal–methyl interactions is further present in the solid-state structure of $\text{Yb}[\text{CH}(\text{SiMe}_3)_2]_3\text{Li}(\text{thf})_4$ (Figure 3).⁴² The solvent separated ion pair consists of a $\{\text{Li}(\text{thf})_4\}$ cationic unit and a $\{\text{Yb}[\text{CH}(\text{SiMe}_3)_2]_3\}$ anion. A trigonal pyramidal environment about the ytterbium atom is accomplished and each of the $[\text{CH}(\text{SiMe}_3)_2]$ groups shows one additional close Yb methyl contact (Figure 3). Other than the lithium and potassium containing ate complexes, the sodium compound was stable at $-30\text{ }^\circ\text{C}$ but slowly decomposed at ambient temperature.

The coordinating Et_2O molecules in neutral $\text{Yb}[\text{CH}(\text{SiMe}_3)_2]_2(\text{Et}_2\text{O})_2$ can easily be displaced by a chelating 1,2-bis(dimethylphosphino)ethane (dmpe), to yield the respective $\text{Yb}[\text{CH}(\text{SiMe}_3)_2]_2(\text{dmpe})$.⁴¹ The observed reactivity is in good agreement with loosely bound diethylether donors.

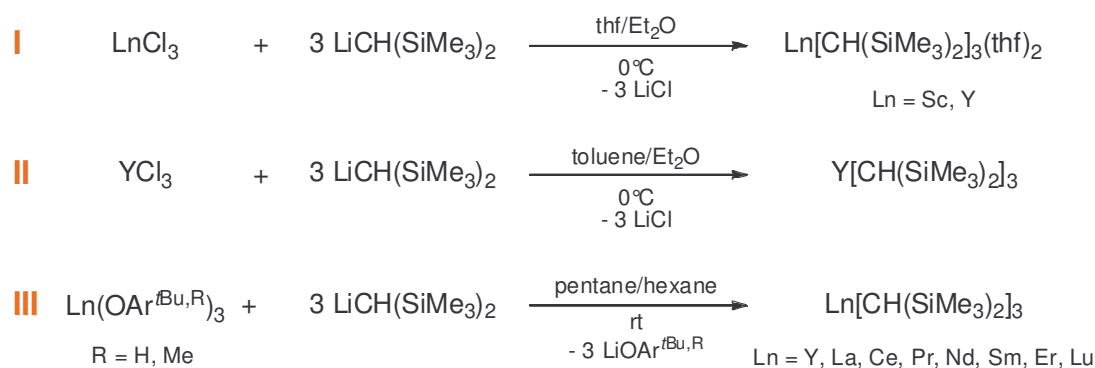
Exchange of one alkyl ligand in an alkane elimination reaction was found when reacting $\text{Yb}[\text{CH}(\text{SiMe}_3)_2]_2(\text{Et}_2\text{O})_2$ with *N,N*-bis(trimethylsilyl)-1,4-phenylenediamine (Scheme 4).⁴¹



The mixed ytterbium(II) mono(alkyl)-mono(aryloxy) Yb[CH(SiMe₃)₂](OAr^{tBu,Me})(thf)₃ was obtained when Yb(OAr^{tBu,Me})₂(thf)₃ was treated with one equivalent of KCH(SiMe₃)₂ in thf. So far the organometallic chemistry of low-valent lanthanides carrying the [CH(SiMe₃)₂] ligand has been limited to the smallest ytterbium(II) metal center. Apparently, the ligand does not provide enough steric and electronic protection to satisfy the larger metal centers Eu(II) and Sm(II).

2.2 Synthesis, Structure, and Properties of Ln(III)[CH(SiMe₃)₂]₃ and Ln(III)[CH(SiMe₃)(SiMe₂OMe)]₃

Cation size limitations have not been observed for the bis(trimethylsilyl)methyl complexes of the trivalent rare-earth metals. Already the first publication on Ln[CH(SiMe₃)₂]₃ (**C**) described the synthesis of Sc[CH(SiMe₃)₂]₃(thf)₂ as the respective compound of the smallest rare-earth metal.²² Salt metathesis reaction of LnCl₃ and the organolithium compound LiCH(SiMe₃)₂ in a mixture of thf and Et₂O further yielded the yttrium analogue as a thf solvate (Scheme 5, I).²² Solvent-free Y[CH(SiMe₃)₂]₃ could be obtained from a toluene/diethylether mixture, remarkably, the first successful synthesis of a neutral homoleptic solvent free lanthanide alkyl compound (Scheme 5, II).²² As ate complex formation under these reaction conditions is favored with increasing size of the metal cation, salt metathesis of Ln(OAr^{tBu})₃ and LiCH(SiMe₃)₂ became the predominant synthesis route (Scheme 5, III).⁴³ Insolubility of the byproduct Li(OAr^{tBu}) in hydrocarbon solvents allows for easy separation and additionally moves the equilibrium to the product side. Applying this procedure, complexes Ln[CH(SiMe₃)₂]₃ have been synthesized for Ln = Y,⁴⁴ La,⁴³ Ce,⁴⁵ Pr,⁴⁶ Nd,⁴⁶ Sm,⁴³ Er,⁴⁷ and Lu⁴⁴ covering the whole cation size range of the rare-earth metals.



Scheme 5: Synthesis of Ln(III)[CH(SiMe₃)₂]₃(solv)_x (**C**).

The solid-state structures of Ln[CH(SiMe₃)₂]₃ (Ln = Y,⁴⁵ La,⁴³ Ce,⁴⁵ and Sm⁴³) have been determined and revealed isomorphous structures with a pyramidal geometry about the metal center. The deviation from the anticipated planarity might be rationalized on

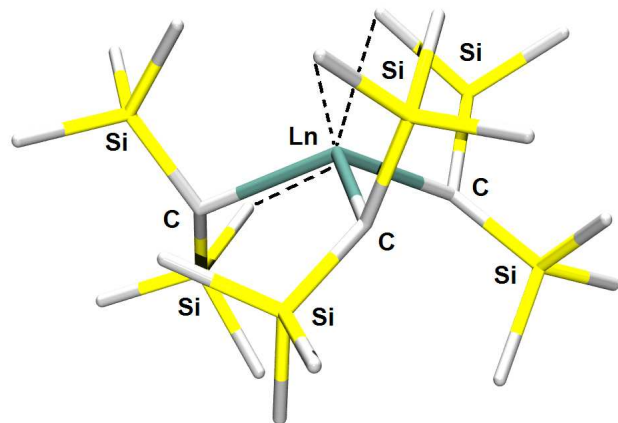
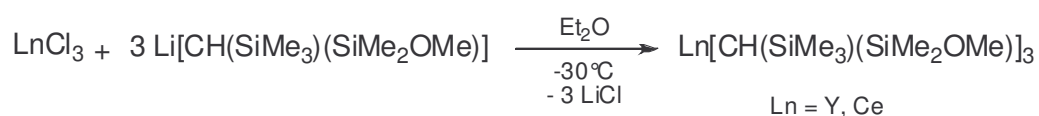


Figure 5: Solid-state structure of Ln[CH(SiMe₃)₂]₃.

steric reasons. By adopting a pyramidal structure, repulsion between the ligands is minimized and the ligand-metal attractions are maximized. Indeed, each metal center achieves coordination saturation by forming three additional close Ln-CH₃ contacts. Based on DFT calculations of La[CH(SiMe₃)₂]₃ the most likely explanation for the observed short contacts are agostic (Si-C_β)...Ln rather than (C_γ-H)...Ln

interactions.^{48,49} Due to dynamic exchange processes, the different methyl groups can not be distinguished by solution NMR even at low temperature. The ¹³C CPMAS NMR spectrum of La[CH(SiMe₃)₂]₃, however, showed two peaks for the trimethylsilyl groups.⁵⁰ Compounds Ln[CH(SiMe₃)₂]₃ are soluble in hydrocarbon, aromatic, and ethereal solvents but thermal instability has been reported. Accordingly, the thermal stability decreases with increasing size of the rare-earth metal center and decomposition leads to formation of CH₂(SiMe₃)₂ and insoluble material, which has not been further characterized.

The methoxy analogues Ln(III)[CH(SiMe₃)(SiMe₂OMe)]₃ (**D**) were synthesized from anhydrous LnCl₃ (Ln = Y, Ce) and Li[CH(SiMe₃)(SiMe₂OMe)] (Scheme 6).⁴⁵ Interestingly, no LiCl containing products were obtained from this reaction which is attributed to the intramolecular interaction of the OMe group with the rare-earth metal center.



Scheme 6: Synthesis of Ln(III)[CH(SiMe₃)(SiMe₂OMe)]₃ (**D**).

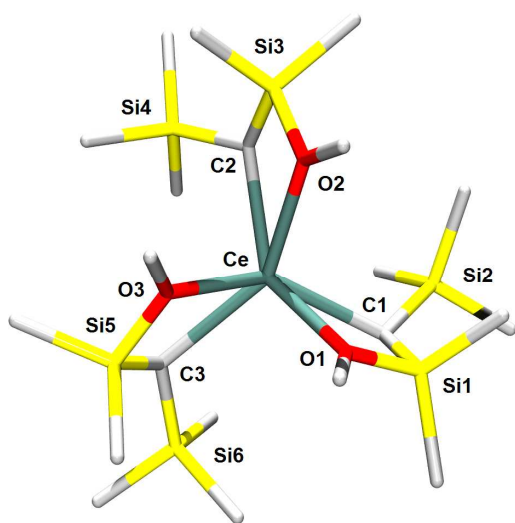
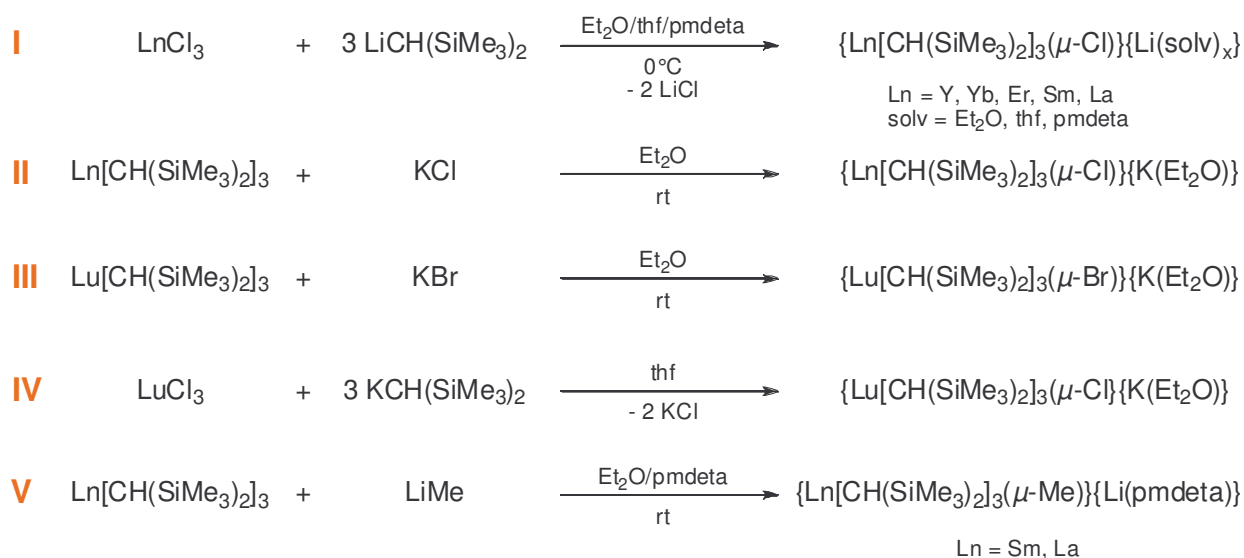


Figure 6: Solid-state structure of $\text{Ce}[\text{CH}(\text{SiMe}_3)(\text{SiMe}_2\text{OMe})]_3$.

The solid-state structures of the yttrium and cerium compounds are isostructural (Figure 6).⁴⁵ The rare-earth metal center is surrounded by the three chelating alkyl ligands in a distorted trigonal prismatic geometry. Solution NMR experiments revealed an equilibrium of two different isomers with *cis*- and *trans*-OMe groups.

As mentioned earlier the usability of $\text{LiCH}(\text{SiMe}_3)_2$ as starting material for the synthesis of neutral $\text{Ln}[\text{CH}(\text{SiMe}_3)_2]_3$ is limited. Particularly in the presence of polar donor solvents, ate complexes are the most favored reaction products. Such ionic compounds have been obtained throughout the entire rare-earth metal series (Scheme 7, I).^{51,52} The molecular structure of $\{\text{La}[\text{CH}(\text{SiMe}_3)_2]_3(\mu\text{-Cl})\}\{\text{Li}(\text{pmdeta})\}$ shows a monomer where the La and the Li atoms are linked via a single almost linear chloride bridge.⁵¹ The chloride atom sits in the vacant coordination site of $\text{La}[\text{CH}(\text{SiMe}_3)_2]_3$ without significant distortion of the $\text{La}[\text{CH}(\text{SiMe}_3)_2]_3$ skeleton.



Scheme 7: Synthesis of ate complexes $\{\text{Ln}[\text{CH}(\text{SiMe}_3)_2]_3(\mu\text{-X})\}\{\text{M}(\text{solv})_x\}$ (E) and $\{\text{Ln}[\text{CH}(\text{SiMe}_3)_2]_3(\mu\text{-Me})\}\{\text{M}(\text{solv})_x\}$ (F).

Alkali metal halide containing $\{\text{Ln}[\text{CH}(\text{SiMe}_3)_2]_3(\mu\text{-X})\}\{\text{K}(\text{Et}_2\text{O})\}$ ($\text{X} = \text{Cl}, \text{Br}$) can further be synthesized by direct adduct formation of KX and $\text{Ln}[\text{CH}(\text{SiMe}_3)_2]_3$ (Scheme 7, II and III).⁵³ The coordinating ether can readily be removed by heating the solid compound under reduced pressure. With toluene the solvent-free compound $\{\text{Lu}[\text{CH}(\text{SiMe}_3)_2]_3(\mu\text{-Cl})\}\{\text{K}\}$ formed a solvent adduct with two toluene molecules coordinated in an η^6 mode. Interestingly, the reaction of $\text{Ln}[\text{CH}(\text{SiMe}_3)_2]_3$ with one equivalent LiMe in the presence of *pmdeta* yielded monomeric $\{\text{Ln}[\text{CH}(\text{SiMe}_3)_2]_3(\mu\text{-Me})\}\{\text{Li}(\text{pmdeta})\}$ (**F**).⁵⁴ Characterization of the samarium complex by X-ray diffraction showed a structure isomorphous to μ -chloro compound $\{\text{La}[\text{CH}(\text{SiMe}_3)_2]_3(\mu\text{-Cl})\}\{\text{Li}(\text{pmdeta})\}$ with an almost linear but asymmetric $\text{Sm}-\text{CH}_3 \cdots \text{Li}$ bridge.

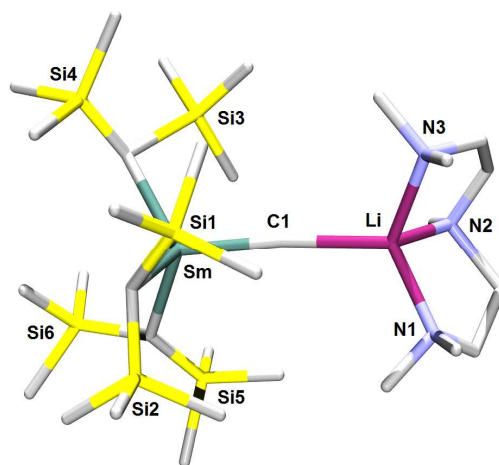


Figure 7: Solid-state structure of $\{\text{Sm}[\text{CH}(\text{SiMe}_3)_2]_3(\mu\text{-Me})\}\{\text{Li}(\text{pmdeta})\}$.

2.3 Ln(III)[CH(SiMe₃)₂]₃ as Synthesis Precursors

Homoleptic rare-earth metal alkyls $\text{Ln}[\text{CH}(\text{SiMe}_3)_2]_3$ (**C**) are valuable precursors allowing for protonolysis reactions with a variety of protic substrates under mild conditions. Their “alkyl-only” nature prevents salt coordination as well as the coordination of donor-solvents. $[\text{CH}(\text{SiMe}_3)_2]$ exchange reactions are usually kinetically controlled and very sensitive to the reactivity and steric hindrance of the reactants. Thus, alkane elimination reactions are basically limited to the early and middle lanthanide tris(alkyls).

Aiming at the synthesis of a mono(cyclopentadienyl) bis(alkyl) complex, $(\text{C}_5\text{Me}_5)\text{H}$ has been reacted with $\text{Ln}[\text{CH}(\text{SiMe}_3)_2]_3$ ($\text{Ln} = \text{La}, \text{Ce}$) to give mixtures of $(\text{C}_5\text{Me}_5)_2\text{Ln}[\text{CH}(\text{SiMe}_3)_2]$ (**2**), $(\text{C}_5\text{Me}_5)\text{Ln}[\text{CH}(\text{SiMe}_3)_2]_2$ (**3**) and $\text{Ln}[\text{CH}(\text{SiMe}_3)_2]_3$ (**C**).⁵⁵

The mixture of products was found to be the result of a competitive introduction of cyclopentadienyl ligands rather than disproportionation of (C₅Me₅)Ln[CH(SiMe₃)₂]₂. Reaction of (C₅Me₅)H with the sterically more congested Y[CH(SiMe₃)₂]₃ revealed a high kinetic barrier for the introduction of a cyclopentadienyl ligand and did not give the desired product.

The thermal stability of lanthanidocene and half-lanthanidocene complexes **2** and **3** is low and (C₅Me₅)Ln[CH(SiMe₃)₂]₂ decomposes already at ambient temperature under formation of CH₂(SiMe₃)₂ and a complex mixture of organolanthanide compounds.⁵⁶

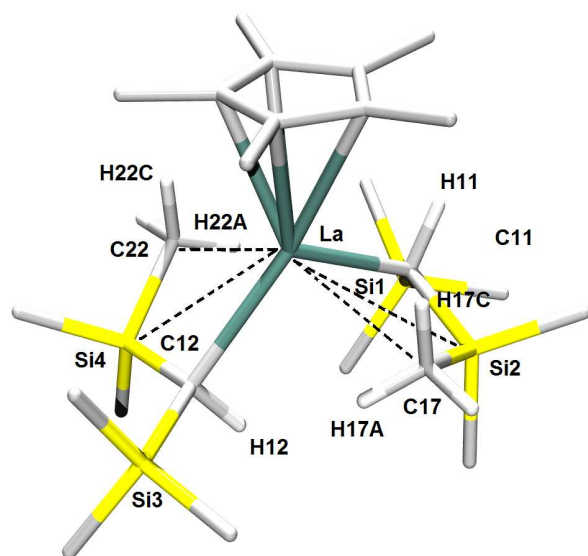


Figure 8: Solid-state structure of (C₅Me₅)La[CH(SiMe₃)₂]₂.

X-ray crystallographic investigation of (C₅Me₅)Ln[CH(SiMe₃)₂]₂ (Ln = La, Ce)^{57,58} and single crystal neutron diffraction of the lanthanum derivative⁵⁹ provided interesting insight into the alkyl ligand's interaction with the lanthanide metal center (Figure 8). The coordinative unsaturation of the metal center is relieved by secondary Ln...Si and Ln...C interactions causing a significant elongation of the agostic Si_β-C_γ bonds. Surprisingly, the methyl group hydrogen atoms of the

interacting groups are tilted away from the lanthanide metal center which is in marked contrast to agostic β- and γ-CH systems. These species may be viewed as models for the early stages of β-methyl elimination reactions.

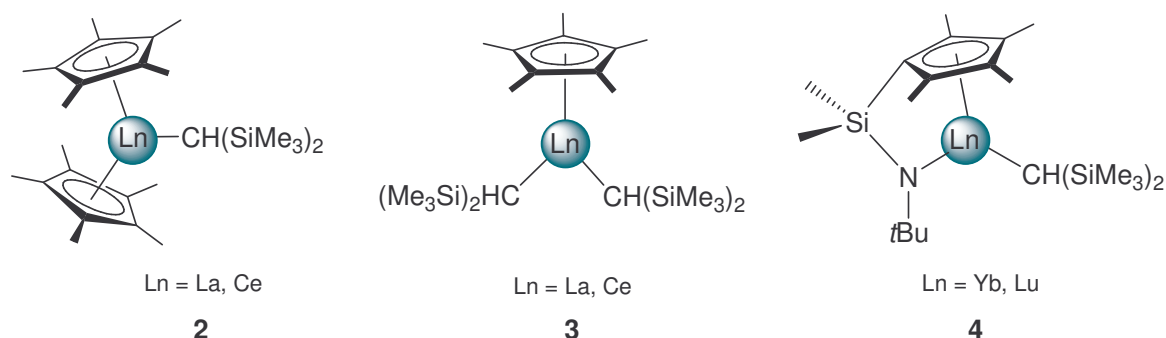


Figure 9: Lanthanidocene (**2**), half-lanthanidocene (**3**), and constrained geometry complexes (**4**) derived from Ln[CH(SiMe₃)₂]₃ (**C**).

Remarkably, homoleptic alkyls Ln[CH(SiMe₃)₂]₃ of the late lanthanide metals ytterbium and lutetium reacted with Me₂Si(C₅Me₄H)(tBuNH) to form constrained geometry complexes **4** (Figure 9).⁶⁰ However, heating was necessary to activate the tetramethylcyclopentadiene C–H group for alkane elimination. Complexes **4** are active catalysts for aminoalkene hydroamination/cyclization. The attempted synthesis of a mono(alkyl) compound using a linked alkoxide-cyclopentadienyl ligand and in situ prepared Y(OAr^{tBu})[CH(SiMe₃)₂]₂ only yielded the “alkyl-free” ate complex {η⁵:η¹-C₅H₄[CH₂CO(3,5-C₆H₃(CF₃)₂)₂]₂YLi(thf)_n (**5**).⁶¹

SCHAVERIEN ET AL. first reported the applicability of Ln[CH(SiMe₃)₂]₃ for the synthesis of non-cyclopentadienyl complexes. The reaction of octaethylporphyrin (OEPH₂) and Ln[CH(SiMe₃)₂]₃ (Ln = Y, Lu) afforded purple, hexane-soluble [OEP]Ln[CH(SiMe₃)₂] (**6**) in good yields.⁴⁴ The solid-state structure of the lutetium compound revealed an approximately square pyramidal coordination geometry at the lutetium metal with the apical site occupied by the [CH(SiMe₃)₂] ligand (Figure 10). In contrast to the geometries found for other [CH(SiMe₃)₂] containing complexes, the bis(trimethylsilyl)methyl ligand shows no interaction with the lutetium metal center.

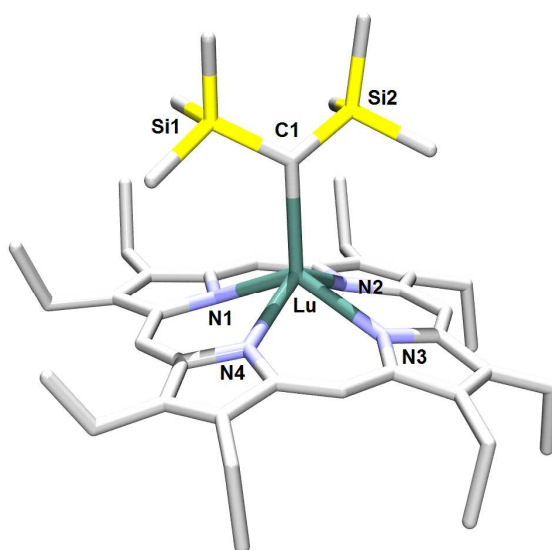


Figure 10: Solid-state structure of [OEP]Lu[CH(SiMe₃)₂] (**6**).

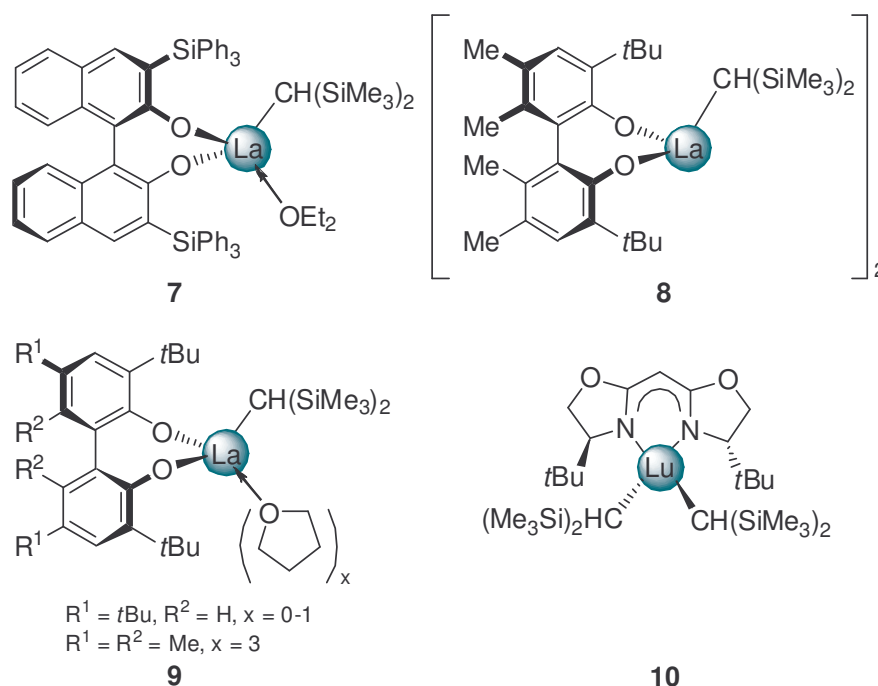


Figure 11: Bis(oxazolinato), biphenolate, and binaphtholate complexes derived from Ln[CH(SiMe₃)₂]₃ (**C**).

Mild protonolysis reactions of La[CH(SiMe₃)₂]₃ and chiral, chelating binaphtholes and biphenols resulted in the smooth formation of mono(alkyl) binaphtholate lanthanum complex **7** and mono(alkyl) biphenolate lanthanum complexes **8** and **9**, respectively (Figure 11).^{62,63} While biphenolate **8** revealed a dimeric structure in the absence of donor-solvents, the sterically quite undemanding ancillary ligand allows for coordination of up to three donor molecules in the presence of thf (**9**). Compounds **7-9** show good catalytic activity for the hydroamination/cyclization of aminoalkenes but the practical use for asymmetric hydroamination is limited by the low enantiomeric excess in the produced heterocycles.

A rare example of an enantioselective non-metallocene hydroamination catalyst is the C₂ symmetric bis(oxazolinato)lanthanide complex [(4*S*)-*t*BuBox]Lu[CH(SiMe₃)₂]₂ (**10**) synthesized via alkane elimination from Lu[CH(SiMe₃)₂]₃.⁶⁴

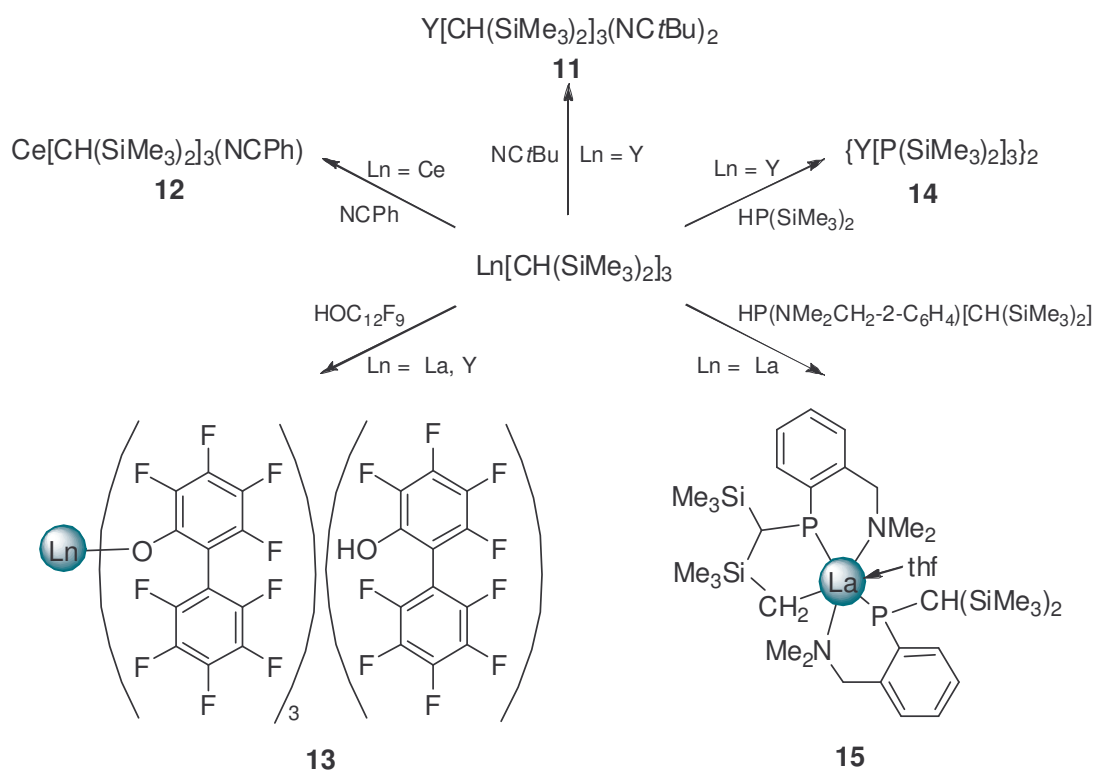
Contrary to the formation of Yb(II) 1-azaallyl and β -diketiminates when reacting divalent Yb[CH(SiMe₃)₂]₂(Et₂O)₂ with nitriles NPh and N*t*Bu, respectively,⁴⁵ only 1:2 (**11**) and 1:1 (**12**) adducts of the nitrile to the rare-earth metal center have been observed starting from trivalent Ln[CH(SiMe₃)₂]₃ (Scheme 8).⁴⁵ Even when heated in toluene no nitrile-insertion into the Ln–C bond was evidenced, presumably due to effective steric shielding and the resulting high kinetic barrier for the insertion reaction.

Acid-base reaction of Ln[CH(SiMe₃)₂]₃ (Ln = La, Y) with perfluorobiphenols quantitatively produced compounds **13** (Scheme 8) capable of forming stable ion pairs with metallocene dimethyls. Such ion pairs provided extremely active ethylene polymerization catalysts.⁶⁵

Complete ligand exchange was further observed for the reaction of bis(trimethylsilyl)phosphane and Y[CH(SiMe₃)₂]₃ yielding dimeric {Y[P(SiMe₃)₂]₃}₂ (**14**) and CH₂(SiMe₃)₂ (Scheme 8).⁶⁶

MARKS ET AL. found that homoleptic Ln[CH(SiMe₃)₂]₃ catalyze the phosphinoalkyne cyclization with turn-over frequencies comparable to the most active lanthanidocene catalysts. In an initiating step complete Ln-[CH(SiMe₃)₂] protonolysis is observed according to ¹H NMR spectroscopic investigations.⁶⁷

The treatment of lanthanum tris(alkyl) La[CH(SiMe₃)₂]₃ with two equivalents of the secondary phosphine HP(NMe₂CH₂-2-C₆H₄)[CH(Me₃Si)₂], however, revealed the product of a cyclometalation reaction (**15**) with the intramolecular elimination of CH₂(SiMe₃)₂ from transiently formed {[CH(SiMe₃)₂](C₆H₄-2-CH₂NMe₂)P}₂La[CH(SiMe₃)₂] (Scheme 8).⁶⁸

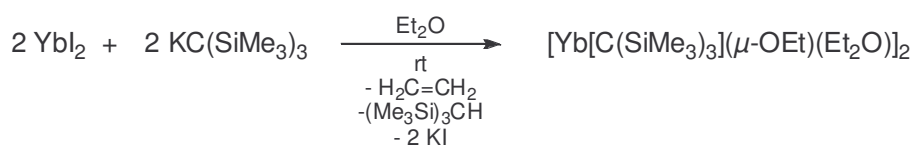


Scheme 8: Derivatization of Ln[CH(SiMe₃)₂]₃ (C).

3 Ln(II)[C(SiMe₃)₃]₂ and Ln(II)[C(SiMe₃)₂(SiMe₂R)]₂

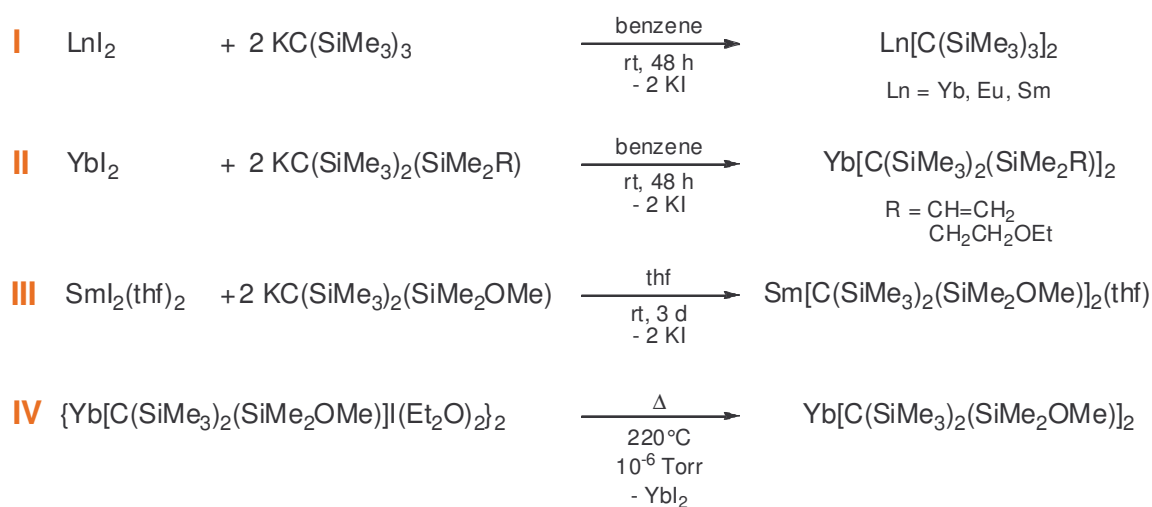
Extending the series of trimethylsilyl-substituted methyl ligands to the highest possible substitution at the methyl-carbon atom leads to extremely bulky [C(SiMe₃)₃] ligands.²³ Due to their high steric demand such ligands are well suited to stabilize lanthanide metal centers in the divalent state. While ate complex formation was indicative of insufficient steric protection for the divalent ytterbium complexes carrying [CH(SiMe₃)₂] ligands, such salt formation is effectively suppressed in EABORN complexes Ln(II)[C(SiMe₃)₃]₂ (**G**).

However, the first attempt to synthesize a homoleptic ytterbium alkyl complex applying the reaction conditions yielding Yb[CH(SiMe₃)₂]₃(Et₂O)₂ (**A**) were not successful. Reaction of YbI₂ with two equivalents of KC(SiMe₃)₃ in Et₂O rather gave orange-red crystals of the dimeric ether cleavage product {Yb[C(SiMe₃)₃](μ-OEt)(Et₂O)}₂ (**16**) than the putative Yb[C(SiMe₃)₃]₂ (Scheme 9).^{40,41}



Scheme 9: Synthesis of [Yb[C(SiMe₃)₃](μ-OEt)(Et₂O)]₂ (**16**).

Further attempts to synthesize Yb[C(SiMe₃)₃]₂ were undertaken in the absence of ether solvents. A suspension of YbI₂ in benzene reacted with a solution of KC(SiMe₃)₃ to yield the homoleptic, solvent free ytterbium alkyl complex Yb[C(SiMe₃)₃]₂ (Scheme 10, **I**).²³



Scheme 10: Synthesis of Ln(II)[C(SiMe₃)₃]₂ (**G**) and Ln(II)[C(SiMe₃)₂(SiMe₂R)]₂ (**H**).

The respective europium(II)⁶⁹ and samarium(II)⁷⁰ complexes were synthesized the same way, with yields decreasing with increasing size of the metal cation (Yb > Eu > Sm). The crystal structures of all three compounds have been determined and revealed solvent-free monomers (Figure 12 and Figure 13).

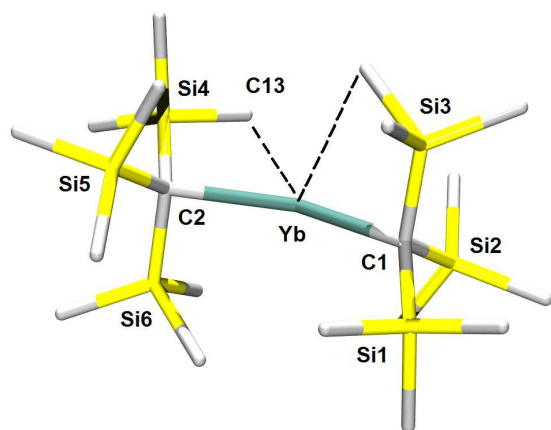


Figure 12: Solid-state structure of Yb[C(SiMe₃)₃]₂.

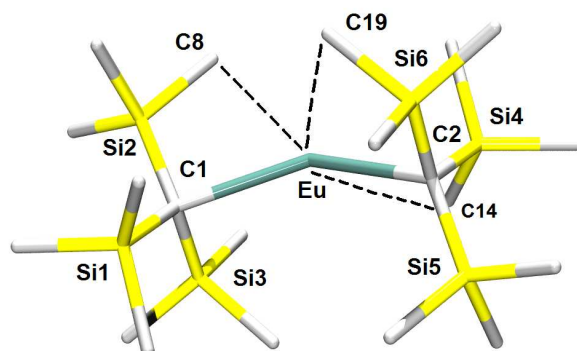


Figure 13: Solid-state structure of Eu[C(SiMe₃)₃]₂.

The most interesting feature of the solid-state structures are the bent C–Ln–C angles (137°, Yb; 136°, Eu; 143°, Sm). Similar bending is also observed for the respective bis(cyclopentadienyls) Ln(C₅Me₅)₂.⁷¹⁻⁷⁴ There has been intensive discussion whether the bending is caused by electronic factors^{75,76} or by ligand interactions.⁷⁷ As the latter would be significantly reduced by lengthening the metal-carbon bond, the similarity of the observed angles in the ytterbium and europium compounds suggest that the factor determining the C–Ln–C angles is electronic rather than steric. A contribution of the metal d-orbitals has been discussed.⁶⁹

The mean metal–carbon distances in complexes Ln[C(SiMe₃)₃]₂ are long compared to those observed in other linear divalent species,^{78,79} reducing the interactions between the SiMe₃ groups. The ytterbium compound shows two short Yb–methyl interactions in the solid state, which contribute to a stabilization of the molecule (Figure 12).²³ Three similar interactions were observed for the larger europium metal center (Figure 13).⁶⁹ Attempts to distinguish methyl groups by low-temperature NMR spectroscopy were not successful. All protons appeared to be equivalent even at –95 °C.

In order to provide further stabilization of complexes Ln[C(SiMe₃)₃]₂ a series of ligand modifications has been carried out and the ligand contribution on complex stability and reactivity has been studied.⁶⁹ Reaction of YbI₂ with the modified potassium salts KC(SiMe₃)₂(SiMe₂R) (R = CH=CH₂ and CH₂CH₂OEt) in benzene afforded Yb[C(SiMe₃)₂(SiMe₂R)]₂ in good yields (Scheme 10, II). A methoxy derivative of ytterbium was obtained by heating {Yb[C(SiMe₃)₂(SiMe₂OMe)](Et₂O)₂}₂ (Scheme 10, IV) under reduced pressure. More intuitive seems the synthesis of the samarium analogue starting from SmI₂(thf)₂ and the potassium salt KC(SiMe₃)₂(SiMe₂OMe) (Scheme 10,

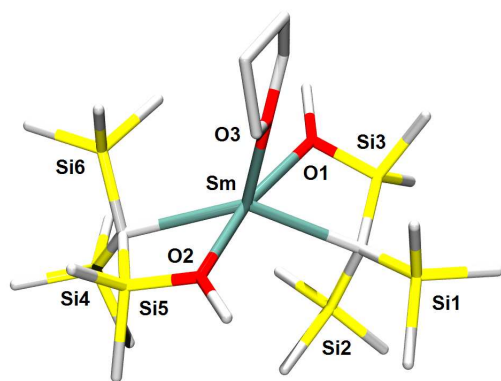


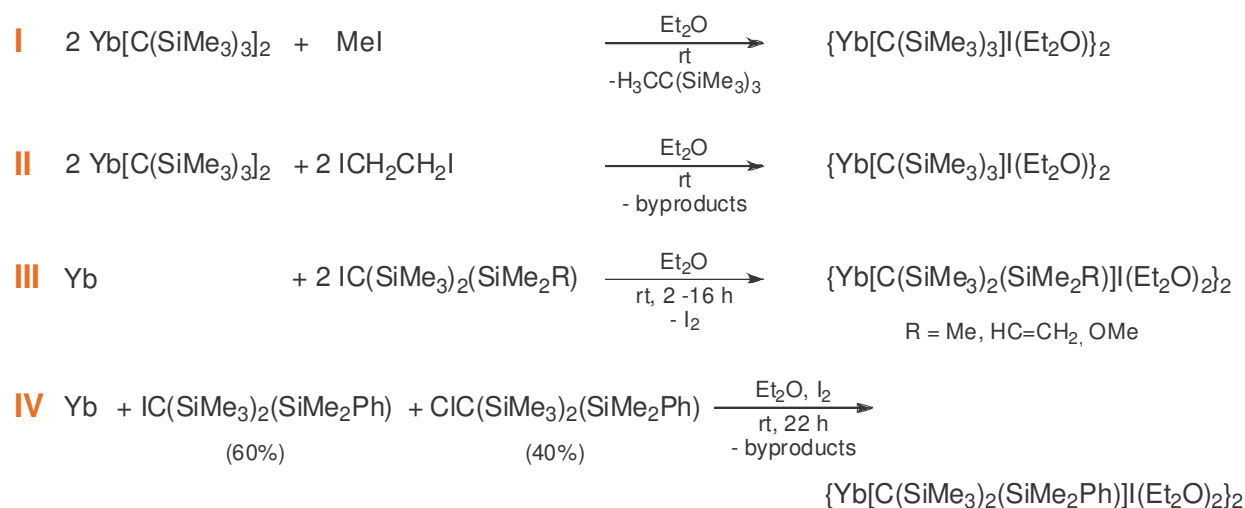
Figure 14: Solid-state structure of Sm[C(SiMe₃)₂(SiMe₂OMe)]₂(thf).

III).⁸⁰ Sm[C(SiMe₃)₂(SiMe₂OMe)]₂(thf) could be obtained in high yield as green-black single crystals grown from cyclohexane (Figure 14). The five coordinate samarium metal center is surrounded by the two chelating alkyl ligands and one thf molecule. Additional coordination of the OMe groups results in the formation of two four-membered chelate rings.

Due to the higher coordination numbers of the divalent metal center, the tendency to ether cleavage as found for Yb[C(SiMe₃)₃]₂ (Scheme 9) could be reduced dramatically. The additional interaction with the chelating ligand, even the weak vinyl–Yb interaction (for R = CH=CH₂), inhibits the coordination of Et₂O and consecutive ether cleavage reactions.

SmI₂ is a commonly used reagent in organic syntheses. Presumably, organosamarium intermediates play a key role in the SmI₂ mediated addition of alkylhalogenides to ketones (Samarium BARBIER Reaction (SBR)). The reactivity of Sm[C(SiMe₃)₂(SiMe₂OMe)]₂(thf) toward benzophenone has therefore been investigated but revealed the formation of a ketyl-radical anion complex Sm[C(SiMe₃)₂(SiMe₂OMe)]₂(OCPh₂) (**17**) rather than a GRIGNARD-like addition product.⁸⁰

A series of GRIGNARD reagent analogues with the general formula {Yb[C(SiMe₃)₂(SiMe₂R)](Et₂O)₂}₂ (J) has been reported. The reaction of Yb[C(SiMe₃)₃]₂ with iodomethane led to the cleavage of one Yb–C bond and formation of {Yb[C(SiMe₃)₃](Et₂O)₂}₂ (Scheme 11, I).²³



Scheme 11: Synthesis of $\{\text{Yb}[\text{C}(\text{SiMe}_3)_2(\text{SiMe}_2\text{R})]\text{I}(\text{Et}_2\text{O})_2\}_2$ (**J**).

The multiplicity of products/byproducts arising from this reaction, especially the formation of side-product $\text{HC}(\text{SiMe}_3)_3$, suggests a radical reaction pathway (not shown in Scheme 11). The same compound was isolated from the reaction between $\text{Yb}[\text{C}(\text{SiMe}_3)_3]_2$ and an excess of $\text{ICH}_2\text{CH}_2\text{I}$ as well as the reaction with $\text{IC}(\text{SiMe}_3)_3$ in Et_2O , respectively (Scheme 11, II and III).²³ The use of alkyl-iodides and Yb powder further allowed for the synthesis of derivatives $\{\text{Yb}[\text{C}(\text{SiMe}_3)_2(\text{SiMe}_2\text{R})]\text{I}(\text{Et}_2\text{O})_2\}_2$ (R = CH=CH₂, OMe) (Scheme 11, III).⁶⁹ $\{\text{Yb}[\text{C}(\text{SiMe}_3)_2(\text{SiMe}_2\text{Ph})]\text{I}(\text{Et}_2\text{O})_2\}_2$ was obtained from a mixture of the respective iodoalkyl and the chloroalkyl (Scheme 11, IV).⁶⁹ All “lanthanide GRIGNARD” reagents (**K**) are stable in Et_2O solutions and can be stored as such for several weeks. The alkyl ytterbium iodides decompose when heated under reduced pressure to

give $\text{Yb}[\text{C}(\text{SiMe}_3)_2(\text{SiMe}_2\text{R})]_2$ and YbI_2 (see Scheme 10, IV). In unpolar organic solvents all GRIGNARD-type ytterbium complexes exist in a typical SCHLENK equilibrium.

The solid-state structures of several alkyl iodides have been determined all substantiating dimeric structures (Figure 15).^{23,69} The molecules usually have a center of symmetry due to an almost square-planar Yb_2I_2 ring.

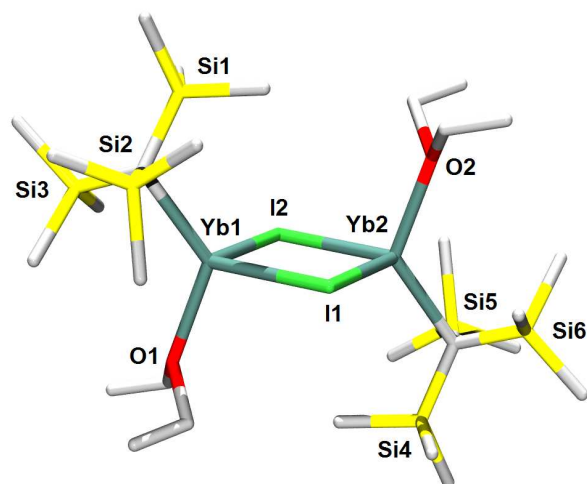


Figure 15: Solid-state structure of $\{\text{Yb}[\text{C}(\text{SiMe}_3)_3]\text{I}(\text{Et}_2\text{O})\}_2$.

Analogue structures are adopted by a number of GRIGNARD reagents.

Besides their occurrence in organic synthesis (*in situ* formation), the probably most interesting application of complexes Ln[C(SiMe₃)₃]₂ is the polymerization of methylmethacrylate and acrylonitrile.^{70,81,82} Of several tested divalent ytterbium alkyl, amide, and alkynide complexes, Yb[C(SiMe₃)₃]₂ produced poly(MMA) with the highest isotacticity (97%) and excellent yield. The obtained polymer showed high molecular weights ($M_n = 51 \cdot 10^4$ g/mol) and very narrow molecular weight distributions ($M_w/M_n = 1.1$).⁷⁰

3.1 Related Ln(II) Silylmethyl Complexes

In 1999 a closely related bidentate ligand [(Me₃Si)₂CSiMe₂CH₂CH₂SiMe₂C(SiMe₃)₂] had been introduced to low-valent lanthanide organometallic chemistry.⁸³ This ligand can be regarded to as two trimethylsilyl groups (“trisyl”) joined together like Siamese twins and thus is referred to as “trisamyl” ligand. Treatment of YbI₂ with the potassium salt of the trisamyl ligand gave the solvent-free chelate complex Yb[(Me₃Si)₂CSiMe₂CH₂CH₂SiMe₂C(SiMe₃)₂] (**18**) (Figure 16). Due to high disorder detailed structural data could not be obtained. The reaction of **18** with Et₂O was investigated and was found to be slower than the one with Yb[C(SiMe₃)₃]₂.

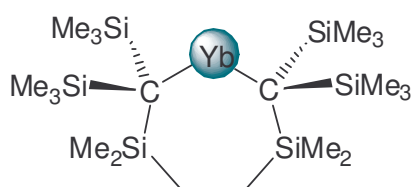
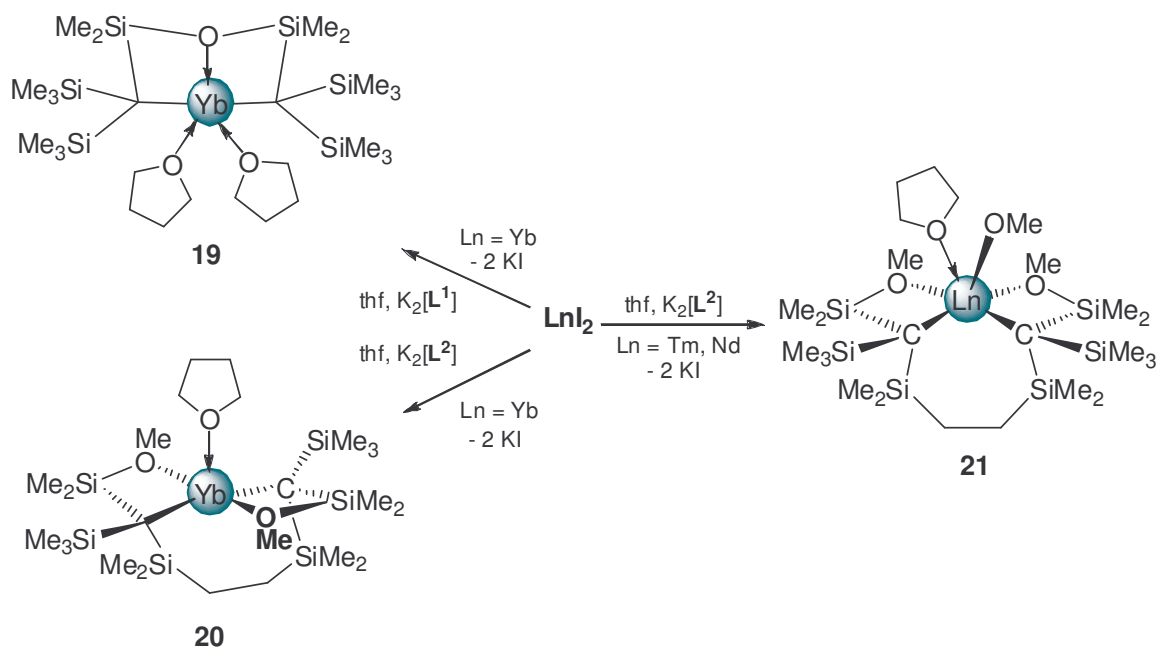


Figure 16: Structure of Yb[(Me₃Si)₂CSiMe₂CH₂CH₂SiMe₂C(SiMe₃)₂] (**18**).

Very recently the ytterbium(II) complexes of dicarbanionic sterically hindered, O-functionalized ligands [L¹] and [L²] have been reported (Scheme 12).⁸⁴ YbI₂ and either of the dipotassium agents K₂[L¹] and K₂[L²] cleanly formed the corresponding bisalkylytterbium(II) compounds **19** and **20**.



Scheme 12: Synthesis of Yb(II), Tm(III), and Nd(III) complexes with $[\text{L}^1]$ and $[\text{L}^2]$.

Both compounds react instantaneously with Et_2O as known for $\text{Yb}[\text{C}(\text{SiMe}_3)_3]_2$ (Scheme 9), but can be isolated as thf adducts. Upon standing at ambient temperature for several days, **19** partly forms a paramagnetic Yb(III) species, as evidenced by NMR experiments.

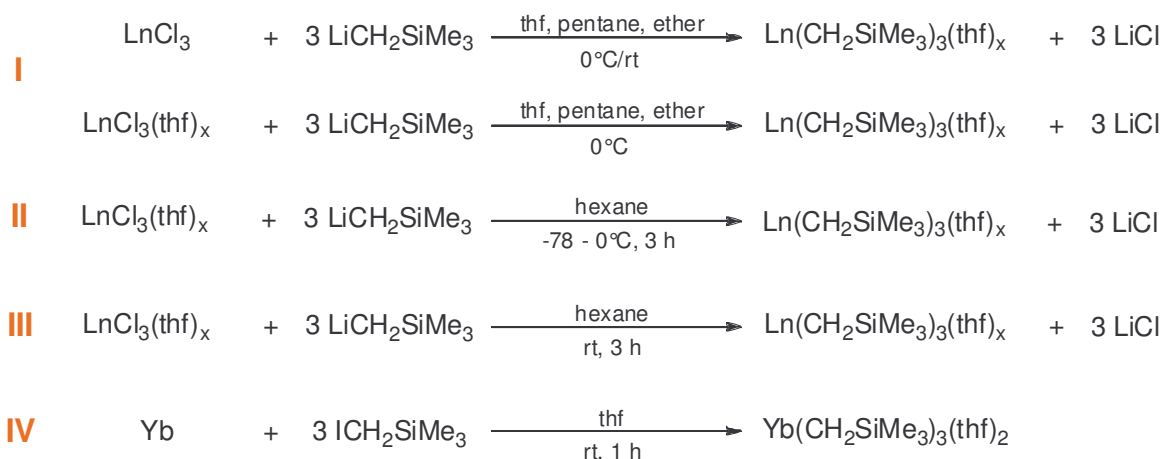
In contrast to the ready isolation of ytterbium(II) compounds, reactions between LnI_2 ($\text{Ln} = \text{Tm}, \text{Nd}$) were accompanied by oxidation of the divalent metal center to form Tm(III) and Nd(III) complexes **21** (Scheme 12). The additional metal methoxy ligand coordinated to the metal in **21** is most likely derived from Si–O cleavage of a second dicarbanion ligand.

4 Homoleptic Tris(trimethylsilyl)methyl Complexes

Ln(III)(CH₂SiMe₃)₃(thf)_x

4.1 Synthesis, Structure, and Properties

The application of homoleptic tris(trimethylsilyl)methyl rare-earth metal complexes Ln(CH₂SiMe₃)₃(thf)_x (**K**) underwent an exceptional development during the last decade. Acting as alkyl precursors they are among the most widely used starting materials in organorare-earth metal chemistry. First synthesized as early as 1973 by LAPPERT ET AL.,²¹ detailed investigations on structure and reactivity of these lanthanide hydrocarbyls were presented only recently.



Scheme 13: Synthesis of Ln(CH₂SiMe₃)₃(thf)_x (**K**).

The initial synthesis of group 3 tris(trimethylsilyl)methyl complexes Sc(CH₂SiMe₃)₃(thf)₂ and Y(CH₂SiMe₃)₃(thf)₂²¹ was extended to the lanthanide metals some years later. Main contributions were made by LAPPERT and SCHUMANN ET AL. describing the respective lutetium,⁸⁵ ytterbium,⁸⁶ thulium, erbium,^{86,87} and terbium⁸⁶ compounds. The representative of the medium-sized lanthanide metal center samarium⁸⁵ was described and characterized in 2002 marking the upper cation size limit for isolable compounds Ln(CH₂SiMe₃)₃(thf)_x.

Several synthesis procedures for Ln(CH₂SiMe₃)₃(thf)_x have been described, the majority following a salt metathesis reaction of the anhydrous rare-earth metal halides LnCl₃ or the thf adducts LnCl₃(thf)_x and three equivalents of LiCH₂SiMe₃ (Scheme 13, I - III). The original synthesis reported by LAPPERT and SCHUMANN follows eq. I in Scheme 13 using

hexane (pentane)/diethylether mixtures combined with (stoichiometric) amounts of thf.^{21,87} Reactions were performed at ca. 0 °C and ambient temperature, respectively. With the introduction of compounds Ln(CH₂SiMe₃)₃(thf)_x as rare-earth metal alkyl precursors, slightly modified synthesis protocols II and III have been applied using hexane suspensions of LnCl₃(thf)_x and LiCH₂SiMe₃.

Synthesis route IV starting from Yb chips and ICH₂SiMe₃ is limited to this redox active Yb metal center.⁸⁸ In situ preparation of the rare-earth metal alkyls has also proved suitable when further reacting Ln(CH₂SiMe₃)₃(thf)_x in alkane elimination reactions with protic reagents. Table 1 summarizes the reported synthesis approaches, the number of coordinating thf molecules, yields, and characterization of compounds **K**.

Table 1: Ln(CH₂SiMe₃)₃(thf)_x (**K**): Synthesis, thf coordination, yield, and characterization.

| Ln | Synthesis | thf _{coord.} (x) | Yield | Characterization | Ref. |
|----|-----------|---------------------------|-------|---|-------|
| Sc | I | 2 | | ¹ H, ¹³ C, IR, EA, mp | 21 |
| | II | 2 | | | |
| | III | 2 | 71% | | 89 |
| Y | I | 2 | | ¹ H, ¹³ C, ²⁹ Si, IR, EA, mp, X-ray | 21 |
| | II | 2 | 82% | | |
| | III | 3 | 69% | (x = 3) | 89 |
| Lu | I | 2 | | ¹ H, ¹³ C, IR, EA, X- ray | 91 |
| | II | 2 | 63% | | |
| | III | 2 | 65% | | 89 |
| Yb | I | 2 | | ¹ H, IR, EA, mp, X- ray | 86,91 |
| | II | 2 | | | |
| | IV | 2 | 48% | | 88 |
| Tm | I | 2 | | IR, EA | 91,92 |
| | II | 2 | | | |
| Er | I | 2 | 29% | IR, EA, mp, X-ray | 86 |
| | | | | | 87 |
| Tb | I | 2 | | IR, mp, EA | 86 |
| | II | 2 | | | |
| Sm | I | 3 | 50% | ¹ H, ¹³ C, IR, EA, mp, X-ray | 85 |

Due to inefficient steric shielding of the rare-earth metal center by the [CH₂SiMe₃] ligands complexes **K** require stabilizing donor molecules, usually thf. The number of additional thf molecules coordinated thus increases with increasing size of the rare-earth metal cation (Table 1).

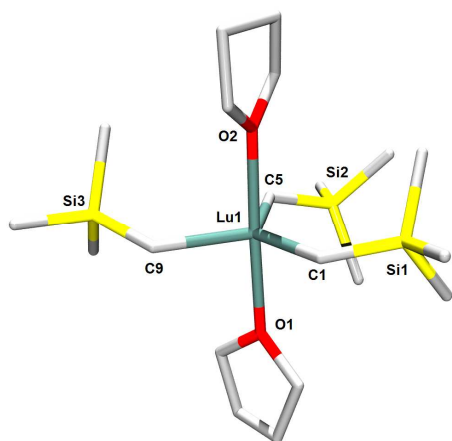


Figure 18: Molecular structure of Lu(CH₂SiMe₃)₃(thf)₂.

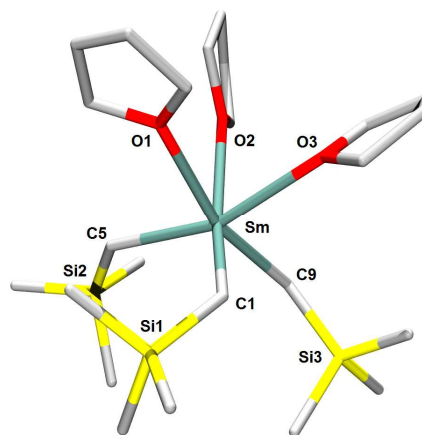
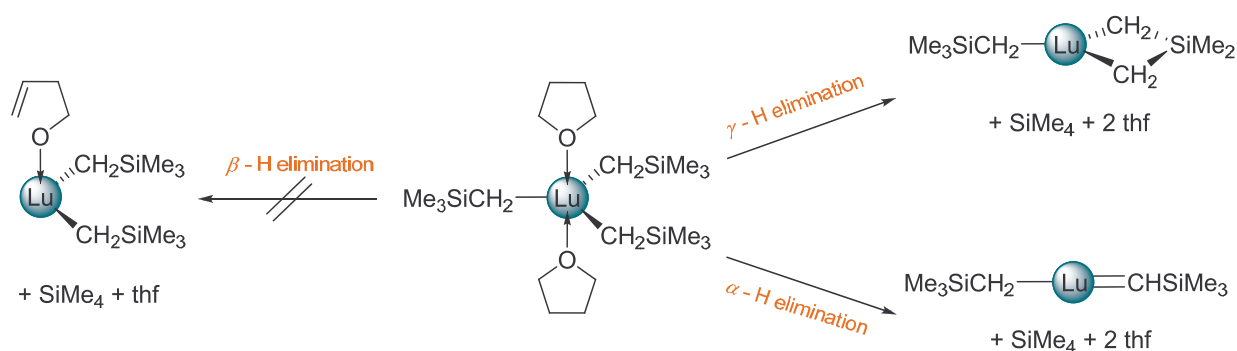


Figure 17: Molecular structure of Sm(CH₂SiMe₃)₃(thf)₃.

Solvation affects the solid-state structures of Ln(CH₂SiMe₃)₃(thf)_x (Figure 17 and Figure 18). The representatives of the smaller rare-earth metals Ln(CH₂SiMe₃)₃(thf)₂ (Ln = Lu,⁸⁵ Yb,⁸⁸ and Er⁸⁵) feature a five coordinate metal center with the three [CH₂SiMe₃] ligands occupying the equatorial and the thf oxygens occupying the axial positions of a trigonal bipyramid (Figure 18). A propeller like arrangement of the alkyl ligands around the metal center (C_{3h} symmetry) is not realised. Rather, two of the silyl groups are facing each other causing non-uniform angles C–Ln–C (max. 110°–134°) and Ln–C distances. X-ray structure analysis of Y(CH₂SiMe₃)₃(thf)₃⁹⁰ and Sm(CH₂SiMe₃)₃(thf)₃⁸⁵ revealed a distorted *fac*-octahedral coordination of alkyl ligands and the three donor thf molecules (Figure 17). The angles O–Ln–O (74°–81°) are considerably smaller than angles C–Ln–C (101°–108°). Such octahedral coordination can also be enforced by thf → diglyme ligand exchange as reported for Lu(CH₂SiMe₃)₃(thf)(diglyme).⁹³

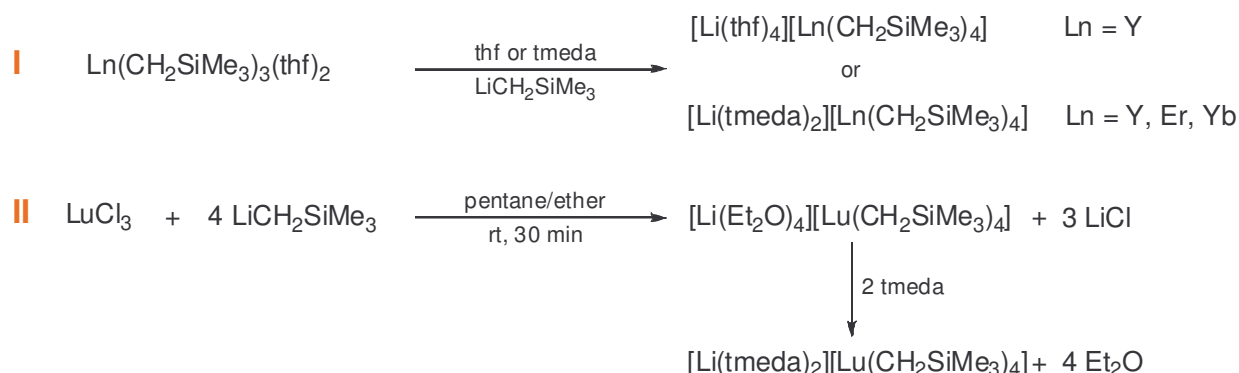
A major drawback of homoleptic alkyls **K** is their thermal instability. At ambient temperature solid and dissolved samples of Ln(CH₂SiMe₃)₃(thf)_x decompose within hours leading to oily insoluble products and the formation of SiMe₄.⁸⁵ Especially the derivatives of the larger lanthanides are prone to ligand degradation reactions, limiting the availability of these useful precursors to the small and middle-sized rare-earth metals (Sc - Sm). Nevertheless, the synthesis of Nd(CH₂SiMe₃)₃ was published in 1980.

The authors claimed a dimeric structure of the insufficiently characterized product.⁹⁴ The synthesis of the neodymium compound, however, has not been reproduced so far. Three reasonable elimination pathways have been proposed for the thermal decomposition of Ln(CH₂SiMe₃)₃(thf)_x all involving the evolution of SiMe₄ (Scheme 14).⁹³ While α -H elimination from a [Ln-CH₂Si] moiety was first assumed to be the favorable decomposition pathway,⁸⁷ more detailed investigations on the thermal degradation of Lu(CH₂SiMe₃)₃(thf)₂ corroborate γ -H elimination to be predominant. The “face to face” arrangement of two of the SiMe₃ groups in trigonal bipyramidal compounds **K** (Figure 18) seems to impede the α -H elimination of SiMe₄ and octahedrally coordinated Lu(CH₂SiMe₃)₃(thf)(diglyme) proved to be thermally robust.⁹³ A β -H elimination mechanism could be ruled out by studies on Lu(CH₂SiMe₃)₃(thf-*d*₈)₂.



Scheme 14: Thermal decomposition pathways of Lu(CH₂SiMe₃)₃(thf)₂ (according to reference ⁹³).

Besides thermal instability ate complex formation is a hampering side-effect in the synthesis of **K**. Already the earliest publications report the occurrence of anionic complexes [Li(solvent)₄][Ln(CH₂SiMe₃)₄] (**L**) regardless of the stoichiometry of LnCl₃ and LiCH₂SiMe₃.^{86,91} Direct synthesis of the lithium salts **L** was achieved by reaction of Ln(CH₂SiMe₃)₃(thf)_x with LiCH₂SiMe₃ (Scheme 15, I)⁸⁶ and LnCl₃ with four equivalents of LiCH₂SiMe₃ (Scheme 15, II),⁹¹ respectively (Scheme 15). The ate complexes are insoluble in non-polar solvents but are readily soluble in ethers. The diethylether adducts [Li(Et₂O)₄][Ln(CH₂SiMe₃)₄] are kinetically labile and follow an α -H elimination pathway leading to lanthanide alkylidenes Li[Ln(CH₂SiMe₃)₂(CHSiMe₃)], but can be stabilized by donor exchange with tmeda (Scheme 15, II).⁹¹ However, such ate complexes are not found to be suitable alkyl precursors.



Scheme 15: Formation of ate complexes [Li(solv)_x][Ln(CH₂SiMe₃)₄] (**L**).

The attempted synthesis of the samarium alkyl **K_{Sm}** by treatment of Sm(OAr^{*i*Pr,H})₃(thf)₂ (OAr^{*i*Pr,H} = OC₆H₃-2,6-*i*Pr₂) with three equivalents of LiCH₂SiMe₃ in toluene did not yield the desired product but [Li(thf)]₂[Sm(OAr^{*i*Pr,H})₃(CH₂SiMe₃)₂] (see also chapter 6.2).⁹⁵

4.2 Ln(CH₂SiMe₃)₃(thf)_x as Synthesis Precursors

Despite the afore-mentioned drawbacks (cation size restrictions, thermal instability, and ate complex formation) Ln(CH₂SiMe₃)₃(thf)_x (**K**) are widely used rare-earth metal alkyl synthesis precursors. Protonolysis of one, two or all three [CH₂SiMe₃] ligands under loss of SiMe₄ allowed for the synthesis of an impressive variety of heteroleptic rare-earth metal (alkyl) compounds. Particularly, the access to catalytically highly active alkyl compounds including cationic variants led to extensive derivatization of Ln(CH₂SiMe₃)₃(thf)_x.

4.2.1 Cationic Complexes [Ln(CH₂SiMe₃)_{3-n}(solv)_x]ⁿ⁺[anion]ⁿ⁻

OKUDA found that toluene solutions of Ln(CH₂SiMe₃)₃(thf)₂ (Ln = Y, Tm, Er, Ho, Dy, and Tb) effectively catalyze the polymerization of ethylene upon activation with BRØNSTED acid [PhNMe₂H][B(C₆F₅)₄] in the presence of Al/Bu₃.⁹⁶ Hereby, polymerization activities were well correlated to the effective ionic radius of the rare-earth metal. Mono(cationic) complexes [Ln(CH₂SiMe₃)₂(solv)_x][B(C₆F₅)₄] (**22**) and di(cationic) compounds [Ln(CH₂SiMe₃)(solv)_x][B(C₆F₅)₄]₂ (**23**) were discussed as the catalytically active species and a series of such ionic rare-earth metal alkyl compounds was investigated.⁹⁶⁻⁹⁸ While

cationic rare-earth metal alkyls $[\text{Ln}(\text{CH}_2\text{SiMe}_3)_{3-n}(\text{solv})_x]^{n+}[\text{anion}]^{n-}$ are insoluble in hydrocarbons and aromatic solvents, they were reported to be soluble and stable in the presence of donor solvents (thf, pyridine). Equimolar amounts of $\text{Y}(\text{CH}_2\text{SiMe}_3)_3(\text{thf})_2$ and LEWIS acidic $\text{Al}(\text{CH}_2\text{SiMe}_3)_3$ formed the ion pair $[\text{Y}(\text{CH}_2\text{SiMe}_3)_2(\text{thf})_4][\text{Al}(\text{CH}_2\text{SiMe}_3)_4]$ (**24**) which could be further activated by $[\text{PhNMe}_2\text{H}][\text{B}(\text{C}_6\text{F}_5)_4]$ providing high activity in the polymerization of ethylene. Single crystals of **24** were obtained from a pentane/thf mixture, revealing a distorted octahedral coordination geometry about the yttrium metal center (Figure 19).⁹⁶ The two remaining alkyl ligands of the cationic unit are arranged in a *cis* fashion while four thf donor molecules stabilize the cationic yttrium metal center.

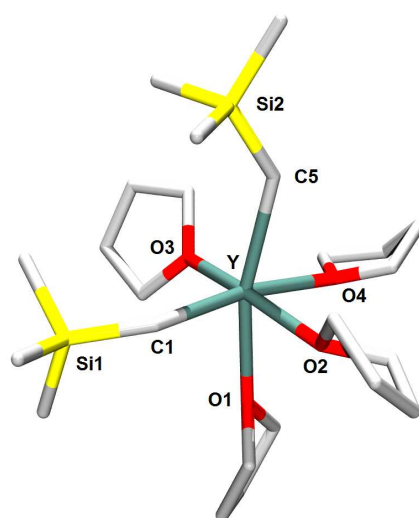
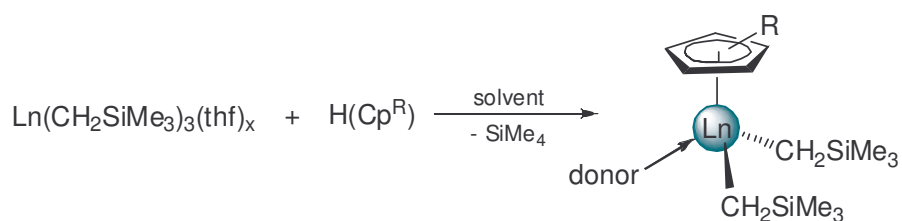


Figure 19: Solid-state structure of the cationic moiety of $[\text{Y}(\text{CH}_2\text{SiMe}_3)_2(\text{thf})_4][\text{Al}(\text{CH}_2\text{SiMe}_3)_4]$ (**24**).

4.2.2 Half-Sandwich Complexes

Structurally well characterized organo-rare-earth metal complexes based on cyclopentadienyl ligands are of considerable interest, particularly in the catalytic hydroamination and as homogeneous polymerization catalysts for both nonpolar and polar monomers. Compared with bis(cyclopentadienyl) complexes, half-sandwich rare-earth metal complexes which contain only one cyclopentadienyl ligand show an increased potential for functionalization at the metal center. Allowing for two σ -bound alkyl ligands such compounds retain one alkyl ligand upon mono(cationization). Hence, they display potential catalyst precursors in polymerization or organic transformation reactions. The conventional synthesis of mono(cyclopentadienyl) rare-earth metal complexes by salt metathesis reactions is often hampered by ate complex formation

with concomitant alkali metal salt incorporation.⁹⁹⁻¹⁰¹ Alkane elimination was found to be a facile synthesis route to complexes of the type (Cp^R)Ln(CH₂SiMe₃)₂(donor)_x. Reaction of Ln(CH₂SiMe₃)₃(thf)_x (**K**) with the respective substituted cyclopentadiene H(Cp^R) (Scheme 16) gave access to a variety of mono(cyclopentadienyl)-bis(alkyl) complexes (Figure 20 and Table 2). Remarkably, metallocene-formation even in the presence of excess H(Cp^R) was not observed when silicon-containing cyclopentadienes were employed.¹⁰² The use of silicon-free cyclopentadienes H(C₅Me₅) and H(C₅Me₄H) often results in mixtures of mono- and bis(cyclopentadienyl) complexes.



Scheme 16: General synthesis procedure for half-sandwich complexes from Ln(CH₂SiMe₃)₃(thf)_x (**K**).

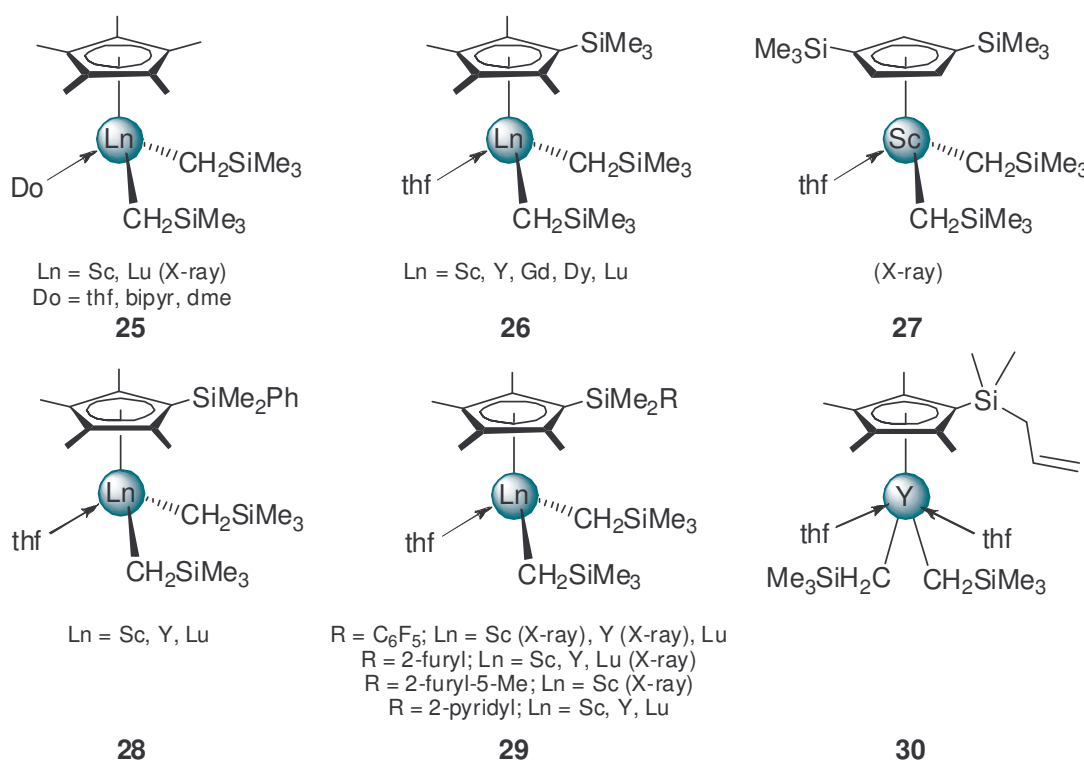


Figure 20: Complexes (Cp^R)Ln(CH₂SiMe₃)₂(donor)_x derived from Ln(CH₂SiMe₃)₃(thf)_x (**K**).

Table 2: Further application of half-sandwich complexes (Cp^R)Ln(CH₂SiMe₃)₂(donor)_x.

| Compound | Further application | Ref. |
|-----------|--|------|
| 25 | ▪ [CH ₂ SiMe ₃] exchange reactions | 103 |
| | ▪ Formation of mono(cations) | 104 |
| | ▪ Alternating ethylene-norbornene copolymerization | |
| 26 | ▪ Synthesis of hydrido compounds | 102 |
| | ▪ Formation of mono(cations) | 105 |
| | ▪ Syndiospecific polymerization of styrene | 104 |
| | ▪ Ethylene-styrene copolymerization | 106 |
| | ▪ Ethylene-norbornene copolymerization (alternating and poly(ethylene- <i>alt</i> -norbornene) block-copolymers) | 107 |
| | ▪ Homo- and alternating copolymerization of cyclohexene oxide with CO ₂ | 108 |
| | ▪ Polymerization of isoprene (3,4 enriched) | 109 |
| 27 | ▪ Formation of mono(cations) | 104 |
| | ▪ Ethylene-norbornene copolymerization | |
| 28 | ▪ Synthesis of hydrido compounds | 107 |
| | ▪ Formation of mono(cations) | 110 |
| | ▪ Syndiospecific polymerization of styrene | |
| 29 | ▪ Formation of mono(cations) | 110 |
| | ▪ Syndiospecific polymerization of styrene | 111 |
| | | 112 |
| 30 | ▪ Insertion of CO ₂ | 90 |
| | ▪ Formation of a cyclopentadienyl-allyl ligand by multiple metalation | |

Mono(cyclopentadienyl) complexes **26** and **28** can undergo hydrolysis of both alkyl ligands affording isolable hydrido clusters.^{107,108} The *in situ* generation of cationic mono(cyclopentadienyl) rare-earth metal complexes by alkyl abstraction using borate reagents [Ph₃C][B(C₆F₅)₄] and [PhNMe₂H][B(C₆F₅)₄], respectively, results in highly active polymerization catalysts (Table 2). Scandium bis(alkyl) complex **26**_{Sc} shows excellent activity for syndiospecific styrene homopolymerization (activity: 1.36 · 10⁴ kg sPS/(mol Sc h); *M*_w/*M*_n = 1.37) and the copolymerization of ethylene and styrene.¹⁰⁵ Very high activities are further observed in the copolymerization of ethylene and norbornene.¹⁰⁴

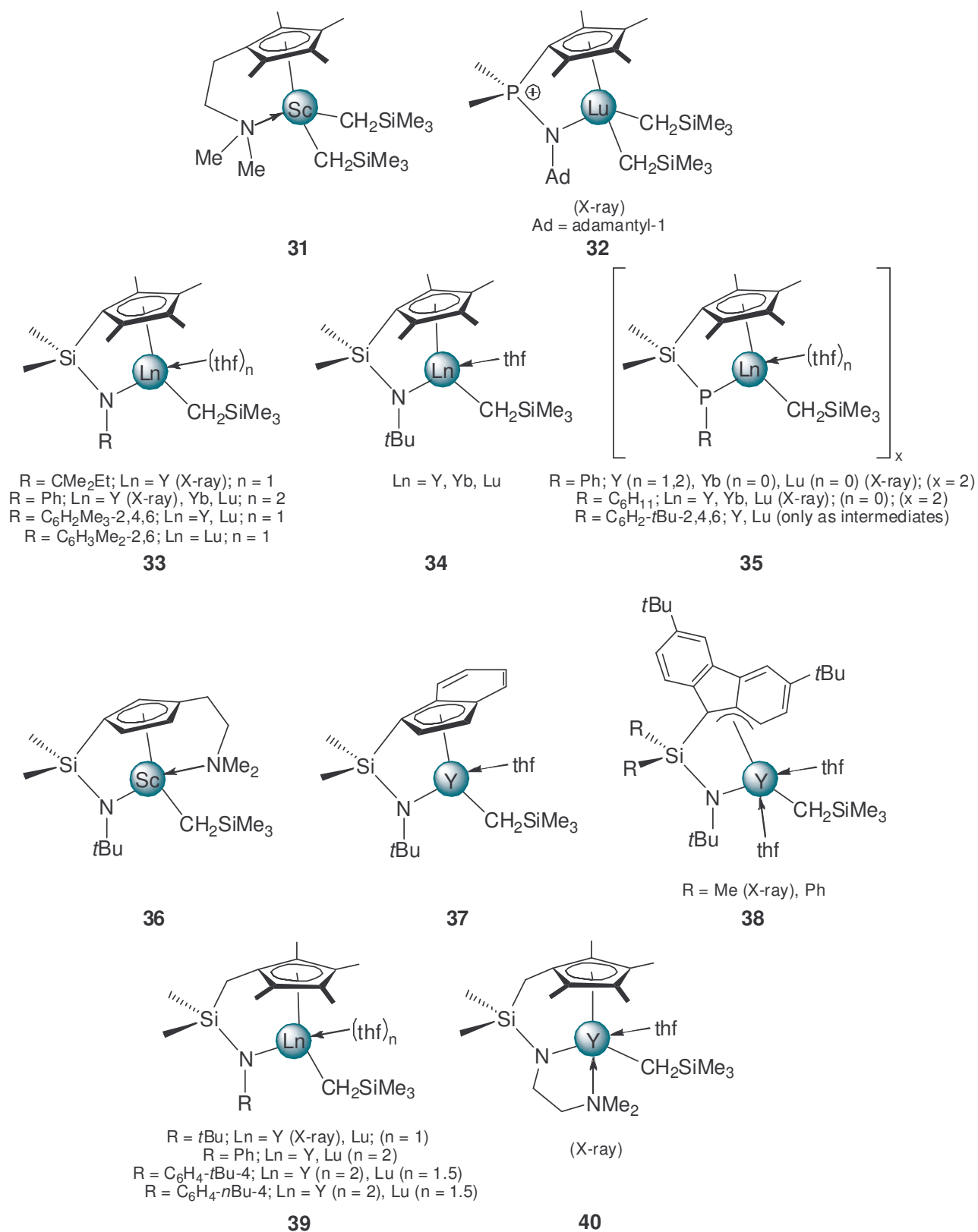
4.2.3 Complexes with Functionalized Cp^R Ligands

Figure 21: Complexes with functionalized Cp^R ligands derived from Ln(CH₂SiMe₃)₃(thf)_x(K).

Incorporation of the cyclopentadienyl ancillary ligand into a chelate array of donor-functionalities gives access to a variety of modifications of the parent Cp. Such a pendant ligand system is the linked amido-cyclopentadienyl ligand, which has, since the original introduction by the BERCAW group, advanced to be one of the most versatile ligands for group 4 metal polymerization catalysts.¹¹³ Catalysts based on this type of ligand provide a constrained ligand environment but are anticipated to be more active toward sterically demanding monomers than metallocenes. Donor-functionalized cyclopentadienes react with Ln(CH₂SiMe₃)₃(thf)_x (**K**) according to an alkane elimination reaction as shown in Scheme 16. Depending on the nature of the additional-functionality (neutral or monoanionic) two or one [CH₂SiMe₃] ligands are retained allowing for further derivatization (Figure 21).

In the presence of Ph₃SiH or H₂ complexes **33-40** form dimeric hydrido complexes,^{102,114-116} showing high potential in the catalytic hydrosilylation of olefins.¹¹⁷⁻¹¹⁹ Catalytic activities and stereoselectivities are hereby influenced by the length of the link between the cyclopentadienyl and the amido-functionality and the substituents at the amido-nitrogen.¹¹⁷ Remarkable catalytic activity was observed for complexes **35**^{Cyclohexyl}. Upon activation with equimolar amounts of [Ph₃C][B(C₆F₅)₄] such compounds polymerized ethylene and isoprene regiospecifically yielding 3,4-polyisoprene with isotactic-rich stereo microstructures and relatively narrow molecular weight distribution ($M_w/M_n = 1.8$).¹²⁰ Complex **34_r** was found to initiate the polymerization of the polar monomers *tert*-butyl acrylate and acrylonitrile, however, yielding atactic polymeric products.¹⁰²

Table 3: Further application of complexes with functionalized Cp^R ligands.

| Compound | Further application | Ref. |
|-----------|--|---------|
| 31 | ▪ Formation of mono(cation) | 121 |
| | ▪ Polymerization of ethylene | |
| 32 | ▪ No further application | 122 |
| 33 | ▪ Synthesis of hydrido compounds | 114 |
| | ▪ Dimerization of terminal alkynes | 115 |
| | ▪ Catalytic addition of amine N-H bonds to carbodiimines | 117 |
| | ▪ Hydrosilylation of olefins | 123,124 |
| 34 | ▪ Synthesis of hydrido compounds | 102 |
| | ▪ Polymerization of <i>t</i> Bu-acrylate | 115 |
| | ▪ Polymerization of acrylonitrile | 114 |
| | ▪ Dimerization of terminal alkynes | |

Table 3 (continued): Further application of complexes with functionalized Cp^R ligands.

| Compound | Further application | Ref. |
|-----------|--|------|
| 35 | ▪ Synthesis of hydrido compounds | 119 |
| | ▪ Hydrosilylation of olefins | 109 |
| | ▪ Polymerization of ethylene | |
| | ▪ Isospecific 3,4-polymerization of isoprene | |
| 36 | ▪ Synthesis of hydrido compounds | 125 |
| 37 | ▪ Synthesis of hydrido compounds | 114 |
| 38 | ▪ Synthesis of hydrido compounds | 126 |
| | ▪ Polymerization of methyl methacrylate (low activity) | |
| 39 | ▪ Synthesis of hydrido compounds | 118 |
| | ▪ Hydrosilylation of olefins | 117 |
| 40 | ▪ Synthesis of hydrido compounds | 116 |
| | ▪ Hydrosilylation of olefins | |

4.2.4 Complexes with Neutral Nitrogen- and Oxygen-based Ligands

While early work in organorare-earth metal chemistry was dominated by complexes supported by cyclopentadienyl type ligands of varying substitution and modification, the limitations inherent to these ligand sets triggered the development of alternative ancillary ligands. Particularly in the last 15 years advanced ligand design gave access to a wide variety of rare-earth metal complexes supported by non-cyclopentadienyl ligand environments. Due to the LEWIS acidic nature of the rare-earth metal ions, ligands based on the hard donor elements oxygen and nitrogen are most commonly used, while some notable exceptions have been reported. To avoid ligand redistribution, multidentate ligands are generally favored. Since rare-earth metal cations are invariable in the +3 oxidation state (except Eu(II), Sm(II), Yb(II), and Ce(IV)), neutral, monoanionic or dianionic ligand sets are the most desirable.

Neutral macrocyclic and tripodal ancillary ligands containing oxygen, nitrogen, or sulfur donors were found suitable to stabilize tris(alkyl) rare-earth metal complexes (Figure 22). Moreover, such facially coordinating ancillary ligands allow for the formation of stable mono(cationic) and in some cases even di(cationic) rare-earth metal alkyl species.

Complexes **41-50** were prepared by the reaction of tris(alkyl) precursors Ln(CH₂SiMe₃)₃(thf)_x (**K**) with equimolar amounts of the respective neutral donor-ligand (Figure 22 and Table 4).

In situ formation of mono- and di(cationic) rare-earth metal alkyl species by treatment with [Ph₃C][B(C₆F₅)₄], [PhNMe₂H][B(C₆F₅)₄], or B(C₆F₅)₃, respectively, was reported for compounds **41-45**, **47**, **49**, and **50**.^{92,97,127-133} The borate/borane activated complexes (except **41-43**) polymerized ethylene with moderate to high activities. Activated complex **45** stabilized by 1,4,7-trithiacyclononane further initiated the polymerization of 1-hexene and styrene with very high activities but yielded atactic polymers with poor control of the molecular weights.¹³¹

Bis(cations) formed by **50_{Sc}** and two equivalents [Ph₃C][B(C₆F₅)₄] are highly active in the polymerization of 1-hexene producing highly isotactic poly(1-hexene) (2030 kg/(mol h); *mmmm* = 90%).¹³³

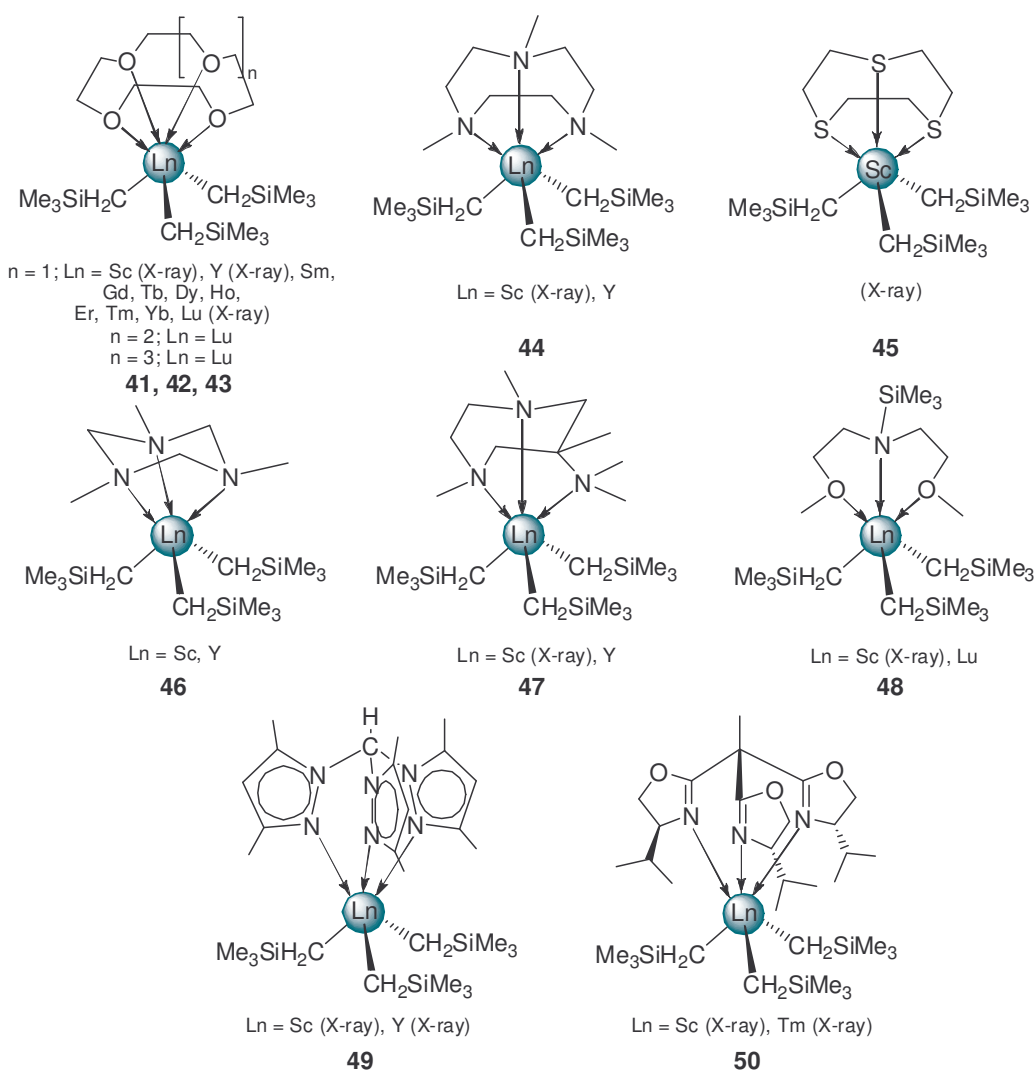


Figure 22: Ln(CH₂SiMe₃)₃(thf)_x derivatives containing neutral [0000], [00000], [000000], [NNN], [SSS], and [ONO] ligands.

Table 4: Further application of complexes containing neutral N- and O-based ligands.

| Compound | Further application | Ref. |
|-----------|--|--------|
| 41 | ▪ Formation of mono- and di(cations) | 127 |
| 42 | ▪ Formation of mono(cation) | 128 |
| 43 | ▪ Formation of mono(cation) | 97 |
| 44 | ▪ Formation of mono(cations) | 129 |
| | ▪ Polymerization of ethylene | 130 |
| 45 | ▪ Formation of mono- and di(cations) | 131 |
| | ▪ Polymerization of ethylene | |
| | ▪ Polymerization of 1-hexene | |
| | ▪ Polymerization of styrene | |
| 46 | ▪ No further application | 130 |
| 47 | ▪ Formation of mono(cation) | 132 |
| | ▪ Polymerization of ethylene | |
| 48 | ▪ Synthesis of hydrido compounds | 134 |
| | ▪ Dimerization of terminal alkynes | |
| | ▪ Catalytic addition of amine N-H bonds to carbodiimines | |
| 49 | ▪ Formation of mono(cation) | 129 |
| | ▪ Polymerization of ethylene | 130 |
| 50 | ▪ Formation of mono- and di(cations) | 92,133 |
| | ▪ Polymerization of α -alkenes | |

4.2.5 Complexes with Monoanionic Nitrogen-, Oxygen-, and Phosphorus-based Ligands

A large number of monoanionic ancillary ligand sets has been developed, well suitable to stabilize alkyl complexes of the rare-earth metals. The monoanionic ancillary ligand allows for organometallic rare-earth metal complexes with two hydrocarbyl or hydrido ligands which can be converted into the corresponding cationic mono(alkyl) species by activation with borate/borane reagents like [Ph₃C][B(C₆F₅)₄], [PhNMe₂H][B(C₆F₅)₄], or B(C₆F₅)₃. The resulting cationic species have demonstrated encouraging catalytic activities for a range of polymerization reactions including olefins, conjugated dienes, and polar monomers. Homoleptic Ln(CH₂SiMe₃)₃(thf)_x (**K**) are the most widely used alkyl precursors for the synthesis of rare-earth metal bis(alkyl) complexes supported by such

monoanionic ancillary ligands. Alkane elimination reaction of usually equimolar amounts of the respective protonated ligand and Ln(CH₂SiMe₃)₃(thf)_x gave access to a large variety of complexes [Ligand]Ln(CH₂SiMe₃)_x(thf)_n (Figure 23-Figure 26).

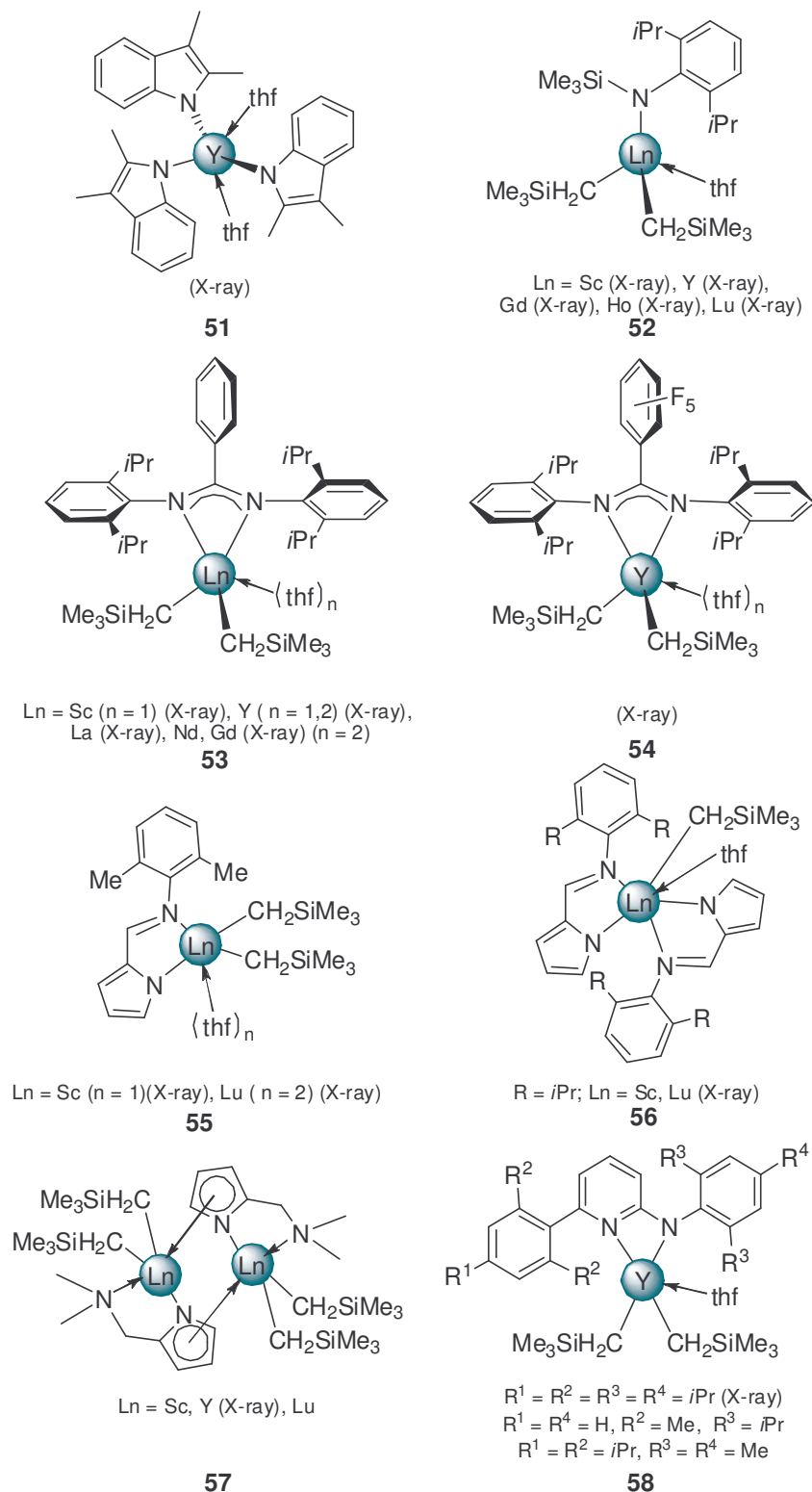


Figure 23: Ln(CH₂SiMe₃)₃(thf)_x derivatives containing monoanionic [N], and [NN] ligands.

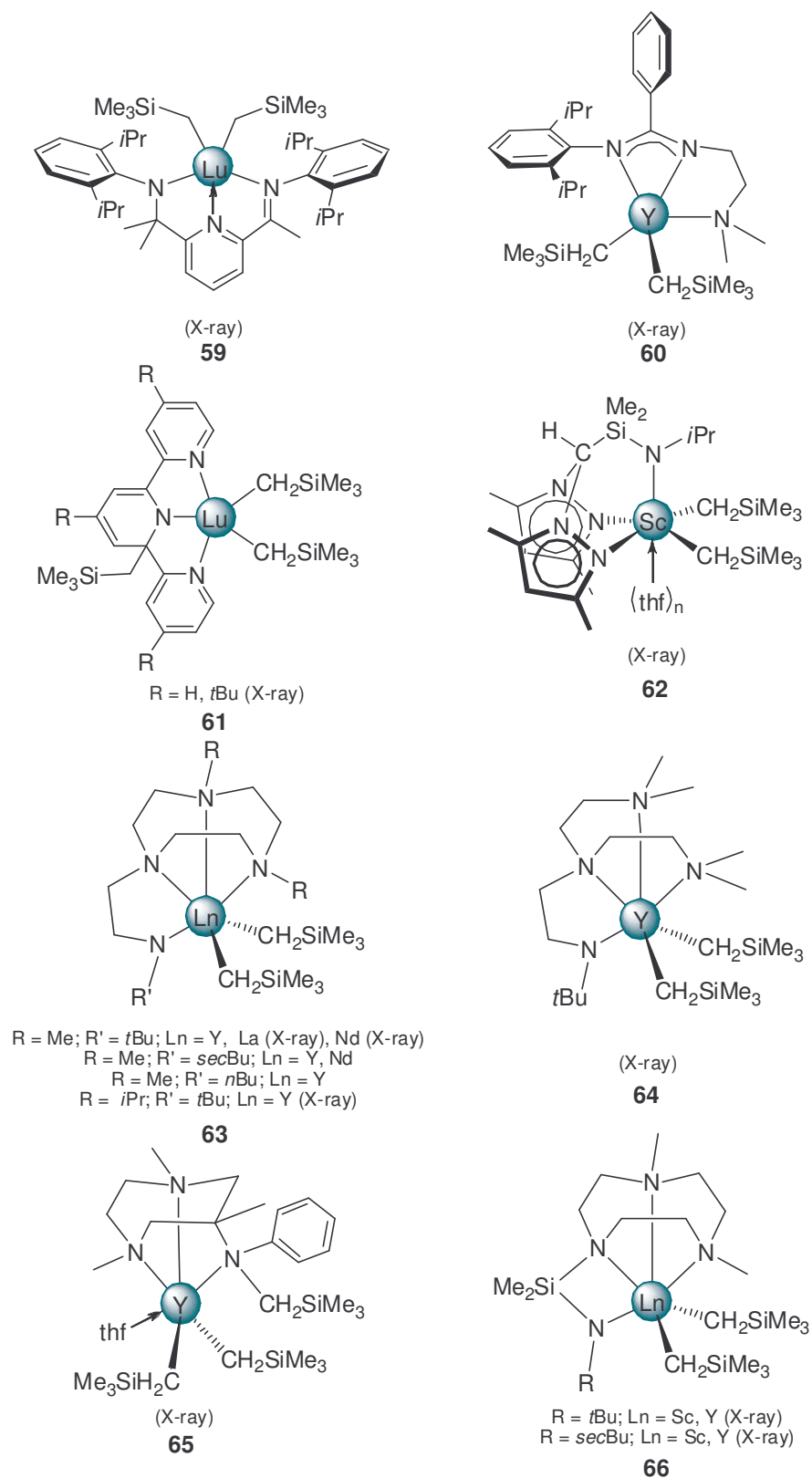


Figure 24: Ln(CH₂SiMe₃)₃(thf)_x derivatives containing monoanionic [NNN], [NNN], and [NNNN] ligands.

One of the first monoanionic nitrogen-donor ancillaries applied in this alkane elimination reaction is the benzamidinato ligand. The HESSEN group reported benzamidinato-bis(alkyl) complexes **53** and **54** as well as the formation of cationic species upon activation with [PhNMe₂H][B(C₆F₅)₄].¹³⁵⁻¹³⁷ *In situ* prepared cations effectively catalyzed the polymerization of ethylene yielding polyethylene with a narrow polydispersity (**53**_v/[PhNMe₂H][B(C₆F₅)₄]/TiBAO: 3 · 10³kg/(mol bar h); *M_w*/*M_n* = 2.0).¹³⁵

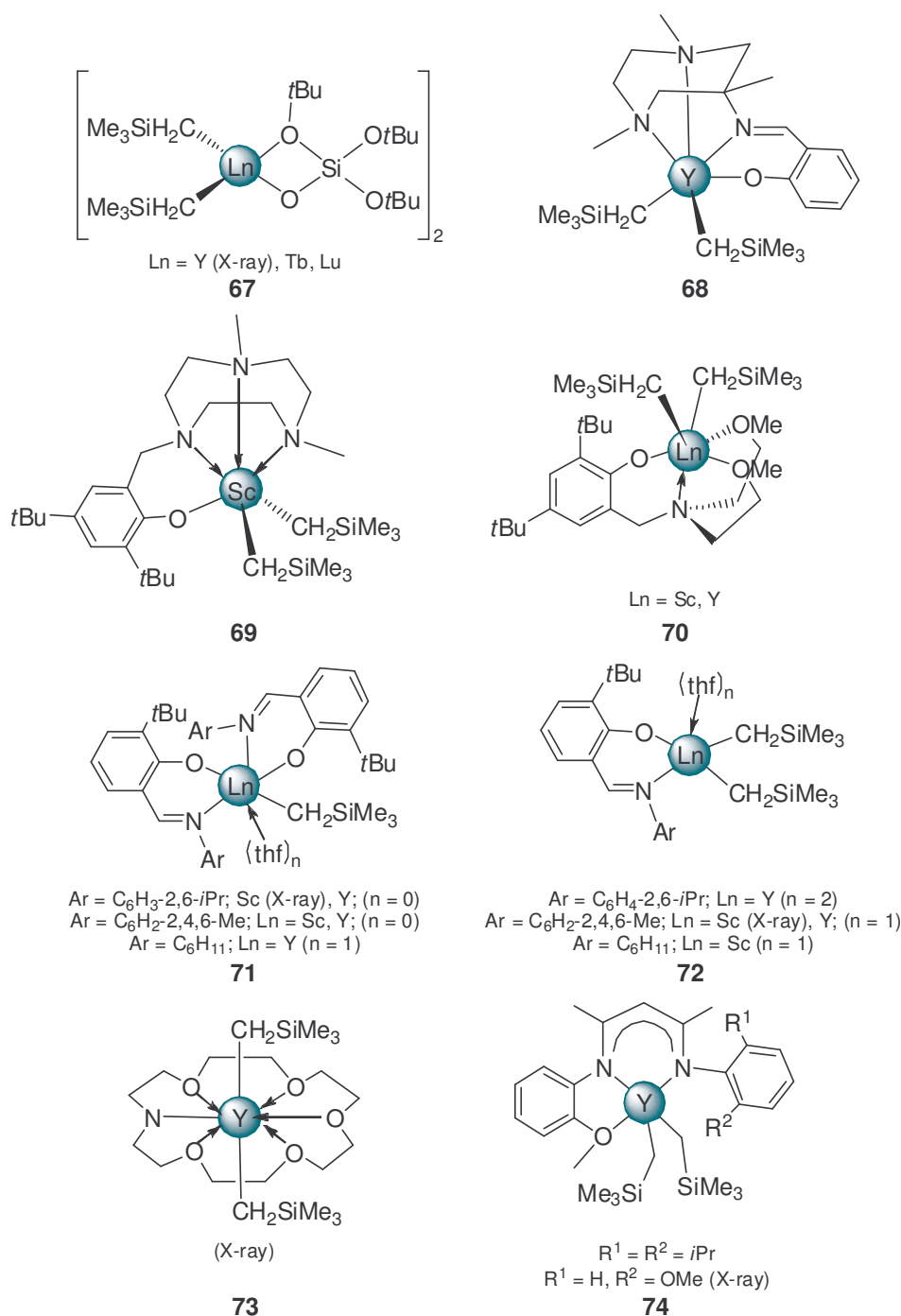


Figure 25: Ln(CH₂SiMe₃)₃(thf)_x derivatives containing monoanionic [OO], [ONN], [ONNN], [ONOO], and [N00000] ligands.

Remarkably, the benzamidinato ligand proved suitable to form bis(alkyl) complexes of the entire rare-earth metal cation size-range. One-pot reaction of LaBr₃(thf)₄, NdCl₃(thf)₃, or GdCl₃(thf)₃ with three equivalents of LiCH₂SiMe₃ and one equivalent of the amidine yielded the respective complexes **53_{La}**, **53_{Nd}**, and **53_{Gd}** - the first neosilyl-complexes of the early lanthanide metals.¹³⁶

Active ethylene polymerization catalysts were further obtained from complexes **58**,¹³⁸ **63**,¹³⁹ **64**,¹⁴⁰ **66**,¹⁴¹ and **70**¹⁴² when activated with borate reagents. While cationic species derived from **55** and [Ph₃C][B(C₆F₅)₄] showed no activity in the polymerization of isoprene, addition of AlEt₃ as a third component resulted in versatile activity depending on the molar ratio of [Al]/[Ln], however, producing polyisoprene with low stereoregularity.¹⁴³ High *cis*-1,4-polyisoprene (*cis*-1,4: 99%; *M_w*/*M_n* = 1.05-1.13) could be obtained from catalyst mixtures **75**/[PhNMe₂H][B(C₆F₅)₄] and **75**/[Ph₃C][B(C₆F₅)₄], rare examples of high catalytic activity in the absence of an organoaluminum cocatalyst.¹⁴⁴

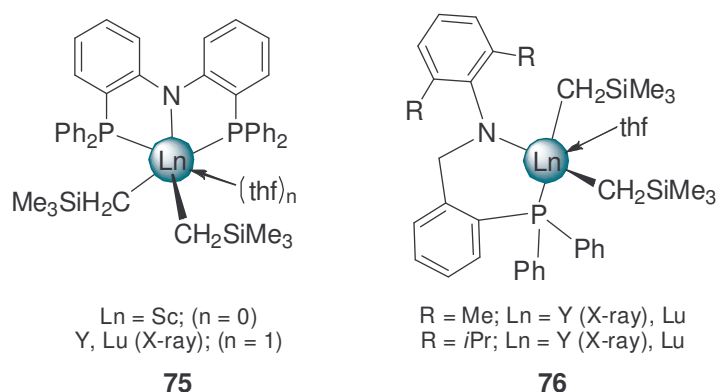


Figure 26: Ln(CH₂SiMe₃)₃(thf)_x derivatives containing monoanionic [PNP]⁻ and [NP]⁻ ligands.

Neutral complexes **56**, **74**, and **76** are active catalysts for the ring-opening polymerization (ROP) of D,L-lactide^{143,145,146} and **71** and **72** polymerize ε-caprolactone.¹⁴⁷

Table 5: Further application of complexes containing monoanionic N-, O- and P-based ligands.

| Compound | Further application | Ref. |
|----------|--|------------|
| 51 | ▪ No further application | 148 |
| 52 | ▪ Formation of mono(cations) ▪ Polymerization of isoprene | 149 |
| 53 | ▪ Formation of mono(cations) ▪ Polymerization of ethylene | 135 136 |
| 54 | ▪ Formation of mono(cations) ▪ Polymerization of ethylene | 137 |
| 55 | ▪ Formation of mono(cations) ▪ Polymerization of isoprene | 143 |
| 56 | ▪ Formation of mono(cations) ▪ ROP of D,L-lactide | 150 143 |
| 57 | ▪ No further application | 143 |
| 58 | ▪ Formation of mono(cations) ▪ Polymerization of ethylene | 138 |
| 59 | ▪ Formation of mono(cations) | 151 |
| 60 | ▪ No further application | 137 |
| 61 | ▪ No further application | 152 |
| 62 | ▪ Formation of mono(cations) | 153 |
| 63 | ▪ Formation of mono(cations) ▪ Polymerization of ethylene | 139 141 |
| 64 | ▪ Formation of mono(cations) ▪ Polymerization of ethylene | 140 |
| 65 | ▪ No further application | 132 |
| 66 | ▪ Formation of mono(cations) ▪ Polymerization of ethylene | 141 |
| 67 | ▪ No further application | 154 |
| 68 | ▪ No further application | 132 |
| 69 | ▪ No further application | 155 |
| 70 | ▪ Formation of mono(cations) ▪ Polymerization of ethylene | 142 |

Table 5 (continued): Further application of complexes containing monoanionic N-, O- and P-based ligands.

| Compound | Further application | Ref. |
|-----------|--|------|
| 71 | ▪ Hydrido compounds | 156 |
| | ▪ ROP of ϵ -caprolactone | 147 |
| | | 157 |
| 72 | ▪ ROP of ϵ -caprolactone | 156 |
| | | 147 |
| 73 | ▪ Formation of mono(cations) | 158 |
| | ▪ Insertion of CO | |
| 74 | ▪ ROP of <i>rac</i> lactide | 145 |
| 75 | ▪ Formation of mono(cations) | 144 |
| | ▪ Polymerization of isoprene and butadiene | |
| | ▪ Copolymerization of isoprene and butadiene | |
| 76 | ▪ Polymerization of D,L-lactide | 146 |

4.2.6 Complexes with Dianionic Nitrogen- and Oxygen-based Ligands

Reaction of Ln(CH₂SiMe₃)₃(thf)_x (**K**) with multidentate ligand precursors containing two acidic functionalities yielded a series of very stable mono(alkyl) rare-earth metal complexes (Figure 27 and Figure 28). The dianionic ligand set allows for the preparation of complexes related to those supported by the bis(cyclopentadienyl) platform.

However, the presence of only one alkyl ligand prevents the formation of stable cationic rare-earth metal species. Application of complexes supported by dianionic ancillary ligands therefore depends on the initiating property of the remaining alkyl-actor ligand. Compound **77_{Sc}** bearing a tridentate diamido-pyridine ancillary ligand initiated the polymerization of the polar monomer methyl methacrylate (MMA). The resulting PMMA showed a narrow molecular weight distribution ($M_w/M_n = 1.28$) but low control of the tacticity.¹⁵⁹ Aminotroponiminato complex **80** performed as catalyst for the regiospecific intramolecular hydroamination/cyclization of terminal amino-olefins.¹⁶⁰

Polyactides are among the most promising biodegradable and biocompatible synthetic macromolecules. Such polymers are most conveniently accessible by ring-opening polymerization of lactide. Mono(alkyl) complexes **87** and **90-92** displayed living-polymerization of *rac*-lactide under mild conditions.^{145,161,162} Remarkably, the polymers produced show very high stereoselectivity affording heterotactic polyactide from racemic lactide mixtures.

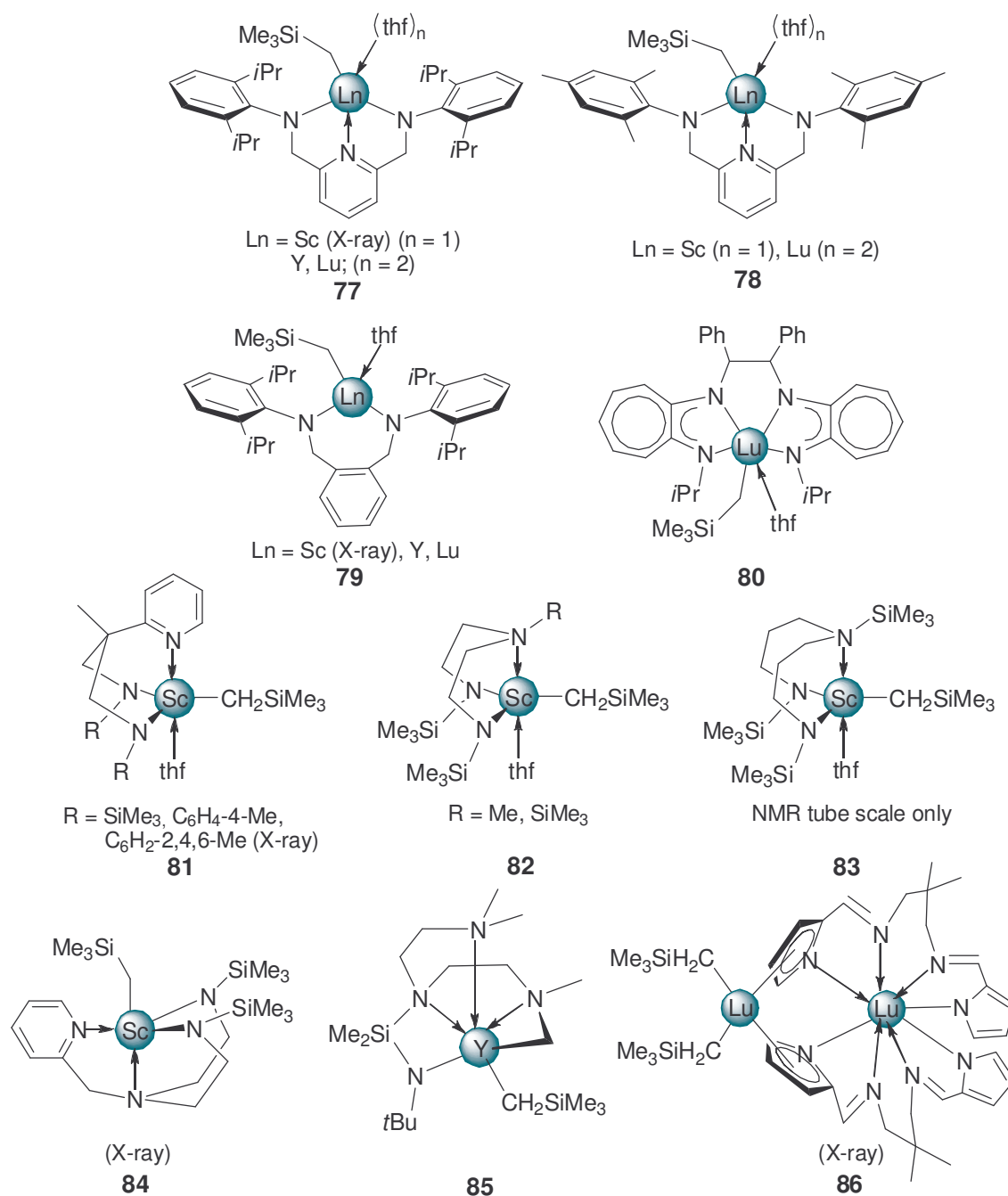


Figure 27: Ln(CH₂SiMe₃)₃(thf)_x derivatives containing dianionic [NN]²⁻, [NNN]²⁻, and [NNNN]²⁻ ligands.

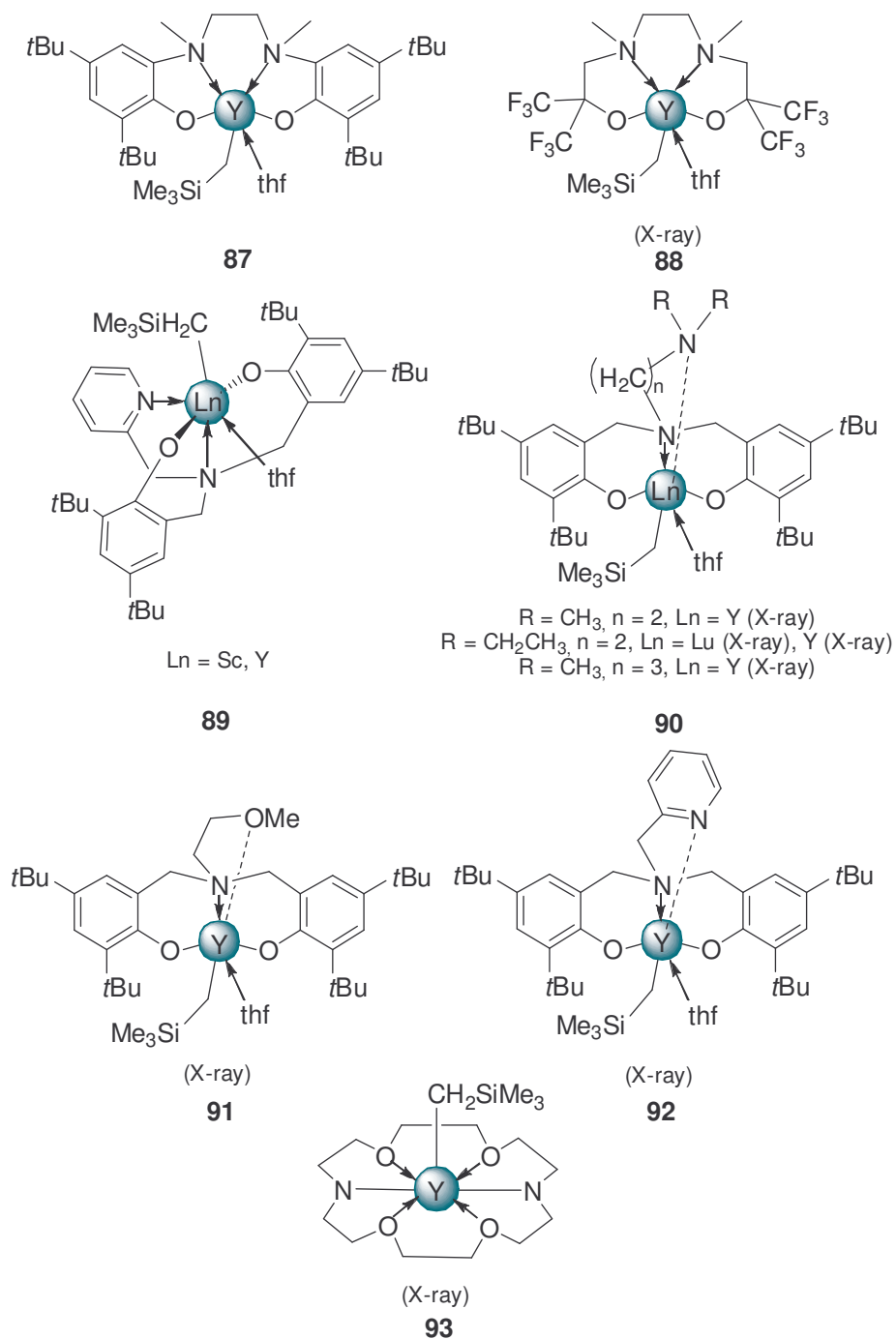


Figure 28: Ln(CH₂SiMe₃)₃(thf)_x derivatives containing dianionic [ONNO]²⁻, [ONOO]²⁻, and [NOOOO]²⁻ ligands.

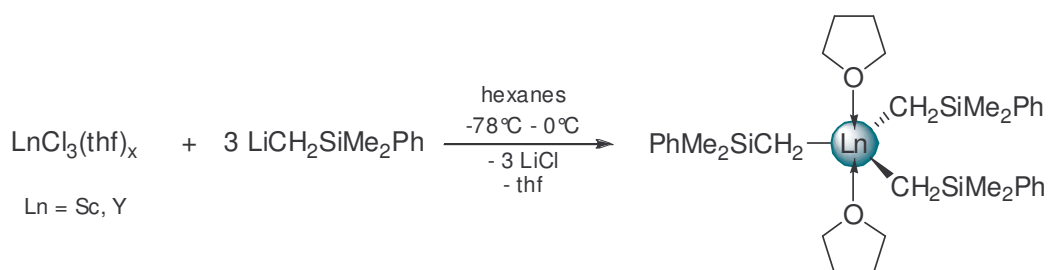
Table 5: Further application of complexes containing dianionic N- and O- based ligands.

| Compound | Further application | Ref. |
|-----------|--|------------|
| 77 | ▪ Polymerization of methyl methacrylate | 159 |
| 78 | ▪ No further applications | 159 |
| 79 | ▪ No further applications | 159 |
| 80 | ▪ Hydroamination/cyclization of terminal amino-olefins | 160 |
| 81 | ▪ No further applications | 163 |
| 82 | ▪ No further applications | 163 |
| 83 | ▪ No further applications | 163 |
| 84 | ▪ No further applications | 155 |
| 85 | ▪ No further applications | 140 |
| 86 | ▪ Polymerization of isoprene | 143 |
| 87 | ▪ ROP of <i>rac</i> lactide | 145 |
| 88 | ▪ No further applications | 164 |
| 89 | ▪ No further applications | 155 165 |
| 90 | ▪ ROP of <i>rac</i> lactide | 145 |
| 91 | ▪ ROP of <i>rac</i> lactide | 161 162 |
| 92 | ▪ ROP of <i>rac</i> lactide | 145 |
| 93 | ▪ No further applications | 166 |

5 Ln(CH₂SiMe₂Ph)₃(thf)₂

5.1 Synthesis, Structure, and Properties

Tempted by the thermal instability of lanthanide alkyls Ln(CH₂SiMe₃)₃(thf)_x (**K**) more bulky [CH₂SiMe₂Ph] groups have been introduced to prepare homoleptic alkyls Ln(CH₂SiMe₂Ph)₃(thf)₂ (**M**). The scandium and yttrium derivatives were first reported in 2002 by PIERS as easily accessible by salt metathesis reaction of LnCl₃(thf)_x and LiCH₂SiMe₂Ph (Scheme 17).^{156,167}



Scheme 17: Synthesis of Ln(CH₂SiMe₂Ph)₃(thf)₂ (**M**).

The [CH₂SiMe₂Ph] ligands impart higher stability of complexes **M** reflected in high isolable yields and significantly reduced thermal degradation. However, decomposition giving an unidentified, insoluble brown precipitate accompanied by loss of Me₃SiPh occurred after 24 h at 65 °C in toluene-*d*₈. The lower solubility of compounds Ln(CH₂SiMe₂Ph)₃(thf)₂ compared to Ln(CH₂SiMe₃)₃(thf)_x facilitates crystallization and

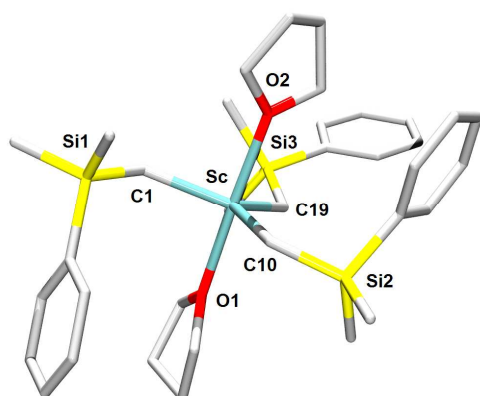


Figure 29: Molecular structure of Sc(CH₂SiMe₂Ph)₃(thf)₂.

purification of these alkyl derivatives. In the solid-state, Sc(CH₂SiMe₂Ph)₃(thf)₂ features a trigonal bipyramidal coordination geometry upon the scandium metal center.¹⁵⁶ The two thf molecules are axially coordinated while the alkyl groups are arranged in a pinwheel array (Figure 29). The trigonal bipyramid is nearly regular and the Sc–C bond lengths are essentially identical.

According to NMR spectroscopic studies the solid-state structure is also retained in solution. Very recently the respective thulium compound Tm(CH₂SiMe₂Ph)₃(thf)₂ has been synthesized following the procedure depicted in Scheme 17.⁹² Due to the unexpected low stability compound **M_{Tm}** was not isolated but used *in situ* at -80 °C in an alkane elimination reaction. Attempts to synthesize complexes **M** with the larger rare-earth metals have not been reported so far.

LiCH₂SiMe₂Ph is commercially not available and has to be synthesized from Me₂PhSiCH₂Cl and lithium powder. This and the low volatility of the Me₃SiPh side-product of alkane elimination reactions (bp. 170 °C vs 27 °C SiMe₄) are obvious disadvantages of the presented lanthanide alkyls.¹⁵⁶

5.2 Ln(CH₂SiMe₂Ph)₃(thf)₂ as Synthesis Precursors

Like their less bulky analogues, complexes Ln(CH₂SiMe₂Ph)₃(thf)₂ have been used as starting materials for alkane elimination reactions. The number of reported applications, however, is so far limited to monoanionic multidentate N,O-donor and neutral multidentate N-donor ligands (Figure 30).

A series of salicylaldiminato complexes **94-100** has been investigated with respect to the ancillary ligand-impact on the (thermal) stability of complexes [L³]₂Ln(CH₂SiMe₂Ph)(thf)_x (Ln = Sc, Y) (**94-97**) and [L³]Y(CH₂SiMe₂Ph)₂(thf)_x (x = 1, 2) (**98**) ([L³] = salicylaldiminato ligand).^{156,157,167} A mono([L³]) complex could only be obtained for the yttrium metal center and the bulkiest salicylaldiminato ligand (**98**). Complex **98** is thermally stable at ambient temperature but undergoes clean ligand redistribution upon heating to 60 °C to give bis[L³] complex **97_Y** and Me₃SiPh. The stability of bis[L³] complexes **94-100** increases with increasing steric bulk on the aldimine functionality. Insufficient steric shielding and elevated temperatures lead to rapid decomposition via ligand metalation and/or 1,3- migration of the entire [CH₂SiMe₂Ph] group to the aldimine carbon.

Tris[L³] complexes can be realised by performing alkane elimination with three equivalents of H[L³] yielding **99** and five-coordinate scandium complex **100**.

A series of monoanionic, tripodal ancillary ligands featuring various neutral O-, N-, and S-donors has been synthesized in the group of BERCAW.¹⁴² The reaction of *in situ* generated Ln(CH₂SiMe₂Ph)₃(thf)₂ (**M**) (Ln = Sc, Y) with the respective ligand precursors cleanly produced compounds **101-104**. Cationization of compounds **101-104** with

[PhNMe₂H][B(C₆F₅)₄] and/or MAO generated mono(alkyl) species providing low activity in the polymerization of ethylene.

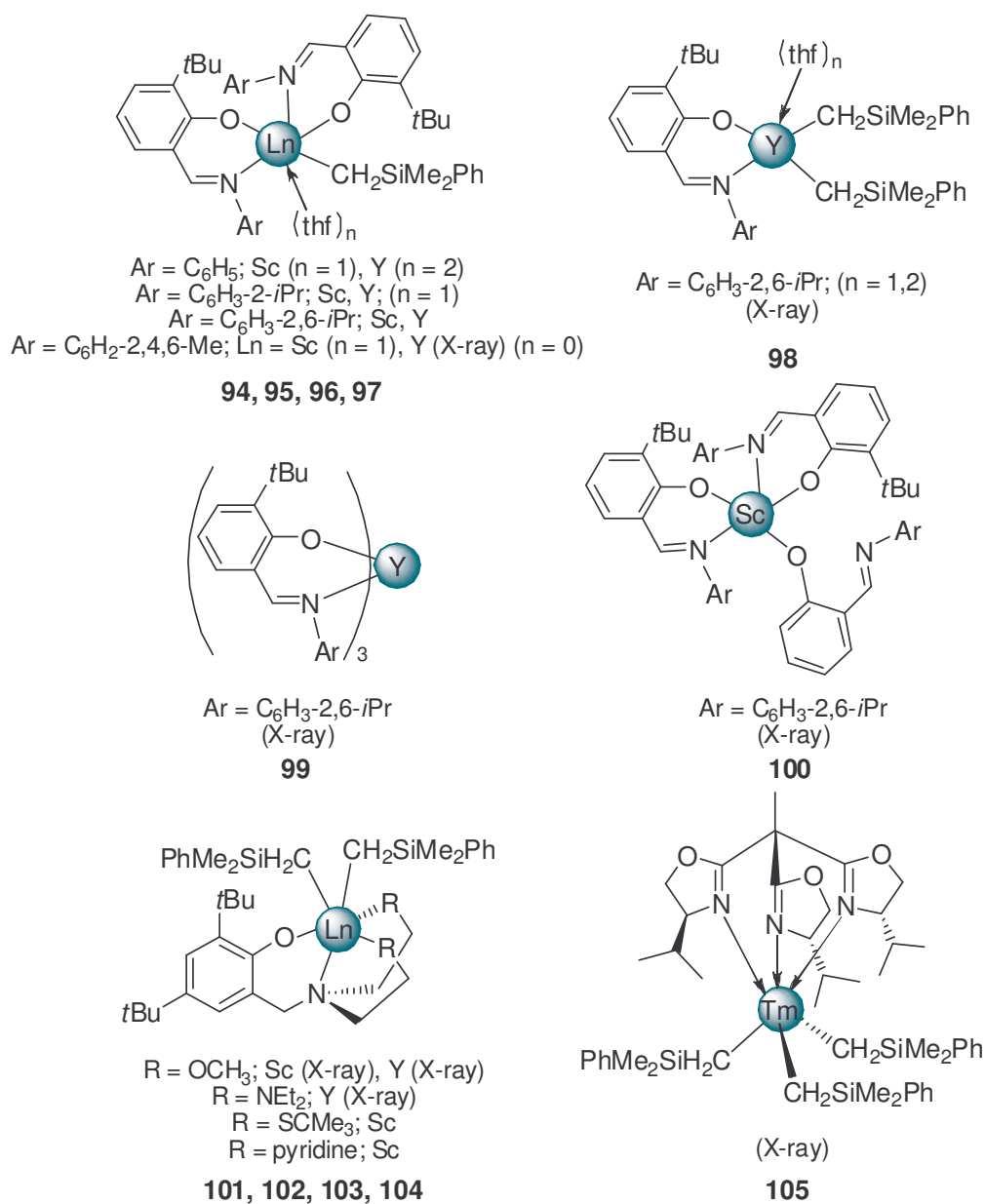


Figure 30: Ln(CH₂SiMe₂Ph)₃(thf)₂ derivatives containing neutral N-donor- and monoanionic N,O-ancillary ligands.

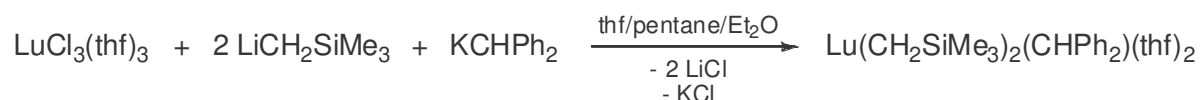
With the objective to obtain a catalytically active cationic lanthanide alkyl species, *in situ* prepared Tm(CH₂SiMe₂Ph)₃(thf)₂ was treated with the C₃-chiral tris(oxazoliny)ethane to form donor-free **105**.⁹² The reaction of **105** with either one or two equivalents of [Ph₃C][B(C₆F₅)₄], however, failed to produce an active catalyst for the polymerization of 1-hexene, 1-heptene, or 1-octene.

6 Heteroleptic Alkyl, Alkyl/Aryloxo and Alkyl/Alkoxo Compounds

6.1 Lu(CH₂SiMe₃)₂(CHPh₂)(thf)₂

The [CHPh₂] anion appeared to be a promising candidate for the synthesis of stable alkyl lanthanide complexes. Due to its steric demand and the flexible bonding modes it was expected to saturate the coordination sphere of the metal center. The anticipated formation of homoleptic complexes Ln(CHPh₂)₃(solv)_x, however, was not observed.¹⁶⁸ Attempted synthesis by reaction of two/three equivalents of KCHPh₂ and YbI₂(thf)₂, LuCl₃, YbCl₃, and YCl₃, respectively, only resulted in dark colored oils.

The heteroleptic lutetium alkyl complex Lu(CH₂SiMe₃)₂(CHPh₂)(thf)₂ (**106**) could be obtained according to the equation depicted in Scheme 18.¹⁶⁸



Scheme 18: Synthesis of Lu(CH₂SiMe₃)₂(CHPh₂)(thf)₂ (**106**).

The mixed alkyl lutetium compound shows a solid-state structure comparable to its homoleptic analogue Lu(CH₂SiMe₃)₃(thf)₂ (cf., Figure 18). The three alkyl ligands occupy the equatorial positions of a distorted trigonal bipyramid (Figure 31).

Due to the steric requirement of the benzylhydryl ligand, the lutetium methine carbon distance (Lu–C1, 2.45 Å) is considerably longer than the lutetium methylene carbon distances in the same molecule (Lu–C14, 2.35 Å; Lu–C18, 2.34 Å).

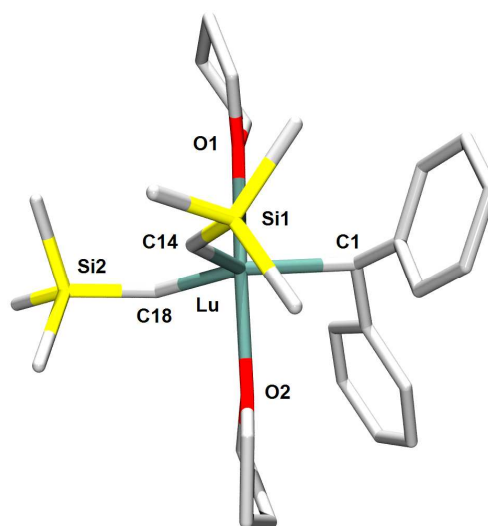


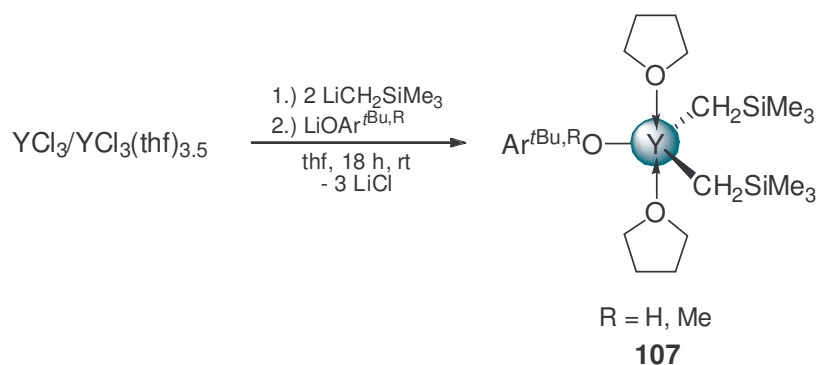
Figure 31: Solid-state structure of Lu(CH₂SiMe₃)₂(CHPh₂)(thf)₂ (**106**).

The alkyl compound is extremely air- and water sensitive but is stable for some days if kept in evacuated sealed tubes. So far literature provides no further information on derivatization or reactivity of Lu(CH₂SiMe₃)₂(CHPh₂)(thf)₂.

6.2 Alkyl/Aryloxo

Due to the formation of a strong metal oxygen bond, alkoxide and aryloxo ligands display attractive ligands for stabilization of electropositive rare-earth metals. A few mixed alkyl/aryloxo and alkyl/alkoxide complexes have been reported in literature. The availability and stability of such compounds is sensitively balanced by the steric bulk of the respective alkyl and aryloxo/alkoxide ligands but steric saturation is commonly achieved by ate complex formation.

Use of a sterically highly demanding aryloxo in combination with small $[\text{CH}_2\text{SiMe}_3]$ ligands allowed for the formation of the neutral yttrium alkyl/aryloxo species $\text{Y}(\text{CH}_2\text{SiMe}_3)_2(\text{OAr}^{\text{tBu,H}})(\text{thf})_2$ (**107^H**) ($\text{OAr}^{\text{tBu,H}} = \text{OC}_6\text{H}_3\text{-2,6-tBu}$).¹⁶⁹ As depicted in Scheme 19 the reaction of YCl_3 with two equivalents of $\text{LiCH}_2\text{SiMe}_3$ followed by addition of one equivalent of $\text{LiOAr}^{\text{tBu,H}}$ in thf readily forms this neutral complex.



Scheme 19: Synthesis of heteroleptic mono(aryloxo)-bis(alkyl)-complexes **107^H** and **107^{Me}**.

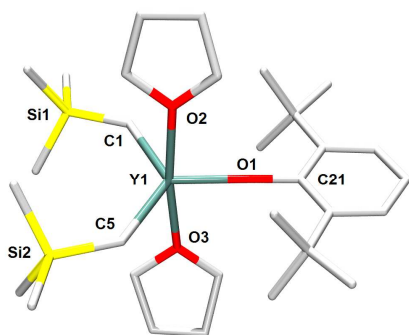
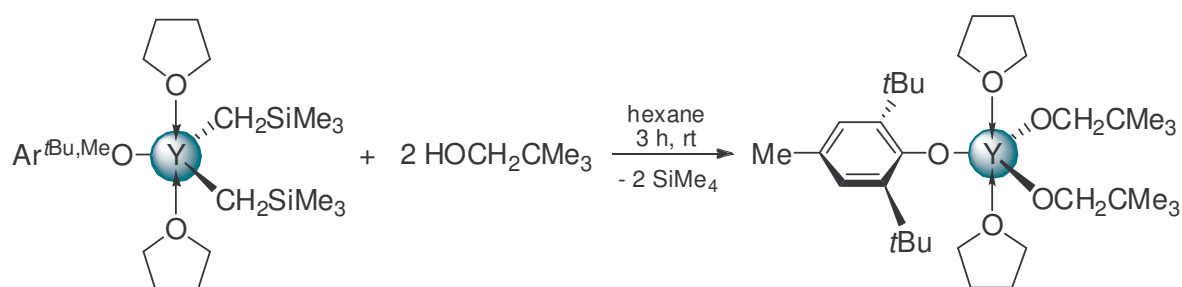


Figure 32: Solid-state structure of $\text{Y}(\text{CH}_2\text{SiMe}_3)_2(\text{OAr}^{\text{tBu,H}})(\text{thf})_2$.

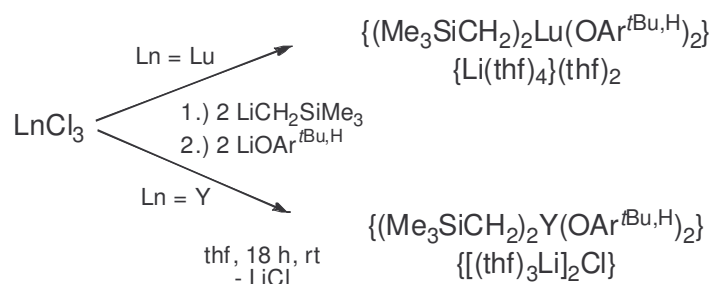
Based on this original synthesis the analogous $\text{Y}(\text{CH}_2\text{SiMe}_3)_2(\text{OAr}^{\text{tBu,Me}})(\text{thf})_2$ (**107^{Me}**) ($\text{OAr}^{\text{tBu,Me}} = \text{OC}_6\text{H}_2\text{-4-Me-2,6-tBu}$) was prepared in a one-pot synthesis protocol starting from $\text{YCl}_3(\text{thf})_{3.5}$, $\text{LiCH}_2\text{SiMe}_3$, and $\text{LiOAr}^{\text{tBu,Me}}$.¹⁷⁰ The mono(aryloxo)-bis(alkyl) complex **107^H** adopts a slightly distorted trigonal bipyramid in the solid-state (Figure 32) with a 172.6° angle between the axial ligands ($\text{O2}(\text{thf})\text{-Y-O3}(\text{thf})$).¹⁶⁹ The largest ligands occupy the equatorial positions as expected.

Convenient acid-base reaction of the alkylated aryloxide **107^{Me}** with two equivalents of neopentanol gave heteroleptic alkoxide **108** in good yield (Scheme 20).¹⁷⁰



Scheme 20: Synthesis of heteroleptic mono(aryloxo)-bis(alkoxo) complex **108**.

Changing the molar ratio of $\text{LnCl}_3/\text{LiCH}_2\text{SiMe}_3/\text{LiOAr}^{\text{tBu,H}}$ to 1:2:2 yielded the anticipated anionic bis(alkyl)-bis(aryloxide) complexes $\{(\text{Me}_3\text{SiCH}_2)_2\text{Ln}(\text{OAr}^{\text{tBu,H}})_2\}^-$ (**109**) for yttrium and lutetium (Scheme 21).¹⁷¹ The four-coordinate anionic moieties in **109** crystallize with nearly identical distorted tetrahedral geometries at the yttrium and lutetium metal centers. The cationic moieties are formed by the unusual cation $\{[(\text{thf})_3\text{Li}]_2\text{Cl}\}^+$ (**109_Y**) and the commonly observed cation $\{\text{Li}(\text{thf})_4\}^+$ (**109_{Lu}**), respectively (Scheme 21).



Scheme 21: Synthesis of ate complexes **109**.

Neutral **107^H** and ion-pairs **109** catalyze the ring-opening polymerization of ϵ -caprolactone.¹⁷¹ $\text{Y}(\text{CH}_2\text{SiMe}_3)_2(\text{OAr}^{\text{tBu,H}})(\text{thf})_2$ further initiates the polymerization of ethylene, exhibits metalation reactivity with phenylacetylene and pyridine, and evidences insertion of CNtBu, CO, and CO₂.¹⁷¹

As already mentioned in chapter 4.1 the attempt to synthesize homoleptic $\text{Sm}(\text{CH}_2\text{SiMe}_3)_3(\text{thf})_3$ by alkylation of the monomeric aryloxide $\text{Sm}(\text{OAr}^{i\text{Pr,H}})_3(\text{thf})_2$ with three equivalents of $\text{LiCH}_2\text{SiMe}_3$ gave the mixed aryloxide-alkyl ate complex $[\text{Li}(\text{thf})]_2[\text{Sm}(\text{OAr}^{i\text{Pr,H}})_3(\text{CH}_2\text{SiMe}_3)_2]$ (**110**) in moderate yield.⁹⁵ The ionic compound can rather be described as the product of an addition reaction of two equivalents $\text{LiCH}_2\text{SiMe}_3$ than that of a ligand substitution reaction. The solid-state structure displays a distorted square-based pyramidal samarium metal ligated by one terminal and one bridging $[\text{CH}_2\text{SiMe}_3]$ ligand. The three $[\text{OAr}^{i\text{Pr,H}}]$ ligands are bridging between the lanthanide metal and the lithium cations.

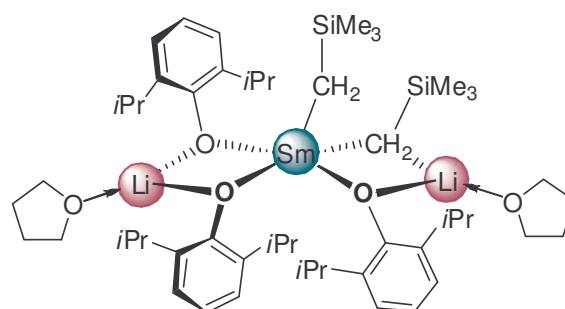


Figure 33: Structure of $[\text{Li}(\text{thf})]_2[\text{Sm}(\text{OAr}^{i\text{Pr,H}})_3(\text{CH}_2\text{SiMe}_3)_2]$ (**110**).

The observed addition reaction of the lithium alkyl reagent is contrary to the reactivity of $\text{Ln}(\text{OAr}^{t\text{Bu,H}})_2/\text{LiCH}(\text{SiMe}_3)_2$ mixtures reported by LAPPERT (see chapter 2.2). Reduced steric requirement of the $[\text{OAr}^{i\text{Pr,H}}]$ ligands, the higher solubility of $\text{LiOAr}^{i\text{Pr,H}}$ in hexane, and the presence of thf as a potential donor in the starting material were held responsible for the differing reactivity. More straight-forward was the formation of $\text{Nd}(\text{CH}_2\text{SiMe}_3)(\text{OAr}^{t\text{Bu,Me}})_2(\text{thf})_2$ (**111**) when reacting $\text{Nd}(\text{OAr}^{t\text{Bu,Me}})_3(\text{thf})$ and $\text{Mg}(\text{CH}_2\text{SiMe}_3)_2(\text{Et}_2\text{O})$ (1 : 1) in an attempt to isolate the active species of polymerization catalyst mixtures $\text{Nd}(\text{OAr}^{t\text{Bu,Me}})_3(\text{thf})/\text{MgR}_2$ (Figure 34).¹⁷² The solid-state structure of **111** features the metal center coordinated in a slightly distorted trigonal bipyramidal mode by one equatorial $[\text{CH}_2\text{SiMe}_3]$ ligand and two equatorial $[\text{OAr}^{t\text{Bu,Me}}]$ ligands. Due to the enhanced bulkiness of these ligands the angle between the axial thf molecules is lower than the theoretical value ($\text{O}(\text{thf})-\text{Nd}-\text{O}(\text{thf}) = 165.5^\circ$). The isolated species does, however, not initiate the polymerization of ethylene under the conditions used for the *in situ* prepared compounds. Blockage of the active site by the coordinated thf was claimed.

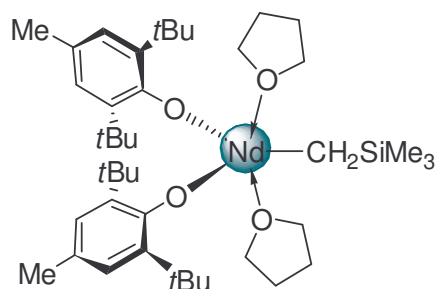
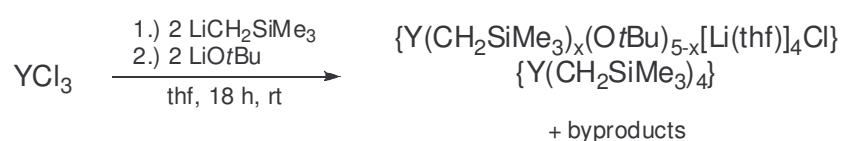


Figure 34: Structure of $\text{Nd}(\text{CH}_2\text{SiMe}_3)(\text{OAr}^{t\text{Bu,Me}})_2(\text{thf})_2$ (**111**).

6.3 Alkyl/Alkoxide

Interesting reactivity patterns were observed when combining $[\text{CH}_2\text{SiMe}_3]$ and alkoxide ligands. In an attempt to make a mixed alkyl/alkoxide compound starting from YCl_3 with two equivalents of $\text{LiCH}_2\text{SiMe}_3$ and two equivalents of LiOtBu the product of a nearly complete segregation of alkyl and alkoxide ligands into anionic and cationic compounds was observed (Scheme 22).¹⁷³



Scheme 22: Formation of $\{\text{Y}(\text{CH}_2\text{SiMe}_3)_x(\text{OtBu})_{5-x}[\text{Li}(\text{thf})_4\text{Cl}]\}\{\text{Y}(\text{CH}_2\text{SiMe}_3)_4\}$ **112**.

X-ray crystallography revealed the ion-pair $\{\text{Y}(\text{CH}_2\text{SiMe}_3)_x(\text{OtBu})_{5-x}[\text{Li}(\text{thf})_4\text{Cl}]\}\{\text{Y}(\text{CH}_2\text{SiMe}_3)_4\}$ (**112**) to be the outcome of this complex reaction.

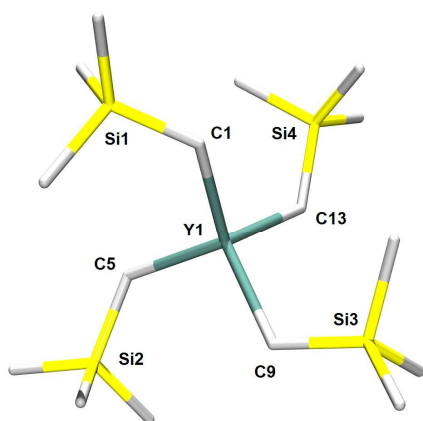


Figure 35: Solid-state structure of anionic $\{\text{Y}(\text{CH}_2\text{SiMe}_3)_4\}$ in **112**.

While the cationic unit shows a complex structure of a central five-coordinate yttrium atom surrounded by $[\text{OtBu}]$ ligands (the cation contains a disordered ligand which is a mixture of approx. 75% OtBu and 25% CH_2SiMe_3), the anionic part contains a homoleptic yttrium tetrakis-(trimethylsilyl)methyl complex. The geometry about the Y central metal describes a tetrahedron with C–Y–C angles ranging from 105.9° to 113.2° (Figure 35).

The stoichiometrically expected product could be obtained when using the bulkier $[\text{CH}(\text{SiMe}_3)_2]$ ligand in combination with *tert*-butoxide. Under similar reaction conditions the ate complex $\text{Y}[\text{CH}(\text{SiMe}_3)_2]_2(\mu\text{-OtBu})_2\text{Li}(\text{thf})$ (**113**) formed and could be isolated in moderate yields.¹⁶⁹ Consistent with the relative size of the ligands, the solid-state structure of **113** revealed terminal alkyl ligands and alkoxide moieties bridging between the yttrium and the lithium atom. Salt formation and the lower reactivity of bridging alkoxide ligands (vs. terminal) is assumed to stabilize this well-defined species. Attempts to prepare a neutral analogue containing these ligands were not successful.

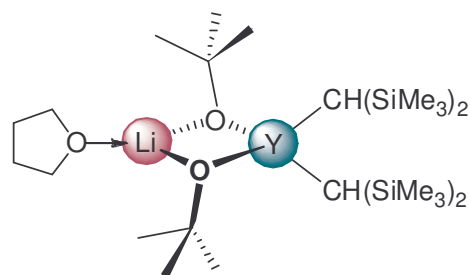
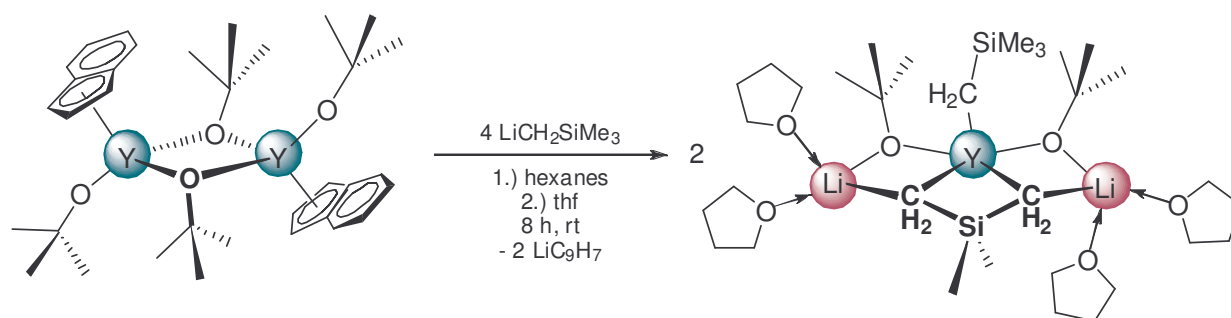


Figure 36: Structure of $\text{Y}[\text{CH}(\text{SiMe}_3)_2]_2(\mu\text{-OtBu})_2\text{Li}(\text{thf})$ (**113**).

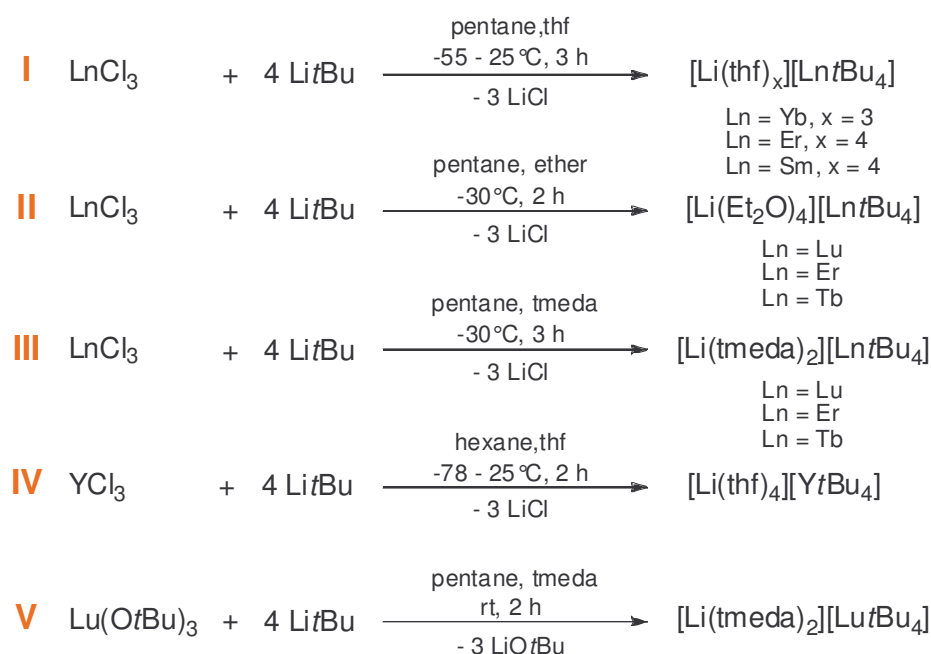
Unexpected reactivity was observed when reacting a mixed indenyl-yttrium alkoxide with four equivalents of $\text{LiCH}_2\text{SiMe}_3$ (Scheme 23). Partly alkylation accompanied by elimination of lithium indenide yielded the indenyl free alkyl alkoxide complex $\text{Y}(\text{CH}_2\text{SiMe}_3)[(\mu\text{-CH}_2)_2\text{SiMe}_2][(\mu\text{-OtBu})\text{Li}(\text{thf})_2]_2$ (**114**) (Scheme 23).¹⁷⁴ The crystallographic investigation of **114** revealed the formation of a remarkable $[(\mu\text{-CH}_2)_2\text{SiMe}_2]$ ligand formally derived by metalation of a methyl group of a $[\text{CH}_2\text{SiMe}_3]$ ligand. The extended steric protection generated by this metallacyclobutane ring possibly explains the low coordination number of five at the yttrium metal center. Synthetic utilization of compound **114** in further derivatization reactions is hampered by the advanced synthesis protocol.



Scheme 23: Formation of $\text{Y}(\text{CH}_2\text{SiMe}_3)[(\mu\text{-CH}_2)_2\text{SiMe}_2][(\mu\text{-OtBu})\text{Li}(\text{thf})_2]_2$ (**114**).

7 [Li(solv)_x][LnⁿTBu₄]

One of the major challenges in organorear-earth metal chemistry remains the synthesis of unsolvated, homoleptic tris(alkyl) complexes. The desire of the large rare-earth metal ion to adopt high coordination numbers very often cannot be satisfied with simple alkyl ligands. For rare-earth metal complexes carrying [tBu] ligands stereoelectronic saturation is achieved by ate complex formation. The first synthesis of [Li(solv)_x][LnⁿTBu₄] (**N**) was reported in 1978 by EVANS for ytterbium, erbium, and samarium.¹⁷⁵ Following the synthesis approach in Scheme 24, I, thf adducts [Li(thf)_x][LnⁿTBu₄] have been isolated and characterized by means of elemental analysis, IR spectroscopy, magnetic susceptibility and ¹H NMR spectroscopy (Sm).



Scheme 24: Synthesis of [Li(solv)_x][LnⁿTBu₄] (**N**).

Several years later SCHUMANN ET AL. synthesized the ether analogues [Li(Et₂O)₄][LnⁿTBu₄] of lutetium, erbium, and terbium (Scheme 24, II).¹⁷⁶ Ate complex formation was reported regardless of the stoichiometric ratio of the starting materials. Exchanging the ether donors by tmeda allowed for the isolation of compounds [Li(tmeda)₂][LnⁿTBu₄] (Scheme 24, III).¹⁷⁶ An alternative synthesis protocol starting from Ln(OtBu)₃ and four equivalents of LiⁿtBu in the presence of tmeda yielded products of the same composition (Scheme 24, V).¹⁷⁶

Compounds [Li(solv)_x][LnⁿTBu₄] are insoluble in hydrocarbons and form oils in aromatic solvents. They are completely soluble in ethereal solvents (Et₂O, thf).

The solid-state structure of [Li(tmeda)₂][LuⁿTBU₄] (**N**_{Lu-tmeda}) revealed a solvent separated ion pair (Figure 37).¹⁷⁷ The lutetium atom in the anionic unit is tetrahedrally coordinated by the four *tert*-butyl ligands. The Lu–C distances (2.32 - 2.43 Å) and the C–Lu–C angles (107.3 - 109°) are in the expected range.

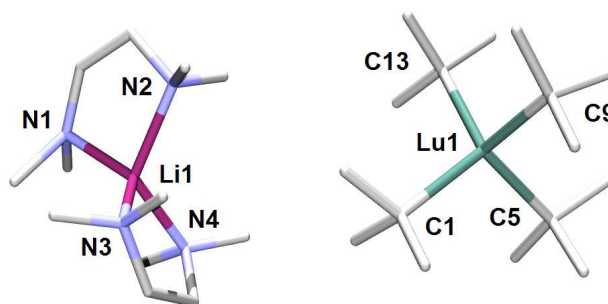
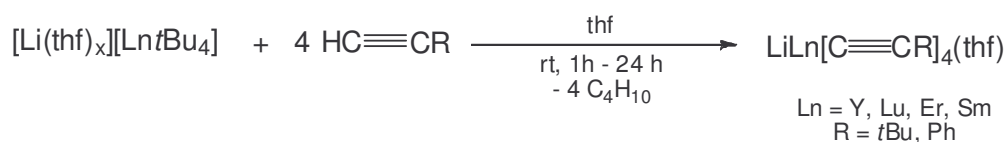


Figure 37: Solid-state structure of [Li(tmeda)₂][LuⁿTBU₄] (**N**_{Lu-tmeda}).

Despite of the presence of β -hydrogen atoms, compounds [Li(solv)_x][LnⁿTBU₄] provide relatively high stability. [Li(thf)_x][LnⁿTBU₄] (Ln = Yb, Sm) were reported to be stable for several days at ambient temperature.¹⁷⁵ Thermal decomposition of the respective samarium compound was monitored by NMR spectroscopy and suggested that dissociation of LiⁿTBU occurs as one of the initial decomposition steps. The absence of equivalent quantities of 2-methylpropene and 2-methylpropane after decomposition led to the conclusion that β -hydride elimination is not the most facile degradation pathway.¹⁷⁸ This phenomenon is in contrast to transition organometallic chemistry, where β -hydride elimination usually prevents the formation of stable *t*Bu species.

[Li(thf)_x][LnⁿTBU₄] react with alkynes according to an acid-base reaction under formation of tetra(alkynide) anions [Ln(C \equiv CR)₄]⁻. The *t*Bu ligands are hereby completely displaced under concomitant formation of 2-methylpropane.^{179,180}

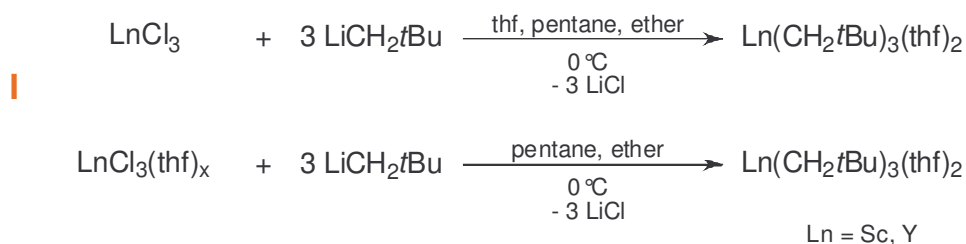


Scheme 25: Reactivity of [Li(thf)_x][LnⁿTBU₄] (**N**) toward alkynes.

Already under mild reaction conditions [Li(tmeda)₂][Ln⁺tBu₄] react with α,β unsaturated aldehydes and ketones under formation of 1,2 addition products.¹⁷⁷ All four *t*Bu groups can be transferred, but lanthanide containing reaction intermediates could not be isolated.

8 Ln(CH₂*t*Bu)₃(thf)₂

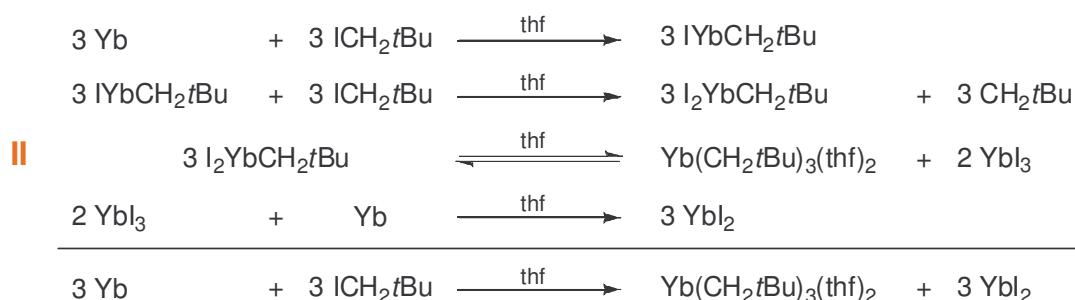
LAPPERT ET AL. reported the first group 3 neopentyl complexes Ln(CH₂*t*Bu)₃(thf)₂ (**O**) together with their silyl-analogues Ln(CH₂SiMe₃)₃(thf)₂ (**K**) in 1973.²⁴ A trigonal bipyramidal arrangement of the ligands around the metal center was anticipated by the ¹H NMR spectra of Sc(CH₂*t*Bu)₃(thf)₂ and Y(CH₂*t*Bu)₃(thf)₂, but final structural proof was not supplied until 30 years later when NIEMEYER successfully crystallized the respective ytterbium compound Yb(CH₂*t*Bu)₃(thf)₂.¹⁸¹



Scheme 26: Synthesis of Ln(CH₂*t*Bu)₃(thf)₂ (**O**) by salt metathesis.

While LAPPERT followed the widely used synthesis procedure starting from lanthanide tris(halogenides) and lithium alkyl reagents (Scheme 26), Yb(CH₂*t*Bu)₃(thf)₂ was synthesized directly from Yb metal and organohalides (Scheme 27).¹⁸¹

Such a direct approach is more common for the synthesis of divalent organolanthanide complexes and reaction mixtures often provide complex mixtures of Ln(II) and Ln(III) organyls. Purple crystals of Yb(CH₂*t*Bu)₃(thf)₂ were obtained from reaction mixtures containing Yb chips and 2,2-dimethylpropyl iodide (neopentyl iodide).



Scheme 27: Synthesis of Yb(CH₂*t*Bu)₃(thf)₂ (**O_{Yb}**).

¹H NMR spectroscopy and magnetic susceptibility measurements confirmed the presence of a paramagnetic Yb(III) metal center. The expected trigonal bipyramidal structure could finally be proven by X-ray structure determination (Figure 38).¹⁸¹ Structural details are in very good agreement with those found in the respective Yb(CH₂SiMe₃)₃(thf)₂ structure. The O–Yb–O angle (178.8°) between the axial thf donor molecules is very close to the ideal value but the highest possible C_{3h} symmetry is not accomplished. Two [CH₂tBu] ligands are facing each other. Steric repulsion is reflected in the non-uniform C–Yb–C angles (110.3° - 133.5°) and Yb–C bond lengths (2.36 - 2.39 Å).

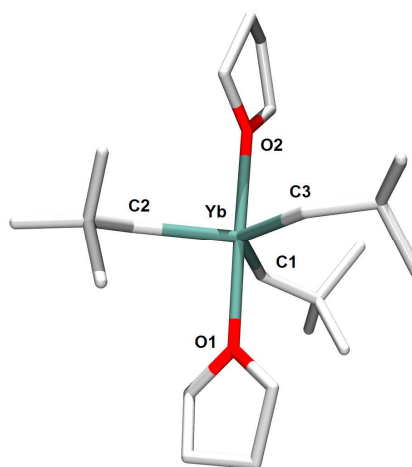
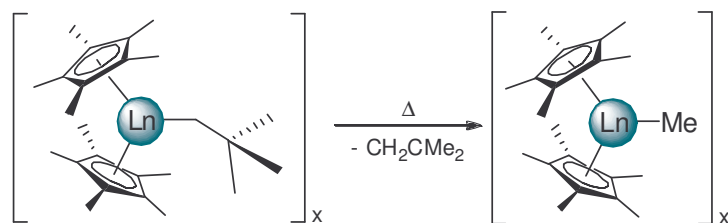


Figure 38: Solid-state structure of Yb(CH₂tBu)₃(thf)₂ (**O_{Yb}**).

Very little is known about rare-earth metal neopentyl complexes. Considering the wide application of the respective tris(trimethylsilyl)methyl complexes, this is especially surprising. Further derivatization of lanthanide alkyls Ln(CH₂tBu)₃(thf)₂ by means of alkane elimination have not been reported so far. Low thermal stability of [CH₂tBu] containing compounds could be a reasonable explanation for the low number of reported representatives. Metallocenes (C₅Me₅)₂Ln(CH₂tBu) (**115**) (Ln = Sc, Lu) could be obtained by salt metathesis reaction of [(C₅Me₅)₂LnCl]_x and LiCH₂tBu.^{182,183} Such compounds decompose at ambient temperature and their solutions are sensitive to ambient light. The stability of **115** is hereby decreasing with increasing size of the lanthanide cation and decomposition occurs under formation of the β-methyl elimination products [(C₅Me₅)₂LnMe]_x (Scheme 28).^{182,183} No α-agostic interaction of the neopentyl ligand and the lanthanide metal center - providing further stabilization - was observed in the solid-state structure of



Scheme 28: Decomposition of [(C₅Me₅)₂Ln(CH₂tBu)]_x (**115**) via β-methyl elimination.

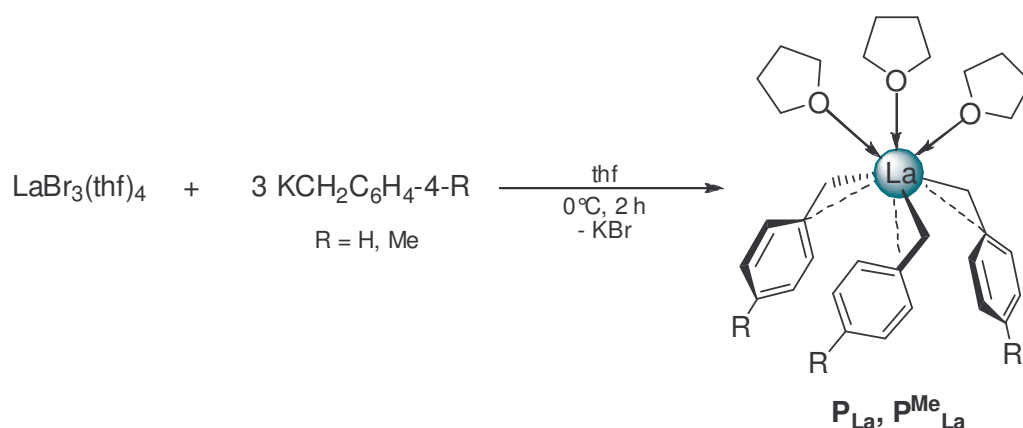
monomeric (C₅Me₅)₂Sc(CH₂tBu).

These findings substantiate low thermal stability of the homoleptic compounds and demonstrate possible decomposition pathways, regardless of the absence of a β-hydrogen atom.

9 Lanthanide Benzyl Complexes

9.1 La(CH₂Ph)₃(thf)₃ and La(CH₂C₆H₄-4-Me)₃(thf)₃

Due to the need for suitable homoleptic alkyl precursors especially of the larger rare-earth metals, benzyl ligands [CH₂Ph] experienced a revival as potential ligands. First reports on homoleptic tris(benzyl) complexes of neodymium¹⁸⁴ and lanthanum¹⁸⁵ were published in the 1980s but were inconclusive as to the existence of these species. Both compounds were characterized as (thermally) labile and decomposition to the alkylidene [PhCH₂Nd=CHPh] species was proposed for the neodymium compound, while the formation of [PhCH₂La(H)OCH=CH₂(thf)₂] was suggested in the lanthanum case. Very recently, the straightforward synthesis of neutral, salt-free lanthanum tris(benzyl) complexes La(CH₂Ph)₃(thf)₃ (**P_{La}**) and La(CH₂C₆H₄-4-Me)₃(thf)₃ (**P^{Me}_{La}**) was described by the group of HESSEN (Scheme 29).¹⁸⁶



Scheme 29: Synthesis of La(CH₂Ph)₃(thf)₃ (**P_{La}**) and La(CH₂C₆H₄-4-Me)₃(thf)₃ (**P^{Me}_{La}**).

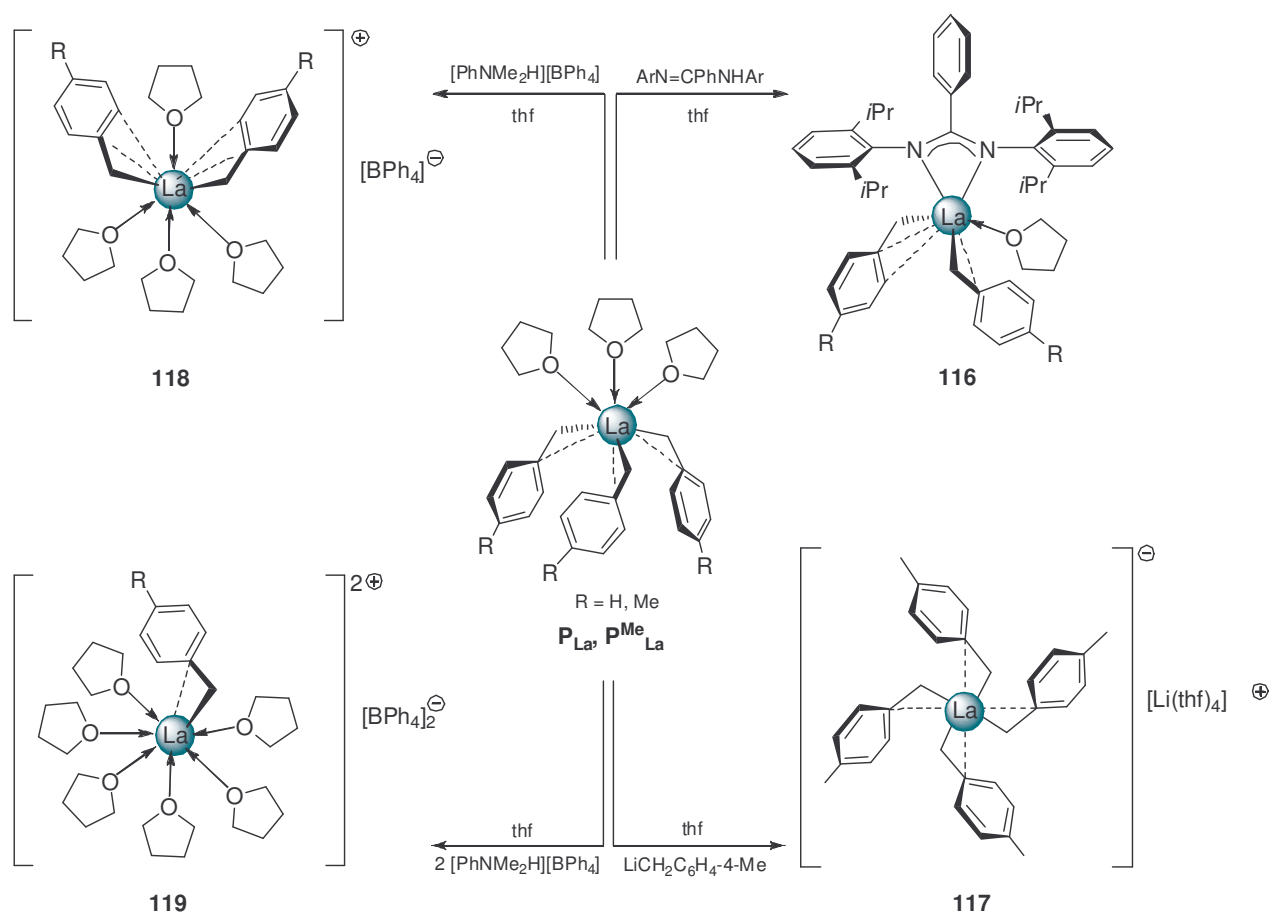
Reaction of LaBr₃(thf)₄ with three equivalents of potassium benzyls KCH₂C₆H₄-4-R (R = H, Me) in thf afforded lanthanum tris(benzyls) **P_{La}** and **P^{Me}_{La}** as orange-yellow crystals. Crystal structure determination revealed an η² coordination of each benzyl group to the lanthanum metal center. Three thf molecules are located in a facial arrangement on one side of the molecule. La(CH₂Ph)₃(thf)₃ and La(CH₂C₆H₄-4-Me)₃(thf)₃ are poorly soluble in hydrocarbons but can be dissolved in thf. On the NMR time scale all benzyl methylene protons are equivalent suggesting an average C_{3v} symmetric solution structure.

Application of lanthanum benzyls **P** and **P^{Me}** as alkyl precursors in a series of derivatization reactions demonstrated the versatility and synthetic value of these

compounds (Scheme 30).¹⁸⁶ Acid-base reaction with the amidine ArN=CPhNHAr (Ar = C₆H₃-2,6-*i*Pr) in thf generated the mono(amidinate)-bis(benzyl) complexes [PhC(NAr)₂]La(CH₂C₆H₄-R)₂(thf)_n (**116** and **116^{Me}**) and one equivalent of toluene or *p*-xylene, respectively.

In complexes **116** one benzyl ligand is coordinated in an η^2 mode while the second benzyl ligand is significantly tilted suggesting an η^3 like bonding.

Reactions of the tris(benzyl) complex **P^{Me}_{La}** with LiCH₂C₆H₄-4-Me in thf led to the formation of the ionic compound [La(CH₂C₆H₄-4-Me)₄][Li(thf)₄] (**117**). Crystal structure determination again revealed a stabilizing η^2 coordination of all four benzyl ligands in the anionic unit.



Scheme 30: Derivatization reactions of La(CH₂Ph)₃(thf)₃ (**P_{La}**) and La(CH₂C₆H₄-4-Me)₃(thf)₃ (**P^{Me}_{La}**).

Interestingly, mono(cationic) and di(cationic) lanthanum benzyl species could be obtained when reacting **P_{La}** and **P^{Me}_{La}** with one or two equivalents of the BRØNSTED acid [PhNMe₂H][B(C₆F₅)₄]. To facilitate crystallization of the ionic lanthanum compounds the corresponding tetraphenylborate salts were prepared using [PhNMe₂H][BPh₄]. Remarkably, both mono(cation) **118** and di(cation) **119** could be crystallized and

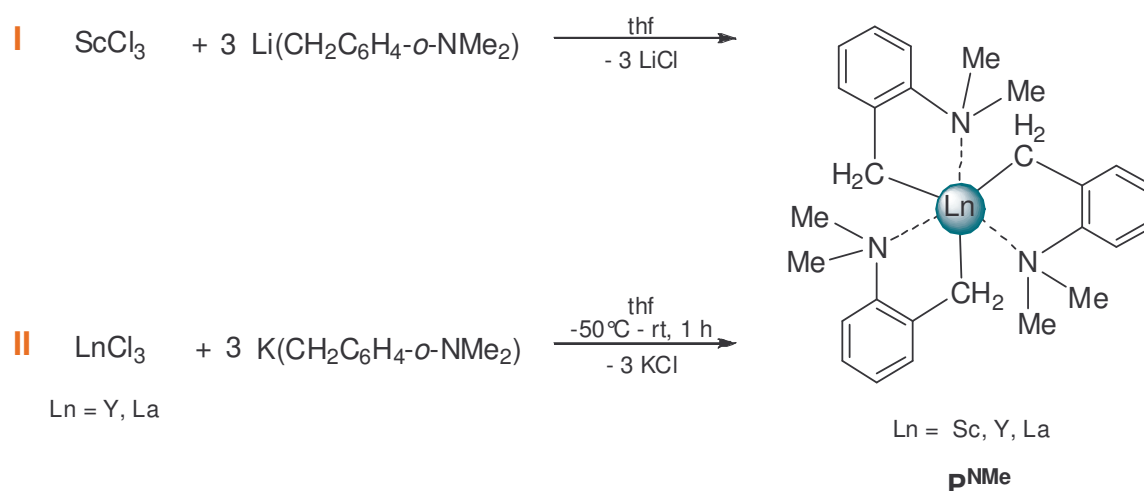
showed two tilted η^3 coordinated benzyl groups in the mono(cationic) species **118** while the remaining benzyl ligand in di(cation) **119** is essentially η^2 bonded. In both molecules the environment of the lanthanum metal center is saturated by thf molecules.

9.2 Ln(CH₂C₆H₄-o-NMe₂)₃ and Ln(CH₂C₆H₄-o-SiMe₃)₃

Moreover, donor-functionalized benzyl ligands have attracted attention very recently. The [CH₂C₆H₄-o-NMe₂] ligand had especially been developed to provide stability and steric shielding in complexes of the early transition metals. Due to its “built-in” chelating amino group it was found suitable to stabilize homoleptic and heteroleptic titanium and chromium complexes.¹⁸⁷

With the synthesis of the homoleptic solvent-free scandium compound Sc(CH₂C₆H₄-o-NMe₂)₃ MANZER introduced these bidentate benzyl ligands to group 3 chemistry.^{187,188}

Straightforward synthesis starting from ScCl₃ and Li(CH₂C₆H₄-o-NMe₂) yielded the envisaged product as an extremely air-sensitive, pale-yellow, crystalline solid (Scheme 31, I). Further purification, however, was described as exceedingly difficult.



Scheme 31: Synthesis of Ln(CH₂C₆H₄-o-NMe₂)₃ (**P^{NMe}**).

Almost thirty years later HARDER rediscovered the synthetic potential of Ln(CH₂C₆H₄-o-NMe₂)₃ (**P^{NMe}**).¹⁸⁹ Applying slightly modified reaction conditions and using the potassium salt K(CH₂C₆H₄-o-NMe₂) rather than the lithium analogue he succeeded in preparing the yttrium and lanthanum derivatives Y(CH₂C₆H₄-o-NMe₂)₃ and La(CH₂C₆H₄-o-NMe₂)₃ (Scheme 31, II). The solid-state structures of the isostructural compounds revealed a paddle-wheel structure with prismatic coordinated metal centers (Figure 39).

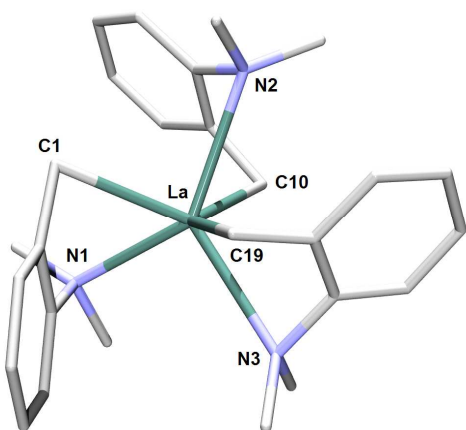


Figure 39: Solid-state structure of La(CH₂C₆H₄-o-NMe₂)₃ (**PNMe_eLa**).

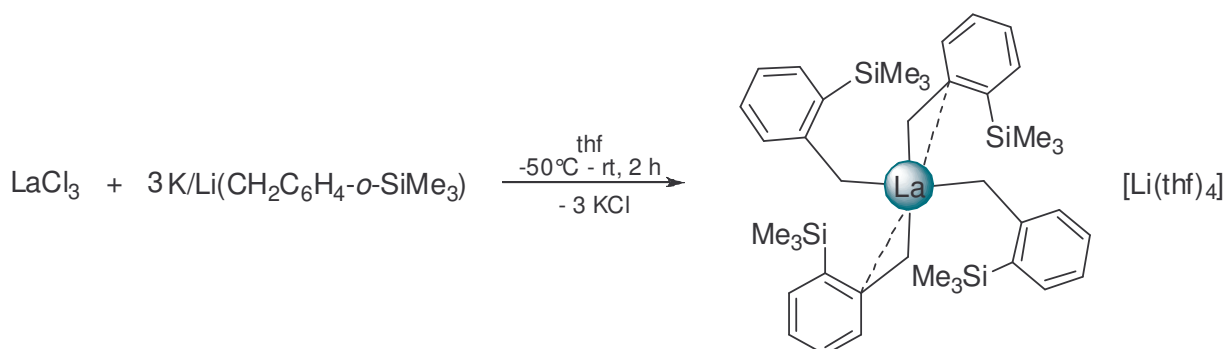
The bidentate ligand has a bite angle of 68.8° (Y) and 64.7° (La), respectively. Remarkably, the La-C_{ipso} and La-C_{ortho} distances are shorter than expected, demonstrating a pronounced multihapto bonding with increasing metal size. The benzyl ligands show a hybridization of the CH₂ group between sp² and sp³.

Compounds Ln(CH₂C₆H₄-o-NMe₂)₃ are insoluble in hydrocarbons, but are moderately soluble in aromatic

solvents and thf. Sc(CH₂C₆H₄-o-NMe₂)₃ reacts violently with chlorinated solvents.¹⁸⁸ Noteworthy is the thermal stability of complexes **PNMe_e**. Toluene solutions can be stored at ambient temperature for several months with only negligible decomposition. Even heated solutions show only minor decomposition.

Variation of the donor functionality at the benzyl ligands *ortho*-position, and the effect on complex stabilization was also investigated. SiMe₃ substituents were anticipated to provide extended steric shielding of the rare-earth metals coordination sphere and additional stabilization by possible agostic Si–Me–Ln interactions.

The attempted preparation of a neutral homoleptic lanthanum compound by reaction of LaCl₃ with K(CH₂C₆H₄-o-SiMe₃) in thf yielded the ionic complex [La(CH₂C₆H₄-o-SiMe₃)₄][Li(thf)₄] (**PSiMe_eLa**) due to lithium impurities in the starting material (Scheme 32).¹⁸⁹



Scheme 32: Synthesis of ionic complex [La(CH₂C₆H₄-o-SiMe₃)₄][Li(thf)₄] (**PSiMe_eLa**).

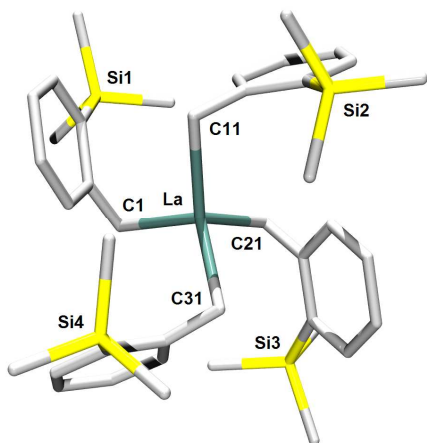
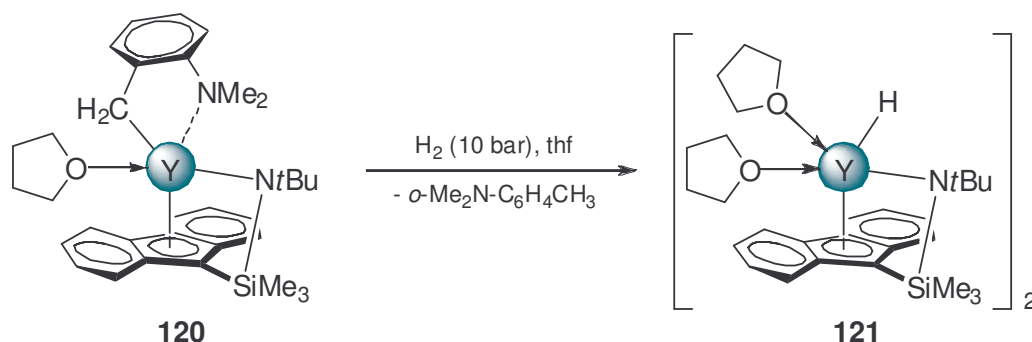


Figure 40: Solid-state structure of the [La(CH₂C₆H₄-o-SiMe₃)₄] anion in **P^{Si}Me₃La**.

The solid-state structure of [La(CH₂C₆H₄-o-SiMe₃)₄][Li(thf)₄] shows a pseudo *S*₄ symmetric [La(CH₂C₆H₄-o-SiMe₃)₄] anion with a distorted tetrahedral geometry about the lanthanum metal center (Figure 40). Two of the La–C bonds are distinctively shorter than the other two, substantiating a tendency toward η² bonding.

Despite of the stereoelectronic saturation by three N-donors, compounds Ln(CH₂C₆H₄-o-NMe₂)₃ (**P^NMe**) are prone to ligand exchange reactions. The yttrium derivative has been shown to deprotonate fluorenes and alkylamines and has been used as precursor in the synthesis of a constrained geometry yttrium benzyl compound (**120**) which could easily be converted into a yttrium-hydrido species (**121**) (Scheme 33).¹⁸⁹

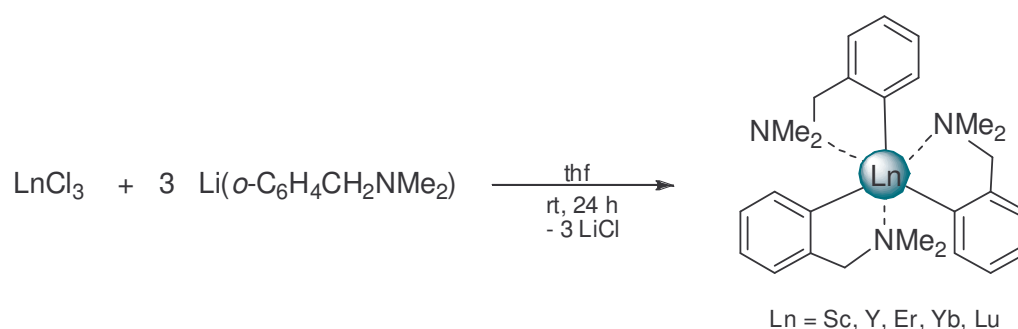


Scheme 33: Synthesis of a constrained geometry yttrium benzyl complex.

10 Ln(o-C₆H₄CH₂NMe₂)₃

[(Dimethylamino)methyl]-phenyl ligands [o-C₆H₄CH₂NMe₂] were developed parallel to the donor substituted benzyl ligands described in chapter 9.2.¹⁸⁸ They are structurally strongly related to the previously mentioned alkyl complexes and will therefore be accounted on here. The first [(dimethylamino)methyl]-phenyl lanthanide complex was reported in 1978.¹⁸⁸ Scandium compound Sc(o-C₆H₄CH₂NMe₂)₃ (**Q_{Sc}**) was prepared from ScCl₃ and Li(o-C₆H₄CH₂NMe₂) in refluxing thf and could be obtained as a white, insoluble compound which decomposes violently in dichloromethane and methanol.

In 1984 WAYDA ET AL. extended this synthesis protocol to the lanthanide metals lutetium, ytterbium, and erbium (Scheme 34).¹⁹⁰ Good isolable yields, purity, and easy characterization by standard analytical and spectroscopic techniques were reported. Crystal structure determination of the respective Lu(o-C₆H₄CH₂NMe₂)₃ finally proved the proposed structure and composition of compounds **Q** (Figure 41). Attempts to further extend the series to the early and middle lanthanide metals were not successful. Reaction of LnCl₃ (Ln = Pr, Nd, Sm, Tb) with the lithium salt Li(o-C₆H₄CH₂NMe₂) only produced uncharacterizable mixtures of products.¹⁹¹



Scheme 34: Synthesis of Ln(o-C₆H₄CH₂NMe₂)₃ (**Q**).

Phenyl complexes Ln(o-C₆H₄CH₂NMe₂)₃ are extremely air- and moisture-sensitive and marginally soluble in alkane solvents. They are, however, soluble in aromatic and ethereal solvents. In the solid-state, the three bidentate phenyl ligands of Lu(o-

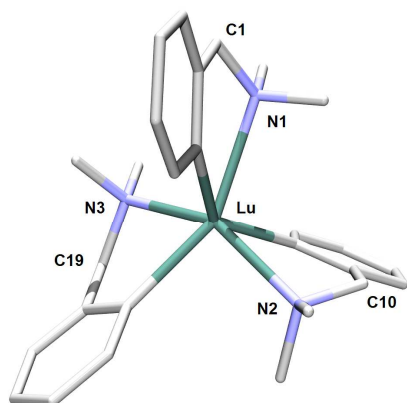


Figure 41: Solid state structure of Lu(o-C₆H₄CH₂NMe₂)₃ (**QLu**).

C₆H₄CH₂NMe₂)₃ (**QLu**) surround the lutetium metal center in a pedal-wheel manner (Figure 41).¹⁹⁰ Interestingly, the Lu–N distances fall into a two-short-one-long pattern. The origin was discussed to be of steric nature or due to packing effects.

Attempted hydrogenolysis of Lu(o-C₆H₄CH₂NMe₂)₃ with molecular hydrogen and reaction with simple olefins did not reveal the envisaged products. With terminal alkynes Lu(o-C₆H₄CH₂NMe₂)₃ formed the metalation product, though (see chapter 11.2).¹⁹¹

In an arene elimination reaction of Y(O-C₆H₄CH₂NMe₂)₃ with H(C₅Me₅) the group of TEUBEN successfully synthesized a mono(cyclopentadiene)-bis(phenyl) yttrium complex (**122**) (Figure 42) and investigated thermal decomposition pathways of such compounds.^{55,192}

Besides the formation of cyclopentadienyl complexes, compounds **Q** were found to be suitable precursors for the synthesis of lanthanide complexes with multidentate binaphthol (**123**) and amino-amido (**124**) ligands.¹⁹³⁻¹⁹⁵ Compounds **123** and **124** (Figure 42) have successfully been applied as catalysts in the (asymmetric) hydroamination.

With the intention to synthesize a heteroleptic mono(phosphor-ylide), Y(O-C₆H₄CH₂NMe₂)₃ was reacted with Ph₃P=CH-(o-CH₃OC₆H₄) but **125** was rather obtained as the product of exhaustive protonolysis of the phosphoranylidene ligand (Figure 42).¹⁹⁶

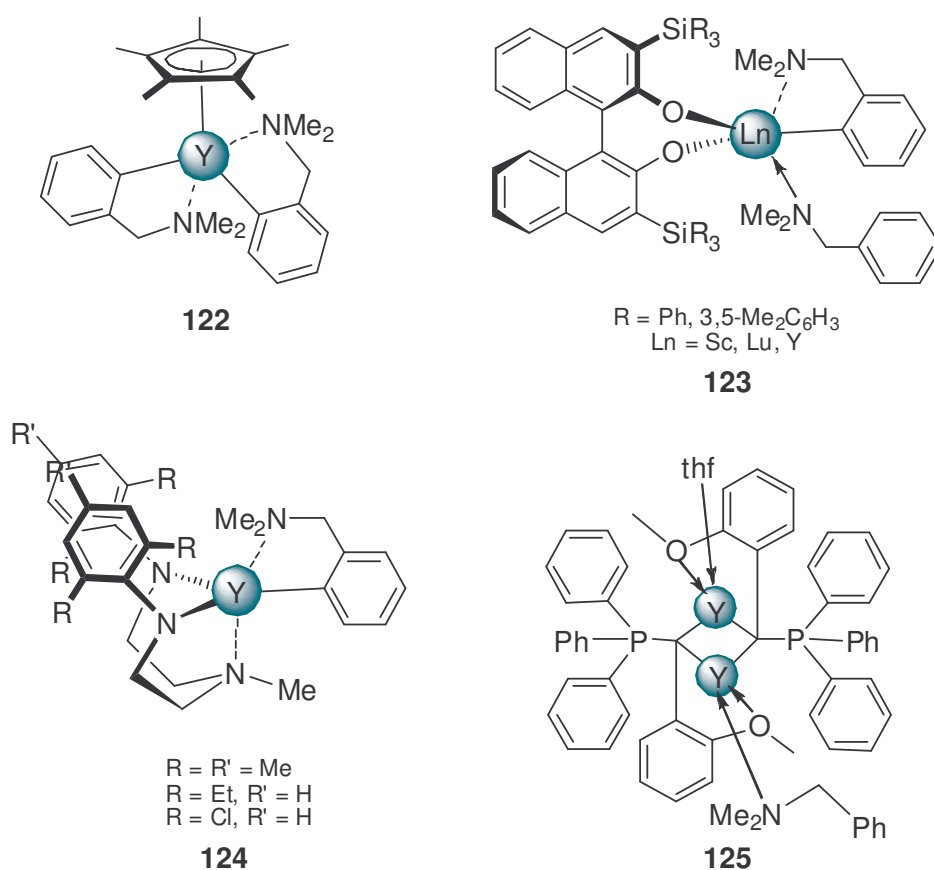


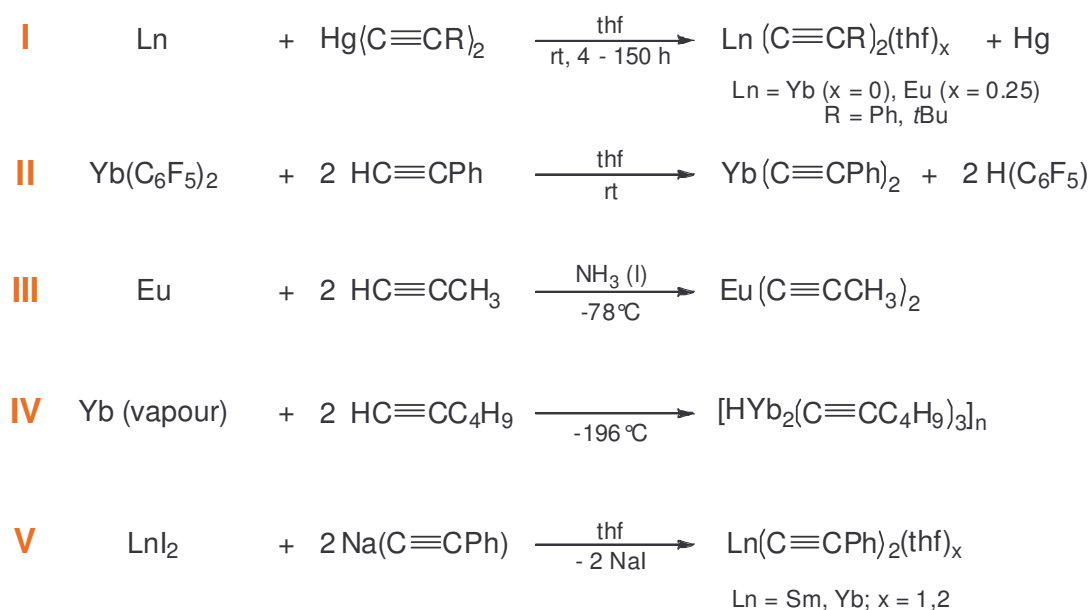
Figure 42: Complexes obtained from arene elimination reactions with Ln(O-C₆H₄CH₂NMe₂)₃ (**Q**).

11 Lanthanide Alkynides

11.1 Ln(II) Alkynides

The organometallic chemistry of the low-valent lanthanides featuring σ -bonded ligands is strongly connected to lanthanide alkynides. Even though first examples of divalent lanthanide alkynides have been reported more than 30 years ago, the chemistry of these σ -bonded hydrocarbyls developed sluggishly. This can partly be assigned to the advanced synthesis, the high reactivity of the divalent metal center (“hot oxidation state”), and to the challenging characterization.

Until today a large variety of synthesis procedures has been developed, allowing access to alkynide complexes of Yb(II), Eu(II), and Sm(II) (**R**) (Scheme 35). Major contributions to the early developments were made by DEACON ET AL. introducing transmetalation reactions of organomercurials as a route to organolanthanides.^{197,198} Bis(phenylethyne) ytterbium and europium have been prepared by such transmetalations and were isolated solvent-free (Ln = Yb) or as $\text{Eu}(\text{C}\equiv\text{CPh})_2(\text{thf})_{0.25}$ (**R^{Ph}**) (Scheme 35, I). Following the same protocol the respective $\text{Ln}(\text{C}\equiv\text{C}t\text{Bu})_2$ (**R^{tBu}**) compounds were accessible, even though bis(3,3-dimethylbut-1-ynide) mercury is less reactive than bis(phenylethyne) mercury.¹⁹⁹ Attempts to obtain the divalent samarium compounds and tris(alkynide)lanthanides by transmetalation failed.¹⁹⁹



Scheme 35: Synthesis of Ln(II) alkynides (**R**).

Bis(phenylethyne) ytterbium could further be prepared by ligand exchange of $\text{Yb}(\text{C}_6\text{F}_5)_2$ with phenylacetylene (Scheme 35, II).¹⁹⁷ Although reaction of $\text{Eu}(\text{C}_6\text{F}_5)_2$ and $\text{Ln}(\text{C}\equiv\text{CtBu})_2$ with phenylacetylene was indicated by IR and the hydrolysis behavior, no defined products could be isolated from such mixtures.

A very early report describes the reaction of metallic europium and ytterbium in liquid ammonia with propyne. Complex $\text{Eu}(\text{C}\equiv\text{CCH}_3)_2$ ($\text{R}^{\text{Me}}_{\text{Eu}}$) could be isolated from a blue solution, while in the ytterbium case a mixture of the desired product $\text{Yb}(\text{C}\equiv\text{CCH}_3)_2$ and $\text{Yb}(\text{NH}_2)_2$ was obtained.²⁰⁰

In an effort to investigate the extend of low-valent lanthanide chemistry EVANS ET AL. applied the metal vaporization technique to examine zero-valent lanthanide metal reactivity.²⁰¹ Co-condensation of ytterbium metal vapor with 1-hexyne at -196°C generated a black matrix of which several very similar products could be extracted with thf (Scheme 35, IV). IR spectroscopy indicated terminal hexynide ligands and chemical reactivity the presence of hexynide and hydride ligands. Isopiestic molecular weight studies revealed the existence of highly associated complexes. The oligomerization presumably occurs via alkyne bridges as depicted in Figure 43 a. Analogue reactions with the larger metal centers europium and samarium provided trivalent lanthanide species (*vide infra*).

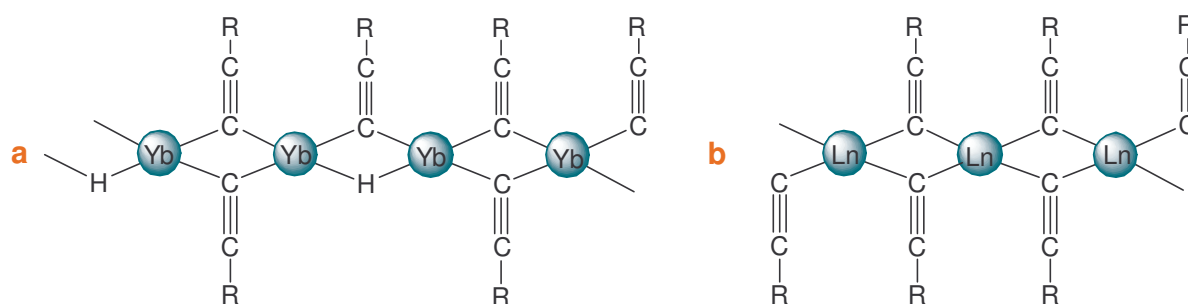


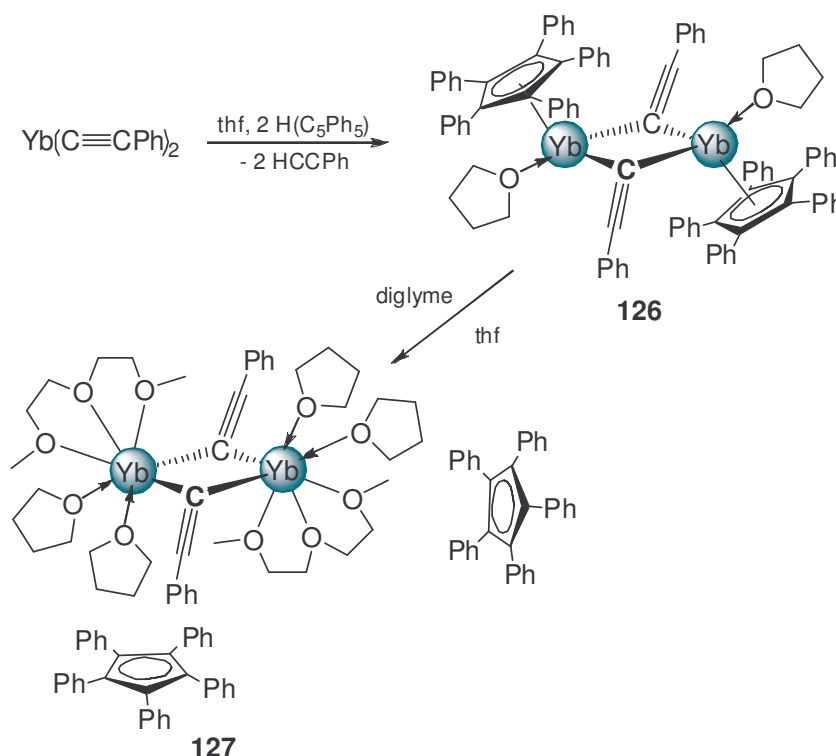
Figure 43: Proposed oligomeric structure of a) $[\text{HYb}_2(\text{C}\equiv\text{CR})_3]_n$ and b) $[\text{Ln}(\text{C}\equiv\text{CR})_2]_n$.

Salt metathesis of divalent lanthanide iodides and phenylethyne sodium as applied by BOCHKAREV yielded the solvated $\text{Ln}(\text{C}\equiv\text{CPh})_2(\text{thf})_x$ compounds (R^{Ph}) ($\text{Ln} = \text{Yb}, \text{Sm}$) (Scheme 35, V). This is the only report of a samarium bis(alkynide) compound.²⁰²

The alkyne complexes of the low-valent lanthanides are indefinitely stable in inert atmosphere but extremely sensitive to oxygen and moisture.¹⁹⁷ $\text{Ln}(\text{C}\equiv\text{CR})_2$ are insoluble in non-polar solvents but can be dissolved in thf. A trimeric-tetrameric structure was found in boiling thf indicative of an associated solid-state structure.¹⁹⁹ This associate structure is further confirmed by significantly low $\nu(\text{C}\equiv\text{C})$ frequencies which can be assigned to bridging alkyne groups (Figure 43 b). So far all attempts to obtain structural information by crystallography have been frustrated by the inability to grow suitable crystals.

Alkyne ligands can be exchanged according to an acid-base reaction. For example the $[\text{C}\equiv\text{CtBu}]$ ligand in $\text{Yb}(\text{C}\equiv\text{CtBu})_2$ reacts with two equivalents of the stronger BRØNSTED acid $\text{HC}\equiv\text{CPh}$ to give $\text{Yb}(\text{C}\equiv\text{CPh})_2$.¹⁹⁹ Considering the relatively high acidity of terminal alkynes, ligand exchange reactions are of minor synthetic value, though.

Interesting reactivity was recently reported by DEACON when reacting sterically very demanding $\text{H}(\text{C}_5\text{Ph}_5)$ with a thf solution of $\text{Yb}(\text{C}\equiv\text{CPh})_2$ (or *in situ* generated $\text{Yb}(\text{C}\equiv\text{CPh})_2$) (Scheme 36).²⁰³



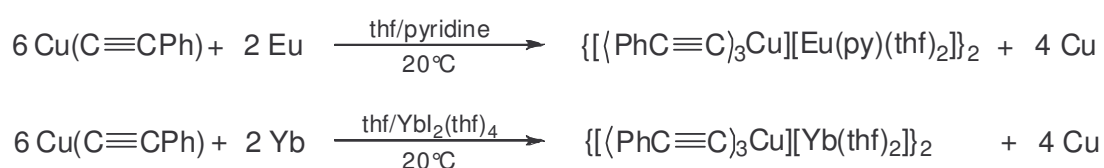
Scheme 36: Reaction of $\text{Yb}(\text{C}\equiv\text{CPh})_2$ with $\text{H}(\text{C}_5\text{Ph}_5)$.

The resulting mono(cyclopentadienyl) complex $[\text{Yb}(\text{C}_5\text{Ph}_5)(\mu\text{-C}\equiv\text{CPh})(\text{thf})]_2$ (**126**) revealed a dimeric structure with bridging $[\text{C}\equiv\text{CPh}]$ ligands. Slow addition of diglyme to **126** yielded solvent separated ion pair $[\text{Yb}(\mu\text{-C}\equiv\text{CPh})(\text{diglyme})(\text{thf})_2]_2[\text{C}_5\text{Ph}_5] \cdot (\text{thf})_4$ (**127**).

The $[\text{C}_5\text{Ph}_5]$ anions are not bound to the metal but reside in the crystal lattice. A similar pattern was also observed in $[\text{Eu}(\mu\text{-C}\equiv\text{CPh})(\text{diglyme})_2]_2[\text{P}_2\text{C}_3\text{tBu}_3]_2 \cdot \text{C}_6\text{D}_6 \cdot (\text{diglyme})_{0.5}$ (**128**).

Alkynides $\text{Ln}(\text{C}\equiv\text{CR})_2$ act as effective carbanion sources in reactions with aldehydes and ketones and can further act as reducing agents.²⁰⁴ Commonly *in situ* generated, such compounds are valuable reagents in organic synthesis. Most widely used are organosamariums for carbon–carbon bond formations (Samarium BARBIER reaction, Samarium GRIGNARD reaction), due to their advantage of rapid, mild, and chemoselective reduction of organohalides.²⁰⁵⁻²⁰⁷ Both inter- and intramolecular versions of these reactions using primary and secondary alkyl halides have been well established.

A speciality of so far no further synthetic value is the formation of cuprate complexes of europium and ytterbium (**S**) (Scheme 37).²⁰⁸ Redox transmetalation reaction of the lanthanide metals with organocopper compound $\text{CuC}\equiv\text{CPh}$ yielded the lanthanide cuprate complexes $\{[(\text{C}\equiv\text{CPh})_3\text{Cu}][\text{Eu}(\text{py})(\text{thf})_2]\}_2$ and $\{[(\text{C}\equiv\text{CPh})_3\text{Cu}][\text{Yb}(\text{thf})_2]\}_2$. The outcome of the reactions is essentially dependent on the solvents used and the reaction conditions. While reactions performed in pyridine/thf mixtures readily gave complexes **S**, same reactions in thf need the presence of catalytic amounts of $\text{YbI}_2(\text{thf})_4$. The solid-state structure of cuprates **S** revealed two $\text{Eu}(\text{py})(\text{thf})_2$ units and two $\text{Yb}(\text{thf})_4$ units, respectively, that are bonded by two bridging $\text{Cu}(\text{C}\equiv\text{CPh})_3$ fragments.

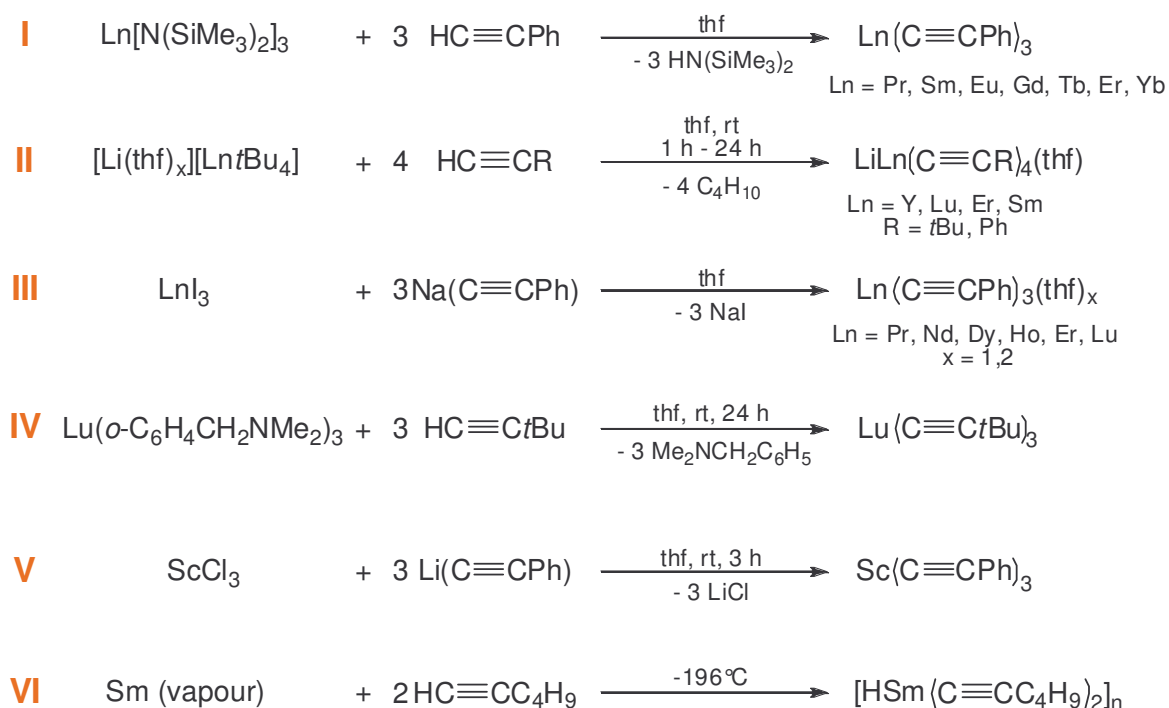


Scheme 37: Synthesis of Eu and Yb cuprate complexes (**S**).

11.2 Ln(III) Alkynides

Compared to their divalent analogues, trivalent homoleptic alkynides are even less studied. The number of reports on compounds $\text{Ln}(\text{C}\equiv\text{CR})_3$ (**T**) is basically limited to reports on synthesis approaches. Since transmetalation reactions did not afford alkynides of the trivalent rare-earth metals,¹⁹⁹ amine elimination, alkane elimination, and salt metathesis are potential synthesis procedures.

Synthesis according to the commonly used “silylamide route” was performed for a wide size-range of rare-earth metal cations and gave compounds $\text{Ln}(\text{C}\equiv\text{CPh})_3$ (**T**) in high yields (Scheme 38, I).^{209,210} When investigating the general reactivity of Ln–C σ -bonds, the reactivity of ate complexes $[\text{Li}(\text{thf})_x][\text{Ln}t\text{Bu}_4]$ (**N**) toward substrates containing acidic hydrogens was tested. Complete ligand exchange was observed with terminal alkynes $\text{HC}\equiv\text{CPh}$ and $\text{HC}\equiv\text{C}t\text{Bu}$ yielding alkynide ate complexes $\text{LiLn}(\text{C}\equiv\text{CR})_4$ (Scheme 38, II).^{179,180}



Scheme 38: Synthesis of Ln(III) alkynides (**T**).

Reactivity studies further revealed that treatment of $\text{Lu}(\text{o-C}_6\text{H}_4\text{CH}_2\text{NMe}_2)_3$ with $\text{HC}\equiv\text{CtBu}$ give solvent free $\text{Lu}(\text{C}\equiv\text{CtBu})_3$ ($\text{T}^{\text{tBu}}_{\text{Lu}}$) and *N,N*-dimethylbenzylamine (Scheme 38, IV).¹⁹¹ Starting from ScCl_3 and lithium alkyne a representative of the smallest rare-earth metal scandium $\text{Sc}(\text{C}\equiv\text{CPh})_3$ ($\text{T}^{\text{Ph}}_{\text{Sc}}$) could be obtained (Scheme 38, V).¹⁶ Surprisingly, solutions of LnI_3 in thf react with $\text{Na}(\text{C}\equiv\text{CPh})$ under elimination of NaI to give the solvated lanthanide alkynides $\text{Ln}(\text{C}\equiv\text{CPh})_3(\text{thf})_x$ (T^{Ph}) (Scheme 38, III).²¹¹ Even though the donor solvent was present in all other reported synthesis routes only solvent-free products have been reported.

In contrast to the reactivity observed for ytterbium (chapter 11.1, Ln(II) alkynides), co-condensation of samarium metal with 1-hexyne at -196°C produced an orange-black matrix from which a trivalent alkynide hydride of the possible composition $[\text{HSm}(\text{C}\equiv\text{CC}_4\text{H}_9)_2]_n$ ($\text{HT}^{\text{C}_4\text{H}_9}_{\text{Sm}}$) could be extracted (Scheme 38, VI).²⁰¹ Like for the divalent ytterbium compound a highly associate solid-state structure is anticipated (Figure 43 a). Application of alkynide hydride $\text{HT}^{\text{C}_4\text{H}_9}_{\text{Sm}}$ in the catalytic hydrogenation of 3-hexyne revealed formation of 3-hexene with low rates.

An exceptional organoerbium complex ligated by dendritic acetylide ligands has been published by M. BOCHKAREV ET AL. (Figure 44). Reacting $\text{Er}[\text{N}(\text{SiMe}_3)_2]_3$ with three equivalents of phenylacetylene in toluene gave $\text{Er}[\text{C}\equiv\text{CC}_6\text{H}_3(\text{C}\equiv\text{CPh})_{2-3,5}]_3$ in good yield ($\text{T}^{\text{dend}}_{\text{Er}}$).²¹²

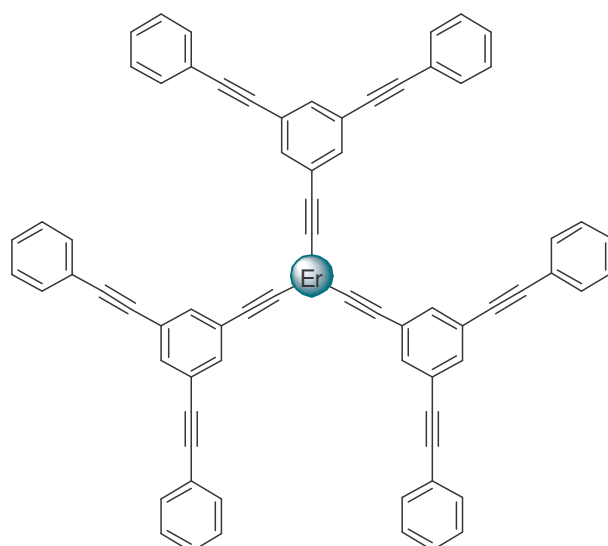


Figure 44: Proposed structure of $\text{Er}[\text{C}\equiv\text{CC}_6\text{H}_3(\text{C}\equiv\text{CPh})_{2-3,5}]_3$ ($\text{T}^{\text{dend}}_{\text{Er}}$).

The second generation organoerbium dendrimer $\text{Er}[\text{C}\equiv\text{CC}_6\text{H}_3[\text{C}\equiv\text{CC}_6\text{H}_3(\text{C}\equiv\text{CPh})_{2-3,5}]_2-3,5]_3$ could be prepared in a similar manner.²¹²

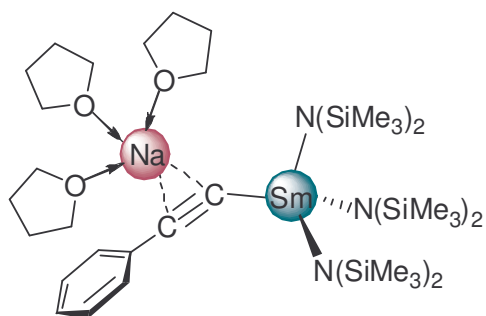


Figure 45: Structure of $\{\text{Na}(\text{thf})_3\}\{\text{Sm}[\text{N}(\text{SiMe}_3)_2]_3(\text{C}\equiv\text{CPh})\}$ ($\mathbf{129}_{\text{Sm}}$).

Reacting the tris(amides) $\text{Ln}[\text{N}(\text{SiMe}_3)_2]_3$ of cerium, samarium, and europium with phenylacetylene in the presence of one equivalent $\text{NaN}(\text{SiMe}_3)_2$ produced ion pairs $\{\text{Na}(\text{thf})_3\}\{\text{Ln}[\text{N}(\text{SiMe}_3)_2]_3(\text{C}\equiv\text{CPh})\}$ ($\mathbf{129}$) ($\text{Ln} = \text{Ce}, \text{Sm}, \text{Eu}$).²¹³ The solvated sodium ion binds side-on to the acetylide ligand of the heteroleptic tris(amide)-mono(alkynide) complex (Figure 45). The cation interaction bends the $\text{Sm}-\text{C}\equiv\text{C}$ angle in $\mathbf{129}_{\text{Sm}}$ to a value of only 151.4° .

Heteroleptic bis(aryloxy)-mono(acetylide) complexes were recently reported by DEACON ET AL.²¹⁴ Due to extreme steric bulk provided by $\text{HOAr}^{\text{tBu,OMe}}$ ($\text{Ar}^{\text{tBu,OMe}} = \text{C}_6\text{H}_2\text{-4-OMe-2,6-tBu}$) transmetalation reaction of $\text{Hg}(\text{C}\equiv\text{CPh})_2$ with the smaller rare-earth elements Y, Er, and Lu in the presence of the aryl-alcohol cleanly produced $\text{Ln}(\text{OAr}^{\text{tBu,OMe}})_2(\text{C}\equiv\text{CPh})(\text{thf})_2$ ($\mathbf{130}$). Isolation of these mixed-ligand complexes was attributed to steric inhibition of the cleavage of the final $\text{Ln}(\text{C}\equiv\text{CPh})$ group. Under the same reaction conditions Yb with $\text{Hg}(\text{C}\equiv\text{CPh})_2$ and $\text{HOAr}^{\text{tBu,OMe}}$ gave divalent $\text{Yb}(\text{OAr}^{\text{tBu,OMe}})_2(\text{thf})_3$ ($\mathbf{131}$) which could be oxidized by additional $\text{Hg}(\text{C}\equiv\text{CPh})_2$ to complete the series by $\text{Yb}(\text{OAr}^{\text{tBu,OMe}})_2(\text{C}\equiv\text{CPh})$ ($\mathbf{132}$). The observed reactivity is remarkably as the homoleptic alkynides of the trivalent rare-earth metals were not accessible by transmetalation reaction (*vide supra*).¹⁹⁹

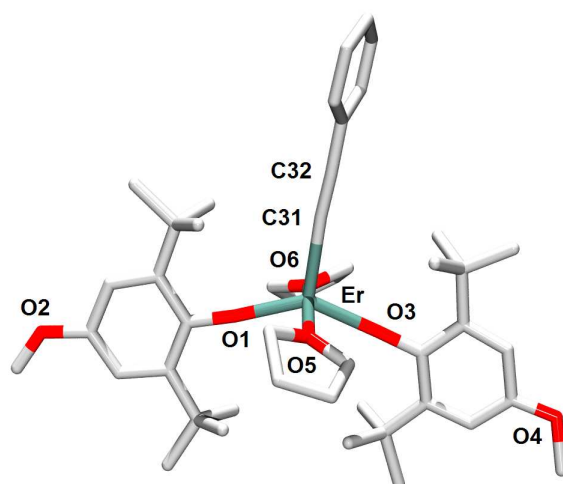


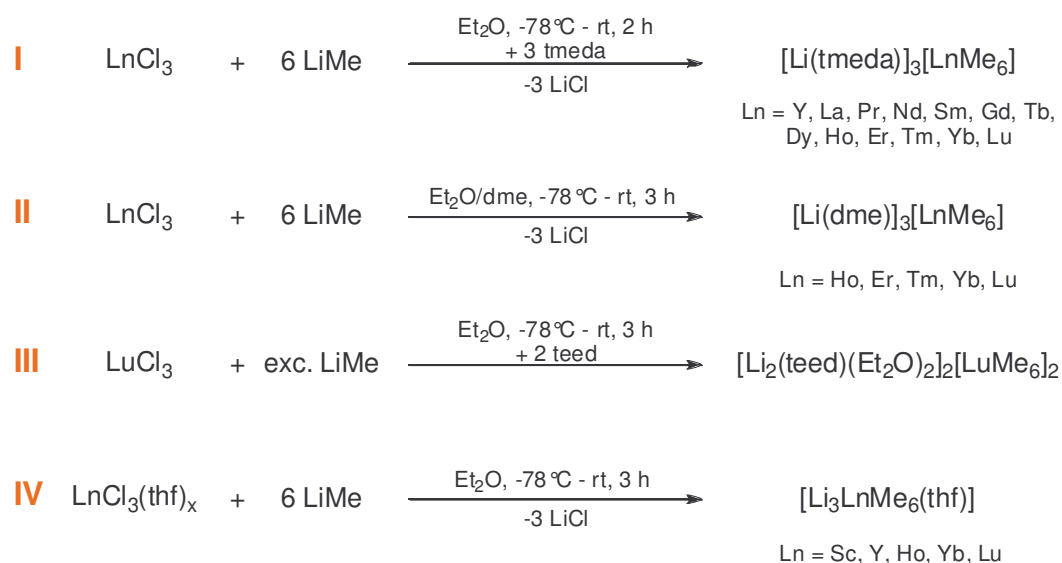
Figure 46: Solid-state structure of $\text{Er}(\text{OAr}^{\text{tBu,OMe}})_2(\text{C}\equiv\text{CPh})(\text{thf})_2$ ($\mathbf{130}_{\text{Er}}$).

12 [Li(donor)]₃[LnMe₆] and [LnMe₃]_n

Unsolvated methyl complexes are classified as the most reactive organorare-earth metal compounds. Enhanced basicity and the small size of the methyl ligand promote extraordinary reactivity^{215,216} enabling, e.g. methane activation²¹⁷ and multiple hydrogen abstraction.²¹⁸ Permethylated transition-metal complexes, as represented by neutral M(CH₃)_n and anionic [M(CH₃)_n]^{m-}, have attracted considerable interest not only for displaying the simplest organometallic derivatives but also for their intrinsic bonding phenomena.^{215,219} While structural and theoretical investigations on homoleptic group 4, 5, 6, and 7 derivatives proceeded remarkably, group 3 and lanthanide congeners remained elusive until very recently.^{20,219}

Commonly, stable homoleptic rare-earth alkyl compounds involve sterically demanding or chelating alkyl groups to meet the rare-earth metal's need for steric saturation. Apparently, the small methyl ligand can not provide such stereoelectronic protection often resulting in fast secondary reactions and decomposition.

Early attempts to obtain permethylated rare-earth metal complexes by reaction of methyllithium with LnCl₃ gave evidence for the formation of such compounds, isolation from ethereal solutions, however, was not successful.^{16,17} In the 1980s SCHUMANN ET AL. reported the synthesis of thermally stable ionic permethylated complexes [Li(donor)]₃[LnMe₆] (**U**) stabilized by chelating bases (donor = tmeda (*N,N,N',N'*-tetramethylethylenediamine), dme (1,2-dimethoxyethane), and teed (tetraethyl-ethylenediamine)).^{19,176,220}



Scheme 39: Synthesis of ionic [Li(donor)]₃[LnMe₆] and [Li₃LnMe₆(thf)] (**U**).

Dropwise addition of ethereal MeLi-solutions to suspensions of the rare-earth metal trichlorides in the presence of stoichiometric amounts of the respective donor molecules resulted in the formation of hexamethyl complexes for the entire series of rare-earth metals except Ce, Pm, and Eu (Scheme 39, I - III).

Following a slightly modified synthesis procedure using LnCl₃(thf)_x as rare-earth metal source OKUDA obtained [Li₃LnMe₆(thf)] as powdery solids (Scheme 39, IV).²²¹

Compounds [Li(donor)]₃[LnMe₆] are soluble in ethereal solvents, slightly soluble in aromatic solvents but insoluble in hydrocarbons.¹⁷⁶ The thermal stability is decreasing with increasing effective radius of the rare-earth metal cation. Hence, derivatives of the small ions (Lu-Ho) decompose over 120 °C, while all larger ions form complexes that are less stable.¹⁷⁶ In the solid-state the rare-earth metal ion is surrounded by six methyl groups in a slightly distorted octahedral arrangement (Figure 47 and Figure 48). The lithium atoms are located at the center of tetrahedra made up of two methyl groups and the two nitrogen or oxygen donors of tmeda and dme, respectively.^{176,220}

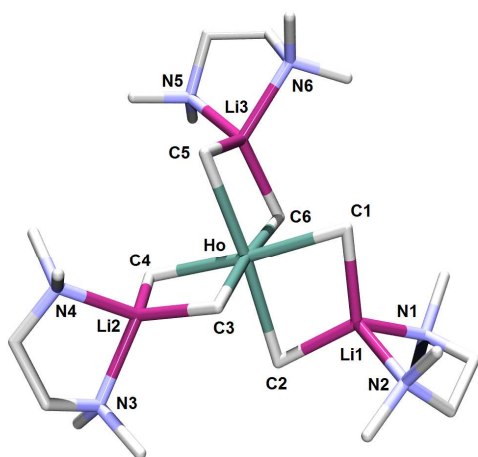


Figure 48: Solid-state structure of [Li(tmeda)]₃[HoMe₆] (**U_{Ho-tmeda}**).

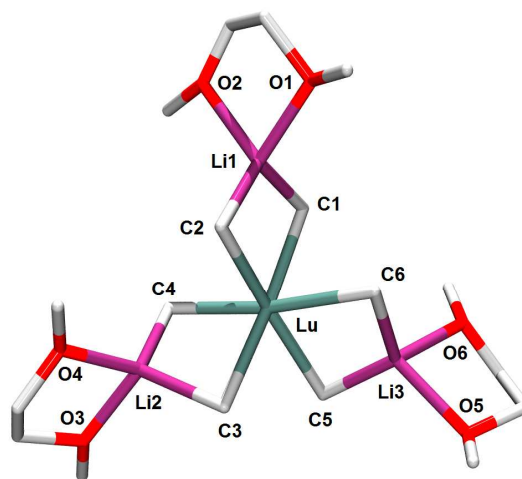
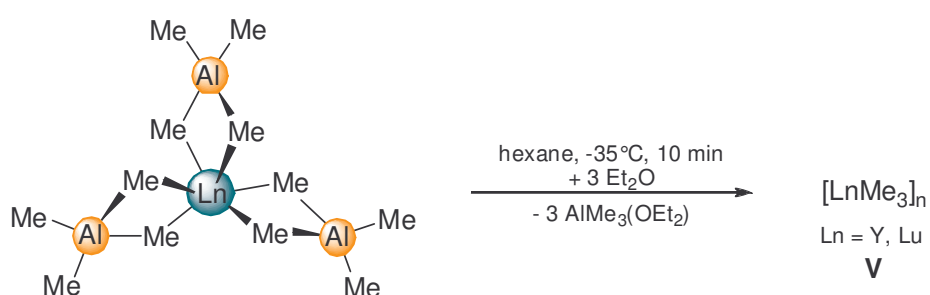


Figure 47: Solid-state structure of [Li(dme)]₃[LuMe₆] (**U_{Lu-dme}**).

Hexamethyl rare-earth metal complexes are extremely sensitive toward moisture and oxygen. On hydrolysis all ligands are replaced from the rare-earth metal with concurrent formation of Ln(OH)₃, CH₄, and tmeda/dme/teed. Further investigations on the chemical reactivity of [Li(donor)]₃[LnMe₆] (**U**) are limited to preliminary studies on methylation of α,β -unsaturated ketones and aldehydes. 1,2-Methylation was found to be favored over 1,4-methylation of the tested substrates.¹⁷⁶ Protonolysis of compounds

[Li₃LnMe₆(thf)] with borate reagents yielded active isoprene polymerization catalysts that will be accounted on later (*vide infra*).²²¹

Twenty years after SCHUMANN'S discovery of ionic permethylated compounds [Li(donor)]₃[LnMe₆] ANWANDER succeeded in the synthesis of neutral homoleptic trimethylttrium and trimethyllutetium (**V**).²⁰ Adding stoichiometric amounts of thf (3 equivalents) to a solution of Ln(AlMe₄)₃ (**Y^{Me}**) in hexane instantly produced a white precipitate of [LnMe₃]_n (**V**). Optimized conditions for the donor-induced tetramethylaluminate cleavage reaction (see also chapter 14.3) comprise the use of freshly sublimed Ln(AlMe₄)₃ as well as the less LEWIS basic donor diethylether, and low reaction temperature (Scheme 40).



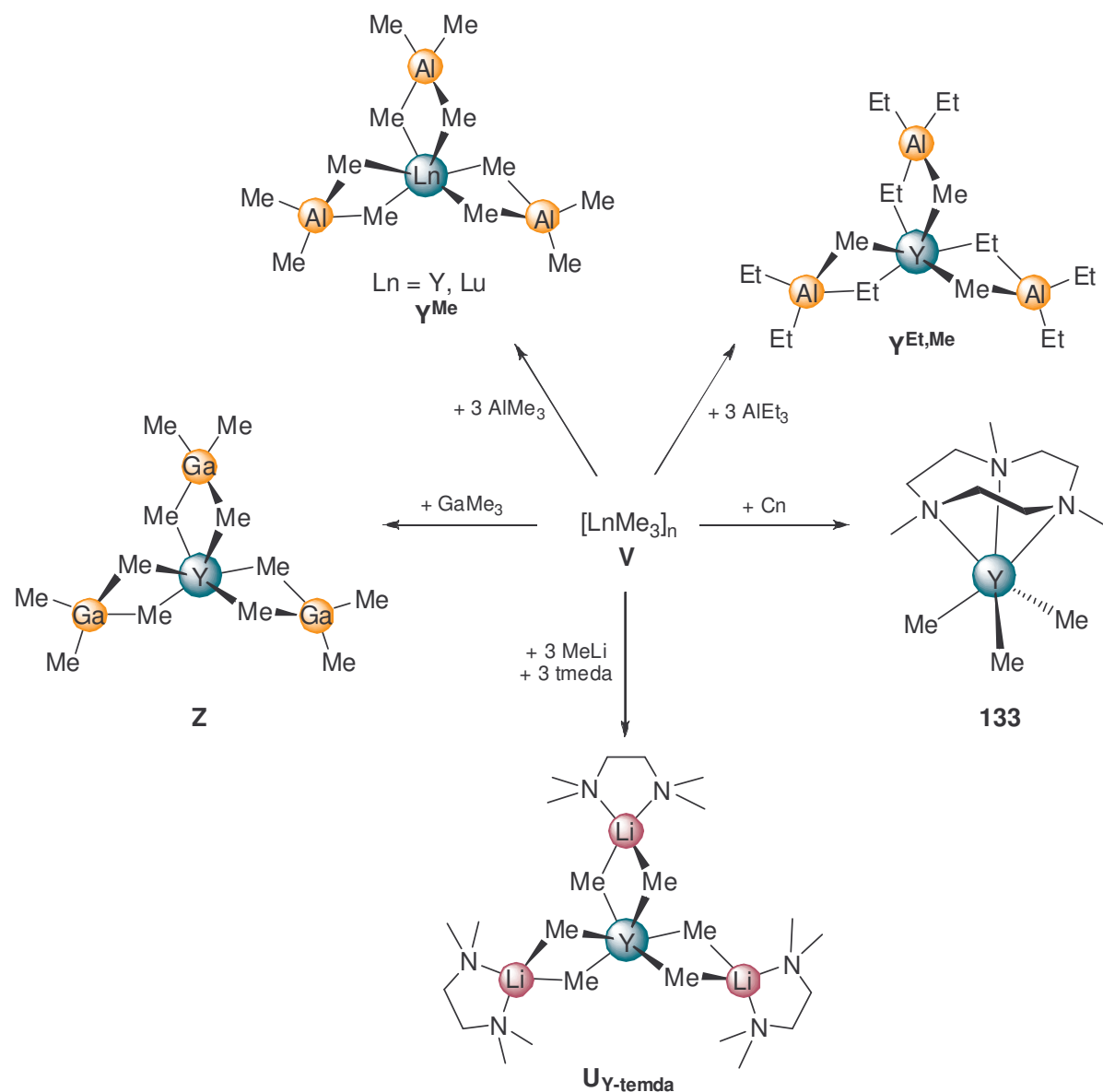
Scheme 40: Synthesis of [LnMe₃]_n (**V**).

Compounds [LnMe₃]_n are insoluble in aliphatic and aromatic solvents and slowly decompose in the presence of donor solvents (thf, Et₂O). Insolubility prevents the characterization of [LnMe₃]_n by solution NMR spectroscopy and single crystal X-ray diffraction studies. Solid-state FTIR and MAS NMR spectroscopy revealed a uniform coordination environment at the rare-earth metal center suggesting a polymeric network of rare-earth metals connected by bridging methyl groups.

So far only trimethylttrium and trimethyllutetium could be obtained following the synthesis route depicted in Scheme 40.

The donor-cleavage reaction was found to be completely reversible. Treatment of [LnMe₃]_n with three equivalents of AlMe₃ led to quantitative re-formation of Ln(AlMe₄)₃ (**Y^{Me}**) (Scheme 41).²⁰ Accordingly, other strong LEWIS acids like AlEt₃ and GaMe₃ re-dissolved [YMe₃]_n to yield heterobimetallic Y(Al₃Me₃Et₉) (**Y^{Et,Me}**) and Y(GaMe₄)₃ (**Z_Y**),^{20,222} respectively. In the presence of tmeda as donor solvent [YMe₃]_n and three equivalents of MeLi SCHUMANN'S ate-complex [Li(tmeda)]₃[YMe₆] (**U_{Y-tmeda}**) formed in moderate yield.

Reaction with 1,4,7-trimethyl-1,4,7-triazacyclononane (Cn) gave [CnYMe₃] (**133**) as previously prepared in the group of BERCAW (Scheme 41).



Scheme 41: Derivatization of $[LnMe_3]_n$ (**V**) by donor addition.

Homoleptic $[LnMe_3]_n$ further proved to react with BRØNSTED acids $HN(SiHMe_2)_2$ and $HOCHtBu_2$ forming homoleptic solvent-free amides $\{Y[N(SiHMe_2)_2]_3\}_2$ (**134**)²²² and alkoxides $Y(OCHtBu_2)_3$ (**135**),²⁰ respectively. Highly efficient methylation of the carbonylic functionality in 9-fluorenone (high yield, high group transfer economy) was observed, demonstrating the multifaceted applicability of $[LnMe_3]_n$ as rare-earth metal precursor and in organic synthesis.²²²

Donor(thf)-induced tetramethylaluminate cleavage of Ln(AIME₄)₃ accompanied by protonolysis with excess [NEt₃H][BPh₄] generated the ion triple [YMe(thf)₆]²⁺[BPh₄]₂ (**136**) in crystalline form (Figure 49).²²¹ The similar methyl di(cation) was obtained when applying five equivalents of [NEt₃H][BPh₄] to a thf solution of ionic [Li₃YMe₆(thf)]. Respective dicationic complexes of Sc, Ho, Yb, and Lu were prepared similarly.²²¹

Owing to the difficult separation of the LiBPh₄ byproduct upon using [Li₃YMe₆(thf)], dimethyl mono(cation) [YMe₂(thf)_x]⁺ (**137**) rather had to be generated from homoleptic Y(AIME₄)₃ and one equivalent of [NEt₃H][BPh₄] in thf.^{96,221}

The solid-state structure of ion pair [YMe₂(thf)₅][BPh₄] (**137**) revealed a pentagonal bipyramidal coordination geometry around the yttrium metal center (Figure 50).⁹⁶ The two methyl groups are *trans*-disposed. Replacing one methyl group by thf leads to the solid-state structure of ion triple [YMe(thf)₆][BPh₄]₂ (**136**) showing a similar geometric arrangement of ligand and donors around the Y metal center (Figure 49).²²¹ The remaining methyl group occupies the apical position of the pentagonal bipyramid.

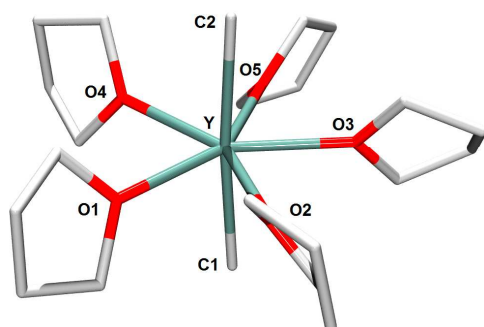


Figure 50: Solid-state structure of cation [YMe₂(thf)₅]⁺ in [YMe₂(thf)₅][BPh₄] (**137**).

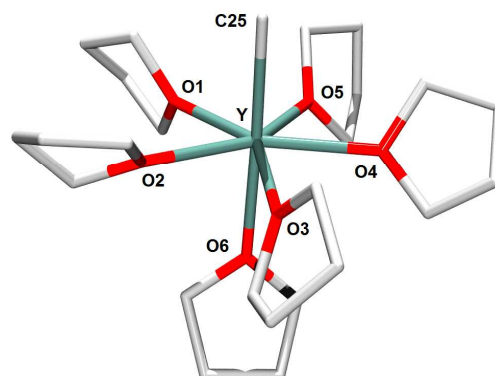


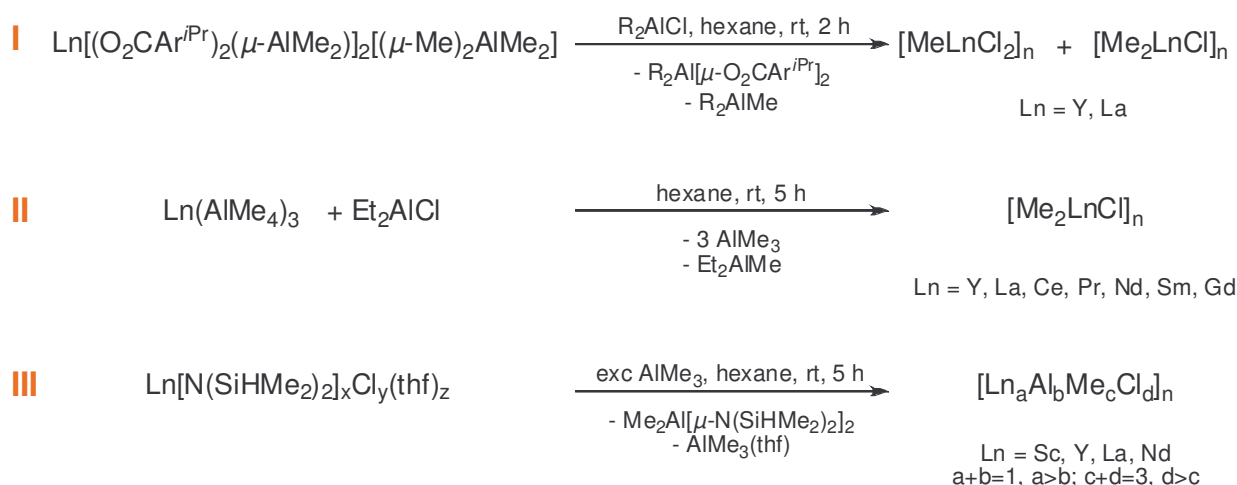
Figure 49: Solid-state structure of bis(cation) [YMe(thf)₆]²⁺ in [YMe(thf)₆][BPh₄]₂ (**136**).

In situ generated di(cations) [YMe(solv)_n]²⁺ (**136**) (solv = toluene) catalyzed the polymerization of 1,3 dienes when applying [PhNMe₂H][B(C₆F₅)₄] as cationizing agent, while the activation by [PhNMe₂H][BPh₄] did not result in catalytically active species.²²¹ This marked reactivity difference was attributed to the comparatively weak coordination of fluorinated anions resulting in solvent separated ion pairs in aromatic solvents. Contrary, a strong η⁶-coordination of the [BPh₄] anions would lead to inactive contact ion pairs.

Investigating the catalytic performance of in situ prepared $[\text{YMe}_2(\text{solv})_n]^+$ (**137**) and $[\text{YMe}(\text{solv})_n]^{2+}$ (**136**) toward dienes revealed remarkably higher activity and *cis*-selectivity for the dicationic species (monocation: 90% *cis*-PBD; dication 97% *cis*-PBD). Activities and polymer properties further displayed a strong dependence on the use of Al/Bu_3 as a scavenger (100 eq.).

13 Mixed Methyl/Chloride Rare-Earth Metal Compounds

During the studies on the stereospecific polymerization of 1,3-dienes catalyzed by Ln/Al heterobimetallic complexes, the group of ANWANDER observed the precipitation of insoluble rare-earth metal containing products upon “cationization” with R_2AlCl reagents ($\text{R} = \text{Me}, \text{Et}$).²²³⁻²²⁵ The formation of such precipitates occurred irrespective of the precatalysts involved and, hence, was found for active catalyst mixtures $\text{Ln}[(\text{O}_2\text{CAr}^{i\text{Pr}})_2(\mu\text{-AlMe}_2)]_2[(\mu\text{-Me})_2\text{AlMe}_2]/\text{R}_2\text{AlCl}$,²²⁴ $\text{Ln}(\text{OR}')_3(\text{AlMe}_3)_n/\text{R}_2\text{AlCl}$ ($\text{R}' = \text{neopentyl}, 2,6\text{-tBu}_2\text{C}_6\text{H}_3, 2,6\text{-iPr}_2\text{C}_6\text{H}_3$),²²⁵ and $\text{Ln}(\text{AlMe}_4)_3/\text{R}_2\text{AlCl}$,²²³ respectively (Scheme 42, I and II). Attempted characterization of the insoluble material by elemental analyses was not satisfactory, but the amount of isolated products pointed at the formation of polymeric/ionic $[\text{Me}_2\text{LnCl}]_n/[\text{MeLnCl}_2]_n$ (**W**) as a possible polymerization-initiating species.²²⁴

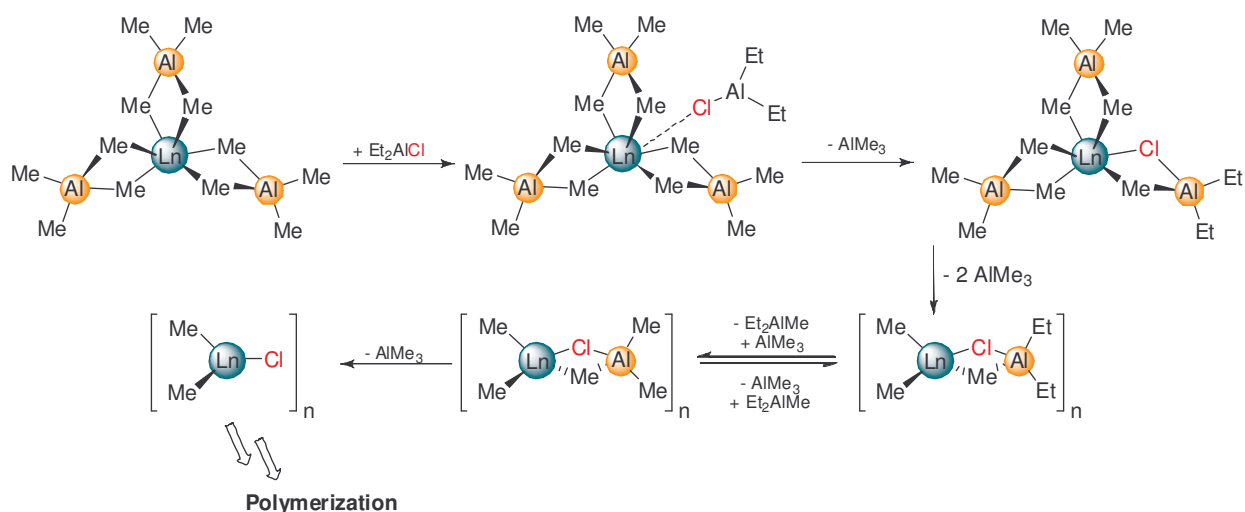


Scheme 42: Synthesis of mixed methyl/chloride rare-earth metal compounds $[\text{Ln}_a\text{Al}_b\text{Me}_c\text{Cl}_d]_n$, $[\text{MeLnCl}_2]_n$, and $[\text{Me}_2\text{LnCl}]_n$ (**W**).

A direct approach toward the synthesis of mixed methyl/chloride species **W** was published very recently.²²⁶ Alkylation of heteroleptic amido/chloride rare-earth metal complexes comprising preformed Ln–Cl moieties with excess AlMe₃ resulted in the formation of amorphous solids identified as [Ln_aAl_bMe_cCl_d]_n (a+b = 1, a>b; c+d = 3, d>c) (Scheme 42, III). The ¹³C MAS NMR spectrum suggests bridging methyl groups as the predominant carbon species, while terminal methyl groups seem to be absent.

The polymeric mixed methyl/chloride rare-earth metal compounds are insoluble in hydrocarbons and aromatic solvents, but dissolve in ethereal solvents (Et₂O, thf). However, scrambling of methyl and chloride ligands was apparent when dissolving [Y_aAl_bMe_cCl_d]_n in thf.

Based on NMR spectroscopic investigations and catalytic studies a mechanistic scenario for the formation of [Me₂LnCl]_n from Ln(AlMe₄)₃ and Et₂AlCl has been developed (Scheme 43).²²⁶ Mechanistic proposals for the respective Ln-carboxylate²²⁴ or Ln-alkoxide/aryloxide systems²²⁵ have also been published.



Scheme 43: Mechanistic scenario for the formation of [Me₂LnCl]_n from Ln(AlMe₄)₃ and Et₂AlCl.

Testing the reactivity of compounds [Ln_aAl_bMe_cCl_d]_n (**W**) toward BRØNSTED acidic substrates (*t*Bu-substituted phenols, H(C₅Me₅)) revealed no protonolysis reactions. Neither was alkylation of 9-fluorenone observed.²²⁶

Remarkably, the neodymium derivative (**W**_{Nd}) was found to initiate the stereospecific polymerization of isoprene with very high activities. The resulting polyisoprene shows very high *cis*-1,4 content (99%) and narrow molecular weight distributions ($M_n/M_w = 2.11$).²²⁶

14 Homoleptic Rare-Earth Metal Tetraalkylaluminates

14.1 Synthesis, Structure, and Properties of Ln(II)(AIR₄)₂

Early investigations by ANDERSEN regarding the reactivity of dimeric {Yb(II)[N(SiMe₃)₂]₂}₂ toward molecules with LEWIS acidic sites fundamentally contributed to the development of lanthanide tetraalkylaluminate compounds.²²⁷ Reaction of {Yb(II)[N(SiMe₃)₂]₂}₂ with equimolar amounts of AIR₃ (R = Me, Et) resulted in the formation of bis(trialkylaluminum)-adducts Yb[N(SiMe₃)₂]₂(AIR₃)₂ (**138**). Determination of the solid-state structure of Yb(II)[N(SiMe₃)₂]₂(AlMe₃)₂ revealed a monomeric Yb[N(SiMe₃)₂]₂ fragment in which each lone pair of electrons on the nitrogen atoms is coordinated to aluminum atoms (Figure 51).²²⁷ Steric saturation of the large divalent ytterbium metal center is achieved by four additional γ-CH agostic interactions with adjacent methyl-protons.

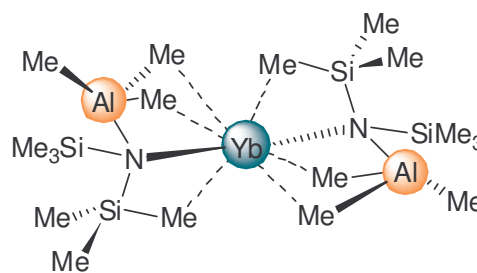
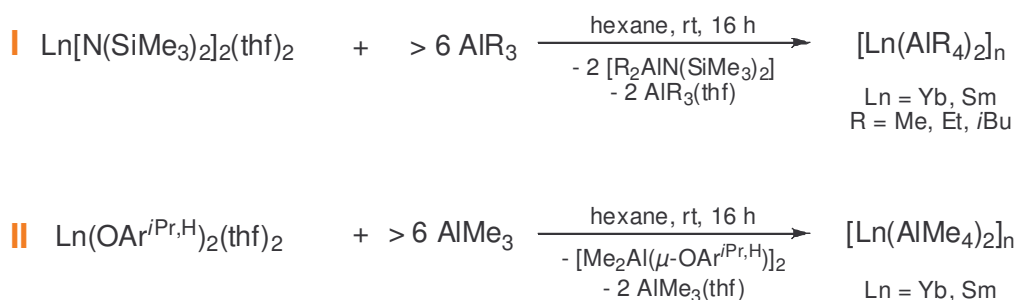


Figure 51: Structure of Yb(II)[N(SiMe₃)₂]₂(AlMe₃)₂.

In 2001 the above mentioned reactions were reinvestigated by the group of ANWANDER using an excess of the trialkylaluminum reagents (Scheme 44, I).^{228,229} The obtained peralkylated heterobimetallic complexes Ln(II)(AIR₄)₂ (**X**) (R = Me, Et, *i*Bu) are the products of a complete [amide] → [alkyl] transformation, proceeding via intermediately formed AIR₃-adducts as found by ANDERSEN (Figure 51).²²⁷



Scheme 44: Synthesis of Ln(II)(AIR₄)₂ (**X**).

While the methyl derivatives (**X^{Me}**) precipitate quantitatively from hexane reaction mixtures to give analytically pure powders, Ln(II)(AlEt₄)₂ (**X^{Et}**) and Ln(II)(Al*i*Bu₄)₂ (**X^{iBu}**)

display excellent solubility in hexane and can be separated from the byproduct [R₂AlN(SiMe₃)₂] by fractional crystallization.^{228,229}

Homoleptic Ln(II)(AlMe₄)₂ (X^{Me}) could further be obtained by complete alkylation of lanthanide(II) bis(2,6-diisopropylphenolates) with an excess of AlMe₃ (Scheme 44, II).²³⁰ Structure determination of the methyl derivatives Ln(II)(AlMe₄)₂ is frustrated by the insolubility in aliphatic and aromatic solvents but single crystals suitable for X-ray crystallographic structure determination could be obtained for the higher alkylated congeners Ln(II)(AlEt₄)₂ (X^{Et}).^{228,231} Both divalent metal centers ytterbium and samarium show isomorphous structures in the solid-state consisting of a polymeric network of interconnected anionic [Ln(AlEt₄)₃]⁻ (Figure 53) and cationic [Ln(AlEt₄)]⁺ (Figure 52) fragments. In the anionic unit the lanthanide(II) metal center is coordinated by six bridging carbon atoms facilitating a pseudo octahedral geometry (Figure 53). Each [AlEt₄]⁻ unit is coordinated in an η² fashion. While the [AlEt₄] coordination in the cationic moiety [Yb(AlEt₄)]⁺ was described as a slightly distorted η³-coordination,²²⁸ the respective samarium containing unit rather showed a bent η²-coordination mode (Figure 52).²³¹

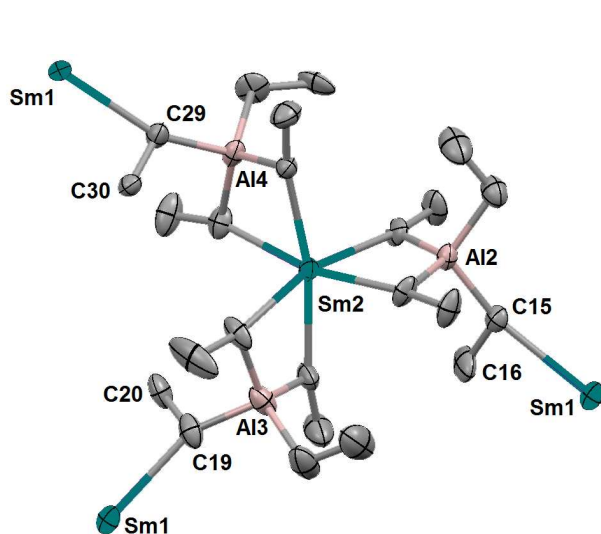


Figure 53: Solid-state structure of the anionic molecular fragment [Sm(AlEt₄)₃]⁻ showing the interconnection of the formally anionic and cationic fragments.

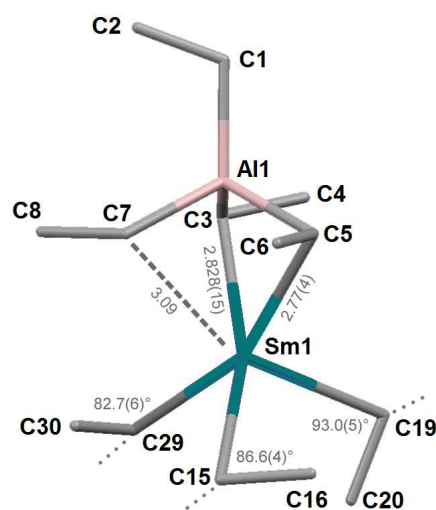


Figure 52: Solid-state structure of the cationic molecular fragment [Sm(AlEt₄)]⁺ showing the interconnection of the formally anionic and cationic fragments.

Interconnection of the formally anionic and cationic molecular fragments into a three-dimensional network is accomplished via the “terminal” ethyl groups of [Ln(AlEt₄)₃]⁻ resulting in an overall μ, η¹:η² coordination mode.

Due to dynamic exchange processes in solution (see chapter 14.2), the ¹H NMR spectrum of diamagnetic Yb(II)(AlEt₄)₂ exhibits only two resonances for the [AlEt₄] ligands.²³¹ Variable temperature ¹H NMR studies did not reveal decoalescence of the proton signals for the bridging and non-bridging alkyl groups over the temperature range of -100 to +90 °C.

CP MAS NMR spectroscopic investigations on insoluble Yb(II)(AlMe₄)₂ were indicative of two distinct bridging methyl groups in the solid-state.²³¹

Unlike homoleptic Ln(AlMe₄)₃ (Y^{Me}) of the trivalent rare-earth metal centers, donor-induced aluminate cleavage²³² (see chapter 14.3) does not occur at lanthanide(II) metal centers. Contrary, interaction of polymeric [Ln(II)(AlR₄)₂]_n with donor molecules of varying bonding strength and bonding mode (donor = thf, pyridine, phenanthroline) leads to the formation of discrete monomeric lanthanide donor-adducts Ln(AlR₄)₂(donor)_n (**139** and **140**) (Figure 55 and Figure 54).²²⁹

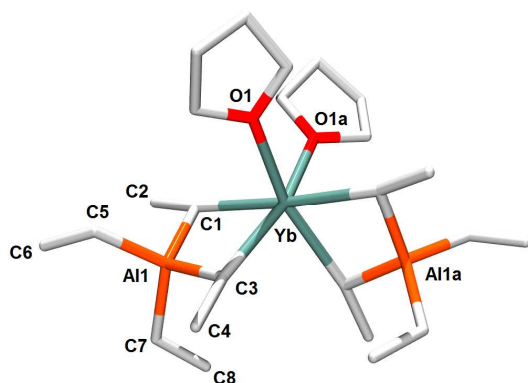


Figure 55: Solid-state structure of Yb(AlEt₄)₂(thf)₂ (**139**).

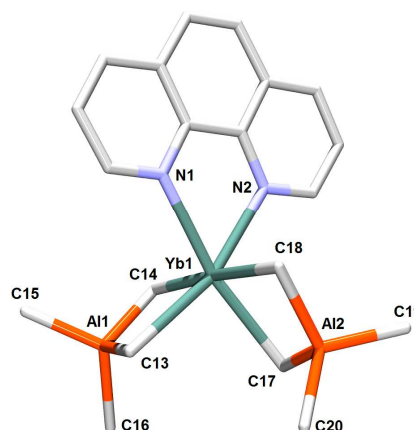


Figure 54: Solid-state structure of Yb(AlMe₄)₂(phen) (**140**).

The observed divergent reactivity of heterobimetallic homoleptic Ln(II)(AlR₄)₂ and Ln(III)(AlMe₄)₃ toward LEWIS basic molecules accounts for a different nature of the lanthanide-carbon bonding. While the latter display true aluminate complexes (E_N scale according to PAULING: Ln(III) = 1.1-1.3, Al(III) = 1.6) divalent derivatives are better described as lanthanidate complexes [AlEt₂]₂[LnEt₄(donor)_n] similar to [Li(donor)_n]₃[Ln(III)Me₆] (see chapter 12). The Ln-C bonding nature can not be rationalized on the basis of PAULING's electronegativity scale^{233,234} and the LEWIS acidity criterion (Al(III) > Ln(III) > Ln(II)) commonly considered as the driving force for

AlR₃(donor) separation can not be applied either. Increased covalent contributions to the Ln(II)–C bonds rather seem to control the observed Lewis base addition reactions. Studies on the reactivity of peralkylated [Ln(II)(AlR₄)₂]_n (**X**) toward protic substrates were performed only recently. Remarkably, a suspension of [Yb(AlMe₄)₂]_n in thf reacted with

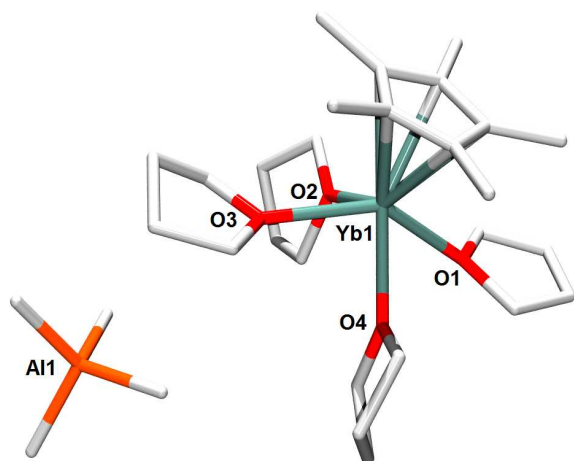
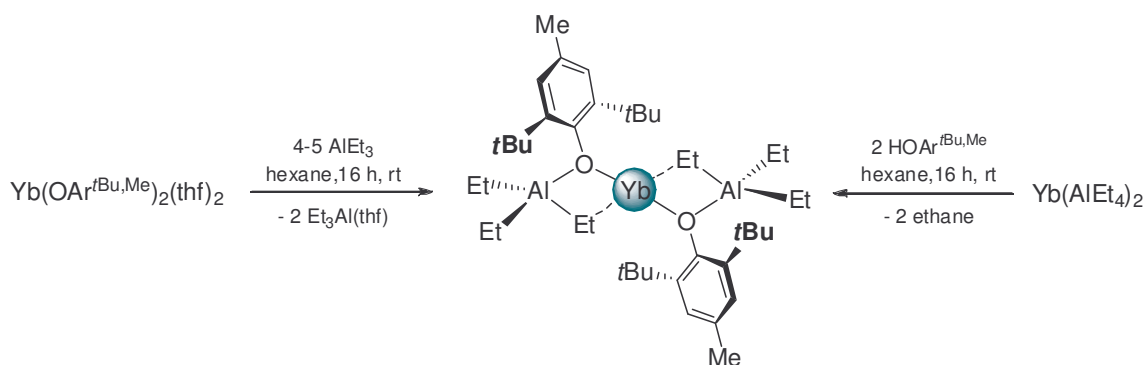


Figure 56: Solid-state structure of [(C₅Me₅)Yb(thf)₄][AlMe₄] (**141**).

excess H(C₅Me₅) yielding [(C₅Me₅)Yb(thf)₄][AlMe₄] (**141**) according to a methane elimination reaction.²³⁵ The solid-state structure revealed a solvent separated ion pair consisting of a [(C₅Me₅)Yb(thf)₄] cation and a non coordinating [AlMe₄] anion (Figure 56). A similar structural motif had previously been found in the solid-state structure of [η⁵-(fluorenyl)Yb(thf)₄][AlMe₄].²³⁶

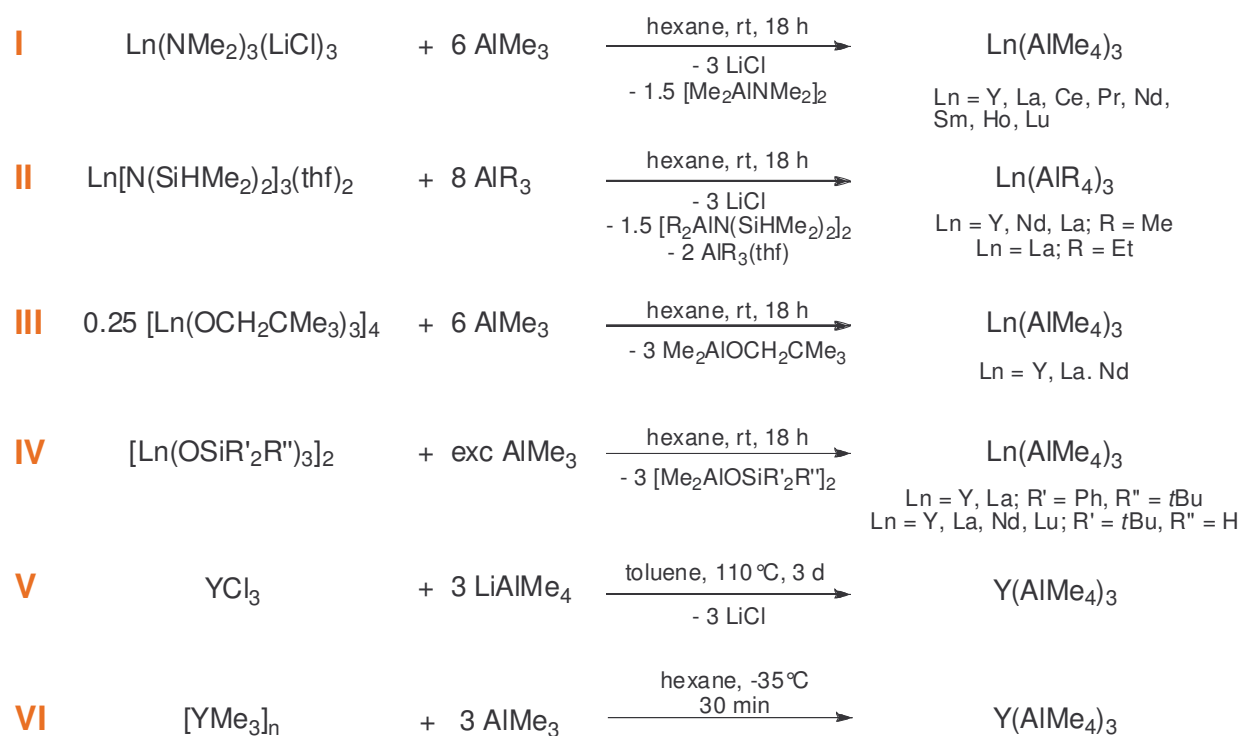
Alkane elimination reaction at the [AlR₄] ligands also occurs in the presence of sterically demanding aryloxides HOAr^{R,R'}. Accordingly, reaction mixtures of [Yb(AlEt₄)_n] and two equivalents of HOAr^{tBu,Me} (OAr^{tBu,Me} = OC₆H₂-4-Me-2,6-tBu) produce triethylaluminum adducts Yb(μ-OAr^{tBu,Me})₂[(μ-Et)AlEt₂]₂ (**142**) under concomitant evolution of ethane (Scheme 45).²³⁵ Interestingly, similar compounds have earlier been reported by ANWANDER as the result of a AlR₃ (R = Me, Et) adduct-formation at homoleptic Yb(OAr^{tBu,Me})₂(thf)₂ (Scheme 45).^{170,230}



Scheme 45: Synthesis of a Yb(II) bis(aryloxide)-bis(triethylaluminum) adduct **142**.

14.2 Synthesis, Structure, and Properties of Ln(III)(AIR₄)₃

When investigating the reactivity of homoleptic rare-earth metal alkylamides toward LEWIS acidic highly reactive organoaluminum reagents, EVANS ET AL. discovered the formation of heterobimetallic Ln(III)/Al alkyl species.²³⁷⁻²³⁹ The degree of alkylation in the generated heterobimetallic compounds is hereby strongly dependent on the amount of alkylaluminum reagent present in the reaction mixture and the stereoelectronic properties of the alkylamide ligands. While homoleptic AlMe₃ adducts Ln[(μ-NMe₂)(μ-Me)AlMe₂]₃ (**143**) were isolated from Ln(NMe₂)₃(LiCl)₃ in the presence of three equivalents AlMe₃,²³⁷ peralkylated tris(tetramethylaluminates) Ln(AlMe₄)₃ (**Y**) formed with excess of trimethylaluminum.²³⁸ Such AlMe₃-mediated complete [NR₂]₃→[AlMe₄]₃ transformations were found to be a viable route for the synthesis of several tetramethylaluminate containing organorare-earth metal complexes.^{240,241}



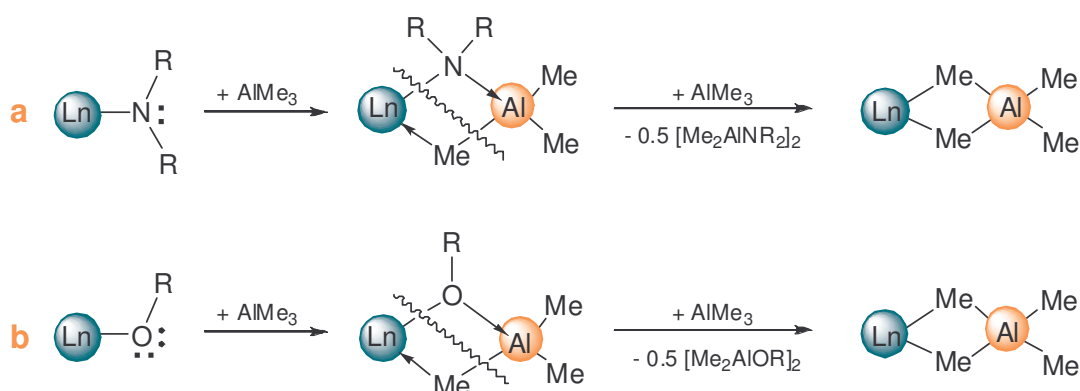
Scheme 46: Synthesis of homoleptic Ln(III)(AIR₄)₃ (**Y**).

As first reported in 1995, the general synthesis of homoleptic Ln(III) tris(tetramethylaluminates) **Y** is based on the alkylation of Ln(NMe₂)₃(LiCl)₃ with excess AlMe₃ (Scheme 46, I).²³⁸ Following this synthesis route Ln(AlMe₄)₃ of the entire group 3 metal and lanthanide series except scandium and promethium were obtained in good yields (**Paper II**). However, several crystallization steps are necessary to obtain

crystalline, trimethylaluminum-free Ln(AlMe₄)₃. The high volatility of the alkylated amide byproduct [Me₂AlNMe₂]₂ is one of the main advantages of this synthesis strategy, allowing for easy separation of the desired product.

Although rare-earth metal tetramethylaluminates are accessible by alkylation of a number of other Ln(III) precursors like silylamide complexes Ln[N(SiHMe₂)₂]₃(thf)₂,²⁴² tetrameric [Ln(OCH₂CMe₃)₃]₄,¹⁷⁰ aryloxide [Y(OAr^{iPr,H})₃]₂,²³⁰ and siloxides [Ln(OSiR'₂R'')₃]₂,²⁴³ separation of the peralkylated Ln(AlMe₄)₃ products from the alkylated byproducts has proved to be difficult (Scheme 46, II-IV). Due to the high solubility of tetramethylaluminate complexes Ln(AlEt₄)₃, separation from residual AlEt₃ and the byproduct [Et₂AlNR₂]₂ was not successful. Only reaction of La[N(SiHMe₂)₂]₃(thf)₂ with AlEt₃ produced separable single-crystals of La(AlEt₄)₃ (Y^{Et}_{La}) (Scheme 46, II).²²³ Salt metathesis as a one-step synthesis protocol for the preparation of Ln(AlMe₄)₃ could be applied for anhydrous YCl₃ and three equivalents of lithium tetramethylaluminate (Paper II). Suspensions in toluene yielded 7% of Y(AlMe₄)₃ after seven days (Scheme 46, V). Derivatives of the larger rare-earth metals could not be obtained by this method. Alternatively, Y(AlMe₄)₃ of very high purity can be obtained by AlMe₃-adduct formation to the polymeric yttrium-methyl compound [YMe₃]_n (V). Adding three equivalents AlMe₃ to a hexane suspension of [YMe₃]_n yielded crystalline Y(AlMe₄)₃ in almost quantitative yield (Scheme 46, VI).²⁰

Formation of tetramethylaluminate ligands by [amide] → [methyl] or [OR] → [methyl] exchange, respectively, likely proceeds via a two-step mechanistic scenario (Scheme 47).



Scheme 47: Two-step mechanistic scenario for the formation of tetramethylaluminate ligands by a) [amide] → [methyl] or b) [OR] → [methyl] exchange.

In a first step, the strong Lewis acid AlMe₃ coordinates to the basic amido-nitrogen/OR. Such adduct formation apparently results in a weakening of the originally strong Ln–N/Ln–O bond. Intermediate formation of a four-membered Ln–N–Al–Me ring^{227,237,239} (Ln–O–Al–Me)^{224,225,230,243,244} containing a bridging methyl group allows for partly saturation of the highly Lewis acidic rare-earth metal center. Addition of a second AlMe₃ molecule results in the complete [amide] → [methyl] ([OR] → [methyl]) exchange under formation of a tetramethylaluminate ligand and thermodynamically very stable [Me₂AlNR₂]₂ ([Me₂OR]₂).²⁴⁵⁻²⁴⁸

The [amide/OR] → [alkyl] transformation is a versatile synthesis procedure, reported for several heteroleptic Ln/Al heterobimetallic rare-earth organometallic complexes. A high yield synthesis of lanthanide tetramethylaluminates underlies steric restrictions, though,

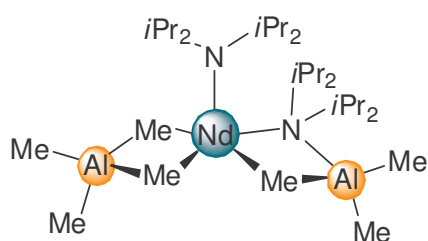


Figure 57: Structure of Nd(NiPr₂)[(μ-NiPr₂)(μ-Me)AlMe₂][(μ-Me)₂AlMe₂] (**144**).

and the choice of monoanionic lanthanide amide/OR precursors is often limited to small functionalities (NMe₂, NEt₂). The influence of the amido R group is impressively demonstrated in Nd(NiPr₂)[(μ-NiPr₂)(μ-Me)AlMe₂][(μ-Me)₂AlMe₂] (**144**) containing three different types of ligands. Stepwise addition of four equivalents AlMe₃ to Nd(NiPr₂)₃(thf) produced this mixed ligand compound, acting as a model for the two-step tetramethylaluminate formation. Contrary to

divalent Ln(II)[N(SiMe₃)₂]₂(thf)₂, steric constraints hamper the adduct formation/alkylation when using homoleptic Ln(III)[N(SiMe₃)₂]₃.^{242,249}

The solid-state structures of homoleptic Y,²³⁸ La, Pr, Nd,²³⁸ Sm, and Lu tetramethylaluminates have been determined, showing a rare-earth metal cation size dependent aluminate coordination (**Paper I**). Ln(AlMe₄)₃ of the small to middle-sized Ln(III) ions (Lu–Sm) crystallize in the centrosymmetric space group C2/c (Figure 59). The slightly larger praseodymium and neodymium derivatives (monoclinic space group P2₁/c) crystallize with two independent molecules in the unit cell. All solid-state structures show a sixfold coordination of carbon atoms around the Ln(III) metal centers resulting in a pseudo-octahedral coordination geometry (Figure 59). Each [AlMe₄] unit coordinates to the central Ln metal through two bridging methyl groups forming planar or almost planar [Ln(μ-Me)₂Al] metalacycles.

The bridging carbon atoms revealed a heavily distorted trigonal-bipyramidal coordination geometry. Due to steric unsaturation of the rare-earth metal center, two of the three H atoms in each bridging methyl group are directed toward the Ln atom.

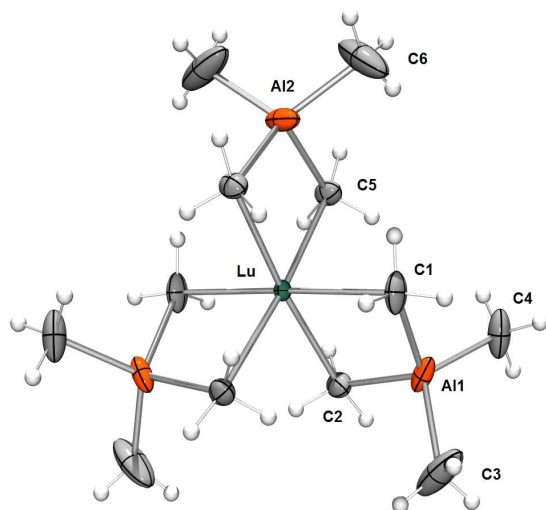


Figure 59: Solid-state structure of $\text{Lu}[(\mu\text{-Me})_2\text{AlMe}_2]_3$ (YMe_{Lu}).

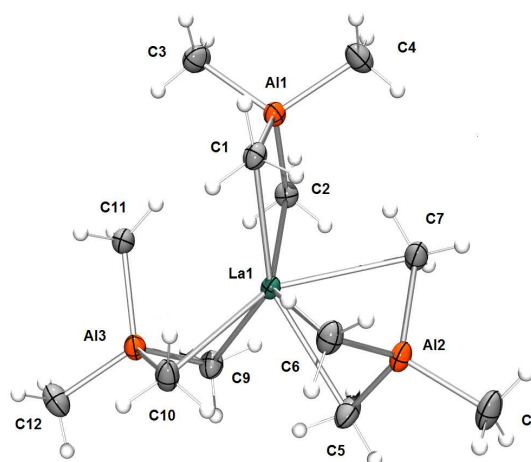


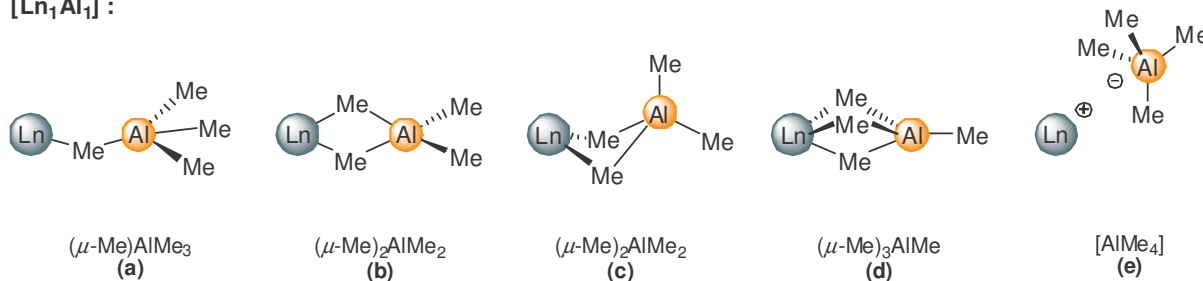
Figure 58: Solid state structure of $\text{La}[(\mu\text{-Me})_2\text{AlMe}_2]_2[(\mu\text{-Me})_3\text{AlMe}]$ (YMe_{La}).

X-Ray crystallographic structure analysis of $\text{La}(\text{AlMe}_4)_3$ revealed the presence of three different $[\text{AlMe}_4]$ coordination modes in a single molecule, namely $\text{La}[(\mu\text{-Me})_2\text{AlMe}_2][(\mu\text{-Me})_3\text{AlMe}]$ (Figure 58). While one ligand coordinates in the routinely observed η^2 fashion to form an almost planar $[\text{La}(\mu\text{-Me})_2\text{Al}]$ heterobimetallic unit, the second $[\text{AlMe}_4]$ ligand shows a bent η^2 coordination with an additional $\text{La}-(\mu\text{-Me})$ contact. The third tetramethylaluminate ligand coordinates through three bridging methyl groups to the lanthanum metal center, providing additional stereoelectronic saturation (**Paper I**).

In the course of X-ray crystallographic investigations of homoleptic and heteroleptic organorare-earth metal complexes containing tetramethylaluminate ligands, different types of $[\text{AlMe}_4]$ coordination modes were observed (Figure 60). Among these, terminal (**b**) and bridging $\eta^1:\eta^1$ coordinated ligands (**f**) seem to be favored as evidenced for homoleptic $\text{Ln}(\text{AlMe}_4)_3$ (**Paper I**),²³⁸ heteroleptic non-metallocene mono- and bis(aluminates)^{224,230} as well as lanthanidocene complexes.²⁵⁰⁻²⁵² However, in the presence of sterically highly unsaturated rare-earth metal centers additional bonding modes were observed. Bent $[\text{Ln}(\mu\text{-Me})_2\text{Al}]$ moieties (**c**)^{241,253} as well as terminal (**d**) and bridging $(\mu\text{-Me})\text{AlMe}(\mu\text{-Me})_2$ -coordinated aluminate ligands (**g**) appeared in $\text{La}(\text{AlMe}_4)_3$ (**Paper I**) and alkylated polynuclear chloride clusters.²⁵⁴ Non-coordinating $[\text{AlMe}_4]^-$ units

(e) were found in fluorenyl lanthanide(II) complexes and in [(C₅Me₅)Yb(thf)₄][AlMe₄] (**141**) (chapter 14.1).^{235,236} A rare example of a terminal η^1 coordinated [AlMe₄] ligand (**a**) was reported for a diamido-pyridine complex [NNN]La[(μ -Me)AlMe₃](thf) (**Paper III**).

[Ln₁Al₁] :



[Ln₂Al₁] :

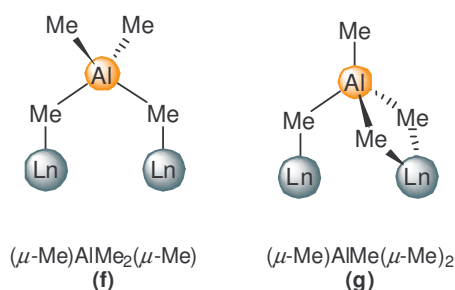


Figure 60: Structurally characterized coordination modes of the [AlMe₄] ligand in organorare-earth metal chemistry.

Homoleptic tris(tetramethylaluminates) Ln(AlMe₄)₃ are soluble in aliphatic and aromatic solvents. Due to immediate donor-induced aluminate cleavage ethereal solvents have to be avoided.

Despite of their different solid-state structures, the ¹H NMR spectra of Ln(AlMe₄)₃ show only one signal for the [AlMe₄] moieties at ambient temperature (**Paper I**).²³⁸ This is indicative of a very fast exchange of bridging and terminal methyl groups (Figure 61). However, different types of methyl groups could be resolved at lower temperature for complexes of the smaller Ln(III) metals. In consistence with increased steric unsaturation and therefore more rapid alkyl exchange, decoalescence temperatures decreased with increasing size of the rare-earth metal center (Lu = 278 K, Y = 229 K, Sm = 216 K) (**Paper I**).

The methyl group exchange mechanism was studied by dynamic NMR spectroscopy and line-shape analysis, revealing activation parameters indicative of an associative methyl group exchange for Ln(AlMe₄)₃ (Ln = Sm, Y, Lu) (**Paper I**).

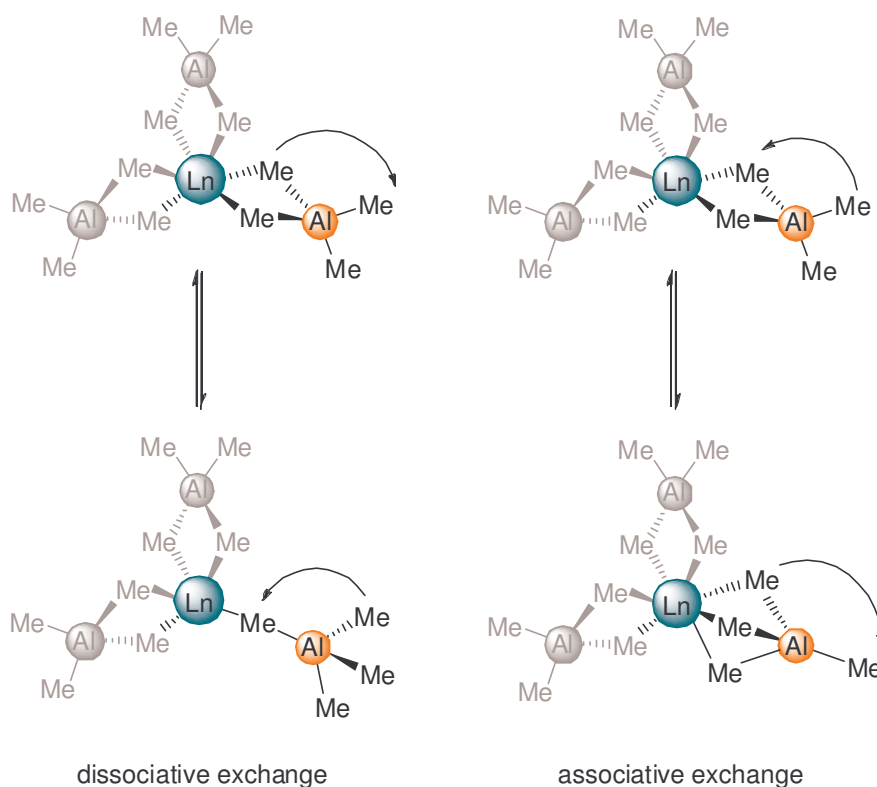
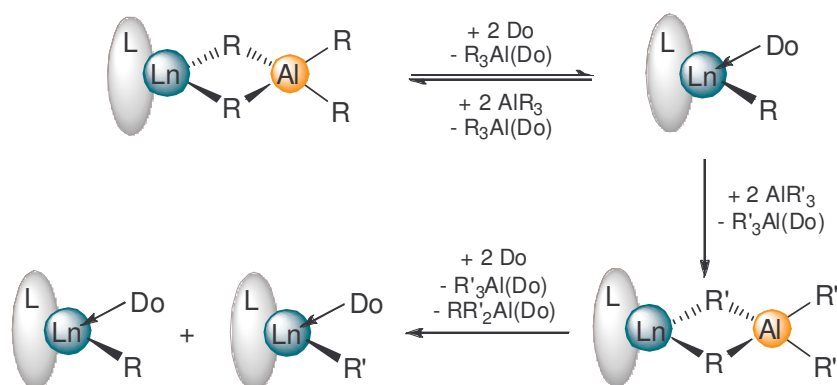


Figure 61: Dissociative *versus* associative methyl exchange in homoleptic Ln(AlMe₄)₃ complexes.

14.3 Ln(III)(AlMe₄)₃ as Synthesis Precursors

An important reactivity concept of heterobimetallic Ln/Al alkyl complexes, the donor(Do)-induced aluminate cleavage was reported as early as 1979 by LAPPERT (Scheme 48).²³²

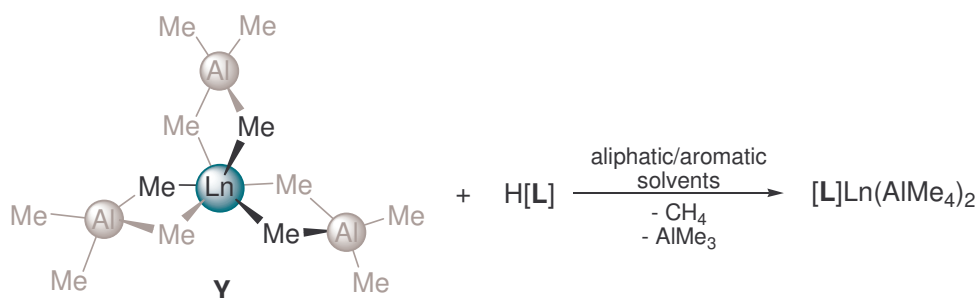


Scheme 48: Donor(Do)-induced aluminate cleavage and the reversibility phenomena in aluminate chemistry.

Originally applied for lanthanidocene complexes (C₅H₅)₂Ln(AlMe₄) the donor(pyridine)-cleavage gave access to dimeric (μ-Me)₂-bridged complexes [(C₅H₅)₂Ln(μ-Me)]₂.²³² LAPPERT'S concept of donor-induced aluminate cleavage recently allowed for the generation of solvent free [LnMe₃]_n (**V**) from homoleptic Ln(AlMe₄)₃ (Ln = Y, Lu)²⁰ (chapter 12) as well as half-lanthanidocene^{218,253} and lanthanidocene methyl²⁵⁵ derivatives carrying the bulky (C₅Me₅) ligand. The previously mentioned formation of [YMe₂(thf)₅][BPh₄] (**137**) and ion triple [YMe(thf)₆][BPh₄]₂ (**136**) (chapter 12) can also be assigned to a donor(thf)-induced cleavage of Y(AlMe₄)₃ followed by protonolysis reaction with [NEt₃H][BPh₄].^{96,221}

The reversibility of the tetraalkylaluminate cleavage reaction is another important detail of the early work by LAPPERT.²³² It was later exploited for the synthesis of mixed-alkylated complexes, e.g mixed methyl/ethyl aluminate complexes.²⁴⁰

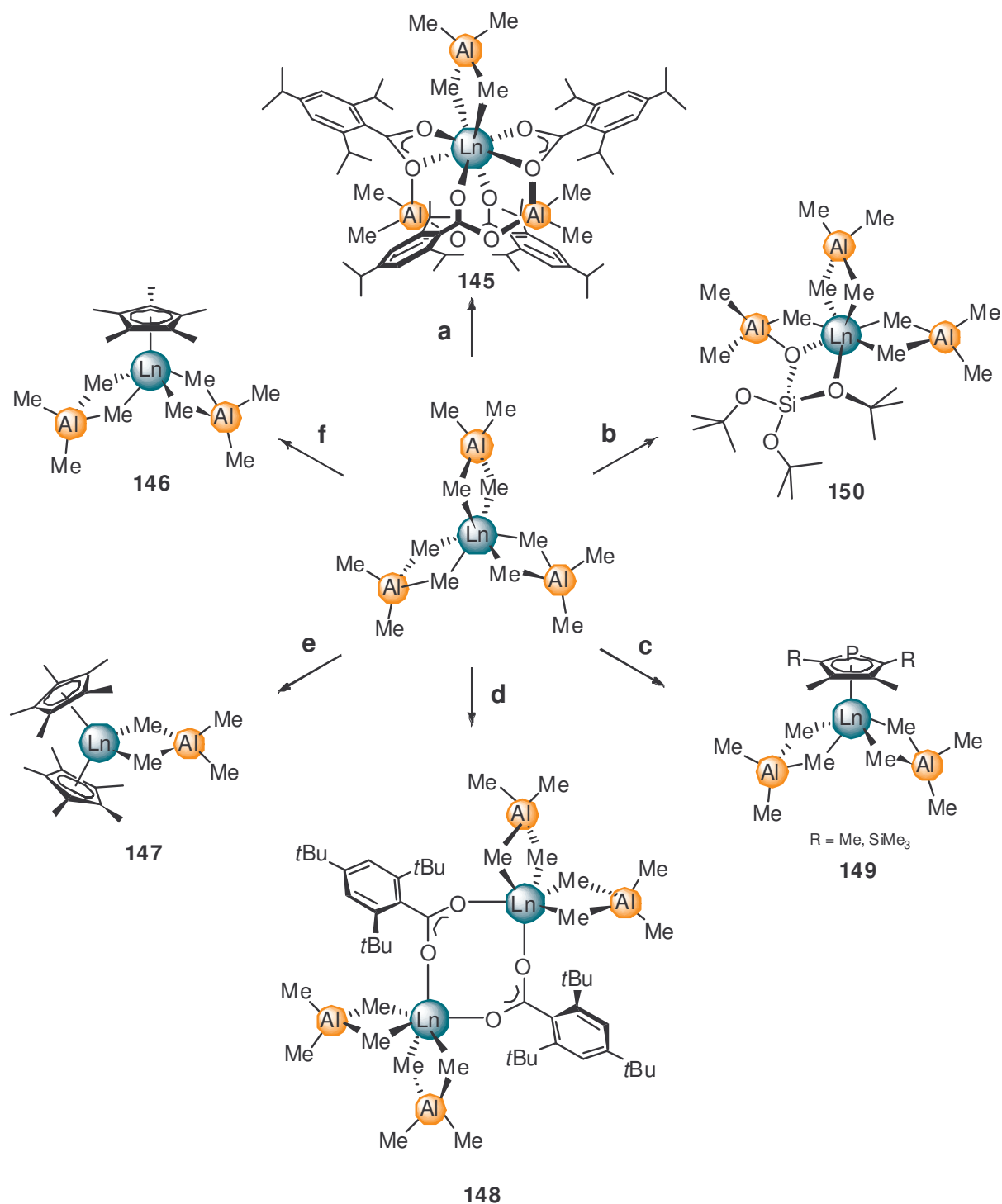
Homoleptic tris(tetramethylaluminate) complexes Ln(AlMe₄)₃ further are convenient synthesis precursors for the generation of various heteroleptic heterobimetallic Ln/Al complexes. The above-mentioned donor-induced cleavage reactions imply another important concept of the [AlMe₄] moiety. Thus, tetramethylaluminates can also be described as adducts LnMe₃(AlMe₃)₃ ("alkyls in disguise"). In accordance with this bonding feature several alkane elimination reactions have been reported, leading to heteroleptic Ln/Al tetramethylaluminate rare-earth metal complexes (Scheme 49).



Scheme 49: General reaction of Ln(AlMe₄)₃ (= LnMe₃(AlMe₃)₃) with protic substrates.

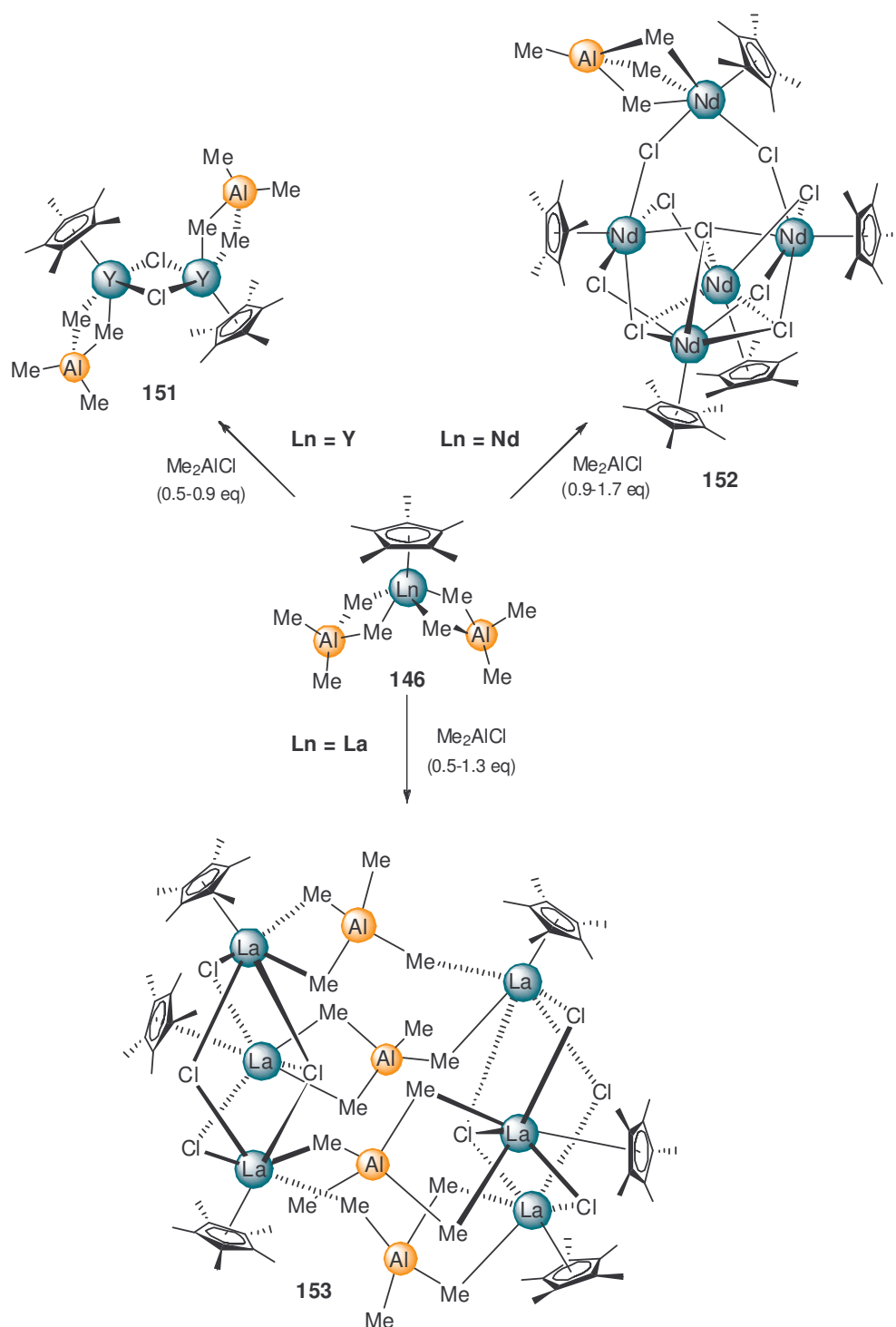
Homoleptic Ln(AlMe₄)₃ readily undergo protonolysis reactions with BRØNSTED acidic O-donors, including phenols, alcohols, silanols, and carboxylic acids to generate heteroleptic Ln/Al bimetallic complexes (Scheme 50, **a**, **b** and **d**).^{170,223,224} These complexes were extensively used as model systems to study structure-reactivity relationships in commonly used ZIEGLER-type catalysts.

Methane elimination reaction with H(C₅Me₅) involving one or two tetramethylaluminate ligands produced half-lanthanidocene bis(aluminate) or lanthanidocene mono(aluminate) complexes (**146** and **147**), respectively (Scheme 50, **e** and **f**).^{253,256}



Scheme 50: Alkane elimination and salt metathesis in $\text{Ln}(\text{AlMe}_4)_3$ chemistry: **(a)** + $\text{HO}_2\text{CC}_6\text{H}_2-2,4,6-i\text{Pr}$, - CH_4 , - alkylated byproducts; **(b)** + $\text{HOSi}(\text{OtBu})_3$, - CH_4 , - AlMe_3 ; **(c)** + $\text{K}[\text{PC}_4\text{Me}_4]$ or $\text{K}[\text{PC}_4\text{Me}_2(\text{SiMe}_3)_2]$, - KAlMe_4 ; **(d)** + $\text{HO}_2\text{CC}_6\text{H}_2-2,4,6-t\text{Bu}$, - CH_4 , - AlMe_3 ; **(e)** + $2 \text{H}(\text{C}_5\text{Me}_5)$, - 2CH_4 , - 2AlMe_3 ; **(f)** + $\text{H}(\text{C}_5\text{Me}_5)$, - CH_4 , - AlMe_3 .

Very recently, the reaction of $\text{Ln}(\text{AlMe}_4)_3$ with potassium salts $\text{K}[\text{PC}_4\text{Me}_4]$ and $\text{K}[\text{PC}_4\text{Me}_2(\text{SiMe}_3)_2]$ was found to produce mono($\text{PC}_4\text{Me}_2\text{R}_2$) bis(tetramethylaluminate) complexes **149** under concomitant formation of KAlMe_4 (Scheme 50, c).²⁵⁷ This remarkable reaction adds another bonding concept describing the $[\text{AlMe}_4]$ moiety as purely anionic $[\text{AlMe}_4]$ ligand which undergoes ligand exchange via salt metathesis reactions.

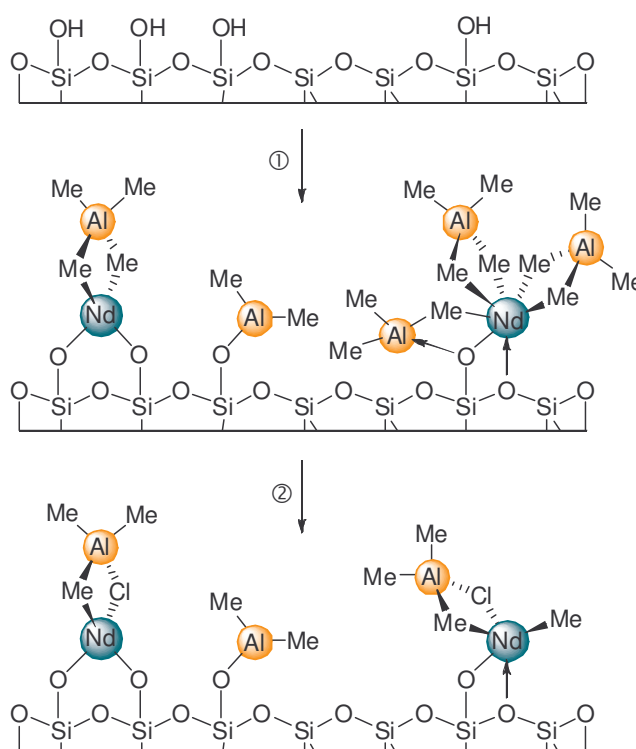


Scheme 51: [Alkyl] \rightarrow [chloride] interchange reactions of $(\text{C}_5\text{Me}_5)\text{Ln}(\text{AlMe}_4)_2$ (**146**).

As presented in chapter 13 homoleptic $\text{Ln}(\text{AlMe}_4)_3$ react with R_2AlCl under formation of polymeric mixed methyl/chloride rare-earth metal compounds (**W**).^{223,226} Such compounds are discussed as possible polymerization-initiating species in the stereospecific polymerization of dienes. A mechanistic proposal for the observed [alkyl] \rightarrow [chloride] exchange was presented earlier (see chapter 13).

Direct structural evidence of an [alkyl] \rightarrow [chloride] interchange reaction was obtained from half-lanthanidocene model compounds.²⁵⁴ Alkylated $[\text{Y}_2\text{Al}_2]$ (**151**), $[\text{Nd}_5\text{Al}]$ (**152**) and $[\text{La}_6\text{Al}_4]$ (**153**) cluster compounds were isolated from binary $(\text{C}_5\text{Me}_5)\text{Ln}(\text{AlMe}_4)_2/\text{Me}_2\text{AlCl}$ mixtures (Scheme 51). Apparently, subtle changes in the rare-earth metal size considerably affect the [aluminate] \rightarrow [chloride] exchange reaction and the coordination behavior of the $[\text{AlMe}_4]$ moiety.

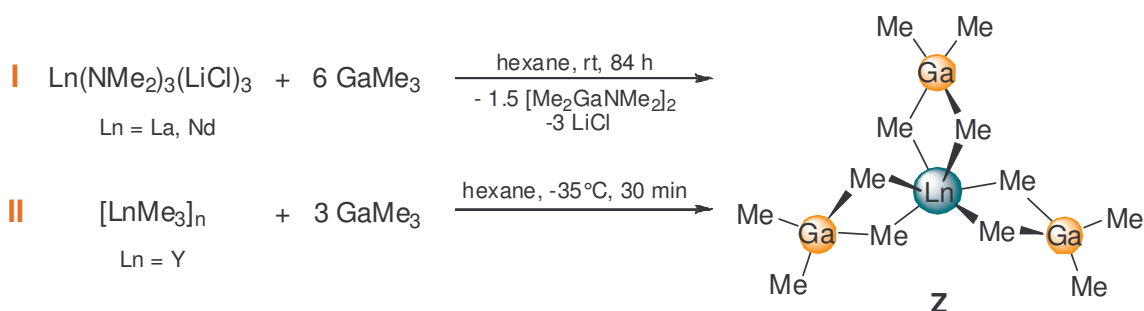
In a preliminary study, cubic MCM-48 featuring a three-dimensional mesopore system was applied to heterogenize binary $[\text{Nd}(\text{AlMe}_4)_3/\text{Et}_2\text{AlCl}]$ precatalysts systems.²²³ The organometallic-inorganic hybrid material was characterized by means of FTIR spectroscopy, elemental analysis, and nitrogen physisorption. The neodymium-grafted materials performed as efficient single-component catalysts in the slurry polymerization of isoprene. Polymer analysis revealed high-*cis*-1,4-stereospecificities (>99% *cis*) and narrow molecular weight distributions ($M_n/M_w = 1.33 - 1.88$).



Scheme 52: Proposed surface species of hybrid materials after immobilization of $\text{Nd}(\text{AlMe}_4)_3$ and Et_2AlCl on dehydrated MCM-48.

15 Homoleptic Ln(III) Tris(tetramethylgallates) Ln(GaMe₄)₃

In 1994 EVANS ET AL. reported the synthesis and molecular structure of neodymium(III) tris(tetramethylgallate) (**Z**) as the first structurally characterized molecular lanthanide-gallium heterobimetallic complex.²³⁷ The reaction of six equivalents or an excess of GaMe₃ with a suspension of Nd(NMe₂)₃(LiCl)₃ in hexane afforded the solvent-free heterobimetallic alkyl compound Nd(GaMe₄)₃. (Scheme 53, I).



Scheme 53: Synthesis of Ln(GaMe₄)₃ (**Z**).

The formation of tetramethylgallate ligands is likely to occur through intermediate coordination of LEWIS acidic GaMe₃ to the basic amido-nitrogens of Ln(NMe₂)₃(LiCl)₃. An additional equivalent of GaMe₃ triggers the complete [amide] → [methyl] exchange leading to [GaMe₄] ligands (see chapter 14.2). Successful isolation and characterization of the GaMe₃ adduct Nd(NMe₂)₃(GaMe₃)₃ (**154**) (Figure 62) and partially exchanged complex La(GaMe₄)[(NMe₂)(GaMe₃)₂]₂ (**155**) (Figure 62) support the proposed stepwise mechanism.²³⁷

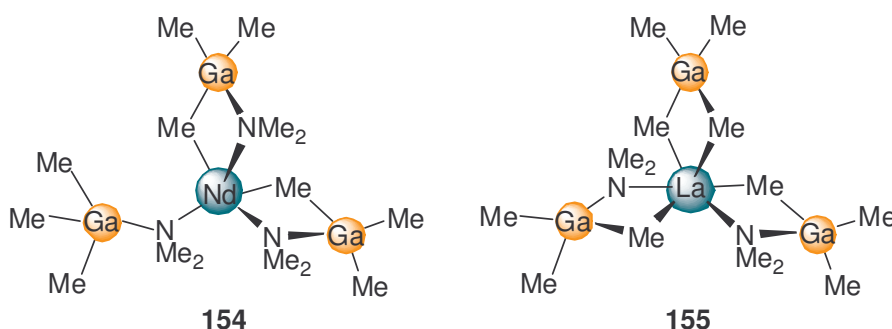


Figure 62: Isolated reaction intermediates occurring during the formation of Ln(GaMe₄)₃.

Ligand transformation is further driven by the formation of very stable [Me₂GaNMe₂]₂ which can be separated from Ln(GaMe₄)₃ by fractional crystallization. With the discovery

of [LnMe₃]_n (**V**) by the group of ANWANDER an alternative and economic synthesis route toward homoleptic Ln(GaMe₄)₃ evolved.^{20,222} The polymeric yttrium-methyl compound [YMe₃]_n could be re-dissolved by GaMe₃ yielding very pure Y(GaMe₄)₃ in almost quantitative yield (Scheme 53, II). The stoichiometric use of expensive trimethylgallium and the avoidance of undesired gallium-containing byproducts are clearly favorable attributes. However, the applicability of this synthesis approach is so far limited to yttrium as a rare-earth metal center.

Tris(tetramethylgallates) of the rare-earth metals are soluble in hydrocarbons and aromatic solvents. Donor-solvents lead to immediate donor-cleavage of the [GaMe₄]

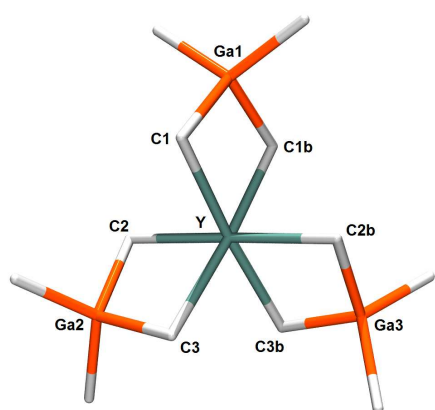
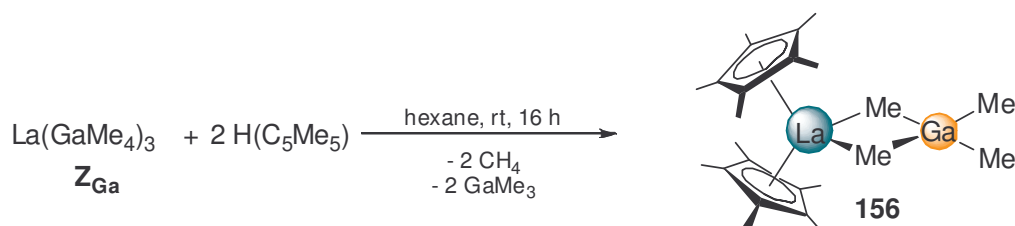


Figure 63: Solid-state structure of Y(GaMe₄)₃ (**Z**).

ligand (see chapter 14.3). Single crystals of the neodymium and yttrium derivatives have been obtained from hexane solutions and revealed octahedrally coordinated rare-earth metal cations and a tetrahedral geometry about the gallium metal centers (Figure 63).^{222,237} All three Ln–C–Ga–C rings are almost planar and two of the hydrogen atoms at the five-coordinate bridging carbon atoms are tilted toward the rare-earth metal center (see chapter 14.2). Compared with structurally related Ln(AlMe₄)₃ the Ln⋯Ga distances are considerably shorter than the respective Ln⋯Al distances which is further reflected in less acute C–Ln–C angles.

Little is known about the reactivity of Ln(GaMe₄)₃ but similar reactivity patterns as provided by compounds Ln(AlMe₄)₃ are anticipated based on their structural analogy. The ability of Ln(GaMe₄)₃ to react according to an alkane elimination reaction could recently be proven by the formation of lanthanidocene (C₅Me₅)₂La(GaMe₄) (**156**) when stirring a mixture of La(GaMe₄)₃ and H(C₅Me₅) (Scheme 54).²⁵⁸



Scheme 54: Derivatization of La(GaMe₄)₃.

B

Summary

Since the early 1980s organometallic chemistry of the rare-earth metals has witnessed a spectacular growth. A central aspect of this development is the quest for defined molecular rare-earth metal based catalysts and, strongly related, the development of molecular models enabling insight into system-inherent structure-reactivity relationships. Rare-earth metal alkyl compounds occupy a decisive position, particularly, within ZIEGLER-type polymerization catalysis. Accordingly, lanthanidocene alkyl complexes were successfully employed for clarifying key steps such as initiation, propagation, and termination.²⁵⁹⁻²⁶² While early research in rare-earth metal related polymerization catalysis was dominated by rigid cyclopentadienyl ligands, alternative non-cyclopentadienyl (post-lanthanidocene) catalyst families mainly based on functionalized chelating nitrogen and oxygen donor ligands have evolved during the past 15 years. Despite major advances in ancillary ligand design, significant catalytic activity still remains dependent on the use of suitable system-activating co-catalysts, namely aluminum alkyl and borane/borate reagents. Insight into intricate pre-catalyst/co-catalyst interactions is fundamental to catalyst optimization and development. In particular, heterobimetallic Ln/Al rare-earth metal alkyl compounds were proposed to model interactions of group 4 and rare-earth metals with aluminum alkyl activators.

This thesis is devoted to the study of heteroleptic rare-earth metal alkyl compounds mainly containing heterobimetallic Ln/Al alkyl moieties. Based on a detailed study concerning the intrinsic properties of homoleptic $\text{Ln}(\text{AlMe}_4)_3$, the potential of such “alkyls in disguise” as rare-earth metal precursors for post-lanthanidocene chemistry is investigated. The characterization of rare-earth metal products, reaction intermediates, side-products, and decomposition products illustrates the complexity of post-lanthanidocene/aluminum alkyl interactions. Systematic investigation of the pre-catalysts/co-catalyst interplay and extensive polymerization experiments give insight into activation mechanisms and provide a “single-component” catalyst for the polymerization of 1,3-dienes.

1 Homoleptic Rare-Earth Metal(III) Tetramethylaluminates

Homoleptic tris(tetramethylaluminate) complexes $\text{Ln}(\text{AlMe}_4)_3$, first reported in 1995,²³⁸ found entry into organorare-earth metal synthesis only recently. Their straightforward high-yield synthesis for the entire size range of rare-earth metal cations, except scandium, is presented in **Paper I**. Various synthesis routes toward $\text{Ln}(\text{AlMe}_4)_3$ were attempted confirming the [amide] \rightarrow [alkyl] transformation to be the optimal synthesis approach. A series of X-ray structure analyses revealed a rare-earth metal cation size-

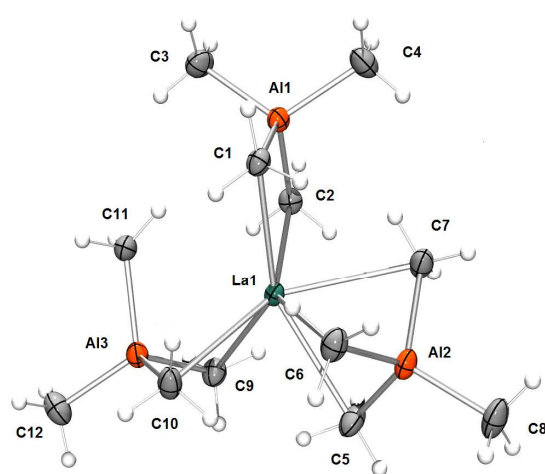


Figure S1: Solid-state structure of $\text{La}[(\mu\text{-Me})_2\text{AlMe}_2]_2[(\mu\text{-Me})_3\text{AlMe}]$.

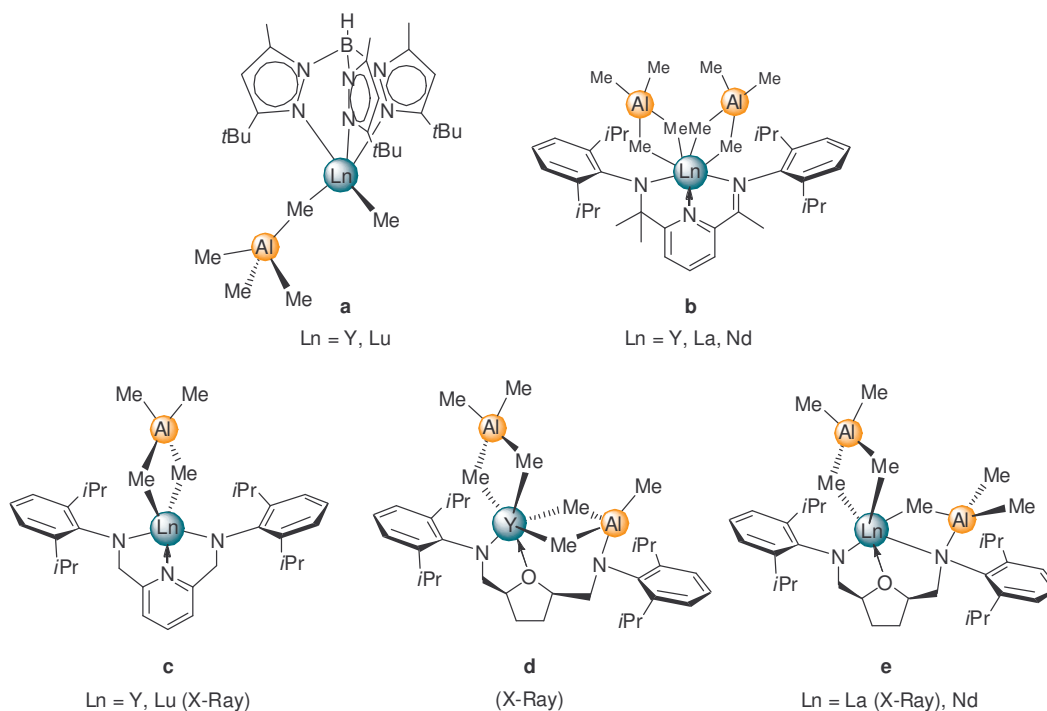
dependent coordination of the $[\text{AlMe}_4]$ moieties. $[\text{AlMe}_4]$ ligands willingly adapt to stereoelectronic requirements by undergoing $\eta^2 \rightarrow \eta^3$ (steric unsaturation, **Paper I**) and $\eta^2 \rightarrow \eta^1$ coordination shifts (steric oversaturation, **Paper III**). Figure S1 shows the solid-state structure of $\text{La}[(\mu\text{-Me})_2\text{AlMe}_2]_2[(\mu\text{-Me})_3\text{AlMe}]$ as the representative of the largest rare-earth metal center. Stereoelectronic saturation is realized by $[\text{AlMe}_4]$ ligands in three different η^2/η^3

coordination modes (vs. $\text{Ln}[(\mu\text{-Me})_2\text{AlMe}_2]_3$ for Nd-Lu). Such structurally evidenced $\eta^2 \rightarrow \eta^3$ coordination mode shifts further characterize the dynamic behavior of tetramethylaluminate ligands in solution. Dynamic ^1H and ^{13}C NMR spectroscopy combined with line-shape analysis revealed a very fast exchange of terminal and bridging methyl groups in $\text{Ln}(\text{AlMe}_4)_3$. Regardless of the rare-earth metal size, methyl group exchange proceeds with activation parameters indicating an associative mechanism with higher ordered η^3 transient states. Exchange rates k , however, decrease significantly with decreasing size of the Ln^{3+} cation. Despite an anticipated highly ionic character of $\text{Ln}-[\text{AlMe}_4]$ bonds, one dimensional ^{89}Y NMR and two-dimensional ^1H - ^{89}Y HMQC NMR spectroscopy clearly revealed a scalar ^1H - ^{89}Y coupling providing evidence for a significant degree of covalency of the Ln-aluminate bonding.

2 Ln(AIME₄)₃ as Synthesis Precursors for Post-Lanthanidocene Chemistry

A primary objective of this work was to investigate the suitability of homoleptic Ln(AIME₄)₃ as rare-earth metal alkyl precursors for non-cyclopentadienyl (post-lanthanidocene) compounds. In the presence of BRØNSTED acidic substrates, Ln(AIME₄)₃ can react according to an alkane elimination reaction yielding heteroleptic rare-earth metal complexes containing [AIME₄] functionalities. Such functionalities are of considerable interest, as cationic bimetallic species [LM(μ-R)₂AIR₂]⁺ are discussed as catalyst resting states for MAO-activated group 4 polymerization initiators.^{263,264} Moreover, such species are important intermediates in chain transfer and catalyst deactivation processes.²⁶⁵⁻²⁶⁸ Given the intrinsic interrelation between group 4 and group 3/lanthanide metal polymerization chemistry, rare-earth metal complexes proved to be ideal model systems for ZIEGLER catalysts.

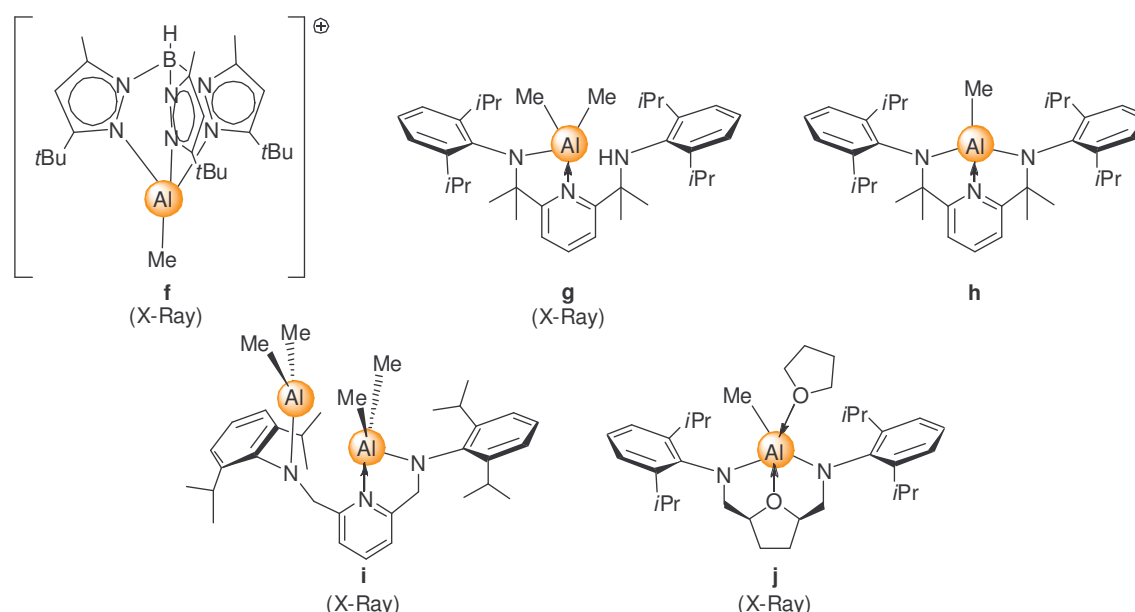
Accordingly, the reactivity of Ln(AIME₄)₃ toward several chelating nitrogen donor ligands has been investigated, namely monoanionic tris(pyrazolylborate) (**Paper V**), monoanionic imino-amido-pyridine (**Paper III**), dianionic diamido-pyridine (**Paper IV**), and dianionic diamido-tetrahydrofuran ligands (**Paper II**).



Scheme S1: Post-lanthanidocene complexes derived from Ln(AIME₄)₃ (adapted from **Papers II-IV**).

Reaction of the particular protonated ligand precursor with $\text{Ln}(\text{AlMe}_4)_3$ in all cases led to the formation of rare-earth metal complexes containing one or two $[\text{AlMe}_4]$ moieties, respectively (Scheme S1).

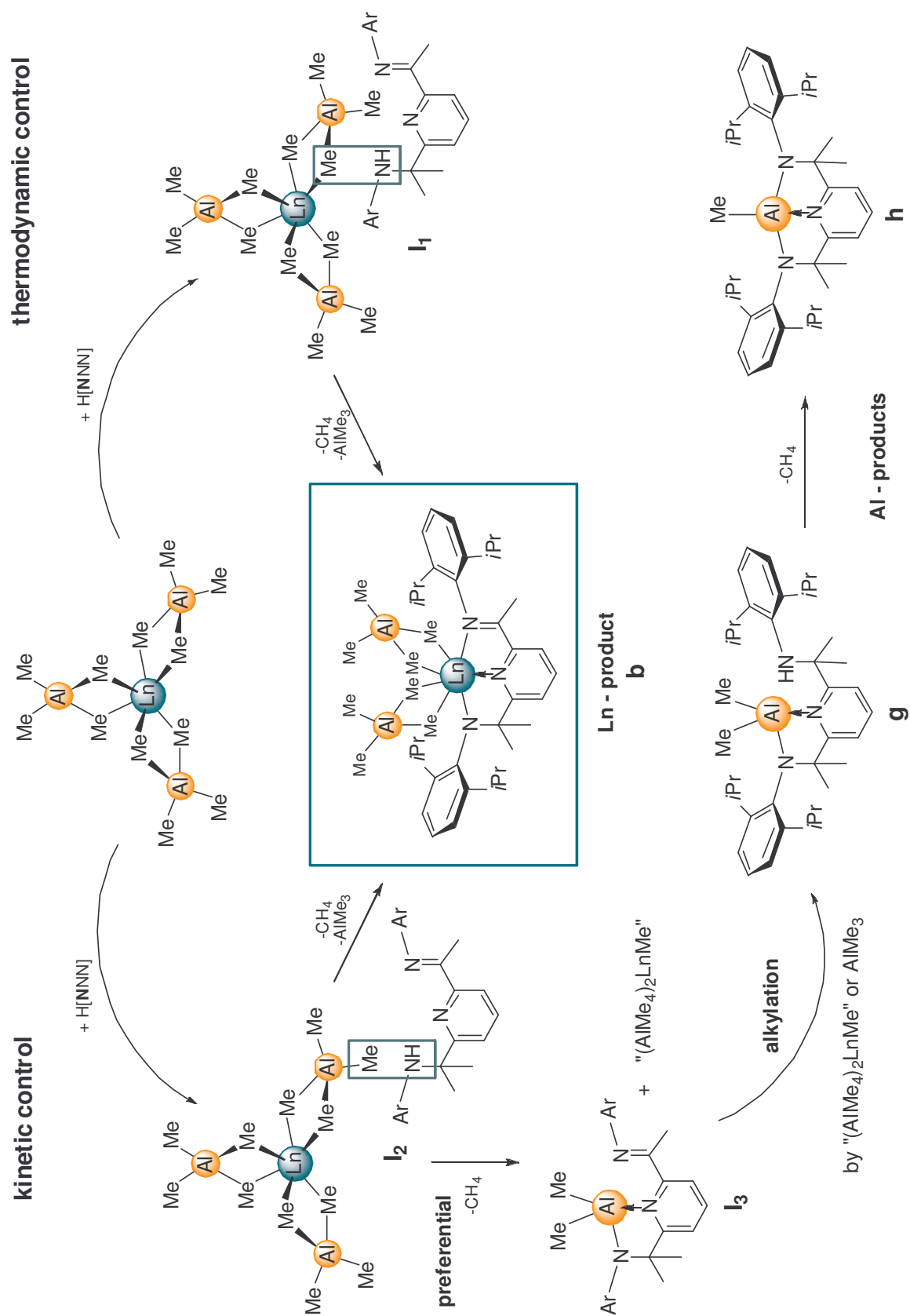
The overall yields of rare-earth metal containing products **a-e**, however, were significantly dependent on the rare-earth metal size and did not exceed 80% (calculated on Ln). Competitive formation of aluminum complexes appeared to be intrinsic to the interaction of nitrogen donor ancillary ligands and $\text{Ln}(\text{AlMe}_4)_3$. The respective aluminum compounds have been separated and fully characterized (Scheme S2).



Scheme S2: Aluminum complexes that competitively formed in the reaction of N-donor ligands and $\text{Ln}(\text{AlMe}_4)_3$. **f** shows only the cationic part of the obtained ion pair, (adapted from **Papers III-IV**).

Closer investigation of the Ln^{3+} size dependent formation of aluminum compounds **f-j** resulted in a universal mechanistic proposal explaining the product distributions as result of kinetically controlled reaction sequences. As a representative, Scheme S3 shows the proposed mechanism for the formation of **b/g/h**. The key feature is the kinetically controlled initial attack of the ancillary ligand's amine functionality at a bridging or terminal methyl group of one tetramethylaluminate moiety. In the presence of easily accessible bridging methyl groups, particularly for the larger rare-earth metal centers

(La - Nd), methane elimination reaction between a bridging methyl group and the amine functionality (Scheme S3, **I₁**) results in the formation of thermodynamically stable Ln-N(ancillary ligand) bonds (\rightarrow **b**).



Scheme S3: Proposed mechanistic scenario of kinetically and thermodynamically controlled ligand attack occurring in reactions between the imino-amido-pyridine ligand precursor and $\text{Ln}(\text{AlMe}_4)_3$ ($\text{H}[\text{NNN}]$ = imino-amido-pyridine; according to **Paper III**).

Due to enhanced steric crowding the thermodynamically less favored attack at a terminal methyl group appears to be pronounced for $\text{Ln}(\text{AlMe}_4)_3$ of the small rare-earth metal centers (Lu - Y) (Scheme S3, **l**₂). Consequent bond formation to the adjacent aluminum atom proceeds under loss of methane and leads to preferential formation of the respective aluminum complexes (**l**₃ → **g** → **h**). A significantly increased yield of aluminum side-products with decreasing metal cation size ($\text{La} < \text{Nd} < \text{Y} \ll \text{Lu}$) is inherent to all investigated systems substantiating the proposed mechanistic scenario. Structural evidence could further be obtained by X-ray crystallographic investigation of complexes **d** and **e** (Scheme S1) revealing the kinetic (Y, **d**) and thermodynamic product (La, **e**), respectively.

3 Reactivity of Post-Lanthanidocene Tetramethylaluminate Complexes

Hydrogen abstraction from methyl groups via formation of methylene and methine functionalities is structurally evidenced by a few rare examples in group 4 and rare-earth metal chemistry.^{218,269-274} Apparently, the presence of trimethylaluminum is of special importance. Such C–H activation reactions are intensely discussed as deactivation pathways in ZIEGLER-type polymerization catalysis.

Post-lanthanidocene related C–H activation has been studied for diamido-pyridine complexes **c** (Paper IV). Thermal decomposition via σ -bond metathetical loss of

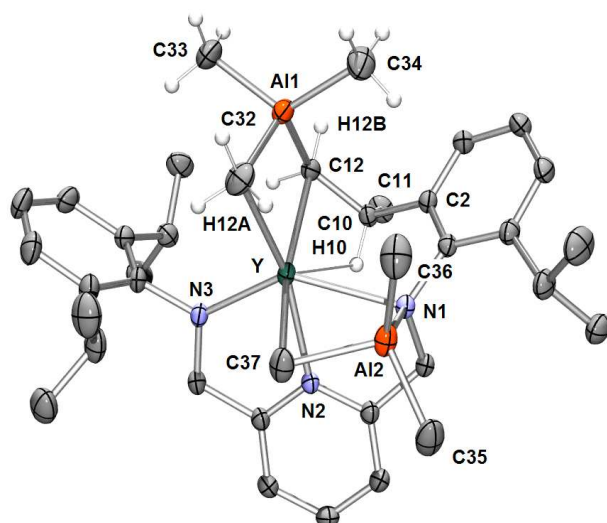


Figure S2: Solid-state structure of the cyclometalation product **k** (adapted from Paper IV).

methane occurred for the respective yttrium compound (**c**_Y) only in the presence of trimethylaluminum. The solid-state structure of the cyclometalation product **k** (Figure S2) revealed ligand metalation via a four-membered transition state involving an *i*Pr-methyl group and one bridging methyl group of the $\text{Y}[(\mu\text{-Me})_2\text{AlMe}_2]$ unit in **c**_Y. The initial formation of a heterobridging $[\text{Y}(\mu\text{-NR}_2)(\mu\text{-Me})\text{AlMe}_2]$ unit was found to be vital to facilitate the metalation reaction pathway. The latter can be rationalized on the basis

of kinetic (due to steric constraint) or thermodynamic control. Ligand degradation was not observed for complexes **c** containing the smaller Sc and Lu, and the larger La metal center. Clearly, such cation size dependent reactivity emphasizes the impact of the rare-earth metal center on the complex stability.

The path breaking investigation by WATSON ET AL., substantiating the capability of Ln–methyl functionalities to engage in the activation of C–H bonds, is meanwhile well established.^{260,261} Donor-induced cleavage of tetramethylaluminate complexes offers a

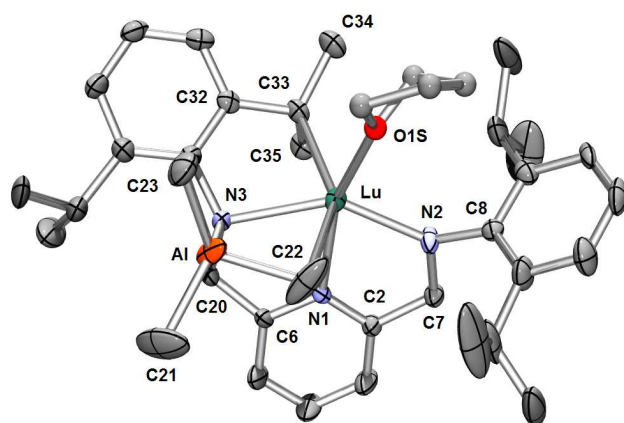


Figure S3: Solid-state structure of donor-cleavage product **I** (adapted from **Paper IV**).

convenient synthesis approach toward highly reactive [Ln–Me] moieties. Accordingly, donor-cleavage of the tetramethylaluminate ligand in compounds **c** resulted in the intermediate formation of [Ln–Me] moieties. Due to extraordinary reactivity complexes containing [Ln–Me] units could not be isolated but extensive ligand degradation (Sc, Y, La) or C–H abstraction at a methine group of the ancillary ligand (Lu) was observed (Figure S3). C–H abstraction

at a tertiary carbon atom as found in lutetium complex **I** is statistically and kinetically disfavored and reflects the high reactivity of small alkyl groups.

Donor-induced cleavage of imino-amido-pyridine complex **b**_{La} revealed the product of an “incomplete” donor cleavage (**Paper III**, Figure S4). Contrary to an anticipated organoaluminum-free methyl derivative, lanthanum complex **m** features an intact tetramethylaluminate in a novel η^1 coordination mode, remarkably, in the presence of the cleaving agent thf. Formation of **m** is assumed to originate from fast sequential processes involving initial donor-induced

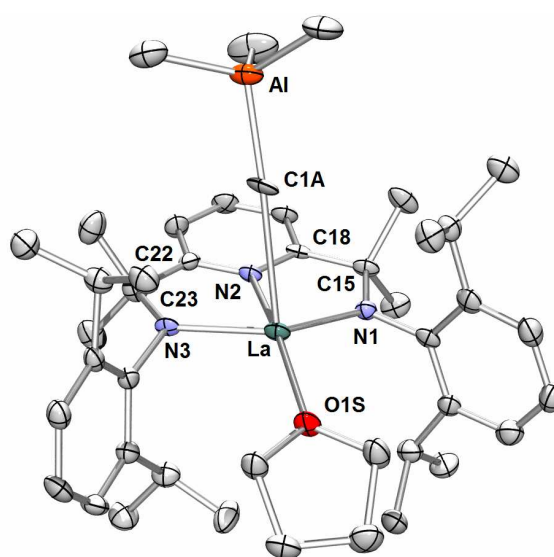


Figure S4: Solid-state structure of donor-cleavage product **m** (adapted from **Paper III**).

cleavage of one tetramethylaluminate ligand in complex **b_{La}** to produce a reactive methyl group. The transient [Ln–Me] species undergoes methyl migration from the metal center to the imino carbon atom implying additional anionization of the ligand and concomitant quaternization of the former imino carbon atom yielding lanthanum complex **m**.

Despite the enhanced reactivity, [Ln–Me] species can be isolated when kinetically protected by a sterically shielding ancillary ligand. Complexes **a** (Scheme S1), comprising [Ln–(AlMe₄)] and [Ln–Me] moieties, are effectively stabilized by the bulky [Tp^{tBu,Me}] ligand (Paper V). The methyl group is presumably formed by intra- (via a κ²-coordinated [Tp^{tBu,Me}] ligand) or intermolecular N-donor cleavage (via [Tp^{tBu,Me}]H) of one tetramethylaluminate ligand.

However, the high potential of [Ln–(AlMe₄)]/[Ln–Me] containing reaction mixtures to activate C–H bonds was substantiated by the competitive formation of salt-like {[Tp^{tBu,Me}]AlMe}{Y(AlMe₄)[(μ-CH₂)(μ-Me)AlMe₂]₂(AlMe₂)} (**n**) (Figure S5). While the detailed mechanistic scenario leading to this mixed metal compound remains obscure, reactivity patterns can be recognized. The present two methylidene containing [(μ-CH₂)(μ-Me)AlMe₂] moieties are strong reminders of the prominent TEBBE reagent [Cp₂Ti[(μ-CH₂)(μ-Cl)AlMe₂] and its derivative [Cp₂Ti[(μ-CH₂)(μ-Me)AlMe₂] obtained by reaction of [Cp₂TiMe₂] and AlMe₃.

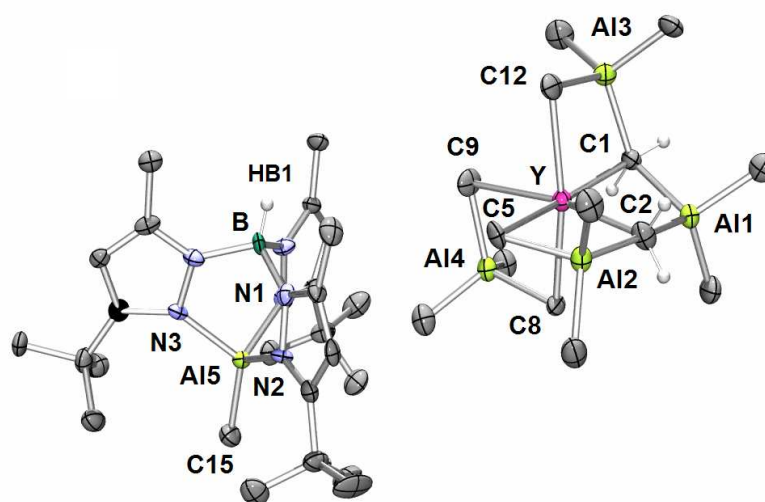


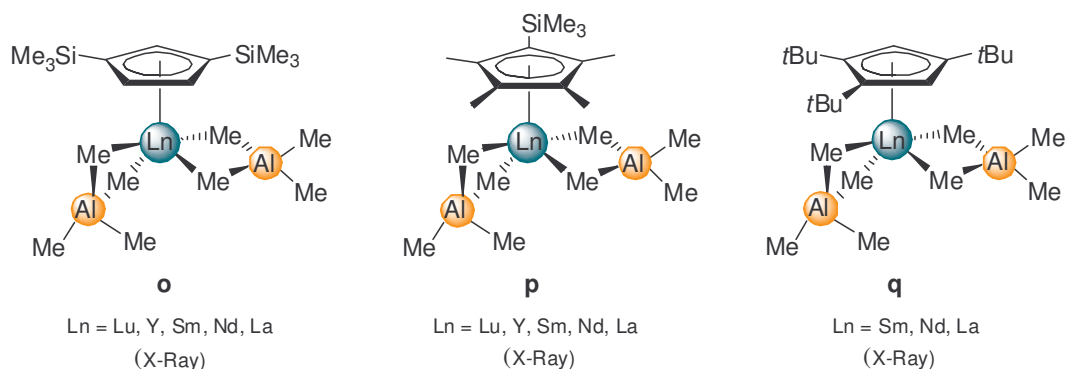
Figure S5: Solid-state structure of ion pair {[Tp^{tBu,Me}]AlMe}{Y(AlMe₄)[(μ-CH₂)(μ-Me)AlMe₂]₂(AlMe₂)} (**n**) (adapted from Paper V).

Preliminary reactivity studies of complex **a** revealed highly efficient methylation of carbonylic functionalities and promising reactivity in alkane elimination reactions.

4 Pre-Catalyst/Co-Catalyst Interactions of $\text{Cp}^{\text{R}}\text{Ln}(\text{AlMe}_4)_2$

The nature of the active rare-earth metal species of ZIEGLER mixed catalysts has been a matter of dispute since the early discovery of their superior performance in the stereospecific polymerization of 1,3-dienes.^{275,276,277} It is commonly accepted that the active rare-earth metal center is obtained in a two-step activation sequence involving the formation of a reactive Ln–alkyl or Ln–hydride bond and Al→Ln chloride transfer (“cationization”). Preformed Ln/Al heterobimetallic complexes such as carboxylates $\text{Ln}[(\text{O}_2\text{CAr}^i\text{Pr})_2(\mu\text{-AlMe}_2)]_2(\text{AlMe}_4)$, siloxides $\text{Ln}[\text{OSi}(\text{OtBu})_3](\text{AlMe}_3)(\text{AlMe}_4)_2$, and homoleptic $\text{Ln}(\text{AlMe}_4)_3$ can be considered as alkylated intermediates which, upon further activation with Et_2AlCl , give highly efficient initiators for the *cis*-1,4 selective isoprene polymerization (**Paper I**).^{223,225} The catalyst mixtures containing homoleptic tetramethylaluminates $\text{Ln}(\text{AlMe}_4)_3$ and two equivalents of Et_2AlCl show highest activities and perform superior to carboxylate and siloxide derivatives. An intrinsic rare-earth metal size effect is observed entailing highest catalytic activities for praseodymium and neodymium metal centers.

Intrigued by the reported exceptional catalytic performance of cationic monocyclopentadienyl complexes,²⁷⁸ a series of half-lanthanidocene tetramethylaluminate complexes has been synthesized and characterized (**Paper VII**). Methane elimination reactions of $\text{Ln}(\text{AlMe}_4)_3$ with one equivalent of substituted HCp^{R} yielded the bis(aluminate) complexes $\text{Cp}^{\text{R}}\text{Ln}(\text{AlMe}_4)_2$ **o–q** (Scheme S4). Elevated temperatures and extended reaction times were necessary when using the sterically bulky and deactivated cyclopentadiene [1,2,4-(Me_3C)₃ C_5H_3]. The X-ray crystallographic analyses of **o–q** revealed solid-state structures featuring one routinely observed planar η^2 coordinated $[\text{AlMe}_4]$ ligand while the second one shows a bent η^2 coordination allowing for an additional close C–Ln contact.



Scheme S4: Synthesized and characterized half-sandwich complexes $\text{Cp}^{\text{R}}\text{Ln}(\text{AlMe}_4)_2$ (adapted from **Paper VII**).

“Cationization” of half-sandwich complexes **o-q** with 1-3 equivalents Et_2AlCl did not provide active catalysts for the polymerization of isoprene. In the presence of one

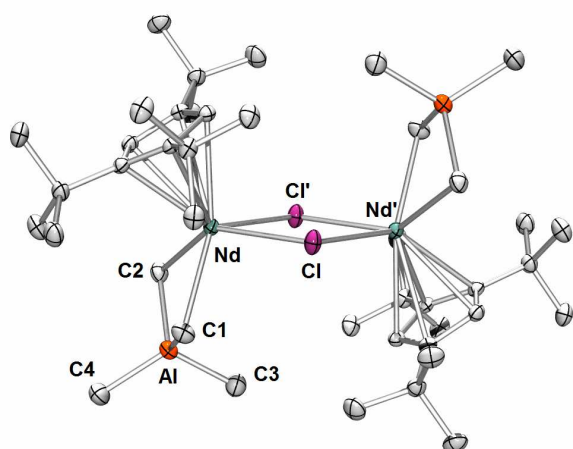


Figure S6: Solid-state structure of $\{[1,2,4\text{-(Me}_3\text{C)}_3\text{C}_5\text{H}_2]\text{Nd}(\text{AlMe}_4)(\mu\text{-Cl})\}_2$ (**r**) (adapted from **Paper VII**).

equivalent Me_2AlCl , [aluminate] \rightarrow [chloride] exchange was observed yielding discrete and stable mixed methyl/chloride compounds $[\text{Cp}^{\text{R}}\text{Ln}(\text{AlMe}_4)(\mu\text{-Cl})]_2$ irrespective of the substituents at the cyclopentadienyl ring and the size of the rare-earth metal center. Isostructural chloride-bridged dimers formed exclusively (Figure S6), while cluster formation as previously found for analogue $(\text{C}_5\text{Me}_5)\text{Ln}(\text{AlMe}_4)_2/\text{Me}_2\text{AlCl}$ ($\text{Ln} = \text{La}, \text{Nd}$) reactions was not observed.

Contrary to the catalytic inactivity of $\text{Cp}^{\text{R}}\text{Ln}(\text{AlMe}_4)_2/\text{Et}_2\text{AlCl}$ mixtures, a systematic study involving $\text{Cp}^{\text{R}}\text{Ln}(\text{AlMe}_4)_2$ and fluorinated borate and borane activators gave access to initiators for the controlled living isoprene polymerization (**Paper VI** and **Paper VII**). NMR spectroscopic studies of mixtures $\text{Cp}^{\text{R}}\text{Ln}(\text{AlMe}_4)_2/[\text{Ph}_3\text{C}][\text{B}(\text{C}_6\text{F}_5)_4]$ and $\text{Cp}^{\text{R}}\text{Ln}(\text{AlMe}_4)_2/[\text{PhNMe}_2\text{H}][\text{B}(\text{C}_6\text{F}_5)_4]$

clearly revealed the formation of tight ion pairs $[\text{Cp}^{\text{R}}\text{Ln}(\text{AlMe}_4)]^+[\text{B}(\text{C}_6\text{F}_5)_4]^-$ for all investigated Cp^{R} . The stability of these cationic species, however, significantly depends on the substituents on the Cp ligand ($(\text{C}_5\text{Me}_5) \gg (\text{C}_5\text{Me}_4\text{SiMe}_3) > [1,2,4\text{-(Me}_3\text{C)}_3\text{C}_5\text{H}_2] \gg [1,3\text{-(Me}_3\text{Si)}_2\text{C}_5\text{H}_3]$) as well as the lanthanide cation size ($\text{La} \gg \text{Nd} > \text{Y}$). Activation of half-sandwich complexes $\text{Cp}^{\text{R}}\text{Ln}(\text{AlMe}_4)_2$ with one equivalent of LEWIS acidic $\text{B}(\text{C}_6\text{F}_5)_3$ proceeds via fast sequential $\text{CH}_3/\text{C}_6\text{F}_5$ exchange processes accompanied by the formation of BMe_3 . Treatment of $(\text{C}_5\text{Me}_5)\text{La}(\text{AlMe}_4)_2$ with one equivalent

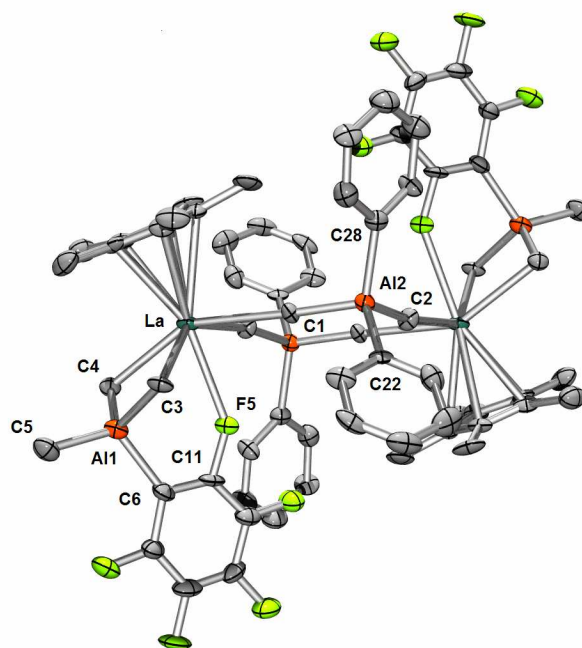


Figure S7: Solid-state structure of $\{[(\text{C}_5\text{Me}_5)\text{La}[(\mu\text{-Me})_2\text{AlMe}(\text{C}_6\text{F}_5)]^+][\text{Me}_2\text{Al}(\text{C}_6\text{F}_5)_2]\}_2$ (**s**) (adapted from **Paper VI**).

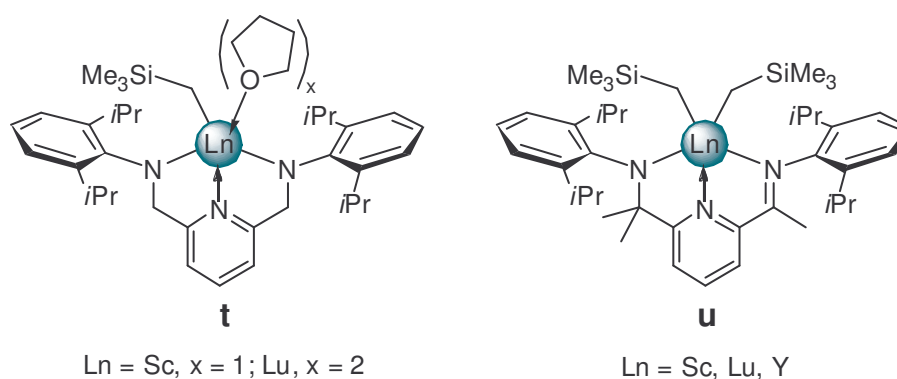
$B(C_6F_5)_3$ quantitatively yielded ion pair $\{[(C_5Me_5)La[(\mu-Me)_2AlMe(C_6F_5)]]^+[Me_2Al(C_6F_5)_2]_2\}^-$ (**s**) (Figure S7). Facile alkyl/ C_6F_5 group exchange is a favorable reaction observed in several catalytic systems based on MAO/ AlR_3 and $M(C_6F_5)_3$ ($M = Al, B$) activators and is commonly discussed as an undesirable catalyst deactivation pathway.²⁷⁹⁻²⁸²

However, the cationic species generated in situ upon treatment of $Cp^R Ln(AlMe_4)_2$ with one equivalent of $[Ph_3C][B(C_6F_5)_4]$, $[PhNMe_2H][B(C_6F_5)_4]$, or $B(C_6F_5)_3$, respectively, showed good to excellent activities for the *trans*-1,4 selective polymerization of isoprene. The stereoregularity of the produced polyisoprene corresponds very well to the stability of the cationic species (*vide supra*) and appears to be strongly dependent on the substitution pattern of the Cp^R ligand, the rare-earth metal cation size, and the boron activator involved. The *trans*-1,4 selectivity increases significantly with increasing size of the rare-earth metal cation, and when using $B(C_6F_5)_3$ as co-catalyst. Ligand effects are less pronounced but correspond to the ligand's proneness toward ligand degradation reactions. Polyisoprene with very high *trans*-1,4 content (99.5%) and very narrow molecular weight distributions ($M_w/M_n = 1.18$) could be obtained from a $(C_5Me_5)La(AlMe_4)_2/B(C_6F_5)_3$ catalyst mixture. Employing the isolated cationic complex **s** as catalyst under the same reaction conditions afforded high-*trans*-1,4 polyisoprene with almost similar polymer properties supporting the assumption that well-defined **s** (Figure S7) serves as catalytically active species in the *in situ* prepared catalyst mixture.

5 Structure-Reactivity Relationships of Amido-Pyridine Supported Rare-Earth Metal Alkyl Complexes

Post-lanthanidocene complexes based on nitrogen-donor ligands have been successfully employed for the synthesis of discrete organorare-earth metal complexes. The number of reported active catalyst systems, however, remains limited. Remarkable catalytic activity was found for complexes containing $[CH_2SiMe_3]$ actor ligands, usually upon cationization with borate and/or organoaluminum activators.

A series of structurally related mono(alkyl) diamido-pyridine and bis(alkyl) imino-amido-pyridine rare-earth metal complexes has been synthesized (Scheme S5) and their initiating performance in the polymerization of ethylene, styrene, and methyl methacrylate has been tested (Paper VIII).



Scheme S5: Synthesized diamido-pyridine (**t**) and imino-amido-pyridine (**u**) alkyl complexes (adapted from **Paper VIII**).

While the neutral alkyl complexes were inactive toward ethylene, cationic derivatives of compound **u** polymerized ethylene with moderate yields. The initiating performance is governed by the rare-earth metal size ($\text{Sc} > \text{Lu}$) and the nature of the co-catalyst. Routinely used fluorinated borate co-catalysts $[\text{Ph}_3\text{C}][\text{B}(\text{C}_6\text{F}_5)_4]$ and $[\text{PhNMe}_2\text{H}][\text{B}(\text{C}_6\text{F}_5)_4]$ produced catalytically active species, while cationization with *N*-[tris(pentafluorophenyl)borane]-3*H*-indole gave inactive species, most likely due to π -coordination of the $[\text{B}(\text{indolyl})(\text{C}_6\text{F}_5)_3]$ anion to the cationic lanthanide metal center. The availability of an initiating alkyl group is essential to provide catalytic performance, as supported by the complete inactivity of cationic species derived from the dianionic diamido-pyridine ligand. Contrary, the homo-polymerization of MMA is only initiated by the neutral mono(alkyl) diamido-pyridine complexes **t**. Neither the neutral bis(alkyl) imino-amido-pyridine complexes **u** nor their cationic variants gave positive polymerization protocols.

C

Concluding Remarks

In 1974 LAPPERT introduced the $[\text{CH}(\text{SiMe}_3)_2]$ ligand to group 3 chemistry marking the beginning of a new era of organolanthanide chemistry. Ever since rare-earth metal alkyl chemistry developed to one of the most prolific areas within rare-earth metal chemistry. The usually high reactivity of $[\text{Ln-alkyl}]$ moieties gives valuable access to a wide variety of heteroleptic rare-earth metal alkyl derivatives and importantly provides an efficient entry into organo-rare-earth metal mediated catalysis.

Despite remarkable advances regarding accessibility and stability, rare-earth metal alkyl chemistry still meets various challenges. One major challenge remains the Ln cation size dependent availability and stability of rare-earth metal alkyl precursors.

In the present work, homoleptic rare-earth metal tris(tetramethylaluminates) $\text{Ln}(\text{AlMe}_4)_3$, also referred to as “alkyls in disguise”, have been investigated with respect to their intrinsic structural and chemical properties as well as to their suitability to act as rare-earth metal alkyl precursors.

Homoleptic tetramethylaluminates can be obtained as solvent-free, alkyl-only compounds for the entire size range of rare-earth metal cations, except scandium. The remarkable adaptability of $[\text{AlMe}_4]$ ligands to the respective stereoelectronic requirements allows for the stabilization of both sterically constrained and sterically open rare-earth metal complexes. A characterization of the rare-earth metal tetramethylaluminate bonding comprehends ionic and covalent bonding. Accordingly, tetramethylaluminate ligands are susceptible to ligand exchange via salt metathesis as well as to alkane elimination reactions in the presence of protic substrates. The $[\text{AlMe}_4]$ moiety is characterized by a highly dynamic behavior. The very fast exchange of bridging and terminal methyl groups proceeds via an associative exchange mechanism ($\eta^2 \rightarrow \eta^3$ coordination shifts).

Recent publications emphasized the suitability of homoleptic $\text{Ln}(\text{AlMe}_4)_3$ for the high yield synthesis of half-lanthanidocene and lanthanidocene complexes. Considering the increasing importance of non-cyclopentadienyl ancillary ligands, a central aspect of this work concerns the implementation of $\text{Ln}(\text{AlMe}_4)_3$ as alkyl precursors in post-lanthanidocene chemistry. Following an alkane elimination protocol, the synthesis of post-lanthanidocene complexes with several multidentate nitrogen donor ligands has been achieved. Inherent to all investigated ancillary ligand systems is the competitive formation of ancillary ligand supported aluminum complexes. The high affinity of LEWIS acidic aluminum cations for nitrogen donors combined with a kinetically controlled initial attack of bulky nitrogen ligands at a terminal methyl group of the

tetramethylaluminate ligand is held responsible for the observed reactivity. The presence of AlMe_3 released in the acid-base reaction between the respective ligand precursor and $\text{Ln}(\text{AlMe}_4)_3$ needs special consideration, particularly for ligands containing functionalities prone to nucleophilic attack.

Enhanced reactivity can be assigned to $[\text{AlMe}_4]$ ligands. Thermal degradation of rare-earth metal complexes containing a tetramethylaluminate ligand was found to proceed via H-abstraction at the ancillary ligand yielding stable cyclometalation products. Particularly $[\text{Ln}-\text{Me}]$ moieties, transiently formed by donor-induced aluminate cleavage showed extraordinary reactivity enabling C-H activation at *tertiary* carbon atoms, ligand alkylation via alkyl-migration, and the formation of TEBBE-like methylidene moieties.

Reasonably, the observed reactivity patterns of $\text{Ln}-[\text{AlMe}_4]$ moieties can serve as valuable models for catalyst deactivation processes in intricate group 4/MAO (organoaluminum) catalyst mixtures.

Homoleptic $\text{Ln}(\text{AlMe}_4)_3$ as well as carboxylate and siloxide complexes derived thereof initiate the polymerization of 1,3-dienes upon cationization with chlorinating Et_2AlCl . Polyisoprenes are produced with very high *cis*-1,4 selectivity ("chloride effect"). The catalyst activities, however, show a strong dependency on the rare-earth metal cation size and the pre-catalyst/co-catalyst ratio. Highest activities and selectivities are found for mixtures containing praseodymium and two equivalents of Et_2AlCl .

Contrary, mixtures of Et_2AlCl and half-sandwich complexes $\text{Cp}^{\text{R}}\text{Ln}(\text{AlMe}_4)_2$ do not provide catalytically active systems, presumably due to the formation of well defined and stable dimers $[\text{Cp}^{\text{R}}\text{Ln}(\text{AlMe}_4)\text{Cl}]_2$.

Treatment of complexes $\text{Cp}^{\text{R}}\text{Ln}(\text{AlMe}_4)_2$ with fluorinated borate and borane reagents, however, reveals the formation of distinct cationic rare-earth metal species. While $[\text{Ph}_3\text{C}][\text{B}(\text{C}_6\text{F}_5)_4]$ and $[\text{PhNMe}_2\text{H}][\text{B}(\text{C}_6\text{F}_5)_4]$ yield tight ion pairs $[\text{Cp}^{\text{R}}\text{Ln}(\text{AlMe}_4)]^+[\text{B}(\text{C}_6\text{F}_5)_4]^-$, activation of half-sandwich complexes $\text{Cp}^{\text{R}}\text{Ln}(\text{AlMe}_4)_2$ with one equivalent of LEWIS acidic $\text{B}(\text{C}_6\text{F}_5)_3$ proceeds via fast sequential $\text{CH}_3/\text{C}_6\text{F}_5$ exchange processes. The structural characterization of the resulting ion pair $\{[(\text{C}_5\text{Me}_5)\text{La}[(\mu\text{-Me})_2\text{AlMe}(\text{C}_6\text{F}_5)]]^+[\text{Me}_2\text{Al}(\text{C}_6\text{F}_5)_2]^- \}_2$ evidences the complexity of catalyst mixtures containing organoaluminum and borate/borane reagents. Extensive use of organoaluminum scavengers in the presence of boron activators has to be put into perspective.

Remarkably, borate/borane activation generates catalytically highly active species initiating the *trans*-1,4 selective polymerization of isoprene. *Trans*-selectivities are strongly associated to the relative stability of the respective cationic rare-earth metal

species, which increases with increasing rare-earth metal size, and with the chemical innocence and stability of the Cp^{R} ligand. The choice of co-catalyst has a major impact on the catalyst activities and selectivities - highest *trans*-selectivities are connected to the use of $\text{B}(\text{C}_6\text{F}_5)_3$. Accordingly, catalyst mixtures $(\text{C}_5\text{Me}_5)\text{La}(\text{AlMe}_4)_2/\text{B}(\text{C}_6\text{F}_5)_3$ yielded polyisoprene with very high *trans*-1,4 content (99.5%) and very narrow molecular weight distributions ($M_w/M_n = 1.18$). Employing the isolated cationic complex $\{[(\text{C}_5\text{Me}_5)\text{La}[(\mu\text{-Me})_2\text{AlMe}(\text{C}_6\text{F}_5)]]^+[\text{Me}_2\text{Al}(\text{C}_6\text{F}_5)_2]_2\}$ as single-component catalyst afforded high-*trans*-1,4 polyisoprene with almost similar polymer properties supporting the assumption that the ion pair serves as catalytically active species in the *in situ* prepared catalyst mixture.

Catalytic activity is achieved by sensitively balancing a multitude of factors. Among these complex stability, the nature of ancillary and actor ligands, and pre-catalyst/co-catalyst interactions are the most apparent approaches to catalyst optimization. While extensive work was performed on pre-catalyst (rare-earth metal complex) design, still little is known about the diversity and complexity of pre-catalyst/co-catalyst interplay. Generalizations have to be treated carefully even for closely related systems. Small variations, particularly of multicomponent systems, allow for unexpected and intricate reaction sequences challenging the insight into the nature of active species but, moreover, open up for novel pathways of modern catalysis.

D

Bibliography

- (1) Frankland, P. F. *J. Chem. Soc.* **1848-1849**, 2, 263.
- (2) Coates, G. E.; Wade, K. In *Organometallic Compounds*; 3rd ed.; Coates, G. E., Green, M. L. H., Wade, K., Eds.; Methuen: London, 1967; Vol. 1.
- (3) Cotton, F. A. *Chem. Rev.* **1955**, 55, 551.
- (4) Jaffe, H. H.; Doak, G. O. *J. Chem. Phys.* **1953**, 21, 627.
- (5) Green, M. L. H. In *Organometallic Compounds*; 3rd ed.; Coates, G. E., Green, M. L. H., Wade, K., Eds.; Methuen: London, 1968; Vol. 2.
- (6) Clauss, K.; Beermann, C. *Angew. Chem.* **1959**, 71, 627.
- (7) Berthold, H. J.; Groh, G. *Z. Anorg. Allg. Chem.* **1963**, 319, 230.
- (8) Berthold, H. J.; Groh, G. *Angew. Chem. Int. Ed.* **1966**, 5, 516.
- (9) Collier, M. R.; Lappert, M. F.; Truelock, M. M. *J. Organomet. Chem.* **1970**, 25, C36.
- (10) Collier, M. R.; Lappert, M. F.; Pearce, R. *J. Chem. Soc., Dalton Trans.* **1973**, 445.
- (11) Yagupsky, G.; Shortland, A.; Wilkinson, G. *Chem. Commun.* **1970**, 1369.
- (12) Mowat, W.; Shortland, A.; Yagupsky, G.; Hill, N. J.; Yagupsky, M.; Wilkinson, G. *J. Chem. Soc., Dalton Trans.* **1972**, 533.
- (13) Plets, V. M. *Dokl. Akad. Nauk SSSR* **1938**, 20, 27.
- (14) Gilman, H.; Jones, R. G. *J. Org. Chem.* **1945**, 10, 505.
- (15) Hart, F. A.; Saran, M. S. *J. Chem. Soc.; Chem. Commun.* **1968**, 1614.
- (16) Hart, F. A.; Massey, A. G.; Saran, M. S. *J. Organomet. Chem.* **1970**, 21, 147-154.
- (17) Müller, J. Dr. Thesis, Technische Universität Berlin, 1978.
- (18) Schumann, H. *J. Organomet. Chem.* **1985**, 281, 95-110.
- (19) Schumann, H.; Müller, J. *Angew. Chem. Int. Ed.* **1978**, 17, 276.
- (20) Dietrich, H. M.; Raudaschl-Sieber, G.; Anwander, R. *Angew. Chem. Int. Ed.* **2005**, 44, 5303-5306.

- (21) Lappert, M. F.; Pearce, R. J. *Chem. Soc., Chem. Commun.* **1973**, 126.
- (22) Barker, G. K.; Lappert, M. F. *J. Organomet. Chem.* **1974**, 76, C45-C46.
- (23) Eaborn, C.; Hitchcock, P. B.; Izod, K.; Smith, J. D. *J. Am. Chem. Soc.* **1994**, 116, 12071-12072.
- (24) Thompson, L. C. In *Handbook on the physics and chemistry of the rare earths*; Gschneidner Jr., K. A., Eyring, L., Eds.; North-Holland Publishing Company: Amsterdam, 1979.
- (25) Freeman, A. J.; Watson, R. E. *Phys. Rev.* **1962**, 127, 2058.
- (26) Seth, M.; Dolg, M.; Fulde, P.; Schwerdtfeger, P. *J. Am. Chem. Soc.* **1995**, 117, 6597.
- (27) Gibson, J. K. *J. Phys. Chem. A* **2003**, 107, 7891-7899.
- (28) Cornehl, H. H.; Heinemann, C.; Schröder, D.; Schwarz, H. *Organometallics* **1995**, 14, 992-999.
- (29) Schinzel, S.; Bindl, M.; Visseaux, M.; Chermette, H. *J. Phys. Chem. A* **2006**, 110, 11324-11331.
- (30) Eaborn, C.; Eidenschink, R.; Jackson, P. M.; Walton, D. R. M. *J. Organomet. Chem.* **1975**, 101, C40.
- (31) Schleyer, P. v. R.; Clark, T.; Kos, A. J.; Spitznagel, G. W.; Rohde, C.; Arad, D.; Houk, K. N.; Rondan, N. G. *J. Am. Chem. Soc.* **1984**, 106, 6467-6475.
- (32) Brinkman, E. A.; Berger, S.; Brauman, J. I. *J. Am. Chem. Soc.* **1994**, 116, 8304-8310.
- (33) Römer, B.; Gatev, G. G.; Zhong, M.; Brauman, J. I. *J. Am. Chem. Soc.* **1998**, 120, 2919-2924.
- (34) Fu, Y.; Liu, L.; Li, R. Q.; Liu, R.; Guo, Q. X. *J. Am. Chem. Soc.* **2004**, 126, 814-822.
- (35) Nolan, S. P.; Stern, D.; Marks, T. J. *J. Am. Chem. Soc.* **1989**, 111, 7844-7853.
- (36) Bordwell, F. G. *Acc. Chem. Res.* **1988**, 21, 456-463.

- (37) Bordwell, F. G.; <http://www.chem.wisc.edu/areas/reich/pkatable/index.htm>.
- (38) Wetzel, D. M.; Brauman, J. I. *J. Am. Chem. Soc.* **1988**, *110*, 8333-8336.
- (39) Collier, M. R.; Kingston, B. M.; Lappert, M. F.; Truelock, M. M. Britain, 1969.
- (40) Hitchcock, P. B.; Holmes, S. A.; Lappert, M. F.; Tian, S. *J. Chem. Soc., Chem. Commun.* **1994**, 2691-2692.
- (41) Van den Hende, J. R.; Hitchcock, P. B.; Holmes, S. A.; Lappert, M. F.; Tian, S. *J. Chem. Soc., Dalton Trans.* **1995**, 3933-3939.
- (42) Hitchcock, P. B.; Khvostov, A. V.; Lappert, M. F. *J. Organomet. Chem.* **2002**, *663*, 263-268.
- (43) Hitchcock, P. B.; Lappert, M. F.; Smith, R. G.; Bartlett, R. A.; Power, P. P. *J. Chem. Soc., Chem. Commun.* **1988**, 1007-1009.
- (44) Schaverien, C. J.; Orpen, A. G. *Inorg. Chem.* **1991**, *30*, 4968-4978.
- (45) Avent, A. G.; Caro, C. F.; Hitchcock, P. B.; Lappert, M. F.; Li, Z.; Wei, X.-H. *Dalton Trans.* **2004**, 1567-1577.
- (46) Guttenberger, C.; Amberger, H. D. *J. Organomet. Chem.* **1997**, *545-546*, 601-606.
- (47) Reddmann, H.; Guttenberger, C.; Amberger, H.-D. *J. Organomet. Chem.* **2000**, *602*, 65-71.
- (48) Perrin, L.; Maron, L.; Eisenstein, O.; Lappert, M. F. *New J. Chem.* **2003**, *27*, 121.
- (49) Clark, D. L.; Gordon, J. C.; Hay, P. J.; Martin, R. L.; Poli, R. *Organometallics* **2002**, *21*, 5000-5006.
- (50) Schaverien, C. J.; Nesbitt, G. J. *J. Chem. Soc., Dalton Trans.* **1992**, 157-167.
- (51) Atwood, J. L.; Lappert, M. F.; Smith, R. G.; Zhang, H. M. *J. Chem. Soc., Chem. Commun.* **1988**, 1308-1309.
- (52) Westerhausen, M.; Hartmann, M.; Pfitzner, A.; Schwarz, W. Z. *Anorg. Allg. Chem.* **1995**, *621*, 837-850.

- (53) Schaverien, C. J.; Van Mechelen, J. B. *Organometallics* **1991**, *10*, 1704-1709.
- (54) Hitchcock, P. B.; Lappert, M. F.; Smith, R. G. *J. Chem. Soc., Chem. Commun.* **1989**, 369-371.
- (55) Booij, M.; Kiers, N. H.; Heeres, H. J.; Teuben, J. H. *J. Organomet. Chem.* **1989**, *364*, 79-86.
- (56) Booij, M.; Meetsma, A.; Teuben, J. H. *Organometallics* **1991**, *10*, 3246-3252.
- (57) Van der Heijden, H.; Schaverien, C. J.; Orpen, A. G. *Organometallics* **1989**, *8*, 255-258.
- (58) Heeres, H. J.; Meetsma, A.; Teuben, J. H. *Organometallics* **1989**, *8*, 2637-2646.
- (59) Klooster, W. T.; Brammer, L.; Schaverien, C. J.; Budzelaar, P. H. M. *J. Am. Chem. Soc.* **1999**, *121*, 1381-1382.
- (60) Tian, S.; Arredondo, V. M.; Stern, C. L.; Marks, T. J. *Organometallics* **1999**, *18*, 2568-2570.
- (61) Gendron, R. A. L.; Berg, D. J.; Shao, P.; Barclay, T. *Organometallics* **2001**, *20*, 4279-4286.
- (62) Schaverien, C. J.; Meijboom, N.; Orpen, A. G. *J. Chem. Soc., Chem. Commun.* **1992**, 124-126.
- (63) Gribkov, D. V.; Hampel, F.; Hultsch, K. C. *Eur. J. Inorg. Chem.* **2004**, *2004*, 4091-4101.
- (64) Hong, S.; Tian, S.; Metz, M. V.; Marks, T. J. *J. Am. Chem. Soc.* **2003**, *125*, 14768-14783.
- (65) Metz, M. V.; Sun, Y.; Stern, C. L.; Marks, T. J. *Organometallics* **2002**, *21*, 3691-3702.
- (66) Westerhausen, M.; Hartmann, M.; Schwarz, W. *Inorg. Chim. Acta* **1998**, *269*, 91-100.
- (67) Kawaoka, A. M.; Douglass, M. R.; Marks, T. J. *Organometallics* **2003**, *22*, 4630-4632.

- (68) Izod, K.; Liddle, S. T.; McFarlane, W.; Clegg, W. *Organometallics* **2004**, *23*, 2734-2743.
- (69) Eaborn, C.; Hitchcock, P. B.; Izod, K.; Lu, Z. R.; Smith, J. D. *Organometallics* **1996**, *15*, 4783-4790.
- (70) Qi, G.; Nitto, Y.; Saiki, A.; Tomohiro, T.; Nakayama, Y.; Yasuda, H. *Tetrahedron* **2003**, *59*, 10409-10418.
- (71) Schaverien, C. J. *Adv. Organomet. Chem.* **1994**, *36*, 283-362.
- (72) Andersen, R. A.; Boncella, J. M.; Burns, C. J.; Blom, R.; Haaland, A.; Volden, H. V. *J. Organomet. Chem.* **1986**, *312*, C49-C52.
- (73) Andersen, R. A.; Blom, R.; Boncella, J. M.; Burns, C. J.; Volden, H. V. *Acta. Chem. Scand.* **1987**, *A41*, 24-35.
- (74) Evans, W. J.; Hughes, L. A.; Hanusa, T. P. *Organometallics* **1986**, *5*, 1285-1291.
- (75) DeKock, R. L.; Peterson, M. A.; Timmer, L. K.; Baerends, E. J.; Vernooijs, P. *Polyhedron* **1990**, *9*, 1919-1934.
- (76) Kaupp, M.; Schleyer, P. v. R.; Dolg, M.; Stoll, H. *J. Am. Chem. Soc.* **1992**, *114*, 8202-8208.
- (77) Hollis, T. K.; Burdett, J. K.; Bosnich, B. *Organometallics* **1993**, *12*, 3385-3386.
- (78) Al-Juaid, S. S.; Eaborn, C.; Hitchcock, P. B.; McGeary, C. A.; Smith, J. D. *J. Chem. Soc., Chem. Commun.* **1989**, 273-274.
- (79) Al-Juaid, S. S.; Eaborn, C.; Hitchcock, P. B.; Izod, K.; Mallien, M.; Smith, J. D. *Angew. Chem. Int. Ed.* **1994**, *33*, 1268-1270.
- (80) Clegg, W.; Eaborn, C.; Izod, K.; O'Shaughnessy, P.; Smith, J. D. *Angew. Chem.* **1997**, *109*, 2925-2926.
- (81) Yasuda, H. *J. Polym. Sci. Part A: Polym. Chem.* **2001**, *39*, 1955-1959.
- (82) Yasuda, H. *J. Organomet. Chem.* **2002**, *647*, 128-138.

- (83) Eaborn, C.; Hill, M. S.; Hitchcock, P. B.; Smith, J. D.; Zhang, S.; Ganicz, T. *Organometallics* **1999**, *18*, 2342-2348.
- (84) Bowman, L. J.; Izod, K.; Clegg, W.; Harrington, R. W. *Organometallics* **2007**, *26*, 2646-2651.
- (85) Schumann, H.; Freckmann, D. M. M.; Dechert, S. Z. *Anorg. Allg. Chem.* **2002**, *628*, 2422-2426.
- (86) Atwood, J. L.; Hunter, W. E.; Rogers, R. D.; Holton, J.; McMeeking, J.; Pearce, R.; Lappert, M. F. *J. Chem. Soc., Chem. Commun.* **1978**, 140-142.
- (87) Schumann, H.; Müller, J. J. *Organomet. Chem.* **1978**, *146*, C5-C7.
- (88) Niemeyer, M. *Acta Cryst.* **2001**, *E57*, m578-m580.
- (89) Estler, F. Dr. Thesis, Technische Universität München, 2002.
- (90) Evans, W. J.; Brady, J. C.; Ziller, J. W. *J. Am. Chem. Soc.* **2001**, *123*, 7711-7712.
- (91) Schumann, H.; Müller, J. J. *Organomet. Chem.* **1979**, *169*, C1-C4.
- (92) Lukesova, L.; Ward, B. D.; Bellemin-Laponnaz, S.; Wadepohl, H.; Gade, L. H. *Dalton Trans.* **2007**, 920-922.
- (93) Rufanov, K. A.; Freckmann, D. M. M.; Kroth, H.-J.; Schutte, S.; Schumann, H. Z. *Naturf. B: Chem. Sci.* **2005**, *60*, 533-537.
- (94) Vollershtein, E. L.; Yakovlev, V. A.; Tinyakova, E. I.; Dolgoplosk, B. A. *Dokl. Akad. Nauk SSSR* **1980**, *250*, 365.
- (95) Clark, D. L.; Gordon, J. C.; Huffman, J. C.; Watkin, J. G.; Zwick, B. D. *Organometallics* **1994**, *13*, 4266-4270.
- (96) Arndt, S.; Spaniol, T. P.; Okuda, J. *Angew. Chem. Int. Ed.* **2003**, *42*, 5075-5079.
- (97) Arndt, S.; Spaniol, T. P.; Okuda, J. *Chem. Commun.* **2002**, 896-897.
- (98) Nakajima, Y.; Okuda, J. *Organometallics* **2007**, *26*, 1270-1278.
- (99) Sulfab, Y.; Al-Shatti, N. J. *Inorg. Chim. Acta* **1984**, *87*, L23.

- (100) Margerum, D. W. *Pure Appl. Chem.* **1983**, *55*, 23-34.
- (101) Diddario, L. L.; Robinson, W. R.; Margerum, D. W. *Inorg. Chem.* **1983**, *22*, 1021.
- (102) Hultsch, K. C.; Spaniol, T. P.; Okuda, J. *Angew. Chem. Int. Ed.* **1999**, *38*, 227-230.
- (103) Cameron, T. M.; Gordon, J. C.; Scott, B. L. *Organometallics* **2004**, *23*, 2995-3002.
- (104) Li, X.; Baldamus, J.; Hou, Z. *Angew. Chem. Int. Ed.* **2005**, *44*, 962-965.
- (105) Luo, Y.; Baldamus, J.; Hou, Z. *J. Am. Chem. Soc.* **2004**, *126*, 13910-13911.
- (106) Cui, D.; Nishiura, M.; Hou, Z. *Macromolecules* **2005**, *38*, 4089-4095.
- (107) Hultsch, K. C.; Voth, P.; Spaniol, T. P.; Okuda, J. *Z. Anorg. Allg. Chem.* **2003**, *629*, 1272-1276.
- (108) Tardif, O.; Nishiura, M.; Hou, Z. *Organometallics* **2003**, *22*, 1171-1173.
- (109) Zhang, W. X.; Nishiura, M.; Hou, Z. *J. Am. Chem. Soc.* **2005**, *127*, 16788-16789.
- (110) Hitzbleck, J.; Beckerle, K.; Okuda, J.; Halbach, T.; Mülhaupt, R. *Macromol. Symp.* **2006**, *236*, 23-29.
- (111) Arndt, S.; Spaniol, T. P.; Okuda, J. *Organometallics* **2003**, *22*, 775-781.
- (112) Hitzbleck, J.; Okuda, J. *Z. Anorg. Allg. Chem.* **2006**, *632*, 1947-1949.
- (113) Shapiro, P. J.; Bunel, E. E.; Schaefer, W. P.; Bercaw, J. E. *Organometallics* **1990**, *9*, 867.
- (114) Hultsch, K. C.; Voth, P.; Beckerle, K.; Spaniol, T. P.; Okuda, J. *Organometallics* **2000**, *19*, 228-243.
- (115) Arndt, S.; Voth, P.; Spaniol, T. P.; Okuda, J. *Organometallics* **2000**, *19*, 4690-4700.
- (116) Voth, P.; Spaniol, T. P.; Okuda, J. *Organometallics* **2003**, *22*, 3921-3926.
- (117) Robert, D.; Trifonov, A. A.; Voth, P.; Okuda, J. *J. Organomet. Chem.* **2006**, *691*, 4393-4399.

- (118) Trifonov, A. A.; Spaniol, T. P.; Okuda, J. *Organometallics* **2001**, *20*, 4869-4874.
- (119) Tardif, O.; Nishiura, M.; Hou, Z. *Tetrahedron* **2003**, *59*, 10525-10539.
- (120) Zhang, L.; Luo, Y.; Hou, Z. *J. Am. Chem. Soc.* **2005**, *127*, 14562-14563.
- (121) Canich, J. A. M.; Schaffer, T. D.; Christopher, J. N.; Squire, K. R.; World Pat. W00018808 ed.; Exxon, Ed., 2000; Vol. 1.
- (122) Rufanov, K. A.; Petrov, A. R.; Kotov, V. V.; Laquai, F.; Sundermeyer, J. *Eur. J. Inorg. Chem.* **2005**, *2005*, 3805-3807.
- (123) Nishiura, M.; Hou, Z.; Wakatsuki, Y.; Yamaki, T.; Miyamoto, T. *J. Am. Chem. Soc.* **2003**, *125*, 1184-1185.
- (124) Zhang, W. X.; Nishiura, M.; Hou, Z. *Chem. Eur. J.* **2007**, *13*, 4037-4051.
- (125) Mu, Y.; Piers, W. E.; MacQuarrie, D. C.; Zaworotko, M. J.; Young, V. G. *Organometallics* **1996**, *15*, 2720-2726.
- (126) Kirillov, E.; Toupet, L.; Lehmann, C. W.; Razavi, A.; Carpentier, J. F. *Organometallics* **2003**, *22*, 4467-4479.
- (127) Arndt, S.; Zeimentz, P. M.; Spaniol, T. P.; Okuda, J.; Honda, M.; Tatsumi, K. *Dalton Trans.* **2003**, 3622-3627.
- (128) Elvidge, B. R.; Arndt, S.; Zeimentz, P. M.; Spaniol, T. P.; Okuda, J. *Inorg. Chem.* **2005**, *44*, 6777-6788.
- (129) Lawrence, S. C.; Ward, B. D.; Dubberley, S. R.; Kozak, C. M.; Mountford, P. *Chem. Commun.* **2003**, 2880-2881.
- (130) Tredget, C. S.; Lawrence, S. C.; Ward, B. D.; Howe, R. G.; Cowley, A. R.; Mountford, P. *Organometallics* **2005**, *24*, 3136-3148.
- (131) Tredget, C. S.; Bonnet, F.; Cowley, A. R.; Mountford, P. *Chem. Commun.* **2005**, 3301-3303.
- (132) Ge, S.; Bambirra, S.; Meetsma, A.; Hessen, B. *Chem. Commun.* **2006**, 3320-3322.

- (133) Ward, B. D.; Bellemin-Lapponnaz, S.; Gade, L. H. *Angew. Chem. Int. Ed.* **2005**, *44*, 1668-1671.
- (134) Zeimentz, P. M.; Spaniol, T. P.; Okuda, J. *Inorg. Chim. Acta* **2006**, *359*, 4769-4773.
- (135) Bambirra, S.; Leusen, D. v.; Meetsma, A.; Hessen, B.; Teuben, J. H. *Chem. Commun.* **2003**, 522-523.
- (136) Bambirra, S.; Bouwkamp, M. W.; Meetsma, A.; Hessen, B. *J. Am. Chem. Soc.* **2004**, *126*, 9182-9183.
- (137) Bambirra, S.; Otten, E.; van Leusen, D.; Meetsma, A.; Hessen, B. *Z. Anorg. Allg. Chem.* **2006**, *632*, 1950-1952.
- (138) Kretschmer, W. P.; Meetsma, A.; Hessen, B.; Schmalz, T.; Qayyum, S.; Kempe, R. *Chem. Eur. J.* **2006**, *12*, 8969-8978.
- (139) Bambirra, S.; Leusen, D. v.; Meetsma, A.; Hessen, B.; Teuben, J. H. *Chem. Commun.* **2001**, 637-638.
- (140) Bambirra, S.; Boot, S. J.; vanLeusen, D.; Meetsma, A.; Hessen, B. *Organometallics* **2004**, *23*, 1891-1898.
- (141) Bambirra, S.; vanLeusen, D.; Tazelaar, C. G. J.; Meetsma, A.; Hessen, B. *Organometallics* **2007**, *26*, 1014-1023.
- (142) Marinescu, S. C.; Agapie, T.; Day, M. W.; Bercaw, J. E. *Organometallics* **2007**, *26*, 1178-1190.
- (143) Yang, Y.; Liu, B.; Lv, K.; Gao, W.; Cui, D.; Chen, X.; Jing, X. *Organometallics* **2007**, *26*, 4575-4584.
- (144) Zhang, L.; Suzuki, T.; Luo, Y.; Nishiura, M.; Hou, Z. *Angew. Chem. Int. Ed.* **2007**, *46*, 1909-1913.
- (145) Liu, X.; Shang, X.; Tang, T.; Hu, N.; Pei, F.; Cui, D.; Chen, X.; Jing, X. *Organometallics* **2007**, *26*, 2747-2757.
- (146) Liu, B.; Cui, D.; Ma, J.; Chen, X.; Jing, X. *Chem. Eur. J.* **2007**, *13*, 834-845.

- (147) Lara-Sanchez, A.; Rodriguez, A.; Hughes, D. L.; Schormann, M.; Bochmann, M. *J. Organomet. Chem.* **2002**, *663*, 63-69.
- (148) Evans, W. J.; Brady, J. C.; Ziller, J. W. *Inorg. Chem.* **2002**, *41*, 3340-3346.
- (149) Luo, Y.; Nishiura, M.; Hou, Z. *J. Organomet. Chem.* **2007**, *692*, 536-544.
- (150) Yang, Y.; Li, S.; Cui, D.; Chen, X.; Jing, X. *Organometallics* **2007**, *26*, 671-678.
- (151) Cameron, T. M.; Gordon, J. C.; Michalczyk, R.; Scott, B. L. *Chem. Commun.* **2003**, 2282-2283.
- (152) Jantunen, K. C.; Scott, B. L.; Hay, P. J.; Gordon, J. C.; Kiplinger, J. L. *J. Am. Chem. Soc.* **2006**, *128*, 6322-6323.
- (153) Howe, R. G.; Tredget, C. S.; Lawrence, S. C.; Subongkoj, S.; Cowley, A. R.; Mountford, P. *Chem. Commun.* **2006**, 223-225.
- (154) Elvidge, B. R.; Arndt, S.; Spaniol, T. P.; Okuda, J. *Dalton Trans.* **2006**, 890-901.
- (155) Skinner, M. E. G.; Tyrrell, B. R.; Ward, B. D.; Mountford, P. *J. Organomet. Chem.* **2002**, *647*, 145-150.
- (156) Emslie, D. J. H.; Piers, W. E.; Parvez, M.; McDonald, R. *Organometallics* **2002**, *21*, 4226-4240.
- (157) Emslie, D. J. H.; Piers, W. E.; Parvez, M. *Dalton Trans.* **2003**, 2615-2620.
- (158) Lee, L.; Berg, D. J.; Einstein, F. W.; Batchelor, R. *J. Organometallics* **1997**, *16*, 1819-1821.
- (159) Estler, F.; Eickerling, G.; Herdtweck, E.; Anwander, R. *Organometallics* **2003**, *22*, 1212-1222.
- (160) Meyer, N.; Zulys, A.; Roesky, P. W. *Organometallics* **2006**, *25*, 4179-4182.
- (161) Cai, C.-X.; Toupet, L.; Lehmann, C. W.; Carpentier, J.-F. *J. Organomet. Chem.* **2003**, *683*, 131-136.
- (162) Amgoune, A.; Thomas, C. M.; Roisnel, T.; Carpentier, J.-F. *Chem. Eur. J.* **2006**, *12*, 169-179.

- (163) Ward, B. D.; Dubberley, S. R.; Maise-Francois, A.; Gade, L. H.; Mountford, P. J. *Chem. Soc., Dalton Trans.* **2002**, 4649-4657.
- (164) Lavanant, L.; Chou, T. Y.; Chi, Y.; Lehmann, C. W.; Toupet, L.; Carpentier, J. F. *Organometallics* **2004**, *23*, 5450-5458.
- (165) Boyd, C. L.; Toupance, T.; Tyrrell, B. R.; Ward, B. D.; Wilson, C. R.; Cowley, A. R.; Mountford, P. *Organometallics* **2005**, *24*, 309-330.
- (166) Lee, L.; Berg, D. J.; Bushnell, G. W. *Organometallics* **1995**, *14*, 8-10.
- (167) Emslie, D. J. H.; Piers, W. E.; MacDonald, R. J. *Chem. Soc., Dalton Trans.* **2002**, 293-294.
- (168) Schumann, H.; Freckmann, D. M. M.; Dechert, S. *Organometallics* **2006**, *25*, 2696-2699.
- (169) Evans, W. J.; Broomhall-Dillard, R. N. R.; Ziller, J. W. *Organometallics* **1996**, *15*, 1351-1355.
- (170) Fischbach, A. Dr. Thesis, Technische Universität München, 2003.
- (171) Evans, W. J.; Broomhall-Dillard, R. N. R.; Ziller, J. W. *J. Organomet. Chem.* **1998**, *569*, 89-97.
- (172) Gromada, J.; Mortreux, A.; Nowogrocki, G.; Leising, F.; T., M.; Carpentier, J.-F. *Eur. J. Inorg. Chem.* **2004**, *2004*, 3247-3253.
- (173) Evans, W. J.; Shreeve, J. L.; Broomhalldillard, R. N. R.; Ziller, J. W. *J. Organomet. Chem.* **1995**, *501*, 7-11.
- (174) Evans, W. J.; Boyle, T. J.; Ziller, J. W. *J. Organomet. Chem.* **1993**, *462*, 141-148.
- (175) Wayda, A. L.; Evans, W. J. *J. Am. Chem. Soc.* **1978**, *100*, 7119-7121.
- (176) Schumann, H.; Müller, J.; Bruncks, N.; Lauke, H.; Pickardt, J. *Organometallics* **1984**, *3*, 69-74.
- (177) Schumann, H.; Genthe, W.; Hahn, E.; Pickardt, J.; Schwarz, H.; Eckart, K. *J. Organomet. Chem.* **1986**, *306*, 215-225.

- (178) Qian, C.; Ye, C.; Li, Y. *J. Organomet. Chem.* **1986**, 302, 171-179.
- (179) Evans, W. J.; Drummond, D. K.; Hanusa, T. P.; Olofson, J. M. *J. Organomet. Chem.* **1989**, 376, 311-320.
- (180) Evans, W. J.; Wayda, A. L. *J. Organomet. Chem.* **1980**, 202, C6-C8.
- (181) Niemeyer, M. Z. *Anorg. Allg. Chem.* **2000**, 626, 1027-1029.
- (182) Sadow, A. D.; Tilley, T. D. *J. Am. Chem. Soc.* **2003**, 125, 7971-7977.
- (183) Evans, W. J.; Champagne, T. M.; Ziller, J. W.; Kaltsoyannis, N. *J. Am. Chem. Soc.* **2006**, 128, 16178-16189.
- (184) Chigir, N. N.; Guzman, I. S.; Sharaev, O. K.; Tinyakova, E. I.; Dolgoplosk, B. A. *Dokl. Akad. Nauk SSSR* **1982**, 263, 375.
- (185) Thiele, K. H.; Unverhau, K.; Geitner, M.; Jacob, K. Z. *Anorg. Allg. Chem.* **1987**, 548, 175-179.
- (186) Bambirra, S.; Meetsma, A.; Hessen, B. *Organometallics* **2006**, 25, 3454-3462.
- (187) Manzer, L. E. *J. Organomet. Chem.* **1977**, 135, C6-C9.
- (188) Manzer, L. E. *J. Am. Chem. Soc.* **1978**, 100, 8068-8073.
- (189) Harder, S. *Organometallics* **2005**, 24, 373-379.
- (190) Wayda, A. L.; Atwood, J. L.; Hunter, W. E. *Organometallics* **1984**, 3, 939-941.
- (191) Wayda, A. L.; Rogers, R. D. *Organometallics* **1985**, 4, 1440-1444.
- (192) Booij, M.; Klers, N. H.; Meetsma, A.; Teuben, J. H. *Organometallics* **1989**, 8, 2454-2461.
- (193) Hultsch, K. C.; Hampel, F.; Wagner, T. *Organometallics* **2004**, 23, 2601-2612.
- (194) Gribkov, D. V.; Hultsch, K. C. *Chem. Commun.* **2004**, 730-731.
- (195) Gribkov, D. V.; Hultsch, K. C.; Hampel, F. *J. Am. Chem. Soc.* **2006**, 128, 3748-3759.

- (196) Rufanov, K. A.; Muller, B. H.; Spannenberg, A.; Rosenthal, U. *New J. Chem.* **2006**, *30*, 29-31.
- (197) Deacon, G. B.; Koplick, A. J. *J. Organomet. Chem.* **1978**, *146*, C43-C45.
- (198) Deacon, G. B.; Koplick, A. J.; Raverty, W. D.; Vince, D. G. *J. Organomet. Chem.* **1979**, *182*, 121-141.
- (199) Deacon, G. B.; Koplick, A. J.; Tuong, T. D. *Aust. J. Chem.* **1982**, *35*, 941-949.
- (200) Murphy, E.; Toogood, G. E. *Inorganic and Nuclear Chemistry Letters* **1971**, *7*, 755-759.
- (201) Evans, W. J.; Engerer, S. C.; Coleson, K. M. *J. Am. Chem. Soc.* **1981**, *103*, 6672-6677.
- (202) Gailiunas, G.; Biktimirov, R. K.; Nurtdinova, G. V.; Monakov, Y. B.; Tolstikov, G. A. *Izvestiya Akademii Nauk SSSR, Seriya Khimicheskaya* **1984**, *6*, 1435.
- (203) Forsyth, C. M.; Deacon, G. B.; Field, L. D.; Jones, C.; Junk, P. C.; Kay, D. L.; Masters, A. F.; Richards, A. F. *Chem. Commun.* **2006**, 1003-1005.
- (204) Deacon, G. B.; Tuong, T. D. *J. Organomet. Chem.* **1981**, *205*, C4-C6.
- (205) Utimoto, K.; Nakamura, A.; Matsubara, S. *J. Am. Chem. Soc.* **1990**, *112*, 8189-8190.
- (206) Kunishima, M.; Tanaka, S.; Kono, K.; Hioki, K.; Tani, S. *Tetrahedron Letters* **1995**, *36*, 3707-3710.
- (207) Kunishima, M.; Nakata, D.; Tanaka, S.; Hioki, K.; Tani, S. *Tetrahedron* **2000**, *56*, 9927-9935.
- (208) Bochkarev, L. N.; Druzhkova, O. N.; Zhiltsov, S. F.; Zakharov, L. N.; Fukin, G. K.; Khorshev, S. Y.; Yanovsky, A. I.; Struchkov, Y. T. *Organometallics* **1997**, *16*, 500-502.
- (209) Shustov, S. B.; Bochkarev, L. N.; Zhiltsov, S. F. *Metalloorganicheskaya Khimiya* **1990**, *3*, 624-628.

- (210) Bochkarev, L. N.; Shustov, S. B.; Guseva, T. V.; Zhiltsov, S. F. *Zhurnal Obshchei Khimii* **1988**, *58*, 923-924.
- (211) Druzhkova, O. N.; Pimanova, N. A.; Bochkarev, L. N. *Russ. J. Gen. Chem.* **1999**, *69*, 1724-1725.
- (212) Bochkarev, M. N.; Katkova, M. A.; Khorshev, S. Y.; Makarenko, N. P. *Russ. Chem. Bull.* **1998**, *47*, 349-351.
- (213) Karl, M.; Seybert, G.; Massa, W.; Harms, K.; Agarwal, S.; Maleika, R.; Stelter, W.; Greiner, A.; Heitz, W.; Neumüller, B.; Dehnicke, K. *Z. Anorg. Allg. Chem.* **1999**, *625*, 1301-1309.
- (214) Deacon, G. B.; Fallon, G. D.; Forsyth, C. M.; Harris, S. C.; Junk, P. C.; Skelton, B. W.; White, A. H. *Dalton Trans.* **2006**, 802-812.
- (215) Davidson, P. J.; Lappert, M. F.; Pearce, R. *Chem. Rev.* **1976**, *76*, 219-242.
- (216) Ziegler, T.; Folga, E.; Berces, A. J. *J. Am. Chem. Soc.* **1993**, *115*, 636-646.
- (217) Watson, P. L. *J. Am. Chem. Soc.* **1983**, *105*, 6491-6493.
- (218) Dietrich, H. M.; Grove, H.; Törnroos, K. W.; Anwander, R. *J. Am. Chem. Soc.* **2006**, *128*, 1458-1459.
- (219) Seppelt, K. *Acc. Chem. Res.* **2003**, *36*, 147-153.
- (220) Schumann, H.; Lauke, H.; Hahn, E.; Pickardt, J. *J. Organomet. Chem.* **1984**, *263*, 29-35.
- (221) Arndt, S.; Beckerle, K.; Zeimentz, P. M.; Spaniol, T. P.; Okuda, J. *Angew. Chem. Int. Ed.* **2005**, *44*, 7473-7477.
- (222) Dietrich, H. M.; Meermann, C.; Törnroos, K. W.; Anwander, R. *Organometallics* **2006**, *25*, 4316-4321.
- (223) Fischbach, A.; Klimpel, M. G.; Widenmeyer, M.; Herdtweck, E.; Scherer, W.; Anwander, R. *Angew. Chem. Int. Ed.* **2004**, *43*, 2234-2239.
- (224) Fischbach, A.; Perdih, F.; Herdtweck, E.; Anwander, R. *Organometallics* **2006**, *25*, 1626-1642.

- (225) Fischbach, A.; Meermann, C.; Eickerling, G.; Scherer, W.; Anwander, R. *Macromolecules* **2006**, *39*, 6811-6816.
- (226) Meermann, C.; Törnroos, K. W.; Nerdal, W.; Anwander, R. *Angew. Chem. Int. Ed.* **2007**, *46*, 6508-6513.
- (227) Boncella, J. M.; Andersen, R. A. *Organometallics* **1985**, *4*, 205-206.
- (228) Klimpel, M. G.; Anwander, R.; Tafipolsky, M.; Scherer, W. *Organometallics* **2001**, *20*, 3983-3992.
- (229) Schrems, M. G.; Dietrich, H. M.; Tornroos, K. W.; Anwander, R. *Chem. Commun.* **2005**, 5922-5924.
- (230) Fischbach, A.; Herdtweck, E.; Anwander, R.; Eickerling, G.; Scherer, W. *Organometallics* **2003**, *22*, 499-509.
- (231) Sommerfeldt, H.-M.; Meermann, C.; Schrems, M. G.; Törnroos, K. W.; Frøystein, N. Å.; Miller, R. J.; Scheidt, E.-W.; Scherer, W.; Anwander, R. *Dalton Trans.* **2008**, 1899-1907.
- (232) Holton, J.; Lappert, M. F.; Ballard, D. G. H.; Pearce, R.; Atwood, J. L.; Hunter, W. E. *J. Chem. Soc., Dalton Trans.* **1979**, 54-61.
- (233) Pauling, L. *The Nature of the Chemical Bond*; 3 ed.; Cornell University press: Ithaca, 1960.
- (234) Allred, A. L. *J. Inorg. Nucl. Chem.* **1961**, *17*, 215.
- (235) Sommerfeldt, H.-M. Master Thesis, University of Bergen, 2008.
- (236) Nakamura, H.; Nakayama, Y.; Yasuda, H.; Maruo, T.; Kanehisa, N.; Kai, Y. *Organometallics* **2000**, *19*, 5392-5399.
- (237) Evans, W. J.; Anwander, R.; Doedens, R. J.; Ziller, J. W. *Angew. Chem. Int. Ed.* **1994**, *33*, 1641.
- (238) Evans, W. J.; Anwander, R.; Ziller, J. W. *Organometallics* **1995**, *14*, 1107-1109.
- (239) Evans, W. J.; Anwander, R.; Ziller, J. W.; Khan, S. I. *Inorg. Chem.* **1995**, *34*, 5927-5930.

- (240) Klimpel, M. G.; Eppinger, J.; Sirsch, P.; Scherer, W.; Anwander, R. *Organometallics* **2002**, *21*, 4021-4023.
- (241) Anwander, R.; Klimpel, M. G.; Dietrich, H. M.; Shorokhov, D. J.; Scherer, W. *Chem. Commun.* **2003**, 1008-1009.
- (242) Anwander, R.; Runte, O.; Eppinger, J.; Gerstberger, G.; Herdtweck, E.; Spiegler, M. *J. Chem. Soc., Dalton Trans.* **1998**, 847-858.
- (243) Fischbach, A.; Eickerling, G.; Scherer, W.; Herdtweck, E.; Anwander, R. *Z. Naturf. B: Chem. Sci.* **2004**, *59*, 1353-1364.
- (244) Fischbach, A.; Perdih, F.; Sirsch, P.; Scherer, W.; Anwander, R. *Organometallics* **2002**, *21*, 4569-4571.
- (245) Nagl, I.; Widenmeyer, M.; Herdtweck, E.; Raudaschl-Sieber, G.; Anwander, R. *Microporous Mesoporous Mat.* **2001**, *44*, 311-319.
- (246) Byers, J. J.; Pennington, W. T.; Robinson, G. H.; Hrnčir, D. C. *Polyhedron* **1990**, *9*, 2205-2210.
- (247) Hess, H.; Hinderer, A.; Steinhauser, S. *Z. Anorg. Allg. Chem.* **1970**, *377*, 1-10.
- (248) McLaughlin, G. M.; Smith, J. D.; Sim, G. A. *J. Chem. Soc., Dalton Trans.* **1972**, 2197.
- (249) Klimpel, M. G. Dr. Thesis, Technische Universität München, 2001.
- (250) Holton, J.; Lappert, M. F.; Ballard, D. G. H.; Pearce, R.; Atwood, J. L.; Hunter, W. E. *J. Chem. Soc., Chem. Commun.* **1976**, 425-426.
- (251) Busch, M. A.; Harlow, R.; Watson, P. L. *Inorg. Chim. Acta* **1987**, *140*, 15-20.
- (252) Evans, W. J.; Kozimor, S. A.; Brady, J. C.; Davis, B. L.; Nyce, G. W.; Seibel, C. A.; Ziller, J. W.; Doedens, R. J. *Organometallics* **2005**, *24*, 2269-2278.
- (253) Dietrich, H. M.; Zapilko, C.; Herdtweck, E.; Anwander, R. *Organometallics* **2005**, *24*, 5767-5771.
- (254) Dietrich, H. M.; Schuster, O.; Törnroos, K. W.; Anwander, R. *Angew. Chem. Int. Ed.* **2006**, *45*, 4858-4863.

- (255) Evans, W. J.; Chamberlain, L. R.; Ulibarri, T. A.; Ziller, J. W. *J. Am. Chem. Soc.* **1988**, *110*, 6423-6432.
- (256) Dietrich, H. M.; Törnroos, K. W.; Anwander, R., unpublished results.
- (257) Le Roux, E.; Nief, F.; Jaroschik, F.; Törnroos, K. W.; Anwander, R. *Dalton Trans.* **2007**, 4866-4870.
- (258) Dietrich, H. M.; Herdtweck, E.; Törnroos, K. W.; Anwander, R., unpublished results.
- (259) Watson, P. L.; Parshall, G. W. *Acc. Chem. Res.* **1985**, *18*, 51-56.
- (260) Watson, P. L. *J. Am. Chem. Soc.* **1982**, *104*, 337-339.
- (261) Watson, P. L.; Roe, D. C. *J. Am. Chem. Soc.* **1982**, *104*, 6471-6473.
- (262) Burger, B. J.; Thompson, M. E.; Cotter, W. D.; Bercaw, J. E. *J. Am. Chem. Soc.* **1990**, *112*, 1566.
- (263) Brintzinger, H. H.; Fischer, D.; Mühlhaupt, R.; Rieger, B.; Waymouth, R. W. *Angew. Chem. Int. Ed. Engl.* **1995**, *34*, 1143.
- (264) Bochmann, M. *J. Organomet. Chem.* **2004**, 689, 3982.
- (265) Bochmann, M.; Lancaster, S. J. *Angew. Chem. Int. Ed. Engl.* **1994**, *33*, 1634.
- (266) Britovsek, P.; Cohen, S. A.; Gibson, V. C.; van Meurs, M. *J. Am. Chem. Soc.* **2004**, *126*, 10701.
- (267) Petros, R. A.; Norton, J. R. *Organometallics* **2004**, *23*, 5105.
- (268) Lyakin, O. Y.; Bryliakov, K. P.; Semikolenova, N. M.; Lebedev, A. Y.; Voskoboynikov, A. Z.; Zakharov, V. A.; Talsi, E. P. *Organometallics* **2007**, *26*, 1536.
- (269) Tebbe, F. N.; Parshall, G. W.; Reddy, G. S. *J. Am. Chem. Soc.* **1978**, *100*, 3611.
- (270) Dietrich, H. M.; Törnroos, K. W.; Anwander, R. *J. Am. Chem. Soc.* **2006**, *128*, 9298-9299.
- (271) Kickham, J. E.; Guérin, F.; Stephan, D. *J. Am. Chem. Soc.* **2002**, *124*, 11486.

- (272) Guérin, F.; Stephan, D. *Angew. Chem. Int. Ed.* **1999**, *38*, 3698.
- (273) Kickham, J. E.; Guérin, F.; Steward, J. C.; Stephan, D. *Angew. Chem. Int. Ed.* **2000**, *39*, 3263.
- (274) Wei, P.; Stephan, D. *Organometallics* **2003**, *22*, 1992.
- (275) Friebe, L.; Nuyken, O.; Obrecht, W. *Adv. Polym. Sci.* **2006**, *204*, 1.
- (276) Fischbach, A.; Anwander, R. *Adv. Polym. Sci.* **2006**, *204*, 155.
- (277) Taube, R.; Sylvester, G. In *Applied Homogeneous Catalysis with Organometallic Compounds*; Cornils, B., Herrmann, W. A., Eds.; Wiley-VCH: Weinheim, 2002.
- (278) Hou, Z.; Luo, Y.; Li, X. *J. Organomet. Chem.* **2006**, *691*, 3114.
- (279) Kim, J. S.; Wojcinski II, L. M.; Liu, S.; Sworen, J. C.; Sen, A. *J. Am. Chem. Soc.* **2000**, *122*, 5668.
- (280) Klosin, J.; Roof, G. R.; Chen, E. Y.-X. *Organometallics* **2000**, *19*, 4684.
- (281) Bochmann, M.; Sarsfield, M. *J. Organometallics* **1998**, *17*, 5908.
- (282) Hayes, P. G.; Piers, W. E.; Parvez, M. *Organometallics* **2005**, *24*, 1173.

Paper I

Homoleptic Rare-Earth Metal(III) Tetramethylaluminates: Structural Chemistry, Reactivity, and Performance in Isoprene Polymerization

Melanie Zimmermann,^[a] Nils Åge Frøystein,^[a] Andreas Fischbach,^[b] Peter Sirsch,^[c] H. Martin Dietrich,^[a] Karl W. Törnroos,^[a] Eberhardt Herdtweck,^[d] and Reiner Anwander*^[a]

Abstract: The complexes $[\text{Ln}(\text{AlMe}_4)_3]$ ($\text{Ln} = \text{Y}, \text{La}, \text{Ce}, \text{Pr}, \text{Nd}, \text{Sm}, \text{Ho}, \text{Lu}$) have been synthesized by an amide elimination route and the structures of $[\text{Lu}\{(\mu\text{-Me})_2\text{AlMe}_2\}_3]$, $[\text{Sm}\{(\mu\text{-Me})_2\text{AlMe}_2\}_3]$, $[\text{Pr}\{(\mu\text{-Me})_2\text{AlMe}_2\}_3]$, and $[\text{La}\{(\mu\text{-Me})_2\text{AlMe}_2\}_2\{(\mu\text{-Me})_3\text{AlMe}\}]$ determined by X-ray crystallography. These structures reveal a distinct Ln^{3+} cation size-dependency. A comprehensive insight into the intrinsic properties and solution coordination phenomena of $[\text{Ln}(\text{AlMe}_4)_3]$ complexes has been gained from extended dynamic ^1H and ^{13}C NMR spectroscopic studies, as well as 1D ^{89}Y , 2D $^1\text{H}/^{89}\text{Y}$, and ^{27}Al NMR spectroscopic investigations. $[\text{Ce}(\text{AlMe}_4)_3]$ and $[\text{Pr}(\text{AlMe}_4)_3]$ have been used as alkyl precursors for the synthesis of heterobimetallic alkylated rare-

earth metal complexes. Both carboxylate and siloxide ligands can be introduced by methane elimination reactions that give the heterobimetallic complexes $[\text{Ln}\{(\text{O}_2\text{C}\text{Ar}^{\text{Pr}})_2(\mu\text{-AlMe}_2)\}_2(\text{AlMe}_4)(\text{C}_6\text{H}_{14})_n]$ and $[\text{Ln}\{\text{OSi}(\text{O}t\text{Bu})_3\}(\text{AlMe}_3)(\text{AlMe}_4)_2]$, respectively. $[\text{Pr}\{\text{OSi}(\text{O}t\text{Bu})_3\}(\text{AlMe}_3)(\text{AlMe}_4)_2]$ has been characterized by X-ray structure analysis. All of the cerium and praseodymium complexes are used as precatalysts in the stereospecific polymerization of isoprene (1–3 equivalents of Et_2AlCl as co-catalyst) and compared to the corresponding neodymi-

um-based initiators reported previously. The superior catalytic performance of the homoleptic complexes leads to quantitative yields of high-*cis*-1,4-polyisoprene (>98%) in almost all of the polymerization experiments. In the case of the binary catalyst mixtures derived from carboxylate or siloxide precatalysts quantitative formation of polyisoprene is only observed for $n_{\text{Ln}}:n_{\text{Cl}} = 1:2$. The influence of the metal size is illustrated for the heterobimetallic lanthanum, cerium, praseodymium, neodymium, and gadolinium carboxylate complexes, and the highest activities are observed for praseodymium as a metal center in the presence of one equivalent of Et_2AlCl .

Keywords: aluminum • homogeneous catalysis • lanthanides • NMR spectroscopy • polymerization

Introduction

Since the first successful isolation of organometallic derivatives of the rare-earth elements (Ln),^[1] the synthesis of homoleptic alkyl complexes (LnR_3) has posed a continual challenge in the field of experimental organolanthanide chemistry.^[2–4] Simple alkyl ligands such as methyl and ethyl have been found to be incapable of coping with the stereoelectronic demands of the large and highly oxophilic Ln^{3+} metal centers, and it was not until the late 1980s that donor-free LnR_3 compounds containing very bulky alkyl ligands ($\text{R} = \text{CH}(\text{SiMe}_3)_2$) were isolated and characterized.^[5] Donor (D)-solvated alkyl derivatives $[\text{LnR}_3(\text{D})_n]$ are routinely used as precursor compounds for the synthesis of heteroleptic derivatives $[\text{L}_x\text{LnR}_y(\text{D})_m]$ ($x + y = 3$) that provide an efficient entry into organolanthanide-based catalysis as well as unique model systems for studying elementary processes in

[a] M. Zimmermann, Dr. N. Å. Frøystein, Dr. H. M. Dietrich, Prof. Dr. K. W. Törnroos, Prof. Dr. R. Anwander
Department of Chemistry, University of Bergen
Allégaten 41, 5007 Bergen (Norway)
Fax: (+47)555-89-490
E-mail: reiner.anwander@kj.uib.no

[b] Dr. A. Fischbach
Current address: OXEA Deutschland GmbH
Otto-Roelen-Strasse 3, 46147 Oberhausen (Germany)

[c] Dr. P. Sirsch
Department of Chemistry, University of New Brunswick
Fredericton, NB E3B 6E2 (Canada)

[d] Dr. E. Herdtweck
Department Chemie, Lehrstuhl für Anorganische Chemie
Technische Universität München
Lichtenbergstrasse 4, 85747 Garching bei München (Germany)

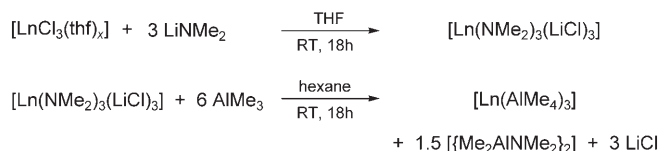
olefin polymerization.^[4] However, their implementation in this area has been hampered by several factors. Thus, besides the formation of polymeric network structures,^[6] “ate” complexes,^[7] and the need for stabilizing donor molecules,^[8–11] the availability and stability of rare-earth metal alkyl precursors is very much dependent on the size of the Ln³⁺ ion. To date, [LnMe₃]_x (Ln=Y, Ho, Lu),^[6] [Ln(CH₂SiMe₃)₃(thf)_x] (Ln=Sc, Y, Er, Yb, Lu, x=2; Ln=Y, Sm, x=3),^[8] [Ln(CH₂SiMe₂Ph)₃(thf)₂] (Ln=Sc, Y),^[9] [Ln(CH₂tBu)₃(thf)₂] (Ln=Sc, Y, Yb),^[8a,10] [La(CH₂Ph)₃(thf)₃], [La(CH₂Ph-4-Me)₃(thf)₃],^[11] [La{CH(PPh₂)₂}₃],^[12] [Ln(*o*-Me₂NC₆H₄CH₂)₃] (Ln=Sc, Y, La, Lu),^[13] and [Ln{CH(SiMe₃)₂}₃] (Ln=Y, La, Nd, Sm, Lu)^[5] are the only fully characterized rare-earth metal tris(alkyl) complexes. Their suitability for alkane-elimination reactions, however, is affected by the low stability and unavailability of the envisaged large or small Ln³⁺ ion in many cases.

Homoleptic tris(tetramethylaluminate) complexes [Ln(AlMe₄)₃] found entry into organolanthanide synthesis only recently, some 10 years after their discovery.^[14,15] Their straightforward high-yield synthesis and their availability for the entire Ln³⁺ size-range, except scandium, without ate complex formation make these “metal alkyls in disguise” versatile synthetic precursors for the generation of a variety of heterobimetallic Ln/Al complexes.^[16,17] Recent publications in this field have emphasized the suitability of [Ln(AlMe₄)₃] complexes for both the synthesis of half-lanthanidocene^[18] and lanthanidocene complexes^[19] and also post-lanthanidocene derivatives.^[20,21] Thus, [Ln(AlMe₄)₃] complexes can undergo protonolysis reactions—[AlMe₄][−]→[ligand-H] exchange—that lead to the formation of methane and trimethylaluminum as the only by-products,^[16,18] as well as salt-metathesis reactions involving [AlMe₄][−]→[ligand[−]] exchange.^[22] The formation of distinct heteroleptic tetramethylaluminate complexes depending on the Ln³⁺ size^[20,21] has been ascribed to different reaction pathways arising from attack at either the bridging or terminal methyl groups of a Ln-bonded [AlMe₄][−] ligand, therefore comprehensive insight into the intrinsic properties and solution/solid-state coordination phenomena of [Ln(AlMe₄)₃] complexes seems to be crucial for understanding their enhanced reactivity, be it in alkane elimination,^[23,24] methyl group transfer (alkylation) reactions,^[21] or catalytic diene polymerization.^[17]

Herein, we would like to discuss a detailed study of homoleptic rare-earth metal tris(tetramethylaluminate) complexes that involves varying the synthetic approach, several X-ray structure analyses, and dynamic and heteronuclear NMR spectroscopy. Furthermore, [Ln(AlMe₄)₃] complexes have been used as alkyl precursors for the synthesis of rare-metal metal carboxylate and siloxide tetramethylaluminate complexes and their catalytic performance as binary isoprene polymerization catalysts has been investigated.

Results and Discussion

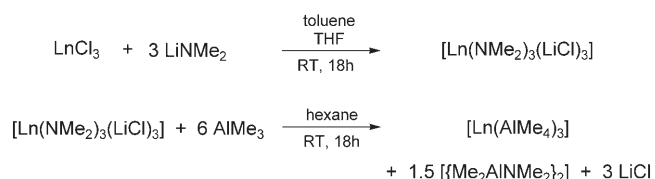
Synthesis of Ln³⁺ tetramethylaluminate complexes: The general synthesis of homoleptic [Ln(AlMe₄)₃] complexes, first reported for the metals yttrium, neodymium, and samarium in 1995 (Scheme 1),^[14,17] gave the trimethylaluminum



Scheme 1. Synthesis of homoleptic rare-metal metal(III) tetramethylaluminates (Ln=Y (**1a**), La (**1b**), Nd (**1e**), Sm (**1f**), Ho (**1g**), and Lu (**1h**)).

inclusion products [Ln(AlMe₄)₃(Al₂Me₆)_{0.5}]. The Ln³⁺ tetramethylaluminate complexes of Y (**1a**), La (**1b**), Nd (**1e**), Sm (**1f**), Ho (**1g**), and Lu (**1h**) were obtained in good overall yields by following this original procedure. Several crystallization steps were necessary to obtain crystalline, trimethylaluminum-free Ln(AlMe₄)₃ complexes, with the actual number of steps depending on the size of the Ln³⁺ ion (Lu ≫ Y, Ho > Nd, Sm, La). Compounds **1** were dried in vacuo prior to each recrystallization to allow co-crystallized AlMe₃ to evaporate. (**CAUTION:** Volatiles containing trimethylaluminum react violently when exposed to air). [Y(AlMe₄)₃] (**1a**), [Ho(AlMe₄)₃] (**1g**), and [Lu(AlMe₄)₃] (**1h**) were further purified by sublimation under the conditions reported in an earlier publication.^[6] ¹H, ¹³C, and ²⁷Al NMR spectroscopy as well as elemental analysis and IR spectroscopy confirmed the absence of AlMe₃ in complexes **1**. Due to efficient paramagnetic relaxation caused by the Ho³⁺ metal center, NMR spectroscopy was not informative for compound **1g**.

The cerium and praseodymium derivatives (**1c** and **1d**, respectively) were obtained following a slightly modified procedure (Scheme 2). Thus, commercially available anhydrous

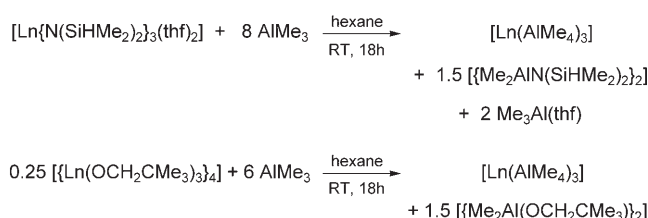


Scheme 2. Synthesis of homoleptic rare-earth metal(III) tetramethylaluminates (Ln=Ce (**1c**), Pr (**1d**)).

metal trichlorides were used without previous activation by Soxhlet extraction.^[25] After slow addition of THF to their toluene suspensions, three equivalents of solid LiNMe₂ were added to generate the dimethylamido ate complexes [Ln(NMe₂)₃(LiCl)₃]. A subsequent AlMe₃-mediated [NMe₂][−]→[AlMe₄][−] exchange in hexane gave compounds **1c** and **1d** in good yields. These tetramethylaluminate complexes were obtained as pale yellow (**1c**, 67%) or pale green (**1d**, 74%)

needles by recrystallization from saturated hexane solutions at -30°C . Their compositions were confirmed by ^1H , ^{13}C , and ^{27}Al NMR spectroscopy (**1d**), elemental analysis, and IR spectroscopy. Due to efficient paramagnetic relaxation caused by the Ce^{3+} metal center, NMR spectroscopy was not informative for **1c**.

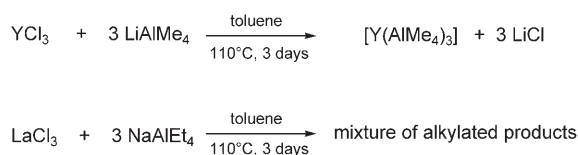
The high volatility of the alkylated amide by-product $[\{\text{Me}_2\text{AlNMe}_2\}_2]$ is one of the main advantages of this synthetic strategy. Although tetramethylaluminates are accessible by alkylation of a number of other Ln^{3+} precursor compounds, such as the readily available silylamide complexes $[\text{Ln}\{\text{N}(\text{SiHMe}_2)_2(\text{thf})\}_2]$ ^[26] or the tetrameric rare-earth metal neopentolates $[\{\text{Ln}(\text{OCH}_2\text{CMe}_3)_3\}_4]$,^[27] separation of the desired products from the alkylated by-products $[\{\text{Me}_2\text{AlN}(\text{SiHMe}_2)_2\}_2]$ and $[\{\text{Me}_2\text{Al}(\text{OCH}_2\text{CMe}_3)_2\}_2]$, respectively, which are non-volatile at ambient temperature, can prove difficult. For example, several recrystallizations from hexane solution at -30°C are necessary to give pure $[\text{Y}\{(\mu\text{-Me})_2\text{AlMe}_2\}_3]$ when synthesized according to Scheme 3. Fur-



Scheme 3. Alternative syntheses of homoleptic rare-earth metal tetramethylaluminates.

thermore, due to the higher bond energies of $[\text{Ln}-\text{O}]$ versus $[\text{Ln}-\text{N}]$ moieties, much larger excesses of AlMe_3 than the theoretical amount of six equivalents (Scheme 3) have to be added to give complexes **1** in acceptable yields.

We also examined the feasibility of salt-metathesis reactions as one-step synthetic protocols for the preparation of complexes **1**. Thus, anhydrous (non-activated) YCl_3 and three equivalents of lithium tetramethylaluminate (LiAlMe_4) were suspended in a small amount of toluene and heated to 110°C . However, after three days only 7% of $[\text{Y}\{(\mu\text{-Me})_2\text{AlMe}_2\}_3]$ (**1a**) had formed as the only hexane-soluble rare-earth metal-containing product (Scheme 4). At-



Scheme 4. Attempted syntheses of homoleptic rare-earth metal tetraalkylaluminate complexes by direct salt metathesis routes.

tempts to synthesize the derivatives of the larger metals lanthanum and praseodymium failed. The reaction of anhydrous LaCl_3 with three equivalents of the toluene-soluble

sodium tetraethylaluminate (NaAlEt_4), on the other hand, gave a small amount of a mixture of alkylated products (Scheme 4). Crystallization of the resulting products did not prove possible due to their high solubility.

X-ray crystallographic studies of $\text{Ln}(\text{AlMe}_4)_3$: Single crystals of the homoleptic lutetium (**1h**), samarium (**1f**), praseodymium (**1d**), and lanthanum (**1b**) tetramethylaluminates suitable for X-ray crystallographic structure determinations were grown from saturated hexane solutions at -30°C . This series covers the entire Ln^{3+} size range and thus allows an insight into any size-dependent aluminate coordination in the solid state. Isostructural $[\text{Lu}\{(\mu\text{-Me})_2\text{AlMe}_2\}_3]$ (**1h**) and $[\text{Sm}\{(\mu\text{-Me})_2\text{AlMe}_2\}_3]$ (**1f**), which represent the small to middle-sized Ln^{3+} ions, crystallize in the centrosymmetric space group $C2/c$ (Figure 1, Table 1).

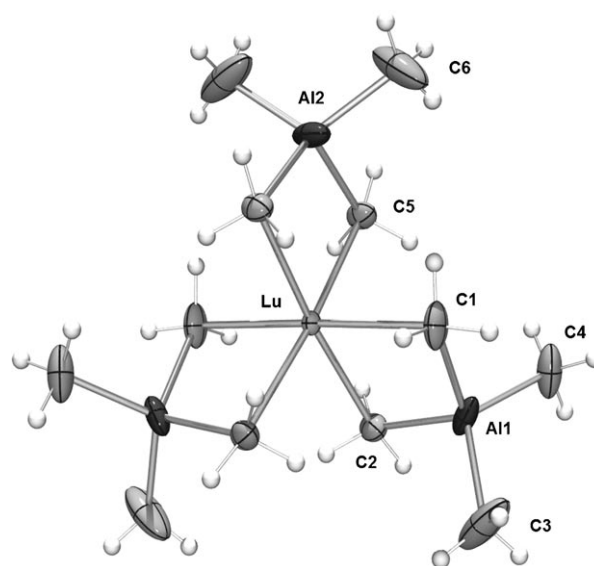


Figure 1. Molecular structure of **1h** (atomic displacement parameters set at the 50% level).

$[\text{Pr}\{(\mu\text{-Me})_2\text{AlMe}_2\}_3]$ (**1d**), which features a slightly larger Pr^{3+} metal center (compared to Sm^{3+}), is isostructural with the previously reported neodymium derivative **1e** (monoclinic space group $P2_1/c$)^[14] and crystallizes with two independent molecules in the unit cell (Figure 2, Table 2).

The solid-state structures of $[\text{Ln}(\text{AlMe}_4)_3]$ complexes ($\text{Ln} = \text{Lu}, \text{Sm}, \text{Pr}, \text{Nd}$) show a sixfold coordination of carbon atoms around the Ln^{3+} metal centers which results in a pseudo-octahedral geometry. Each $[\text{AlMe}_4]$ unit is coordinated to the central Ln metal through two methyl groups that bridge in an η^2 fashion and form planar or almost planar $[\text{Ln}(\mu\text{-CH}_3)_2\text{Al}]$ metallacycles (max. departure from least-squares planes: **1d**: $-0.054(1)$ (Al4); **1f**: $-0.0126(5)$ (Al1); **1h**: $0.001(1)$ Å (Al1)). Notably, the deviation from planarity, that is, the bending of the tetramethylaluminate ligand, increases with increasing metal size ($\text{Pr}^{3+} \approx \text{Nd}^{3+} > \text{Sm}^{3+} > \text{Lu}^{3+}$). All hydrogen atoms at the bridging methyl

Table 1. Selected bond lengths [Å] and angles [°] in compounds **1f** and **1h**.^[a]

| | [Sm(AlMe ₄) ₃] (1f) | [Lu(AlMe ₄) ₃] (1h) |
|------------|--|--|
| Ln–C1 | 2.566(1) | 2.466(2) |
| Ln–C2 | 2.573(1) | 2.471(2) |
| Ln–C5 | 2.555(1) | 2.455(2) |
| Al1–C1 | 2.086(1) | 2.084(2) |
| Al1–C2 | 2.084(1) | 2.078(2) |
| Al1–C3 | 1.968(2) | 1.961(4) |
| Al1–C4 | 1.964(2) | 1.964(2) |
| Al2–C5 | 2.091(2) | 2.089(2) |
| Al2–C6 | 1.963(2) | 1.961(5) |
| Ln–Al1 | 3.1323(3) | 3.0176(5) |
| Ln–Al2 | 3.1207(5) | 3.0062(8) |
| C1–Ln–C2 | 82.87(3) | 86.30(7) |
| C1–Ln–C5 | 92.33(4) | 89.01(7) |
| C1–Ln–C5' | 90.25(4) | 92.30(7) |
| C5–Ln–C5' | 83.55(5) | 87.05(7) |
| C1–Al1–C2 | 109.31(4) | 108.44(9) |
| C5–Al2–C5' | 108.93(6) | 108.08(5) |
| C3–Al1–C4 | 118.69(6) | 118.7(1) |
| C6–Al2–C6' | 119.9(1) | 119.7(2) |

[a] Symmetry codes for equivalent atoms ('): $-x+1, y, 1/2-z$ for **1f** and $-x, y, 1/2-z$ for **1h**.

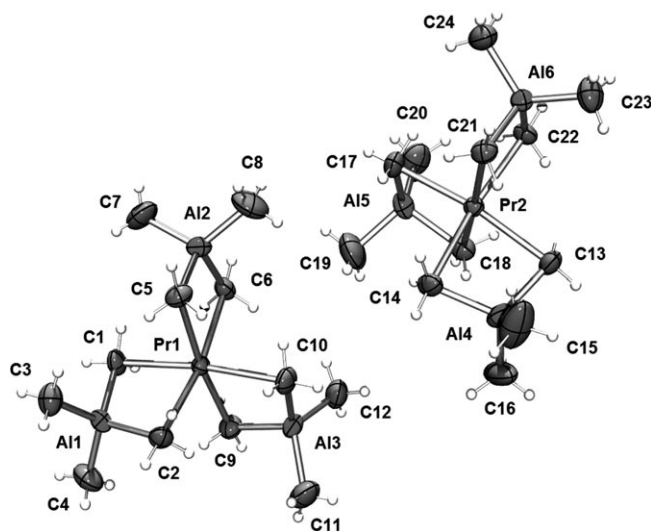


Figure 2. Molecular structure of **1d** (atomic displacement parameters set at the 50% level).

groups were located and refined to give five-coordinate carbon atoms with a heavily distorted trigonal-bipyramidal coordination geometry. Due to the steric unsaturation of the rare-earth metal center, two of the three H atoms in each bridging methyl group are directed toward the Ln atom. These hydrogen atoms and the aluminum occupy the equatorial positions of the trigonal bipyramid whereas the third hydrogen and the Ln metal are in the apical positions (e.g., Lu–C1–H13 169(2)°; Sm1–C1–H1B 168(1)°; Pr1–C1–H1C 172(2)°). The Ln–C(μ -Me) and Ln–Al bond lengths increase with increasing Ln³⁺ size but are shorter than the bonds in their half-metallocene [(C₅Me₅)Lu{(μ-Me)₂-AlMe₂}]₂ (av. Lu–C(μ) 2.505(3) and Lu–Al 3.0612(9) Å)^[28]

and metallocene [(C₅Me₅)₂Sm{(μ-Me)AlMe₂(μ-Me)}₂Sm(C₅Me₅)₂] (av. Sm–C(μ) 2.75(1) and av. Sm–Al 4.792(5) Å)^[29] derivatives. In accordance with the larger size of the Pr³⁺ ion compared to the neodymium derivative,^[14] all of the Pr–C(μ -Me) bonds are slightly elongated (av. 2.604 Å (**1d**) vs. 2.589 Å (**1e**)).

[La(AlMe₄)₃] (**1b**), which contains the largest Ln³⁺ ion, crystallizes in the monoclinic space group *P*2₁/*n* with only one molecule in the unit cell. It exhibits an extraordinary solid-state structure (Figure 3) that features three different [AlMe₄] coordination modes in a single molecule, namely [La{(μ-Me)₂AlMe₂}]₂{(μ-Me)₃AlMe}. One AlMe₄[−] ligand coordinates in the routinely observed η² fashion to form an almost planar heterobimetallic [La(μ-CH₃)₂Al] unit with a La1–C1–Al1–C2 torsion angle of 2.1(1)°. The second AlMe₄[−] ligand shows a bent η²-coordination (La1–C9–Al3–C10 49.0(1)°) with an additional La–(μ-CH₃) contact (La1–C11 3.154(3) Å). The La–(μ-CH₃) bond lengths in this bent AlMe₄[−] ligand are elongated ($\Delta_{\text{La-C}}$ is approximately 0.119 Å) and the La1–Al3 distance is shortened ($\Delta_{\text{La-Al}}$ is approximately 0.232 Å). A similar structural motif has previously been found in the solid-state structures of [(C₅Me₅)La(AlMe₄)₂]^[18] and [(C₅Me₅)Lu(AlMe₄)₂]^[28]. Interestingly, the third AlMe₄[−] ligand coordinates through three bridging methyl groups to the lanthanum metal center. The La–(μ-CH₃) bonds (av. 2.882(6) Å) of this η³-coordinated ligand are significantly longer than the bonds of the η²-coordinated [AlMe₄] moieties in **1b** and [(C₅Me₅)La(AlMe₄)₂] (av. 2.749(7) Å).^[18] In contrast, the La1–Al2 distance is shorter (2.995(1) Å) than the La1–Al1 (3.264(1) Å) and La1–Al3 (3.032(1) Å) distances. The differently coordinated tetramethylaluminate ligands lead to a coordination number of between seven and eight. As a comparison, chloroaluminate complexes of the type [Ln(AlCl₄)₃] (Ln = Tb, Dy, Ho) exhibit a coordination number of eight by adopting a square-antiprismatic coordination geometry.^[30] Very recently, the only other solid-state structure featuring such a true η³-coordination of an [AlMe₄] group to a rare-earth metal center was reported for the pentaneodymium cluster [Cp*₅Nd₅{(μ-Me)₃AlMe}(μ₄-Cl)(μ₃-Cl)₂(μ₂-Cl)₆].^[31] The solid-state structure of [La{(μ-Me)₂AlMe₂}]₂{(μ-Me)₃AlMe} proves the high coordinational flexibility of the tetramethylaluminate ligand and its ability to adapt perfectly to the given stereoelectronic requirements of the rare-earth metal center.

NMR spectroscopic investigations of [Ln(AlMe₄)₃]

Variable-temperature NMR studies and dynamic behavior: Despite their different solid-state structures, the ¹H NMR spectra of [Ln{(μ-Me)₂AlMe₂}]₃ (Ln = Lu, Y, Sm, Nd) and [La{(μ-Me)₂AlMe₂}]₂{(μ-Me)₃AlMe} show only one signal for the [AlMe₄] moieties at ambient temperature. This is indicative of a very fast exchange of bridging and terminal methyl groups. However, two different types of methyl groups with an integral ratio of 1:1 could be resolved at lower temperature for the smaller Ln³⁺ complexes (Figure 4). Variable-temperature (VT) ¹H NMR experi-

Table 2. Selected bond lengths [\AA] and angles [$^\circ$] in compounds **1e**^[14] and **1d**.

| | [Nd(AlMe ₄) ₃] (1e) molecule 1 | [Pr(AlMe ₄) ₃] (1d) | | [Nd(AlMe ₄) ₃] (1e) molecule 2 | [Pr(AlMe ₄) ₃] (1d) |
|------------|--|--|-------------|--|--|
| Ln1–C1 | 2.578(13) | 2.603(3) | Ln2–C13 | 2.581(14) | 2.604(3) |
| Ln1–C2 | 2.563(14) | 2.593(3) | Ln2–C14 | 2.596(13) | 2.606(3) |
| Ln1–C5 | 2.605(13) | 2.618(3) | Ln2–C17 | 2.566(14) | 2.616(3) |
| Ln1–C6 | 2.609(14) | 2.615(3) | Ln2–C18 | 2.595(14) | 2.595(3) |
| Ln1–C9 | 2.601(14) | 2.606(3) | Ln2–C21 | 2.594(13) | 2.594(3) |
| Ln1–C10 | 2.595(13) | 2.601(3) | Ln2–C22 | 2.588(13) | 2.619(3) |
| Al1–C1 | 2.067(14) | 2.087(3) | Al4–C13 | 2.075(14) | 2.085(3) |
| Al1–C2 | 2.078(14) | 2.092(3) | Al4–C14 | 2.076(13) | 2.082(3) |
| Al1–C3 | 1.956(16) | 1.958(3) | Al4–C15 | 1.971(18) | 1.952(3) |
| Al1–C4 | 1.967(14) | 1.961(3) | Al4–C16 | 1.944(15) | 1.961(3) |
| Ln1–Al1 | 3.149(4) | 3.1733(8) | Ln2–Al4 | 3.144(4) | 3.1665(7) |
| Ln1–Al2 | 3.153(5) | 3.1700(8) | Ln2–Al5 | 3.170(4) | 3.1866(7) |
| Ln1–Al3 | 3.155(5) | 3.1735(8) | Ln2–Al6 | 3.159(4) | 3.1784(7) |
| C1–Ln1–C2 | 81.8(4) | 81.82(8) | C13–Ln2–C14 | 82.0(4) | 81.63(8) |
| C1–Ln1–C5 | 92.2(4) | 92.35(8) | C13–Ln2–C17 | 94.7(4) | 93.82(9) |
| C1–Ln1–C6 | 173.2(4) | 172.67(9) | C13–Ln2–C18 | 174.4(5) | 173.50(9) |
| C1–Ln1–C9 | 92.6(4) | 93.06(8) | C13–Ln2–C21 | 92.4(4) | 92.21(9) |
| C1–Ln1–C10 | 93.9(4) | 93.55(9) | C13–Ln2–C22 | 91.2(4) | 91.19(9) |
| C5–Ln1–C6 | 82.0(4) | 81.19(9) | C17–Ln2–C18 | 81.0(4) | 81.39(9) |
| C9–Ln1–C10 | 82.5(4) | 81.33(9) | C21–Ln2–C22 | 81.4(4) | 81.22(8) |
| C1–Al1–C2 | 108.6(6) | 109.05(10) | C13–Al4–C14 | 109.8(5) | 109.63(10) |
| C1–Al1–C3 | 107.3(6) | 106.66(12) | C13–Al4–C15 | 106.8(7) | 106.22(15) |
| C1–Al1–C4 | 107.4(6) | 107.68(13) | C13–Al4–C16 | 107.6(7) | 107.42(13) |
| C3–Al1–C4 | 118.9(7) | 119.07(14) | C15–Al4–C16 | 119.1(8) | 119.15(16) |

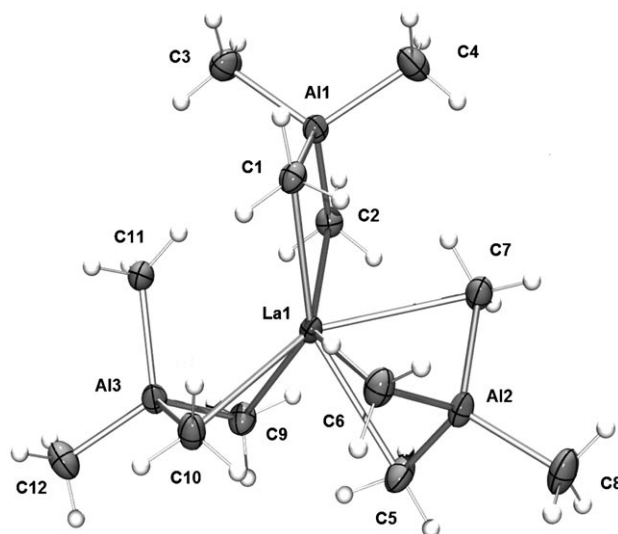


Figure 3. Molecular structure of **1b** (atomic displacement parameters set at the 50% level). Selected bond lengths [\AA] and angles [$^\circ$]: La1–C1 2.696(3), La1–C2 2.701(3), La1–C5 2.772(3), La1–C6 2.980(3), La1–C7 2.892(3), La1–C9 2.735(3), La1–C10 2.902(3), La1–C11 3.154(3), Al1–C1 2.080(3), Al1–C2 2.080(3), Al1–C3 1.972(3), Al1–C4 1.965(4), Al2–C5 2.056(4), Al2–C6 2.040(4), Al2–C7 2.036(4), Al2–C8 1.959(4), Al3–C9 2.072(4), Al3–C10 2.048(4), Al3–C11 2.001(3), Al3–C12 1.955(4), La1–Al1 3.264(1), La1–Al2 2.996(1), La1–Al3 3.032(1); C1–La1–C2 78.8(1), C1–La1–C5 114.4(1), C1–La1–C6 143.3(1), C1–La1–C7 80.3(1), C1–La1–C9 139.4(1), C1–La1–C10 80.9(1), C1–Al1–C2 110.9(2), C1–Al1–C3 106.6(2), C1–Al1–C4 109.2(2), C3–Al1–C4 114.3(2), C5–Al2–C6 107.1(1), C5–Al2–C7 103.6(2), C5–Al2–C8 112.5(2), C6–Al2–C8 112.6(2), C7–Al2–C8 114.8(2), C9–Al3–C10 108.1(2), C9–Al3–C11 103.8(2), C9–Al3–C12 112.7(2), C10–Al3–C11 106.1(2), C10–Al3–C12 110.55(2).

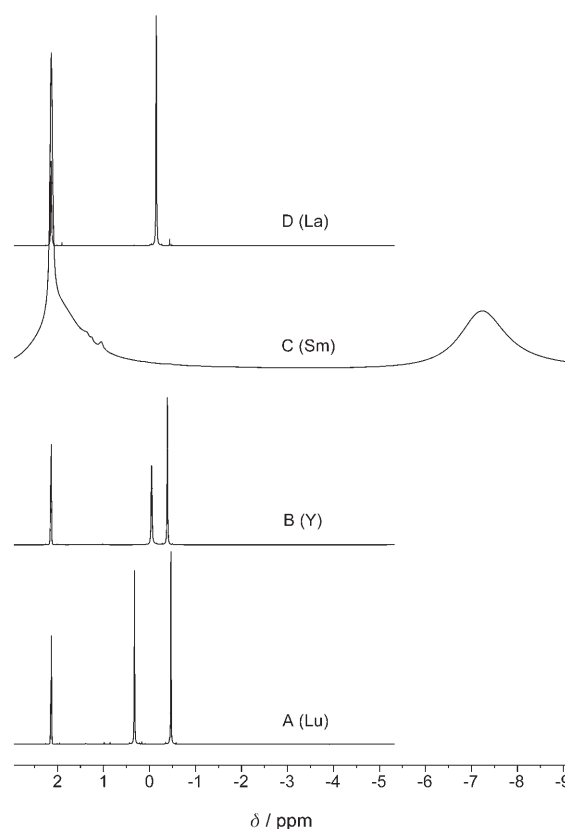


Figure 4. Low-temperature ^1H NMR spectra (500.13 MHz) of the methyl groups in A) [Lu(AlMe₄)₃] (225 K), B) [Y(AlMe₄)₃] (193 K), C) [Sm(AlMe₄)₃] (191 K), and D) [La(AlMe₄)₃] (193 K) in [D₈]toluene (the residual protons of the toluene methyl group appear at $\delta = 2.1$ ppm).

ments in $[D_8]$ toluene revealed decoalescence of the methyl resonances at a temperature, T_c , that decreases with increasing Ln^{3+} size ($Lu=278 > Y=229 > Sm=216$ K). This is consistent with increased steric unsaturation and therefore more rapid alkyl exchange at the larger rare-earth metal centers.

Narrow signals with a 1:1 integral ratio for the two different methyl groups of $[Ln(\mu-Me)_2AlMe_2]_3$ ($Ln=Lu, Y, Sm$) were observed below 193 K (Figure 4). Broadening of the low-field methyl resonance of $[Y\{(\mu-Me)_2AlMe_2\}_3]$ due to a two-bond $^1H-^{89}Y$ scalar coupling ($^2J_{Y,H}=2.5$ Hz) was observed; this clearly shows that this signal is that of the bridging $[(\mu-Me)_2Al]$ moiety. Signal splitting of a considerably narrowed 1H NMR resonance of the methyl groups occurred at temperatures well above coalescence (Figure 5a). This splitting, which reached optimal resolution at approximately 316 K, is clearly attributable to $^2J_{Y,H}$ coupling. Exceedingly fast methyl group exchange effectively decouples the proton resonance at even higher temperatures, and at 348 K only a narrow singlet appears. It is noteworthy that the ^{13}C NMR spectrum at 193 K also shows two signals at $\delta=13.7$ and -8.5 ppm (Figure 5b). A $^{13}C-^{89}Y$ scalar cou-

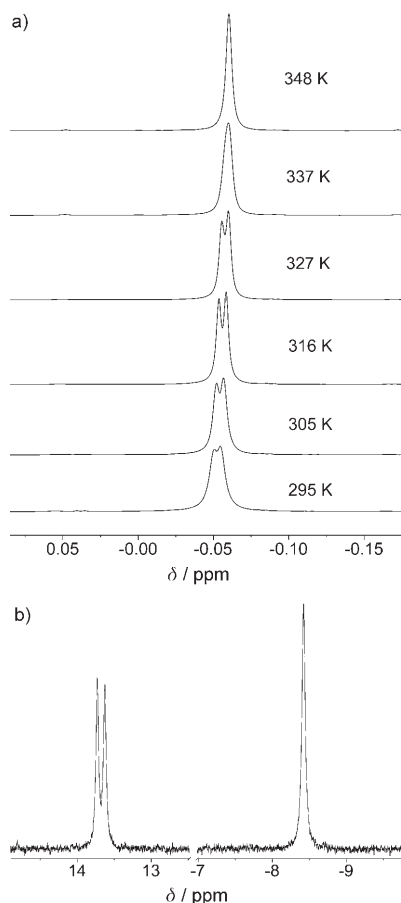


Figure 5. a) Variable-temperature 1H NMR spectra (500.13 MHz) of $[Y\{(\mu-Me)_2AlMe_2\}_3]$ (**1a**) dissolved in $[D_3]$ chlorobenzene in the temperature range 295–348 K; b) ^{13}C NMR spectrum (125.77 MHz) of **1a** dissolved in $[D_8]$ toluene at 193 K.

pling ($^1J_{Y,C}=12.8$ Hz) unambiguously confirms the low-field resonance as being that of the bridging $[(\mu-Me)_2Al]$ moiety. No decoalescence of the $[AlMe_4]$ resonance was observed in the accessible temperature range (down to 183 K) for the largest lanthanide metal centers (Pr, Nd, and La). These findings are in good agreement with earlier investigations on the thermal behavior of $[Ln(AlMe_4)_3]$ complexes.^[14]

Structural evidence for a η^3 - $[AlMe_4]$ coordination in the solid state (see above) and the highly fluxional behavior of compounds **1** in solution suggest transient η^3 -coordinated $[AlMe_4]$ moieties for the larger Ln centers. A sterically unsaturated rare-earth metal center therefore allows for an associative methyl exchange, as depicted on the right-hand side of Figure 6, whereas in sterically hindered complexes

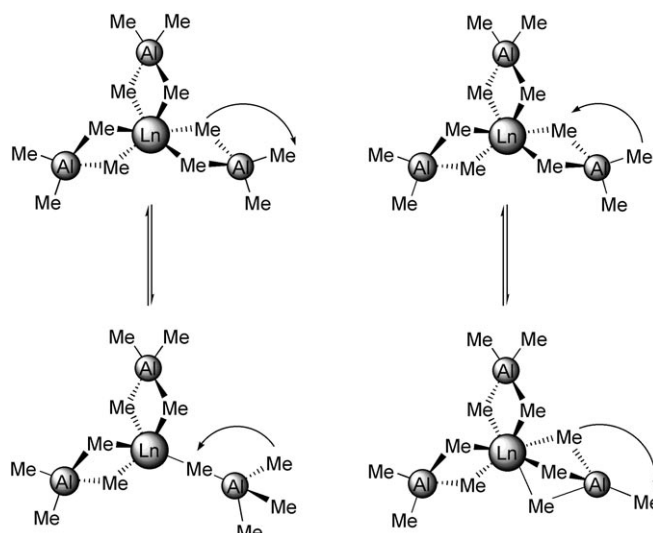


Figure 6. Dissociative (left) versus associative methyl exchange (right) in homoleptic $[Ln(AlMe_4)_3]$ complexes.

such as $[\{(O_2CAR^{iPr})_2(\mu-AlMe_2)_2\}Y(AlMe_4)]^{[16]}$ (**2a**) and $[Al_2Me_6]^{[32]}$ intramolecular methyl group exchange occurs via a dissociative mechanism with transient η^1 -coordinated $[AlMe_4]$ moieties, as shown on the left-hand side of Figure 6. The existence of such η^1 -coordinated tetramethylaluminum ligands was recently confirmed by the solid-state structure of the diamidopyridine complex $[(NNN)La\{(\mu-Me)AlMe_3\}(thf)]$ (NNN = diamidopyridine).^[21]

Dynamic NMR spectroscopy and line-shape analysis have proved to be a convenient tool for studying fast exchange processes in or between molecules and they have been successfully used to determine methyl exchange rates and activation parameters for several heteroleptic rare-earth metal tetramethylaluminate complexes.^[16,28,33] A better understanding of the exchange mechanisms, kinetics, and thermodynamics of the homoleptic tetramethylaluminate complexes $[Ln(AlMe_4)_3]$ could therefore be anticipated by applying dynamic NMR spectroscopy.

The 1H NMR spectra of $[Y(AlMe_4)_3]$ (**1a**), $[Sm(AlMe_4)_3]$ (**1f**), and $[Lu(AlMe_4)_3]$ (**1h**), as well as the ^{13}C NMR spectra

of $[\text{Y}(\text{AlMe}_4)_3]$ (**1a**), were examined in different temperature ranges for solutions in $[\text{D}_8]$ toluene. The rate constants of the methyl group exchange were obtained by simulating the NMR spectra with the program MEXICO.^[34] This program simulates complex exchange spectra by taking into account homonuclear as well as heteronuclear scalar coupling and variations of the relative ^1H and ^{13}C chemical shifts of the two exchanging sites with temperature. A good fit to the experimental data parameters was obtained by using a procedure based on simplex iterations with a two-site mutual exchange model. Figures 7 and 8 show the experimental and

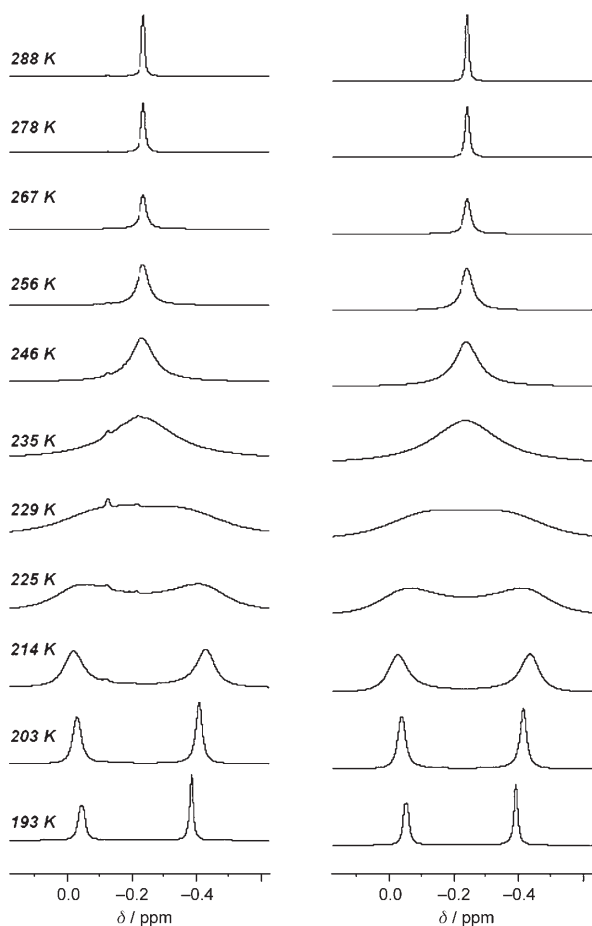


Figure 7. Experimental (left) and simulated (right) ^1H NMR spectra (500.13 MHz) of $[\text{Y}\{(\mu\text{-Me})_2\text{AlMe}_2\}_3]$ (**1a**) in $[\text{D}_8]$ toluene at different temperatures.

simulated line-shapes for the ^1H (500.13 MHz) and ^{13}C NMR (125.77 MHz) spectra of $[\text{Y}\{(\mu\text{-Me})_2\text{AlMe}_2\}_3]$ (**1a**), respectively, at varying temperatures. The rate constants and values of the relevant thermodynamic parameters obtained in this work are summarized in Tables 3 and 4.

Even though the signal-to-noise ratios of some of the ^{13}C NMR spectra are very low, most notably close to coalescence, the calculated exchange rates show reasonable correspondence with those obtained by fitting the exchange model to the ^1H NMR spectra.

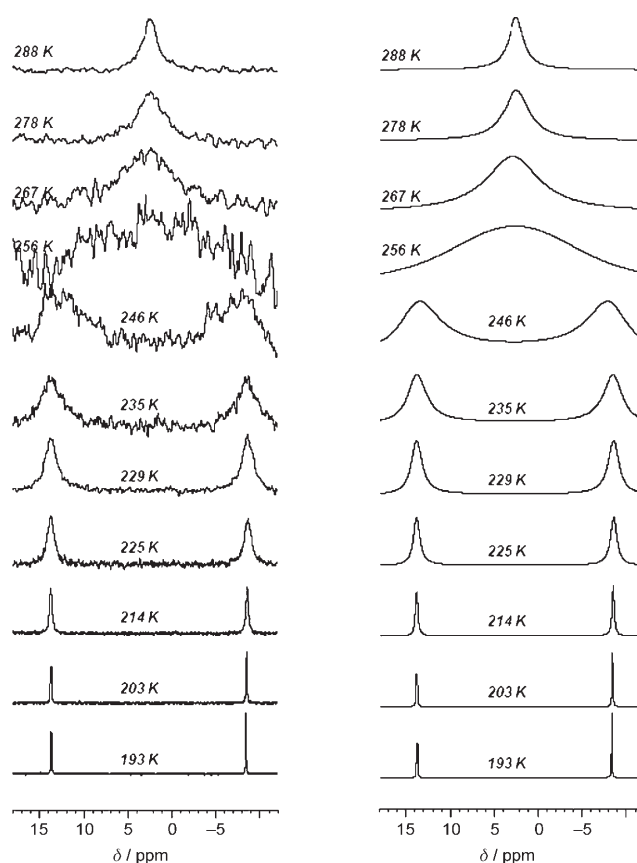


Figure 8. Experimental (left) and simulated (right) ^{13}C NMR spectra (125.77 MHz) of $[\text{Y}\{(\mu\text{-Me})_2\text{AlMe}_2\}_3]$ (**1a**) in $[\text{D}_8]$ toluene at different temperatures.

Surprisingly, the aluminate methyl group exchange proceeds with activation parameters (calculated using the Eyring equation; see also Figure 9) that indicate an associative methyl group exchange (right-hand side of Figure 6) for all $[\text{Ln}(\text{AlMe}_4)_3]$ complexes investigated. The negative activation entropies propose a higher ordered transition state, which implies an η^3 -coordinated $[\text{AlMe}_4^-]$ ligand, for the complete series of Ln^{3+} ions. The activation entropy increases with decreasing size of the metal center, but appears to be lower for the smallest metal center lutetium than for yttrium. This could be due to strong secondary interactions, for example $\text{Ln}\cdots\text{CH}_3$ agostic interactions, originating from the most Lewis acidic Lu^{3+} center. For comparison, a dissociative methyl group exchange (positive ΔS^\ddagger) has been reported for the $[\text{Al}_2\text{Me}_6]$ dimer^[32] and the sterically crowded heteroleptic yttrium carboxylate complex **2a** (Table 4).^[16] Moreover, the low ΔH^\ddagger values suggest relatively weak aluminate bonding.

In agreement with previous findings,^[16] the free enthalpy decreases with increasing Ln^{3+} size, which is indicative of a weakening of the $\text{Ln}-\text{C}$ bond for the larger metal centers. The comparatively higher free activation energy ΔG^\ddagger for the smallest metal center Lu compared to that for Sm at a given temperature corresponds to a slowing of the methyl group exchange. For example, a $\Delta(\Delta G^\ddagger)$ value of

Table 3. Exchange rates k and free energies of activation (ΔG^\ddagger) for [Lu(AlMe₄)₃] (**1h**), [Sm(AlMe₄)₃] (**1f**), and [Y(AlMe₄)₃] (**1a**) obtained by line-shape analysis. The estimated uncertainty for the free energies of activation is 0.3 kJ mol⁻¹.

| [Lu(AlMe ₄) ₃] (1h) | | | [Sm(AlMe ₄) ₃] (1f) | | | [Y(AlMe ₄) ₃] (1a ; ¹ H NMR) | | | [Y(AlMe ₄) ₃] (1a ; ¹³ C NMR) | |
|--|---------------------------|--|--|---------------------------|--|---|---------------------------|--|--|--|
| T [K] | k [s ⁻¹] | ΔG^\ddagger [kJ mol ⁻¹] | T [K] | k [s ⁻¹] | ΔG^\ddagger [kJ mol ⁻¹] | T [K] | k [s ⁻¹] | ΔG^\ddagger [kJ mol ⁻¹] | k [s ⁻¹] | ΔG^\ddagger [kJ mol ⁻¹] |
| 225 | 8.9 | 50.4 | 176 | 2.2 × 10 ² | 34.4 | 193 | 1.6 × 10 ¹ | 42.1 | 1.4 × 10 ¹ | 42.3 |
| 235 | 2.3 × 10 ¹ | 51.0 | 178 | 2.2 × 10 ² | 34.9 | 203 | 3.3 × 10 ¹ | 43.3 | 3.4 × 10 ¹ | 43.2 |
| 246 | 6.7 × 10 ¹ | 51.2 | 180 | 2.6 × 10 ² | 35.0 | 214 | 1.0 × 10 ² | 43.6 | 1.1 × 10 ² | 43.5 |
| 262 | 3.0 × 10 ² | 51.4 | 185 | 4.7 × 10 ² | 35.2 | 225 | 3.3 × 10 ² | 43.6 | 3.3 × 10 ² | 43.7 |
| 267 | 4.9 × 10 ² | 51.4 | 191 | 8.4 × 10 ² | 35.3 | 228 | 4.8 × 10 ² | 43.6 | 4.8 × 10 ² | 43.6 |
| 272 | 7.6 × 10 ² | 51.5 | 196 | 6.7 × 10 ² | 36.7 | 228 | 4.9 × 10 ² | 43.7 | 4.7 × 10 ² | 43.7 |
| 274 | 8.9 × 10 ² | 51.5 | 201 | 1.3 × 10 ³ | 36.6 | 229 | 5.2 × 10 ² | 43.6 | 6 × 10 ² | 43.5 |
| 275 | 9.7 × 10 ² | 51.5 | 207 | 5.0 × 10 ³ | 35.3 | 229 | 5.5 × 10 ² | 43.7 | 6 × 10 ² | 43.7 |
| 276 | 1.2 × 10 ³ | 51.3 | 212 | 4.8 × 10 ³ | 36.4 | 230 | 5.7 × 10 ² | 43.7 | 6 × 10 ² | 43.7 |
| 278 | 1.0 × 10 ³ | 51.8 | 217 | 5.0 × 10 ³ | 37.3 | 235 | 9.3 × 10 ² | 43.8 | 1.0 × 10 ³ | 43.7 |
| 279 | 1.1 × 10 ³ | 51.8 | 222 | 7.3 × 10 ³ | 37.5 | 246 | 2.2 × 10 ³ | 44.1 | 2.1 × 10 ³ | 44.2 |
| 288 | 2.1 × 10 ³ | 52.2 | 228 | 1.1 × 10 ⁴ | 37.7 | 256 | 5.2 × 10 ³ | 44.2 | 8 × 10 ³ | 43.3 |
| 299 | 4.0 × 10 ³ | 52.6 | 233 | 1.7 × 10 ⁴ | 37.7 | 256 | 4.9 × 10 ³ | 44.4 | 7 × 10 ³ | 43.8 |
| 309 | 7.3 × 10 ³ | 53.0 | 244 | 1.8 × 10 ⁴ | 39.4 | 267 | 1.1 × 10 ⁴ | 44.5 | 1.5 × 10 ³ | 43.9 |
| 320 | 1.3 × 10 ⁴ | 53.3 | 254 | 3.0 × 10 ⁴ | 40.1 | 278 | 2.2 × 10 ⁴ | 44.8 | 2.9 × 10 ⁴ | 44.1 |
| 331 | 2.4 × 10 ⁴ | 53.5 | 265 | 4.8 × 10 ⁴ | 40.9 | 288 | 3.7 × 10 ⁴ | 45.3 | 5 × 10 ⁴ | 44.5 |
| 341 | 4.2 × 10 ⁴ | 53.7 | 275 | 5.9 × 10 ⁴ | 42.1 | | | | | |
| 352 | 5.7 × 10 ⁴ | 54.6 | 286 | 9.3 × 10 ⁴ | 42.8 | | | | | |
| 362 | 1.1 × 10 ⁵ | 54.5 | 297 | 1.2 × 10 ⁵ | 43.8 | | | | | |

Table 4. Thermodynamic data for the exchange of bridging and terminal methyl groups in [Ln(AlMe₄)₃]- and [AlMe₄]-containing compounds. The activation parameters shown are only based on the variable ¹H NMR spectra.

| Compound | T_c [K] | $\Delta G^\ddagger(T_c)$ [kJ mol ⁻¹] | ΔH^\ddagger [kJ mol ⁻¹] | ΔS^\ddagger [JK ⁻¹ mol ⁻¹] |
|---|-----------|---|--|--|
| [Lu{(μ-Me) ₂ AlMe ₂ }] ₃ (1h) | 279 | 51.8(3) | 44(1) | -30(3) |
| [Y{(μ-Me) ₂ AlMe ₂ }] ₃ (1a) | 229 | 43.6(3) | 38(1) | -26(4) |
| [Sm{(μ-Me) ₂ AlMe ₂ }] ₃ (1f) | 216 | 37.3(3) | 20.2(6) | -78(3) |
| [(L ¹) ₂ Y{(μ-Me) ₂ AlMe ₂ }] (2a) ^[a,d] | 263 | 53(3) ^[e] | 73(4) | 66(3) |
| [(L ¹) ₂ La{(μ-Me) ₂ AlMe ₂ }] (2b) ^[a,d] | 213 | 45(2) ^[e] | 28(2) | -58(3) |
| [(L ²)Y{(μ-Me) ₂ AlMe ₂ }] ^[b,e] | | 63.0 ^[c] | 24.3 | -130 |
| [Me ₂ Al{(μ-Me) ₂ AlMe ₂ }] ^[f] | | 44.8 ^[c] | 81.5 | 123.1 |

[a] L¹ = (O₂CAr^{Pr})₂(μ-AlMe₂). [b] L² = Me₂Si(2-MeBenzInd)₂. [c] At 298 K. [d] See ref. [16]. [e] See ref. [33]. [f] See ref. [32]

9.4 kJ mol⁻¹ at 275 K corresponds to a slowing by a factor 61 (Table 3).

1D ⁸⁹Y and 2D ¹H-⁸⁹Y NMR spectra of [Y(AlMe₄)₃]: Metal-centered NMR spectroscopy is a particularly suitable probe of chemical reactivity as it is element specific and is applicable to any metal of the periodic table that has an isotope with a nuclear spin.^[35] Additionally, metal nuclei have very large shielding (chemical shift) ranges and hence are very sensitive to small changes in geometry and coordination numbers, thereby revealing subtle changes in the solution composition of complexes. The properties of the monoisotopic ⁸⁹Y nucleus (100% abundance, $I = -1/2$, and a wide chemical shift range of approx. 1300 ppm) make it attractive for NMR studies. However, its routine use in the characterization of yttrium complexes is impaired by its low receptivity (0.681 relative to ¹³C), low resonance frequency

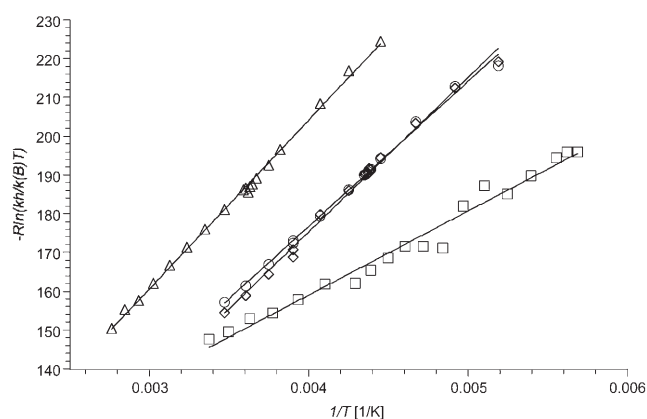


Figure 9. Linearized Eyring plots ($-R\ln(kh/k_B T) = -\Delta S^\ddagger + \Delta H^\ddagger/T$) for the exchange of bridging and terminal methyl groups in [Y(AlMe₄)₃] ((\circ), ¹H NMR data; (\circ), ¹³C NMR data), [Lu(AlMe₄)₃] (Δ), and [Sm(AlMe₄)₃] (\square).

(24.5 MHz at a magnetic field strength of 11.7 T (¹H = 500 MHz)), and extremely long T_1 relaxation times (typically of the order of 60 s), which leads to lengthy experiments and saturation difficulties.

Contrary to chemical shift correlations in beryllium and aluminum complexes,^[36,37] the correlation between ⁸⁹Y chemical shifts and the metal coordination number is unclear. Nevertheless, there are clear trends regarding the influence of various ligands on ⁸⁹Y chemical shifts. Thus, an increased electronegativity and π -donating ability of the ligated groups is correlated with increased ⁸⁹Y nuclear shielding and resonance shifts to higher field.^[38] The chemical shifts of organoyttrium compounds extend over a very large range, with the most shielded cyclopentadienyl species in the range of about $\delta = -370$ (for [Y(C₅H₄Me)₃(thf)]) to 80 ppm; the

purely “ σ -bound”, and therefore most deshielded, species $[\text{Y}\{\text{CH}(\text{SiMe}_3)_2\}_3]$ has the largest reported chemical shift of +895 ppm (Table 5).

The ^{89}Y NMR spectrum of $[\text{Y}(\text{AlMe}_4)_3]$ (**1a**) as a 0.25 M solution in $[\text{D}_6]$ benzene at 298 K shows a very narrow signal at $\delta = +394$ ppm (Figure 10). This value is best compared to the dicationic complexes $[\text{Y}(\text{CH}_2\text{SiMe}_3)(\text{thf})_4][\text{BPh}_4]_2$ ($\delta = 409.2$ ppm) and $[\text{YMe}(\text{thf})_6][\text{BPh}_4]_2$ ($\delta = 433.2$ ppm) (Table 5), which are shifted substantially upfield from their neutral species. The relatively low-field shift of the ^{89}Y signal in the spectrum of $[\text{Y}(\text{AlMe}_4)_3]$ supports the conclusion that the aluminate bonding shows a significant degree of covalency.

This finding is in agreement with computational studies on the bonding nature in $[\text{Y}(\text{AlMe}_4)_3]^{[42]}$ and this covalent contribution to the Ln–C bond is further substantiated by the presence of a scalar ^1H – ^{89}Y coupling. The resolvable $^2J_{\text{Y,H}}$ coupling was efficiently exploited in a two-dimensional

^1H – ^{89}Y HMQC NMR experiment (0.25 M solution of **1a** in $[\text{D}_6]$ benzene; Figure 10), which actually proved less time-consuming than the 1D ^{89}Y experiment (7 min vs. 2 h 20 min). Polarization transfer from ^1H to ^{89}Y greatly enhances the sensitivity and allows a much faster data accumulation rate which, in this case, is not restricted by the very long T_1 of ^{89}Y but rather the much shorter T_1 of ^1H .

^{27}Al NMR spectra of $[\text{Ln}(\text{AlMe}_4)_3]$ complexes: ^{27}Al NMR spectroscopy appears to be a very attractive technique for the study of Ln/Al heterobimetallic compounds as the ^{27}Al nucleus (100 % abundance) has a relatively high magnetogyric ratio (similar to ^{13}C). However, the aluminum nucleus possesses a quadrupolar moment ($I = 5/2$) and hence often produces quite broad signals in the NMR spectra, with the linewidth depending heavily upon the coordination geometry of the aluminum metal center. The chemical shift range of ^{27}Al is approximately 450 ppm and chemical shifts can be

categorized according to the ligand symmetry about the aluminum atom.^[43] Aluminum species with tetrahedral symmetry, as in $[\text{Ln}(\text{AlMe}_4)_3]$ complexes, are found in an intermediate region of the chemical shift scale. Complexes with this symmetry are normally found at high frequency relative to $[\text{Al}(\text{H}_2\text{O})_6]^{3+}$, with a chemical shift range extending from $\delta = -28$ ppm for $[\text{AlH}_4]^-$ to about $\delta = 220$ ppm for alkylaluminum complexes (Al_2R_6) and their adducts (Table 6).

Good quality ^{27}Al NMR spectra of $[\text{Ln}(\text{AlMe}_4)_3]$ (Ln = Y, La, Pr, Nd, Sm, and Lu) complexes as 0.25 M solutions in $[\text{D}_6]$ benzene could be acquired at 25 °C within a short time (Figure 11). All spectra show a single ^{27}Al NMR peak with linewidths between $\Delta\nu_{1/2} = 1836$ Hz for $[\text{Sm}(\text{AlMe}_4)_3]$ and 3150 Hz for $[\text{Y}(\text{AlMe}_4)_3]$. Since all the Al atoms maintain their fourfold coordination, these relatively large linewidths could arise from associative methyl group exchange, which would lead to a pronounced distortion from tetrahedral symmetry.^[47] The chemical shifts of the Lu ($\delta = 163$ ppm), Y ($\delta = 167$ ppm), Sm ($\delta = 163$ ppm), and La ($\delta = 165$ ppm) derivatives are in the expected region for tetrahedral-

Table 5. Alkylttrium complexes and their corresponding ^{89}Y NMR chemical shifts.

| Complex | δ_{exp} [ppm] | CN ^[a] | Solvent | Ref |
|--|-----------------------------|-------------------|-------------------------|------|
| $[\text{Y}(\text{C}_5\text{H}_4\text{Me})_2(\mu\text{-C}\equiv\text{CCMe}_3)_2]$ | –74 | 8 | $[\text{D}_8]$ THF | [39] |
| $[\text{Y}(\text{C}_5\text{H}_4\text{Me})_2(\mu\text{-Me})_2]$ | –15 | 8 | $[\text{D}_8]$ toluene | [39] |
| $[\text{Y}(\text{H}_2\text{O})_8]^{3+}$ | 0.00 (reference) | 6 | D_2O | |
| $[\text{Y}(\text{C}_5\text{H}_4\text{Me})_2(\text{Me})(\text{thf})]$ | 40 | 8 | $[\text{D}_8]$ THF | [39] |
| $[\text{Y}(\text{C}_5\text{Me}_5)_2\text{CH}(\text{SiMe}_3)_2]$ | 78.9 | 4 | $[\text{D}_6]$ benzene | [38] |
| $[\text{Y}(\text{CH}_2\text{SiMe}_3)(\text{thf})_4][\text{BPh}_4]_2$ | 409.2 | 5 | $[\text{D}_8]$ THF | [41] |
| $[\text{YMe}(\text{thf})_6][\text{BPh}_4]_2$ | 433.2 | 7 | $[\text{D}_5]$ pyridine | [41] |
| $[\text{Y}\{1,3\text{-(SiMe}_3)_2\text{C}_3\text{H}_5\}_3]$ | 470.5 | 3 | $[\text{D}_6]$ benzene | [40] |
| $[\text{Y}(\text{CH}_2\text{SiMe}_3)_2(\text{thf})_4][\text{BPh}_4]$ | 660.0 | 6 | $[\text{D}_8]$ THF | [41] |
| $[\text{Y}(\text{CH}_2\text{SiMe}_3)_2(\text{thf})_4][\text{BPh}_3(\text{CH}_2\text{SiMe}_3)]$ | 660.2 | 6 | $[\text{D}_8]$ THF | [41] |
| $[\text{Y}(\text{CH}_2\text{SiMe}_3)_2(\text{thf})_4][\text{Al}(\text{CH}_2\text{SiMe}_3)_4]$ | 666.4 | 6 | $[\text{D}_8]$ THF | [41] |
| $[\text{Y}(\text{CH}_2\text{SiMe}_3)_3(\text{thf})_2]$ | 882.7 | 5 | $[\text{D}_8]$ THF | [41] |
| $[\text{Y}\{\text{CH}(\text{SiMe}_3)_2\}_3]$ | 895.0 | 3 | $[\text{D}_8]$ toluene | [38] |

[a] CN = coordination number.

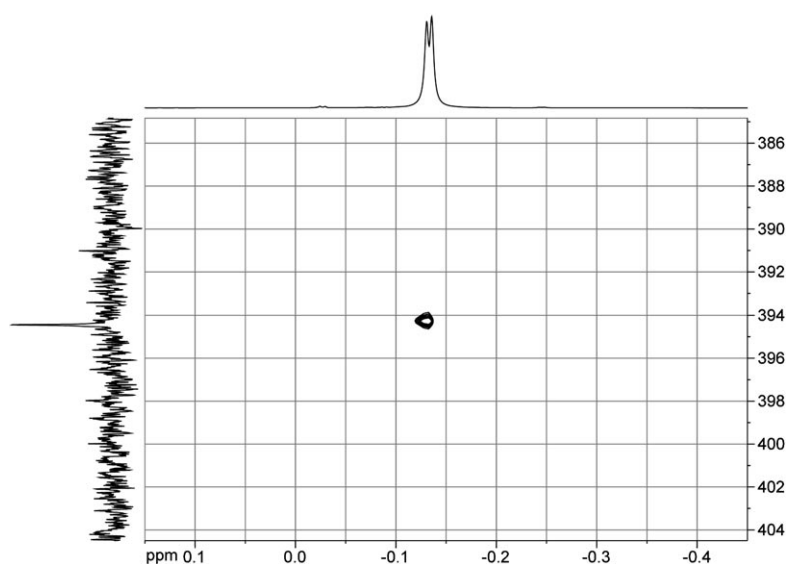
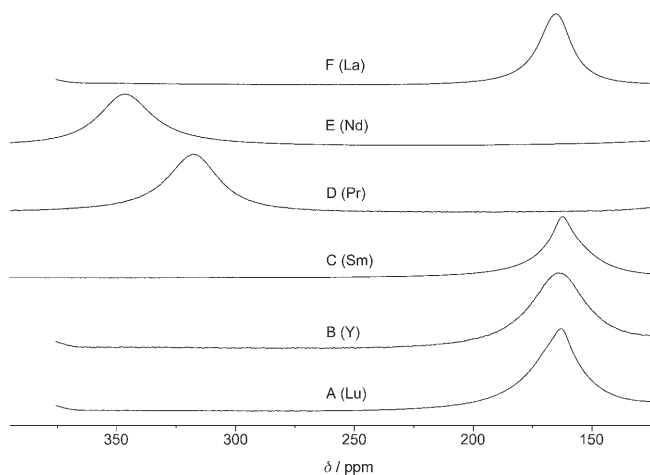


Figure 10. Two-dimensional ^1H – ^{89}Y HMQC NMR spectrum of $[\text{Y}(\text{AlMe}_4)_3]$ (**1a**) dissolved in $[\text{D}_6]$ benzene at 298 K. The 1D ^{89}Y NMR spectrum (24.51 MHz) is shown on the left edge of the contour plot and the 1D ^1H NMR spectrum (500.13 MHz) of the methyl region is shown at the top.

Table 6. Aluminum compounds and their corresponding ^{27}Al chemical shifts and linewidths.

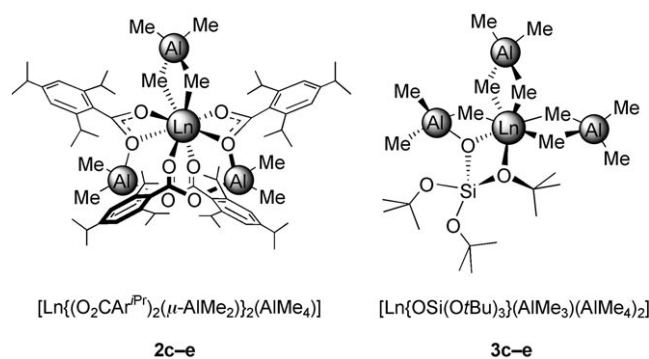
| Compound | δ_{exp} [ppm] | Solvent | Linewidth [Hz] | Ref |
|--|-----------------------------|---------------------------|----------------|------|
| $\text{Et}_3\text{Al}\cdot\text{SEt}_2$ | +221 | C_6H_{12} | 1890 | [44] |
| $[\text{Al}_2\text{iBu}_6]$ | +220 | C_6H_{12} | 6000 | [45] |
| $\text{Et}_3\text{Al}\cdot\text{thf}$ | +176 | C_6H_{12} | 1280 | [44] |
| $[\text{AlH}\text{iBu}_2]_n$ | +162 | | 10000 | [45] |
| $[\text{Al}_2\text{Et}_6]$ | +171 | C_6H_{12} | 1700 | [45] |
| $[\text{Al}_2\text{Me}_6]$ | +156 | neat | 450 | [45] |
| $[\text{Al}(\text{H}_2\text{O})_6]^{3+}$ | 0 | H_2O | 3 | [46] |

Figure 11. ^{27}Al NMR spectra (130.32 MHz) of $[\text{Lu}(\text{AlMe}_4)_3]$ (A), $[\text{Y}(\text{AlMe}_4)_3]$ (B), $[\text{Sm}(\text{AlMe}_4)_3]$ (C), $[\text{Pr}(\text{AlMe}_4)_3]$ (D), $[\text{Nd}(\text{AlMe}_4)_3]$ (E), and $[\text{La}(\text{AlMe}_4)_3]$ (F) dissolved in $[\text{D}_6]\text{benzene}$ at 298 K.

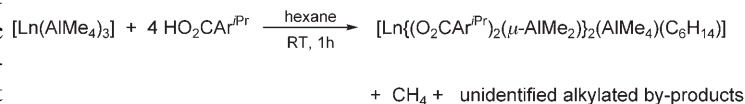
ly coordinated alkylaluminum complexes and they differ only slightly from the chemical shifts reported for $[\text{Al}_2\text{Me}_6]$ and $[\text{Al}_2\text{Et}_6]$ (Table 6). Exceptionally low-field shifts of $\delta = 317$ and 346 ppm, most likely caused by the paramagnetic metal centers, were obtained for $[\text{Pr}(\text{AlMe}_4)_3]$ (**1d**) and $[\text{Nd}(\text{AlMe}_4)_3]$ (**1e**), respectively. The paramagnetic shift effect on the ^{27}Al signal in $[\text{Sm}(\text{AlMe}_4)_3]$ is negligible. The paramagnetic Ln^{3+} metal centers influence the ^{27}Al NMR spectra differently, and these differences are probably due to the varying relaxation behavior of the unpaired electron spins belonging to the paramagnetic metal centers. Pr^{3+} and Nd^{3+} seem to cause a significant paramagnetic shift for the ^{27}Al resonances, although no broadening effect is observed. Neither of these influences are pronounced for the ^{27}Al signals of $[\text{Sm}(\text{AlMe}_4)_3]$, although possible paramagnetic shifts and broadening effects are observed in the ^1H (Figure 4) and ^{13}C NMR spectra (not shown) of $[\text{Sm}(\text{AlMe}_4)_3]$. None of the various paramagnetic effects were investigated further. As expected, due to fast (T_2) relaxation of the ^{27}Al nuclear spin and the concomitant line-broadening, spin-spin coupling was not observed in the NMR spectra.

Reactivity toward carboxylic acids and silanols: As shown previously, homoleptic $[\text{Ln}(\text{AlMe}_4)_3]$ complexes readily un-

dergo protonolysis reactions with a variety of Brønsted acidic O-donors, including phenols, alcohols, silanols, and carboxylic acids, to generate heteroleptic Ln/Al heterobimetallic complexes.^[16,17] These complexes not only show an interesting structural chemistry but can also act as model systems to study structure–reactivity relationships in commonly used Ziegler-type catalysts. The alkylated heterobimetallic lanthanide carboxylate complexes $[\text{Ln}\{(\text{O}_2\text{CAr}^{\text{Pr}})_2(\mu\text{-AlMe}_2)_2(\text{AlMe}_4)(\text{C}_6\text{H}_{14})\}]$ (Figure 12) and $[\text{Ln}(\text{O}_2\text{CC}_6\text{H}_2\text{-}i\text{Bu}_3\text{-}2,4,6)\{(\mu\text{-Me})_2\text{AlMe}_2\}_2]$, derived from the sterically bulky 2,4,6-triisopropyl- and 2,4,6-tri-*tert*-butylbenzoic acids, respectively, have been prepared from **1** in good to quantitative yields by methane elimination reactions.^[16]

Figure 12. Heteroleptic carboxylate and siloxide complexes of Ce, Pr, and Nd synthesized from **1** by methane elimination and used as precatalysts in isoprene polymerization.

This strategy was also successfully employed here to synthesize the cerium and praseodymium complexes **2c** and **2d**, respectively (Scheme 5). Thus, homoleptic tetramethylalumi-

Scheme 5. Synthesis of alkylaluminum lanthanide carboxylates ($\text{Ar}^{\text{Pr}} = \text{C}_6\text{H}_2\text{iPr}_3\text{-}2,4,6$; $\text{Ln} = \text{Ce}$ (**2c**), Pr (**2d**), Nd (**2e**)).

nate complexes **1c** and **1d** were treated with four equivalents of solid 2,4,6-triisopropylbenzoic acid. After the evolution of methane had ceased (<5 min) the clear solutions were stirred for one hour, concentrated, and finally stored overnight at -30°C to give pale-yellow ($\text{Ln} = \text{Ce}$ (**2c**)) or pale-green ($\text{Ln} = \text{Pr}$ (**2d**)) crystalline solids in good yields.

The elemental analyses of **2c** and **2d** were in good agreement with the formation of hexane inclusion compounds, and one equivalent of hexane remained confined within the crystal lattice even under high vacuum. The same observation has previously been made for the derivatives of lanthanum, neodymium, and gadolinium and proven by means of elemental analysis and NMR spectroscopy (for $\text{Ln} = \text{La}$).^[16] On the other hand, hexane-insoluble homologues with no

residual solvent molecules have been obtained for the smaller metal centers yttrium and lutetium.^[48]

The reaction of homoleptic tetramethylaluminate complexes **1c**, **1d**, and **1e** with one equivalent of tris(*tert*-butoxy)silanol (HOSi(*Ot*Bu)₃) afforded the heteroleptic siloxide complexes [Ln{OSi(*Ot*Bu)₃}(AlMe₃)(AlMe₄)₂] (**3c–e**) (Figure 13 and Scheme 6).^[17,49] The new cerium and praseo-

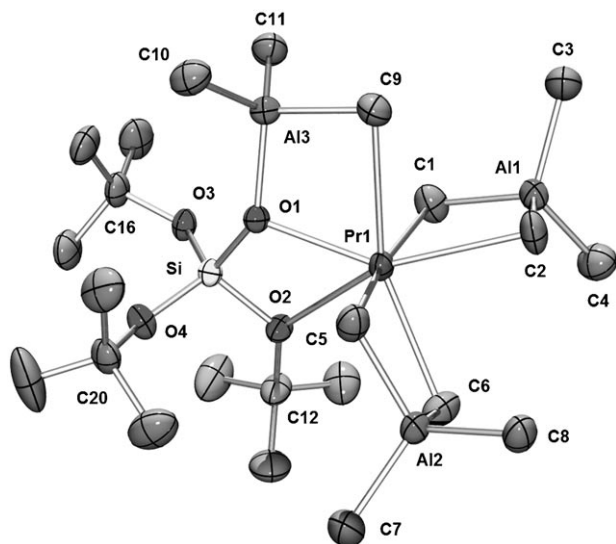
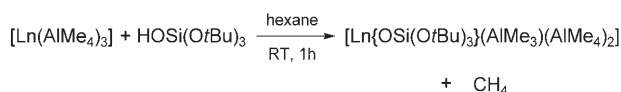


Figure 13. Molecular structure of **3d** (atomic displacement parameters set at the 50% level). Hydrogen atoms have been omitted for clarity. Selected bond lengths [Å] and angles [°]: Pr1–C1 2.619(3), Pr1–C2 2.795(3), Pr1–C5 2.676(3), Pr1–C6 2.621(3), Pr1–C9 2.754(3), Pr1–O1 2.357(2), Pr1–O2 2.714(2), Al1–C1 2.082(4), Al1–C2 2.070(4), Al1–C3 1.967(4), Al1–C4 1.965(4), Al3–C9 2.042(4), Al3–C10 1.952(3), Al3–C11 1.968(3), Al3–O1 1.854(2), Si–O1 1.629(2), Si–O2 1.660(2), Si–O3 1.600(2), Si–O4 1.595(2); C1–Pr1–C2 78.6(1), C1–Pr1–C5 167.8(1), C1–Pr1–C6 101.1(1), C1–Pr1–C9 88.1(1), C2–Pr1–C5 89.6(1), C2–Pr1–C6 79.1(1), C2–Pr1–C9 76.0(1), C5–Pr1–C6 79.2(1), C5–Pr1–C9 86.2(1), C6–Pr1–C9 151.1(1), O1–Pr1–O2 57.13(6), O1–Pr1–C1 99.5(1), O1–Pr1–C2 146.6(1), O1–Pr1–C5 88.7(1), O1–Pr1–C6 133.1(1), O1–Pr1–C9 70.6(1), O2–Pr1–C1 84.8(1), O2–Pr1–C2 152.9(1), O2–Pr1–C5 107.3(1), O2–Pr1–C6 83.4(1), O2–Pr1–C9 125.0(1).



Scheme 6. Synthesis of alkylaluminum lanthanide siloxides (Ln = Ce (**3c**), Pr (**3d**), Nd (**3e**)).

dium derivatives **3c** (Ln = Ce) and **3d** (Ln = Pr) were obtained in good yields. Recrystallization from saturated hexane solutions at –30 °C gave pale yellow (**3c**) and pale green (**3d**) crystals which gave correct elemental analyses.

The single crystals of **3d** proved to be suitable for an X-ray crystallographic structure determination. As reported previously for the lanthanum derivative,^[17,49] the praseodymium metal center is seven-coordinated by five AlCH₃

carbon atoms and two oxygen atoms of an asymmetrically η²-coordinated siloxide ligand (Figure 13). One of the tetramethylaluminate units is asymmetrically coordinated due to the pseudo-*trans* positions of the siloxide ligand within the distorted pentagonal bipyramid. A significantly elongated Pr1–C2 bond (2.795(3) Å) is present compared to the average Pr–C(μ-Me) distances in **1d** (2.606 Å) and **3d** (2.667 Å, AlMe₄ units except for Pr1–C2). This distance is even larger than the Pr1–C9 distance of the coordinated AlMe₃ molecule (2.754(3) Å). Nevertheless, both [Pr(μ-Me)₂AlMe₂] metallacycles remain planar, with sums of the inner bond angles of 359.9(2)° and 359.8(2)°, respectively.

Type-3 siloxide derivatives have been discussed as possible model complexes for the reaction of **1** with a dehydrated silica surface, and grafting of the binary [Nd(AlMe₄)₃]/Et₂AlCl precatalyst system onto mesoporous silica MCM-48 has yielded a very efficient single-component catalyst for the *cis*-stereospecific polymerization of isoprene.^[17,50]

Polymerization of isoprene: Complexes **1**, **2**, and **3** (Figure 12) were employed as precatalysts in the *cis*-stereospecific polymerization of isoprene. Diethylaluminum chloride (Et₂AlCl) was used as a co-catalyst and the formation of high-*cis*-1,4-polyisoprene (>98%) was proven by ¹³C NMR spectroscopy. Emphasis was placed on the impact of the metal center and the *n*_{Ln}:*n*_{Cl} ratios on polymer yields, molecular weights, and molecular weight distributions. The polymerization results are summarized in Table 7 along with the data for the neodymium-based catalysts taken from previous studies, which were performed under similar conditions (see Experimental Section).^[16,17] All of the precursor molecules display *n*_{Ln}:*n*_{Al} ratios of 1:3, although the heterobimetallic carboxylate complexes **2** contain oxygen-bonded “deactivated” dimethylaluminum bridges.

Impact of the metal center on the catalytic activity: The metal centers cerium, praseodymium, and neodymium were selected to investigate the intrinsic “neodymium effect” more systematically. In previous studies we have shown that neodymium alkylaluminate complexes greatly outperform their corresponding lanthanum and gadolinium congeners (Figure 14).^[16] Unsurprisingly for complexes derived from large rare-earth metal centers, the cerium and praseodymium derivatives **1–3** are also highly active initiators in isoprene polymerization.^[51,52] Almost all of the tetramethylaluminate complexes **1** gave quantitative yields of high-*cis*-1,4-polyisoprenes in the presence of between one and three equivalents of the alkylaluminum chloride co-catalyst (Table 7, runs 1–9). The slightly lower activities of the carboxylate- and siloxide-based initiators allow for a more detailed discussion of the metal effect. For example, the heterobimetallic lanthanide carboxylate complexes **2** produce polyisoprenes in yields of 79% (**2c**, Ln = Ce, run 10), 98% (**2d**, Ln = Pr, run 13), and 77% (**2e**, Ln = Nd, run 16) upon addition of one equivalent of Et₂AlCl. These findings “complete” a previous study where catalysts derived from larger (Ln = La, 12%) and smaller metal centers (Ln = Gd, 24%) gave lower yields of isolated polymer (Figure 14).^[16]

Table 7. Results of the polymerization of isoprene using compounds **1–3** in combination with different amounts of Et₂AlCl as co-catalyst.

| Run ^[a] | Precatalyst | Et ₂ AlCl ^[b] [equiv] | Yield [%] | M _n ^[c] (×10 ³) | M _w ^[c] (×10 ³) | PDI ^[c] |
|--------------------|----------------|--|--------------|--|--|--------------------|
| 1 | 1c (Ce) | 1 | >99 | 160 | 386 | 2.41 |
| 2 | 1c (Ce) | 2 | >99 | 152 | 469 | 3.08 |
| 3 | 1c (Ce) | 3 | 13 | 66 | 241 | 3.66 |
| 4 | 1d (Pr) | 1 | >99 | 386 | 732 | 1.90 |
| 5 | 1d (Pr) | 2 | >99 | 320 | 735 | 2.30 |
| 6 | 1d (Pr) | 3 | >99 | 345 | 704 | 2.02 |
| 7 | 1e (Nd) | 1 | >99 | 228 | 788 | 3.45 |
| 8 | 1e (Nd) | 2 | >99 | 117 | 326 | 2.78 |
| 9 | 1e (Nd) | 3 | >99 | 113 | 329 | 2.92 |
| 10 | 2c (Ce) | 1 | 79 | 187 | 418 | 2.24 |
| 11 | 2c (Ce) | 2 | >99 | 149 | 532 | 3.59 |
| 12 | 2c (Ce) | 3 | 97 | 256 | 494 | 1.93 |
| 13 | 2d (Pr) | 1 | 98 | 573 | 863 | 1.51 |
| 14 | 2d (Pr) | 2 | >99 | 158 | 650 | 4.11 |
| 15 | 2d (Pr) | 3 | >99 | 476 | 778 | 1.64 |
| 16 | 2e (Nd) | 1 | 77 | 165 | 575 | 3.48 |
| 17 | 2e (Nd) | 2 | >99 | 271 | 621 | 2.29 |
| 18 | 2e (Nd) | 3 | 98 | 194 | 410 | 2.11 |
| 19 | 3c (Ce) | 1 | 18 | 414 | 744 | 1.80 |
| 20 | 3c (Ce) | 2 | >99 | 535 | 807 | 1.51 |
| 21 | 3c (Ce) | 3 | 33 | 72 | 366 | 5.08 |
| 22 | 3d (Pr) | 1 | 21 | 303 | 718 | 2.37 |
| 23 | 3d (Pr) | 2 | >99 | 446 | 762 | 1.71 |
| 24 | 3d (Pr) | 3 | 88 | 354 | 707 | 2.00 |
| 25 | 3e (Nd) | 1 | 92 | 355 | 744 | 2.10 |
| 26 | 3e (Nd) | 2 | >99 | 223 | 453 | 2.03 |
| 27 | 3e (Nd) | 3 | 38 | 107 | 371 | 3.46 |

[a] General polymerization procedure: 0.02 mmol of precatalyst, 8 mL of hexane, 0.02–0.06 mmol of Et₂AlCl (1–3 equiv), 20 mmol of isoprene; 24 h, 40 °C. [b] Catalyst pre-formation: 30 min at ambient temperature. [c] Determined by size-exclusion chromatography (SEC) against polystyrene standards.

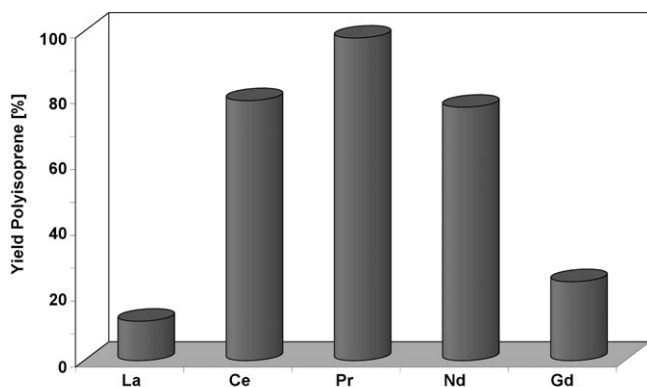


Figure 14. Yields of isolated polyisoprene obtained with carboxylate precatalysts **2** and one equivalent of Et₂AlCl co-catalyst. Data for the La, Nd, and Gd polymerizations are taken from previous studies performed under similar conditions.^[17]

No neodymium effect was observed in the presence of three equivalents of the co-catalyst for either carboxylate (Table 7, runs 12, 15, and 18) or siloxide precatalysts (Table 7, runs 21, 24, and 27).

Impact of the metal center on the polymer properties: Higher molecular weights were obtained, on average, for

praseodymium-based initiators with identical ligand environments and the same amount of co-catalyst. For example, homoleptic tetramethylaluminate complexes **1** gave molecular weights, M_w , of 241 000 (Ln=Ce, run 3), 704 000 (Ln=Pr, run 6), and 329 000 g mol⁻¹ (Ln=Nd, run 9) upon activation with three equivalents of Et₂AlCl. The polydispersities do not show any clear trend and range from 1.51 (runs 13 and 20) to 5.08 (run 21).

Impact of the ligand on the catalytic activity: Quantitative polymer formation was observed in almost all of the experiments based on **1** (Table 7, runs 1–9), thus showing the superior performance of the homoleptic complexes compared to all of the other precatalysts employed in this and earlier studies.^[17] Only in the presence of **1c** (Ln=Ce) and three equivalents of the chloride co-catalyst, a drastically lower activity with an isolated yield of only 13% was observed (run 3). For comparison, the slightly larger metal center lanthanum gave catalytically inactive mixtures under similar conditions.^[17] The carboxylate- and particularly the siloxide-derived initiators revealed significantly lower catalytic activities in the presence of one or three equivalents of the co-catalyst. Surprisingly, higher activities were observed for the mono(tetramethylaluminate) complexes **2** (Table 7, runs 10–18) than for the bis(tetramethylaluminate) complexes **3** (Table 7, runs 19–27).

Impact of the ligand on the polymer properties: Despite the stereoelectronic differences between alkylaluminate, carboxylate, and siloxide ligands, the molecular weights and molecular weight distributions are very similar, although slightly shorter polymer chains are generally produced by the most reactive tetramethylaluminate precatalysts **1** (Table 7, runs 1–9).

Impact of the catalyst-to-co-catalyst ratio on the catalytic activities: As reported previously for a variety of different initiator systems based on halide, carboxylate, alkoxide, and phosphate ligands, the highest polymer yields were obtained in the presence of two equivalents of the Et₂AlCl co-catalyst.^[53–57] Quantitative yields of *cis*-1,4-polyisoprene were obtained for all of the precatalysts, regardless of the size of the lanthanide metal center or the type of ligand system. This study demonstrates once again that the presence of two equivalents of the chloride source seems to be crucial for optimal activation of the rare-earth metal centers. Lower reactivities were observed in the presence of three equivalents of the chloride source due to the formation of larger amounts of perhalogenated, and therefore catalytically inactive, LnCl₃.

Impact of the catalyst-to-co-catalyst ratio on the polymer properties: The molecular weights and molecular weight distributions of all the polymers obtained seem to follow no general trend—both values are actually more dependent on the size of the metal center and the type of ligand environment under similar conditions (see above).

Conclusion

Amide elimination has been confirmed as the optimal approach to homoleptic rare-earth metal tris(tetramethylaluminate) complexes. $[\text{Ln}(\text{AlMe}_4)_3]$ complexes with metals in the $\text{La}^{3+} \rightarrow \text{Lu}^{3+}$ size range can be straightforwardly obtained by the reaction of $[\text{Ln}(\text{NMe}_2)_3(\text{LiCl})_3]$ with trimethylaluminum. X-ray structure analyses of the lutetium, samarium, praseodymium, and lanthanum tetramethylaluminates have revealed a Ln^{3+} cation size-dependent coordination of the $[\text{AlMe}_4]$ moieties. The exceptional solid-state structure of the lanthanum derivative can best be described by the formula $[\text{La}\{(\mu\text{-Me})_2\text{AlMe}_2\}_2\{(\mu\text{-Me})_3\text{AlMe}\}]$, which involves AlMe_4^- ligands coordinating in three different coordination modes. The resulting higher coordination number of the lanthanum center (6 \rightarrow 7/8) certainly reflects the larger La^{3+} size, but also corroborates the high coordinational flexibility of the tetramethylaluminate ligand. AlR_4^- ligands therefore seem to willingly adapt to the stereoelectronic requirements of the complex they find themselves in, gradually changing along the Ln series by undergoing $\eta^2 \rightarrow \eta^3$ (steric unsaturation, this work) and $\eta^2 \rightarrow \eta^1$ coordination shifts (steric oversaturation). The former $\text{Ln}\{(\mu\text{-Me})_2\text{AlMe}_2\} \rightarrow \text{Ln}\{(\mu\text{-Me})_3\text{AlMe}\}$ ($\eta^2 \rightarrow \eta^3$) coordination mode shift characterizing the associative methyl exchange between bridging and terminal methyl groups has also been observed by dynamic ^1H and ^{13}C NMR spectroscopy by utilizing line-shape analysis in which higher ordered transient states (η^3) are indicated by negative values of ΔS^\ddagger . The presence of a $^2J_{\text{Y,H}}$ (2.5 Hz) and a $^1J_{\text{Y,C}}$ (12.8 Hz) scalar coupling provides evidence for a significant degree of covalency of the Ln-aluminate bonding. In addition, the $^2J_{\text{Y,H}}$ coupling allows for a fast and thereby sensitive alternative to obtaining ^{89}Y chemical shifts. The ^{27}Al NMR spectra of $[\text{Ln}(\text{AlMe}_4)_3]$ complexes have revealed a drastic low-field shift for the paramagnetic neodymium and praseodymium derivatives. Finally, isoprene polymerization utilizing three types of structurally well-defined heterobimetallic rare-earth metal complexes of the large metal centers Ce, Pr, and Nd with alkylaluminate, carboxylate, and siloxide ligands has revealed: a) high activities in the presence of diethylaluminum chloride as a co-catalyst (optimal ratio $n_{\text{Ln}}:n_{\text{cocatalyst}}=1:2$), b) a *cis* stereospecificity for all the initiators of more than 98%, c) the superior performance of homoleptic $[\text{Ln}(\text{AlMe}_4)_3]$ complexes compared to carboxylate and siloxide derivatives, and d) that the “intrinsic neodymium effect”, that is, the fact that the highest activities in diene polymerizations so far have been observed for neodymium-based catalyst systems, has to be put into perspective.

Experimental Section

General remarks: All operations were performed with rigorous exclusion of air and water using standard Schlenk, high-vacuum, and glove box techniques (MBraun MBLab; <1 ppm O_2 , <1 ppm H_2O). Hexane, THF, and toluene were purified with Grubbs columns (MBraun SPS, solvent

purification system) and stored in a glove box. $[\text{D}_6]$ Benzene was obtained from Aldrich, degassed, dried with Na for 24 h, and filtered. AlMe_3 and Et_2AlCl were purchased from Aldrich and used as received. Isoprene was obtained from Aldrich, dried several times over activated molecular sieves (3 Å) and distilled prior to use. Complexes **1b**,^[17] **1h**,^[6] **2e**,^[48] and **3e**^[17] were synthesized according to previously published procedures. LiAlMe_4 and NaAlEt_4 were prepared according to literature procedures.^[58,59] IR spectra were recorded with a NICOLET Impact 410 FTIR spectrometer and a Perkin-Elmer 1650 FTIR spectrometer as Nujol mulls sandwiched between CsI plates. Elemental analyses were performed with an Elementar Vario EL III.

General procedure for the synthesis of lanthanide(III) tris(tetramethylaluminate)s 1a, 1e, 1f, and 1g: A THF solution of three equivalents of LiNMe_2 (10 mL) was added slowly to a suspension of $[\text{LnCl}_3(\text{thf})_x]$ in THF (15 mL) and the mixture was stirred at ambient temperature for 18 h. The solvent was then removed in vacuo. The remaining solid was suspended in hexane, a solution containing eight equivalents of AlMe_3 diluted with hexane was added, and the resulting mixture stirred at ambient temperature. After 18 h the solvent was removed under reduced pressure, the residue extracted several times with hexane, and the product separated by crystallization at -30°C . The $[\text{Ln}(\text{AlMe}_4)_3]$ complex was recrystallized several times from hexane at -30°C to obtain AlMe_3 -free crystals, which were dried in vacuo prior to each recrystallization cycle.

Yttrium(III) tris(tetramethylaluminate) (1a): Following the procedure described above, $[\text{YCl}_3(\text{thf})_{3.5}]$ (6.10 g, 13.62 mmol), LiNMe_2 (2.09 g, 40.87 mmol), and AlMe_3 (7.86 g, 108.99 mmol) yielded **1a** as colorless crystals (4.30 g, 12.26 mmol, 90%). ^1H NMR (600 MHz, $[\text{D}_6]$ benzene, 25°C): $\delta = -0.25$ (s, $\text{Al}(\text{CH}_3)_4$) ppm. ^1H NMR (500 MHz, $[\text{D}_8]$ toluene, 25°C): $\delta = -2.4$ (s, $\text{Al}(\text{CH}_3)_4$) ppm. ^{13}C NMR (151 MHz, $[\text{D}_6]$ benzene, 25°C): $\delta = 2.8$ (brs, $\text{Al}(\text{CH}_3)_4$) ppm. ^{27}Al NMR (130 MHz, $[\text{D}_6]$ benzene, 25°C): $\delta = 167$ (brs, $\Delta\nu_{1/2} = 3150$ Hz, $\text{Al}(\text{CH}_3)_4$) ppm. IR (nujol): $\tilde{\nu} = 1463$ (vs, nujol), 1385 (vs, nujol), 1303 (w), 1225 (s), 1204 (vs), 971 (w), 899 (w), 852 (w), 733 (vs), 707 (vs), 578 (vs), 557 cm^{-1} (vs). Elemental analysis (%) calcd for $\text{C}_{12}\text{H}_{36}\text{Al}_3\text{Y}$ (350.27): C 41.15, H 10.36; found: C 41.27, H 10.48.

Neodymium(III) tris(tetramethylaluminate) (1e): Following the procedure described above, $[\text{NdCl}_3(\text{thf})_{1.75}]$ (5.47 g, 14.50 mmol), LiNMe_2 (2.22 g, 43.51 mmol), and AlMe_3 (8.36 g, 116.03 mmol) yielded **1e** as blue crystals (5.35 g, 13.20 mmol, 91%). ^1H NMR (500 MHz, $[\text{D}_6]$ benzene, 25°C): $\delta = 10.53$ (brs, $\Delta\nu_{1/2} = 40$ Hz, $\text{Al}(\text{CH}_3)_4$) ppm. ^{13}C NMR (151 MHz, $[\text{D}_6]$ benzene, 25°C): $\delta = 281.5$ (brs, $\Delta\nu_{1/2} = 180$ Hz, $\text{Al}(\text{CH}_3)_4$) ppm. ^{27}Al NMR (130 MHz, $[\text{D}_6]$ benzene, 25°C): $\delta = 346$ (brs, $\Delta\nu_{1/2} = 2874$ Hz, $\text{Al}(\text{CH}_3)_4$) ppm. IR (nujol): $\tilde{\nu} = 1455$ (vs, nujol), 1378 (vs, nujol), 1306 (w), 1212 (vs), 1129 (w), 1052 (w), 975 (w), 925 (w), 892 (w), 859 (w), 726 (vs), 699 (vs), 561 (vs), 541 cm^{-1} (vs). Elemental analysis (%) calcd for $\text{C}_{12}\text{H}_{36}\text{Al}_3\text{Nd}$ (405.60): C 35.54, H 8.95; found: C 35.27, H 8.70.

Samarium(III) tris(tetramethylaluminate) (1f): Following the procedure described above, $[\text{SmCl}_3(\text{thf})_2]$ (5.48 g, 13.66 mmol), LiNMe_2 (2.09 g, 40.99 mmol), and AlMe_3 (7.88 g, 109.30 mmol) yielded **1f** as yellow crystals (4.52 g, 10.99 mmol, 80%). ^1H NMR (500 MHz, $[\text{D}_6]$ benzene, 25°C): $\delta = -3.06$ (brs, $\Delta\nu_{1/2} = 10$ Hz, $\text{Al}(\text{CH}_3)_4$) ppm. ^1H NMR (500 MHz, $[\text{D}_8]$ toluene, 25°C): $\delta = -2.83$ (brs, $\Delta\nu_{1/2} = 14$ Hz, $\text{Al}(\text{CH}_3)_4$) ppm. ^{13}C NMR (151 MHz, $[\text{D}_6]$ benzene, 25°C): $\delta = -31.5$ (brs, $\Delta\nu_{1/2} = 54$ Hz, $\text{Al}(\text{CH}_3)_4$) ppm. ^{27}Al NMR (130 MHz, $[\text{D}_6]$ benzene, 25°C): $\delta = 163$ (brs, $\Delta\nu_{1/2} = 1836$ Hz, $\text{Al}(\text{CH}_3)_4$) ppm. IR (nujol): $\tilde{\nu} = 1458$ (vs, nujol), 1380 (vs, nujol), 1303 (w), 1199 (vs), 966 (w), 940 (w), 919 (w), 852 (w), 723 (vs), 697 (vs), 572 (vs), 547 cm^{-1} (vs). Elemental analysis (%) calcd for $\text{C}_{12}\text{H}_{36}\text{Al}_3\text{Sm}$ (411.72): C 35.01, H 8.81; found: C 35.32, H 8.63.

Holmium(III) tris(tetramethylaluminate) (1g): Following the procedure described above, $[\text{HoCl}_3(\text{thf})_{3.33}]$ (0.460 g, 0.90 mmol), LiNMe_2 (0.138 g, 2.70 mmol), and AlMe_3 (0.519 g, 7.20 mmol) yielded **1g** as pink crystals (0.307 g, 0.72 mmol, 80%). IR (nujol): $\tilde{\nu} = 1458$ (vs, nujol), 1380 (vs, nujol), 1308 (w), 1220 (s), 1204 (w), 1090 (w), 966 (w), 899 (w), 847 (w), 728 (vs), 692 (vs), 562 cm^{-1} (vs). Elemental analysis (%) calcd for $\text{C}_{12}\text{H}_{36}\text{Al}_3\text{Ho}$ (426.29): C 33.81, H 8.51; found: C 33.67, H 8.48.

Lanthanum(III) tris(tetramethylaluminate) (1b): The synthesis of this complex has been reported previously.^[17] ^1H NMR (500 MHz,

[D₈]toluene, 25 °C): $\delta = 0.05$ (s, Al(CH₃)₄) ppm. ²⁷Al NMR (130 MHz, [D₆]benzene, 25 °C): $\delta = 165$ (brs, $\Delta\nu_{1/2} = 1928$ Hz, Al(CH₃)₄) ppm.

Lutetium(III) tris(tetramethylaluminate) (1h): The synthesis of this complex has been reported previously.¹⁶¹ ¹H NMR (500 MHz, [D₈]toluene, 25 °C): $\delta = 0.16$ (brs, $\Delta\nu_{1/2} = 72$ Hz, Al(CH₃)₄) ppm. ²⁷Al NMR (130 MHz, [D₆]benzene, 25 °C): $\delta = 163$ (brs, $\Delta\nu_{1/2} = 2262$ Hz, Al(CH₃)₄) ppm.

General procedure for the synthesis of lanthanide(III) tris(tetramethylaluminate)s 1c and 1d: THF (10 mL) was slowly added to a suspension of LnCl₃ in toluene (5 mL) at ambient temperature. LiNMe₂ was then slowly added as a solid and the mixture stirred at ambient temperature for 18 h. The solvent was removed in vacuo and the residue re-suspended in hexane (10 mL). AlMe₃ (7.5 equiv) was slowly added to this suspension and the mixture stirred for another 18 h at ambient temperature. It was then centrifuged and filtered through Celite to remove the insoluble LiCl. Solvent, excess AlMe₃, and the volatile by-product [(Me₂Al(μ-NMe₂)₂)₂] were removed in vacuo and the residue was finally crystallized from hexane at -30 °C.

Cerium(III) tris(tetramethylaluminate) (1c): Following the procedure described above, CeCl₃ (1.48 g, 6.00 mmol), LiNMe₂ (0.92 g, 18.0 mmol), and AlMe₃ (3.26 g, 45.00 mmol) yielded **1c** as pale yellow crystals (1.18 g, 2.90 mmol, 74 %). IR (nujol): $\tilde{\nu} = 1458$ (vs, nujol), 1380 (vs, nujol), 1303 (w), 1196 (s), 1033 (m), 692 (s), 571 (s), 551 (s), 470 cm⁻¹ (m). Elemental analysis (%) calcd for C₁₂H₃₆Al₃Ce (401.84): C 35.90, H 9.04; found: C 35.90, H 9.31.

Praseodymium(III) tris(tetramethylaluminate) (1d): Following the procedure described above, PrCl₃ (0.99 g, 4.0 mmol), LiNMe₂ (0.61 g, 12.00 mmol), and AlMe₃ (2.16 g, 30.00 mmol) yielded **1d** as pale green crystals (1.184 g, 2.90 mmol, 74 %). ¹H NMR (500 MHz, [D₆]benzene, 25 °C): $\delta = 8.43$ (brs, $\Delta\nu_{1/2} = 22$ Hz, Al(CH₃)₄) ppm. ¹³C NMR (126 MHz, [D₆]benzene, 25 °C): $\delta = 207.0$ (brs, $\Delta\nu_{1/2} = 56$ Hz, Al(CH₃)₄) ppm. ²⁷Al NMR (130 MHz, [D₆]benzene, 25 °C): $\delta = 317.4$ (brs, $\Delta\nu_{1/2} = 2876$ Hz, Al(CH₃)₄) ppm. IR (nujol): $\tilde{\nu} = 1458$ (vs, nujol), 1380 (vs, nujol), 1304 (w), 1197 (s), 1019 (w), 693 (s), 568 (s), 550 (s), 468 cm⁻¹ (m). Elemental analysis (%) calcd for C₁₂H₃₆Al₃Pr (402.28): C 35.83, H 9.02; found: C 35.91, H 9.45.

[Ce(O₂CC₆H₄iPr₃-2,4,6)(μ-AlMe₂)₂(AlMe₃)(C₆H₁₄)] (2c): Solid 2,4,6-triisopropyl benzoic acid (0.534 g, 2.15 mmol, 4.0 equiv) was slowly added to a well-stirred solution of **1c** (0.216 g, 0.54 mmol) in hexane (10 mL) at ambient temperature. After the evolution of methane had ceased the slightly yellow solution was stirred for a further hour at ambient temperature. The solvent was then reduced to about one half and the mixture was stored overnight at -30 °C. The mother liquid was separated from the pale yellow crystalline solid, which was washed with a small amount of cold hexane and finally dried in vacuo to give analytically pure **2c** (0.628 g, 0.44 mmol, 82 %). IR (nujol): $\tilde{\nu} = 1619$ (s), 1575 (w), 1528 (s), 1427 (s), 1365 (s), 1351 (s), 1332 (s), 1317 (s), 1197 (m), 1154 (m), 1109 (m), 1087 (w), 940 (w), 878 (m), 779 (m), 699 (s), 632 (m), 592 (w), 490 (w), 459 cm⁻¹ (w). Elemental analysis (%) calcd for C₇₈H₁₃₀Al₃CeO₈ (1417.0): C 66.12, H 9.25; found: C 65.91, H 9.71.

[Pr(O₂CC₆H₄iPr₃-2,4,6)(μ-AlMe₂)₂(AlMe₃)(C₆H₁₄)] (2d): Following the procedure described above for **2c**, **1d** (0.205 g, 0.51 mmol), and 2,4,6-triisopropylbenzoic acid (0.506 g, 2.04 mmol, 4 equiv) gave **2d** as a pale green crystalline solid (0.620 g, 0.44 mmol, 86 %). IR (nujol): $\tilde{\nu} = 1621$ (s), 1575 (w), 1528 (s), 1351 (s), 1332 (s), 1317 (s), 1196 (m), 1154 (m), 1109 (m), 1087 (w), 940 (w), 878 (m), 779 (m), 699 (s), 631 (m), 591 (w), 490 (w), 458 cm⁻¹ (w). Elemental analysis (%) calcd for C₇₈H₁₃₀Al₃PrO₈ (1417.7): C 66.08, H 9.24; found: C 66.27, H 9.67.

[Ce(OSi(O*t*Bu)₃(AlMe₃)(AlMe₄)₂)] (3c): Solid HOSi(O*t*Bu)₃ (0.158 g, 0.60 mmol, 1.0 equiv) was slowly added to a well-stirred solution of **1c** (0.239 g, 0.60 mmol) in hexane (7 mL) at ambient temperature. After the evolution of methane had ceased the bright yellow solution was stirred for a further hour at ambient temperature. The solvent was then removed in vacuo and the residue redissolved in hexane (3 mL). This solution was filtered through a pad of Celite and left to crystallize overnight at -30 °C. The mother liquid was then removed and the yellow crystalline solid washed with a small amount of cold hexane and dried in vacuo to give **3c** as a yellow crystalline solid (0.306 g, 0.47 mmol, 78 %). IR (nujol): $\tilde{\nu} = 1369$ (s), 1304 (w), 1246 (m), 1190 (s), 1090 (s), 1063 (s), 1028

(m), 945 (w), 922 (m), 899 (s), 832 (w), 822 (w), 803 (w), 705 (s), 604 (w), 574 (m), 530 (m), 489 (m), 436 cm⁻¹ (w). Elemental analysis (%) calcd for C₂₃H₆₀Al₃CeO₄Si (649.88): C 42.51, H 9.31; found: C 42.60, H 9.55.

[Pr(OSi(O*t*Bu)₃(AlMe₃)(AlMe₄)₂)] (3d): Following the procedure described above for **3c**, **1d** (0.196 g, 0.49 mmol), and HOSi(O*t*Bu)₃ (0.129 g, 0.49 mmol, 1 equiv) gave **3d** as a pale green crystalline solid (0.237 g, 0.36 mmol, 75 %). IR (nujol): $\tilde{\nu} = 1370$ (s), 1304 (w), 1245 (m), 1190 (s), 1171 (m), 1091 (s), 1062 (s), 1028 (m), 948 (w), 922 (m), 897 (s), 832 (w), 822 (w), 803 (w), 692 (s), 602 (w), 574 (m), 528 (m), 488 (m), 435 cm⁻¹ (w). Elemental analysis (%) calcd for C₂₃H₆₀Al₃PrO₄Si (650.67): C 42.46, H 9.29; found: C 42.58, H 9.49.

Polymerization of isoprene: All manipulations were performed in a glove box under argon. A detailed polymerization procedure (run 10 of Table 7) is described here as a typical example. Et₃AlCl (2.5 μL, 0.02 mmol, 1 equiv) was added to a solution of **2c** (27.7 mg, 0.02 mmol) in hexane (8 mL) and the mixture was "aged" for 30 min. The polymerization was carried out at 40 °C for 24 h after addition of isoprene (2.0 mL, 20 mmol). The polymerization mixture was then poured into a large quantity of acidified isopropanol containing 0.1 % (w/w) 2,6-di-*tert*-butyl-4-methylphenol as a stabilizer. The polymer was washed with isopropanol and dried in vacuo at ambient temperature to constant weight. The monomer conversion was determined gravimetrically.

Polymer analyses: The molar masses (*M_w*, *M_n*) of the polymers were determined by size-exclusion chromatography (SEC) with an SEC apparatus fitted with a pump supplied by Waters (Waters 510) and Ultrastaygel columns with pore sizes of 500, 1000, 10000, and 100000 Å (eluent: CHCl₃; flow rate: 0.5 mL min⁻¹). Sample solutions (1.0 mg of polymer per milliliter of CHCl₃) were filtered through a 0.2 μm syringe filter prior to injection. The signals were detected with a differential refractometer (Waters 410) and calibrated against polystyrene standards from Fluka (*M_w*/*M_n* < 1.15). The microstructure of polyisoprenes was examined by ¹³C NMR spectroscopy in CDCl₃.

NMR spectroscopy

Sample preparation: [Ln(AlMe₄)₃] was dissolved in [D₈]toluene for the low temperature studies, in [D₅]chlorobenzene for the high temperature studies, and in [D₆]benzene for multinuclear studies at ambient temperature with a concentration of approximately 0.25 M.

High-resolution NMR spectra were acquired with Bruker Biospin AV500 and AV600 spectrometers equipped with narrow-bore UltraShieldPlus magnets. A 5-mm broadband probe head equipped with a z-gradient coil was used on the AV500. The temperature was set and stabilized with a Bruker B-VT 3000 temperature controller unit regulating the boil-off rate of liquid nitrogen for the variable temperature experiments or the heating of the gas flow from a BCU5 cooling unit for the other NMR experiments. A 5-mm triple resonance (¹H, ¹³C, ¹⁵N) inverse CryoProbe was used on the AV600. Only ¹H (600.13 MHz) and broadband ¹H-decoupled ¹³C (150.91 MHz) spectra at 298 K were recorded on the AV600. Variable-temperature ¹H (500.13 MHz) and broadband ¹H-decoupled ¹³C (125.77 MHz) spectra were acquired on the AV500. The temperature scales on both spectrometers were calibrated against a standard sample (Bruker) containing 4 % methanol in [D₄]methanol. The average estimated uncertainty of the real temperature inside the NMR tubes was 1 K. The sample temperatures were kept at 298 K for all other than the variable-temperature experiments. The ⁸⁹Y NMR spectra of [Y(AlMe₄)₃] dissolved in [D₈]toluene were acquired at 24.51 MHz on the AV500. For the 1D ⁸⁹Y experiment, the pulse width was 9 μs (approx. 55° flip angle), the recycling delay 30 s, and 176 scans were averaged. ¹H inverse-gated decoupling was used to minimize any possible intensity loss from negative NOE effects on ⁸⁹Y. The total experimental time for the ⁸⁹Y NMR experiment was 2 h 20 min. A two-dimensional ¹H-detected ¹H-⁸⁹Y HMQC^{60,61} spectrum was acquired in the pure-absorption mode. Since ⁸⁹Y is present at 100 % natural abundance, no gradients were required for coherence selection. A total of 32 *t_i* increments were collected. Four transients were averaged for each increment and the recycling delay was 2 s. The experiment was optimized for ²J_{H,Y} = 2.5 Hz. Broadband ⁸⁹Y decoupling (composite pulse decoupling) was used during the acquisition. The total experimental time was 7 min. ²⁷Al spectra of [Ln(AlMe₄)₃] were recorded on the AV500 at 130.33 MHz. 2000 scans were averaged. The

NMR spectroscopic data were processed and displayed using iNMR^[62] and Bruker's TopSpin software. The residual ¹H signal of the deuterated solvents and ¹³C solvent signals were used as secondary chemical shift references, and the chemical shifts are thus referenced to internal solvent resonances and reported in parts per million relative to TMS. The \mathcal{E} -scale was used to reference the ⁸⁹Y chemical shift.^[63] Thus, $\mathcal{E} = 4.900198$ MHz for ⁸⁹Y and the measured absolute frequency at $\delta = 0.00$ ppm for ¹H when using the secondary reference, gives a reference frequency for the ⁸⁹Y chemical shifts. The ²⁷Al chemical shifts are reported relative to an external reference, namely a solution of AlCl₃ in D₂O with a drop of concentrated HCl [Al(D₂O)₆]³⁺.

The MEXICO program^[34] was used to analyze the variable temperature ¹H and ¹³C NMR spectra by line-shape analyses of the methyl regions of the spectra. The spectral regions were fitted to a mutual two-site exchange model (equal populations) using a simplex-based iterative procedure. The MEXICO program takes into account the (slight) variations of the ¹H and ¹³C chemical shifts with temperature and the heteronuclear ²J_{Y,H} and ¹J_{Y,C} couplings. Based on variations seen in the rate constants upon adjusting some model parameters, and the quality of the fits (based on χ^2), the average uncertainties for the rate constants are estimated at 10% and 20% for the ¹H and ¹³C spectral series, respectively. The varying contribution from inhomogeneities and the natural linewidths, as well as the limited spectral signal-to-noise ratios, especially for the ¹³C spectra, all contribute to the uncertainties. The QtiPlot program was used to plot, fit, and extract the activation parameters from the kinetic data.^[64] A linear least-squares fitting procedure was used to calculate the activation parameters from the Eyring equation. The uncertainties in the activation parameters were calculated with error propagation formulae.^[65,66] In addition, a comparison was made with results from nonlinear fitting schemes (with and without weighting of the data points). This comparison revealed moderate deviations between the values obtained from the

various fitting schemes, and also suggested that the uncertainties found using the error propagation formulas were reasonable.

Single-crystal X-ray structures

Crystal data and details of the structure determination are presented in Table 8.

Compounds 1d, 1h, and 3d: A suitable single crystal was transferred into a Lindemann capillary, fixed, and sealed. Data collection was carried out on an area detecting system (Nonius, MACH3, κ -CCD) at the window of a rotating anode (Nonius, FR591) with graphite monochromated MoK α radiation ($\lambda = 0.71073$ Å) at 173, 123, and 153 K, respectively (Oxford Cryosystems). Nine data sets were measured in rotation scan modus with $\Delta\phi/\Delta\omega = 1.0^\circ$. The structure was solved using SIR92 and full-matrix least-squares refinement made with SHELXL-97.^[67] All hydrogen positions were refined with individual isotropic displacement parameters for **1h**. Noncoordinating methyl groups in **1d** and **3d** were refined as rigid and rotating (difference Fourier density optimization) CH₃ groups around the respective C–Al bonds. Coordinating methyl groups were refined as rigid pyramidal groups with the same C–H and H–H distances as for the previous, but with the threefold axis of the pyramidal rigid group allowed to be nonparallel to the C–Al bond axis. The isotropic displacement parameters for all H atoms were set to be 1.5 times that of the pivot C atom.

Compounds 1b and 1f: The crystals were placed in a nylon loop containing Paratone oil (Hampton Research) and mounted directly into the N₂ cold stream (Oxford Cryosystems Series 600) on a Bruker AXS SMART 2 K CCD diffractometer. Data were collected by means of 0.3° ω -scans in four orthogonal φ -settings using MoK α radiation ($\lambda = 0.71073$ Å). Data collection was controlled by the program SMART, data integration by SAINT, and structure solution and model refinement were performed with SHELXS-97^[68b] and SHELXL-97,^[67] respectively. Noncoordinating

Table 8. Crystallographic data for compounds **1b**, **1d**, **1f**, **1h**, and **3d**.

| | 1b | 1d | 1f | 1h | 3d |
|--|--|--|--|--|---|
| formula | C ₁₂ H ₃₆ Al ₃ La | C ₁₂ H ₃₆ Al ₃ Pr | C ₁₂ H ₃₆ Al ₃ Sm | C ₁₂ H ₃₆ Al ₃ Lu | C ₂₃ H ₆₀ Al ₃ O ₄ PrSi |
| Fw | 400.26 | 402.26 | 411.723 | 436.32 | 650.65 |
| color/habit | colorless/prism | pale green/needle | yellow/needle | colorless/fragment | pale green/plate |
| crystal dimensions [mm ³] | 0.40 × 0.38 × 0.30 | 0.62 × 0.30 × 0.21 | 0.57 × 0.22 × 0.12 | 0.25 × 0.30 × 0.58 | 0.33 × 0.31 × 0.31 |
| cryst system | monoclinic | monoclinic | monoclinic | monoclinic | monoclinic |
| space group | P2 ₁ /n | P2 ₁ /c | C2/c | C2/c | P2 ₁ /c |
| a [Å] | 15.4744(14) | 7.4567(1) | 10.8844(4) | 10.8848(1) | 10.2408(1) |
| b [Å] | 7.3837(7) | 17.9165(1) | 15.9478(6) | 15.6948(1) | 17.2826(2) |
| c [Å] | 17.5984(16) | 32.5452(2) | 12.6732(5) | 12.4838(1) | 20.0699(2) |
| β [°] | 91.753(2) | 92.0119(2) | 102.932(1) | 101.8067(3) | 104.7609(6) |
| V [Å ³] | 2009.8(3) | 4345.29(7) | 2144.05(14) | 2087.55(3) | 3434.90(6) |
| Z | 4 | 8 | 4 | 4 | 4 |
| T [K] | 123(2) | 173(2) | 123(2) | 123(1) | 153(2) |
| ρ_{calcd} [mg m ⁻³] | 1.323 | 1.230 | 1.275 | 1.388 | 1.258 |
| μ [mm ⁻¹] | 2.238 | 2.347 | 2.845 | 4.838 | 1.552 |
| F(000) | 816 | 1648 | 836 | 872 | 1368 |
| θ range [°] | 1.73/30.11 | 2.20/26.27 | 2.31/30.08 | 2.31/25.29 | 2.10/26.38 |
| index ranges | −21 ≤ h ≤ 21, −10 ≤ k ≤ 10, −24 ≤ l ≤ 24 | −9 ≤ h ≤ 9, −22 ≤ k ≤ 21, −40 ≤ l ≤ 39 | −15 ≤ h ≤ 15, −22 ≤ k ≤ 22, −17 ≤ l ≤ 17 | −13 ≤ h ≤ 13, −18 ≤ k ≤ 18, −14 ≤ l ≤ 14 | −12 ≤ h ≤ 12, −21 ≤ k ≤ 21, −25 ≤ l ≤ 23 |
| no. of rflns collected | 33 491 | 45 964 | 18 226 | 25 693 | 84 999 |
| no. of indep rflns/R _{int} | 5902/0.0261 | 8676/0.0415 | 3146/0.0163 | 1901/0.040 | 6887/0.0657 |
| No. of obsd rflns (I > 2 σ (I)) | 5626 | 7696 | 3088 | 1892 | 5486 |
| data/restraints/ params | 5902/48/221 | 8676/72/409 | 3146/18/104 | 1901/0/147 | 6887/30/365 |
| R1/wR2 (I > 2 σ (I)) ^[a] | 0.0275/0.0743 | 0.0225/0.0448 | 0.0103/0.0276 | 0.0102/0.0248 | 0.0314/0.0576 |
| R1/wR2 (all data) ^[a] | 0.0287/0.0747 | 0.0287/0.0466 | 0.0107/0.0278 | 0.0103/0.0248 | 0.0503/0.0624 |
| GOF (on F ²) ^[a] | 1.284 | 1.077 | 1.110 | 1.113 | 1.054 |
| largest diff peak and hole [e Å ⁻³] | 1.464/−0.867 | 0.409/−0.423 | 0.274/−0.662 | 0.46/−0.50 | 1.100/−0.602 |

[a] R1 = $\Sigma(|F_o| - |F_c|) / \Sigma |F_o|$; wR2 = $\{\Sigma[w(F_o^2 - F_c^2)^2] / \Sigma[w(F_o^2)^2]\}^{1/2}$; GOF = $\{\Sigma[w(F_o^2 - F_c^2)^2] / (n - \dots)\}^{1/2}$.

methyl groups were refined as rigid and rotating (difference Fourier density optimization) CH₃ groups around the respective C–Al bonds. Coordinating methyl groups were refined as rigid pyramidal groups with the same C–H and H–H distances as for the previous, but with the threefold axis of the pyramidal rigid group allowed to be nonparallel to the C–Al bond axis. The isotropic displacement parameters for all H atoms were set to be 1.5 times that of the pivot C atom.

CCDC-642735–CCDC-642739 contain the supplementary crystallographic data for this paper. These data can be obtained free of charge from the Cambridge Crystallographic Data Center via www.ccdc.cam.ac.uk/data_request/cif.

Acknowledgments

Financial support from the Norwegian Research Council (project no. 171245V30) and the program Nanoscience@UiB is gratefully acknowledged. We also thank Dr. L. Friebe (c/o Prof. O. Nuyken) for GPC analysis and Rannveig Litlabø for providing a sample of [Pr(AlMe₄)₃].

- [1] a) J. M. Birmingham, G. Wilkinson, *J. Am. Chem. Soc.* **1954**, *76*, 6210; b) J. M. Birmingham, G. Wilkinson, *J. Am. Chem. Soc.* **1956**, *78*, 42.
- [2] H. Gilman, R. G. Jones, *J. Am. Chem. Soc.* **1945**, *67*, 505.
- [3] F. A. Hart, A. G. Massey, M. S. Saran, *J. Organomet. Chem.* **1970**, *21*, 147.
- [4] Reviews: a) F. T. Edelmann, *Top. Curr. Chem.* **1996**, *179*, 247; b) H. Yasuda, *Top. Organomet. Chem.* **1999**, *2*, 255; c) R. Anwander in *Applied Homogeneous Catalysis with Organometallic Compounds* (Eds.: B. Cornils, W. A. Herrmann), Wiley-VCH, Weinheim, **2002**, p. 974; d) F. T. Edelmann, D. M. M. Freckmann, H. Schumann, *Chem. Rev.* **2002**, *102*, 1851.
- [5] a) G. K. Barker, M. F. Lappert, *J. Organomet. Chem.* **1974**, *76*, C45; b) P. B. Hitchcock, M. F. Lappert, R. G. Smith, R. A. Bartlett, P. P. Power, *J. Chem. Soc. Chem. Commun.* **1988**, 1007.
- [6] H. M. Dietrich, G. Raudaschl-Sieber, R. Anwander, *Angew. Chem.* **2005**, *117*, 5437; *Angew. Chem. Int. Ed.* **2005**, *44*, 5303.
- [7] a) H. Schumann, J. Müller, *Angew. Chem.* **1978**, *90*, 307; *Angew. Chem. Int. Ed. Engl.* **1978**, *17*, 276; b) H. Schumann, J. Pickardt, N. Bruncks, *Angew. Chem.* **1981**, *93*, 127; *Angew. Chem. Int. Ed. Engl.* **1981**, *20*, 120; c) H. Schumann, J. Müller, N. Bruncks, H. Lauke, J. Pickardt, H. Schwarz, K. Eckart, *Organometallics* **1984**, *3*, 69; d) H. Schumann, H. Lauke, E. Hahn, J. Pickardt, *J. Organomet. Chem.* **1984**, *263*, 29; e) A. L. Wayda, W. J. Evans, *J. Am. Chem. Soc.* **1978**, *100*, 7119; f) J. L. Atwood, M. F. Lappert, H. Zhang, *J. Chem. Soc. Chem. Commun.* **1988**, 1308.
- [8] a) M. F. Lappert, R. Pearce, *J. Chem. Soc. Chem. Commun.* **1973**, 126; b) J. L. Atwood, W. E. Hunter, R. D. Rogers, J. Holton, J. McMeeking, R. Pearce, M. F. Lappert, *J. Chem. Soc. Chem. Commun.* **1978**, 140; c) H. Schumann, J. Müller, *J. Organomet. Chem.* **1978**, *146*, C5; d) H. Schumann, D. M. M. Freckmann, S. Dechert, *Z. Anorg. Allg. Chem.* **2002**, *628*, 2422; e) M. Niemeyer, *Acta Crystallogr. Sect. A* **2001**, *E57*, m553; f) W. J. Evans, J. C. Brady, J. W. Ziller, *J. Am. Chem. Soc.* **2001**, *123*, 7711.
- [9] D. J. H. Emslie, W. E. Piers, M. Parvez, R. McDonald, *Organometallics* **2002**, *21*, 4226.
- [10] M. Niemeyer, *Z. Anorg. Allg. Chem.* **2000**, *626*, 1027.
- [11] S. Bambirra, A. Meetsma, B. Hessen, *Organometallics* **2006**, *25*, 3454.
- [12] H. H. Karsch, A. Appelt, G. Müller, *Angew. Chem.* **1986**, *98*, 832; *Angew. Chem. Int. Ed. Engl.* **1986**, *25*, 823.
- [13] a) M. Boojj, N. H. Kiers, H. J. Heeres, J. H. Teuben, *J. Organomet. Chem.* **1989**, *364*, 79; b) A. L. Wayda, R. D. Rogers, *Organometallics* **1985**, *4*, 1440; c) L. E. Manzer, *J. Am. Chem. Soc.* **1978**, *100*, 8068; d) S. Harder, *Organometallics* **2005**, *24*, 373.
- [14] a) W. J. Evans, R. Anwander, J. W. Ziller, *Organometallics* **1995**, *14*, 1107; b) W. T. Klooster, R. S. Lu, R. Anwander, W. J. Evans, T. E. Koetzle, R. Bau, *Angew. Chem.* **1998**, *110*, 1326; *Angew. Chem. Int. Ed.* **1998**, *37*, 1268.
- [15] A. Fischbach, R. Anwander, *Adv. Polym. Sci.* **2006**, *204*, 155.
- [16] A. Fischbach, F. Perdih, E. Herdtweck, R. Anwander, *Organometallics* **2006**, *25*, 1626.
- [17] A. Fischbach, M. G. Klimpel, M. Widenmeyer, E. Herdtweck, W. Scherer, R. Anwander, *Angew. Chem.* **2004**, *116*, 2284; *Angew. Chem. Int. Ed.* **2004**, *43*, 2234.
- [18] H. M. Dietrich, C. Zapolko, E. Herdtweck, R. Anwander, *Organometallics* **2005**, *24*, 5767.
- [19] H. M. Dietrich, M. Zimmermann, R. Anwander, unpublished results.
- [20] M. Zimmermann, K. W. Törnroos, R. Anwander, *Organometallics* **2006**, *25*, 3593.
- [21] M. Zimmermann, K. W. Törnroos, R. Anwander, *Angew. Chem.* **2007**, *119*, 3187; *Angew. Chem. Int. Ed. Engl.* **2007**, *46*, 3126.
- [22] E. Le Roux, F. Jaroschik, F. Nief, K. W. Törnroos, R. Anwander, unpublished results.
- [23] H. M. Dietrich, K. W. Törnroos, R. Anwander, *J. Am. Chem. Soc.* **2006**, *128*, 9298.
- [24] H. M. Dietrich, H. Grove, K. W. Törnroos, R. Anwander, *J. Am. Chem. Soc.* **2006**, *128*, 1458.
- [25] Due to the low solubilities of the trichlorides of the larger lanthanide metals, Soxhlet extraction with thf to generate the activated [LnCl₃(thf)_x] complexes is time consuming.
- [26] R. Anwander, O. Runte, J. Eppinger, G. Gerstberger, E. Herdtweck, M. Spiegler, *J. Chem. Soc. Dalton Trans.* **1998**, 847.
- [27] D. M. Barnhart, D. L. Clark, J. C. Gordon, J. C. Huffman, J. G. Watkin, B. D. Zwick, *J. Am. Chem. Soc.* **1993**, *115*, 8461.
- [28] R. Anwander, M. G. Klimpel, H. M. Dietrich, D. J. Shorokhov, W. Scherer, *Chem. Commun.* **2003**, 1008.
- [29] W. J. Evans, L. R. Chamberlain, T. A. Ulibarri, J. W. Ziller, *J. Am. Chem. Soc.* **1988**, *110*, 6423.
- [30] G. R. Patzke, R. Wartchow, W. Urland, *Z. Anorg. Allg. Chem.* **2000**, *626*, 789.
- [31] H. M. Dietrich, O. Schuster, K. W. Törnroos, R. Anwander, *Angew. Chem.* **2006**, *118*, 4977; *Angew. Chem. Int. Ed.* **2006**, *45*, 4858.
- [32] M. E. O'Neill, K. Wade in *Comprehensive Organometallic Chemistry* (Eds.: G. Wilkinson, F. G. A. Stone, E. W. Abel), Pergamon Press, New York, **1982**, p. 593.
- [33] J. Eppinger, *PhD Thesis*, **1999**, Technische Universität München.
- [34] a) A. D. Bain, G. J. Duns, *Can. J. Chem.* **1996**, *74*, 819; b) A. D. Bain, D. M. Rex, R. N. Smith, *Magn. Reson. Chem.* **2001**, *39*, 122.
- [35] W. von Philipsborn, *Chem. Soc. Rev.* **1999**, *28*, 95.
- [36] P. G. Plioger, K. D. John, T. S. Keizer, T. M. McCleskey, A. K. Burell, R. L. Martin, *J. Am. Chem. Soc.* **2004**, *126*, 14651.
- [37] P. J. Shapiro, *Coord. Chem. Rev.* **1999**, *189*, 1.
- [38] C. J. Schaverien, *Organometallics* **1994**, *13*, 69.
- [39] W. J. Evans, J. H. Meadows, A. G. Kostka, G. L. Closs, *Organometallics* **1985**, *4*, 324.
- [40] R. E. White, T. P. Hanusa, *Organometallics* **2006**, *25*, 5621.
- [41] S. Arndt, J. Okuda, *Adv. Synth. Catal.* **2005**, *347*, 339.
- [42] M. G. Klimpel, R. Anwander, M. Tafipolsky, W. Scherer, *Organometallics* **2001**, *20*, 3983.
- [43] R. Benn, E. Janssen, H. Lehmkuhl, A. Rufinska, K. Angermund, P. Betz, R. Goddard, C. Krüger, *J. Organomet. Chem.* **1991**, *411*, 37.
- [44] H. E. Swift, C. P. Pole, J. F. Itzel, *J. Phys. Chem.* **1964**, *68*, 2509.
- [45] D. E. O'Reilly, *J. Chem. Phys.* **1960**, *32*, 1007.
- [46] B. W. Epperlein, O. Lutz, *Z. Naturforsch. A* **1968**, *23*, 1413.
- [47] J. W. Akitt, *Annu. Rep. NMR Spectrosc.* **1972**, *5A*, 465.
- [48] A. Fischbach, F. Perdih, P. Sirsch, W. Scherer, R. Anwander, *Organometallics* **2002**, *21*, 4569.
- [49] A. Fischbach, G. Eickerling, W. Scherer, E. Herdtweck, R. Anwander, *Z. Naturforsch. B* **2004**, *59*, 1353.
- [50] R. Anwander, *Chem. Mater.* **2001**, *13*, 4419.
- [51] Z. Shen, J. Ouyang, F. Wang, Z. Hu, Y. Fu, B. Qian, *J. Polym. Sci.: Polym. Chem. Ed.* **1980**, *18*, 3345.

- [52] Y. B. Monakov, N. G. Marina, I. G. Savel'eva, L. E. Zhiber, V. G. Kozlov, S. R. Rafikov, *Dokl. Akad. Nauk SSSR* **1982**, 265, 1431; *Chem. Abstr.* **1983**, 98, 54523.
- [53] J. Witte, *Angew. Makromol. Chem.* **1981**, 94, 119.
- [54] L. Friebe, O. Nuyken, H. Windisch, W. Obrecht, *Macromol. Chem. Phys.* **2002**, 203, 1055.
- [55] A. Pross, P. Marquardt, K. H. Reichert, W. Nentwig, T. Knauf, *Angew. Makromol. Chem.* **1997**, 249, 59.
- [56] L. Friebe, O. Nuyken, W. Obrecht, *J. Macromol. Sci. Pure Appl. Chem.* **2005**, 42, 839.
- [57] C. Boisson, F. Barbotin, R. Spitz, *Macromol. Chem. Phys.* **1999**, 200, 1163.
- [58] J. Yamamoto, C. A. Wilkie, *Inorg. Chem.* **1971**, 10, 1129.
- [59] H. Tani, T. Konomi, *J. Polym. Sci., Part A* **1966**, 4, 301.
- [60] L. Müller, *J. Am. Chem. Soc.* **1979**, 101, 4481.
- [61] A. Bax, R. H. Griffey, B. L. Hawkins, *J. Magn. Reson.* **1983**, 55, 301.
- [62] Nucleomatica, <http://www.inmr.net/index.html>
- [63] R. K. Harris, E. D. Becker, S. M. Cabral de Menezes, R. Goodfellow, P. Granger, *Pure Appl. Chem.* **2001**, 73, 1795.
- [64] <http://soft.proindependent.com/qtiplot.html>
- [65] P. M. Morse, M. D. Spencer, S. R. Wilson, G. S. Girolami, *Organometallics* **1994**, 13, 1646.
- [66] Q. D. Shelby, W. Lin, G. S. Girolami, *Organometallics* **1999**, 18, 1904.
- [67] a) Data Software for NONIUS Collection κ -CCD devices, Delft (The Netherlands) **1997**; b) Z. Otwinowski, W. Minor, *Methods Enzymol.* **1997**, 276, 307; c) *International Tables for Crystallography*, (Eds: T. Hahn, A. J. C. Wilson), Kluwer Academic Publisher, Dordrecht, Boston, London, **1992**; d) A. L. Spek, PLATON: A Multipurpose Crystallographic Tool, Utrecht University, Utrecht (The Netherlands) **2007**; e) SIR92: A. Altomare, G. Casciarano, C. Giacovazzo, A. Guagliardi, M. C. Burla, G. Polidori, M. Camalli, *J. Appl. Cryst.* **1994**, 27, 435; f) G. M. Sheldrick, SHELXL-97, University of Göttingen, Germany, **1998**.
- [68] a) SMART, Ver. 5.054, **1999** and SAINT, Ver. 6.45a, Bruker AXS Inc., Madison, Wisconsin (USA), **2001**; b) G. M. Sheldrick, SHELXS-97, University of Göttingen, Germany, **2003**.

Received: April 4, 2007
Published online: July 24, 2007

Paper II

Implementation of Ln(AlMe₄)₃ as Precursors in Postlanthanidocene Chemistry

Melanie Zimmermann, Karl W. Törnroos, and Reiner Anwander*

Department of Chemistry, University of Bergen, Allégaten 41, N-5007, Bergen, Norway

Received March 17, 2006

cis-2,5-Bis[*N,N*-((2,6-diisopropylphenyl)amino)methyl]tetrahydrofuran (H₂BDPPthf) was obtained from LiNH(2,6-*i*-Pr₂C₆H₃) and *cis*-2,5-bis((tosyloxy)methyl)tetrahydrofuran in high yield and employed as a new [NON]²⁻ ancillary ligand for rare-earth metal centers. The reaction of H₂BDPPthf with homoleptic tetramethylaluminates Ln(AlMe₄)₃ (Ln = Y, Nd, La) quantitatively yielded heterobimetallic complexes (BDPPthf)Ln(AlMe₄)(AlMe₃) via alkane elimination. X-ray structure analysis of (BDPPthf)Ln(AlMe₄)(AlMe₃) (Ln = Y, La) revealed different coordination modes of BDPPthf, AlMe₄⁻, and AlMe₃. The yttrium derivative displays an η²-coordination of BDPPthf and insertion of AlMe₃ into one of the Ln–N anilido bonds to form a novel [Ln^{III}(μ-Me)₂AlMe(NR₂)] moiety. In contrast, BDPPthf coordinates the larger lanthanum center in an η³ fashion involving a heterobridging [La(μ-NR₂)(μ-Me)AlMe₂] moiety. The AlMe₄⁻ ligand adopts an unusual distorted μ:η³- (La) and a routine μ:η²-coordination mode (Y) depending on the size of the metal center. The intrinsic [NON]²⁻ ligand functionality for the first time implied the formation and structural identification of a kinetically favored aluminate/HR protonolysis product (Y), whereas the thermodynamically favored Ln–amido contact is found for the lanthanum derivative. All organolanthanide complexes were fully characterized by NMR and FTIR spectroscopy and elemental analysis.

Introduction

The quest for new, highly active and selective polymerization catalysts continues to stimulate research directed toward ancillary ligand and metal precursor design.¹ Recent developments in organolanthanide chemistry have focused on the use of non-cyclopentadienyl ancillary ligands, with much of the interest in “postlanthanidocene” chemistry being linked to the formation of cationic alkyl species.² In general, the activity and selectivity of a catalyst is related to precatalyst stability and the active species derived therefrom. To date, chelating diamido ligands of the type [NDoN]²⁻, such as [NNN]²⁻,³ [NON]²⁻,⁴ and [NPN]²⁻,⁵ have proved to be particularly useful in the formation of discrete and stable lanthanide complexes. In a previous study we reported the synthesis of a series of [NNN]LnR(THF)_x (Ln = Sc, Y, Lu; R = CH₂SiMe₃, N^{*i*}Pr₂, N(SiHMe₂)₂, NEt₂) complexes derived from H₂BDPPpyr (2,6-bis((2,6-diisopropylphenyl)amino)methyl)pyridine)^{3b} and the applicability of the scandium derivatives for the living polymerization of methyl methacrylate (MMA).

The successful complexation of such diamido ligands is limited by the availability of suitable precursors (namely, alkyl

species) for the entire lanthanide series.⁶ To date, Ln(CH₂-SiMe₃)₃(THF)_x (x = 2, 3),⁷ Ln[CH(SiMe₃)₂]₃,⁸ Ln(CH₂SiMe₂-Ph)₃(THF)₂,⁹ and Ln(*o*-Me₂NC₆H₄CH₂)₃¹⁰ represent the most commonly used lanthanide alkyl precursors that facilitate the formation of postlanthanidocene complexes via an alkane elimination reaction.

We have recently shown that homoleptic complexes Ln(AlMe₄)₃ (Ln = Y, La, Nd, Lu) are convenient synthetic precursors en route to mononuclear bis(tetraalkylaluminate) half-sandwich complexes of the type (C₅Me₅)Ln(AlMe₄)₂.¹¹ Herein, we describe the use of Ln(AlMe₄)₃ as precursors for the synthesis of postlanthanidocene complexes using *cis*-2,5-bis[*N,N*-((2,6-diisopropylphenyl)amino)methyl]tetrahydrofuran (H₂BDPPthf, H₂[1]) as a new donor-functionalized diamido ligand.

Results and Discussion

[NDoN]²⁻ Ancillary Ligand Library. Our initial investigations into [NDoN]²⁻ diamido-based postlanthanidocene chemistry revealed an unexpected beneficial effect of an additional donor (Do) functionality in the ligand backbone.^{3b} While five-coordinate complexes [^{*i*}PrNNN^{*i*}Pr]ScR(THF) initiated the living polymerization of MMA, four-coordinate [^{*i*}PrNN^{*i*}Pr]ScR(THF), lacking a donor functionality, did not show any polymerization activity. We also found that the stability of complexes [^{*i*}PrNNN^{*i*}Pr]-

* Corresponding author. Fax: +47 555 89490. E-mail: reiner.anwander@kj.uib.no.

(1) (a) Schrock, R. R. *Acc. Chem. Res.* **1997**, *30*, 9. (b) Kempe, R. *Angew. Chem., Int. Ed.* **2000**, *39*, 468. (c) Gade, L. H. *Acc. Chem. Res.* **2002**, *35*, 575. (d) Piers, W. E.; Emslie, D. J. H. *Coord. Chem. Rev.* **2002**, *233–234*, 131. (e) Gibson, V. C.; Spitzmesser, S. K. *Chem. Rev.* **2003**, *103*, 283.

(2) Arndt, S.; Okuda, J. *Adv. Synth. Catal.* **2005**, *347*, 339.

(3) (a) Skinner, M. E. G.; Tyrell, B. R.; Ward, B. D.; Mountford, P. J. *Chem. Soc., Dalton Trans.* **2002**, 1694. (b) Estler, F.; Eickerling, G.; Herdtweck, E.; Anwander, R. *Organometallics* **2003**, *22*, 1212. (c) Sugiyama, H.; Korobkov, I.; Gambarotta, S.; Möller, A.; Budzelaar, P. H. M. *Inorg. Chem.* **2004**, *43*, 5771.

(4) Graf, D. D.; Davis, W. M.; Schrock, R. R. *Organometallics* **1998**, *17*, 5820.

(5) Fryzuk, M. D.; Yu, P.; Patrick, B. O. *Can. J. Chem.* **2001**, *79*, 1194.

(6) Bamber, S.; Bouwkamp, M. W.; Meetsma, A.; Hessen, B. J. *Am. Chem. Soc.* **2004**, *126*, 9182.

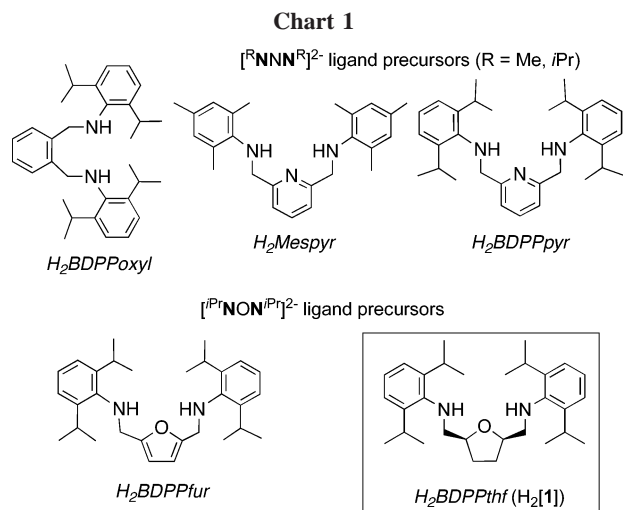
(7) Lappert, M. F.; Pearce, R. J. *Chem. Soc., Chem. Commun.* **1973**, 126.

(8) Hitchcock, P. B.; Lappert, M. F.; Smith, R. G.; Bartlett, R. A.; Power, P. P. *J. Chem. Soc., Chem. Commun.* **1988**, 1007.

(9) Emslie, D. J. H.; Piers, W. E.; Parvez, M.; McDonald, R. *Organometallics* **2002**, *21*, 4226.

(10) Harder, S. *Organometallics* **2005**, *24*, 373.

(11) Dietrich, H. M.; Zapilko, C.; Herdtweck, E.; Anwander, R. *Organometallics* **2005**, *24*, 5767.



$\text{LnR}(\text{THF})_x$ ($\text{Ln} = \text{Sc}$, $x = 1$; $\text{Ln} = \text{Lu}$, Y , $x = 2$) is governed by a metal size-dependent match/mismatch of the rigid tridentate ancillary ligand ($\text{Sc} \approx \text{Lu} \gg \text{Y}$) and by the steric shielding of the metal center via the ancillary ligand periphery ($[\textit{iPr}^{\text{NNN}}\textit{iPr}] \gg [\text{Me}^{\text{NNN}}\text{Me}]$). To get more insight into any structure–reactivity relations, we are currently attempting to complement this library by O-donor-functionalized ligands $[\textit{iPr}^{\text{NON}}\textit{iPr}]^{2-}$ as shown in Chart 1.

It can be anticipated that the complexation ability of rare-earth metal centers is markedly affected by (a) a smaller ring size in the ligand backbone, (b) an enhanced coordinative flexibility of the saturated tetrahydrofuran derivative, and (c) oxygen versus nitrogen donor coordination. While the “methyl” variant H_2BMPthf has previously been used for the synthesis of postzirconocene complex $[\text{Me}^{\text{NON}}\text{Me}]\text{ZrMe}_2$,¹² $\text{H}_2\text{BDPPthf}$ and $\text{H}_2\text{BDPPfur}$ ¹³ appear to be new ligand precursors. $\text{H}_2\text{BDPPthf}$ ($\text{H}_2[1]$) was prepared in four steps from 5-hydroxymethylfuraldehyde following the manner reported by Flores et al.¹² In the last step of the synthesis *cis*-2,5-bis((tosyloxy)methyl)tetrahydrofuran was treated with $\text{LiNH}(2,6\text{-}i\text{Pr}_2\text{C}_6\text{H}_3)$ to yield diamine $\text{H}_2[1]$ as a white solid (93%). ^1H and ^{13}C NMR spectra of $\text{H}_2[1]$ are in accordance with the *cis*-configuration of the molecule (mirror plane) and a highly flexible structure, as evidenced by rapid rotation of the aryl rings about the $\text{N}-\text{C}_{\text{ipso}}$ bond.

Synthesis and Characterization of Aluminato Complexes Derived from $\text{H}_2\text{BDPPthf}$ ($\text{H}_2[1]$). Compounds $(\text{BDPPthf})\text{-Ln}(\text{AlMe}_4)(\text{AlMe}_3)$ (Y , **3a**; La , **3b**; and Nd , **3c**) were prepared by slow addition of a hexane solution of $\text{Ln}(\text{AlMe}_4)_3$ to a solution of $\text{H}_2\text{BDPPthf}$ in hexane (Scheme 1).

The reaction was evidenced by instant gas evolution and the precipitation of **3** as analytically pure white solids for the yttrium and lanthanum derivative (**3a,b**) and as a blue-green solid for the neodymium compound (**3c**), respectively. The lanthanide complexes were obtained in nearly quantitative yields. In an attempt to examine the implications of the metal size for the complex formation, Y , Nd , and La were chosen as representative of smaller- and larger-sized rare-earth metal centers.

Single crystals of **3a** and **3b** suitable for X-ray structure analysis were grown from a hexane/toluene mixture (Figures 1

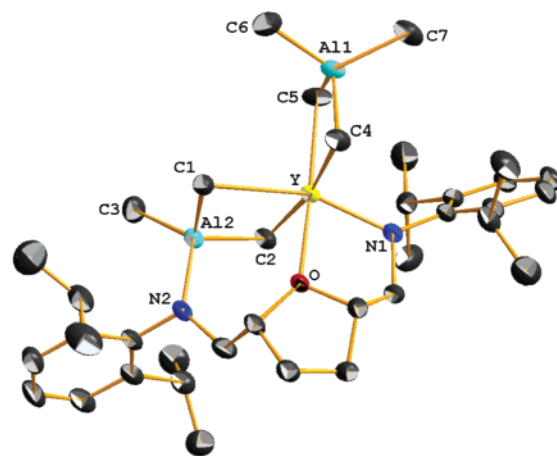


Figure 1. ORTEP drawing of $(\text{BDPPthf})\text{Y}(\text{AlMe}_4)(\text{AlMe}_3)$ (**3a**) in the solid state. Thermal ellipsoids are drawn at the 50% probability level. Hydrogen atoms are omitted for clarity. Atomic labels are given for selected atoms.

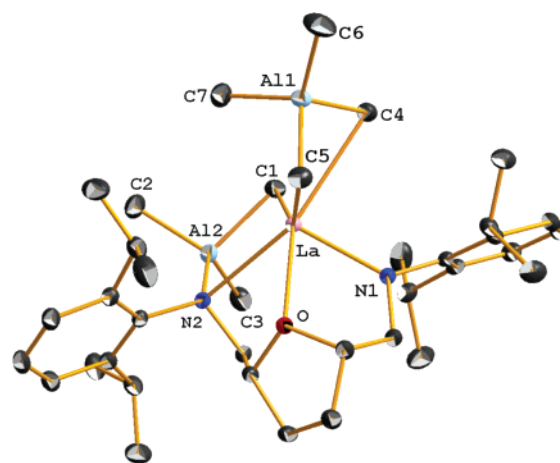
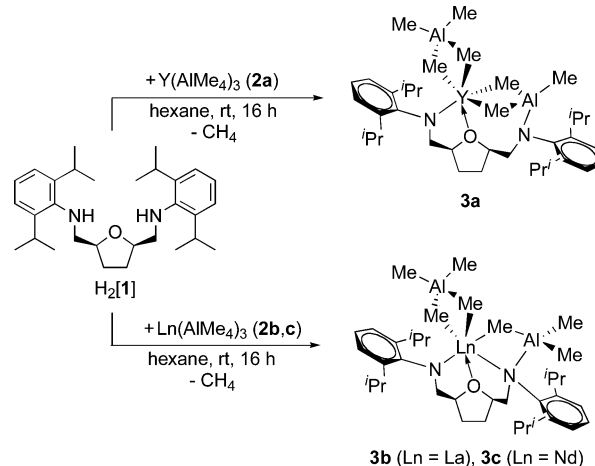


Figure 2. ORTEP drawing of $(\text{BDPPthf})\text{La}(\text{AlMe}_4)(\text{AlMe}_3)$ (**3b**) in the solid state. Thermal ellipsoids are drawn at the 50% probability level. Hydrogen atoms are omitted for clarity. Atomic labels are given for selected atoms.

Scheme 1. Synthesis of $(\text{BDPPthf})\text{Ln}(\text{AlMe}_4)(\text{AlMe}_3)$ ($\text{Ln} = \text{Y}$, La , and Nd) (3**) from $\text{H}_2\text{BDPPthf}$ (**1**) and $\text{Ln}(\text{AlMe}_4)_3$ ($\text{Ln} = \text{Y}$, La , and Nd) (**2**)**



(12) Flores, M. A.; Manzoni, M. R.; Baumann, R.; Davis, W. M.; Schrock, R. R. *Organometallics* **1999**, *18*, 3220.

(13) Zimmermann, M.; Herdtweck, E.; Anwender, R. Abstracts of Papers; 229th ACS National Meeting, San Diego, CA; American Chemical Society: Washington, DC, 2005; INOR 856.

and **2**). Selected bond distances and angles are listed in Table 1. Both complexes reveal the same net molecular composition of $(\text{BDPPthf})\text{Ln}(\text{AlMe}_4)(\text{AlMe}_3)$ with six-coordinate metal centers, however, a distinct organoaluminum coordination.

Table 1. Selected Interatomic Distances and Angles for (BDPPthf)Y(AlMe₄)(AlMe₃) (3a) and (BDPPthf)La(AlMe₄)(AlMe₃) (3b)

| | 3a (Ln = Y) | 3b (Ln = La) |
|-------------------|-------------|--------------|
| Bond Lengths (Å) | | |
| Ln–N1 | 2.178(2) | 2.333(2) |
| Ln–N2 | | 2.817(2) |
| Ln–O | 2.3376(15) | 2.493(2) |
| Ln···Al1 | 3.0972(8) | 3.0661(6) |
| Ln···Al2 | 3.1110(7) | 3.3939(7) |
| Ln–C1 | 2.607(3) | 2.696(2) |
| Ln–C2 | 2.584(3) | |
| Ln–C4 | 2.573(3) | 2.920(2) |
| Ln–C5 | 2.516(3) | 2.780(2) |
| Ln–C7 | | 3.236(3) |
| Al1–C4 | 2.065(3) | 2.055(3) |
| Al1–C5 | 2.072(3) | 2.065(3) |
| Al1–C6 | 1.967(3) | 1.958(3) |
| Al1–C7 | 1.960(3) | 2.006(3) |
| Al2–N2 | 1.832(2) | 1.951(2) |
| Al2–C1 | 2.062(3) | 2.075(2) |
| Al2–C2 | 2.056(3) | 1.971(3) |
| Al2–C3 | 1.958(3) | 1.987(3) |
| Bond Angles (deg) | | |
| N1–Ln–N2 | | 109.5(1) |
| O–Ln–C5 | 176.7(1) | |
| O–Ln–N1 | 76.1(1) | 69.3(1) |
| O–Ln–N2 | | 67.5(1) |
| O–Ln–C1 | 81.9(1) | 134.7(1) |
| O–Ln–C2 | 86.5(1) | |
| O–Ln–C4 | 95.0(1) | 140.9(1) |
| N1–Ln–C1 | 158.0(1) | |
| N1–Ln–C2 | 96.3(1) | |
| N2–Ln–C1 | | 72.8(1) |
| N2–Ln–C4 | | 151.5(1) |
| N2–Ln–C5 | | 127.7(1) |
| C4–Ln–C5 | 83.1(1) | 71.2(1) |
| C4–Al1–C5 | 109.4(1) | 107.4(1) |
| Ln–C4–Al1 | 83.0(1) | 73.8(1) |
| Ln–C5–Al1 | 84.3(1) | 76.9(1) |
| Ln–C1–Al2 | 82.7(1) | 89.7(1) |
| Ln–C2–Al2 | 83.4(1) | |
| C1–Ln–C2 | 80.9(1) | |
| C1–Al2–C2 | 109.8(1) | |

The yttrium complex **3a** adopts a distorted octahedral coordination geometry, with the Do-oxygen and one of the tetramethylaluminato carbons in the apical positions ($\angle\text{O–Y–C5} = 176.7^\circ$). The BDPPthf ancillary ligand is coordinated to the yttrium center in a η^2 fashion with very short Y–N1 (2.178(2) Å) and Y–O (2.338(2) Å) bond lengths. For comparison, the corresponding Y–[NON]²⁻ bond lengths in the five-coordinate complex [tBu-d₆-N-o-C₆H₄)₂O]Y[CH(SiMe₃)₂](THF) are 2.290 (av) and 2.337(8) Å.⁴ The AlMe₄⁻ ligand coordinates in a η^2 fashion with an almost planar heterobimetallic [Y(μ -Me)₂Al] moiety ($\angle\text{C4–Y–C5–Al1} = -3.3^\circ$, interplanar angle C4YC5–C4Al1C5 = 5.7°). The Y–C bond lengths are in the expected range (Y–C1/C2 = 2.596 Å (av)).¹⁴ The AlMe₃ unit appears inserted into a fictitious Y–N2 bond, resulting in a novel [Ln^{III}(μ -Me)₂AlMe(NR₂)] moiety with slightly shortened Y–(μ -CH₃) bond lengths (Y–C4/C5 = 2.545 Å (av)). The [Y(μ -Me)₂Al] moiety is slightly bent toward the N2 atom ($\angle\text{C1–Y–C2–Al2} = -11.7^\circ$, interplanar angle C1YC2–C1Al2C2 = 20.4°). To the best of our knowledge Yb^{III}-[N(SiMe₃)₂]₂(AlMe₃)₂ is the only structure featuring a comparable [Ln(μ -Me)₂AlMe(NR₂)] unit.¹⁵

The lanthanum complex **3b** represents a rare example of a [NDoN]²⁻ postlanthanidocene complex with a large Ln(III)

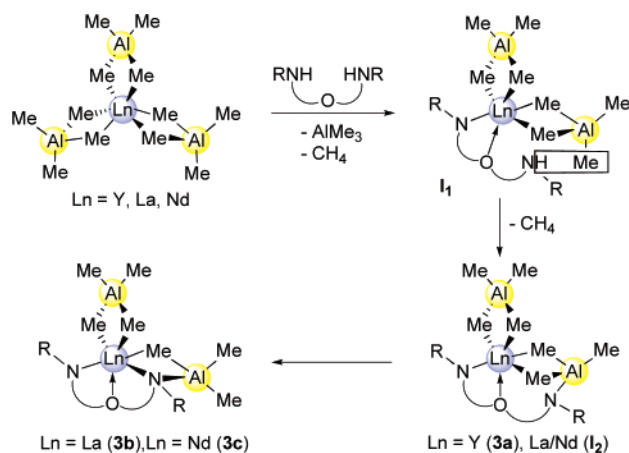
metal center.^{3,16} In contrast to yttrium complex **3a** the BDPPthf is coordinated to the lanthanum center in a η^3 fashion. One anilido nitrogen (N2) and one of the tetramethylaluminato methyl carbons (C4) occupy the apical positions of a strongly distorted octahedral coordination geometry ($\angle\text{N2–La–C4} = 151.5^\circ$). The two La–N bond lengths differ considerably due to the formation of one heterobridging [La(μ -NR₂)(μ -Me)Al] moiety, involving an extremely long La–N2 bond of 2.817(2) Å. For comparison, the bridging, terminal, and donor La–N bond distances in six-coordinate La[(μ -Me)₂GaMe₂][(μ -Me)-(μ -NMe₂)GaMe₂]₂¹⁷ and eight-coordinate (C₅Me₅)₂La(NHMe)-(H₂NMe)¹⁸ are 2.448 (av), 2.32(1), and 2.70(1) Å, respectively. Similar heterobridging moieties were described for Nd[NⁱPr₂]-[(μ -NⁱPr₂)(μ -Me)AlMe₂][(μ -Me)₂AlMe₂],¹⁹ [(Me₂Al(μ -Me)₂)₂Nd-(μ_3 -NC₆H₅)(μ -Me)AlMe₂]₂,²⁰ and [(μ -NC₆H₃ⁱPr₂-2,6)Sm(μ -NHC₆H₃ⁱPr₂-2,6)(μ -Me)AlMe₂]₂.²¹ The La–N1 bond of 2.333(2) Å is considerably shorter than those in six-coordinate La complexes supported by a diaminopyridine [NNN]²⁻-type ligand (2.409 Å).^{3c} As with the yttrium compound **3a** a strong interaction of the donor in the ligand backbone with the metal center is indicated by a relatively short La–O bond length of 2.493(2) Å, cf. La–O in five-coordinate La[N(SiHMe₂)₂]₃-(THF)₂ of 2.564(4) and 2.583(4) Å.²²

The AlMe₄⁻ ligand shows structural features similar to those recently found for (C₅Me₅)La(AlMe₄)₂.¹¹ It provides an atypically bent heterobimetallic [La(μ -Me)₂Al] moiety ($\angle\text{C4–La–C5–Al1} = -32.8^\circ$, interplanar angle C4LaC5–C4Al1C5 = 63.2°) with an additional La···(μ -CH₃) contact of 3.236(3) Å (La···C7), due to the steric unsaturation of the large lanthanum metal center. This pronounced La···C7 contact is also evidenced by differing bond angles $\angle\text{La–Al–C}_{\text{terminal}}$ of the bent ($\angle\text{La–Al1–C6/7} = 167.2^\circ$, 76.1°) compared to the η^2 -bonded aluminate ligands ($\angle\text{Y–Al1–C6/7} = 117.2^\circ$, 123.7°) of the analogous yttrium complex **3a**. Hence, the bent AlMe₄⁻ ligand accomplishes a distorted η^3 coordination mode comparable to that in (C₅Me₅)La(AlMe₄)₂.¹¹ The other La–(μ -CH₃) bond lengths range from 2.695(2) to 2.920(2) Å, with the heterobridging moiety forming the shortest contact, cf., La–(μ -CH₃) in (C₅Me₅)La(AlMe₄)₂ of 2.694(3)–2.802(4) Å.¹¹

The ¹H NMR spectra of complexes **3a** and **3b** in C₆D₆ revealed a rigid coordination of the BDPPthf ligand at ambient temperature, indicating a large rotational barrier for the aryl groups around the N–C_{ipso} bond. The signals for the N-methylene protons (**3a**: 3.79 ppm; **3b**: 3.53 ppm) and the CH_{thf} (**3a**: 4.75, 4.65 ppm; **3b**: 4.82, 4.05 ppm) are shifted significantly downfield compared to H₂[1] (3.07 ppm res. 2.98 ppm). The isopropyl groups of the [NON]²⁻ ligand also exhibit two significantly downfield shifted multiplets for the methine groups (**3a**: 3.79, 3.48 ppm; **3b**: 3.76, 3.53 ppm) compared to H₂[1] (3.54 and 2.66 ppm), as well as four doublets for the methyl groups. The ¹H NMR spectrum of **3a** in C₆D₆ clearly revealed four signals in the alkyl region at 25 °C, suggesting enhanced fluxionality of the [AlMe₄] and [AlMe₃] moieties in solution (cf., seven methyl resonances would have been expected for an

(16) Izod, K.; Liddle, S. T.; Clegg, W. *Chem. Commun.* **2004**, 1748.(17) Evans, W. J.; Anwender, R.; Doedens, R. J.; Ziller, J. W. *Angew. Chem., Int. Ed. Engl.* **1994**, *33*, 1641.(18) Gagné, M. R.; Stern, C. L.; Marks, T. J. *J. Am. Chem. Soc.* **1992**, *114*, 275.(19) Evans, W. J.; Anwender, R.; Ziller, J. W. *Inorg. Chem.* **1995**, *34*, 5930.(20) Evans, W. J.; Ansari, M. A.; Ziller, J. W.; Khan, S. I. *Inorg. Chem.* **1996**, *35*, 5435.(21) Gordon, J. C.; Giesbrecht, G. R.; Clark, D. L.; Hay, P. J.; Keogh, D. W.; Poli, R.; Scott, B. L.; Watkin, J. G. *Organometallics* **2002**, *21*, 4726.(22) Anwender, R.; Runte, O.; Eppinger, J.; Gerstberger, G.; Herdtweck, E.; Spiegler, M. *J. Chem. Soc., Dalton Trans.* **1998**, 847.(14) Evans, W. J.; Anwender, R.; Ziller, J. W. *Organometallics* **1995**, *14*, 1107.(15) Boncella, J. M.; Anderson, R. A. *Organometallics* **1985**, *4*, 205.

Scheme 2. Kinetically versus Thermodynamically Controlled "Aluminate Elimination" Mediated by a Chelating Diamido Ligand



entirely nonfluxional arrangement, as proposed by the fully asymmetric solid-state structure). The terminal methyl groups of $[\text{AlMe}_4]$ show a broad singlet at -0.15 ppm at ambient temperature, whereas the signal for the bridging methyl groups can clearly be assigned by a characteristic doublet at -0.13 ppm ($^2J_{\text{Y,H}} = 2.4$ Hz). These resonances are shifted to lower field in comparison with the homoleptic precursor **2a** (-0.27 ppm). Various temperature NMR studies in toluene- d_8 support this assignment by coalescence of the $[\text{AlMe}_4]$ methyl resonances due to rapid exchange of bridging and terminal methyl groups at elevated temperatures. Two separate signals at 0.12 and -0.38 ppm (integral ratio 6:3) can be assigned to the $[\text{AlMe}_3]$ methyl groups. Curiously, the methyl group appearing at -0.38 ppm indicates an interaction with the yttrium center ($^2J_{\text{Y,H}} = 2.8$ Hz), which is opposed to the solid-state structure of **3a**, however would be more in favor of a methyl group arrangement as detected in the solid-state structure of **3b**. Coalescence of the $[\text{AlMe}_3]$ methyl resonances was not observed at elevated temperatures, consistent with an increased rigidity compared to **3b** due to enhanced steric crowding at the yttrium center. In contrast, the ^1H NMR spectrum of **3b** at 25°C showed only two signals in the methyl alkyl region. The signal at 0.01 ppm can be assigned to the $[\text{AlMe}_4]$ moiety and the signal at -0.05 ppm is the resonance of the $[\text{AlMe}_3]$ methyl groups. Both signals are shifted to lower field compared to the homoleptic precursor **2b** (-0.20 ppm), and the $[\text{La}(\mu\text{-Me})\text{AlMe}]$ moieties indicate a rapid exchange of bridging and terminal methyl groups. These results are consistent with an increased steric unsaturation at the larger lanthanum metal center. Elemental analysis, IR data, and a well-resolved ^{13}C NMR spectrum of paramagnetic **3c** clearly indicate the formation of complex $(\text{BDPPthf})\text{Nd}(\text{AlMe}_4)(\text{AlMe}_3)$. The size similarity of the neodymium and lanthanum metal centers suggests a solid-state structure of **3c** analogous to **3b**.

Based on the structural and dynamic features of complexes **3** a consecutive aluminate/diamido ligand exchange can be rationalized as shown in Scheme 2. Accordingly, the first amino functionality can easily approach the six-coordinate metal center of the homoleptic precursor via displacement of one AlMe_4^- ligand and formation of a strongly bonded $[\text{NO}]^-$ -chelating ligand, intermediate **I1**; this is also evidenced by the facile reaction of $\text{Ln}(\text{AlMe}_4)_3$ with donor molecules.²³ Subsequently, the dangling second amino group reacts with a terminal methyl

group of another AlMe_4^- ligand, affording the kinetically favored product **I2**. Such a derivative was isolated for Y as compound **3a**. Apparently, due to enhanced steric hindrance, the second amino functionality is unable to approach the smaller yttrium center to form a second thermodynamically favored Ln–amido contact, as found in the lanthanum derivative **3b**.

Conclusion

Homoleptic alkyl complexes $\text{Ln}(\text{AlMe}_4)_3$ display a high potential as precursors for postlanthanidocene chemistry. The new ancillary ligand precursor $\text{H}_2\text{BDPPthf}$ has been successfully employed for the preparation of the first postlanthanidocene complexes featuring both small and large Ln^{III} metal centers as well as tetramethylaluminate actor ligands. Moreover, the intrinsic $[\text{NON}]^{2-}$ ligand functionality for the first time implied the formation of a kinetically favored aluminate/HR protonolysis product and the identification of a $[\text{Ln}(\mu\text{-Me})_2\text{AlMe}(\text{NR}_2)]$ heterobimetallic moiety unprecedented in organolanthanide(III) chemistry. Complexes $(\text{BDPPthf})\text{Ln}(\text{AlMe}_4)(\text{AlMe}_3)$ are the subject of very promising reactivity and activity studies.

Experimental Details

General Procedures. All reactions and manipulations with air-sensitive compounds were performed under dry argon, using standard Schlenk and glovebox techniques (MB Braun MBLab; <1 ppm O_2 , <1 ppm H_2O). Hexane, THF, and toluene were purified by using Grubbs columns (MBraun SPS, solvent purification system). All solvents were stored in a glovebox. Deuterated solvents were degassed and dried over Na/K alloy and stored in a glovebox. Reagents were obtained from commercial suppliers and used without further purification, unless otherwise noted. Homoleptic $\text{Ln}(\text{AlMe}_4)_3$ ($\text{Ln} = \text{Y}, \text{La}$)¹⁴ and *cis*-2,5-bis((tosyloxy)methyl)-tetrahydrofuran¹² were synthesized according to the literature method. NMR spectra were recorded at 25°C on a Bruker-AVANCE-DMX400 (^1H : 400.13 MHz; ^{13}C : 100.62 MHz). ^1H and ^{13}C shifts are referenced to internal solvent resonances and reported in parts per million relative to TMS. IR spectra were recorded on a Nicolet-Impact 410 FTIR spectrometer as Nujol mulls sandwiched between CsI plates. Elemental analyses were performed on an Elementar Vario EL III, with samples that have been dried in vacuo.

***cis*-2,5-Bis[*N,N*-(2,6-diisopropylphenyl)amino)methyl]-tetrahydrofuran ($\text{H}_2\text{BDPPthf}$, $\text{H}_2[1]$).** A solution of lithium 2,6-diisopropylanilide (2.36 g, 12.98 mmol) in THF (15 mL) was added slowly to a stirred solution of *cis*-2,5-bis((tosyloxy)methyl)-tetrahydrofuran (2.86 g, 6.49 mmol) in THF (100 mL) at -78°C . The mixture was warmed to ambient temperature and stirred for 40 h, and all volatile components were then removed in vacuo. The residue was extracted with toluene (3×50 mL), and the extract was dried in vacuo. The product was purified by column chromatography (silica, pentane/ethyl acetate = 95/05 as eluent) to give $\text{H}_2[1]$ as a white solid (2.72 g, 6.03 mmol, 93%). IR (Nujol, cm^{-1}): 3387 m N–H, 1916 w, 1856 w, 1796 w, 1621 m, 1586 m, 1459 vs Nujol, 1377 vs Nujol, 1363 s, 1308 w, 1255 m, 1220 w, 1190 m, 1178 s, 1082 s, 1056 m, 946 w, 885 w, 851 w, 802 m, 755 s, 665 m, 621 w, 573 w, 555 w, 530 w, 430 w. ^1H NMR (400 MHz, C_6D_6 , 25°C): δ 7.14 (m, 6 H, ar), 3.98 (m, 2 H, CH_{thf}), 3.56 (s br, 2 H, N–H), 3.54 (sp, 4 H, ar–CH), 3.07 (dd, $^2J \cong 12.8$ Hz, $^3J \cong 4.0$ Hz, 2 H, N– CH_2), 2.98 (dd, $^2J \cong 12.8$ Hz, $^3J \cong 6.0$ Hz, 2 H, N– CH_2), 1.53 (m, 2 H, thf), 1.40 (m, 2 H, thf), 1.29 (d, $^3J \cong 6.0$ Hz, 24 H, CH_3). ^1H NMR (400 MHz, CDCl_3 , 25°C): δ 7.22 (m, 6 H, ar), 4.31 (m, 2 H, CH_{thf}), 3.50 (sp, 4 H, ar–CH), 3.47 (s br, 2 H, N–H), 3.18 (dd, $^2J \cong 12.4$ Hz, $^3J \cong 3.3$ Hz, 2 H, N– CH_2), 3.08 (dd, $^2J \cong 12.4$ Hz, $^3J \cong 7.7$ Hz, 2 H, N– CH_2), 2.17 (m, 2 H, thf), 1.91 (m, 2 H, thf), 1.42 (d, $^3J \cong 7.2$ Hz, 24 H, CH_3). ^{13}C NMR (100 MHz, CDCl_3 , 25°C): δ 142.5, 129.0, 122.7, 118.5 (C_{ar}),

(23) Dietrich, H. M.; Raudaschl-Sieber, G.; Anwander, R. *Angew. Chem. Int. Ed.* **2005**, *44*, 5303.

71.5 (C_{thf}), 56.3 (N-CH₂), 29.0 (C_{thf}), 27.6 (ar-CH), 24.3 (CH₃). Anal. Calcd for C₃₀H₄₆N₂O (450.706 g/mol): C, 79.95; H, 10.29; N, 6.22. Found: C, 80.28; H, 10.15; N, 6.07.

General Procedure for the Preparation of (BDPPthf)Ln(AlMe₄)(AlMe₃), 3a–c. In a glovebox, Ln(AlMe₄)₃ (**2a–c**) was dissolved in 5 mL of hexane and added to a stirred solution of 1 equiv of H₂BDPPthf (H₂[1]) in 5 mL of hexane. Instant gas formation was observed. The reaction mixture was stirred another 12 h at ambient temperature while the formation of a precipitate was observed. The product was separated by centrifugation and washed three times with 3 mL of hexane to yield **3** as powdery solids in almost quantitative yields. The remaining solids were crystallized from a hexane/toluene solution at -35 °C to give colorless (**3a**, **3b**) or blue-green crystals (**3c**) in moderate yields suitable for X-ray diffraction.

(BDPPthf)Y(AlMe₄)(AlMe₃) (3a). Following the procedure described above, Y(AlMe₄)₃ (**2a**) (104 mg, 0.30 mmol) and H₂-BDPPthf (H₂[1]) (133 mg, 0.30 mmol) yielded **3a** (105 mg, 0.15 mmol, 50%) as colorless crystals. IR (Nujol, cm⁻¹): 1459 vs Nujol, 1377 vs Nujol, 1307 w, 1248 m, 1216 w, 1188 s, 1183 m, 1124 m, 1055 m, 1015 w, 930 w, 895 w, 858 w, 831 w, 801 w, 781 m, 763 w, 694 m, 651 w, 572 w, 542 w, 497 w, 470 w. ¹H NMR (400 MHz, C₆D₆, 25 °C): δ 7.23 (m, 3 H, ar), 7.19 (m, 3 H, ar), 4.75 (m, 1 H, CH_{thf}), 4.65 (m, 1 H, CH_{thf}), 3.79 (m, 5 H, N-CH₂, ar-CH), 3.48 (sp, 2 H, ar-CH), 2.84 (dd, ²J ≅ 12.4 Hz, ³J ≅ 8.9 Hz, 1 H, N-CH₂), 1.48 (d, ³J ≅ 6.8 Hz, 3 H, CH₃), 1.44 (d, ³J ≅ 6.8 Hz, 3 H, CH₃), 1.42 (d, ³J ≅ 7.2 Hz, 3 H, CH₃), 1.40 (d, ³J ≅ 7.2 Hz, 3 H, CH₃), 1.38 (d, ³J ≅ 7.2 Hz, 3 H, CH₃), 1.29 (d, ³J ≅ 7.2 Hz, 3 H, CH₃), 1.24 (d, ³J ≅ 6.8 Hz, 3 H, CH₃), 1.14 (d, ³J ≅ 6.8 Hz, 3 H, CH₃), 1.18 (m, 2 H, thf), 0.93 (m, 2 H, thf), 0.12 (s, 6 H, Al(CH₃)₃), -0.13 (d, ²J_{Y,H} ≅ 2.4 Hz, 6 H, Al(μ-CH₃)₂(CH₃)₂), -0.15 (s br, 6 H, Al(μ-CH₃)₂(CH₃)₂), -0.38 (d, ²J_{Y,H} ≅ 2.8 Hz, 3 H, Al(CH₃)₃). ¹³C NMR (100 MHz, C₆D₆, 25 °C): δ 151.0, 148.2, 147.1, 144.9, 144.7, 125.1, 124.8, 124.4, 124.1, 123.8 (C_{ar}), 88.2 (C_{thf}), 85.2 (C_{thf}), 65.0 (N-CH₂), 59.6 (N-CH₂), 31.8, 29.4, 28.5, 28.2, 27.4, 25.8, 25.6, 24.9, 24.5, 24.4, 24.1, 23.4 (C_{thf}, ar-CH, CH₃), 2.4 (s br, Al(CH₃)₄), 1.9 (s br, Al(CH₃)₄), 1.1 (s br, Al(CH₃)₃). Anal. Calcd for C₃₇H₆₅N₂OAl₂Y (696.804): C, 63.77; H, 9.40; N, 4.02. Found: C, 64.02; H, 9.27; N, 3.93.

(BDPPthf)La(AlMe₄)(AlMe₃) (3b). Following the procedure described above, La(AlMe₄)₃ (**2b**) (154 mg, 0.39 mmol) and H₂-BDPPthf (H₂[1]) (173 mg, 0.39 mmol) yielded **3b** (193 mg, 0.26 mmol, 66%) as colorless crystals. IR (Nujol, cm⁻¹): 1459 vs Nujol, 1377 vs Nujol, 1309 w, 1252 m, 1219 w, 1196 m, 1171 s, 1083 s, 1054 m, 961 w, 931 w, 892 w, 843 w, 799 m, 755 s, 696 m, 652 w, 564 w, 530 w, 513 w, 466 w. ¹H NMR (400 MHz, C₆D₆, 25 °C): δ 7.26 (m, 3 H, ar), 7.06 (m, 3 H, ar), 4.82 (m, 1 H, CH_{thf}), 4.05 (m, 1 H, CH_{thf}), 3.76 (m, 3 H, N-CH₂, ar-CH), 3.53 (m, 3 H, N-CH₂, ar-CH), 2.65 (dd, ²J ≅ 13.2 Hz, ³J ≅ 4.4 Hz, 1 H, N-CH₂), 2.27 (sp, 1 H, ar-CH), 1.58 (d, ³J ≅ 7.2 Hz, 3 H, CH₃), 1.55 (d, ³J ≅ 7.2 Hz, 3 H, CH₃), 1.47 (d, ³J ≅ 6.8 Hz, 3 H, CH₃), 1.40 (d, ³J ≅ 7.2 Hz, 3 H, CH₃), 1.38 (d, ³J ≅ 6.8 Hz, 3 H, CH₃), 1.34 (d, ³J ≅ 6.8 Hz, 3 H, CH₃), 1.31 (d, ³J ≅ 6.8 Hz, 3 H, CH₃), 1.20 (d, ³J ≅ 6.8 Hz, 3 H, CH₃), 1.15 (m, 2 H, thf), 0.99 (m, 2 H, thf), 0.01 (s, 12 H, Al(CH₃)₄), -0.05 (s, 9 H, Al(CH₃)₃). ¹³C NMR (100 MHz, C₆D₆, 25 °C): δ 149.9, 147.7, 147.3, 144.9, 144.2, 127.1, 125.4, 125.3, 125.1, 124.1 (C_{ar}), 86.6 (C_{thf}), 84.1 (C_{thf}), 65.6 (N-CH₂), 59.5 (N-CH₂), 33.5, 29.7, 28.4, 28.3, 28.2, 27.7, 26.8, 26.1, 25.6, 25.4, 24.9, 24.2, 24.0 (C_{thf}, ar-CH, CH₃), 2.3 (s br, Al(CH₃)₄), 2.0 (s br, Al(CH₃)₃). Anal. Calcd for C₃₇H₆₅N₂OAl₂La (746.633): C, 59.51; H, 8.77; N, 3.75. Found: C, 59.46; H, 8.68; N, 3.72.

(BDPPthf)Nd(AlMe₄)(AlMe₃) (3c). Following the procedure described above, Nd(AlMe₄)₃ (**2c**) (182 mg, 0.45 mmol) and H₂-BDPPthf (H₂[1]) (202 mg, 0.45 mmol) yielded **3c** (237 mg, 0.32 mmol, 70%) as blue-green crystals. IR (Nujol, cm⁻¹): 1459 vs Nujol, 1377 vs Nujol, 1313 w, 1302 s, 1253 m, 1236 s, 1222 w, 1189 m, 1172 s, 1146 w, 1097 s, 1054 s, 1033 w, 1003 w, 988 w,

Table 2. Crystal Data and Data Collection Parameters of Complexes 3a and 3b

| | 3a | 3b |
|---|---|--|
| chem formula | C ₈₁ H ₁₃₈ N ₄ O ₂ Al ₄ Y ₂ | C ₃₇ H ₆₅ N ₂ OAl ₂ La |
| fw | 1485.69 | 746.78 |
| color/shape | colorless/prism | colorless/needle |
| cryst size (mm) | 0.35 × 0.18 × 0.13 | 0.38 × 0.90 × 0.07 |
| cryst syst | triclinic | monoclinic |
| space group | <i>P</i> $\bar{1}$ (no. 2) | <i>P</i> 2 ₁ / <i>n</i> (no. 14) |
| <i>a</i> (Å) | 12.4487(6) | 9.5128(7) |
| <i>b</i> (Å) | 12.4523(6) | 10.8146(8) |
| <i>c</i> (Å) | 14.9992(7) | 40.644(3) |
| α (deg) | 106.758(1) | |
| β (deg) | 90.620(1) | 93.035(1) |
| γ (deg) | 106.356(1) | |
| <i>V</i> (Å ³) | 2125.51(18) | 4175.5(5) |
| <i>Z</i> | 2 | 4 |
| <i>T</i> (K) | 153(2) | 153(2) |
| ρ _{calcd} (g cm ⁻³) | 1.161 | 1.188 |
| μ (mm ⁻¹) | 1.443 | 1.092 |
| <i>F</i> ₀₀₀ | 798 | 1568 |
| θ range (deg) | 2.08–26.37 | 2.01–30.03 |
| data collected (<i>h, k, l</i>) | 15, 15, 18 | 13, 15, 57 |
| no. of reflns collected | 27 908 | 70 529 |
| no. of indep reflns/ <i>R</i> _{int} | 8704 (all)/0.029 | 12 204 (all)/0.035 |
| no. of obsd reflns (<i>I</i> > 2σ(<i>I</i>)) | 7496 (obsd) | 10524 (obsd) |
| no. of params refined | 439 | 403 |
| <i>R</i> ₁ (obsd/all) ^a | 0.0344/0.0447 | 0.0297/0.0373 |
| w <i>R</i> ₂ (obsd/all) ^a | 0.0900/0.0955 | 0.0672/0.0691 |
| GOF (obsd/all) ^a | 1.039/1.173 | 1.075/1.075 |
| largest diff peak and hole (e Å ⁻³) | +0.498/-0.541 | +0.507/-1.731 |

$$^a R_1 = (|F_o| - |F_c|)/|F_o|; wR_2 = \{[w(F_o^2 - F_c^2)]/w(F_o^2)\}^{1/2}; \text{GOF} = \{[w(F_o^2 - F_c^2)]/(n - p)\}^{1/2}.$$

933 w, 923 w, 891 w, 850 w, 833 w, 799 m, 787 m, 769 s, 721 m, 704 w, 560 w, 532 w, 509 w, 462 w. ¹H NMR (600 MHz, C₆D₆, 25 °C): δ 17.52, 17.10, 16.18, 13.17, 12.04, 10.67, 10.20, 10.00, 9.71, 7.03, 7.69, 5.93, 2.11, 2.08, 1.28, 1.08, 0.89, -2.84, -3.69, -4.75, -5.16, -9.88, -11.21, -11.79, -14.96, -16.45. ¹³C NMR (100 MHz, C₆D₆, 25 °C): δ 168.3, 154.5, 144.6, 142.8, 136.4, 129.3, 129.2, 125.5, 124.8 (C_{ar}), 76.0 (C_{thf}), 50.2 (N-CH₂), 41.8, 36.2, 35.4, 31.9, 30.1, 24.5, 22.2, 20.2, 16.7, 15.4 (C_{thf}, ar-CH, CH₃). Anal. Calcd for C₃₇H₆₅N₂OAl₂Nd (752.138): C, 59.09; H, 8.71; N, 3.72. Found: C, 58.92; H, 8.69; N, 3.71.

X-ray Crystallography and Crystal Structure Determination of 3a and 3b. Crystals suitable for diffraction experiments were selected in a glovebox and mounted in Paratone-N inside a nylon loop (Hampton research). Data collection was done on a Bruker AXS SMART 2K CCD diffractometer using graphite-monochromated Mo Kα radiation (λ = 0.71073 Å) performing ω-scans in four φ positions, employing the SMART software package.²⁴ A total of 1888 collected images were processed using SAINT.²⁵ Numerical absorption correction was done using SHELXTL.²⁶ The structures were solved by direct methods and refined with standard difference Fourier techniques.²⁶ The structure of **3a** contains a rotationally disordered toluene molecule lying on an inversion center. This molecule was refined with a 6-fold disorder model using SHELXL command DFIX to constrain the methyl to ring atom C–C distances to 1.52 Å. The FLAT command was applied to the ring atoms. The C atoms in the ring were refined anisotropically. The H atom positions of the AlMe groups are clearly visible in the difference Fourier map. The structure of **3b** contained one heavily disordered solvent molecule (hexane) that could not be

(24) SMART v. 5.054, Data Collection Software for Bruker AXS CCD; Bruker AXS Inc.: Madison, WI, 1999.

(25) SAINT v. 6.45a, Data Integration Software for Bruker AXS CCD; Bruker AXS Inc.: Madison, WI, 2002.

(26) SHELXTL v. 6.14, Structure Determination Software Suite; Bruker AXS Inc.: Madison, WI, 2000.

modeled, and it was therefore subtracted from the intensity data using the routine SQUEEZE as implemented in the program PLATON.²⁷ The subtracted contribution to the total scattering equals 54 electrons. After subtraction PLATON reported a solvent accessible volume of 204 Å³. In both **3a** and **3b**, the H atom positions of the AlMe groups are clearly visible in the difference Fourier map. All H atoms in the structure were geometrically positioned (AFIX 13, 43, 23, and 137) and their U_{iso} constrained to be between 1.2 and 1.5 times that of the parent atom. For further experimental details see Table 2. Crystallographic data (excluding structure factors) for the structures reported in this paper have been deposited with the Cambridge Crystallographic Data Centre as supplementary publication nos. CCDC-292070 (**3a**) and CCDC-292071 (**3b**). Copies of the data can be obtained free of charge on

application to CCDC, 12 Union Road, Cambridge CB2 1EZ, UK (fax: (+44)1223-336-033; e-mail: deposit@ccdc.cam.ac.uk).

Acknowledgment. We thank the Deutsche Forschungsgemeinschaft (SPP 1166), the Fonds der Chemischen Industrie, and the Bayerische Forschungsförderung for generous support. R.A. thanks Warren Piers and Joe Takats for stimulating discussions.

Supporting Information Available: Text giving tables of atomic coordinates, atomic displacement parameters, and bond distances and angles for complexes **3a** and **3b**. This material is available free of charge via the Internet at <http://pubs.acs.org>.

(27) Spek, A. L. *Acta Crystallogr., Sect. A* **1990**, *46*, C34.

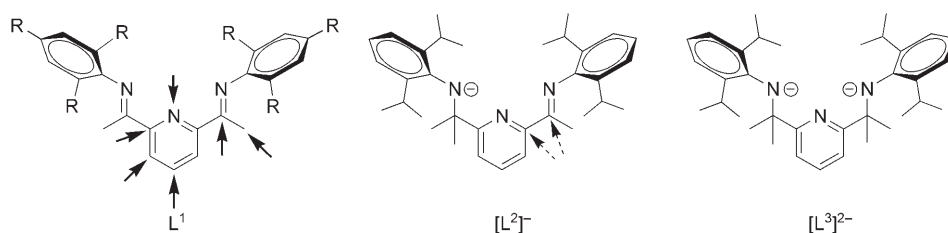
OM060244D

Paper III

Alkyl Migration and an Unusual Tetramethylaluminate Coordination Mode: Unexpected Reactivity of Organolanthanide Imino–Amido–Pyridine Complexes**

Melanie Zimmermann, Karl W. Törnroos, and Reiner Anwander*

Bis(imino)pyridine compounds provide versatile ancillary ligand sets for efficient Ziegler–Natta catalysts based on the late transition metals iron and cobalt^[1] and the earlier transition metals vanadium^[2] and chromium.^[3] Extended studies have outlined the capability of such conjugated [NNN] ligands (L^1 , Scheme 1) to engage in a variety of transformations. In addition to substantial charge-transfer



Scheme 1. The chemical non-innocence of [NNN]ⁿ⁻ ($n=0-2$) ancillary ligands. Known sites of nucleophilic attack/alkylation are indicated by arrows (broken arrows: this work).

interactions of the ligand π system with the transition-metal center, alkylation proneness at various positions of the ligand framework evidence the chemical non-innocence of these diimino ligands. With diverse alkylating agents, alkyl attack at the imino function^[4] or at any position of the pyridine ring,^[2,4a,5] even the pyridine N atom,^[6] and deprotonation of the methyl sidearms have been reported to occur (Scheme 1).^[5b,6b,7] Furthermore, dimerization by C–C bond formation after reduction of the enamine functionality^[5b,8] and cycloaddition of the pyridine ring have been observed.^[5b]

The generally observed decrease of the metal–nitrogen bond energies from late to early transition metals within a given series, combined with the uncharged nature of the bis(imino)pyridine ligand are considered to prevent the formation of stable Group 3 complexes.^[9] The only example of a lanthanide complex stabilized by an assumed neutral

bis(imino)pyridine ligand turned out to be the product of an internal ligand reduction affording a radical anion; attempts to prepare the $LnCl_3$ ($Ln=Nd$) adduct of the bis(imino)pyridine were unsuccessful.^[8b]

The demonstration of a nucleophilic attack of alkylating reagents or cocatalysts such as $AlMe_3$ on the imino carbon of the ligand backbone has in turn provided a new class of monoanionic imino–amido–pyridine [NNN]⁻ ligands (L^2 , Scheme 1).^[4b] These ligands retain the unusual stereoelectronic properties of the bis(imino)pyridine ligand and offer an approach to synthesizing discrete conformationally rigid lanthanide complexes. Starting from $[Lu(CH_2SiMe_3)_3(thf)_2]$ Gordon et al. were able to prepare the first lutetium dialkyl complex stabilized by

$[L^2]^-$.^[10] We have recently shown that homoleptic lanthanide tetramethylaluminates $[Ln(AlMe_4)_3]$ are convenient synthesis precursors for the generation of a variety of heterobimetallic Ln/Al complexes including half-lanthanidocene,^[11] lanthanidocene,^[12] as well as bis(amido)pyridine-derived [NNN]²⁻ organolanthanide complexes.^[13] Herein we present new [NNN]⁻ and [NNN]²⁻ organolanthanide complexes in which the chemical non-innocence of the imino–amido–pyridine ligand facilitates an unprecedented coordination mode of the tetramethylaluminate ligand.

$[Ln(AlMe_4)_3]$ ($Ln=La$ (**1a**), Nd (**1b**) and Y (**1c**)) react with light yellow HL^2 in an alkane elimination reaction (Scheme 2). Instant gas evolution, a color change to dark red and subsequent precipitation of wine-red solid suggested a coordination of the monoanionic imino–amido ligand to a metal center.

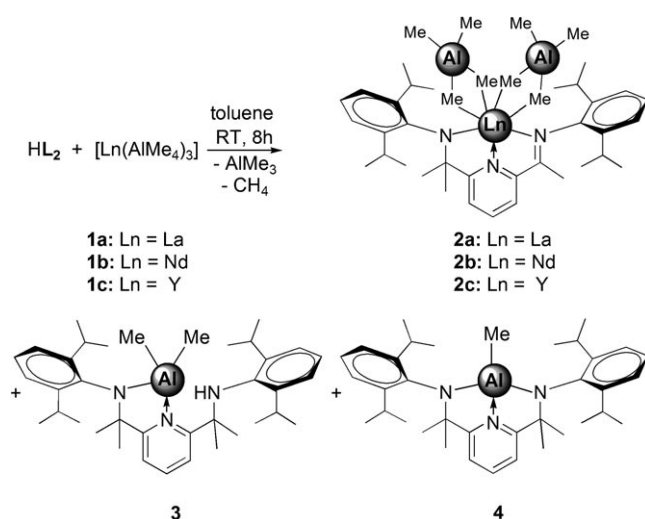
Separation of the precipitate from the reaction mixture afforded complexes **2** as wine-red powders with yields increasing according to the size of the metal cation ($Ln=Y$ 49%; Nd 52%; La 62%). The IR spectra of complexes **2** show a strong absorption at 1582 cm^{-1} (**2a**, **2c**) and 1588 cm^{-1} (**2b**) attributed to the stretching vibration of a metal-coordinated imino group (HL^2 : 1644 cm^{-1}). Similar shifts were observed in bis(imino)pyridine complexes of titanium.^[5a]

The 1H NMR spectra of complexes **2** in C_6D_6 revealed a rigid L^2 coordination at ambient temperature indicating a large rotational barrier for the aryl groups around the $N-C_{ipso}$ bond. Two upfield shifted singlets at $\delta=1.71$ (3H) and

[*] M. Zimmermann, Prof. K. W. Törnroos, Prof. R. Anwander
Department of Chemistry
University of Bergen
Allégaten 41, 5007 Bergen (Norway)
Fax: (+47) 5558-9490
E-mail: reiner.anwander@kj.uib.no

[**] Financial support from the Norwegian Research Council, the program Nanoscience@UiB, and the Fonds der Chemischen Industrie is gratefully acknowledged.

Supporting information for this article is available on the WWW under <http://www.angewandte.org> or from the author.



Scheme 2. Reaction of imino–amino–pyridine ligand HL^2 with $[Ln(AlMe_4)_3]$ (**1**).

1.39 ppm (6H) (**2a**) ($\delta = 1.74$ and 1.35 ppm, **2c**) confirm the maintenance of the imino–amido–pyridine ligand backbone. The 1H NMR spectra show only one broad singlet in the methyl alkyl region at $\delta = -0.25$ (**2a**) and -0.38 ppm (**2c**), respectively, which can be assigned to the $\{AlMe_4\}$ moieties and indicates a rapid exchange of bridging and terminal methyl groups. These resonances are shifted to lower field compared to the homoleptic precursors ($\delta = -0.20$ (**1a**) and -0.27 ppm (**1c**)). The formation of the corresponding paramagnetic neodymium complex **2b** is clearly indicated by elemental analysis, IR data, and a relatively well-resolved 1H NMR spectrum ($\delta_{AlCH_3} = 6.30$ ppm).

The moderate yields of complexes **2** and the striking red color of the soluble fraction made a closer investigation of the supernatant solution necessary. Apart from residual $[Ln(AlMe_4)_3]$, fractional crystallization from hexane afforded analytically pure orange and red crystals of aluminum complexes **3** and **4**, respectively (Scheme 2).

An X-ray structure analysis of complex **3** revealed the unprecedented alkylation of the imino carbon atom of $[L^2]^-$ (Figure 1). The metal center in **3** is in a distorted tetrahedral coordination environment which features a methylated ancillary ligand, η^2 -coordinated to the metal center. The Al–N bonds and the N2–Al–N3 bite angle are in the expected ranges.^[4b,14a,15] Alkylation of the imino carbon atom with the consequent formation of a dianionic bis(amido)pyridine of the $[NNN]^{2-}$ type was not anticipated and is in striking contrast with the reactivity of bis(imino)pyridine ligands and complexes derived there from. For example, treatment of bis(imino)pyridines and their late transition-metal complexes even with an excess of $AlMe_3$ exclusively affords the monoalkylation products.^[4b,14] Hence, the reactivity observed in our system suggests an alkylation sequence via highly reactive $\{Ln-Me\}$ moieties rather than alkylation by $AlMe_3$ released in the acid–base reaction of $[Ln(AlMe_4)_3]$ and HL^2 . At the same time, the Lewis acidic Al^{3+} competes with the lanthanide centers for the $[NNN]^{2-}$ ligand coordination—the strong Lewis acid Al^{3+} has a high affinity for nitrogen

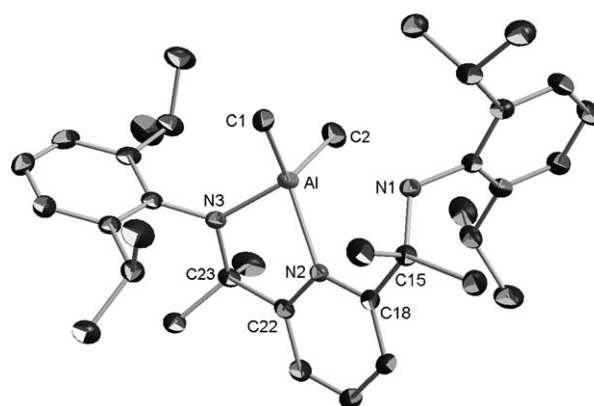


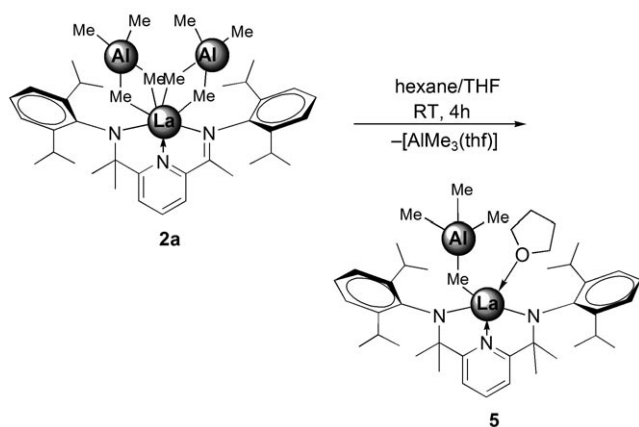
Figure 1. Molecular structure of **3** (anisotropic displacement parameters set at 50% probability). Hydrogen atoms are omitted for clarity. Selected interatomic distances [Å] and angles [°]: Al–N1 2.8056(13), Al–N2 2.0552(13), Al–N3 1.8568(13), Al–C1 1.9814(17), Al–C2 1.9764(18), N1–C15 1.4954(19), N3–C23 1.4738(19), C15–C18 1.530(2), C22–C23 1.525(2); N2–Al–N3 82.27(5), Al–N3–C23 113.30(10), N3–Al–C1 107.82(7), N3–Al–C2 114.74(7), N2–Al–C1 125.28(7), N2–Al–C2 112.38(7), N1–C15–C18 108.59(12), N3–C23–C22 105.89(12).

donors.^[16] The competition is evidenced by the dependency of the aluminum complex formation on the size of the Ln^{3+} ion. The 4:1 ratio of **3**:**4** is indicative of a kinetically (**3**) or thermodynamically (**4**, by CH_4 elimination from **3**) controlled reaction.

Complexes $[L^2Ln(AlMe_4)_2]$ (**2a–c**; Ln = La, Nd, Y) resemble $[(NNN)FeMe(AlMe_4)]$ (NNN = bis(imino)pyridine) which has been discussed as an active site in highly efficient catalytic systems based on bis(imino)pyridine Fe^{2+} complexes activated by methylaluminoxane (MAO) or trialkylaluminum reagents.^[17] Tetramethylaluminate $\{AlMe_4\}$ moieties, also referred to as “alkyls in disguise”, offer a commonly used synthesis approach to highly reactive $\{Ln-Me\}$ derivatives.^[18] The donor-induced cleavage of tetramethylaluminates (donor = THF, diethyl ether, pyridine) has been applied to convert heteroleptic lanthanidocene and half-lanthanidocene complexes, $[Cp'_2Ln(AIR_4)]$ and $[Cp'_2Ln(AIR_4)_2]$ (Cp' = substituted cyclopentadienyl), into complexes $[Cp'_2LnR]$ and $[Cp'_2LnR_2]$, respectively.^[11,18,19]

Addition of an excess of THF to a stirred suspension of the bis(tetramethylaluminate) complex **2a** in hexane (Scheme 3) resulted in instant dissolution of the wine-red solid accompanied by decolorization of the solution.

Colorless single crystals of **5** suitable for X-ray diffraction were grown from a hexane solution and revealed the product of an unexpected “incomplete” donor-induced tetramethylaluminate cleavage (Figure 2).^[15] Contrary to an anticipated organoaluminum-free methyl derivative, lanthanum complex **5** features an intact tetramethylaluminate ligand in a novel (μ -Me) $\{AlMe_3\}$ coordination mode. To our knowledge, this is the first example of a structurally authenticated η^1 -coordinated $\{AlMe_4\}$ moiety—the missing tetramethylaluminate coordination mode to complete the series, the η^2 and η^3 modes have been reported.^[20] Moreover, complex **5** features the cleaving agent THF and a tetramethylaluminate in the same molecule. The only comparable structures reported are $[(C_5Me_5)_2Sm$



Scheme 3. Donor-induced cleavage of one tetramethylaluminate ligand from **2a** with THF.

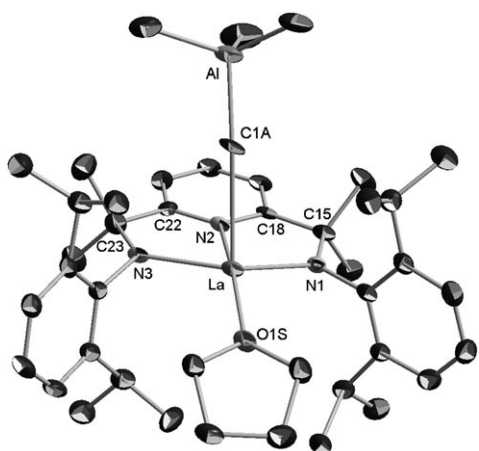


Figure 2. Molecular structure of **5** (anisotropic displacement parameters set at 50% probability). Hydrogen atoms are omitted for clarity. Selected interatomic distances [Å] and angles [°]: La–N1 2.294(5), La–N2 2.516(5), La–N3 2.246(6), La–O1S 2.538(4), La–C1A 2.825(7), Al–C1A 2.024(7), Al–C2A 1.980(9), Al–C3A 1.980(9), Al–C4A 1.963(9), N3–C23 1.475(8), C22–C23 1.511(9), N1–C15 1.475(8), C15–C18 1.481(10); N1–La–N3 127.82(18), N1–La–N2 64.96(18), N2–La–N3 64.15(17), N1–La–O1S 111.86(17), N3–La–O1S 114.68(16), N1–La–C1A 97.85(2), N3–La–C1A 87.56(2), O1S–La–C1A 109.95(2), La–C1A–Al 165.0(4), N1–C15–C18 108.2(5), N3–C23–C22 106.1(5).

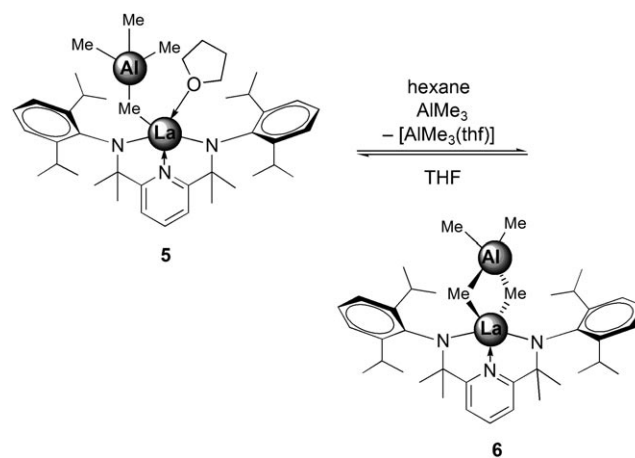
(thf)(μ - η^2 -Et)AlEt₃]^[21] and [(C₅Me₅)₂Yb(η^2 -Et)AlEt₂(thf)]^[22] which involve η^2 -ethyl ligands.^[23] The five-coordinate La center in **5** is further surrounded by the three N atoms of the ancillary ligand which has undergone alkylation in similarity to **3** and **4**. The coordination geometry of the La center is best described as a distorted trigonal bipyramidal with the THF oxygen and the pyridine nitrogen (N2) atoms occupying the apical positions (O1S–La–N2, 166.3°) while the amido nitrogen atoms (N1 and N3) and a tetramethylaluminate carbon atom (C1A) form the equatorial plane.^[15]

The formation of **5** is assumed to originate from fast sequential processes involving initial donor-induced cleavage of one tetramethylaluminate ligand in complex **2a** to produce a highly reactive terminal methyl group. The transient {Ln–

Me} species can undergo methyl migration from the metal center to the imino carbon atom. Such an intramolecular nucleophilic attack on the imino functionality implies additional anionization of the ligand and concomitant quaternization of the former imino carbon atom.^[24] Comparatively short bonds between the lanthanum and the amido nitrogen atoms (La–N1 2.294(5), La–N3 2.246(6) Å) and pyridine nitrogen (N2–La 2.516(5) Å) indicate a strong interaction of the newly formed [NNN]²⁻ ligand with the low-coordinate metal center.^[8b,13] The heterobimetallic {La(μ -Me)Al} moiety features a markedly obtuse La–C1A–Al angle of 165.0(5)° with a La–C bond length of 2.825(7) Å which is in the upper range of η^2 -coordinated tetramethylaluminates (2.694(3) Å–2.802(4) Å).^[11]

The symmetric environment around the metal center imparted by the [NNN]²⁻ ligand is also in accordance with the ¹H NMR spectrum of **5**. In C₆D₆, only one set of signals was observed for the bis(amido)pyridine ligand comprising one multiplet at δ = 3.47 ppm for the methine protons and two duplets at δ = 1.18 and 1.15 ppm for the methyl protons of the isopropyl groups. A relatively sharp singlet at δ = –0.15 ppm is assigned to the {AlMe₄} unit indicating a rapid exchange of the bridging and the terminal methyl groups. Moreover, the significantly upfield shifted multiplets at δ = 2.74 and 0.98 ppm assigned to the THF ligand are in agreement with a strongly bonded THF molecule.

Nevertheless, displacement of the strongly coordinating donor solvent can be achieved by addition of AlMe₃ to a solution of **5** in hexane (Scheme 4). Formation of the donor-



Scheme 4. THF displacement/coordination equilibrium between **5** and **6**.

free tetramethylaluminate complex **6** is quantitative and affords an analytically pure white solid that is sparingly soluble in hexane, [AlMe₃(thf)] is the only byproduct. This displacement of THF is fully reversible and complex **5** can be quantitatively recovered by adding THF to a hexane solution of **6**. Owing to the steric unsaturation of the lanthanum center a η^2 -coordination of the tetramethylaluminate ligand is assumed for compound **6**. However, variable-temperature (VT) NMR spectroscopy could not give final proof, as no

decoalescence of the aluminate signal was observed in the accessible temperature range (−90–25 °C).

Compared to the high degree of delocalization in bis-(imino)pyridine ligands, the conjugation in the imino–amido–pyridine system is restrained. However, it still allows significant internal charge-transfer processes resulting in exceptional reaction pathways, coordination modes, and complex stabilization. The observed reactivity of the imino–amido–pyridine lanthanide complexes not only emphasizes the non-innocence of this ligand system but also the enhanced alkylation capability of {Ln–Me} moieties. The new η¹-tetramethylaluminate coordination substantiates the coordinative flexibility of anionic cocatalysts in Ziegler–Natta-type catalysts and the unpredictable nature of so-called dormant species.

Experimental Section

Representative synthesis of 2a: In a glovebox, [La(AlMe₄)₃] (**1a**, 241 mg, 0.60 mmol) was dissolved in toluene (3 mL) and added to a stirred solution of HL² (300 mg, 0.60 mmol) in toluene (4 mL). The resulting mixture immediately turned red and gas evolution was observed. The reaction mixture was stirred for another 8 h at ambient temperature while the formation of a wine-red precipitate was observed. The product was separated by centrifugation, washed with hexane (4 × 5 mL) and dried under vacuum to yield **2a** as a powdery wine-red solid (303 mg, 0.37 mmol, 62%). ¹H NMR (600 MHz, C₆D₆, 25 °C): δ = 7.18–7.10 (m, 6H, ar), 7.04 (t, ³J = 7.8 Hz, 1H, C₅H₃N-*p*-proton), 6.86 (d, ³J = 7.8 Hz, 1H, C₅H₃N-*m*-proton), 6.85 (d, ³J = 7.8 Hz, 1H, C₅H₃N-*m*-proton), 3.26 (sept, ³J = 6.6 Hz, 2H, ar-CH), 2.62 (sept, ³J = 6.6 Hz, 2H, ar-CH), 1.71 (s, 3H, N=CCH₃), 1.39 (s, 6H, NCCH₃), 1.30 (d, ³J = 6.6 Hz, 6H, CH₃), 1.26 (d, ³J = 6.6 Hz, 6H, CH₃), 1.00 (d, ³J = 6.6 Hz, 6H, CH₃), 0.88 (d, ³J = 6.6 Hz, 6H, CH₃), −0.25 ppm (s, 24H, Al(CH₃)₄). ¹³C NMR (126 MHz, C₆D₆, 25 °C): δ = 175.1, 158.7, 149.4, 140.7, 139.1, 138.4, 125.5, 125.3, 124.9, 117.3, 69.9, 33.7, 29.1, 28.6, 28.1, 26.3, 26.1, 25.5, 25.1, 20.3, 3.1 ppm (s br, Al(CH₃)₄). VT-NMR was unsuccessful due to low solubility of complex **2a** in [D₈]toluene. IR (nujol): ν̄ = 1582 (s, C=N), 1468 (vs, nujol), 1375 (vs, nujol), 1303 (s), 1261 (m), 1220 (w), 1214 (w), 1173 (s), 1095 (w), 1007 (w), 971 (w), 950 (w), 888 (w), 847 (w), 821 (w), 785 (m), 769 (m), 723 (vs), 593 (w), 578 (w), 516 cm^{−1} (w). Elemental analysis (%) calcd for C₄₂H₇₀N₃Al₂La (809.910 g mol^{−1}): C 62.29, H 8.71, N 5.19; found: C 62.21, H 8.77, N 5.13.

5: THF (3 mL) was added dropwise to a stirred suspension of **2a** (126 mg, 0.16 mmol) in hexane (3 mL). The wine-red solid dissolved immediately accompanied by decolorization of the reaction mixture. After stirring for 4 h at ambient temperature the solvent was removed in vacuo to give a white solid which was washed with hexane (3 × 2 mL) and dried under vacuum to yield **5** as a powdery white solid (117 mg, 0.14 mmol, 90%). ¹H NMR (600 MHz, C₆D₆, 25 °C): δ = 7.20–7.11 (m, 6H, ar), 7.06 (t, ³J = 7.8 Hz, 1H, C₅H₃N-*p*-proton), 6.81 (d, ³J = 7.8 Hz, 2H, C₅H₃N-*m*-protons), 3.47 (sept, ³J = 6.6 Hz, 4H, ar-CH), 2.74 (m, 4H, THF), 1.40 (s, 12H, NCCH₃), 1.18 (d, ³J = 6.6 Hz, 12H, CH₃), 1.15 (d, ³J = 6.6 Hz, 12H, CH₃), 0.98 (m, 4H, THF), −0.15 ppm (s, 12H, Al(CH₃)₄). ¹³C NMR (151 MHz, C₆D₆, 25 °C): δ = 174.3, 150.3, 141.3, 139.0, 125.6, 125.0, 117.8, 70.8 (THF), 69.1, 32.8, 31.9, 28.2, 28.0, 25.1, 23.0, 1.7 ppm (s, Al(CH₃)₄). IR (nujol): ν̄ = 1572 (w), 1468 (vs, nujol), 1375 (vs, nujol), 1303 (s), 1256 (w), 1220 (w), 1194 (m), 1158 (m), 1126 (w), 1101 (w), 1044 (w), 1013 (w), 982 (w), 930 (w), 852 (m), 816 (w), 785 (m), 764 (m), 723 (vs), 692 (w), 583 (w), 562 (w), 536 (w), 516 cm^{−1} (w). Elemental analysis (%) calcd for C₄₃H₆₉N₃OAlLa (809.930 g mol^{−1}): C 63.77, H 8.59, N 5.19; found: C 63.37, H 8.58, N 5.02.

6: AlMe₃ (6 mg, 0.09 mmol) was added dropwise to a stirred solution of **5** (71 mg, 0.09 mmol) in toluene (3 mL). After stirring the

colorless reaction mixture for 4 h at ambient temperature the solvent was removed in vacuo to form a white solid which was washed with hexane (3 × 2 mL) and dried under vacuum to yield **6** as a powdery white solid (63 mg, 0.09 mmol, 98%). ¹H NMR (600 MHz, C₆D₆, 25 °C): δ = 7.20–7.16 (m, 6H, ar), 7.14 (t, ³J = 7.8 Hz, 1H, C₅H₃N-*p*-proton), 6.78 (d, ³J = 7.8 Hz, 2H, C₅H₃N-*m*-protons), 3.28 (sept, ³J = 6.6 Hz, 4H, ar-CH), 1.41 (s, 12H, NCCH₃), 1.31 (d, ³J = 6.6 Hz, 12H, CH₃), 1.05 (d, ³J = 6.6 Hz, 12H, CH₃), −0.40 ppm (s, 12H, Al(CH₃)₄). ¹³C NMR (151 MHz, C₆D₆, 25 °C): δ = 175.1, 149.4, 141.5, 139.1, 126.1, 125.3, 117.3, 69.9, 33.7, 28.1, 26.3, 26.1, 2.83 ppm (s, Al(CH₃)₄). IR (nujol): ν̄ = 1577 (w), 1468 (vs, nujol), 1375 (vs, nujol), 1303 (s), 1251 (w), 1240 (w), 1194 (w), 1168 (m), 1095 (w), 1044 (w), 997 (w), 971 (m), 852 (w), 816 (w), 790 (w), 764 (m), 723 (vs), 609 (w), 567 (w), 562 (w), 536 (w), 516 cm^{−1} (w). Elemental analysis (%) calcd for C₃₉H₆₁N₃AlLa (737.824 g mol^{−1}): C 63.49, H 8.33, N 5.70; found: C 63.54, H 8.35, N 5.44.

Full experimental and analytical details for complexes **2–6** are available in the Supporting Information.

Received: November 21, 2006

Revised: December 12, 2006

Published online: March 20, 2007

Keywords: alkylation · aluminum · amide · lanthanides · ligand effects

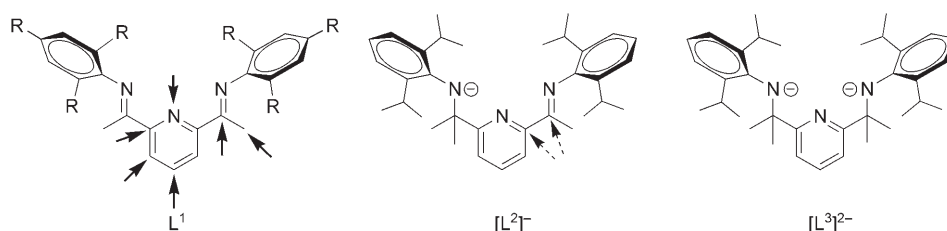
- [1] a) B. L. Small, M. Brookhart, A. M. A. Bennett, *J. Am. Chem. Soc.* **1998**, *120*, 4049; b) G. J. P. Britovsek, V. C. Gibson, B. S. Kimberley, P. J. Maddox, S. J. McTavish, G. A. Solan, A. J. P. White, D. J. Williams, *Chem. Commun.* **1998**, 849; c) G. J. P. Britovsek, M. Bruce, V. C. Gibson, B. S. Kimberley, P. J. Maddox, S. Mastroianni, S. J. McTavish, C. Redshaw, G. A. Solan, S. Strömberg, A. J. P. White, D. J. Williams, *J. Am. Chem. Soc.* **1999**, *121*, 8728.
- [2] D. Reardon, F. Conan, S. Gambarotta, G. Yap, Q. Wang, *J. Am. Chem. Soc.* **1999**, *121*, 9318.
- [3] M. A. Esteruelas, A. M. López, L. Méndez, M. Oliván, E. Oñate, *Organometallics* **2003**, *22*, 395.
- [4] a) J. Scott, S. Gambarotta, I. Korobkov, P. H. M. Budzelaar, *J. Am. Chem. Soc.* **2005**, *127*, 13019; b) M. Bruce, V. C. Gibson, C. Redshaw, G. A. Solan, A. J. P. White, D. J. Williams, *Chem. Commun.* **1998**, 2523; c) S. Milione, G. Cavallo, C. Tedesco, A. Grassi, *J. Chem. Soc. Dalton Trans.* **2002**, 1839.
- [5] a) F. Calderazzo, U. Englert, G. Pampaloni, R. Santi, A. Sommazzi, M. Zinna, *Dalton Trans.* **2005**, 914; b) H. Sugiyama, G. Aharonian, S. Gambarotta, G. P. A. Yap, P. H. M. Budzelaar, *J. Am. Chem. Soc.* **2002**, *124*, 12268.
- [6] a) G. K. B. Clentsmith, V. C. Gibson, P. B. Hitchcock, B. S. Kimberley, C. Rees, *Chem. Commun.* **2002**, 1498; b) I. Khorobkov, S. Gambarotta, G. P. A. Yap, P. H. M. Budzelaar, *Organometallics* **2002**, *21*, 3088; c) I. J. Blackmore, V. C. Gibson, P. B. Hitchcock, C. W. Rees, D. J. Williams, A. J. P. White, *J. Am. Chem. Soc.* **2005**, *127*, 6012.
- [7] a) D. Enright, S. Gambarotta, G. P. A. Yap, P. H. M. Budzelaar, *Angew. Chem.* **2002**, *114*, 4029; *Angew. Chem. Int. Ed.* **2002**, *41*, 3873; b) H. Sugiyama, S. Gambarotta, G. P. A. Yap, D. R. Wilson, S. K.-H. Thiele, *Organometallics* **2004**, *23*, 5054.
- [8] a) J. Scott, S. Gambarotta, I. Korobkov, *Can. J. Chem.* **2005**, *83*, 279; b) H. Sugiyama, I. Korobkov, S. Gambarotta, A. Moeller, P. H. M. Budzelaar, *Inorg. Chem.* **2004**, *43*, 5771.
- [9] a) R. M. Smith, A. E. Martell, *Critical Stability Constants*, Plenum, New York, **1974**; b) A. Dei, P. Paoletti, A. Vacca, *Inorg. Chem.* **1968**, *7*, 865; c) G. Anderegg, *Helv. Chim. Acta* **1960**, *43*, 414; d) G. Anderegg, E. Bottari, *Helv. Chim. Acta* **1965**, *48*, 887; e) G. Anderegg, E. Hubmann, N. G. Podder, F. Wenk, *Helv. Chim. Acta* **1977**, *60*, 123.

- [10] T. M. Cameron, J. C. Gordon, R. Michalczyk, B. L. Scott, *Chem. Commun.* **2003**, 2282.
- [11] H. M. Dietrich, C. Zapolko, E. Herdtweck, R. Anwander, *Organometallics* **2005**, *24*, 5767.
- [12] H. M. Dietrich, M. Zimmermann, R. Anwander, unpublished results.
- [13] M. Zimmermann, K. W. Törnroos, R. Anwander, *Organometallics* **2006**, *25*, 3593.
- [14] a) J. Scott, S. Gambarotta, I. Korobkov, Q. Knijnenburg, B. de Bruin, P. H. M. Budzelaar, *J. Am. Chem. Soc.* **2005**, *127*, 17204; b) Q. Knijnenburg, J. M. M. Smits, P. H. M. Budzelaar, *Organometallics* **2006**, *25*, 1036.
- [15] Compound **3** ($C_{37}H_{56}N_3Al$, $M_r = 569.83$) crystallizes from hexane in the monoclinic space group $P2_1/n$ with $a = 9.4690(3)$, $b = 17.0926(6)$, $c = 21.1610(8)$ Å, $\beta = 91.874(1)^\circ$, $V = 3423.1$ Å³, and $\rho_{\text{calcd}} = 1.106$ g cm⁻³ for $Z = 4$. Data were collected at 123 K on a BRUKER-AXS 2 K CCD system. The structure was solved by direct methods, and least-square refinement of the model based on 6775 (all data) and 5378 reflections ($I > 2\sigma(I)$) converged to final $wR2 = 0.1116$ and $R1 = 0.0396$. Compound **5** ($C_{43}H_{69}N_3AlOLa$, $M_r = 809.90$) crystallizes from hexane in the triclinic space group $P\bar{1}$ with $a = 11.8063(13)$, $b = 12.4658(13)$, $c = 17.1461(18)$ Å, $\alpha = 76.170(2)$, $\beta = 70.824(2)$, $\gamma = 62.452(2)^\circ$, $V = 2101.8(4)$ Å³, and $\rho_{\text{calcd}} = 1.280$ g cm⁻³ for $Z = 2$. Data were collected at 123 K on a BRUKER-AXS 2 K CCD system. The structure was solved by direct methods, and least-square refinement of the model based on 7302 (all data) and 5723 reflections ($I > 2.0\sigma(I)$) converged to final $wR2 = 0.1723$ and $R1 = 0.0617$. CCDC-627911 and CCDC-627912 contain the supplementary crystallographic data for this paper. These data can be obtained free of charge from The Cambridge Crystallographic Data Centre via www.ccdc.cam.ac.uk/data_request/cif.
- [16] R. Duchateau, C. T. van Wee, A. Meetsma, P. T. van Duijnen, J. H. Teuben, *Organometallics* **1996**, *15*, 2279.
- [17] a) E. P. Talsi, D. E. Babushkin, N. V. Semikolenova, V. N. Zudin, V. N. Panchenko, V. A. Zakharov, *Macromol. Chem. Phys.* **2001**, *202*, 2046; b) N. V. Semikolenova, V. A. Zakharov, E. P. Talsi, D. E. Babushkin, A. P. Sobolev, L. G. Echevskay, M. M. Khysniyarov, *J. Mol. Catal. A* **2002**, *182–183*, 283; c) I. I. Zakharov, V. A. Zakharov, *Macromol. Theory Simul.* **2004**, *13*, 583.
- [18] J. Holton, M. F. Lappert, D. G. H. Ballard, R. Pearce, J. L. Atwood, W. E. Hunter, *J. Chem. Soc. Dalton Trans.* **1979**, 54.
- [19] a) M. G. Klimpel, J. Eppinger, P. Sirsch, W. Scherer, R. Anwander, *Organometallics* **2002**, *21*, 4021; b) H. M. Dietrich, G. Raudaschl-Sieber, R. Anwander, *Angew. Chem.* **2005**, *117*, 5437; *Angew. Chem. Int. Ed.* **2005**, *44*, 5303.
- [20] A. Fischbach, R. Anwander, *Adv. Polym. Sci.* **2006**, *204*, 155.
- [21] W. J. Evans, T. M. Champagne, D. G. Giarikos, J. W. Ziller, *Organometallics* **2005**, *24*, 570.
- [22] H. Yamamoto, H. Yasuda, K. Yokota, A. Nakamura, Y. Kai, N. Kasai, *Chem. Lett.* **1988**, 1963.
- [23] Similar binding was found in $[(C_5Me_5)_2Yb(\mu-Me)Be(C_5Me_5)]$: C. J. Burns, R. A. Andersen, *J. Am. Chem. Soc.* **1987**, *109*, 5853.
- [24] Complex **5** is the only alkylation product under the reaction conditions described in the Experimental Section isolable as an analytically pure white solid in very high yields. Nevertheless, when stirring a hexane solution of **5** for 4 days at 40 °C traces of the pyridine *ortho*-alkylation product were found indicating an alkyl migration from the imino carbon to the pyridine *ortho* position.

Organolanthanoid-Imino-Amido-Pyridin-Komplexe mit unerwarteter Reaktivität: Alkylwanderung und ein ungewöhnlicher Tetramethylaluminat-Koordinationsmodus**

Melanie Zimmermann, Karl W. Törnroos und Reiner Anwander*

Bis(imino)pyridine sind vielseitige Hilfsliganden für effiziente Ziegler-Natta-Katalysatoren auf der Basis der späten Übergangsmetalle Eisen und Cobalt^[1] sowie der frühen Übergangsmetalle Vanadium^[2] und Chrom.^[3] Die starke Tendenz dieses konjugierten [NNN]-Liganden (L^1 , Schema 1) zur Beteiligung an vielfältigen Transformationen ist gut do-



Schema 1. Die chemisch „nicht-unschuldigen“ $[\text{NNN}]^{n-}$ -Hilfsliganden ($n=0-2$). Nachgewiesene Angriffspunkte für nucleophile(n) Angriff/Alkylierung sind mit einem Pfeil gekennzeichnet. (gestrichelter Pfeil: vorliegende Arbeit)

kumentiert. Sowohl der beträchtliche Ladungstransfer zwischen dem π -System des Liganden und dem Übergangsmetallzentrum als auch die Alkylierungsneigung mehrerer Positionen des Ligandenrückgrats belegen, dass diese Diiminoliganden „nicht-unschuldig“ sind. In Gegenwart von Alkylierungsmitteln wurden ein Alkylangriff auf die Iminogruppe,^[4] auf jede der Pyridin-Ringpositionen^[2,4a,5] – sogar auf das Pyridin-N-Atom^[6] – sowie Deprotonierung der Methyl-Seitenarme beobachtet (Schema 1).^[5b,6b,7] Auch Dimerisierung durch C-C-Bindungsknüpfung nach Reduktion der Enamineinheit^[5b,8] und Cycloaddition des Pyridinrings wurden gefunden.^[5b]

Die Abnahme der Metall-Stickstoff-Bindungsenergien von späten zu frühen Übergangsmetallen innerhalb einer Reihe in Kombination mit einem neutralen Bis(imino)pyridinliganden verhindert vermutlich die Bildung stabiler

Gruppe-3-Komplexe.^[9] Das einzige Beispiel eines durch einen vermeintlich neutralen Bis(imino)pyridinliganden stabilisierten Lanthanoidkomplexes entpuppte sich als das Ergebnis einer internen Ligandenreduktion unter Bildung eines Radikalanions. Versuche zur Synthese der Bis(imino)pyridin- LnCl_3 -Addukte ($\text{Ln} = \text{Nd}$) verliefen erfolglos.^[8b]

Der Nachweis eines nucleophilen Angriffs von Alkylierungsmitteln oder Cokatalysatoren wie AlMe_3 auf das Imino-C-Atom des Ligandenrückgrats eröffnete zugleich den Zugang zu einer neuen Klasse monoanionischer Imino-Amido-Pyridin- $[\text{NNN}]^-$ -Liganden ($[\text{L}^2]^-$, Schema 1).^[4b] Diese eigneten sich als Ausgangsverbindungen für die Synthese konformativ starrer Lanthanoidkomplexe unter Erhaltung der außerge-

wöhnlichen stereoelektronischen Eigenschaften des Bis(imino)pyridinliganden. Gordon et al. gelang ausgehend von $[\text{Lu}(\text{CH}_2\text{SiMe}_3)_3(\text{thf})_2]$ die Synthese eines Lutetium-Dialkylkomplexes mit $[\text{L}^2]^-$ als stabilisierendem Hilfsliganden.^[10] Wie wir kürzlich zeigen konnten, eignen sich homoleptische Lanthanoidtetramethylaluminat $[\text{Ln}(\text{AlMe}_4)_3]$ sehr gut als Vorstufen für die Synthese vielfältiger Ln/Al -Heterodimetallkomplexe. Dazu zählen sowohl Halb-lanthanoidocene^[11] und Lanthanoidocene^[12] als auch vom Bis(amido)pyridinliganden abgeleitete $[\text{NNN}]^{2-}$ -Organolanthanoidkomplexe.^[13]

Hier stellen wir neuartige $[\text{NNN}]^-$ - und $[\text{NNN}]^{2-}$ -Organolanthanoidkomplexe vor. Hervorgehoben werden sollen dabei die Beteiligung des Imino-Amido-Pyridin-Liganden an der Komplexbildung sowie sein Einfluss auf die Komplexeigenschaften, der zu einem zuvor unbekanntem Koordinationsmodus des Tetramethylaluminatliganden führte.

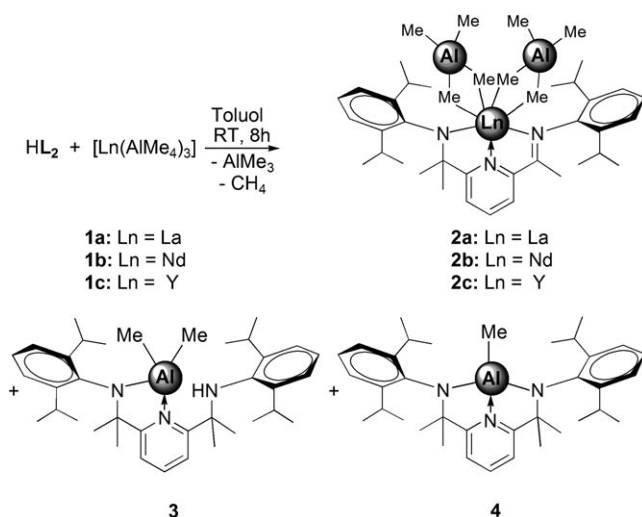
$[\text{Ln}(\text{AlMe}_4)_3]$ [$\text{Ln} = \text{La}$ (**1a**), Nd (**1b**) und Y (**1c**)] reagiert mit hellgelbem HL^2 in Form einer Alkaneliminierung (Schema 2). Die sofortige Gasentwicklung und der Farbwechsel von Hellgelb nach Weinrot, gefolgt von der Bildung eines weinroten Feststoffes, sind ein Hinweis auf die Koordination des monoanionischen Imino-Amido-Liganden an das Metallzentrum.

Die Abtrennung des Feststoffes von der Reaktionsmischung lieferte die weinroten Komplexe **2a-c** als Pulver, wobei die Ausbeute mit der Größe des Metallkations zunahm ($\text{Ln} = \text{Y}$: 49%, Nd : 52%, La : 62%). Die IR-Spektren von **2a-c** zeigen eine starke Absorptionsbande bei 1582 (**2a,c**)

[*] M. Zimmermann, Prof. K. W. Törnroos, Prof. R. Anwander
Department of Chemistry
University of Bergen
Allégaten 41, 5007 Bergen (Norwegen)
Fax: (+47) 5558-9490
E-Mail: reiner.anwander@kj.uib.no

[**] Diese Arbeit wurde vom Norwegian Research Council, dem Programm Nanoscience@UiB und dem Fonds der Chemischen Industrie unterstützt.

Hintergrundinformationen zu diesem Beitrag sind im WWW unter <http://www.angewandte.de> zu finden oder können beim Autor angefordert werden.



Schema 2. Umsetzung des Imino-Amino-Pyridins HL^2 mit $[Ln(AlMe_4)_3]$ (1).

oder 1588 cm^{-1} (**2b**), die der Streckschwingung einer metallkoordinierten Iminogruppe zugeordnet wird (HL^2 : 1644 cm^{-1}). Vergleichbare Verschiebungen wurden bereits bei Bis(imino)pyridinkomplexen des Titans beobachtet.^[5a]

Die 1H -NMR-Spektren von **2a–c** in C_6D_6 bestätigen eine starre L^2 -Koordination und eine hohe Rotationsbarriere für die Arylgruppen um die $N-C_{\text{ipso}}$ -Bindung bei Raumtemperatur. Zwei hochfeldverschobene Singulets bei $\delta = 1.71$ (3H) und 1.39 ppm (6H) (**2a**) [$\delta = 1.74$ und 1.35 ppm (**2c**)] belegen die Erhaltung des Imino-Amido-Pyridin-Ligandenrückgrates. Das 1H -NMR-Spektrum zeigt jeweils nur ein breites Singulett im Methyl-Alkyl-Bereich bei $\delta = -0.25$ (**2a**) bzw. -0.38 ppm (**2c**), das der $\{AlMe_4\}$ -Einheit mit schnell austauschenden verbrückenden und terminalen Methylgruppen zugeordnet werden kann. Gegenüber den Signalen der homoleptischen Vorstufen [$\delta = -0.20$ (**1a**), -0.27 ppm (**1c**)] sind diese Signale zu tiefem Feld verschoben. Die Bildung des paramagnetischen Neodymkomplexes **2b** konnte durch Elementaranalyse, IR-Daten und ein relativ gut aufgelöstes 1H -NMR-Spektrum nachgewiesen werden ($\delta_{AlCH_3} = 6.30$ ppm).

Die moderaten Ausbeuten an **2a–c** und die auffällig rot gefärbte Lösung machten eine genauere Untersuchung des Reaktionsüberstandes unumgänglich. Außer nicht umgesetztem $[Ln(AlMe_4)_3]$ konnten durch fraktionierende Kristallisation die beiden Aluminiumkomplexe **3** und **4** als analytisch reine orangefarbene bzw. rote Verbindungen erhalten werden (Schema 2).

Die Kristallstrukturanalyse des Aluminiumkomplexes **3** offenbarte eine zuvor nicht beobachtete Alkylierung der Iminogruppe von $[L^2]^-$ (Abbildung 1). Das Metallzentrum von **3** ist verzerrt tetraedrisch koordiniert, wobei der methylierte Hilfsligand in η^2 -Form an das Metallzentrum koordiniert. Die Al-N-Bindungslängen und der N2-Al-N3-Winkel liegen im erwarteten Bereich.^[4b,14a,15] Die Alkylierung am Imino-C-Atom und die damit verbundene Bildung eines dianionischen Bis(amido)pyridins des $[NNN]^{2-}$ -Typs waren unerwartet und unterscheiden sich klar von der bekannten Reaktivität der Bis(imino)pyridinliganden und der davon

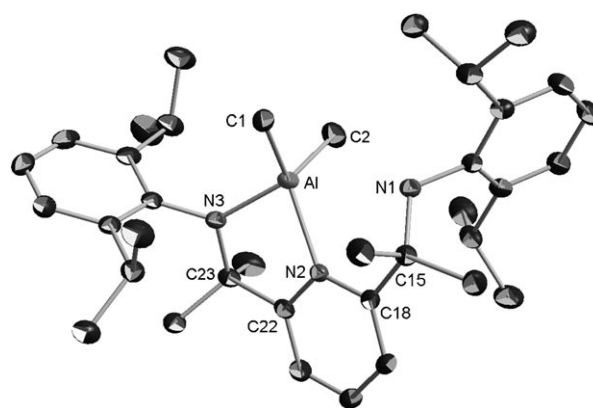


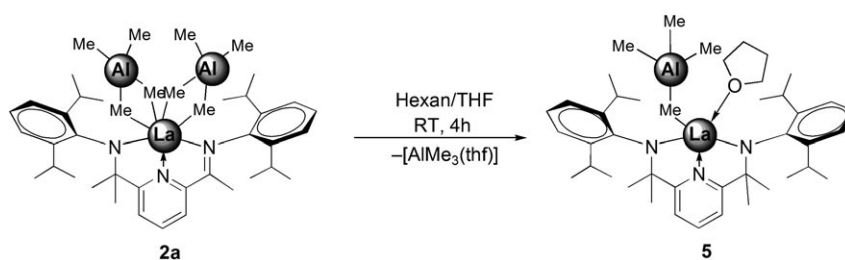
Abbildung 1. Molekülstruktur von **3** (die anisotropen Auslenkungsparameter entsprechen einer Aufenthaltswahrscheinlichkeit von 50%). Wasserstoffatome sind aus Gründen der Übersichtlichkeit nicht dargestellt. Ausgewählte Bindungsabstände [Å] und -winkel [°]: Al...N1 2.8056(13), Al–N2 2.0552(13), Al–N3 1.8568(13), Al–C1 1.9814(17), Al–C2 1.9764(18), N1–C15 1.4954(19), N3–C23 1.4738(19), C15–C18 1.530(2), C22–C23 1.525(2); N2–Al–N3 82.27(5), Al–N3–C23 113.30(10), N3–Al–C1 107.82(7), N3–Al–C2 114.74(7), N2–Al–C1 125.28(7), N2–Al–C2 112.38(7), N1–C15–C18 108.59(12), N3–C23–C22 105.89(12).

abgeleiteten Komplexe. In früheren Arbeiten hatte die Zugabe von $AlMe_3$ zu Bis(imino)pyridinen und ihren Komplexen der späten Übergangsmetalle sogar im Überschuss lediglich das Monoalkylierungsprodukt geliefert.^[4b,14]

Die hier beobachtete Reaktivität lässt deshalb auf einen Alkylierungsmechanismus schließen, der über außerordentlich reaktive $[Ln-Me]$ -Zwischenstufen verläuft und nicht das Ergebnis einer Alkylierung durch das in der Säure-Base-Reaktion von $[Ln(AlMe_4)_3]$ mit HL^2 freigesetzte $AlMe_3$ ist. Gleichzeitig konkurriert das Lewis-saure Al^{3+} um die Koordination an den $[NNN]^{2-}$ -Liganden – die starke Lewis-Säure Al^{3+} hat eine hohe Affinität zu Stickstoffdonoren^[16], was die Abhängigkeit der Aluminiumkomplexbildung von der Ln^{3+} -Größe erklärt. Das 4:1-Verhältnis, in dem die beiden Aluminiumkomplexe gebildet werden, spricht für eine kinetisch (**3**) bzw. thermodynamisch (**4**, durch CH_4 -Eliminierung aus **3**) kontrollierte Reaktion.

Die Komplexe $[L^2Ln(AlMe_4)_2]$ ($Ln = La, Nd, Y$) (**2a–c**) ähneln $[(NNN)FeMe(AlMe_4)]$ ($NNN = \text{Bis(imino)pyridyl}$), das als aktive Spezies in den hocheffizienten, auf Bis(imino)pyridin- Fe^{II} -Komplexen basierenden Katalysatorsystemen diskutiert wird, die durch MAO oder Trialkylaluminiumreagentien aktiviert werden.^[17] Tetramethylaluminat-einheiten $\{AlMe_4\}$ – auch als „maskierte Alkyle“ bezeichnet – bieten eine häufig genutzten Weg zur Synthese hochreaktiver Metallkomplexe mit Lanthanoid- $\{Me\}$ -Derivaten.^[18] Die donorinduzierte Spaltung von Tetramethylaluminaten (Donor: THF, Diethylether, Pyridin) wurde bereits eingesetzt, um heteroleptische Lanthanoidocen- und Halblanthanoidocenkomplexe, $[Cp'_2Ln(AIR_4)]$ bzw. $[Cp'_Ln(AIR_4)_2]$ (Cp' = substituiertes Cyclopentadienyl), in Komplexe vom Typ $[Cp'_2Ln(R)]$ bzw. $[Cp'_Ln(R)_2]$ umzuwandeln.^[11,18,19]

Zugabe eines Überschusses an THF unter Rühren zu einer Suspension des Bis(tetramethylaluminat)-Komplexes **2a** in Hexan (Schema 3) führte zur spontanen Auflösung des weinroten Feststoffes unter Entfärbung der Lösung. Aus



Schema 3. Donorinduzierte Spaltung von **2a** durch THF.

einer Hexanlösung kristallisierten farblose Einkristalle von **5**, die sich für eine Kristallstrukturanalyse eigneten. In der Molekülstruktur zeigte sich eine „unvollständige“ donorinduzierte Tetramethylaluminatspaltung (Abbildung 2).^[15]

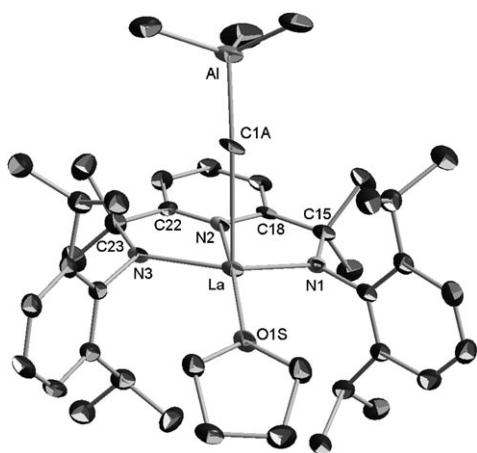


Abbildung 2. Molekülstruktur von **5** (die anisotropen Auslenkungsparameter entsprechen einer Aufenthaltswahrscheinlichkeit von 50%). Wasserstoffatome sind aus Gründen der Übersichtlichkeit nicht dargestellt. Ausgewählte Bindungsabstände [Å] und -winkel [°]: La–N1 2.294(5), La–N2 2.516(5), La–N3 2.246(6), La–O1S 2.538(4), La–C1A 2.825(7), Al–C1A 2.024(7), Al–C2A 1.980(9), Al–C3A 1.980(9), Al–C4A 1.963(9), N3–C23 1.475(8), C22–C23 1.511(9), N1–C15 1.475(8), C15–C18 1.481(10); N1–La–N3 127.82(18), N1–La–N2 64.96(18), N2–La–N3 64.15(17), N1–La–O1S 111.86(17), N3–La–O1S 114.68(16), N1–La–C1A 97.85(2), N3–La–C1A 87.56(2), O1S–La–C1A 109.95(2), La–C1A–Al 165.0(4), N1–C15–C18 108.2(5), N3–C23–C22 106.1(5).

Entgegen einer erwarteten Organoaluminium-freien Verbindung weist der Lanthanokomplex **5** einen intakten Tetramethylaluminatliganden in einem neuartigen $(\mu\text{-Me})\{\text{AlMe}_3\}$ -Koordinationsmodus auf. Unseres Wissens ist dies das erste Beispiel für eine strukturell eindeutig charakterisierte η^1 -koordinierte $\{\text{AlMe}_4\}$ -Einheit und somit der bisher fehlende Tetramethylaluminat-Koordinationsmodus neben den bereits beschriebenen η^2 - und η^3 -Modi.^[20]

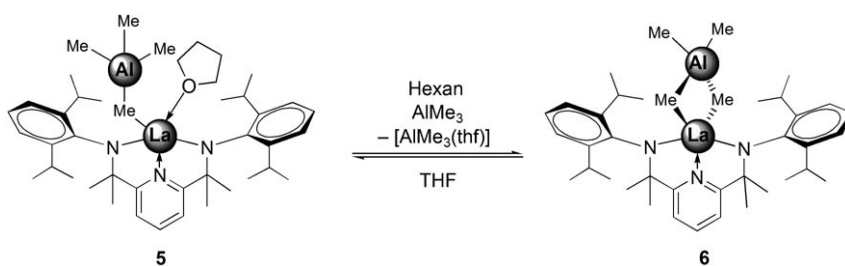
Eine weitere Besonderheit ist das Vorhandensein des Spaltungsreagens THF und eines Tetramethylaluminates im selben Molekül. Die einzigen vergleichbaren Komplexe sind $[(\text{C}_5\text{Me}_5)_2\text{Sm}(\text{thf})(\mu\text{-}\eta^2\text{-Et})\text{AlEt}_3]$ ^[21] und $[(\text{C}_5\text{Me}_5)_2\text{Yb}(\eta^2\text{-Et})\text{AlEt}_2(\text{thf})]$,^[22] die jedoch η^2 -koordinierte Ethylliganden enthalten.^[23] Das fünffach koordinierte La-Zentrum ist außer-

dem von den drei N-Atomen des Hilfsliganden umgeben, der ähnlich wie in **3** und **4** alkyliert wurde. Die Koordinationsumgebung des Lanthanzentrums kann als verzerrt trigonal-bipyramidal beschrieben werden, wobei das THF-O-Atom und das Pyridin-N-Atom (N2) die apikalen Positionen einnehmen (O1S–La–N2 166.3°), während die Amido-N-Atome (N1 und N3) und das Tetramethylaluminat-C-Atom (C1A) die äquatorialen Positionen besetzen.^[15]

Die Bildung von **5** ist vermutlich das Ergebnis einer schnellen Abfolge von Reaktionsschritten, an deren Anfang die donorinduzierte Spaltung eines Tetramethylaluminatliganden in **2a** steht, die zunächst zur Bildung einer hochreaktiven terminalen Methylgruppe führt. Dieses $\{\text{Ln-Me}\}$ -Intermediat vollzieht anschließend eine Methylwanderung vom Metallzentrum zum Imino-C-Atom. Der intramolekulare nucleophile Angriff auf die Iminogruppe verursacht eine weitere Anionisierung des Liganden, die mit einer Quaternisierung des ehemaligen Imino-C-Atoms einhergeht.^[24] Vergleichsweise kurze Bindungen zwischen Lanthan und den Amido-N-Atomen (La–N1 = 2.294(5), La–N3 = 2.246(6) Å) sowie dem Pyridin-N-Atom (N2–La = 2.516(5) Å) lassen auf eine starke Wechselwirkung zwischen dem neu gebildeten $[\text{NNN}]^{2-}$ -Liganden und dem niedrig koordinierten Metallzentrum schließen.^[8b,13] Die $\{\text{La}(\mu\text{-Me})\text{Al}\}$ -Heterodimetalleinheit hat einen ausgesprochen stumpfen La–C1A–Al-Winkel von 165.0(5)°. Die La–C-Bindungslänge liegt mit 2.825(7) Å im Bereich relativ langer Bindungen in η^2 -koordinierten Tetramethylaluminaten (2.694(3)–2.802(4) Å).^[11]

Die symmetrische Umgebung des Metallzentrums durch den $[\text{NNN}]^{2-}$ -Liganden ist auch im ¹H-NMR-Spektrum von **5** erkennbar. In C_6D_6 zeigt der Bis(amido)pyridinligand lediglich einen Signalsatz mit nur einem Multiplett für die Methinprotonen bei $\delta = 3.47$ ppm und zwei Dubletts bei $\delta = 1.18$ und 1.15 ppm für die Methylprotonen der Isopropylgruppen. Ein relativ scharfes Signal bei $\delta = -0.15$ ppm kann der $\{\text{AlMe}_4\}$ -Einheit zugeordnet werden und deutet auf einen schnellen Austausch von verbrückenden und terminalen Methylgruppen hin. Des Weiteren bestätigen die signifikant zu höherem Feld hin verschobenen Multipletts für den THF-Liganden bei $\delta = 2.74$ und 0.98 ppm die starke Bindung des THF-Moleküls an das Metallzentrum.

Trotz seiner starken Koordination kann eine Abdissoziation von THF durch Zugabe von AlMe_3 zu einer Hexanlösung von **5** erreicht werden (Schema 4). Die Bildung des donorfreien Tetramethylaluminatkomplexes **6** erfolgt quantitativ und ergibt einen analytisch reinen weißen Feststoff, der in Hexan schwerlöslich ist. Das einzige Nebenprodukt der Reaktion ist $[\text{AlMe}_3(\text{thf})]$. Die Abdissoziation des THF-Donorliganden ist vollständig reversibel, und **5** kann durch THF-Zugabe zu einer Lösung von **6** in Hexan quantitativ zurückgewonnen werden. Bedingt durch die sterische Untersättigung des Lanthanzentrums wird für **6** eine η^2 -Koordinierung des Tetramethylaluminatliganden angenommen. Ein endgültiger Beweis durch ein VT-NMR-Experiment (VT = variable Temperatur) gelang nicht, da im zugänglichen Temperatur-



Schema 4. THF-Dissoziations-Koordinations-Gleichgewicht zwischen **5** und **6**.

bereich (−90 bis 25 °C) keine Dekoaleszenz des Aluminat-signals beobachtbar war.

Der Imino-Amido-Pyridin-Ligand weist eine wesentlich geringere Konjugation als das Bis(imino)pyridinligandensystem auf. Dennoch lässt er einen signifikanten internen Ladungstransfer zu, der außergewöhnliche Reaktionswege, Koordinationsmodi und Komplexstabilisierung ermöglicht. Die beobachtete Reaktivität der Imino-Amido-Pyridin-Lanthanoid-Komplexe unterstreicht nicht nur das „nicht-unschuldige“ Verhalten dieses Liganden, sondern auch die stark ausgeprägten alkylierenden Eigenschaften von {Ln-Me}-Einheiten. Die neue η^1 -Tetramethylaluminatkoordination ist ein klarer Beleg für die koordinative Flexibilität der anionischen Cokatalsatoren in Ziegler-Natta-Katalysatoren und demonstriert die unvorhersehbare Natur „schlafender“ Katalysatorpezies.

Experimentelles

Repräsentative Synthese von **2a**: In einem Handschuhkasten wurde $[\text{La}(\text{AlMe}_2)_3]$ (**1a**, 241 mg, 0.60 mmol) in 3 mL Toluol gelöst und unter Rühren tropfenweise zu einer Lösung von HL² (300 mg, 0.60 mmol) in 4 mL Toluol gegeben; dabei traten eine sofortige Rotfärbung der Reaktionsmischung und heftige Gasentwicklung ein. Die Reaktionsmischung wurde 8 h bei Raumtemperatur gerührt, wobei sich ein weinroter Feststoff bildete. Das Reaktionsprodukt wurde durch Zentrifugation abgetrennt, viermal mit 5 mL Hexan gewaschen und anschließend am Ölpumpenvakuum getrocknet. **2a** wurde als weinroter Feststoff (303 mg, 0.37 mmol, 62 %) erhalten. ¹H-NMR (600 MHz, C₆D₆, 25 °C): δ = 7.18–7.10 (m, 6H, Ar), 7.04 (t, ³J = 7.8 Hz, 1H, C₅H₃N-*p*-Proton), 6.86 (d, ³J = 7.8 Hz, 1H, C₅H₃N-*m*-Proton), 6.85 (d, ³J = 7.8 Hz, 1H, C₅H₃N-*m*-Proton), 3.26 (sept, ³J = 6.6 Hz, 2H, ArCH), 2.62 (sept, ³J = 6.6 Hz, 2H, ArCH), 1.71 (s, 3H, N=CCH₃), 1.39 (s, 6H, NCCH₃), 1.30 (d, ³J = 6.6 Hz, 6H, CH₃), 1.26 (d, ³J = 6.6 Hz, 6H, CH₃), 1.00 (d, ³J = 6.6 Hz, 6H, CH₃), 0.88 (d, ³J = 6.6 Hz, 6H, CH₃), −0.25 ppm (s, 24H, Al(CH₃)₄). ¹³C-NMR (126 MHz, C₆D₆, 25 °C): δ = 175.1, 158.7, 149.4, 140.7, 139.1, 138.4, 125.5, 125.3, 124.9, 117.3, 69.9, 33.7, 29.1, 28.6, 28.1, 26.3, 26.1, 25.5, 25.1, 20.3, 3.1 ppm (br. s., Al(CH₃)₄). VT-NMR lieferte wegen der geringen Löslichkeit von **2a** in [D₈]Toluol keine Ergebnisse. IR (Nujol): $\tilde{\nu}$ = 1582 (s, C=N), 1468 (vs, Nujol), 1375 (vs, Nujol), 1303 (s), 1261 (m), 1220 (w), 1214 (w), 1173 (s), 1095 (w), 1007 (w), 971 (w), 950 (w), 888 (w), 847 (w), 821 (w), 785 (m), 769 (m), 723 (vs), 593 (w), 578 (w), 516 cm^{−1} (w). Elementaranalyse (%) ber. für C₄₂H₇₀N₃Al₃La (809.910 g mol^{−1}): C 62.29, H 8.71, N 5.19; gef.: C 62.21, H 8.77, N 5.13.

5: Eine Suspension von **2a** (126 mg, 0.16 mmol) in 3 mL Hexan wurde unter Rühren tropfenweise mit 3 mL THF versetzt. Der weinrote Feststoff löste sich sofort unter Entfärbung der Reaktionsmischung auf. Nach vierstündigem Rühren bei Raumtemperatur wurde das Lösungsmittel am Ölpumpenvakuum entfernt, und es wurde ein weißer Feststoff erhalten, der dreimal mit 2 mL Hexan

gewaschen und anschließend am Ölpumpenvakuum getrocknet wurde. **5** wurde als weißer Feststoff (117 mg, 0.14 mmol, 90 %) erhalten. ¹H-NMR (600 MHz, C₆D₆, 25 °C): δ = 7.20–7.11 (m, 6H, Ar), 7.06 (t, ³J = 7.8 Hz, 1H, C₅H₃N-*p*-Proton), 6.81 (d, ³J = 7.8 Hz, 2H, C₅H₃N-*m*-Protonen), 3.47 (sept, ³J = 6.6 Hz, 4H, ArCH), 2.74 (m, 4H, THF), 1.40 (s, 12H, NCCH₃), 1.18 (d, ³J = 6.6 Hz, 12H, CH₃), 1.15 (d, ³J = 6.6 Hz, 12H, CH₃), 0.98 (m, 4H, THF), −0.15 ppm (s, 12H, Al(CH₃)₄). ¹³C-NMR (151 MHz, C₆D₆, 25 °C): δ = 174.3, 150.3, 141.3, 139.0, 125.6, 125.0, 117.8, 70.8 (THF), 69.1, 32.8, 31.9, 28.2, 28.0, 25.1, 23.0, 1.7 ppm (s, Al(CH₃)₄). IR (Nujol): $\tilde{\nu}$ = 1572 (w), 1468 (vs, Nujol), 1375 (vs, Nujol), 1303 (s), 1256 (w), 1220 (w), 1194 (m), 1158 (m), 1126 (w), 1101 (w), 1044 (w), 1013 (w), 982 (w), 930 (w), 852 (m), 816 (w), 785 (m), 764 (m), 723 (vs), 692 (w), 583 (w), 562 (w), 536 (w), 516 cm^{−1} (w). Elementaranalyse (%) ber. für C₄₃H₆₉N₃OAlLa (809.930 g mol^{−1}): C 63.77, H 8.59, N 5.19; gef.: C 63.37, H 8.58, N 5.02.

6: Eine Lösung von **5** (71 mg, 0.09 mmol) in 3 mL Toluol wurde unter Rühren tropfenweise mit AlMe₃ (6 mg, 0.09 mmol) versetzt. Die farblose Reaktionsmischung wurde 4 h bei RT gerührt und das Lösungsmittel anschließend am Ölpumpenvakuum entfernt. Der erhaltene weiße Feststoff wurde dreimal mit 2 mL Hexan gewaschen und am Ölpumpenvakuum getrocknet. **6** wurde als weißer Feststoff (63 mg, 0.09 mmol, 98 %) erhalten. ¹H-NMR (600 MHz, C₆D₆, 25 °C): δ = 7.20–7.16 (m, 6H, Ar), 7.14 (t, ³J = 7.8 Hz, 1H, C₅H₃N-*p*-Proton), 6.78 (d, ³J = 7.8 Hz, 2H, C₅H₃N-*m*-Protonen), 3.28 (sept, ³J = 6.6 Hz, 4H, ArCH), 1.41 (s, 12H, NCCH₃), 1.31 (d, ³J = 6.6 Hz, 12H, CH₃), 1.05 (d, ³J = 6.6 Hz, 12H, CH₃), −0.40 ppm (s, 12H, Al(CH₃)₄). ¹³C-NMR (151 MHz, C₆D₆, 25 °C): δ = 175.1, 149.4, 141.5, 139.1, 126.1, 125.3, 117.3, 69.9, 33.7, 28.1, 26.3, 26.1, 2.83 ppm (s, Al(CH₃)₄). IR (Nujol): $\tilde{\nu}$ = 1577 (w), 1468 (vs, Nujol), 1375 (vs, Nujol), 1303 (s), 1251 (w), 1240 (w), 1194 (w), 1168 (m), 1095 (w), 1044 (w), 997 (w), 971 (m), 852 (w), 816 (w), 790 (w), 764 (m), 723 (vs), 609 (w), 567 (w), 562 (w), 536 (w), 516 cm^{−1} (w). Elementaranalyse (%) ber. für C₃₉H₆₁N₃AlLa (737.824 g mol^{−1}): C 63.49, H 8.33, N 5.70; gef.: C 63.54, H 8.35, N 5.44.

Experimentelle und analytische Details für die Komplexe **2–6** sind als Hintergrundinformationen erhältlich.

Eingegangen am 21. November 2006,
veränderte Fassung am 12. Dezember 2006
Online veröffentlicht am 20. März 2007

Stichwörter: Alkylierungen · Aluminium · Amide · Lanthanoide · Ligandeneffekte

- [1] a) B. L. Small, M. Brookhart, A. M. A. Bennett, *J. Am. Chem. Soc.* **1998**, *120*, 4049; b) G. J. P. Britovsek, V. C. Gibson, B. S. Kimberley, P. J. Maddox, S. J. McTavish, G. A. Solan, A. J. P. White, D. J. Williams, *Chem. Commun.* **1998**, 849; c) G. J. P. Britovsek, M. Bruce, V. C. Gibson, B. S. Kimberley, P. J. Maddox, S. Mastroianni, S. J. McTavish, C. Redshaw, G. A. Solan, S. Strömberg, A. J. P. White, D. J. Williams, *J. Am. Chem. Soc.* **1999**, *121*, 8728.
- [2] D. Reardon, F. Conan, S. Gambarotta, G. Yap, Q. Wang, *J. Am. Chem. Soc.* **1999**, *121*, 9318.
- [3] M. A. Esteruelas, A. M. López, L. Méndez, M. Oliván, E. Oñate, *Organometallics* **2003**, *22*, 395.
- [4] a) J. Scott, S. Gambarotta, I. Korobkov, P. H. M. Budzelaar, *J. Am. Chem. Soc.* **2005**, *127*, 13019; b) M. Bruce, V. C. Gibson, C. Redshaw, G. A. Solan, A. J. P. White, D. J. Williams, *Chem. Commun.* **1998**, 2523; c) S. Milione, G. Cavallo, C. Tedesco, A. Grassi, *J. Chem. Soc. Dalton Trans.* **2002**, 1839.

- [5] a) F. Calderazzo, U. Englert, G. Pampaloni, R. Santi, A. Som-mazzi, M. Zinna, *Dalton Trans.* **2005**, 914; b) H. Sugiyama, G. Aharonian, S. Gambarotta, G. P. A. Yap, P. H. M. Budzelaar, *J. Am. Chem. Soc.* **2002**, *124*, 12268.
- [6] a) G. K. B. Clentsmith, V. C. Gibson, P. B. Hitchcock, B. S. Kimberley, C. Rees, *Chem. Commun.* **2002**, 1498; b) I. Kho-robov, S. Gambarotta, G. P. A. Yap, P. H. M. Budzelaar, *Organometallics* **2002**, *21*, 3088; c) I. J. Blackmore, V. C. Gibson, P. B. Hitchcock, C. W. Rees, D. J. Williams, A. J. P. White, *J. Am. Chem. Soc.* **2005**, *127*, 6012.
- [7] a) D. Enright, S. Gambarotta, G. P. A. Yap, P. H. M. Budzelaar, *Angew. Chem.* **2002**, *114*, 4029; *Angew. Chem. Int. Ed.* **2002**, *41*, 3873; b) H. Sugiyama, S. Gambarotta, G. P. A. Yap, D. R. Wilson, S. K.-H. Thiele, *Organometallics* **2004**, *23*, 5054.
- [8] a) J. Scott, S. Gambarotta, I. Korobkov, *Can. J. Chem.* **2005**, *83*, 279; b) H. Sugiyama, I. Korobkov, S. Gambarotta, A. Moeller, P. H. M. Budzelaar, *Inorg. Chem.* **2004**, *43*, 5771.
- [9] a) R. M. Smith, A. E. Martell, *Critical Stability Constants*, Plenum, New York, **1974**; b) A. Dei, P. Paoletti, A. Vacca, *Inorg. Chem.* **1968**, *7*, 865; c) G. Anderegg, *Helv. Chim. Acta* **1960**, *43*, 414; d) G. Anderegg, E. Bottari, *Helv. Chim. Acta* **1965**, *48*, 887; e) G. Anderegg, E. Hubmann, N. G. Podder, F. Wenk, *Helv. Chim. Acta* **1977**, *60*, 123.
- [10] T. M. Cameron, J. C. Gordon, R. Michalczyk, B. L. Scott, *Chem. Commun.* **2003**, 2282.
- [11] H. M. Dietrich, C. Zapilko, E. Herdtweck, R. Anwander, *Organometallics* **2005**, *24*, 5767.
- [12] H. M. Dietrich, M. Zimmermann, R. Anwander, unveröffent-lichte Ergebnisse.
- [13] M. Zimmermann, K. W. Törnroos, R. Anwander, *Organome-tallics* **2006**, *25*, 3593.
- [14] a) J. Scott, S. Gambarotta, I. Korobkov, Q. Knijnenburg, B. de Bruin, P. H. M. Budzelaar, *J. Am. Chem. Soc.* **2005**, *127*, 17204; b) Q. Knijnenburg, J. M. M. Smits, P. H. M. Budzelaar, *Organometallics* **2006**, *25*, 1036.
- [15] **3** ($C_{37}H_{56}N_3Al$, $M_r = 569.83$) kristallisiert aus Hexan in der monoklinen Raumgruppe $P2_1/n$ mit $a = 9.4690(3)$, $b = 17.0926(6)$, $c = 21.1610(8)$ Å, $\beta = 91.874(1)^\circ$, $V = 3423.1$ Å³ und $\rho_{\text{ber.}} = 1.106$ g cm⁻³ für $Z = 4$. Die Daten wurden bei 123 K auf einem BRUKER-AXS-2-K-CCD-Diffraktometer aufgenommen. Die Strukturlösung erfolgte durch Direkte Methoden und wurde nach der Kleinste-Fehlerquadrat-Methode unter Einbeziehung von 6775 (vollständige Daten) und 5378 Reflexen ($I > 2.0\sigma(I)$) verfeinert; endgültige Werte: $wR2 = 0.1116$, $R1 = 0.0396$. **5** ($C_{43}H_{69}N_3AlOLa$, $M_r = 809.90$) kristallisiert aus Hexan in der triklinen Raumgruppe $P\bar{1}$ mit $a = 11.8063(13)$, $b = 12.4658(13)$, $c = 17.1461(18)$ Å, $\alpha = 76.170(2)$, $\beta = 70.824(2)$, $\gamma = 62.452(2)^\circ$, $V = 2101.8(4)$ Å³ und $\rho_{\text{ber.}} = 1.280$ g cm⁻³ für $Z = 2$. Die Daten wurden bei 123 K auf einem BRUKER-AXS-2-K-CCD-Diffraktometer aufgenommen. Die Strukturlösung erfolgte durch direkte Methoden und wurde nach der Kleinste-Fehlerquadrat-Methode unter Einbeziehung von 7302 (vollständige Daten) und 5723 Reflexen ($I > 2.0\sigma(I)$) verfeinert; endgültige Werte: $wR2 = 0.1723$, $R1 = 0.0617$. CCDC 627911 und 627912 enthalten die ausführlichen kristallographischen Daten zu dieser Veröffentlichung. Die Daten sind kostenlos beim Cambridge Crystallographic Data Centre über www.ccdc.cam.ac.uk/data_request/cif erhältlich.
- [16] R. Duchateau, C. T. van Wee, A. Meetsma, P. T. van Duijnen, J. H. Teuben, *Organometallics* **1996**, *15*, 2279.
- [17] a) E. P. Talsi, D. E. Babushkin, N. V. Semikolenova, V. N. Zudin, V. N. Panchenko, V. A. Zakharov, *Macromol. Chem. Phys.* **2001**, *202*, 2046; b) N. V. Semikolenova, V. A. Zakharov, E. P. Talsi, D. E. Babushkin, A. P. Sobolev, L. G. Echevskay, M. M. Khysniyarov, *J. Mol. Catal. A* **2002**, *182–183*, 283; c) I. I. Zakharov, V. A. Zakharov, *Macromol. Theory Simul.* **2004**, *13*, 583.
- [18] J. Holton, M. F. Lappert, D. G. H. Ballard, R. Pearce, J. L. Atwood, W. E. Hunter, *J. Chem. Soc. Dalton Trans.* **1979**, 54.
- [19] a) M. G. Klimpel, J. Eppinger, P. Sirsch, W. Scherer, R. Anwander, *Organometallics* **2002**, *21*, 4021; b) H. M. Dietrich, G. Raudaschl-Sieber, R. Anwander, *Angew. Chem.* **2005**, *117*, 5437; *Angew. Chem. Int. Ed.* **2005**, *44*, 5303.
- [20] A. Fischbach, R. Anwander, *Adv. Polym. Sci.* **2006**, *204*, 155.
- [21] W. J. Evans, T. M. Champagne, D. G. Giarikos, J. W. Ziller, *Organometallics* **2005**, *24*, 570.
- [22] H. Yamamoto, H. Yasuda, K. Yokota, A. Nakamura, Y. Kai, N. Kasai, *Chem. Lett.* **1988**, 1963.
- [23] Ein ähnliches Bindungsmotiv wurde bei $[(C_5Me_5)_2Yb(\mu-Me)Be(C_5Me_5)]$ beobachtet: C. J. Burns, R. A. Andersen, *J. Am. Chem. Soc.* **1987**, *109*, 5853.
- [24] **5** ist das einzige isolierbare Reaktionsprodukt unter den im experimentellen Teil beschriebenen Reaktionsbedingungen. Die Verbindung kann als analytisch reiner, weißer Feststoff in hohen Ausbeuten erhalten werden. Nach viertägigem Rühren einer Lösung von **5** in Hexan bei 40 °C entstanden jedoch Spuren eines Produktes mit *ortho*-alkyliertem Pyridinring, was auf eine Alkylwanderung vom Imino-C-Atom zur *ortho*-Position des Pyridinrestes hindeutet.



Supporting Information

© Wiley-VCH 2007

69451 Weinheim, Germany

**Alkyl Migration and a new tetramethylaluminate coordination mode:
Unusual reactivity of organolanthanide imino-amido-pyridine complexes**

Melanie Zimmermann, Karl W. Törnroos, and Reiner Anwander*

[*] Prof. Reiner Anwander, Melanie Zimmermann, and Prof. Karl W. Törnroos, Department of Chemistry, University of Bergen, Allégaten 41, N-5007 Bergen, Norway, Fax.Nr.: +47 555 89490, E-mail: reiner.anwander@kj.uib.no

[**] Financial support from the Norwegian Research Council (Project No 171245/V30), the program Nanoscience@UiB, and the Fonds der Chemischen Industrie is gratefully acknowledged.

Experimental Details

General Procedures. All operations were performed with rigorous exclusion of air and water, using standard Schlenk, high-vacuum, and glovebox techniques (MBraun MBLab; <1 ppm O₂, <1 ppm H₂O). Hexane, THF, and toluene were purified by using Grubbs columns (MBraun SPS, solvent purification system) and stored in a glovebox. C₆D₆ was obtained from Aldrich, degassed, dried over Na for 24 h, and filtered. AlMe₃ was purchased from Aldrich and used as received. Homoleptic Ln(AlMe₄)₃ (Ln = La, Nd, Y)^[24] and 2-((2,6-*i*-Pr₂C₆H₃)N=CMe)-6-((2,6-*i*-Pr₂C₆H₃)NHCMe₂)C₅H₃N] (HL₂)^[4b] were synthesized according to the literature method. NMR spectra were recorded at 25 °C on a Bruker-BIOSPIN-AV500 (5 mm BBO, ¹H: 500.13 MHz; ¹³C: 125.77 MHz), and a Bruker-BIOSPIN-AV600 (5 mm cryo probe, ¹H: 600.13 MHz; ¹³C: 150.91 MHz). ¹H and ¹³C shifts are referenced to internal solvent resonances and reported in *parts per million* relative to TMS. IR spectra were recorded on a *NICOLET Impact 410 FTIR* spectrometer as Nujol mulls sandwiched between CsI plates. Elemental analyses were performed on an *Elementar Vario EL III*.

General procedure for the synthesis of complexes 2a-2c

In a glovebox Ln(AlMe₄)₃ (**1**) was dissolved in 3 mL of toluene and added to a stirred solution of 2-((2,6-*i*-Pr₂C₆H₃)N=CMe)-6-((2,6-*i*-Pr₂C₆H₃)NHCMe₂)C₅H₃N] (HL₂) in 4 mL of toluene. The resulting mixture turned red immediately and instant gas formation was observed. The reaction mixture was stirred another 8 h at ambient temperature while the formation of a claret-red precipitate was observed. The product was separated by centrifugation, washed four times with 5 mL of hexane, and dried under vacuum to yield **2** as powdery claret-red solids.

2-((2,6-*i*-Pr₂C₆H₃)N=CMe)-6-((2,6-*i*-Pr₂C₆H₃)NHCMe₂)C₅H₃N]La(AlMe₄)₂ (**2a**).

Following the procedure described above, La(AlMe₄)₃ (**1a**, 241 mg, 0.60 mmol) and HL₂ (300 mg, 0.60 mmol) yielded **2a** as a powdery claret-red solid (303 mg, 0.37 mmol, 62%). ¹H NMR (600 MHz, C₆D₆, 25 °C): d = 7.18-7.10 (m, 6 H, ar), 7.04 (t, ³J ≅ 7.8 Hz, 1 H, C₅H₃N-*p*-proton), 6.86 (d, ³J ≅ 7.8 Hz, 1 H, C₅H₃N-*m*-proton), 6.85 (d, ³J ≅ 7.8 Hz, 1 H, C₅H₃N-*m*-proton), 3.26 (sept, ³J ≅ 6.6 Hz, 2 H, ar-CH), 2.62 (sept, ³J ≅ 6.6 Hz, 2 H, ar-CH), 1.71 (s, 3 H, N=CCH₃), 1.39 (s, 6 H, NCCH₃), 1.30 (d, ³J ≅ 6.6 Hz, 6 H, CH₃), 1.26 (d, ³J ≅ 6.6 Hz, 6 H, CH₃), 1.00 (d, ³J ≅ 6.6 Hz, 6 H, CH₃), 0.88 (d, ³J ≅ 6.6 Hz, 6 H, CH₃), -0.25 (s br, 24 H, Al(CH₃)₄). ¹³C NMR (126 MHz, C₆D₆, 25 °C): d = 175.1, 158.7, 149.4, 140.7, 139.1, 138.4, 125.5, 125.3, 124.9, 117.3, 69.9, 33.7, 29.1, 28.6, 28.1, 26.3,

26.1, 25.5, 25.1, 20.3, 3.1 (s br, Al(CH₃)₄). IR (nujol): 1582 (s, C=N), 1468 (vs, nujol), 1375 (vs, nujol), 1303 (s), 1261 (m), 1220 (w), 1214 (w), 1173 (s), 1095 (w), 1007 (w), 971 (w), 950 (w), 888 (w), 847 (w), 821 (w), 785 (m), 769 (m), 723 (vs), 593 (w), 578 (w), 516 cm⁻¹ (w). Elemental analysis (%) calcd for C₄₂H₇₀N₃Al₂La (809.910 g mol⁻¹): C 62.29; H 8.71; N 5.19; found: C 62.21; H 8.77; N 5.13.

2-((2,6-*i*Pr₂C₆H₃)N=CMe)-6-((2,6-*i*Pr₂C₆H₃)NCMe₂)C₅H₃N]Nd(AlMe₄)₂ (2b).

Following the procedure described above, Nd(AlMe₄)₃ (**1b**, 215 mg, 0.53 mmol) and HL₂ (264 mg, 0.53 mmol) yielded **2b** as a powdery claret-red solid (225 mg, 0.28 mmol, 52%). ¹H NMR (600 MHz, C₆D₆, 25 °C): d = 13.83, 10.60, 6.30, 4.69, 2.10, 1.67, 1.38, 0.89. IR (nujol): 1588 (s, C=N), 1468 (vs, nujol), 1375 (vs, nujol), 1306 (s), 1267 (m), 1234 (w), 1207 (w), 1168 (s), 1102 (w), 1047 (w), 1008 (w), 971 (w), 953 (w), 892 (w), 859 (w), 826 (w), 793 (m), 771 (m), 721 (vs), 599 (w), 572 (w), 533 (w), 528 cm⁻¹ (w). Elemental analysis (%) calcd for C₄₂H₇₀N₃Al₂Nd (815.24 g mol⁻¹): C 61.88; H 8.65; N 5.15; found: C 61.38; H 8.72; N 5.01.

2-((2,6-*i*Pr₂C₆H₃)N=CMe)-6-((2,6-*i*Pr₂C₆H₃)NCMe₂)C₅H₃N]Y(AlMe₄)₂ (2c).

Following the procedure described above, Y(AlMe₄)₃ (**1c**, 121 mg, 0.35 mmol) and HL₂ (172 mg, 0.35 mmol) yielded **2c** as a powdery claret-red solid (129 mg, 0.17 mmol, 49%). ¹H NMR (600 MHz, C₆D₆, 25 °C): d = 7.20-7.11 (m, 6 H, ar), 7.08 (d, ³J ≅ 7.8 Hz, 1 H, C₅H₃N-*m*-proton), 7.01 (t, ³J ≅ 7.8 Hz, 1 H, C₅H₃N-*p*-proton), 6.95 (d, ³J ≅ 7.8 Hz, 1 H, C₅H₃N-*m*-proton), 3.46 (sept, ³J ≅ 6.6 Hz, 2 H, ar-CH), 2.64 (sept, ³J ≅ 6.6 Hz, 2 H, ar-CH), 1.74 (s, 3 H, N=CCH₃), 1.35 (s, 6 H, NCCH₃), 1.34 (d, ³J ≅ 6.6 Hz, 6 H, CH₃), 1.28 (d, ³J ≅ 6.6 Hz, 6 H, CH₃), 1.24 (d, ³J ≅ 6.6 Hz, 6 H, CH₃), 0.92 (d, ³J ≅ 6.6 Hz, 6 H, CH₃), -0.38 (s br, 24 H, Al(CH₃)₄). ¹³C NMR (151 MHz, C₆D₆, 25 °C): d = 177.4, 150.7, 149.4, 141.1, 140.0, 139.2, 139.0, 127.8, 126.4, 124.3, 117.3, 70.7, 31.8, 29.1, 28.3, 27.1, 26.5, 24.9, 24.8, 23.8, 23.0, 3.3 (s br, Al(CH₃)₄). IR (nujol): 1582 (s, C=N), 1468 (vs, nujol), 1375 (vs, nujol), 1300 (s), 1284 (m), 1223 (w), 1207 (w), 1168 (s), 1107 (w), 1019 (w), 975 (w), 936 (w), 897 (w), 859 (w), 826 (w), 798 (m), 776 (m), 721 (vs), 688 (w), 588 (w), 528 cm⁻¹ (w). Elemental analysis (%) calcd for C₄₂H₇₀N₃Al₂Y (759.906 g mol⁻¹): C 66.39; H 9.28; N 5.53; found: C 66.08; H 9.28; N 5.31.

2,6-((2,6-*i*Pr₂C₆H₃)NCMe₂)₂C₅H₃N]AlMe (3).

Following the procedure described for the synthesis of compounds **2**, the supernatant and the hexane washing solutions were combined and dried under vacuum yielding a red-orange powdery solid which was redissolved in hexane. Fractionate crystallization from hexane at -30 °C gave orange crystals of **3** in yields depending on the lanthanide metal size. (Ln = La 8%, Nd 10%, Y 10% calculated on Ln(AlMe₄)₃). ¹H NMR (600 MHz, C₆D₆, 25 °C): d = 7.22-7.20 (m, 6 H, ar), 7.13 (t, ³J ≅ 7.8 Hz, 1 H, C₅H₃N-*p*-proton),

6.73 (d, $^3J \cong 7.8$ Hz, 2 H, C₅H₃N-*m*-proton), 3.65 (sept, $^3J \cong 6.6$ Hz, 4 H, ar-CH), 1.31 (d, $^3J \cong 6.6$ Hz, 12 H, CH₃), 1.29 (d, $^3J \cong 6.6$ Hz, 12 H, CH₃), 1.22 (s, 12 H, NCCH₃) -0.74 (s, 3 H, AlCH₃). ¹³C NMR (151 MHz, C₆D₆, 25 °C): d = 168.3, 149.0, 145.6, 139.5, 124.8, 124.0, 117.3, 60.9, 31.0, 28.4, 26.3, 24.8. IR (nujol): 1592 (s), 1463 (vs, nujol), 1380 (vs, nujol), 1308 (s), 1266 (m), 1251 (m), 1235 (m), 1230 (m), 1204 (w), 1178 (s), 1137 (m), 1085 (m), 1049 (m), 987 (w), 935 (w), 904 (m), 821 (w), 811 (m), 769 (m), 738 (m), 697 (m), 650 (w), 614 (w), 567 (w), 526 cm⁻¹ (w). Elemental analysis (%) calcd for C₃₆H₅₂N₃Al (553.810 g mol⁻¹): C 78.08; H 9.46; N 7.59; found: C 77.70; H 9.09; N 7.35.

2-[(2,6-*i*Pr₂C₆H₃)NCMe₂]-6-[(2,6-*i*Pr₂C₆H₃)NHCMe₂]C₅H₃N]AlMe₂ (4).

Following the procedure described for the synthesis of compounds **2**, the supernatant and the hexane washing solutions were combined and dried under vacuum yielding a red-orange powdery solid which was redissolved in hexane. Fractionate crystallization from hexane at -30 °C gave light red crystals of **4** in yields depending on the lanthanide metal size. (Ln = La 30%, Nd 38%, Y 41% calculated on Ln(AlMe₄)₃). ¹H NMR (600 MHz, C₆D₆, 25 °C): d = 7.27-7.21 (m, 6 H, ar), 6.99 (t, $^3J \cong 7.8$ Hz, 1 H, C₅H₃N-*p*-proton), 6.87 (d, $^3J \cong 7.8$ Hz, 1 H, C₅H₃N-*m*-proton), 6.64 (d, $^3J \cong 7.8$ Hz, 1 H, C₅H₃N-*m*-proton), 4.54 (s, 1 H, N-H), 3.81 (sept, $^3J \cong 6.6$ Hz, 2 H, ar-CH), 2.75 (sept, $^3J \cong 6.6$ Hz, 2 H, ar-CH), 1.49 (s, 6 H, NCCH₃), 1.37 (s, 6 H, NCCH₃), 1.34 (d, $^3J \cong 6.6$ Hz, 12 H, CH₃), 1.09 (d, $^3J \cong 6.6$ Hz, 12 H, CH₃), -0.25 (s, 6 H, Al(CH₃)₂). ¹³C NMR (151 MHz, C₆D₆, 25 °C): d = 175.6, 165.9, 150.7, 145.5, 144.0, 140.0, 139.4, 125.1, 124.2, 123.7, 119.3, 117.3, 62.5, 31.1, 30.3, 28.5, 28.4, 28.1, 26.9, 25.0, 24.6, 0.6 (s br, Al(CH₃)₂). IR (nujol): 3405 (m) (N-H), 1577 (s), 1463 (vs, nujol), 1380 (vs, nujol), 1313 (s), 1251 (m), 1220 (w), 1194 (w), 1142 (w), 1106 (w), 1049 (w), 1018 (w), 987 (w), 971 (w), 919 (w), 868 (w), 826 (w), 769 (m), 723 (vs), 661 (w), 614 (w), 583 cm⁻¹ (w). Elemental analysis (%) calcd for C₃₇H₅₆N₃Al (569.852 g mol⁻¹): C 77.94; H 9.31; N 7.37; found: C 77.69; H 9.09; N 7.41.

2,6-((2,6-*i*Pr₂C₆H₃)NCMe₂)₂C₅H₃N]La(AlMe₄)(THF) (5).

To a stirred suspension of **2a** (126 mg, 0.16 mmol) in 3 mL of hexane 3 mL THF were added dropwise. The claret-red solid dissolved immediately accompanied by decolorization of the reaction mixture. After stirring for 4 h at ambient temperature the solvent was removed in vacuo to form a white solid which was washed three times with 2 mL of hexane and dried under vacuum to yield **5** as a powdery white solid (117 mg, 0.14 mmol, 90%). ¹H NMR (600 MHz, C₆D₆, 25 °C): δ = 7.20-7.11 (m, 6 H, ar), 7.06 (t, ³J ≅ 7.8 Hz, 1 H, C₅H₃N-*p*-proton), 6.81 (d, ³J ≅ 7.8 Hz, 2 H, C₅H₃N-*m*-protons), 3.47 (sept, ³J ≅ 6.6 Hz, 4 H, ar-CH), 2.74 (m, 4 H, THF), 1.40 (s, 12 H, NCCH₃), 1.18 (d, ³J ≅ 6.6 Hz, 12 H, CH₃), 1.15 (d, ³J ≅ 6.6 Hz, 12 H, CH₃), 0.98 (m, 4 H, THF), -0.15 (s, 12 H, Al(CH₃)₄). ¹³C NMR (151 MHz, C₆D₆, 25 °C): δ = 174.3, 150.3, 141.3, 139.0, 125.6, 125.0, 117.8, 70.8 (THF), 69.1, 32.8, 31.9, 28.2, 28.0, 25.1, 23.0, 1.7 (s, Al(CH₃)₄). IR (nujol): 1572 (w), 1468 (vs, nujol), 1375 (vs, nujol), 1303 (s), 1256 (w), 1220 (w), 1194 (m), 1158 (m), 1126 (w), 1101 (w), 1044 (w), 1013 (w), 982 (w), 930 (w), 852 (m), 816 (w), 785 (m), 764 (m), 723 (vs), 692 (w), 583 (w), 562 (w), 536 (w), 516 cm⁻¹ (w). Elemental analysis (%) calcd for C₄₃H₆₉N₃OAlLa (809.930 g mol⁻¹): C 63.77; H 8.59; N 5.19; found: C 63.37; H 8.58; N 5.02.

2,6-((2,6-*i*Pr₂C₆H₃)NCMe₂)₂C₅H₃N]La(AlMe₄) (6).

To a stirred solution of **5** (71 mg, 0.09 mmol) in 3 mL of toluene AlMe₃ (6 mg, 0.09 mmol) was added dropwise. After stirring the colorless reaction mixture for 4 h at ambient temperature the solvent was removed in vacuo to form a white solid which was washed three times with 2 mL of hexane and dried under vacuum to yield **6** as a powdery white solid (63 mg, 0.09 mmol, 98%). ¹H NMR (600 MHz, C₆D₆, 25 °C): δ = 7.20-7.16 (m, 6 H, ar), 7.14 (t, ³J ≅ 7.8 Hz, 1 H, C₅H₃N-*p*-proton), 6.78 (d, ³J ≅ 7.8 Hz, 2 H, C₅H₃N-*m*-protons), 3.28 (sept, ³J ≅ 6.6 Hz, 4 H, ar-CH), 1.41 (s, 12 H, NCCH₃), 1.31 (d, ³J ≅ 6.6 Hz, 12 H, CH₃), 1.05 (d, ³J ≅ 6.6 Hz, 12 H, CH₃), -0.40 (s, 12 H, Al(CH₃)₄). ¹³C NMR (151 MHz, C₆D₆, 25 °C): δ = 175.1, 149.4, 141.5, 139.1, 126.1, 125.3, 117.3, 69.9, 33.7, 28.1, 26.3, 26.1, 2.83 (s, Al(CH₃)₄). IR (nujol): 1577 (w), 1468 (vs, nujol), 1375 (vs, nujol), 1303 (s), 1251 (w), 1240 (w), 1194 (w), 1168 (m), 1095 (w), 1044 (w), 997 (w), 971 (m), 852 (w), 816 (w), 790 (w), 764 (m), 723 (vs), 609 (w), 567 (w), 562 (w), 536 (w), 516 cm⁻¹ (w). Elemental analysis (%) calcd for C₃₉H₆₁N₃AlLa (737.824 g mol⁻¹): C 63.49; H 8.33; N 5.70; found: C 63.54; H 8.35; N 5.44.

[24] W. J. Evans, R. Anwender, J. W. Ziller, *Organometallics* **1995**, *14*, 1107.

Paper IV

Distinct C–H Bond Activation Pathways in Diamido-Pyridine-Supported Rare-Earth Metal Hydrocarbyl Complexes

Melanie Zimmermann,[†] Frank Estler,[‡] Eberhardt Herdtweck,[‡] Karl W. Törnroos,[†] and Reiner Anwander^{*,†}

Department of Chemistry, University of Bergen, Allégaten 41, N-5007, Bergen, Norway, and Department Chemie, Lehrstuhl für Anorganische Chemie, Technische Universität München, Lichtenbergstrasse 4, D-85747 Garching bei München, Germany

Received August 14, 2007

Transition metal precatalyst–organoaluminum cocatalyst interactions are of fundamental importance in Ziegler–Natta polymerization catalysis. Rare-earth metal tetramethylaluminate complexes (BDPPpyr)-Ln(AlMe₄) bearing a [NNN]²⁻ post-metallocene-type ligand (H₂BDPPpyr = 2,6-bis-(((2,6-diisopropylphenyl)amino)methyl)pyridine) were obtained by two different synthesis routes. Reaction of (BDPPpyr)-Ln(NEt₂)(THF) with trimethylaluminum afforded complexes (BDPPpyr)Ln(AlMe₄) of the small rare-earth metals scandium and lutetium. Corresponding compounds of the larger metals yttrium and lanthanum were synthesized according to the tetramethylaluminate route, i.e., the reaction of Ln(AlMe₄)₃ with H₂-BDPPpyr produced (BDPPpyr)Ln(AlMe₄), along with the byproduct (BDPPpyr)(AlMe₂)₂. Dynamic NMR spectroscopy of (BDPPpyr)Ln(AlMe₄) revealed distinct fluxional behavior of the AlMe₄⁻ ligand depending on the metal size (Lu: *associative* via Lu(μ -Me)₃AlMe; Sc: *dissociative* via Sc(μ -Me)AlMe₃). In the presence of trimethylaluminum, the yttrium derivative undergoes a ligand backbone metalation at the isopropyl methyl group yielding (BDPPpyr-**H**)Y[(μ -Me)AlMe₂]₂ featuring a [NNNC]³⁻-type ligand. For the lutetium derivative, addition of THF caused cyclometallation products (BDPPpyr-**H**)Lu[(μ -Me)AlMe₂](THF) and [Lu(BDPPpyr-**H**)₂] involving the isopropyl methine proton. Present studies not only clearly show the enhanced reactivity of rare-earth metal methyl moieties [Ln–Me] but also that excessive use of organoaluminum cocatalysts can result in gradual ligand degradation and concomitant catalyst deactivation. The findings might contribute to a better understanding of activation/deactivation sequences in post-metallocene-promoted olefin polymerization.

Introduction

Ancillary ligand design and metal cationization (= generation of highly electron-deficient metal centers) are most prolific strategies for improving the overall performance of homogeneous polymerization catalysts.¹ The challenge of optimizing the catalyst efficiency, however, often turns into a tightrope walk between ultimate activity (and selectivity) and catalyst deactivation as evidenced by solvent attack and/or self-degradation.² The latter is clearly manifested by (a) (multiple) hydrogen

abstraction occurring in metal-bonded alkyl ligands (e.g., alkylidene formation in *Tebbe*-analogous reagents) accompanied by metal complex clustering³ and (b) ancillary ligand derivatization via inter- and intramolecular C–H bond activation.^{4–13} Early transition metal alkyl and hydride complexes [(Cp')₂MR_x]_y (Cp' = substituted cyclopentadienyl, R = alkyl, hydride)

* Corresponding Author. Prof. Dr. Reiner Anwander, Department of Chemistry, University of Bergen, Allégaten 41, N-5007, Bergen, Norway. E-mail: Reiner.Anwander@kj.uib.no. Tel.: +47 555 89491. Fax: +47 555 89490.

[†] University of Bergen.

[‡] Technische Universität München.

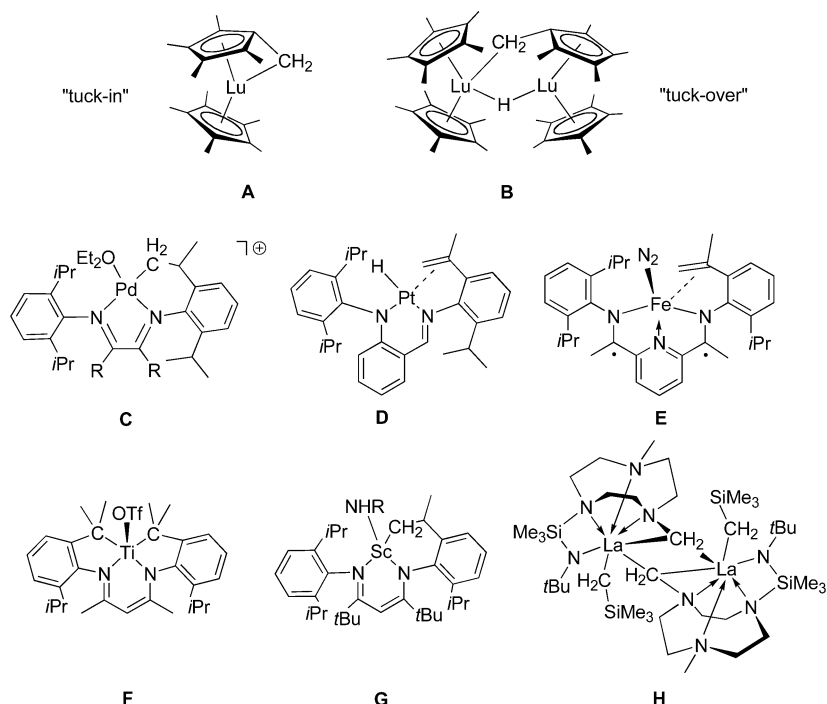
(1) (a) Brintzinger, H. H.; Fischer, D.; Mühlhaupt, R.; Rieger, B.; Waymouth, R. M. *Angew. Chem., Int. Ed. Engl.* **1995**, *34*, 1143. (b) McKnight, A. L.; Waymouth, R. M. *Chem. Rev.* **1998**, *98*, 2587. (c) Alt, H. G.; Köppl, A. *Chem. Rev.* **2000**, *100*, 1205. (d) Hou, Z.; Wakatsuki, Y. *Coord. Chem. Rev.* **2002**, *231*, 1. (e) Gromada, J.; Carpentier, J. F.; Mortreux, A. *Coord. Chem. Rev.* **2004**, *248*, 397. (f) Bochmann, M. *J. Organomet. Chem.* **2004**, *689*, 3982. (g) Hyeon, J. Y.; Gottfriedsen, J.; Edelmann, F. T. *Coord. Chem. Rev.* **2005**, *249*, 2787. (h) Zeimentz, P. M.; Arndt, S.; Elvidge, B. R.; Okuda, J. *Chem. Rev.* **2006**, *106*, 2404, and references therein.

(2) (a) Thompson, M. E.; Baxter, S. M.; Bulls, A. R.; Burger, B. J.; Nolan, M. C.; Santarsiero, B. D.; Schaefer, W. P.; Bercaw, J. E. *J. Am. Chem. Soc.* **1987**, *109*, 203. (b) Ma, K.; Piers, W. E.; Parvez, M. *J. Am. Chem. Soc.* **2006**, *128*, 3303. (c) Jantunen, K. C.; Scott, B. L.; Gordon, J. L.; Kiplinger, J. L. *Organometallics* **2007**, *26*, 2777.

(3) (a) Guérin, F.; Stephan, D. *Angew. Chem., Int. Ed.* **1999**, *38*, 3698. (b) Kickham, J. E.; Guérin, F.; Stewart, J. C.; Stephan, D. *Angew. Chem., Int. Ed.* **2000**, *39*, 3263. (c) Kickham, J. E.; Guérin, F.; Stewart, J. C.; Urbanska, E.; Stephan, D. *Organometallics* **2001**, *20*, 1175. (d) Yue, N.; Hollink, E.; Guérin, F.; Stephan, D. *Organometallics* **2001**, *20*, 4424. (e) Kickham, J. E.; Guérin, F.; Stephan, D. *J. Am. Chem. Soc.* **2002**, *124*, 11486. (f) Stephan, D. *Organometallics* **2005**, *24*, 2548.

(4) (a) Watson, P. L.; Parshall, G. W. *Acc. Chem. Res.* **1985**, *18*, 51. (b) Thompson, M. E.; Bercaw, J. E. *J. Pure Appl. Chem.* **1984**, *56*, 1. (c) Watson, P. L. *J. Chem. Soc., Chem. Commun.* **1983**, 276. (d) Watson, P. L. *J. Am. Chem. Soc.* **1983**, *105*, 6491. (e) Booij, M.; Deelman, B.-J.; Duchateau, R.; Postma, D. S.; Meetsma, A.; Teuben, J. H. *Organometallics* **1993**, *12*, 3531. (f) Deelman, B.-J.; Teuben, J. H.; MacGregor, S. A.; Eisenstein, O. *New J. Chem.* **1995**, *19*, 691. (g) Sadow, A. D.; Tilley, T. D. *J. Am. Chem. Soc.* **2003**, *125*, 7971. (h) Evans, W. J.; Chamberlain, L. R.; Ulibarri, T. A.; Ziller, J. W. *J. Am. Chem. Soc.* **1988**, *110*, 6423. (i) Evans, W. J.; Ulibarri, T. A.; Ziller, J. W. *Organometallics* **1991**, *10*, 134. (j) Evans, W. J.; Perotti, J. M.; Ziller, J. W. *J. Am. Chem. Soc.* **2005**, *127*, 1068. (k) Evans, W. J.; Perotti, J. M.; Ziller, J. W. *J. Am. Chem. Soc.* **2005**, *127*, 3894. (l) Sadow, A. D.; Tilley, T. D. *J. Am. Chem. Soc.* **2005**, *127*, 643. (m) Booij, M.; Meetsma, A.; Teuben, J. H. *Organometallics* **1991**, *10*, 3246. (n) Evans, W. J.; Perotti, J. M.; Ziller, J. W. *Inorg. Chem.* **2005**, *44*, 5820. (o) Evans, W. J.; Champagne, T. M.; Ziller, J. W. *J. Am. Chem. Soc.* **2006**, *128*, 14270. (p) Woodrum, N. L.; Cramer, C. J. *Organometallics* **2006**, *25*, 68. (q) Lewin, J. L.; Woodrum, N. L.; Cramer, C. J. *Organometallics* **2006**, *25*, 5906.

Chart 1



carrying the ubiquitous and robust/rigid cyclopentadienyl ancillary ligand display exceptional potential in the stereoselective polymerization of olefins.¹ The cyclopentadienyl ligand implies highly electron-deficient metal centers facilitating C–H bond activation of the polymer alkyl ligand which either assists (α -agostic interaction) or terminates (β -agostic interaction \rightarrow β -H elimination) chain growth. In addition, intramolecular C–H activation or cyclometallation involving the ancillary ligand backbone is a commonly observed “deactivation” reaction among early transition metal complexes. “Tuck-in” (Chart 1, **A**) and “tuck-over” complexes (Chart 1, **B**) are prominent examples of characteristic C–H bond metalation processes, well documented for rare-earth,^{4b,d,f,h,k–p} group 4,^{2a,5} and group 5⁶ metallocene complexes. Hence, C–H bond activation is a key feature for the mechanistic understanding of chain termination and catalyst deactivation products in *Ziegler-Natta* polymerization.

During the past 15 years new non-metallocene catalyst families (post-metallocenes), mainly based on functionalized chelating nitrogen (imines, amides) and oxygen donor ligands (alkoxides) have evolved and attracted considerable attention in the field of polymer science.¹⁴ Crucially, C–H bond activation pathways seem to be as persistent as for metallocene complexes, whereas C–H bond cleavage can proceed via oxidative addition to an electron-rich and coordinatively unsaturated late transition metal center or via σ -bond metathesis at highly electron-deficient early transition metals. Aside from mechanistic details, the formation of cyclometallation products is a repetitive pattern in post-metallocene chemistry across the entire transition metal series (Chart 1, **C–H**).^{7–11,13} It clearly reflects the ambivalence of very reactive organometallics acting as high-performance catalysts and concurrently favoring catalyst decomposition pathways.

Pyridine diamido ligands of the [NNN]²⁻ divalent type as introduced by *McConville* et al. represent archetypal alternative ligand systems to successfully mimic the stereoelectronic features and polymerization behavior of metallocene complexes of Ti(IV),¹⁵ Zr(IV),¹⁶ and Ta(V).¹⁷ This dianionic tridentate ancillary ligand coordinates exclusively in a meridional fashion to the metal center and provides an extremely rigid and planar

(5) (a) Bercaw, J. E.; Marvich, R. H.; Bell, L. G.; Brintzinger, H.-H. *J. Am. Chem. Soc.* **1972**, *94*, 1219. (b) Pattiasina, J. W.; Hissink, C. E.; de Boer, J. L.; Meetsma, A.; Teuben, J. H. *J. Am. Chem. Soc.* **1985**, *107*, 7758. (c) Bulls, A. R.; Schaefer, W. P.; Serfas, M.; Bercaw, J. E. *Organometallics* **1987**, *6*, 1219. (d) Schock, L. E.; Brock, C. P.; Marks, T. J. *Organometallics* **1987**, *6*, 232. (e) Tjaden, E. B.; Stryker, J. M. *J. Am. Chem. Soc.* **1993**, *115*, 2083. (f) Sun, Y.; Spence, R. E. v. H.; Piers, W. E.; Parvez, M.; Yap, G. P. A. *J. Am. Chem. Soc.* **1997**, *119*, 5132. (g) Pool, J. A.; Bradley, C. A.; Chirik, P. J. *Organometallics* **2002**, *21*, 1271. (h) Bernskoetter, W. H.; Pool, J. A.; Lobkovsky, E.; Chirik, P. J. *Organometallics* **2006**, *25*, 1092.

(6) Riley, P. N.; Parker, J. R.; Fanwick, P. E.; Rothwell, I. P. *Organometallics* **1999**, *18*, 3579.

(7) Tempel, D. J.; Johnson, L. K.; Huff, R. L.; White, P. S.; Brookhart, M. *J. Am. Chem. Soc.* **2000**, *122*, 6686.

(8) Kloek, S. M.; Goldberg, K. I. *J. Am. Chem. Soc.* **2007**, *129*, 3460.

(9) Basuli, F.; Bailey, B. C.; Watson, L. A.; Tomaszewski, J.; Huffman, J. C.; Mindiola, D. J. *Organometallics* **2005**, *24*, 1886.

(10) Bart, S. C.; Bowman, A. C.; Lobkovsky, E.; Chirik, P. J. *J. Am. Chem. Soc.* **2007**, *129*, 7212.

(11) (a) Knight, L. K.; Piers, W. E.; Fleurat-Lessard, P.; Parvez, M.; McDonald, R. *Organometallics* **2004**, *23*, 2087. (b) Knight, L. K.; Piers, W. E.; McDonald, R. *Organometallics* **2006**, *25*, 3289.

(12) Bambirra, S.; Boot, S. J.; van Leusen, D.; Meetsma, A.; Hessen, B. *Organometallics* **2004**, *23*, 1891.

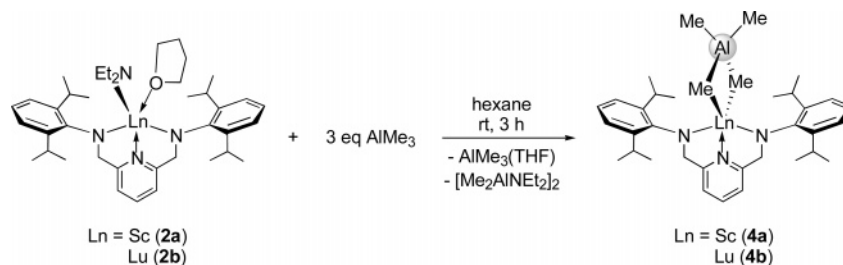
(13) Tazelaar, C. G. J.; Bambirra, S.; van Leusen, D.; Meetsma, A.; Hessen, B.; Teuben, J. H. *Organometallics* **2004**, *23*, 936.

(14) For Reviews see: (a) Britovsek, G. J. P.; Gibson, V. C.; Wass, D. F. *Angew. Chem., Int. Ed.* **1999**, *38*, 428. (b) Kempe, R. *Angew. Chem., Int. Ed.* **2000**, *39*, 468. (c) Gade, L. H. *Acc. Chem. Res.* **2002**, *35*, 575. (d) Piers, W. E.; Emslie, D. J. H. *Coord. Chem. Rev.* **2002**, *233–234*, 131. (e) Gibson, V. C.; Spitzmesser, S. K. *Chem. Rev.* **2003**, *103*, 283.

(15) (a) Guérin, F.; McConville, D. H.; Payne, N. C. *Organometallics* **1996**, *15*, 5085. (b) Guérin, F.; McConville, D. H.; Vittal, J. J. *Organometallics* **1997**, *16*, 1491. (BDPPpyr)Ti([C₄H₂(SiMe₃)₂]₂): N1–Ti1–N2 141.5(3)°.

(16) (a) Guérin, F.; McConville, D. H.; Vittal, J. J. *Organometallics* **1996**, *15*, 5586. (b) Guérin, F.; McConville, D. H.; Vittal, J. J.; Yap, G. A. P. *Organometallics* **1998**, *17*, 5172. (c) Guérin, F.; Del Vecchio, O.; McConville, D. H. *Polyhedron* **1998**, *17*, 917. (BDPPpyr)Zr(C₄H₆): N2–Zr–N2A 140.0(4)°.

(17) (a) Guérin, F.; McConville, D. H.; Vittal, J. J. *Organometallics* **1995**, *14*, 3154. (b) Guérin, F.; McConville, D. H.; Vittal, J. J.; Yap, G. A. P. *Organometallics* **1998**, *17*, 1290. (BDPPpyr)Ta(η^2 -PrC \equiv CCr)Cl: N1–Ta1–N3 137.2(2)°.

Scheme 1. Reaction of (BDPPpyr)Ln(NEt₂)(THF) (2) with AlMe₃

environment. It further proved suitable for accommodating a wide size range of metal centers.^{15–19} The catalytic performance of group 4 complexes supported by pyridine diamido ligands, however, exhibited extreme sensitivity toward the choice of the metal center. Whereas (BDPPpyr)ZrCl₂ (H₂BDPPpyr = 2,6-bis-((2,6-diisopropylphenyl)amino)methyl)pyridine) revealed to be a highly active polymerization initiator upon activation with methylaluminoxane (MAO),^{16a} the corresponding Ti(IV) compound showed only very low activities toward ethylene.^{15a} Catalyst deactivation, due to reduction to Ti(III), was presumed, but interaction of the MAO cocatalyst with the pyridine diamido complex could imply further deactivation pathways. For MAO-activated initiators (typically containing up to 15 wt % AlMe₃), cationic bimetallic species [LM(μ-R)₂AlR₂]⁺ are discussed as catalyst resting states (“dormant species”).^{1a,1f,20} Moreover, these species are important intermediates in chain transfer and catalyst deactivation processes.²⁰ Although such bimetallic group 4 cations have been studied spectroscopically and computationally, it was only recently that Mountford et al. reported the first example of a structurally authenticated group 4 tetramethylaluminate [Ti(NtBu)(Me₃[9]aneN₃)(μ-Me)₂AlMe₂][B(C₆F₅)₄].²¹ Nevertheless, group 4 metallocene and post-metallocene systems often produce intricate catalyst mixtures hampering closer investigations of active species, initiation, propagation as well as catalyst deactivation pathways.²² Given the intrinsic interrelation between group 4 and group 3/lanthanide metal polymerization chemistry, lanthanide complexes proved to be ideal model systems for Ziegler catalysts. Fundamental studies on the interaction of rare-earth metallocene hydrocarbyl derivatives with α-olefins by Watson^{4a,23} and Bercaw²⁴ marked a major breakthrough to understanding mechanistic and kinetic details of olefin insertion and termination processes such as β-H elimination, β-alkyl elimination, or C–H bond activation (“lanthanide model” of Ziegler–Natta polymerization).

(18) Estler, F.; Eickerling, G.; Herdtweck, E.; Anwender, R. *Organometallics* **2003**, *22*, 1212. (BDPPpyr)Sc(CH₂SiMe₃)(THF): N1–Sc–N2 137.04(6)°.

(19) Cruz, C. A.; Emslie, D. J. H.; Harrington, L. E.; Britten, J. F.; Robertson, C. M. *Organometallics* **2007**, *26*, 692. (BDPPpyr)ThCl₂(dme): N1–Th1–N3 128.08°.

(20) (a) Bochmann, M.; Lancaster, S. J. *Angew. Chem., Int. Ed. Engl.* **1994**, *33*, 1634. (b) Britovsek, P.; Cohen, S. A.; Gibson, V. C.; van Meurs, M. J. *Am. Chem. Soc.* **2004**, *126*, 10701. (c) Petros, R. A.; Norton, J. R. *Organometallics* **2004**, *23*, 5105. (d) Lyakin, O. Y.; Bryliakov, K. P.; Semikolenova, N. M.; Lebedev, A. Y.; Voskoboynikov, A. Z.; Zakharov, V. A.; Talsi, E. P. *Organometallics* **2007**, *26*, 1536.

(21) Bolton, P. D.; Clot, E.; Cowley, A. R.; Mountford, P. *Chem. Commun.* **2005**, 3313.

(22) Thiele, H.-K.; Wilson, D. R. *J. Macromol. Sci., Polym. Rev.* **2003**, *C43*, 581.

(23) (a) Watson, P. L. *J. Am. Chem. Soc.* **1982**, *104*, 337. (b) Watson, P. L.; Roe, D. C. *J. Am. Chem. Soc.* **1982**, *104*, 6471.

(24) (a) Burger, B. J.; Thompson, M. E.; Cotter, W. D.; Bercaw, J. E. *J. Am. Chem. Soc.* **1990**, *112*, 1566. (b) Piers, W. E.; Bercaw, J. E. *J. Am. Chem. Soc.* **1990**, *112*, 9406. (c) Burger, B. J.; Cotter, W. D.; Coughlin, E. B.; Chacon, S. T.; Hajela, S.; Herzog, T. A.; Köhn, R.; Mitchell, J.; Piers, W. E.; Shapiro, P. J.; Bercaw, J. E. In *Ziegler Catalysts*; Fink, G., Mühlhaupt R., Brintzinger, H.-H., Eds.; Springer-Verlag: Berlin, 1995; pp 317–331.

Our recent work in the field of heterobimetallic Ln/Al complexes emphasizes the suitability of homoleptic lanthanide tetramethylaluminates Ln(AlMe₄)₃ to act as convenient syntheses precursors,²⁵ offering straightforward entry into donor solvent-free half-lanthanidocene,²⁶ lanthanidocene,²⁷ and post-lanthanidocene chemistry.^{28,29} In this context, we reported the syntheses of lanthanide tetramethylaluminate complexes bearing [NON]²⁻ and [NNN]²⁻ type ancillary ligands. Herein we extend this “tetramethylaluminate route” to the pyridine diamido ligand (BDPPpyr), which we previously used in the synthesis of distinct and stable Ln(III) complexes.¹⁸ Besides solid-state structural features, special emphasis is put on the dynamic behavior of the resulting post-lanthanidocene complexes in solution. Furthermore, we account in detail on the complex stability considering the size of the central lanthanide cation and the composition of the reaction mixtures. Finally, C–H bond activation via σ-bond metathesis is discussed as a possible deactivation pathway in group 3 (lanthanide)/group 4 post-metallocene catalyzed olefin polymerization.

Results and Discussion

Synthesis and Structural Features of (BDPPpyr)Ln(AlMe₄) Complexes. Trimethylaluminum promoted alkylation of lanthanide amide compounds has been found to be a viable route for the synthesis of donor solvent-free rare-earth metal tetramethylaluminates, that is, rare-earth metal hydrocarbyl complexes. Since the first proof of a AlMe₃ mediated complete [NR₂] → [AlMe₄] transformation,³⁰ several publications documented the universal applicability of this synthesis route.^{31–33} A high yield synthesis of lanthanide tetramethylaluminates though is governed by steric restrictions and the choice of monoanionic lanthanide amide precursors is often limited to small amide functionalities (NMe₂, NEt₂). Treatment of (BDPPpyr)Ln(NEt₂)(THF) (Ln = Sc (**2a**), Lu (**2b**)) with 3 eq of AlMe₃ in hexane afforded the tetramethylaluminate complexes (BDPPpyr)Sc(AlMe₄) (**4a**) and (BDPPpyr)Lu(AlMe₄) (**4b**) in almost quantitative yields (Scheme 1). The volatility of

(25) Fischbach, A.; Anwender, R. *Adv. Polym. Sci.* **2006**, *204*, 155.

(26) Dietrich, H. M.; Zapilko, C.; Herdtweck, E.; Anwender, R. *Organometallics* **2005**, *24*, 5767.

(27) Zimmermann, M.; Dietrich, H. M.; Anwender, R. Unpublished results.

(28) Zimmermann, M.; Törnroos, K. W.; Anwender, R. *Organometallics* **2006**, *25*, 3593.

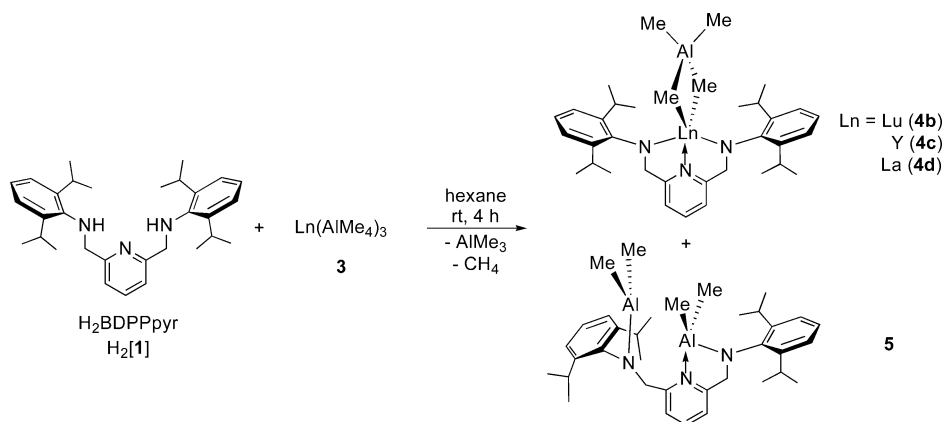
(29) Zimmermann, M.; Törnroos, K. W.; Anwender, R. *Angew. Chem., Int. Ed.* **2007**, *46*, 3126.

(30) Evans, W. J.; Anwender, R.; Ziller, J. W. *Organometallics* **1995**, *14*, 1107.

(31) Anwender, R.; Klimpel, M. G.; Dietrich, H. M.; Shorokhov, D. J.; Scherer, W. *Chem. Commun.* **2003**, 1008.

(32) Klimpel, M. G.; Anwender, R.; Tafipolsky, M.; Scherer, W. *Organometallics* **2001**, *20*, 3983.

(33) Zimmermann, M.; Frøystein, N. Å.; Fischbach, A.; Sirsch, P.; Dietrich, H. M.; Törnroos, K. W.; Herdtweck, E.; Anwender, R. *Chem.–Eur. J.* **2007**, DOI: 10.1002/chem.200700534.

Scheme 2. Reaction of H₂BDPPpyr (H₂[1]) with Ln(AlMe₄)₃ (3)

the byproducts, organoaluminum amide [Me₂AlNEt₂]₂ and THF adduct AlMe₃(THF), allows for an easy separation from complexes **4** (CAUTION: volatiles containing trimethylaluminum react violently when exposed to air). Attempts to synthesize compounds **4a** and **4b** by alkylation of the respective bis(dimethylsilyl)amido or diisopropylamido compounds failed—probably due to effective steric shielding of the (silyl)amide ligands.

Whereas alkylation of the lanthanide amide complexes follows a straightforward high yield synthesis protocol, starting compounds (BDPPpyr)Ln(NEt₂)(THF) (**2**) can only be obtained by a two-step reaction sequence from Ln(CH₂SiMe₃)₃(THF)_x in moderate yields.¹⁸ It is further limited to small to medium sized lanthanide metal centers.³⁴ To access the entire size range of Ln³⁺ cations, homoleptic lanthanide tetramethylaluminates Ln(AlMe₄)₃ (**3**) were employed as alkyl precursors. Ln(AlMe₄)₃ (Ln = Lu (**3b**), Y (**3c**), and La (**3d**)) react with H₂BDPPpyr (H₂[1]) according to an alkane elimination reaction to yield the desired complexes (BDPPpyr)Ln(AlMe₄) (**4**) in a one-step synthesis (Scheme 2).

Instant gas evolution and precipitation of white solid material evidenced coordination of the diamido ligand to the metal center. Separation of the precipitate from the reaction mixture afforded off-white powdery complexes **4b**, **4c**, and **4d** with yields increasing according to the size of the metal cation (Ln = Lu, 73%; Y, 75%; La, 81%). Colorless single crystals of **4b** suitable for X-ray diffraction analysis were grown from hexane solution and revealed the anticipated formation of (BDPPpyr)Lu(AlMe₄) (**4b**) (Figure 1).³⁵ The five-coordinate Lu center is surrounded by three nitrogen atoms of the BDPPpyr ancillary ligand and two methyl carbons of the η²-coordinated tetramethylaluminate moiety. The coordination geometry of the lutetium center is best described as distorted trigonal bipyramidal with the amido nitrogen atoms (N2 and N2') and a tetramethylaluminate carbon (C2) forming the equatorial plane. The pyridine nitrogen N1 and the second tetramethylaluminate carbon C1 occupy the apical positions (N1–Lu–C1, 150.3(1)°). The approximately planar BDPPpyr ligand coordinates in a meridional fashion to the metal center, the ligand bite angle (138.6(1)°) being similar

to those reported for Sc,¹⁸ Th,¹⁹ Ti(IV),¹⁵ Zr(IV),¹⁶ and Ta(V)¹⁷ complexes supported by this pincer ligand. Strong interaction of the [NNN]²⁻ ligand with the central metal is substantiated by a Lu–N2 bond length of 2.186(2) Å. For comparison, the Lu–N bond distances in five-coordinate lutetium amide complex Lu[N(SiHMe₂)₂]₃(THF)₂ are 2.184(3), 2.238(3), and 2.253(3) Å.³⁶ The aryl rings lie perpendicular to the plane of the ligand with an interplanar angle of 82.50(5)°, in a way that the aryl isopropyl groups protect the metal above and below the N₃ plane. Two methyl groups of the [AlMe₄] unit coordinate to the central Lu metal in a classical η² fashion forming a planar [Lu(μ-CH₃)₂Al] heterocycle (torsion angles Lu–C1–Al1–C2, C1–Al1–C2–Lu = 0.00°). The Lu–C1 (2.424(3) Å) and Lu–C2 (2.435(3) Å) bond lengths are comparatively short (Cp*Lu–(AlMe₄)₂, 2.501(3)–2.597(3) Å)³¹ and the consequent short Lu–H distances of an average 2.29(2) Å implicate intramolecular contacts of two of the three H atoms in each bridging methyl group with the sterically unsaturated and Lewis acidic lutetium metal center.

The ¹H NMR spectra of complexes **4** in C₆D₆ are consistent with a rigid meridional coordination of the BDPPpyr ligand to the metal center. The singlet observed for the *N*-methylene protons (4.72 (**4a**), 4.92 (**4b**), 4.80 (**4c**), and 4.99 ppm (**4d**)) as well as only one observed multiplet for the methine groups (3.42 (**4a**), 3.53 (**4b**), 3.43 (**4c**), and 3.20 ppm (**4d**)) are indicative of a highly symmetric environment at the lanthanide metal center. The diastereotopic isopropyl methyl groups show two doublets due to restricted rotation of the aryl groups around the N–C_{ipso} bond. For the lutetium, yttrium, and lanthanum complexes (**4b**–**4d**) the ¹H NMR spectrum shows only one signal in the methyl alkyl region at –0.33 (**4b**), –0.53 (**4c**), and –0.46 ppm (**4d**), respectively, which can be assigned to the [Al(μ-Me)₂Me₂] moieties indicating a rapid exchange of bridging and terminal methyl groups. These resonances are shifted to higher field compared to the homoleptic precursors (–0.09, **3b**; –0.25, **3c**; –0.27 ppm, **3d**). A signal splitting of the ¹H methyl resonance in **4c** is clearly attributable to a ¹H–⁸⁹Y scalar coupling (²J_{YH} = 3 Hz).³⁷ Interestingly, the ¹H NMR spectrum as well as the ¹³C NMR spectrum of the scandium derivative **4a** revealed two different signals for the bridging (¹H, 0.35 ppm; ¹³C, 16.5 ppm) and the terminal methyl groups (¹H, –1.11 ppm; ¹³C, –9.1 ppm) of the [AlMe₄] ligand. Apparently, steric hindrance at the smallest rare-earth metal center scandium results in a significantly lower rate of the methyl group exchange.

(34) (a) Lappert, M. F.; Pearce, R. *J. Chem. Soc., Chem. Commun.* **1973**, 126. (b) Atwood, J. L.; Hunter, W. E.; Rogers, R. D.; Holton, J.; McMeeking, J.; Pearce, R.; Lappert, M. F. *J. Chem. Soc., Chem. Commun.* **1978**, 140. (c) Schumann, H.; Müller, J. *J. Organomet. Chem.* **1978**, 146, C5. (d) Schumann, H.; Freckmann, D. M. M.; Dechert, S. *Z. Anorg. Allg. Chem.* **2002**, 628, 2422. (e) Niemeyer, M. *Acta Crystallogr.* **2001**, E57, m553.

(35) Compound **4b** crystallizes from toluene in the triclinic space group *P* $\bar{1}$ with *a* = 13.0374(1) Å, *b* = 13.6550(1) Å, *c* = 13.8172(1) Å, α = 86.6742(3)°, β = 69.2809(3)°, γ = 74.5579(2)°.

(36) Anwander, R.; Runte, O.; Eppinger, J.; Gerstberger, G.; Herdtweck, E.; Spiegler, M. *J. Chem. Soc., Dalton Trans.* **1998**, 847.

(37) Such signal splitting was also found for Y(AlMe₄)₃ (**3c**) at temperatures well above coalescence (ref 33).

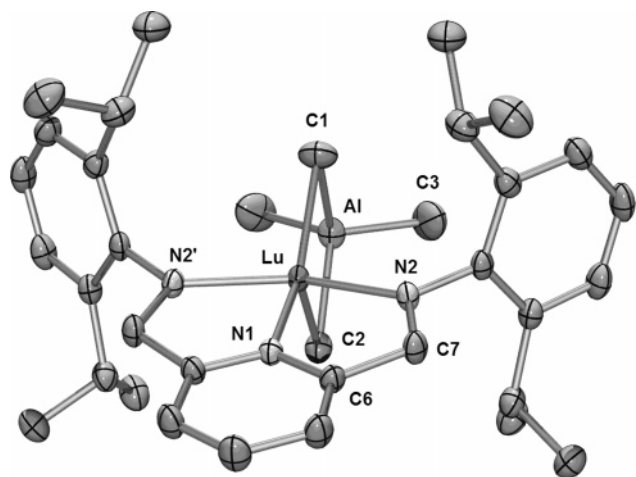
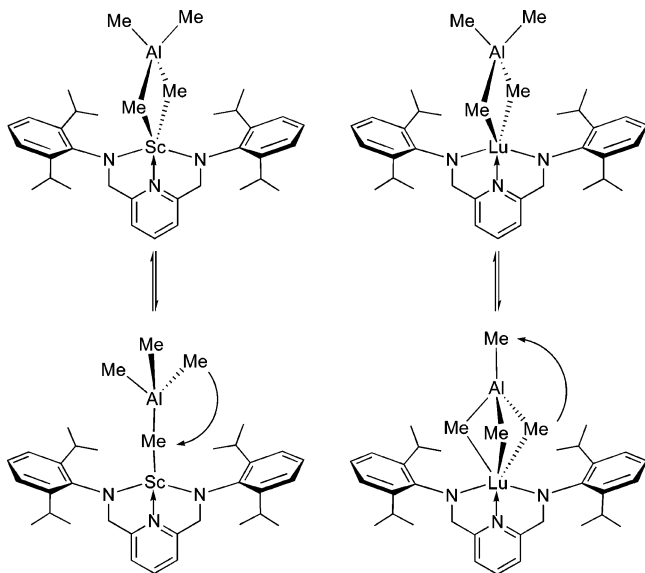


Figure 1. Molecular structure of (BDPPpyr)Lu(AlMe₄) (**4b**) (atomic displacement parameters set at the 50% level). Hydrogen atoms and the solvent molecule are omitted for clarity.

Scheme 3. Dissociative versus Associative Methyl Group Exchange in (BDPPpyr)Ln[(μ-Me)₂AlMe₂] (4**)**



Hence, two separate signals for the different methyl groups of the [Al(μ-Me)₂Me₂] moiety can be assigned at ambient temperature.

These findings suggest two different methyl group exchange mechanisms dependent on the size of the central lanthanide cation. A sterically unsaturated rare-earth metal center allows for an associative methyl group exchange with transient η³ coordinating [AlMe₄] moieties (Scheme 3, right),^{33,38,39} whereas in sterically hindered complexes intramolecular methyl group exchange occurs via a dissociative mechanism with transient η¹ coordination (Scheme 3, left).³⁹

Dynamic NMR spectroscopy has previously been successfully used to determine methyl group exchange rates and activation parameters of several homoleptic and heteroleptic lanthanide tetramethylaluminate complexes.^{33,38,39} Therefore, the ¹H NMR spectra of (BDPPpyr)Sc[(μ-Me)₂AlMe₂] (**4a**) and (BDPPpyr)-Lu[(μ-Me)₂AlMe₂] (**4b**) were examined in different temperature ranges as solutions in toluene-*d*₈. Rate constants *k* of the methyl group exchange were obtained by line shape analysis of the ¹H

Table 1. Selected Structural Parameters for (BDPPpyr)Lu(AlMe₄) (4b**) (Symmetry Code *x*, 1/2-*y*, *z*)**

| Bond Distances (Å) | | | |
|--------------------|----------|----------|----------|
| Lu–N1 | 2.336(2) | Al–C1 | 2.088(4) |
| Lu–N2 | 2.186(2) | Al–C2 | 2.103(3) |
| Lu–C1 | 2.424(3) | Al–C3 | 1.960(3) |
| Lu–C2 | 2.435(3) | N2–C7 | 1.451(3) |
| Lu···Al | 3.001(1) | C6–C7 | 1.503(3) |
| Bond Angles (deg) | | | |
| N1–Lu–N2 | 70.13(4) | Lu–N2–C8 | 125.2(1) |
| N2–Lu–N2' | 138.6(1) | C1–Al–C3 | 107.5(1) |
| N1–Lu–C1 | 150.3(1) | N1–C6–C7 | 115.1(2) |
| N1–Lu–C2 | 122.0(1) | C6–C7–N2 | 111.2(2) |
| Lu–C1–Al | 83.0(1) | | |

methyl signals⁴⁰ and the activation parameters Δ*G*[‡], Δ*H*[‡], and Δ*S*[‡] were calculated from a linearized Eyring equation.⁴¹ Accordingly, the aluminate methyl group exchange in the lutetium compound **4b** proceeds with activation parameters indicative of an associative methyl group exchange (Scheme 3, right; Table 2). The negative activation entropy Δ*S*[‡] = –56(4) J K^{–1} mol^{–1} implies a higher ordered transition state with an η³-coordinated tetramethylaluminate ligand. Relatively weak aluminate bonding is proposed by the low Δ*H*[‡] value (34(1) kJ mol^{–1}). The activation parameters of **4b** are in very good agreement with those found for homoleptic Lu(AlMe₄)₃ (**3b**).³³ The parameters obtained for the scandium complex **4a** have to be treated carefully as coalescence of the aluminate methyl signals (*T*_c = 72 °C) appeared very close to the decomposition temperature of the compound. The amount of available data points is therefore limited. Nevertheless, the activation entropy for this small metal center is clearly positive (Δ*S*[‡] = 122(1) J K^{–1} mol^{–1}) indicating a dissociative methyl group exchange (Scheme 3, left; Table 2) with lower ordering in the transition state (η¹-coordinated tetramethylaluminate ligand). Additionally, the high activation enthalpy Δ*H*[‡] = 109(1) kJ mol^{–1} is in accordance with a very strong bonding of the tetramethylaluminate ligand to the small, Lewis acidic scandium metal center. A dissociative methyl group exchange was also found for the Al₂Me₆ dimer⁴² and a sterically crowded heteroleptic yttrium carboxylate complex (Table 2).³⁹ The comparatively increased free activation energy Δ*G*[‡] for the smaller metal center Sc corresponds to a slowing of the methyl group exchange, e.g., Δ(Δ*G*[‡]) of 23 kJ mol^{–1} at 298 K corresponds to a slowing by a factor of approximately 1 × 10⁴, which is in good agreement with the obtained ¹H NMR spectra of **4a** and **4b**. Owing to enhanced steric unsaturation of the larger metal centers, associative methyl group exchange is assumed for the yttrium (**4c**) and lanthanum derivatives (**4d**).

Whereas compounds **4** precipitate cleanly from the hexane solution when reacting H₂[**1**] with Ln(AlMe₄)₃ (**3**), the orange soluble fraction contains the aluminum complex (BDPPpyr)-(AlMe₂)₂ (**5**) (Scheme 2) as the only byproduct besides unreacted Ln(AlMe₄)₃. Fractional crystallization from hexane afforded analytically pure yellow crystals of **5** suitable for X-ray diffraction analysis. The molecular structure and relevant bond distances and angles of **5** can be found in Figure 2 and Table 3. The solid-state structure revealed a BDPPpyr ligand that is

(40) (a) Gutowsky, H. S.; Holm, C. H. *J. Chem. Phys.* **1956**, *25*, 1228. (b) Allerhand, A.; Gutowsky, H. S.; Jonas, J.; Meinzner, R. A. *J. Am. Chem. Soc.* **1966**, *88*, 3185. (c) Piette, L. H.; Anderson, W. A. *J. Chem. Phys.* **1959**, *30*, 899.

(41) Δ*G*[‡], Δ*H*[‡], and Δ*S*[‡] were obtained from a linearized Eyring plot based on $-R \ln(kh/k_B T) = -\Delta S^\ddagger + \Delta H^\ddagger/T$.

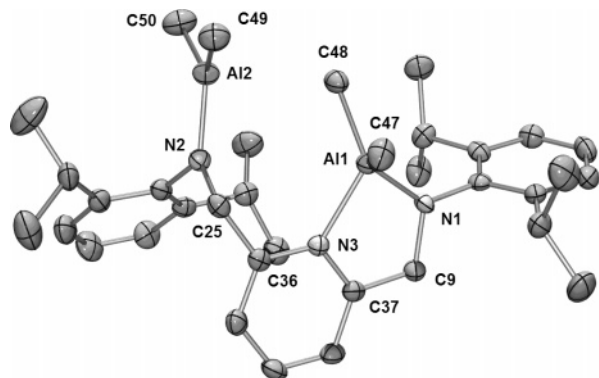
(42) O'Neill, M. E.; Wade, K. In *Comprehensive Organometallic Chemistry*; Wilkinson, G., Stone, F. G. A., Abel, E. W., Eds.; Pergamon Press: New York, 1982; p. 593.

(38) Eppinger, J. *Ph.D. Thesis*, 1999, Technische Universität München.
(39) Fischbach, A.; Perdih, F.; Herdtweck, E.; Anwander, R. *Organometallics* **2006**, *25*, 1626.

Table 2. Thermodynamic Data for the Exchange of Bridging and Terminal Methyl Groups in Tetramethylaluminate Complexes

| compound | T_c [K] | $\Delta G^{\ddagger c}$ [kJ mol ⁻¹] | ΔH^{\ddagger} [kJ mol ⁻¹] | ΔS^{\ddagger} [J K ⁻¹ mol ⁻¹] |
|---|-----------|---|---|--|
| (BDPPpyr)Sc[(μ -Me) ₂ AlMe ₂] (4a) | 345 | 73(1) | 109(1) | 122(1) |
| (BDPPpyr)Lu[(μ -Me) ₂ AlMe ₂] (4b) | 213 | 50(2) | 34(1) | -56(4) |
| Lu[(μ -Me) ₂ AlMe ₂] ₃ (3b) ³³ | 279 | 51.8(3) ^d | 44(1) | -30(3) |
| Y[(μ -Me) ₂ AlMe ₂] ₃ (3c) ³³ | 229 | 43.6(3) ^d | 38(1) | -26(4) |
| [L ¹] ₂ Y[(μ -Me) ₂ AlMe ₂] ^{a,39} | 263 | 53(3) | 73(4) | 66(3) |
| [L ¹] ₂ La[(μ -Me) ₂ AlMe ₂] ^{a,39} | 213 | 45(2) | 28(2) | -58(3) |
| [L ²]Y[(μ -Me) ₂ AlMe ₂] ^{b,38} | | 63.0 | 24.3 | -130 |
| Me ₂ Al(μ -Me) ₂ AlMe ₂ ⁴² | | 44.8 | 81.5 | 123.1 |

^a L¹ = (O₂CAr^{tPr})₂(μ -AlMe₂). ^b L² = Me₂Si(2-MeBenzInd)₂. ^c Uncertainties mainly based on temperature errors. ^d T_c .

**Figure 2.** Molecular structure of (BDPPpyr)(AlMe₂)₂ (**5**) (atomic displacement parameters set at the 50% level). Hydrogen atoms are omitted for clarity.**Table 3.** Selected Structural Parameters for (BDPPpyr)(AlMe₂)₂ (**5**)

| Bond Distances (Å) | | | |
|--------------------|----------|------------|----------|
| Al1–N1 | 1.829(3) | N3–C37 | 1.349(3) |
| Al1–N2 | 1.797(3) | C37–C9 | 1.491(5) |
| Al2–N3 | 2.005(3) | N1–C9 | 1.448(4) |
| Al1–C47 | 1.966(4) | N3–C36 | 1.363(4) |
| Al1–C48 | 1.977(4) | C36–C25 | 1.501(5) |
| Al2–C49 | 1.935(4) | N2–C25 | 1.470(4) |
| Al2–C50 | 1.930(4) | | |
| Bond Angles (deg) | | | |
| N1–Al1–N3 | 85.1(1) | C9–C37–N3 | 116.3(3) |
| N1–Al1–C47 | 119.5(1) | N2–Al2–C49 | 115.7(2) |
| N1–Al1–C48 | 114.3(1) | N2–Al2–C50 | 118.3(2) |
| N3–Al1–C47 | 106.3(2) | Al2–N2–C25 | 121.6(2) |
| N3–Al1–C48 | 119.1(1) | N2–C25–C36 | 113.6(3) |
| Al1–N1–C9 | 115.7(2) | C25–C36–N3 | 118.0(3) |
| N1–C9–C37 | 110.4(3) | | |

coordinated to two aluminum metal centers in an η^2 (N1 and N3) and an η^1 fashion (N2). All Al–N bond lengths and the N1–Al1–N3 bite angle are in the expected ranges.^{29,43} To accommodate the second [AlMe₂] moiety, one CH₂N sidearm is tilted 74.6(4)° (torsion angle N3–C36–C25–N2) out of the plane of the ligand backbone. Broad signals for the CH₂N and aryl isopropyl hydrogen atoms in the ¹H NMR spectrum of **5** indicate high fluxionality of the ligand backbone in C₆D₆.

Formation of organoaluminum byproducts has occurred earlier during the reaction of an imino-amino-pyridine with homoleptic lanthanide tetramethylaluminates **3**.²⁹ So far it is not clear whether the byproduct formation is a result of an intermolecular reaction between H₂BDPPpyr and AlMe₃ released in the acid–base reaction of H₂[**1**] and Ln(AlMe₄)₃ or rather that of an intramolecular competition between the Lewis acidic Al³⁺ and the lanthanide metal centers for the BDPPpyr

ligand. The strong Lewis acid Al³⁺ has a high affinity for nitrogen donors.⁴⁴ The evidenced Ln³⁺ size dependency of the aluminum complex formation supports the latter mechanistic scenario.²⁹

C–H Bond Activation and Cyclometallation Pathways of (BDPPpyr)Ln(AlMe₄) Complexes. Upon stirring the reaction mixture of H₂[**1**] and Y(AlMe₄)₃ (**3c**) at ambient temperature, the intermediately formed (BDPPpyr)Y(AlMe₄) (**4c**) is gradually undergoing an intramolecular metalation process with one of the aryl-isopropyl methyl groups (Scheme 4).

The transformation is accompanied by evolution of one equivalent CH₄ and formation of a yellow solid material with slightly higher solubility in hexane than “reaction intermediate **4c**”. Full and clean conversion to compound **6** was accomplished within 24 h and yellow single crystals suitable for X-ray diffraction analysis were grown from a hexane solution (Figure 3, Table 4). The molecular structure of **6** revealed the product of a ligand metalation via σ -bond metathesis between the C–H bond of the *i*Pr-methyl group and a bridging Y–CH₃ bond of the Y[(μ -CH₃)₂Al(CH₃)₂] unit, showing the overall composition (BDPPpyr-**H**)Y[(μ -Me)AlMe₂]₂. As a result, the BDPPpyr ligand coordinates in an η^4 fashion to the six-coordinate yttrium metal center. The pyridine nitrogen (N2) and one bridging carbon of the former tetramethylaluminate ligand (C32) occupy the apical positions (N2–Y–C32 = 161.94(5)°) of a strongly distorted octahedral coordination geometry. Due to the formation of one heterobridging [Y(μ -NR₂)(μ -Me)AlMe₂] moiety, the Y–N bond lengths differ considerably involving a very long Y–N1 (2.485(1) Å) and a very short Y–N3 bond of 2.191(1) Å.^{28,45} Similar heterobridging units were previously described for (BDPPthf)La[(μ -Me)₂AlMe₂][(μ -Me)AlMe₂],²⁸ Nd(NiPr₂)-[(μ -NiPr₂)(μ -Me)AlMe₂][(μ -Me)₂AlMe₂],⁴⁶ { [Me₂Al(μ -Me)₂]-Nd(μ -NC₆H₅)(μ -Me)AlMe₂]₂,⁴⁷ and [(μ -NC₆H₅iPr₂-2,6)Sm(μ -NHC₆H₅iPr₂-2,6)(μ -Me)AlMe₂]₂.⁴⁸ For better understanding of the AlMe₃ impact on the formation of **6**, a suspension of (BDPPpyr)Y(AlMe₄) (**4c**) in hexane was stirred for 18 h at ambient temperature without and in the presence of 1 eq of AlMe₃ (Scheme 4).

In the absence of the organoaluminum compound neither metalation nor decomposition of **4c** took place, whereas complete conversion of **4c** into metalated compound **6** was found in the presence of AlMe₃. Therefore, it is the initial formation of the heterobridging [Y(μ -NR₂)(μ -Me)AlMe₂] unit that facilitates this metalation reaction pathway. The latter can be rationalized on the basis of kinetic (due to steric constraint)

(44) Duchateau, R.; van Wee, C. T.; Meetsma, A.; van Duijnen, P. T.; Teuben, J. H. *Organometallics* **1996**, *15*, 2279.

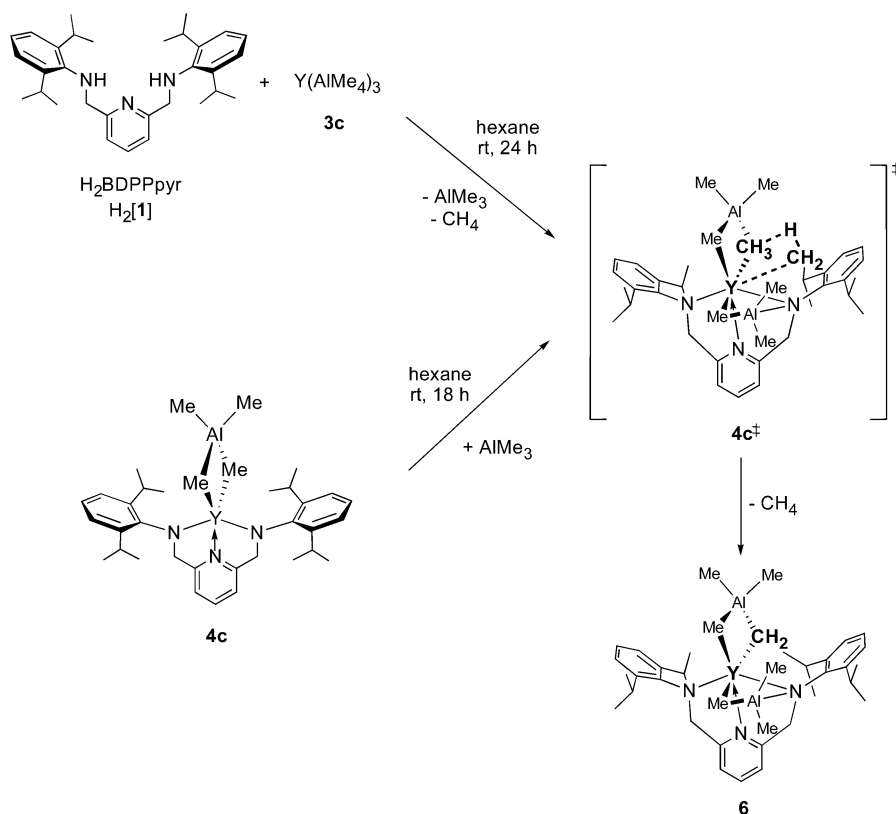
(45) Graf, D. D.; Davis, W. M.; Schrock, R. R. *Organometallics* **1998**, *17*, 5820.

(46) Evans, W. J.; Anwender, R.; Ziller, J. W. *Inorg. Chem.* **1995**, *34*, 5930.

(47) Evans, W. J.; Ansari, M. A.; Ziller, J. W.; Khan, S. I. *Inorg. Chem.* **1996**, *35*, 5435.

(48) Gordon, J. C.; Giesbrecht, G. R.; Clark, D. L.; Hay, P. J.; Keogh, D. W.; Poli, R.; Scott, B. L.; Watkin, J. G. *Organometallics* **2002**, *21*, 4726.

(43) (a) Bruce, M.; Gibson, V. C.; Redshaw, C.; Solan, G. A.; White, A. J. P.; Williams, D. J. *Chem. Commun.* **1998**, 2523. (b) Scott, J.; Gambarotta, S.; Korobkov, I.; Knijnenburg, Q.; de Bruin, B.; Budzelaar, P. H. M. *J. Am. Chem. Soc.* **2005**, *127*, 17204.

Scheme 4. Ligand Metalation of 4c via σ -bond Metathesis

or thermodynamic control. Since the path breaking investigation by Watson et al.,²³ the capability of Ln–methyl functionalities to engage in the activation of C–H bonds has been well established. Recently, single and multiple C–H bond activation was evidenced for lanthanide mono- C_5Me_5 complexes containing tetramethylaluminate functionalities $[\text{AlMe}_4]$.^{49,50} In 6, the interaction of one bridging methyl group of the tetramethylaluminate ligand with the aryl-*i*Pr group led to σ -bond metathetical loss of methane and concomitantly to the formation of a six-membered metalacycle as well as a mixed alkylaluminate species.

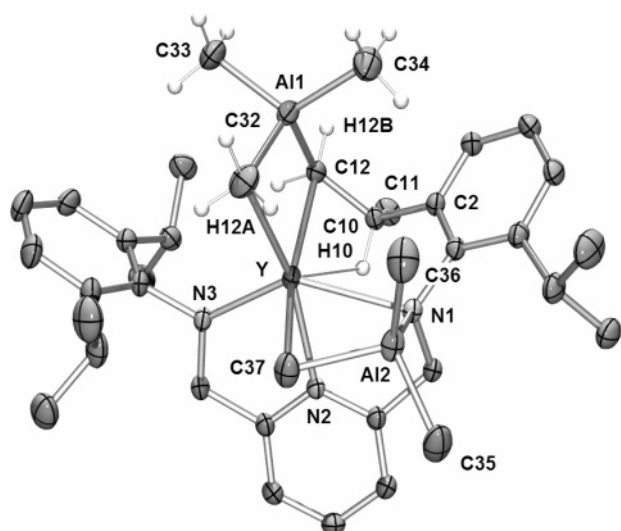


Figure 3. Molecular structure of $(\text{BDPPpyr-H})\text{Y}[(\mu\text{-Me})\text{AlMe}_2]_2$ (6) (atomic displacement parameters set at the 50% level). Hydrogen atoms (except for H10, H12A–B, H32A–C, H33A–C, and H34A–C) are omitted for clarity.

Table 4. Selected Structural Parameters for Complex $(\text{BDPPpyr-H})\text{Y}[(\mu\text{-Me})\text{AlMe}_2]_2$ (6)

| Bond Distances (Å) | | | |
|--------------------|-----------|-----------------|-----------|
| Y–N1 | 2.485(1) | Al2–C36 | 1.983(2) |
| Y–N2 | 2.397(1) | Al2–C37 | 2.063(2) |
| Y–N3 | 2.191(1) | C12–C10 | 1.554(2) |
| Y–C12 | 2.553(1) | C10–C2 | 1.523(2) |
| Y–C32 | 2.545(1) | C10–C11 | 1.538(2) |
| Y–C37 | 2.651(2) | C10–H10 | 1.00(2) |
| Al2–N1 | 1.970(1) | C12–H12A | 1.00(2) |
| Al1–C12 | 2.102(2) | C12–H12B | 0.93(2) |
| Al1–C32 | 2.057(2) | Y \cdots H10 | 2.33(2) |
| Al1–C33 | 1.968(2) | Y \cdots H12A | 2.74(2) |
| Al1–C34 | 1.970(2) | Y \cdots Al1 | 3.0769(5) |
| Al2–C35 | 1.974(4) | Y \cdots Al2 | 3.1350(4) |
| Bond Angles (deg) | | | |
| N1–Y–N3 | 139.30(4) | C37–Al2–C35 | 103.01(7) |
| N1–Y–N2 | 69.42(3) | C37–Al2–C36 | 105.74(7) |
| N2–Y–N3 | 69.88(4) | Y–C12–C10 | 81.83(7) |
| N2–Y–C12 | 114.00(4) | C12–C10–C2 | 110.7(1) |
| N2–Y–C32 | 161.94(5) | C12–C10–C11 | 111.6(1) |
| N2–Y–C37 | 78.43(5) | Y–C12–H12A | 89.9(9) |
| C12–Y–C37 | 161.88(5) | Y–C12–H12B | 163(1) |
| Y–C12–Al1 | 82.14(5) | C12–C10–H10 | 109.3(9) |
| Y–C32–Al1 | 83.20(6) | C11–C10–H10 | 103.0(9) |
| C32–Al1–C33 | 104.38(8) | Y–N1–C1 | 110.39(7) |
| C32–Al1–C34 | 107.54(8) | Y–N3–C20 | 124.12(8) |
| Y–C37–Al2 | 82.36(5) | | |

The hydrogen atoms at the bridging methyl group (C32) and at C12 were located and refined and unequivocally proved the formation of a bridging methylene group (CH_2^-) (Figure 3). Similar reactivity has been documented for LScR_2 and $\text{LScR}(\text{NHR}')$ complexes supported by Nacnac^- ligands carrying bulky 2,6-diisopropylphenyl substituents (Chart 1, G).^{11,51}

(49) Dietrich, H. M.; Törnroos, K. W.; Anwender, R. *J. Am. Chem. Soc.* **2006**, *128*, 9298.

(50) Dietrich, H. M.; Grove, H.; Törnroos, K. W.; Anwender, R. *J. Am. Chem. Soc.* **2006**, *128*, 1458.

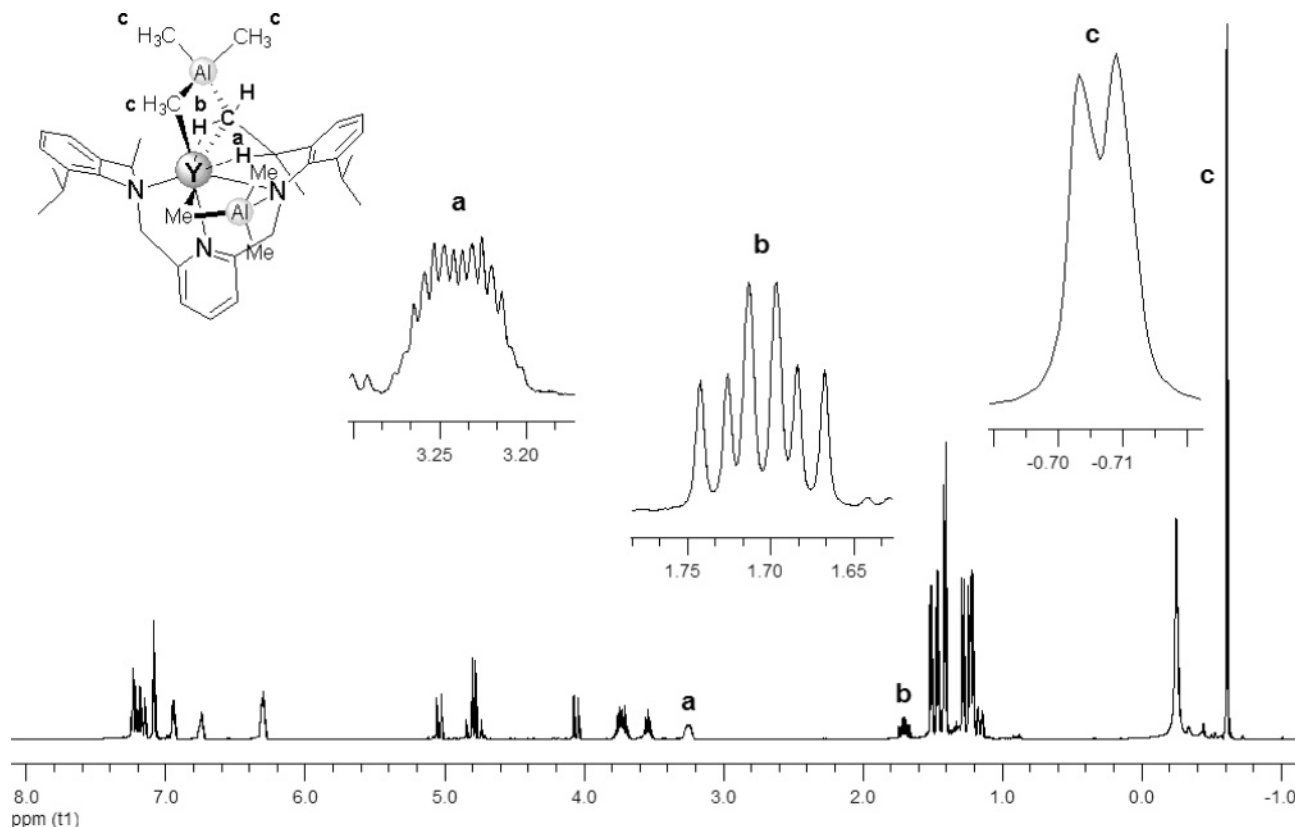


Figure 4. ^1H NMR spectrum (500.13 MHz) of **6** as a solution in C_6D_6 at 298 K.

The characteristic pattern of four methine multiplets and seven methyl doublets for the *i*Pr groups in the ^1H NMR spectrum of **6** in C_6D_6 are clearly indicative of the outcome of this reaction (Figure 4). A doublet of doublets at 1.16 ppm ($^2J_{\text{HH}} = 15.5$ Hz, $^3J_{\text{HH}} = 3.5$ Hz) can be assigned to one of the diastereotopic Y–CH₂ methylene protons, whereas the second methylene proton appears as a doublet of doublets of doublets (1.71 ppm), due to an additional scalar ^1H – ^{89}Y coupling ($^2J_{\text{HH}} = 15.5$ Hz, $^3J_{\text{HH}} = 8.0$ Hz, $^1J_{\text{YH}} = 15.5$ Hz) (Figure 4, **b**).⁵² Scalar coupling with the ^{89}Y nucleus ($^1J_{\text{YH}} = 14.0$ Hz) also leads to a doublet splitting of the multiplet at 3.24 ppm derived from the methine proton involved in the metalacycle (H10) (Figure 4, **a**). The presence of a scalar ^1H – ^{89}Y coupling was further proven by ^{89}Y NMR spectroscopy (no decoupling) and 2D ^1H – ^{89}Y HMQC NMR spectroscopy, showing a multiplet at 426 ppm and cross-peaks in the HMQC, respectively (Figure 5). The close Y···H10 contact (2.33(2) Å) in the solid-state structure of **6** is in the range of covalent Y–H bond lengths⁵³ and suggests an appreciable interaction in the solid state, which is retained in solution as indicated by the NMR spectroscopic investigations. A broad singlet at –0.25 ppm and a doublet at –0.71 ppm ($^2J_{\text{YH}} = 1.2$ Hz) can be assigned to the two [AlMe₃] moieties (Figure 4, **c**). A VT NMR study of compound **6** was hampered by its rapid crystallization in toluene-*d*₈ below –30 °C.

(51) Hayes, P. G.; Piers, W. E.; Lee, L. W. M.; Knight, L. K.; Parvez, M.; Elsegood, M. R. J.; Clegg, W. *Organometallics* **2001**, *20*, 2533.

(52) $^1J_{\text{YH}}$ coupling constants are in the range of 15–30 Hz: Rheder, D. In *Transition Metal Nuclear Magnetic Resonance*; Pregostin, P. S., Ed.; Elsevier: Amsterdam, 1991; pp 4–51.

(53) Examples of Y–H bond lengths from X-Ray diffraction data include the following: (a) 2.19/2.17 Å in [(C₅H₄Me)₂Y(μ-H)(THF)]₂: Evans, W. J.; Meadows, J. H.; Wayda, A. L.; Hunter, W. E.; Atwood, J. L. *J. Am. Chem. Soc.* **1982**, *106*, 2008. (b) 2.35 Å in [(C₅H₅)₂Y(μ-Cl)]₂(μ-H)AlH₂(OEt)₂: Lobovskii, B.; Soloveichik, G. L.; Erofeev, A. B.; Bulichev, B. M.; Bel'skii, V. K. *J. Organomet. Chem.* **1982**, *299*, 67. (c) 2.09/2.13 Å in [Me₂Si(2-MeC₉H₅)₂Y(THF)(μ-H)]: Klimpel, M. G.; Sirsch, P.; Scherer, W.; Anwander, R. *Angew. Chem., Int. Ed.* **2003**, *42*, 574.

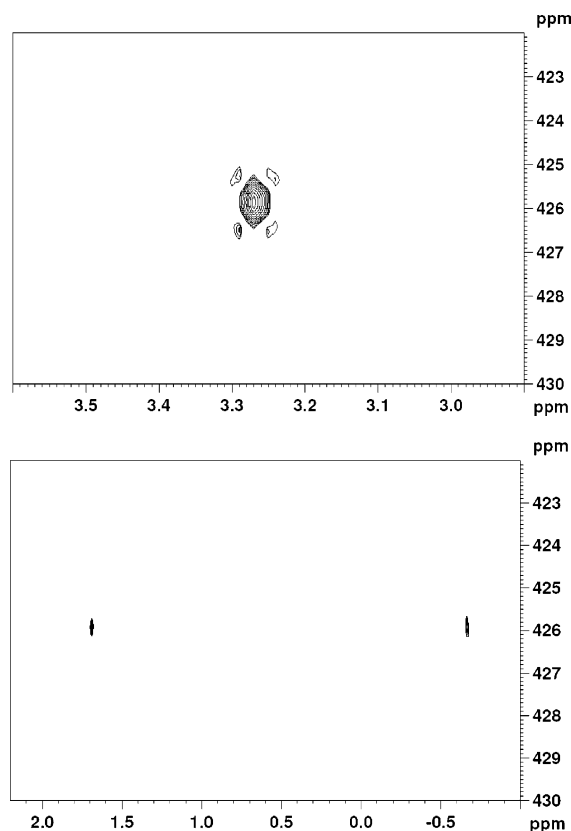
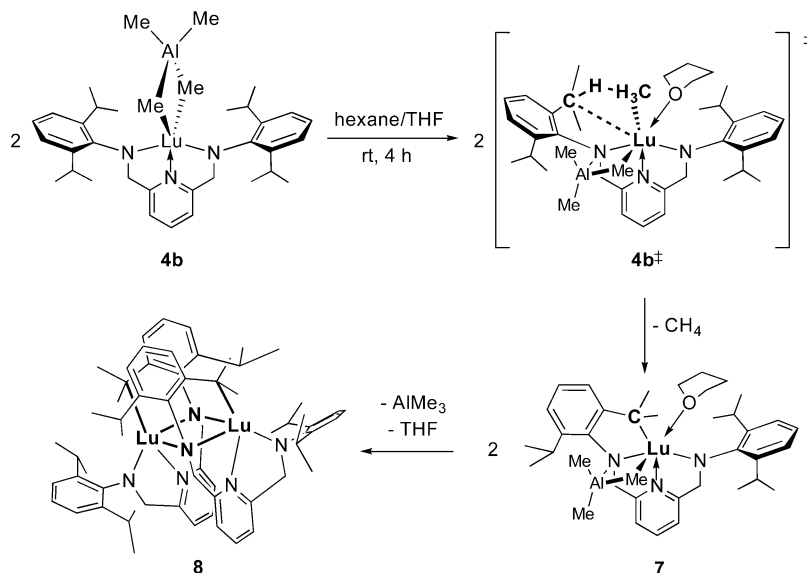


Figure 5. Two-dimensional ^1H – ^{89}Y HMQC NMR spectra of **6** dissolved in toluene-*d*₈ at 298 K. Experiment optimized for $^1J_{\text{YH}} = 14.0$ Hz (top). Experiment optimized for $^2J_{\text{YH}} = 1.5$ Hz (bottom).

In contrast, the formation of analogous metalation products of the smaller and larger lanthanide metal centers scandium, lutetium and lanthanum, respectively, was not observed. Even

Scheme 5. Donor-Induced Cleavage of the Tetramethylaluminate Ligand of **4b Followed by Ligand Metalation via σ -Bond Metathesis**



after stirring hexane suspensions of **4b** and **4d** in the presence of AlMe_3 for several days, the starting compounds could be recovered in almost quantitative yields. Clearly, the observed reactivity emphasizes the impact of the lanthanide cation size on the complex stability of $(\text{BDPPpyr})\text{Ln}(\text{AlMe}_4)$ (**4**).

The donor-induced cleavage of tetramethylaluminate complexes (donor = THF, diethyl ether, pyridine) offers a convenient synthesis approach toward highly reactive $[\text{Ln}-\text{Me}]$ moieties as reported for homoleptic tris(tetramethylaluminate) complexes⁵⁴ and for heteroleptic lanthanidocene and half-lanthanidocene complexes, $[\text{Cp}'_2\text{Ln}(\text{AlR}_4)]$ and $[\text{Cp}'\text{Ln}(\text{AlR}_4)_2]$ (Cp' = substituted cyclopentadienyl; R = Me, Et).^{55,56} When treating a stirred suspension of tetramethylaluminate complex $(\text{BDPPpyr})\text{Lu}(\text{AlMe}_4)$ (**4b**) in hexane with an excess of THF (Scheme 5), instant dissolution of the off-white solid occurred accompanied by a red coloration of the solution. Depending on the reaction and crystallization time, two different batches of yellow single crystals could be harvested from hexane solutions and identified by X-ray diffraction as the cyclometallation products **7** and **8** (Figures 6 and 7). Selected bond distances and angles are listed in Tables 5 and 6.

The formation of final product $[\text{Lu}(\text{BDPPpyr}-\text{H})_2]$ (**8**) originates from sequential processes involving an initial donor-induced cleavage of the tetramethylaluminate ligand in complex **4b** to produce a transition structure **4b**[‡] containing a highly reactive terminal methyl group and a heterobridging $[\text{Lu}(\mu\text{-NR}_2)(\mu\text{-Me})\text{AlMe}_2]$ unit, which seems to be vital to facilitate a metalation reaction pathway. Subsequent σ -bond metathesis between the $\text{Lu}-\text{CH}_3$ bond and the $\text{C}-\text{H}$ bond of one *i*Pr-methine group of the BDPPpyr ligand results in loss of methane and consequent formation of a five-membered metalacycle of the composition $(\text{BDPPpyr}-\text{H})\text{Lu}[(\mu\text{-Me})\text{AlMe}_2](\text{THF})$ (**7**). An X-ray structural analysis of “reaction intermediate” **7** was carried out, revealing the additional coordination of the cleaving agent THF to the lutetium metal center (Figure 6). An increased coordination number of the lutetium metal center

in **7** compared to precursor complex **4b** (CN 6 versus 5) combined with ring strain caused by the fused metalacycles leads to considerably elongated $\text{Lu}-\text{C}$ and $\text{Lu}-\text{N}(\text{amido})$ bond lengths (e.g., $\text{Lu}-\text{C}22$, 2.589(9), $\text{Lu}-\text{N}3$ 2.432(5) Å).⁵⁷

Finally, loss of the heterobridging AlMe_3 unit and displacement of coordinated THF by bridging amido moieties lead to a dimerization to form complex **8**. The two Lu metal centers seem to be perfectly embedded into two new tetradentate $[\text{NNNC}]^{3-}$ ligands which coordinate in a $\mu, \eta^4: \eta^1$ fashion. The coordination geometry of the five-coordinate lutetium centers is best described as strongly distorted trigonal bipyramidal with the two amido nitrogen atoms (N1 and N3) occupying the apical positions ($\text{N}1-\text{Lu}1-\text{N}3 = 138.82(6)^\circ$) and the pyridine N2 atom, the methine carbon (C29), and the bridging amido nitrogen of the second ligand (N3') spanning the equatorial plane. Although the proneness of $\text{Ln}-\text{CH}_3$ bonds to undergo σ -bond metathetical loss of methane is well documented,^{4,23,49–51,58,59} $\text{C}-\text{H}$ abstraction at a methine group (*tert.* carbon) is statistically and kinetically disfavored and therefore exceedingly rare.⁵⁸ To our knowledge, complexes **7** and **8** are the first examples of a structurally authenticated activation of a methine group within organolanthanide chemistry (e.g., derived from Pt, Fe, and Ti, see Chart 1, **D**, **E**, and **F**).^{9,10,60}

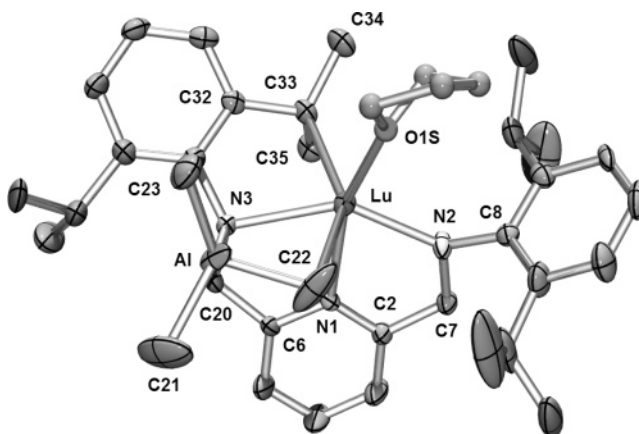


Figure 6. Molecular structure of reaction intermediate $(\text{BDPPpyr}-\text{H})\text{Lu}[(\mu\text{-Me})\text{AlMe}_2](\text{THF})$ (**7**) (atomic displacement parameters set at the 50% level). Hydrogen atoms are omitted for clarity.

(54) Dietrich, H. M.; Raudaschl-Sieber, G.; Anwander, R. *Angew. Chem., Int. Ed.* **2005**, *44*, 5303.

(55) Holton, J.; Lappert, M. F.; Ballard, D. G. H.; Pearce, R.; Atwood, J. L.; Hunter, W. E. *J. Chem. Soc., Dalton Trans* **1979**, 54.

(56) Klimpel, M. G.; Eppinger, J.; Sirsch, P.; Scherer, W.; Anwander, R. *Organometallics* **2002**, *21*, 4021.

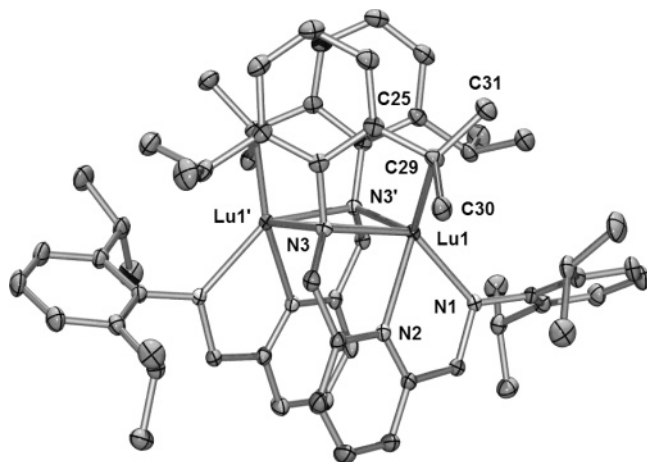


Figure 7. Molecular structure of dimeric $[\text{Lu}(\text{BDPPpyr-H})_2]_2$ (**8**) (atomic displacement parameters set at the 50% level). Hydrogen atoms are omitted for clarity.

Table 5. Selected Structural Parameters for Complex $(\text{BDPPpyr-H})\text{Lu}[(\mu\text{-Me})_2\text{AlMe}_2](\text{THF})$ (**7**)

| Bond Distances (Å) | | | |
|--------------------|------------|------------|-----------|
| Lu–N1 | 2.337(4) | Al–C23 | 1.971(7) |
| Lu–N2 | 2.209(5) | C33–C34 | 1.538(8) |
| Lu–N3 | 2.432(5) | C33–C35 | 1.550(8) |
| Lu–C33 | 2.373(6) | N2–C8 | 1.461(13) |
| Lu–C22 | 2.589(9) | N2–C7 | 1.441(7) |
| Lu–O1S | 2.284(7) | C2–C7 | 1.500(8) |
| Lu \cdots Al | 3.102(2) | N1–C2 | 1.336(7) |
| Lu \cdots H22A | 2.39(8) | N1–C6 | 1.355(7) |
| Al–N3 | 1.955(5) | C6–C20 | 1.494(8) |
| Al–C21 | 1.974(9) | N3–C20 | 1.489(8) |
| Al–C22 | 2.047(9) | | |
| Bond Angles (deg) | | | |
| N2–Lu–N3 | 141.28(16) | Lu–N3–C24 | 109.6(3) |
| N1–Lu–N2 | 70.84(16) | Lu–C33–C32 | 106.6(4) |
| N1–Lu–N3 | 70.44(15) | Lu–N2–C8 | 127.5(12) |
| N1–Lu–O1S | 160.5(2) | N3–Al–C22 | 103.6(3) |
| N1–Lu–C33 | 103.00(18) | C22–Al–Lu | 56.0(2) |

Table 6. Selected Structural Parameters for Complex $[\text{Lu}(\text{BDPPpyr-H})_2]$ (**8**) (Symmetry Code $-x, y, 3/2-z$)

| Bond Distances (Å) | | | |
|--------------------|-----------|-------------|-----------|
| Lu1–N1 | 2.249(2) | Lu1–C29 | 2.399(2) |
| Lu1–N2 | 2.350(2) | C29–C25 | 1.498(3) |
| Lu1–N3 | 2.338(2) | C29–C30 | 1.550(3) |
| Lu1–N3' | 2.318(2) | C29–C31 | 1.530(3) |
| Bond Angles (deg) | | | |
| N1–Lu1–N3 | 138.82(6) | N3–Lu1–N3' | 82.99(6) |
| N1–Lu1–N2 | 70.77(6) | Lu1'–N3–Lu1 | 96.01(6) |
| N2–Lu1–N3 | 68.19(6) | N2–Lu1–C29 | 114.78(6) |
| N1–Lu1–N3' | 105.67(6) | Lu1–C29–C30 | 95.9(1) |
| N2–Lu1–N3' | 106.36(6) | Lu1–C29–C31 | 130.8(2) |

The ^1H NMR spectroscopic investigation of **8** hallmark the metalated compound as the spectrum revealed only three septets at 3.76, 3.68, and 3.11 ppm for the remaining *i*Pr-methine

(57) Representative Lu–C bond lengths from X-ray diffraction data include the following: (a) av. 2.361 Å in 5-coordinate $\text{Lu}(\text{CH}_2\text{SiMe}_3)_2(\text{THF})_2$; ref. 34d. (b) 2.477–2.573 Å in 6-coordinate $\text{LuMe}_3(\text{LiMe}_3)_3(\text{DME})_3$; Schumann, H.; Lauke, H.; Hahn, E.; Pickardt, J. *J. Organomet. Chem.* **1984**, 263, 29.

(58) (a) Crowther, D. J.; Baenziger, N. C.; Jordan, R. F. *J. Am. Chem. Soc.* **1991**, 113, 1455. (b) Den Haan, K. H.; Wielstra, Y.; Teuben, J. H. *Organometallics* **1987**, 6, 2053.

(59) (a) Labinger, J. A.; Bercaw, J. E. *Nature* **2002**, 417, 507. (b) Stahl, S. S.; Labinger, J. A.; Bercaw, J. E. *Angew. Chem., Int. Ed.* **1998**, 37, 2180.

(60) C–H abstraction at both the methine and methyl group occurred for (a) $(\text{Nacnac})\text{Pt}(\text{IV})\text{Me}_3$; Fekl, U.; Goldberg, K. I. *J. Am. Chem. Soc.* **2002**, 124, 6804. (b) $(\text{AnIm})\text{Pt}(\text{IV})\text{Me}_3$; ref. 7.

protons and further two singlets at 1.36 and 1.24 ppm that can be assigned to the noncoupling $\text{LuC}(\text{CH}_3)$ protons. A signal at 95.1 ppm in the ^{13}C CAPT NMR spectrum of **8** further underlines the presence of a quaternary carbon atom.

Attempted donor-induced cleavage of the tetramethylaluminate ligand in the Sc (**4a**), Y (**4c**), and La (**4d**) complexes even with weaker (diethyl ether) or stronger (pyridine) donors than THF did not result in well-defined, characterizable products but in extensive ligand degradation. Again, these findings emphasize a sensitive and distinct cation size/reactivity correlation as well as the extremely high reactivity of terminal Ln–methyl groups.

Conclusions

Complexes $(\text{BDPPpyr})\text{Ln}[(\mu\text{-Me})_2\text{AlMe}_2]$ were synthesized following an amide elimination protocol (Ln = Sc, Lu) or via the “aluminate route” using homoleptic $\text{Ln}(\text{AlMe}_4)_3$ as lanthanide alkyl precursors (Ln = Lu, Y, La). Application of the two synthesis approaches gave access to the entire size range of rare-earth metal centers (Sc–La), thus allowing for comprehensive insight into the intrinsic properties, metal-size dependent dynamic behavior, and reactivity of the resulting tetramethylaluminate complexes. Dynamic ^1H NMR spectroscopy and line-shape analysis evidenced a dissociative exchange of bridging and terminal methyl groups of the tetramethylaluminate ligand in the sterically crowded $(\text{BDPPpyr})\text{Sc}(\text{AlMe}_4)$ (lower ordered transient state, η^1), whereas negative values of $\Delta\delta^\ddagger$ were calculated for the lutetium derivative, substantiating an associative exchange with a η^3 transient state. Because of the intrinsic interrelation of group 4 and group 3/lanthanide metal chemistry, complexes $(\text{BDPPpyr})\text{Ln}(\text{AlMe}_4)$ might be considered as model systems to reveal mechanistic details of post-metallocene based polymerization processes. In the presence of cocatalysts like MAO or organoaluminum reagents, tetraalkylaluminate complexes are proposed as polymerization retarding species (“dormant species”). They are further discussed as important intermediates in chain transfer and termination processes as β -H elimination, β -alkyl elimination via C–H activation and σ -bond metathesis processes. Ancillary ligand degradation via intramolecular σ -bond metathetical C–H activation as herein structurally and spectroscopically evidenced for $(\text{BDPPpyr})\text{Y}(\text{AlMe}_4)$, hence, exhibits a possible catalyst deactivation scenario in the respective group 4 catalyst mixtures. Given that this gradual ligand degradation is initiated by excess of organoaluminum cocatalyst and that it can be very slow, polymerization set-ups involving (prolonged) catalyst aging procedures should be viewed very critically (“single-site” catalysts). The formation of highly reactive $[\text{Ln}–\text{Me}]$ moieties in the presence of small amounts of donor solvent and their unpredictable nature is impressively substantiated by an unprecedented C–H activation of a methine group. Due to the high affinity of Lewis acidic Al^{3+} to nitrogen donors, the formation of aluminum byproducts like the characterized $(\text{BDPPpyr})(\text{AlMe}_2)_2$ should be anticipated for post-metallocene systems, particularly for those derived from *N*-donor ancillary ligands. Their role as possible chain transfer reagents has to be discussed. Clearly, the present (rare-earth) metal-size dependent activation/degradation processes once more emphasize the sensitivity of catalyst/cocatalyst systems to small stereoelectronic modifications and the complexity of Ziegler catalyst mixtures.

Experimental Section

All operations were performed with rigorous exclusion of air and water, using standard Schlenk, high-vacuum, and glovebox

techniques (MBraun MBLab; <1 ppm O₂, <1 ppm H₂O). Hexane, THF, and toluene were purified by using Grubbs columns (MBraun SPS, solvent purification system) and stored in a glovebox. C₆D₆ and toluene-*d*₈ were obtained from Aldrich, degassed, dried over Na for 24 h, and filtered. AlMe₃ was purchased from Aldrich and used as received. (BDPPpyr)Ln(NEt₂)(THF) (Ln = Sc, Lu) (**2**),¹⁸ 2,6-bis((2,6-diisopropylphenyl)amino)methylpyridine (H₂BDPPpyr, H₂[1]),¹⁵ and Ln(AlMe₄)₃ (Ln = Lu, Y, La) (**3**)^{33,54,61} were synthesized according to the literature methods. ¹H and ¹³C NMR spectra were recorded at 25 °C on a Bruker-BIOSPIN-AV500 (5 mm BBO, ¹H: 500.13 Hz; ¹³C: 125.77 MHz) and a Bruker-BIOSPIN-AV600 (5 mm cryo probe, ¹H: 600.13 MHz; ¹³C: 150.91 MHz). ¹H and ¹³C shifts are referenced to internal solvent resonances and reported in parts per million relative to TMS. ⁸⁹Y NMR experiments were performed on the AV500 (24.51 MHz, ¹H inverse gated decoupling). The ¹H-detected ¹H–⁸⁹Y HMQC spectra⁶² were acquired in the pure-absorption mode. Because ⁸⁹Y is present at 100% natural abundance, no gradients were required for coherence selection. Thirty-two *t*₁ increments were collected, 4 transients were averaged for each increment, and the recycling delay was 2 s. The experiment was optimized for ²J_{HY} = 1.5 Hz and ¹J_{HY} = 14 Hz. Broadband ⁸⁹Y decoupling (composite pulse decoupling) was used during the acquisition and the Ξ -scale was used for referencing the ⁸⁹Y chemical shift.⁶³ IR spectra were recorded on a NICOLET Impact 410 FTIR spectrometer as Nujol mulls sandwiched between CsI plates. Elemental analyses were performed on an Elementar Vario EL III.

General Procedure for the Synthesis of (BDPPpyr)Ln(AlMe₄) (4a,b) from (BDPPpyr)Ln(NEt₂)(THF) (2a,b). In a glovebox, 3 eq AlMe₃ were added dropwise to a stirred solution of **2** in 5 mL of hexane at ambient temperature. The reaction mixture was stirred another 3 h at ambient temperature while the formation of a white precipitate was observed. The product was separated by centrifugation and washed three times with 2 mL of hexane to yield **4** as powdery off-white solids in almost quantitative yields. Crystallization from a hexane/toluene solution at –35 °C gave colorless crystals of **4** in moderate yields suitable for X-ray diffraction analysis.

(BDPPpyr)Sc(AlMe₄) (4a). Following the procedure described above, AlMe₃ (32 mg, 0.45 mmol) and (BDPPpyr)Sc(NEt₂)(THF) (**2a**) (97 mg, 0.15 mmol) yielded **4a** (88 mg, 0.15 mmol, 99%) as colorless crystals. ¹H NMR (500 MHz, C₆D₆, 25 °C): δ = 7.2–7.1 (m, 6 H, ar), 6.97 (dd, ³J \approx 8 Hz, 1 H, pyr), 6.51 (d, ³J \approx 8 Hz, 2 H, pyr), 4.72 (s, 4 H, N–CH₂), 3.42 (sp, ³J \approx 7 Hz, 4 H, ar-CH), 1.34 (d, ³J \approx 7 Hz, 12 H, ar-CH₃), 1.17 (d, ³J \approx 7 Hz, 12 H, ar-CH₃), 0.35 (s, 6 H, Al(μ -CH₃)₂(CH₃)₂), –1.11 (s, 6 H, Al(μ -CH₃)₂(CH₃)₂) ppm. ¹³C {¹H} NMR (126 MHz, C₆D₆, 25 °C): δ = 164.7, 149.0, 145.3, 137.6, 125.4, 124.4, 117.4 (C_{ar}), 65.6 (N–CH₂), 28.6, 28.2, 23.3 (CH₃, ar-CH), 16.5 (Al(μ -CH₃)₂(CH₃)₂), –9.1 (Al(μ -CH₃)₂(CH₃)₂) ppm. Anal. calcd for C₃₃H₅₃N₃AlSc (587.763): C, 71.52; H, 9.09; N, 7.15. Found: C, 72.41; H, 9.20; N, 7.6.

(BDPPpyr)Lu(AlMe₄) (4b). Following the procedure described above, AlMe₃ (115 mg, 1.59 mmol) and (BDPPpyr)Lu(NEt₂)(THF) (**2b**) (411 mg, 0.53 mmol) yielded **4b** (379 mg, 0.53 mmol, 99%) as colorless crystals. IR (Nujol, cm^{–1}): 1615 m, 1582 m, 1461 vs Nujol, 1379 vs Nujol, 1306 m, 1245 m, 1185 s, 1162 s, 1129 m, 1102 m, 1069 m, 1041 m, 1024 m, 953 m, 931 w, 897 w, 870 w, 837 w, 809 w, 787 m, 771 s, 726 s, 704 s, 632 m, 577 w, 550 w, 522 w. ¹H NMR (500 MHz, C₆D₆, 25 °C): δ = 7.26–6.95 (m, 6 H, ar), 6.92 (dd, ³J \approx 8 Hz, 1 H, pyr), 6.51 (d, ³J \approx 8.0 Hz, 2 H, pyr), 4.92 (s, 4 H, N–CH₂), 3.53 (sp, ³J \approx 7.0 Hz, 4 H, ar-CH),

1.33 (d, ³J \approx 7.0 Hz, 12 H, ar-CH₃), 1.21 (d, ³J \approx 7.0 Hz, 12 H, ar-CH₃), –0.33 (s br, 12 H, Al(CH₃)₄) ppm. ¹³C {¹H} NMR (126 MHz, C₆D₆, 25 °C): δ = 165.8, 148.7, 146.2, 137.3, 125.0, 124.1, 117.6 (C_{ar}), 66.1 (N–CH₂), 28.5, 28.2, 23.4 (CH₃, ar-CH), 2.6 (Al(CH₃)₄) ppm. Anal. calcd for C₃₅H₅₃N₃AlLu (717.778): C, 58.57; H, 7.44; N, 5.85. Found: C, 58.43; H, 7.20; N, 5.91.

General Procedure for the Synthesis of (BDPPpyr)Ln(AlMe₄) (4b,c,d) from Ln(AlMe₄)₃ (3). In a glovebox, Ln(AlMe₄)₃ (**3**) was dissolved in 3 mL of hexane and added to a stirred solution of 1 equiv H₂BDPPpyr (H₂[1]) in 5 mL of hexane. Instant gas formation was observed. The reaction mixture was stirred another 4 h at ambient temperature while the formation of an off-white precipitate was observed. The product was separated by centrifugation and washed three times with 5 mL of hexane to yield **4** as powdery off-white solids in good yields. The remaining solids were crystallized from a hexane/toluene solution at –35 °C to give colorless crystals of **4** in moderate yields suitable for X-ray diffraction analyses.

(BDPPpyr)Lu(AlMe₄) (4b). Following the procedure described above, Lu(AlMe₄)₃ (**3b**) (221 mg, 0.51 mmol) and H₂BDPPpyr (H₂[1]) (231 mg, 0.51 mmol) yielded **4b** (264 mg, 0.37 mmol, 73%) as colorless crystals.

(BDPPpyr)Y(AlMe₄) (4c). Following the procedure described above, Y(AlMe₄)₃ (**3c**) (227 mg, 0.65 mmol) and H₂BDPPpyr (H₂[1]) (299 mg, 0.65 mmol) yielded **4c** (310 mg, 0.49 mmol, 75%) as colorless crystals. IR (Nujol, cm^{–1}): 1610 m, 1576 m, 1461 vs Nujol, 1379 vs Nujol, 1306 m, 1262 m, 1256 m, 1207 m, 1185 s, 1161 s, 1129 m, 1102 m, 1063 m, 1041 m, 1022 m, 958 m, 936 w, 897 w, 859 w, 815 w, 776 s, 726 s, 594 w. ¹H NMR (500 MHz, C₆D₆, 25 °C): δ = 7.18–7.15 (m, 6 H, ar), 6.97 (dd, ³J \approx 8 Hz, 1 H, pyr), 6.54 (d, ³J \approx 8.0 Hz, 2 H, pyr), 4.80 (s, 4 H, N–CH₂), 3.43 (sp, ³J \approx 7.0 Hz, 4 H, ar-CH), 1.33 (d, ³J \approx 7.0 Hz, 12 H, ar-CH₃), 1.21 (d, ³J \approx 7.0 Hz, 12 H, ar-CH₃), –0.53 (d, ²J_{YH} \approx 3 Hz, 12 H, Al(CH₃)₄) ppm. ¹³C {¹H} NMR (126 MHz, C₆D₆, 25 °C): δ = 165.4, 147.6, 146.0, 137.4, 125.1, 124.3, 117.6 (C_{ar}), 65.9 (N–CH₂), 28.6, 28.3, 23.4 (CH₃, ar-CH), 1.8 (Al(CH₃)₄) ppm. Anal. calcd for C₃₅H₅₃N₃AlY (631.713): C, 66.55; H, 8.46; N, 6.65. Found: C, 66.81; H, 8.85; N, 6.40.

(BDPPpyr)La(AlMe₄) (4d). Following the procedure described above, La(AlMe₄)₃ (**3d**) (105 mg, 0.26 mmol) and H₂BDPPpyr (H₂[1]) (120 mg, 0.26 mmol) yielded **4d** (310 mg, 0.21 mmol, 81%) as colorless crystals. IR (Nujol, cm^{–1}): 1604 m, 1571 m, 1466 vs Nujol, 1378 vs Nujol, 1306 m, 1240 m, 1207 m, 1201 s, 1162 s, 1113 m, 1058 s, 1019 m, 964 w, 936 w, 897 w, 853 w, 804 w, 771 s, 732 s, 621 m, 550 w, 539 w. ¹H NMR (600 MHz, C₆D₆, 25 °C): δ = 7.17–7.01 (m, 6 H, ar), 7.00 (dd, ³J \approx 7.8 Hz, 1 H, pyr), 6.60 (d, ³J \approx 7.8 Hz, 2 H, pyr), 4.99 (s, 4 H, N–CH₂), 3.20 (sp, ³J \approx 7.2 Hz, 4 H, ar-CH), 1.34 (d, ³J \approx 7.2 Hz, 12 H, ar-CH₃), 1.19 (d, ³J \approx 7.2 Hz, 12 H, ar-CH₃), –0.46 (s, 12 H, Al(CH₃)₄) ppm. ¹³C {¹H} NMR (151 MHz, C₆D₆, 25 °C): δ = 165.6, 147.3, 146.3, 137.5, 125.1, 124.7, 117.4 (C_{ar}), 67.4 (N–CH₂), 29.0, 27.7, 24.1 (CH₃, ar-CH), 2.7 (Al(CH₃)₄) ppm. Anal. calcd for C₃₅H₅₃N₃AlLa (681.718): C, 61.67; H, 7.84; N, 6.16. Found: C, 61.46; H, 7.59; N, 5.85.

Synthesis of (BDPPpyr)(AlMe₂)₂ (5). Following the procedure described for the synthesis of compounds **4** from Ln(AlMe₄)₃ (**3**), the orange supernatant and the hexane washing solutions were combined and dried under vacuum yielding a yellow powdery solid which was redissolved in hexane. Crystallization from hexane at –30 °C gave yellow crystals of **5** in yields depending on the lanthanide metal size (Ln = Lu 27%, Y 25%, La 19% calculated on Ln(AlMe₄)₃). IR (Nujol, cm^{–1}): 1615 m, 1576 m, 1455 vs Nujol, 1378 vs Nujol, 1312 m, 1256 m, 1185 m, 1162 m, 1118 m, 1091 m, 1063 m, 1035 m, 1024 w, 964 w, 936 w, 914 w, 853 w, 809 w, 771 s, 732 s, 649 m, 572 w. ¹H NMR (600 MHz, C₆D₆, 25 °C): δ = 7.28–7.02 (m, 6 H, ar), 6.52 (dd, ³J \approx 7.8 Hz, 1 H, pyr), 6.21 (d, ³J \approx 7.8 Hz, 2 H, pyr), 4.51 (s, 2 H, N–CH₂), 4.43 (s, 2 H,

(61) Fischbach, A.; Klimpel, M. G.; Widenmeyer, M.; Herdtweck, E.; Scherer, W.; Anwender, R. *Angew. Chem., Int. Ed.* **2004**, *43*, 2234.

(62) (a) Müller, L. *J. Am. Chem. Soc.* **1979**, *101*, 4481. (b) Bax, A.; Griffey, R. H.; Hawkins, B. L. *J. Magn. Reson.* **1983**, *55*, 301.

(63) Harris, R. K.; Becker, E. D.; Cabral de Menezes, S. M.; Goodfellow, R.; Granger, P. *Pure Appl. Chem.* **2001**, *73*, 1795.

Table 7. Crystallographic Data for Compounds **4b**, **5**, **6**, **7**, and **8**

| compound | 4b | 5 | 6 | 7 | 8 |
|--|---|--|--|--|--|
| formula | C ₃₅ H ₅₃ N ₃ AlLuC ₆ H ₁₄ | C ₃₅ H ₅₃ N ₃ Al ₂ | C ₃₇ H ₅₈ N ₃ Al ₂ Y | C ₃₈ H ₅₇ N ₃ OAlLu | C ₆₂ H ₈₀ N ₆ Lu ₂ |
| fw | 803.93 | 569.76 | 687.73 | 773.82 | 1259.26 |
| color/habit | none/prism | none/lath | none/rhomb | yellow/prism | yellow/prism |
| crystal dim. (mm ³) | 0.25 × 0.25 × 0.15 | 0.25 × .075 × 0.04 | 0.35 × 0.30 × 0.17 | 0.106 × 0.09 × 0.026 | 0.25 × 0.06 × 0.05 |
| crystal system | orthorhombic | monoclinic | monoclinic | monoclinic | monoclinic |
| space group | <i>Pnma</i> | <i>P2₁/c</i> | <i>P2₁/n</i> | <i>P2₁/c</i> | <i>C2/c</i> |
| <i>a</i> , Å | 13.5889(4) | 21.1535(13) | 11.2525(5) | 10.0267(4) | 19.0980(8) |
| <i>b</i> , Å | 16.4035(5) | 9.1668(6) | 23.1905(9) | 12.5492(4) | 17.7147(7) |
| <i>c</i> , Å | 18.5564(6) | 18.287(1) | 15.2776(6) | 28.8528(1) | 17.2840(7) |
| α, deg | 90 | 90 | 90 | 90 | 90 |
| β, deg | 90 | 101.919(1) | 105.627(1) | 94.243(1) | 112.208(1) |
| γ, deg | 90 | 90 | 90 | 90 | 90 |
| <i>V</i> , Å ³ | 4136.3(2) | 3469.6(4) | 3839.3(3) | 3620.5(2) | 5413.7(4) |
| <i>Z</i> | 4 | 4 | 4 | 4 | 4 |
| <i>T</i> , K | 123 | 123 | 123 | 103 | 123 |
| <i>D</i> _{calc} , mg m ⁻³ | 1.291 | 1.091 | 1.190 | 1.420 | 1.545 |
| μ, mm ⁻¹ | 2.437 | 0.110 | 1.592 | 2.783 | 3.671 |
| <i>F</i> (000) | 1672 | 1240 | 1464 | 1592 | 2544 |
| θ range, deg | 2.20–30.26 | 2.28–25.08 | 2.24–30.09 | 2.15–25.06 | 2.30–30.06 |
| index ranges (<i>h</i> , <i>k</i> , <i>l</i>) | –19/19, –23/23, –24/26 | –25/25, –10/10, –21/21 | –15/15, –32/32, –21/21 | –11/11, –14/14, –34/34 | –26/26, –24/24, –24/24 |
| no. of rflns collected | 60008 | 39476 | 64958 | 41264 | 45359 |
| no. of indep rflns/ <i>R</i> _{int} | 6373/0.0321 | 6145/0.1960 | 11275/0.0373 | 6409/0.0501 | 7940/0.0354 |
| no. of obsd rflns (<i>I</i> > 2σ(<i>I</i>)) | 5486 | 3052 | 9194 | 5320 | 6759 |
| data/restraints/params | 6373/14/249 | 6145/0/373 | 11275/9/426 | 6409/226/496 | 7940/0/323 |
| <i>R</i> ₁ / <i>wR</i> ₂ (<i>I</i> > 2σ(<i>I</i>)) ^a | 0.0218/0.0516 | 0.0544/0.0977 | 0.0272/0.0651 | 0.0399/0.0950 | 0.0190/0.0419 |
| <i>R</i> ₁ / <i>wR</i> ₂ (all data) ^a | 0.0303/0.0561 | 0.1560/0.1332 | 0.0410/0.0708 | 0.0522/0.1018 | 0.0283/0.0453 |
| GOF (on <i>F</i> ²) ^a | 1.070 | 0.987 | 1.028 | 1.042 | 1.023 |
| largest diff peak and hole (e Å ⁻³) | 1.79/–0.92 | 0.28/–0.28 | 0.38/–0.51 | 3.18/–0.47 | 0.93/–0.69 |

$$^a R1 = \sum(|F_o| - |F_c|)/\sum|F_o|; wR2 = \{\sum[w(F_o^2 - F_c^2)^2]/\sum[w(F_o^2)^2]\}^{1/2}; GOF = \{\sum[w(F_o^2 - F_c^2)^2]/(n - p)\}^{1/2}.$$

N–CH₂), 3.87 (m, 2 H, ar-CH), 3.33 (m, 2 H, ar-CH), 1.40 (s br, 6 H, ar-CH₃), 1.37 (s br, 6 H, ar-CH₃), 1.16 (s br, 6 H, ar-CH₃), 0.88 (s br, 6 H, ar-CH₃), –0.06 (s br, 6 H, Al(CH₃)₂), –0.38 (s br, 6 H, Al(CH₃)₂) ppm. ¹³C {¹H} NMR (151 MHz, C₆D₆, 25 °C): δ = 157.9, 148.7, 147.7, 145.7, 139.0, 126.3, 126.2, 124.1, 120.8 (C_{ar}), 60.2, 57.7 (N–CH₂), 28.2, 27.6, 26.4, 25.6, 25.5, 24.1 (CH₃, ar-CH), –5.4 (Al(CH₃)₂), –9.0 (Al(CH₃)₂) ppm. Anal. calcd for C₃₅H₅₃N₃Al₂ (569.789): C, 73.78; H, 9.38; N, 7.37. Found: C, 73.98; H, 9.67; N, 7.01.

Synthesis of (BDPPpyr-H)Y[(μ-Me)AlMe₂]₂ (6). In a glovebox, Y(AlMe₄)₃ (**3c**) (180 mg, 0.51 mmol) was dissolved in 3 mL of hexane and added to a stirred solution of 1 equiv H₂BDPPpyr (H₂-[1]) (235 mg, 0.51 mmol) in 5 mL of hexane. Instant gas formation was observed. The reaction mixture was stirred another 24 h at ambient temperature while first the formation of a white precipitate was observed. After approximately 6 h, the white precipitate turned yellowish and partly redissolved. The product was separated by centrifugation and washed three times with 3 mL of hexane to yield **6** (256 mg, 0.37 mmol, 73%) as powdery yellow solid. Crystallization from hexane solution at –35 °C gave yellow crystals of **6** in good yields suitable for X-ray diffraction analysis. IR (Nujol, cm⁻¹): 1602 m, 1575 m, 1461 vs Nujol, 1379 vs Nujol, 1306 m, 1233 m, 1206 m, 1169 m, 1161 m, 1106 m, 1069 m, 1022 m, 969 w, 938 w, 895 w, 848 w, 806 w, 774 s, 721 s, 663 w, 627 w, 579 w, 569 w, 542 w. ¹H NMR (500 MHz, C₆D₆, 25 °C): δ = 7.23–6.93 (m, 6 H, ar), 6.74 (dd, ³*J* ≅ 7.2 Hz, ³*J* ≅ 7.0 Hz, 1 H, pyr), 6.30 (d, ³*J* ≅ 7.0 Hz, 1 H, pyr), 6.29 (d, ³*J* ≅ 7.2 Hz, 1 H, pyr), 5.04 (d, ²*J* ≅ 17 Hz, 1 H, N–CH₂), 4.82 (d, ²*J* ≅ 21 Hz, 1 H, N–CH₂), 4.76 (d, ²*J* ≅ 21 Hz, 1 H, N–CH₂), 4.06 (d, ²*J* ≅ 17 Hz, 1 H, N–CH₂), 3.75 (sp, ³*J* ≅ 6.5 Hz, 1 H, ar-CH), 3.71 (sp, ³*J* ≅ 6.5 Hz, 1 H, ar-CH), 3.54 (sp, ³*J* ≅ 6.5 Hz, 1 H, ar-CH), 3.24 (m, ¹*J*_{YH} ≅ 14.0 Hz, 1 H, ar-CH), 1.71 (dd, ²*J* ≅ 15.5 Hz, ³*J* ≅ 8.0 Hz, ¹*J*_{YH} ≅ 15.5 Hz, 1 H, Y–CH₂), 1.51 (d, ³*J* ≅ 6.5 Hz, 3 H, ar-CH₃), 1.46 (d, ³*J* ≅ 6.5 Hz, 3 H, ar-CH₃), 1.41 (d, ³*J* ≅ 6.5 Hz, 6 H, ar-CH₃), 1.28 (d, ³*J* ≅ 6.5 Hz, 3 H, ar-CH₃), 1.24 (d, ³*J* ≅ 6.5 Hz, 3 H, ar-CH₃), 1.21 (d, ³*J* ≅ 6.5 Hz, 3 H, ar-CH₃), 1.16 (dd, ²*J* ≅ 15.5 Hz, ³*J* ≅ 3.5 Hz, 1 H, Y–CH₂), –0.25 (s br, 9 H, Al(CH₃)₃),

–0.71 (d, ²*J*_{YH} ≅ 1.2 Hz, 9 H, Al(CH₃)₃) ppm. ¹³C {¹H} NMR (126 MHz, C₆D₆, 25 °C): δ = 164.5, 160.2, 147.7, 147.1, 146.7, 146.5, 146.0, 142.6, 139.2, 125.6, 125.0, 124.5, 119.8, 118.4 (C_{ar}), 66.2, 65.5 (N–CH₂), 36.5 (d, ¹*J*_{YC} ≅ 13.2 Hz, Y–CH₂), 31.7, 30.0, 29.0, 28.7, 28.6, 28.2, 28.1, 27.7 (CH₃, ar-CH), –2.5 (s br, Al(CH₃)₃) ppm. Anal. calcd for C₃₇H₅₈N₃Al₂Y (687.756): C, 64.62; H, 8.50; N, 6.11. Found: C, 64.25; H, 8.65; N, 5.94.

Synthesis of (BDPPpyr-H)Lu[(μ-Me)AlMe₂]₂(THF) (7) and [Lu(BDPPpyr-H)]₂ (8). To a stirred suspension of **4b** (102 mg, 0.14 mmol) in 3 mL of hexane 3 mL THF were added dropwise. The white solid dissolved immediately and the reaction mixture turned red. After stirring for 4 h at ambient temperature the solvent was removed in vacuo to form a yellow solid, which was washed three times with 2 mL of hexane and dried under vacuum to yield a powdery yellow solid. Crystallization from hexane solutions yielded two different batches of yellow single crystals. Low-yield product (and intermediate) **7** could be identified by X-ray structure analysis and NMR spectroscopy: ¹H NMR (600 MHz, C₆D₆, 25 °C): δ = 7.33–7.04 (m, 6 H, ar), 7.01 (d, ³*J* ≅ 7.8 Hz, 1 H, pyr), 6.80 (dd, ³*J* ≅ 7.8 Hz, 1 H, pyr), 6.41 (d, ³*J* ≅ 7.8 Hz, 1 H, pyr), 5.50 (d, ²*J* ≅ 18.0 Hz, 1 H, N–CH₂), 5.11 (d, ²*J* ≅ 21.0 Hz, 1 H, N–CH₂), 4.82 (d, ²*J* ≅ 21.0 Hz, 1 H, N–CH₂), 4.73 (d, ²*J* ≅ 18.0 Hz, 1 H, N–CH₂), 4.31 (sp, ³*J* ≅ 6.6 Hz, 1 H, ar-CH), 3.73 (sp, ³*J* ≅ 7.2 Hz, 1 H, ar-CH), 3.55 (sp, ³*J* ≅ 6.6 Hz, 1 H, ar-CH), 3.19 (m, 2 H, THF), 3.10 (m, 2 H, THF), 1.65 (d, ³*J* ≅ 6.6 Hz, 3 H, ar-CH₃), 1.48 (d, ³*J* ≅ 6.6 Hz, 3 H, ar-CH₃), 1.46 (d, ³*J* ≅ 6.6 Hz, 3 H, ar-CH₃), 1.35 (d, ³*J* ≅ 6.6 Hz, 3 H, ar-CH₃), 1.30 (d, ³*J* ≅ 7.2 Hz, 3 H, ar-CH₃), 1.22 (m, 4 H, THF), 1.15 (d, ³*J* ≅ 7.2 Hz, 3 H, ar-CH₃), 0.89 (s, 3 H, ar-CH₃), 0.87 (s, 3 H, ar-CH₃), –0.24 (s br, 9 H, Al(CH₃)₃) ppm. ¹³C {¹H} NMR (151 MHz, C₆D₆, 25 °C): δ = 164.7, 164.0, 157.4, 152.5, 149.8, 147.3, 138.5, 126.7, 124.5, 123.9, 123.4, 122.9, 121.8, 118.6, 118.1 (C_{ar}), 95.2 (C_{quar}), 70.6 (THF), 68.0, 61.7 (N–CH₂), 31.9, 29.0, 28.3, 28.0, 26.4, 25.5, 24.1, 23.9, 23.0 (CH₃, ar-CH, THF), –1.0 (s br, Al(CH₃)₃) ppm. Complex **8** is the thermodynamically favored and preferred crystallization product obtainable in high crystallized yield (128 mg, 0.10 mmol, 74%). IR (Nujol, cm⁻¹): 1613 m, 1577 m, 1458 vs Nujol, 1380 vs

Nujol, 1313 m, 1256 m, 1209 m, 1194 m, 1163 m, 1121 m, 1095 w, 1059 m, 1018 w, 976 m, 940 w, 899 w, 862 w, 811 w, 774 s, 728 s, 629 w, 552 w. ^1H NMR (600 MHz, C_6D_6 , 25 °C): δ = 7.33–6.99 (m, 12 H, ar), 6.83 (dd, $^3J \cong 7.8$ Hz, 2 H, pyr), 6.73 (d, $^3J \cong 7.8$ Hz, 2 H, pyr), 6.64 (d, $^3J \cong 7.8$ Hz, 2 H, pyr), 5.70 (d, $^2J \cong 18.0$ Hz, 2 H, N–CH₂), 5.04 (d, $^2J \cong 19.8$ Hz, 2 H, N–CH₂), 4.62 (d, $^2J \cong 18.0$ Hz, 2 H, N–CH₂), 4.23 (d, $^2J \cong 19.8$ Hz, 2 H, N–CH₂), 3.76 (sp, $^3J \cong 7.2$ Hz, 2 H, ar-CH), 3.68 (sp, $^3J \cong 6.6$ Hz, 2 H, ar-CH), 3.11 (sp, $^3J \cong 6.6$ Hz, 2 H, ar-CH), 1.52 (d, $^3J \cong 7.2$ Hz, 6 H, ar-CH₃), 1.47 (d, $^3J \cong 6.6$ Hz, 6 H, ar-CH₃), 1.42 (d, $^3J \cong 6.6$ Hz, 6 H, ar-CH₃), 1.36 (s, 6 H, ar-CH₃), 1.24 (s, 6 H, ar-CH₃), 1.07 (d, $^3J \cong 6.6$ Hz, 6 H, ar-CH₃), 0.96 (d, $^3J \cong 6.6$ Hz, 6 H, ar-CH₃), 0.95 (d, $^3J \cong 7.2$ Hz, 6 H, ar-CH₃) ppm. ^{13}C { ^1H } NMR (151 MHz, C_6D_6 , 25 °C): δ = 164.6, 164.0, 157.4, 152.5, 149.8, 147.3, 138.4, 126.6, 124.5, 123.9, 123.5, 122.7, 121.6, 118.7, 118.2 (C_{ar}), 95.1 (C_{quat}), 66.2, 65.1 (N–CH₂), 31.9, 29.7, 28.0, 27.2, 26.8, 25.4, 23.8, 23.0 (CH₃, ar-CH) ppm. Anal. calcd for C₆₀H₈₀N₆Lu₂ (1235.275): C, 58.34; H, 6.53; N, 6.80. Found: C, 58.23; H, 6.19; N, 6.64.

Single-Crystal X-Ray Structures. Crystal data and details of the structure determination are presented in Table 7. The crystals were placed in a nylon loop containing Paratone oil (Hampton Research) and mounted directly into the N₂ cold stream (Oxford Cryosystems Series 700) on a Bruker AXS SMART 2K CCD diffractometer. Data were collected by means of 0.3° ω -scans in four orthogonal φ -settings using Mo K α radiation (λ = 0.71073 Å). Data collection was controlled using the program SMART, data

integration using SAINT, and structure solution and model refinement using SHELXS-97 and SHELXL-97,⁶⁴ respectively.⁶⁵ Non-coordinating methyl groups were refined as rigid and rotating (difference Fourier density optimization) CH₃ groups around the respective Al–C bonds. Coordinating methyl groups were refined as rigid pyramidal groups with the same C–H and H–H distances as for the previous, but with the threefold axis of the pyramidal rigid group allowed to be nonparallel with the C–Al bond axis. The isotropic displacement parameters for all methyl H-atoms were set to be 1.5 times that of the pivot C-atom.

Acknowledgment. Financial support from the Norwegian Research Council and the program Nanoscience@UiB is gratefully acknowledged.

Supporting Information Available: CCDC 651955–651958 and CCDC 652609 contain the supplementary crystallographic data for this paper. Copies of the data can be obtained free of charge from The Cambridge Crystallographic Data Centre, via www.ccdc.cam.ac.uk/data_request/cif. This material is available free of charge via the Internet at <http://pubs.acs.org>.

OM700830K

(64) Sheldrick, G. M. *SHELXL-97*, University of Göttingen: Göttingen, Germany, 1998.

(65) (a) *SMART*, version 5.054; Bruker AXS Inc.: Madison, WI, 1999; *SAINT*, version 6.45a; Bruker AXS Inc.: Madison, WI, 2001. (b) Sheldrick, G. M. *SHELXS-97*; University of Göttingen: Göttingen, Germany, 2003.

Paper V

Ln(III) methyl and methylidene complexes stabilized by a bulky hydrotris(pyrazolyl)borate ligand†

Melanie Zimmermann,^a Josef Takats,^b Gong Kiel,^b Karl W. Törnroos^a and Reiner Anwander^{*a}

Received (in Cambridge, UK) 31st August 2007, Accepted 16th November 2007

First published as an Advance Article on the web 30th November 2007

DOI: 10.1039/b713378b

The reaction of $\text{Ln}(\text{AlMe}_4)_3$ with bulky hydrotris(pyrazolyl)borate ($\text{Tp}^{\text{tBu,Me}}$)H proceeds via a sequence of methane elimination and C–H bond activation, affording unprecedented rare-earth metal ligand moieties including $\text{Ln}(\text{Me})[(\mu\text{-Me})\text{-AlMe}_3]$ and X-ray structurally characterized “Tebbe-like” $\text{Ln}[(\mu\text{-CH}_2)_2\text{AlMe}_2]$.

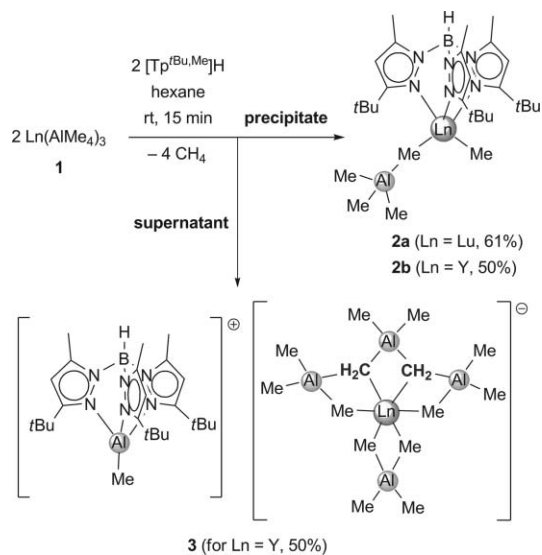
Bulky ancillary ligands give access to low-coordinate organo-lanthanide complexes with small ligands of exceptional reactivity and relevance for olefin polymerization.¹ For example, highly substituted cyclopentadienyl (Cp) and tris(pyrazolyl)borate (Tp) ligands allowed for the isolation and structural characterization of low-molecular hydrido species such as monomeric $(1,3,4\text{-tBu}_3\text{C}_5\text{H}_2)_2\text{Ce}^{\text{III}}\text{H}^2$ and dimeric $[(\text{Tp}^{\text{tBu,Me}})\text{Yb}^{\text{II}}(\mu\text{-H})]_2$,³ respectively. Cp-based ligands have also largely dominated the field of Ln^{III} hydrocarbyl chemistry,⁴ where in particular the $[\text{Ln}^{\text{III}}\text{-CH}_3]$ moiety has demonstrated exceptional reactivity as evidenced by methane activation,⁵ multiple hydrogen abstraction⁶ and α -olefin polymerization.⁷ However, careful design of alternative spectator ligands gave access to a prolific non-cyclopentadienyl organo-lanthanide chemistry.⁸ Anionic tris(3-*R*-5-*R'*-pyrazolyl)borate ligands ($\text{Tp}^{\text{R,R'}}$), formally isoelectronic to the Cp anions, displayed unique versatility as ancillary ligands since their first preparation by Trofimenko 40 years ago.⁹ The steric demand of the $\text{Tp}^{\text{R,R'}}$ ligands can effectively be adjusted by variation of the substituents in the 3-position of the pyrazolyl group (cone angles: $\text{Tp}^{\text{H,H}}$ 184°, $\text{Tp}^{\text{Me,Me}}$ 224°, $\text{Tp}^{\text{tBu,Me}}$ 244°; cf., C_5Me_5 142°).¹⁰ Given the current high impact of half-sandwich Ln^{III} hydrocarbyl complexes,¹¹ trivalent Tp analogues remain scarce.^{12,13} Only two examples of half-sandwich (Tp) Ln^{III} hydrocarbyls have been reported so far.^{14–16} Long and Bianconi described the synthesis of $(\text{Tp}^{\text{Me,Me}})\text{Y}(\text{CH}_2\text{SiMe}_3)_2(\text{thf})$ according to a salt metathesis reaction using $(\text{Tp}^{\text{Me,Me}})\text{YCl}_2(\text{thf})$ and $\text{LiCH}_2\text{SiMe}_3$.¹⁴ Piers *et al.* employed the alternative alkane elimination protocol to obtain scandium compounds $(\text{Tp}^{\text{Me,Me}})\text{Sc}(\text{CH}_2\text{SiMe}_3)_2(\text{thf})$ and $(\text{Tp}^{\text{tBu,Me}})\text{Sc}(\text{CH}_2\text{SiMe}_3)_2$ from $\text{Sc}(\text{CH}_2\text{SiMe}_3)_3(\text{thf})_2$ and $(\text{Tp}^{\text{R,R'}})\text{H}$.¹⁵

Homoleptic tris(tetramethylaluminate) complexes $\text{Ln}(\text{AlMe}_4)_3$ are versatile precursors for the synthesis of heterobimetallic Ln–Al complexes.¹⁷ Protonolysis reaction of such “alkyls in disguise” has been described for a variety of ancillary ligands including cyclopentadienyl, alkoxo and amido ligands.^{18–20} Stimulated by

the potential of these precursors to form highly active Ln–methyl moieties we set out to explore their reactivity toward the acid form of the sterically demanding hydrotris(3-*tert*-butyl-5-methylpyrazolyl)borate, $(\text{Tp}^{\text{tBu,Me}})\text{H}$.

$\text{Ln}(\text{AlMe}_4)_3$ (Ln = Lu (**1a**) and Y (**1b**)) react with $(\text{Tp}^{\text{tBu,Me}})\text{H}$ in hexane according to an alkane elimination reaction as evidenced by instant gas evolution and precipitation of a white solid material (Scheme 1). Separation of the precipitate from the supernatant afforded white powdery compounds identified as $(\text{Tp}^{\text{tBu,Me}})\text{Ln}(\text{AlMe}_4)(\text{Me})$ (Ln = Lu (**2a**), Y (**2b**)). The IR spectra of complexes **2** exhibit $\nu(\text{B-H})$ stretching vibrations at 2561 (**2a**) and 2566 cm^{-1} (**2b**), respectively, indicative of tridentate $\text{Tp}^{\text{tBu,Me}}$ ligands.²¹ ¹H NMR and ¹³C NMR spectra at ambient temperature display one set of resonances for the H-4, the C-5 methyl, and the C-3 *t*Bu groups of the pyrazolyl ligand. The resonances assignable to the $[\text{AlMe}_4]$ and $[\text{Me}]$ moieties appear as broad singlets (Fig. 1). Variable temperature (VT) ¹H NMR studies gave conclusive insight into the exchange processes of the highly fluxional compounds **2**. At 50 °C (decomposition at 60 °C), the ¹H NMR spectrum of lutetium derivative **2a** in toluene-*d*₈ shows only one singlet in the metal alkyl region (−0.15 ppm) accounting for 15 protons of the very fast exchanging AlMe_4 and Me ligands (Fig. 1). Signal decoalescence into two broad singlets at 0.45 ppm (Me, 3H) and −0.23 ppm (AlMe_4 , 12H) occurred at approximately ambient temperature.

Upon cooling to −10 °C the high-field signal decoalesced further and appeared as two distinct singlets in a 3 : 9 ratio. These



Scheme 1

^aDepartment of Chemistry, University of Bergen, Allégaten 41, 5007 Bergen, Norway. E-mail: reiner.anwander@kj.uib.no; Fax: +47 55589490

^bDepartment of Chemistry, University of Alberta, Edmonton, Alberta, Canada T6G 2G2. E-mail: joe.takats@ualberta.ca; Fax: +1 780 4928231

† Electronic supplementary information (ESI) available: Characterization data for **2** and **3** are available. See DOI: 10.1039/b713378b

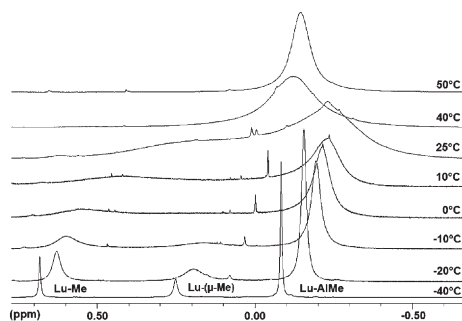


Fig. 1 Variable temperature ^1H NMR spectra (500.13 MHz) of $(\text{Tp}^{\text{tBu,Me}})\text{Lu}(\text{AlMe}_4)(\text{Me})$ (**2a**) dissolved in toluene- d_6 .

findings suggest a $[(\mu\text{-Me})\text{AlMe}_3]$ coordination mode of the tetramethylaluminate ligand in complexes **2** which demonstrates the tendency of the bulky $\text{Tp}^{\text{tBu,Me}}$ ligand to give rise to low coordination numbers.¹⁰ The existence of such η^1 -coordinated tetramethylaluminate ligands was recently confirmed by the solid-state structure of $(\text{NNN})\text{La}[(\mu\text{-Me})\text{AlMe}_3](\text{thf})$ ($\text{NNN} = 2,6\text{-}[\text{2,6-}i\text{Pr}_2\text{C}_6\text{H}_3]\text{NCMe}_2)_2\text{C}_5\text{H}_3\text{N}$).²² The proton resonances of the pyrazolyl ligand showed progressive broadening at lower temperature. The H-4 proton signal already decoalesced well above -40°C into two signals in a 2 : 1 ratio, consistent with a C_s symmetric structure (ESI, Fig. S1–S4†).

Yttrium complex **2b** showed analogous dynamic behaviour. Decoalescence of the AlMe_4 proton signals, however, occurred at lower temperatures (-60°C) consistent with the increasing steric unsaturation at the larger yttrium centre and therefore more rapid methyl group exchange.¹⁷ Attempted crystallization of compounds **2** was hampered by their insolubility in aliphatic solvents and their reactivity toward aromatic solvents (toluene, benzene).

The exceptional formation of rare-earth metal hydrocarbyls **2**, comprising $[\text{Ln}(\text{AlMe}_4)]$ and $[\text{Ln}(\text{Me})]$ moieties, is assumed to originate from a sequence of fast processes. A mechanistic proposal could include the initial formation of a transient bis(tetramethylaluminate) species $(\text{Tp}^{\text{tBu,Me}})\text{Ln}(\text{AlMe}_4)_2$, followed by intra- (from a κ^2 -coordinated $\text{Tp}^{\text{tBu,Me}}$ ligand)²³ or intermolecular (by $(\text{Tp}^{\text{tBu,Me}})\text{H}$) N -donor cleavage of one tetramethylaluminate ligand, producing a terminal methyl group under concomitant release of one equivalent of AlMe_3 .²⁴ Owing to the steric protection by the bulky $\text{Tp}^{\text{tBu,Me}}$ ligand the highly reactive methyl group is kinetically protected and stable complexes **2** can be isolated (Scheme 1).

Cooling the hexane supernatant of the reaction between $\text{Y}(\text{AlMe}_4)_3$ (**1b**) and $(\text{Tp}^{\text{tBu,Me}})\text{H}$ to -30°C reproducibly yielded colourless single crystals of **3** suitable for X-ray structural analysis (Fig. 2).[†] The X-ray diffraction study revealed an unprecedented salt-like compound consisting of a $[(\text{Tp}^{\text{tBu,Me}})\text{AlMe}]^+$ cation and a $[\text{Y}(\text{AlMe}_4)\{(\mu\text{-CH}_2)(\mu\text{-Me})\text{AlMe}_2\}_2(\text{AlMe}_2)]^-$ anion (Scheme 1). While the detailed mechanistic scenario leading to this extraordinary mixed metal compound remains obscure, several reactivity patterns can be recognized. The cationic unit most likely originates from the reaction of $(\text{Tp}^{\text{tBu,Me}})\text{H}$ with one equivalent AlMe_3 released in the acid–base reaction of $(\text{Tp}^{\text{tBu,Me}})\text{H}$ and $\text{Y}(\text{AlMe}_4)_3$ or donor cleavage of $[\text{AlMe}_4]$ (*vide supra*) to form the transient neutral aluminium complex $(\text{Tp}^{\text{tBu,Me}})\text{AlMe}_2$.²² Looney and Parkin previously reported the analogous alkyl aluminium compound $(\text{Tp}^{\text{tBu,H}})\text{AlMe}_2$ with the *t*Bu substituted pyrazole

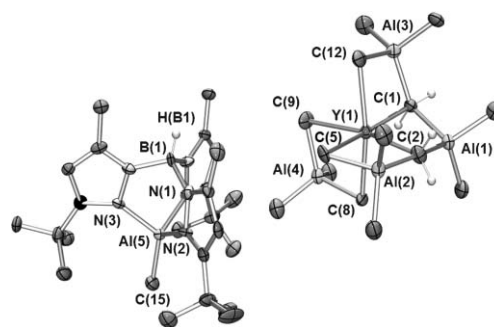


Fig. 2 Molecular structure of **3** (atomic displacement parameters are set at the 50% level). Hydrogen atoms (except for H(B1), H(1A), H(1B), H(2A) and H(2B)) are omitted for clarity. Selected bond distances [Å] and angles [°]: Y(1)–C(1) 2.344(8), Y(1)–C(2) 2.411(9), Y(1)–C(5) 2.582(9), Y(1)–C(8) 2.563(7), Y(1)–C(9) 2.654(8), Y(1)–C(12) 2.589(8), Y(1)⋯Al(1) 2.993(3), Y(1)⋯Al(2) 3.046(2), Y(1)⋯Al(3) 3.031(3), Y(1)⋯Al(4) 3.122(3), Al(1)–C(1) 2.097(7), Al(1)–C(2) 2.093(1), Al(2)–C(2) 2.05(1), Al(2)–C(5) 2.10(1), Al(3)–C(1) 2.068(8), Al(3)–C(12) 2.076(8), Al(4)–C(8) 2.044(8), Al(4)–C(9) 2.06(1), Al(5)–N(1) 1.927(7), Al(5)–N(2) 1.912(6), Al(5)–N(3) 1.909(7), Al(5)–C(15) 1.948(8); N(1)–Al(5)–N(2) 96.4(3), N(1)–Al(5)–N(3) 97.8(3), N(2)–Al(5)–N(3) 97.2(3), N(1)–Al(5)–C(15) 119.4(3), B(1)⋯Al(5)⋯C(15) 179.1(4), C(2)–Y(1)–C(9) 170.2(3), C(1)–Y(1)–C(9) 100.4(3), C(5)–Y(1)–C(9) 90.0(3), C(8)–Y(1)–C(9) 81.4(3), C(9)–Y(1)–C(12) 88.1(3), C(1)–Y(1)–C(2) 85.9(3), C(1)–Al(1)–C(2) 101.4(4), Y(1)–C(1)–Al(3) 86.5(3), Y(1)–C(12)–Al(3) 80.2(3), Y(1)–C(2)–Al(2) 85.8(4), Y(1)–C(5)–Al(2) 80.5(3), C(8)–Al(4)–C(9) 112.0(3).

ligand coordinated in a κ^2 fashion. Coordination of the third pyrazolyl ring is prevented by steric constraints.²⁵ However, this becomes feasible by elimination of one methyl ligand and concomitant cationization as revealed by the formation of the four-coordinate $[(\text{Tp}^{\text{tBu,Me}})\text{AlMe}]^+$ cation in **3**. The Al(5)–N bond distances (av. 1.916(7) Å) differ only slightly, substantiating a κ^3 coordination of the pyrazolylborate ligand in the solid-state. Besides for steric reasons the release of a methyl group might further be driven by the observed C–H bond activation (CH_4 formation) at a $[\text{AlMe}_4]$ unit of unreacted $\text{Y}(\text{AlMe}_4)_3$ producing the anionic part of salt **3**. The two methylidene-containing $[(\mu\text{-CH}_2)(\mu\text{-Me})\text{AlMe}_2]$ moieties are strong reminders of the prominent Tebbe reagent $\text{Cp}_2\text{Ti}[(\mu\text{-CH}_2)(\mu\text{-Cl})\text{AlMe}_2]$ and its derivative $\text{Cp}_2\text{Ti}[(\mu\text{-CH}_2)(\mu\text{-Me})\text{AlMe}_2]$ which can be obtained by reaction of $[\text{Cp}_2\text{TiMe}_2]$ and AlMe_3 .²⁶ It was only recently that rare-earth metal complexes containing such nucleophilic methylidene moieties were obtained as products of C–H bond activation processes.^{27,28} While a more detailed understanding of the reaction pathways leading to compound **3** remains elusive, the reaction stoichiometry comes out even considering the reproducible 50% yield of yttrium complex **2b** and salt **3**. The coordination geometry of the yttrium metal centre in **3** is best described as distorted octahedral with C(2) and C(9) occupying the apical positions (C(2)–Y(1)–C(9), $170.2(3)^\circ$). All hydrogen atoms of coordinating C atoms could be located and refined, unequivocally proving the formation of two bridging methylidene groups ($\mu_3\text{-CH}_2$) (Fig. 2). Compared to the Y–C($\mu\text{-CH}_3$) bond distances in the same molecule the Y–C($\mu\text{-CH}_2$) bonds are significantly shortened (av. 2.378(9) Å vs. 2.597(9) Å). These yttrium methylidene carbon distances are even shorter than the ones found for the trinuclear yttrium cluster $[\text{Cp}^*\text{Y}_3(\mu\text{-Cl})_3(\mu_3\text{-Cl})(\mu_3\text{-CH}_2)(\text{thf})_3]$ (2.424(2)–2.450(2) Å).²⁷ ^1H and ^{13}C NMR spectra of **3** suggest a large

barrier for the exchange of pyrazolyl groups implying a local C_s symmetry of the cationic unit. Signal assignment for the methylenes (^1H : 0.35 and 0.25 ppm; ^{13}C : 31.3 and 31.0 ppm) and methyl groups (^1H : -0.02 – -0.25 , 0.64 ppm; ^{13}C : -0.4 – 2.5 ppm) of the anionic unit was feasible, albeit complex signal patterns made a more detailed interpretation difficult. (ESI, Fig. S5†).

Nucleophilic addition of $[\text{M}-\text{CH}_3]$ moieties to carbonyl functionalities are routine reactions in organic synthesis.²⁹ To test the methylating capability of compounds **2**, reactions with 1–3 eq. of 9-fluorenone in C_6D_6 at ambient temperature were monitored by ^1H NMR spectroscopy. The investigations revealed instant bleaching of the yellow reaction mixture for the addition of 1 and 2 eq. of the ketone, while the addition of a third equivalent led to yellow reaction mixtures containing ill-defined Ln species. Preliminary investigations of the reactivity of **2** toward secondary amines (HNEt_2) evidenced protonolysis of the $[\text{Me}]$ and $[(\mu\text{-Me})\text{AlMe}_3]$ moieties (formation of CH_4 and $\text{Ln}-\text{NEt}_2$) accompanied by competitive formation of $(\text{Tp}^{\text{Bu,Me}})\text{H}$. Furthermore, instant gas evolution was observed when **2** was treated with SiMe_4 in accord with the occurrence of C–H bond activation.

In conclusion, we have demonstrated that protonolysis between $\text{Ln}(\text{AlMe}_4)_3$ and the sterically demanding $(\text{Tp}^{\text{Bu,Me}})\text{H}$ provides a convenient strategy for the synthesis of highly reactive mixed metal Ln^{III} hydrocarbyl complexes, $(\text{Tp}^{\text{Bu,Me}})\text{Ln}(\text{AlMe}_4)(\text{Me})$. The formation of salt-like $[(\text{Tp}^{\text{Bu,Me}})\text{AlMe}]^+[\text{Y}(\text{AlMe}_4)\{(\mu\text{-CH}_2)(\mu\text{-Me})\text{AlMe}_2\}_2(\text{AlMe}_2)]^-$ substantiates the high potential of tetramethylaluminate-containing reaction mixtures to activate C–H bonds. Preliminary reactivity studies revealed highly efficient methylation of carbonyl functionalities and promising reactivity in alkane elimination reactions.

Financial support from the Norwegian Research Council (Project No. 182547) and the program Nanoscience@UiB is gratefully acknowledged. We would also like to thank Jinhua Cheng and Kuburat Saliu for technical assistance.

Notes and references

† Crystal structure determination of complex **3**

Crystal data. $\text{C}_{39}\text{H}_{83}\text{N}_6\text{Al}_5\text{BY}$, $M = 870.73$, orthorhombic, $a = 29.6427(17)$, $b = 9.5879(6)$, $c = 18.0884(11)$ Å, $V = 5140.9(5)$ Å³, $d_{\text{calc}} = 1.125$ g cm⁻³, $T = 123$ K, space group $\text{Pna}2_1$, $Z = 4$. The structure was solved by Patterson methods, and least-square refinement of the model based on 7423 reflections (all data) and 4683 reflections ($I > 2.0\sigma(I)$) converged to a final $R1 = 0.0520$ and $wR2 = 0.1244$, respectively. CCDC 656616. For crystallographic data in CIF or other electronic format see DOI: 10.1039/b713378b

- For reviews, see: H. Yasuda, *Top. Organomet. Chem.*, 1999, **2**, 255; R. Anwander, in *Applied Homogeneous Catalysis with Organometallic Compounds*, ed. B. Cornils and W. A. Herrmann, Wiley-VCH, Weinheim, 2002, p. 974.
- L. Maron, E. V. Werkema, L. Perrin, O. Eisenstein and R. A. Andersen, *J. Am. Chem. Soc.*, 2005, **127**, 279.
- G. M. Ferrence, R. McDonald and J. Takats, *Angew. Chem., Int. Ed.*, 1999, **38**, 2233; G. M. Ferrence and J. Takats, *J. Organomet. Chem.*, 2002, **647**, 84.
- W. J. Evans and B. L. Davis, *Chem. Rev.*, 2002, **102**, 2119.
- P. L. Watson, *J. Am. Chem. Soc.*, 1983, **105**, 6491.
- H. M. Dietrich, H. Grove, K. W. Törnroos and R. Anwander, *J. Am. Chem. Soc.*, 2006, **128**, 1458.

- Z. Hou and Y. Wakatsuki, *Coord. Chem. Rev.*, 2002, **231**, 1; J. Gromada, J.-F. Carpentier and A. Mortreux, *Coord. Chem. Rev.*, 2004, **248**, 397; P. M. Zeimentz, S. Arndt, B. R. Elvridge and J. Okuda, *Chem. Rev.*, 2006, **106**, 2404.
- F. T. Edelmann, D. M. M. Freckmann and H. Schumann, *Chem. Rev.*, 2002, **102**, 1851; W. E. Piers and D. J. H. Emslie, *Coord. Chem. Rev.*, 2002, **233–234**, 131.
- S. Trofimenko, *J. Am. Chem. Soc.*, 1967, **89**, 3170; S. Trofimenko, *Scorpionates: The Coordination Chemistry of Polypyrazolylborate Ligands*, Imperial College Press, London, 1999.
- I. Santos and N. Marques, *New J. Chem.*, 1995, **19**, 551; N. Marques, A. Sella and J. Takats, *Chem. Rev.*, 2002, **102**, 2137; S. Trofimenko, J. C. Calabrese and J. S. Thompson, *Inorg. Chem.*, 1987, **26**, 1507; E. Frauendorfer and H. Brunner, *J. Organomet. Chem.*, 1982, **240**, 371; C. E. Davies, I. M. Gardiner, J. C. Green, M. L. H. Green, N. J. Hazel, P. D. Grebenik, V. S. B. Mtetwa and K. Prout, *J. Chem. Soc., Dalton Trans.*, 1985, 669.
- S. Arndt and J. Okuda, *Chem. Rev.*, 2002, **102**, 1953; Z. Hou, Y. Luo and X. Li, *J. Organomet. Chem.*, 2006, **691**, 3114.
- J. L. Galler, S. Goodchild, J. Gould, R. McDonald and A. Sella, *Polyhedron*, 2004, **23**, 253; A. Sella, S. E. Brown, J. W. Steed and D. A. Tocher, *Inorg. Chem.*, 2007, **46**, 1856.
- For Ln^{II} hydrocarbyls, see: L. Hasinoff, J. Takats, X. W. Zhang, P. H. Bond and R. D. Rogers, *J. Am. Chem. Soc.*, 1994, **116**, 8833.
- D. P. Long and P. A. Bianconi, *J. Am. Chem. Soc.*, 1996, **118**, 12453.
- J. A. Blackwell, C. Lehr, Y. Sun, W. E. Piers, S. D. Pearce-Batchilder, M. J. Zaworotko and V. G. J. Young, *Can. J. Chem.*, 1997, **75**, 702.
- The synthesis of a wide range of $(\text{Tp}^{\text{R,R'}})\text{Ln}(\text{CH}_2\text{SiMe}_2\text{R}'')_2(\text{thf})_{1/0}$ ($\text{R}'' = \text{Me, Ph}$) complexes has been achieved via a combination of protonolysis and Ti-hydrocarbyl elimination: J. Cheng, K. Saliu and J. Takats, unpublished results.
- A. Fischbach and R. Anwander, *Adv. Polym. Sci.*, 2006, **204**, 155; M. Zimmermann, N. Å. Frøystein, A. Fischbach, P. Sirsch, H. M. Dietrich, K. W. Törnroos, E. Herdtweck and R. Anwander, *Chem.–Eur. J.*, 2007, **13**, 8784.
- H. M. Dietrich, C. Zapilko, E. Herdtweck and R. Anwander, *Organometallics*, 2005, **24**, 5767.
- A. Fischbach, M. G. Klimpel, M. Widenmeyer, E. Herdtweck, W. Scherer and R. Anwander, *Angew. Chem., Int. Ed.*, 2004, **43**, 2234.
- M. Zimmermann, K. W. Törnroos and R. Anwander, *Organometallics*, 2006, **25**, 3593.
- M. Akita, K. Ohta, Y. Takahashi, S. Hikichi and Y. Moro-oka, *Organometallics*, 1997, **16**, 4121.
- M. Zimmermann, K. W. Törnroos and R. Anwander, *Angew. Chem., Int. Ed.*, 2007, **46**, 3126.
- X. Zhang, R. McDonald and J. Takats, *New J. Chem.*, 1995, **19**, 573; A. C. Hillier, X. W. Zhang, G. H. Maunder, S. Y. Liu, T. A. Eberspacher, M. V. Metz, R. McDonald, A. Domingos, N. Marques, V. W. Day, A. Sella and J. Takats, *Inorg. Chem.*, 2001, **40**, 5106.
- Donor-induced cleavage of tetramethylaluminates (O-donors, N-donors) offers a convenient synthesis approach toward highly reactive $[\text{Ln}-\text{Me}]$ moieties: J. Holton, M. F. Lappert, D. G. H. Ballard, R. Pearce, J. L. Atwood and W. E. Hunter, *J. Chem. Soc., Dalton Trans.*, 1979, 54.
- A. Looney and G. Parkin, *Polyhedron*, 1990, **9**, 265; D. J. Darensbourg, E. L. Maynard, M. W. Holtcamp, K. K. Klausmeyer and J. H. Reibenspies, *Inorg. Chem.*, 1996, **35**, 2682.
- F. N. Tebbe, G. W. Parshall and G. S. Reddy, *J. Am. Chem. Soc.*, 1978, **100**, 3611.
- H. M. Dietrich, K. W. Törnroos and R. Anwander, *J. Am. Chem. Soc.*, 2006, **128**, 9298.
- M. Zimmermann, F. Estler, E. Herdtweck, K. W. Törnroos and R. Anwander, *Organometallics*, 2007, **26**, 6029.
- J. J. Eisch, in *Comprehensive Organometallic Chemistry II*, ed. G. Wilkinson, F. G. A. Stone and E. W. Abel, Pergamon Press, Oxford, UK, 1995, vol. 11, ch. 6; T. Imamoto, *Pure Appl. Chem.*, 1990, **62**, 747; T. Imamoto, *Lanthanides in Organic Synthesis*, Academic Press, London, 1994.

Supplementary Material

Ln(III) Methyl and Methylidene Complexes Stabilized by a Bulky Hydrotris(pyrazolyl)borate Ligand

Melanie Zimmermann,^a Josef Takats,^b Gong Kiel,^b Karl W. Törnroos^a and Reiner Anwander^{*a}

^a *Department of Chemistry, University of Bergen, Allégaten 41, N-5007 Bergen, Norway. E-mail: reiner.anwander@kj.uib.no.*

^b *Department of Chemistry, University of Alberta, Edmonton, Alberta, Canada T6G 2G2, Canada.*

Experimental Details

General Procedures. All operations were performed with rigorous exclusion of air and water, using standard *Schlenk*, high-vacuum, and glovebox techniques (MBraun MBLab; <1 ppm O₂, <1 ppm H₂O). Hexane and toluene were purified by using *Grubbs* columns (MBraun SPS, solvent purification system) and stored in a glovebox. C₆D₆ and toluene-*d*₈ were obtained from *Aldrich*, degassed, dried over Na for 24 h, and filtered. AlMe₃ was purchased from *Aldrich* and used as received. Homoleptic Ln(AlMe₄)₃ (**1**) (Ln = Lu, Y) were prepared according to literature methods.¹⁷ (Tp^{*t*Bu,Me})H was synthesized by a modification of the published procedure for (PhTp^{*t*Bu})H.³¹ The NMR spectra of air and moisture sensitive compounds were recorded by using *J. Young* valve NMR tubes at 25 °C on a *Bruker*-BIOSPIN-AV500 (5 mm BBO, ¹H: 500.13 Hz; ¹³C: 125.77 MHz) and a *Bruker*-BIOSPIN-AV600 (5 mm cryo probe, ¹H: 600.13 MHz; ¹³C: 150.91 MHz). ¹H and ¹³C shifts are referenced to internal solvent resonances and reported in *parts per million* relative to TMS. ²⁷Al NMR spectra were recorded on the AV500 at 130.33 MHz. 2000 scans were averaged. The ²⁷Al chemical shifts are reported relative to an external reference: a solution of AlCl₃ in D₂O with a drop of concentrated HCl [Al(D₂O)₆³⁺]. ¹¹B NMR (161 MHz) spectra were referenced to an external standard of boron trifluoride diethyl etherate (0.0 ppm, C₆D₆). IR spectra were recorded on a *NICOLET Impact 410 FTIR* spectrometer as Nujol mulls sandwiched between CsI plates. Elemental analyses were performed on an *Elementar Vario EL III*.

General procedure for the synthesis of (Tp^{*t*Bu,Me})Ln(AlMe₄)(Me) (2**):** In a glovebox Ln(AlMe₄)₃ (**1**) was dissolved in 3 mL of hexane and added to a stirred solution of (Tp^{*t*Bu,Me})H in 4 mL of hexane. Instant gas formation and the formation of a white precipitate were observed. The reaction mixture was stirred another 15 min at ambient temperature. The product was separated by centrifugation, washed four times with 5 mL of hexane, and dried under vacuum to yield **2** as powdery white solids.

(Tp^{tBu,Me})Lu(AlMe₄)(Me) (2a): Following the procedure described above, Lu(AlMe₄)₃ (**1a**, 91 mg, 0.21 mmol) and (Tp^{tBu,Me})H (89 mg, 0.21 mmol) yielded **2a** as a powdery white solid (89 mg, 0.13 mmol, 61%).

¹H NMR (500 MHz, C₆D₆, 25 °C): δ = 5.61 (s, Δv_{1/2} = 3 Hz, 3 H, 4-pz-H), 4.44 (d v br, ¹J_{B-H} ≅ 119 Hz, 1 H, BH), 1.93 (s, Δv_{1/2} = 6 Hz, 9 H, pz-CH₃), 1.33 (s, Δv_{1/2} = 2 Hz, 27 H, pz-C(CH₃)₃), 0.07 (s br, Δv_{1/2} = 170 Hz, 3 H, Lu-CH₃), -0.32 (s br, Δv_{1/2} = 110 Hz, 12 H, Al(CH₃)).

¹H NMR (500 MHz, tol-*d*₈, -40 °C): 5.60 (s br, Δv_{1/2} = 30 Hz, 2 H, 4-pz-H), 5.36 (s br, Δv_{1/2} = 57 Hz, 1 H, 4-pz-H), 4.38 (s v br, ¹J_{B-H} ≅ 130 Hz, 1 H, BH), 2.08 (s br, Δv_{1/2} = 30 Hz, 9 H, pz-CH₃), 1.36 (s br, Δv_{1/2} = 19 Hz, 27 H, pz-C(CH₃)₃), 0.46 (s, Δv_{1/2} = 5 Hz, 3 H, Lu-CH₃), 0.03 (s, Δv_{1/2} = 7 Hz, 3 H, Al(μ-CH₃)), -0.31 (s, Δv_{1/2} = 4 Hz, 9 H, Al(CH₃)). ¹³C NMR (126 MHz, C₆D₆, 25 °C): δ = 166.5 (3-pz-C), 148.6 (5-pz-C), 105.0 (4-pz-C), 32.3 (pz-C(CH₃)₃), 31.1 (pz-C(CH₃)₃), 12.9 (pz-CH₃), -5.1 (Lu-CH₃), -6.1 (Al(CH₃)₄). ²⁷Al NMR (130 MHz, C₆D₆, 25 °C): δ = 164 (s br, Al(CH₃)₄) ppm.

¹¹B{¹H} NMR (161 MHz, C₆D₆, 25 °C): δ = -9.1 (s br) ppm. IR (Nujol, cm⁻¹): 2561 m (B-H), 1551 s, 1463 vs Nujol, 1375 vs Nujol, 1323 m, 1246 m, 1204 s, 1163 vs, 1070 s, 1033 s, 987 m, 811 s, 769 s, 728 s, 686 s, 650 m, 588 w, 526 m. Elemental analysis: calculated C (49.72), H (7.91), N (12.00); found C (49.96), H (7.98), N (11.84).

(Tp^{tBu,Me})Y(AlMe₄)(Me) (2b): Following the procedure described above, Y(AlMe₄)₃ (**1b**, 154 mg, 0.44 mmol) and (Tp^{tBu,Me})H (186 mg, 0.44 mmol) yielded **2b** as a powdery white solid (135 mg, 0.22 mmol, 50%).

¹H NMR (500 MHz, C₆D₆, 25 °C): δ = 5.57 (s, 3 H, 4-pz-H), 4.46 (d v br, ¹J_{B-H} ≅ 116 Hz, 1 H, BH), 1.95 (s, Δv_{1/2} = 4 Hz, 9 H, pz-CH₃), 1.32 (s, Δv_{1/2} = 4 Hz, 27 H, pz-C(CH₃)₃), 0.25 (s br, Δv_{1/2} = 100 Hz, 3 H, Y-CH₃), -0.36 (s br, Δv_{1/2} = 30 Hz, 12 H, Al(CH₃)). ¹H NMR (500 MHz, Tol-*d*₈, -60 °C): 5.49 (s br, Δv_{1/2} = 15 Hz, 2 H, 4-pz-H), 5.22 (s br, Δv_{1/2} = 32 Hz, 1 H, 4-pz-H), 4.35 (s v br, Δv_{1/2} = 70 Hz, 1 H, BH), 1.88 (s br, Δv_{1/2} = 13 Hz, 9 H, pz-CH₃), 1.36 (s br, Δv_{1/2} = 13 Hz, 27 H, pz-C(CH₃)₃), 0.43 (s, Δv_{1/2} = 6 Hz, 3 H, Y-CH₃), -0.14 (s, Δv_{1/2} = 20 Hz, 3 H, Al(μ-CH₃)), -0.21 (s, Δv_{1/2} = 10 Hz, 9 H, Al(CH₃)). ¹³C NMR (126 MHz, C₆D₆, 25 °C): δ = 165.4 (3-pz-C), 148.6

(5-pz-C), 104.4 (4-pz-C), 32.2 (pz-C(CH₃)₃), 31.1 (pz-C(CH₃)₃), 12.7 (pz-CH₃), -0.5 (Y-CH₃), -4.3 (Al(CH₃)₄). ²⁷Al NMR (130 MHz, C₆D₆, 25 °C): δ = 162 (s br, Al(CH₃)₄) ppm. ¹¹B{¹H} NMR (161 MHz, C₆D₆, 25 °C): δ = -9.0 (s br) ppm. IR (Nujol, cm⁻¹): 2566 m (B-H), 1551 s, 1458 vs Nujol, 1375 vs Nujol, 1328 s, 1251 m, 1204 s, 1168 vs, 1147 s, 1064 m, 1033 s, 992 m, 904 w, 805 s, 764 s, 728 m, 681 s, 645 m, 593 w, 526 m. Elemental analysis: calculated C (56.68), H (9.02), N (13.68); found C (56.94), H (9.07), N (13.44).

Procedure for the synthesis of {(Tp^{tBu,Me})AlMe}⁺{Y(AlMe₄)[(μ-CH₂)(μ-Me)AlMe₂]₂(AlMe₂)⁻ (3**):**

Following the procedure described for the synthesis of compounds **2b**, the supernatant and the hexane washing solutions were combined and stored at -30 °C. Colorless single crystals of **3** suitable for X-ray diffraction analysis were obtained after four weeks (192 mg, 0.22 mmol, 50% calculated on Y(AlMe₄)₃).

¹H NMR (600 MHz, C₆D₆, 25 °C): δ = 5.80 (s, 1 H, 4-pz-H), 5.56 (s, 2 H, 4-pz-H), 4.30 (s v br, 1 H, BH), 2.19 (s, 3 H, pz-CH₃), 2.02 (s, 6 H, pz-CH₃), 1.37 (s, 9 H, pz-C(CH₃)₃), 1.10 (s, 18 H, pz-C(CH₃)₃), 0.64 (s, 3 H, Al-CH₃), 0.35 (d, ²J_{Y-H} ≅ 3.5 Hz, 2 H, (μ-CH₂)), 0.23 (d, ²J_{Y-H} ≅ 1.2 Hz, 2 H, (μ-CH₂)), -0.02 (d, ²J_{Y-H} ≅ 1.2 Hz, 12 H, Y(Al(CH₃)₄)), -0.06 (d, ²J_{Y-H} ≅ 1.2 Hz, 6 H), -0.15 (s, 6 H), -0.17 (s, 3 H), -0.25 (d, ²J_{Y-H} ≅ 1.8 Hz, 9 H). ¹³C NMR (151 MHz, C₆D₆, 25 °C): δ = 167.0, 164.9 (3-pz-C), 149.7, 147.2 (5-pz-C), 107.0, 106.6 (4-pz-C), 33.0 (pz-C(CH₃)₃), 31.8 (pz-C(CH₃)₃), 31.3, 31.0, (Y-CH₂), 30.7 (pz-C(CH₃)₃), 13.6, 12.7 (pz-CH₃), 2.5, 0.5, 0.3, -0.3, -0.4 (Y-CH₃, Al(CH₃)). ²⁷Al NMR (130 MHz, C₆D₆, 25 °C): δ = 160 (s br, Al(CH₃)₄) ppm. ¹¹B{¹H} NMR (161 MHz, C₆D₆, 25 °C): δ = -7.7 (s br) ppm. Elemental analysis: calculated C (53.80), H (9.61), N (9.65); found C (54.13), H (9.72), N (10.03).

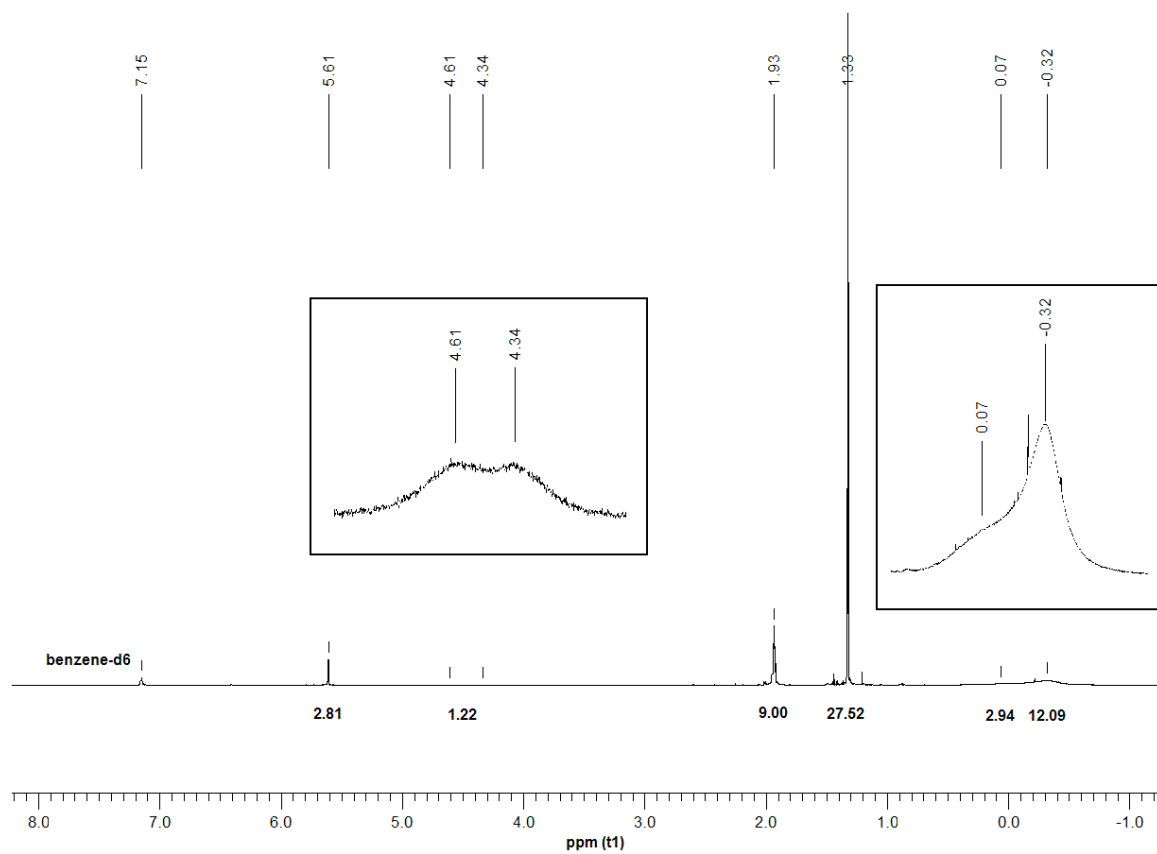


Fig. S1 ^1H NMR spectrum of compound **2a** in benzene- d_6 at 25 °C.

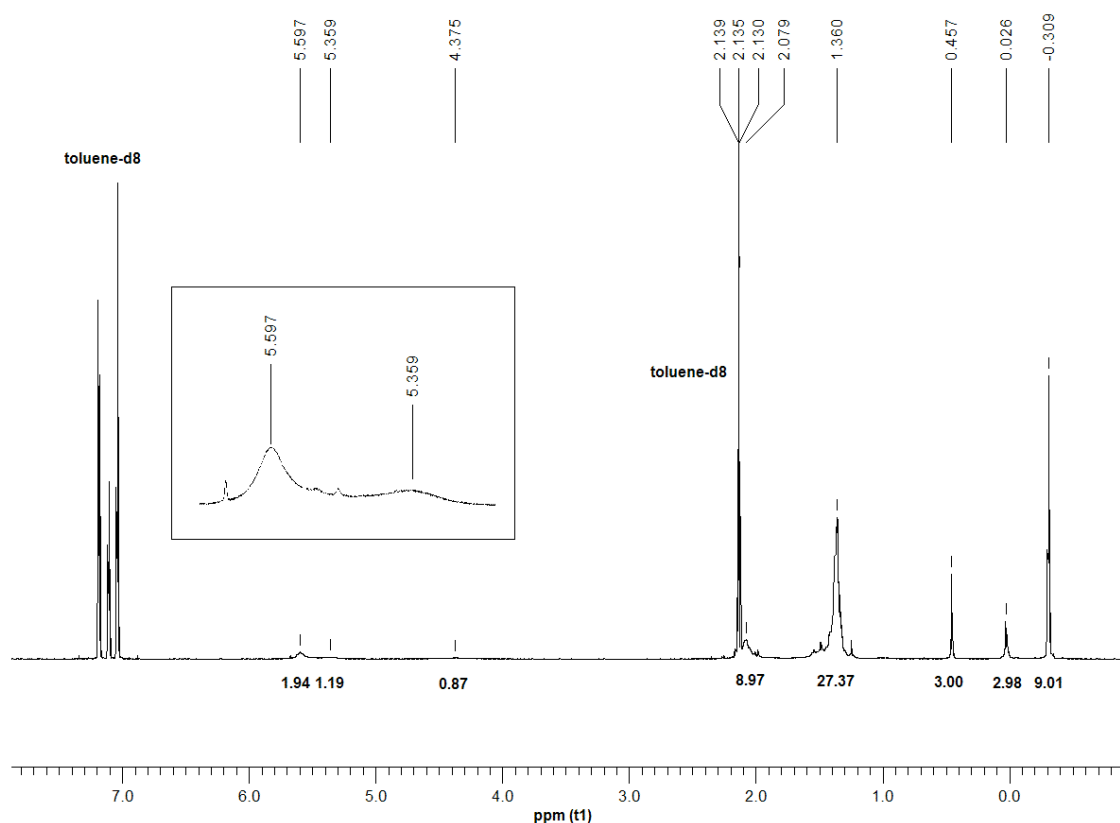


Fig. S2 ¹H NMR spectrum of compound **2a** in toluene-*d*₈ at -40 °C. At -40 °C significant broadening of the resonances associated with the pyrazolylborate ligand is observed. While well-separated signals are already observed for H-4 ($\Delta\nu_{1/2} = 30$ Hz and 57 Hz) the signals for the pZ-*CH*₃ ($\Delta\nu_{1/2} = 30$ Hz) and the pZ-C(*CH*₃)₃ ($\Delta\nu_{1/2} = 19$ Hz) appear only significantly broadened.

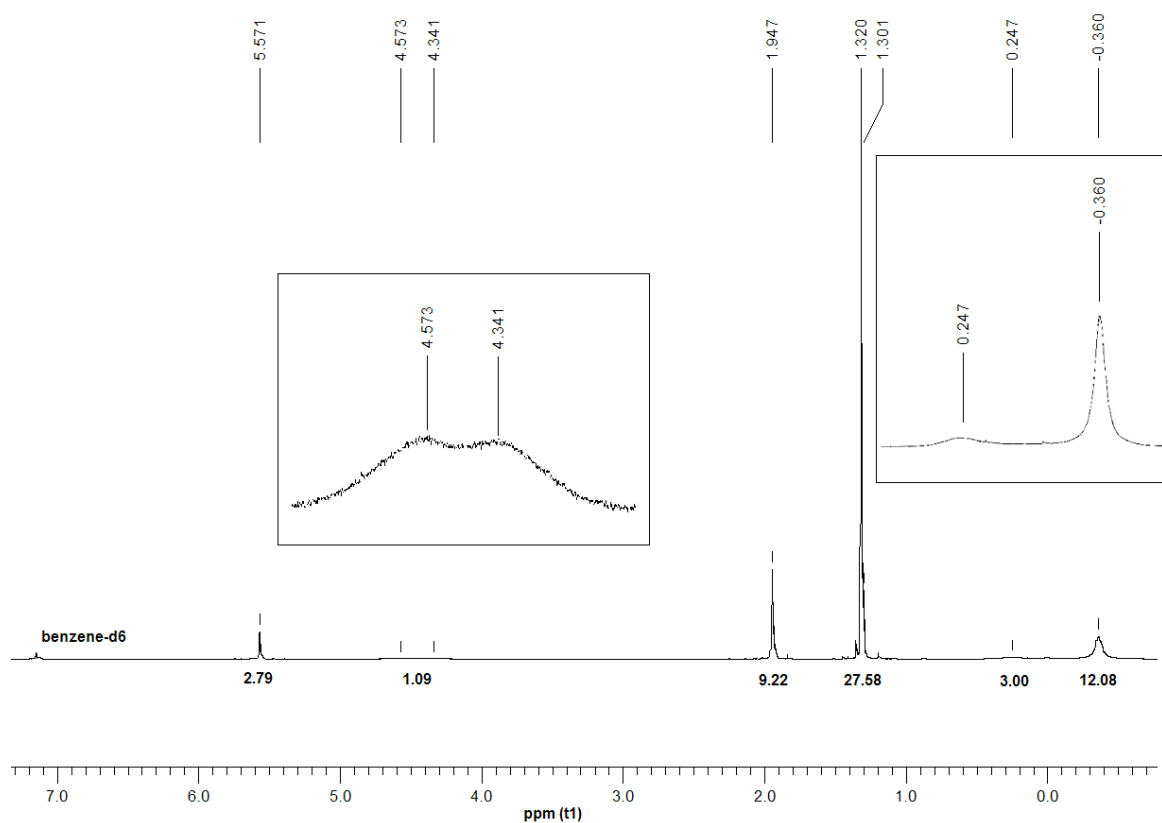


Fig. S3 ^1H NMR spectrum of compound **2b** in benzene- d_6 at 25 °C.

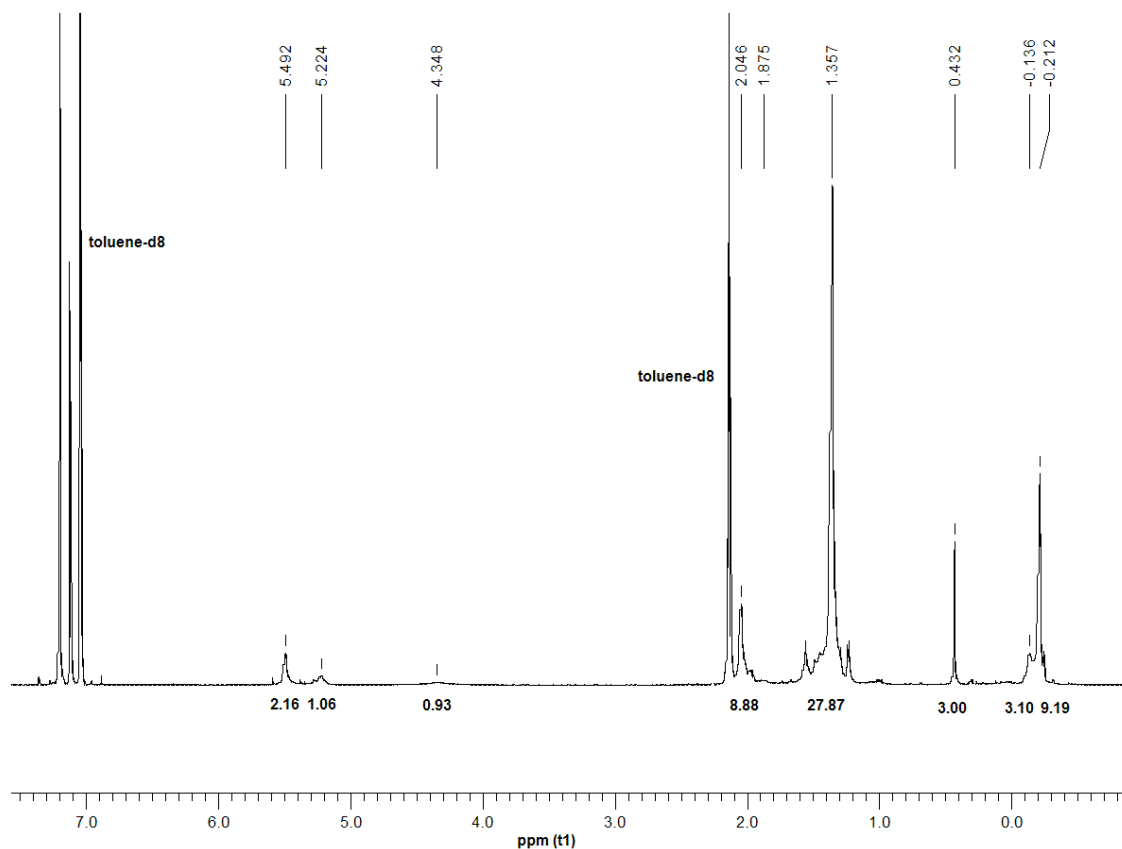


Fig. S4 ^1H NMR spectrum of compound **2b** in $\text{toluene-}d_8$ at $-60\text{ }^\circ\text{C}$. At $-60\text{ }^\circ\text{C}$ significant broadening of the resonances associated with the pyrazolylborate ligand is observed. While well-separated signals are already observed for H-4 ($\Delta\nu_{1/2} = 15\text{ Hz}$ and 32 Hz) the signals for the pz-CH_3 ($\Delta\nu_{1/2} = 13\text{ Hz}$) and $\text{pz-C(CH}_3)_3$ ($\Delta\nu_{1/2} = 13\text{ Hz}$) groups appear only significantly broadened.

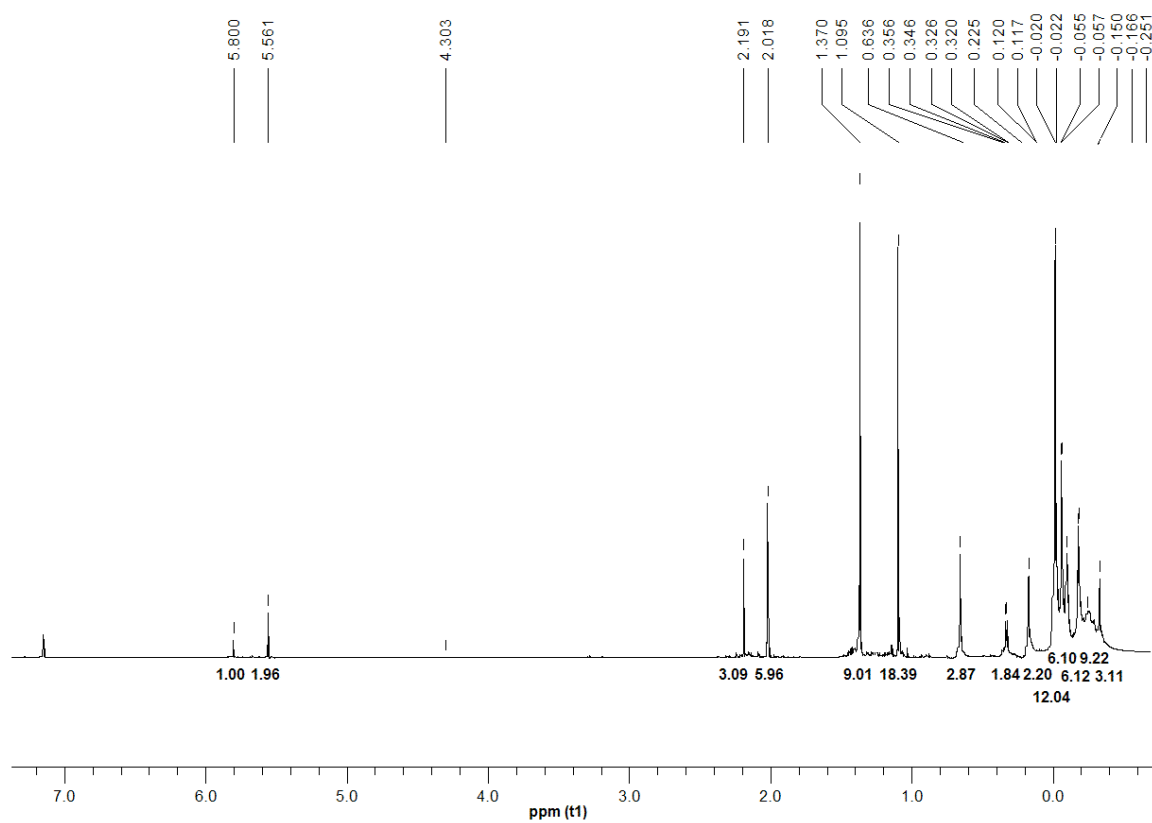


Fig. S5 ^1H NMR spectrum of compound **3** in benzene- d_8 at 25 °C.

Paper VI

Cationic Rare-Earth-Metal Half-Sandwich Complexes for the Living *trans*-1,4-Isoprene Polymerization**

Melanie Zimmermann, Karl W. Törnroos, and Reiner Anwander*

Dedicated to Professor William J. Evans on the occasion of his 60th birthday

Nature provides mankind with highly stereoregular polyterpenes, i.e., polymers of isoprene, featuring distinct properties.^[1] Natural rubber (NR, caoutchouc or *cis*-1,4-polyisoprene, cPIP; > 99% *cis* content, $M_n \approx 2 \times 10^6 \text{ g mol}^{-1}$) is the most important polymer produced by plants and is the raw material for numerous rubber applications. Taking into account new developments in synthetic polymer chemistry, a mechanism for living carbocationic polymerization has recently been proposed for NR biosynthesis.^[2] Gutta-percha obtained from *Palaquium gutta* and several other evergreen trees of East Asia is an isomer of NR displaying an all-*trans* (> 99%) configuration and much lower molecular weight ($M_n = 1.4\text{--}1.7 \times 10^5 \text{ g mol}^{-1}$).^[1] Unlike NR it is a thermoplastic crystalline polymer with a melting point (T_m) of 62 °C. Although for most applications gutta-percha has been superseded by advanced functional polymers, controlled cross-linking of synthetic *trans*-1,4-polyisoprene or its blending (with, for example, natural rubber, styrene-butadiene rubber, and butadiene rubber) and block copolymerization (e.g., with α -olefins) might afford new high-performance materials.^[3]

The synthesis of highly stereoregular cPIP with Ziegler-type catalysts is well established.^[4,5] In particular, catalyst mixtures with rare-earth-metal components such as neodymium represent a prominent class of high-performance catalysts for the industrial stereospecific polymerization (> 98% *cis*-1,4) of 1,3-dienes, even though the molecular weights and molecular weight distributions remain difficult to control.^[6] Molecular systems based on lanthanide metallocene and postmetallocene congeners afford polymers with very narrow molecular weight distributions and very high stereoregularity.^[7–10] A combination of [(C₅Me₅)₂Ln(AlMe₄)]/Al(*i*Bu)₃/[Ph₃C][B(C₆F₅)₄] (Ln = Sm, Gd) gave *cis*-1,4-polybutadiene with excellent stereocontrol (up to 99.9% *cis*) and narrow molecular weight distributions ($M_w/M_n = 1.20\text{--}1.23$), while the polymerization of isoprene was not observed to be living.^[7] cPIP with comparable characteristics (95–99% *cis*-

1,4; $M_w/M_n = 1.3\text{--}1.7$) was obtained with neodymium allyl complexes in the presence of aluminum alkyls as activators^[8,9] as well as with supported catalysts of the type Et₂AlCl@Nd(AlMe₄)₃@MCM-48.^[10] It was only recently that cationic lanthanide alkyl initiators [(PNP^{Ph})Ln(CH₂SiMe₃)(thf)₂]⁺ (PNP^{Ph} = {2-(Ph₂P)C₆H₄]₂N}, Ln = Sc, Y, Lu) were reported to yield high *cis*-1,4 selectivity in the living polymerization of isoprene and butadiene in the absence of any aluminum additive (> 99% *cis*-1,4; $M_w/M_n = 1.05$).^[11] The fabrication of synthetic gutta-percha and gutta-balata has been achieved by utilization of mixed organo-Ln/Mg initiators such as [(CMe₂C₅H₄)₂Sm(C₃H₅)MgCl₂(OEt₂)₂LiCl(OEt₂)] (> 95% *trans*-1,4; $M_w/M_n = 1.32$)^[12] and half-sandwich-based [(C₅Me₅*n*Pr)Nd(BH₄)₂(thf)₂]/Mg(*n*Bu)₂ (Mg/Nd = 0.9; 98.5% *trans*-1,4, $M_w/M_n = 1.15$).^[13–16]

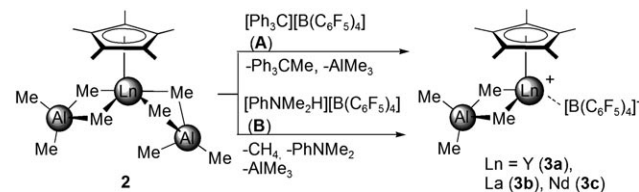
Intrigued by the exceptional catalytic performance of the cationic monocyclopentadienyl complexes [(C₅Me₅)(SiMe₃)Ln(CH₂SiMe₃)(thf)][B(C₆F₅)₄] developed by Hou et al.,^[17] we examined similar cationization reactions of our half-sandwich bis(tetramethylaluminate) complexes [(C₅Me₅)Ln(AlMe₄)₂]. Herein we describe the reactivity of these half-sandwich complexes toward fluorinated borate and borane activators as well as their catalytic performance in the polymerization of isoprene.

Half-sandwich complexes [(C₅Me₅)Ln(AlMe₄)₂] (Ln = Y (**2a**), La (**2b**), Nd (**2c**)) were synthesized according to the alkylaluminate route utilizing [Ln(AlMe₄)₃] (**1**) and [H-(C₅Me₅)].^[6b,18] In small-scale reactions of **2** (in NMR tubes) with one equivalent of [Ph₃C][B(C₆F₅)₄] (**A**) or [PhNMe₂H][B(C₆F₅)₄] (**B**) as solutions in C₆D₆, the NMR signals for **2** disappeared instantly and the quantitative formation of Ph₃CMe and one equivalent AlMe₃ and quantitative formation of PhNMe₂, one equivalent of AlMe₃, and CH₄, respectively, were observed (Scheme 1). New signals for the C₅Me₅ ligand appeared shifted to slightly higher field in accordance with a stronger coordination toward the highly electron-deficient rare-earth-metal cation. High-field shifts were also observed for the signals of the remaining [AlMe₄] ligand. The stability of cationic species **3**, however, signifi-

[*] M. Zimmermann, Prof. K. W. Törnroos, Prof. R. Anwander
 Department of Chemistry
 University of Bergen
 Allégaten 41, 5007 Bergen (Norway)
 Fax: (+47) 5558–9490
 E-mail: reiner.anwander@kj.uib.no

[**] Financial support from the Norwegian Research Council (Project No. 182547/130) and the program Nanoscience@UiB is gratefully acknowledged. We also thank Till Diesing (c/o Dr. Markus Klapper, MPI für Polymerforschung, Mainz (Germany)) for GPC analyses.

Supporting information for this article is available on the WWW under <http://www.angewandte.org> or from the author.

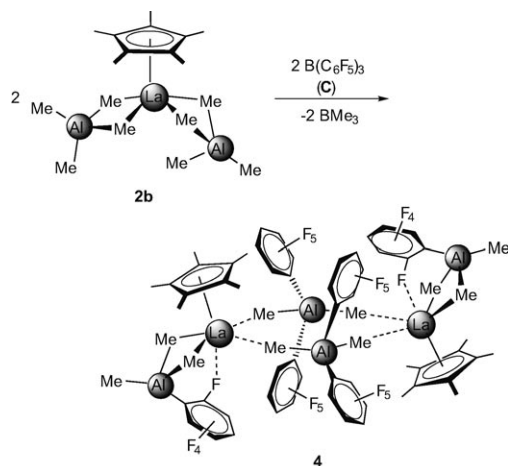


Scheme 1. Cationization of **2** with borate reagents **A** and **B**.

cantly depends on the size of the lanthanide cation ($\text{La} \gg \text{Nd} > \text{Y}$).

Ion pair $[(\text{C}_5\text{Me}_5)\text{La}(\text{AlMe}_4)][\text{B}(\text{C}_6\text{F}_5)_4]$ (**3b**), obtained from **2b** and **A**, dissolves in C_6D_6 or $\text{C}_6\text{D}_5\text{Cl}$, and such solutions are stable for several days enabling closer more-detailed NMR spectroscopic investigations. The ^{11}B NMR spectrum of **3b** in C_6D_6 revealed a broad resonance at $\delta = -16.2$ ppm, which, combined with a ^{19}F chemical shift difference for the *p*- and *m*-F atoms of $\delta = 4.2$ ppm, suggests the existence of a tight ion pair ($\text{C}_6\text{D}_5\text{Cl}$).^[19] A broad singlet at $\delta = -0.30$ ppm (12H) in the ^1H NMR spectrum clearly corresponds to one $[\text{AlMe}_4]$ ligand.^[20]

On the other hand, treatment of $[(\text{C}_5\text{Me}_5)\text{La}(\text{AlMe}_4)_2]$ (**2b**) with one equivalent of Lewis acidic $\text{B}(\text{C}_6\text{F}_5)_3$ (**C**) in $\text{C}_6\text{H}_5\text{Cl}$ at ambient temperature instantly and quantitatively yielded ion pair $[[[(\text{C}_5\text{Me}_5)\text{La}(\mu\text{-Me})_2\text{AlMe}(\text{C}_6\text{F}_5)]][\text{Me}_2\text{Al}(\text{C}_6\text{F}_5)_2]]_2$ (**4**) as the product of very fast sequential $\text{CH}_3/\text{C}_6\text{F}_5$ exchange processes (Scheme 2). **Caution:** Owing to the formation of thermal and shock-sensitive $[\text{Me}_2\text{Al}(\text{C}_6\text{F}_5)_2]^-$, extra caution should be exercised when handling this mixture, especially in higher concentrations.^[21,22]



Scheme 2. Synthesis of **4**.

Layering hexane on the reaction mixture of **2b** and **C** afforded light yellow single crystals of **4**.^[23] The X-ray diffraction study revealed a dimeric contact ion pair, in which two lanthanum-containing cationic units are bridged by two $[\text{Me}_2\text{Al}(\text{C}_6\text{F}_5)_2]$ anions (Figure 1). Comparatively short bonds $\text{La}\cdots\text{C1}$ (2.78(1) Å) and $\text{La}\cdots\text{C2}'$ (2.79(1) Å) suggest a tight interaction of the electron-deficient lanthanum cation with the counterion.^[24,25] (All hydrogen atoms at the sp^3 -hybridized C1 and C2 carbon atoms were located and refined isotropically.) The electron deficiency is further substantiated by significantly shortened $\text{La}-\text{C}(\text{C}_5\text{Me}_5)$ bonds (av. 2.66 Å versus 2.78 Å in **2b**).

Moreover, a $\text{CH}_3/\text{C}_6\text{F}_5$ exchange at the former tetramethylaluminate ligand facilitates a close $\text{La}\cdots\text{F}$ contact ($\text{La}\cdots\text{F5}$ 2.62(1) Å) in the solid state,^[26] which is apparently favored over $\{\text{La}(\mu\text{-Me})_3\text{Al}(\text{C}_6\text{F}_5)\}$ coordination.^[27] This $\text{La}\cdots\text{F}$ interaction results in an almost linear bond angle between the (C_5Me_5) centroid, the lanthanum center, and the adjacent

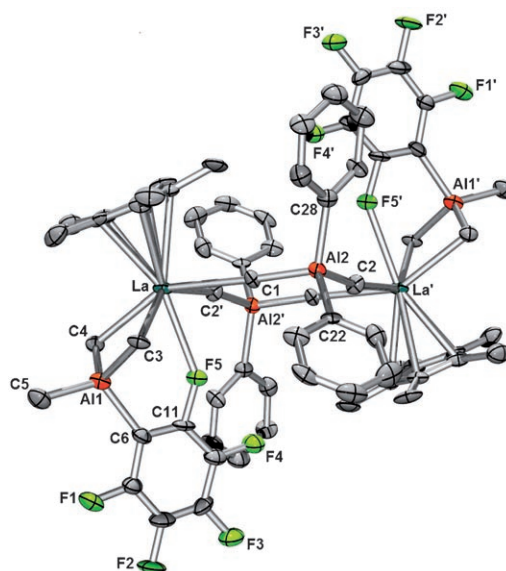


Figure 1. X-ray crystal structure of **4** (atomic displacement parameters set at the 50% level). Hydrogen atoms and fluorine atoms at $\text{Al}(\text{C}_6\text{F}_5)_2$ are omitted for clarity. Selected distances [Å] and angles [°]: $\text{La}-\text{C}(\text{C}_5\text{Me}_5)$ 2.63(1)–2.67(1), $\text{La}\cdots\text{C1}$ 2.78(1), $\text{La}\cdots\text{C2}'$ 2.79(1), $\text{La}-\text{C3}$ 2.62(1), $\text{La}-\text{C4}$ 2.65(1), $\text{La}\cdots\text{Al1}$ 3.16(1), $\text{Al1}-\text{C3}$ 1.99(1), $\text{Al1}-\text{C4}$ 1.98(1), $\text{Al1}-\text{C5}$ 1.88(1), $\text{Al1}-\text{C6}$ 1.95(1), $\text{Al2}-\text{C1}$ 1.96(1), $\text{Al2}-\text{C2}$ 1.95(1), $\text{Al2}-\text{C22}$ 1.95(1), $\text{Al2}-\text{C28}$ 1.96(1), $\text{La}\cdots\text{F5}$ 2.62(1); $\text{C1}\cdots\text{La}\cdots\text{C2}'$ 82.2(3), $\text{C3}-\text{La}-\text{C4}$ 76.8(4), $\text{La}-\text{C3}-\text{Al1}$ 85.1(4), $\text{La}-\text{C4}-\text{Al1}$ 84.5(4), $\text{C3}-\text{Al1}-\text{C5}$ 111.7(6), $\text{C3}-\text{Al1}-\text{C6}$ 101.2(5), $\text{La}-\text{C1}-\text{Al2}$ 169.3(6), $\text{La}-\text{C2}'-\text{Al2}'$ 176.8(5), $\text{La}\cdots\text{F5}-\text{C11}$ 139.8(7), $\text{C3}-\text{Al1}-\text{C4}$ 111.0(5), $\text{C1}-\text{Al2}-\text{C22}$ 108.9(5), $\text{C1}-\text{Al2}-\text{C28}$ 112.1(5), $\text{C2}-\text{Al2}-\text{C22}$ 109.6(5), $\text{C2}-\text{Al2}-\text{C28}$ 110.2(5), (C_5Me_5) (centroid)– $\text{La}\cdots\text{F5}$ 177.2(2) [symmetry code: $1-x, 1-y, 1-z$].

fluorine atom ((C_5Me_5) (centroid)– $\text{La}\cdots\text{F5}$ 177.2(2)°) and a considerable elongation of the C11–F5 bond to 1.35(1) Å. (The lengths of C–F bonds to noncoordinating fluorine atoms average to 1.30 Å).

The ^1H , ^{19}F , and ^{27}Al NMR spectra of **4** indicate a solution structure consistent with that observed in the solid state. Two sets of C_6F_5 resonances with $\Delta\delta_{m,p} = 5.5$ and 4.1 ppm appear in the ^{19}F NMR spectrum at 25 °C which are assigned to the $\{\text{Me}_2\text{Al}(\text{C}_6\text{F}_5)_2\}$ and $\{\text{AlMe}_3(\text{C}_6\text{F}_5)\}$ unit, respectively. However, the $\text{La}\cdots\text{F5}$ interaction appears to be less pronounced in solution, based on the absence of any upfield ^{19}F signals.^[28] Further evidence of two aluminium-containing moieties is provided by the ^{27}Al NMR spectrum, which exhibits two distinct signals at $\delta = 142$ and 157 ppm (**2b**: $\delta = 166$ ppm).^[29] Facile alkyl/ C_6F_5 exchange is a favorable reaction observed in several catalytic systems based on methylaluminumoxane (MAO)/ AlR_3 and $\text{M}(\text{C}_6\text{F}_5)_3$ ($\text{M} = \text{Al}, \text{B}$) activators and is commonly discussed as an undesirable catalyst-deactivation pathway.^[21,22,30]

In contrast, the cationic species generated in situ upon treatment of **2** with one equivalent of **A**, **B**, or **C** showed good to excellent activities for the polymerization of isoprene (Table 1).^[31] The stereoregularity of the produced polyisoprene corresponds very well to the stability of the cationic species (see above) and depends on the size of the rare-earth-metal cation and the boron activator involved. While high *cis*-

Table 1: Effect of Ln size and the cocatalyst on the polymerization of isoprene.

| Entry ^[a] | Precat. | Cocat. ^[b] | t [h] | Yield [%] | Structure ^[c] | | | $M_n(\times 10^5)^{[d]}$ | M_w/M_n | Eff. ^[e] |
|----------------------|----------------|-----------------------|-------|-----------|--------------------------|------------------|------|--------------------------|---------------------|---------------------|
| | | | | | <i>trans</i> -1,4- | <i>cis</i> -1,4- | 3,4- | | | |
| 1 | 2a (Y) | A | 24 | >99 | 20.6 | 60.5 | 18.9 | 0.2 | 8.95 | 3.98 |
| 2 | 2a (Y) | B | 24 | >99 | 28.7 | 43.5 | 27.8 | 0.6 | 1.59 | 1.06 |
| 3 | 2a (Y) | C | 24 | >99 | 93.6 | 1.9 | 4.5 | 0.9 | 1.78 | 0.82 |
| 4 | 2c (Nd) | A | 24 | >99 | 69.7 | 14.0 | 16.3 | 0.3 | 2.87 | 2.11 |
| 5 | 2c (Nd) | B | 24 | >99 | 79.9 | 6.9 | 13.2 | 0.4 | 1.16 | 1.73 |
| 6 | 2c (Nd) | C | 24 | >99 | 92.4 | 3.8 | 3.8 | 1.3 | 1.35 | 0.52 |
| 7 | 2b (La) | A | 24 | >99 | 87.0 | 3.5 | 9.5 | 0.7 | 1.28 | 1.98 |
| 8 | 2b (La) | B | 24 | >99 | 79.5 | 3.4 | 17.1 | 0.6 | 1.22 | 1.08 |
| 9 | 2b (La) | C | 24 | >99 | 99.5 | – | 0.5 | 2.4 | 1.18 | 0.28 |
| 10 | 2b (La) | A | 1 | >99 | 89.4 | 1.2 | 9.4 | 0.7 | 1.28 | 1.04 |
| 11 | 2b (La) | B | 1 | >99 | 87.5 | 2.9 | 9.6 | 0.7 | 1.23 | 1.04 |
| 12 | 2b (La) | C | 18 | >99 | 99.5 | – | 0.5 | 2.4 | 1.18 | 0.28 |
| 13 ^[f] | 2b (La) | A | 2 | >99 | 92.5 | 0.7 | 6.8 | 1.3 | 1.22 | 1.03 |
| 14 ^[f] | 2b (La) | B | 2 | >99 | 89.7 | 1.5 | 8.8 | 1.2 | 1.23 | 1.17 |
| 15 ^[g] | 2b (La) | C | 24 | >99 | 99.4 | – | 0.6 | 4.4 | 1.19 | 0.31 |
| 16 | 4 | – | 24 | >99 | 99.0 | 0.2 | 0.8 | 2.3 | 1.19 | 0.30 |
| 17 ^[h] | 2b (La) | C | 24 | >99 | 98.7 | – | 1.3 | n.d. ^[i] | n.d. ^[i] | – |

[a] Conditions: 0.02 mmol precatalyst, [Ln]/[cocat.] = 1:1, 8 mL toluene, 20 mmol isoprene, 24 h, 40 °C.

[b] Catalyst formed within 20 min at 40 °C. [c] Determined by ¹H and ¹³C NMR spectroscopy in CDCl₃.

[d] Determined by means of size-exclusion chromatography (SEC) against polystyrene standards.

[e] Initiation efficiency = $M_n(\text{calcd})/M_n(\text{found})$. [f] 12 mL toluene; after polymerization of 20 mmol of isoprene for 1 h, another 20 mmol of isoprene were added and the reaction mixture was stirred for another hour. [g] 12 mL toluene; after polymerization of 20 mmol of isoprene for 18 h, another 20 mmol of isoprene were added and the reaction mixture was stirred for another 6 h. [h] 8 mL hexane. [i] Not determined.

1,4 selectivity was a striking feature of tetramethylaluminum-containing catalyst mixtures reported so far (e.g., [Ln-(AlMe₄)₃] (**1**)/Et₂AlCl and [(C₅Me₅)₂Sm(AlMe₄)]/Al(*i*Bu)₃/[Ph₃C][B(C₆F₅)₄]),^[6,7,10] the catalyst systems reported herein afford highly regular *trans*-1,4 PIP.^[12–14] The *trans*-1,4 selectivity increases significantly with increasing size of the rare-earth-metal cation and when B(C₆F₅)₃ is used as the activator (Table 1, entries 1–9). Polyisoprene with very high *trans*-1,4 content (99.5 %) and very narrow molecular weight distributions ($M_w/M_n = 1.18$) could be obtained from a [(C₅Me₅)La(AlMe₄)₂]/B(C₆F₅)₃ catalyst mixture (Table 1, entry 9); this polymeric product has the highest *trans*-1,4 content so far reported for those generated with a homogeneous single-site catalyst.^[12–14] Signals assignable to *cis*-1,4-PIP units were not observed in the ¹³C NMR spectrum. Employing the isolated cationic complex **4** as catalyst under the same reaction conditions afforded *trans*-1,4-PIP with almost the same polymer properties (Table 1, entry 16); this supports the assumption that well-defined **4** serves as the catalytically active species in the catalyst mixture prepared *in situ*.

In accordance with a different activation mechanism, the use of **A** and **B** as activators for [(C₅Me₅)Ln(AlMe₄)₂] led to extremely high activity for the polymerization reactions, however, with lower *trans*-1,4 selectivity than that observed with **C** as the activator (up to 89.4 %, Table 1, entry 10). The highest number of *trans*-1,4 connectivities and very narrow molecular weight distributions were again observed for cationized derivatives of lanthanum precursor **2b** (Table 1, entries 7 and 8).

Catalyst precursor **2b** was therefore examined in more detail. Mixtures **2b/A** and **2b/B** afforded polyisoprene

quantitatively in 1 h (Table 1, entries 10 and 11). In both cases the activities of 68 kg mol⁻¹ h⁻¹ are a factor of 2 higher than those mentioned in literature for similar *trans*-specific polymerizations.^[12–14] Activities obtained for **2b/C** are comparatively low (Table 1, entry 12) because of a long induction period; however, the polymerization rates increase slowly with time (see the Supporting Information). The first insertion of an isoprene monomer into the La–Me bond of the very stable cation **4** appears to be kinetically disfavored and furthermore explains the low initiation efficiency (28 %). Theoretical studies on permethylated lanthanidocene catalysts point to a dependency of the monomer coordination on the steric hindrance around the metal center. Accordingly, the sterically crowded complex **4** is proposed to favor a single η^2 coordination of the diene over an η^4 coordination,

leading to *trans* polymerization.^[32] In any case, the molecular weight of the resulting polymers increased linearly with increasing isoprene conversion. Addition of another 1000 equivalents of monomer to a completed polymerization run yielded PIP with almost double the molecular weight, sustained high *trans*-1,4 selectivity, and narrow molecular weight distributions ($M_w/M_n = 1.19–1.23$, Table 1, entries 13–15).

In conclusion, cationization of donor-solvent-free half-sandwich complexes [(C₅Me₅)Ln(AlMe₄)₂] with fluorinated borate/borane reagents gave access to new initiators for controlled isoprene polymerization. The systematic investigation of the affect of the size of the metal ion and interactions with the cocatalyst (borate vs. borane) resulted in highly active, *trans*-1,4-selective (99.5 %) catalysts for the living polymerization. Successful isolation and structural characterization of the cationic complex **4** give unprecedented insights into the activation mechanism and provide a “single-component” catalyst for the production of polyisoprene with high *trans*-1,4 selectivity. Our findings point to a stabilizing effect of organoaluminum reagents for cationic rare-earth-metal half-sandwich complexes involving the formation of polymerization-active (fluorinated) tetraalkylaluminumate ligands.

Received: August 2, 2007

Revised: September 5, 2007

Published online: December 13, 2007

Keywords: aluminum · cations · isoprene · lanthanides · polymerization

- [1] *Biopolymers, Polyisoprenoids, Vol. 2* (Eds.: E. Koyama, A. Steinbüchel), Wiley-VCH, Weinheim, **2001**.
- [2] J. E. Puskas, E. Gautriaud, A. Deffieux, J. P. Kennedy, *Prog. Polym. Sci.* **2006**, *31*, 533.
- [3] J.-S. Song, B.-C. Huang, D.-S. Yu, *J. Appl. Polym. Sci.* **2001**, *82*, 81.
- [4] a) R. Taube, G. Sylvester in *Applied Homogeneous Catalysis with Organometallic Compounds* (Eds.: B. Cornils, W. A. Herrmann), Wiley-VCH, Weinheim, **2002**, pp. 280–318; b) L. Porri, A. Giarrusso in *Comprehensive Polymer Science, Vol. 4* (Eds.: G. C. Eastmond, A. Ledwith, S. Russo, P. Sigwalt), Pergamon, Oxford, **1989**, pp. 53–108.
- [5] S. K.-H. Thiele, D. R. Wilson, *J. Macromol. Sci. Polym. Rev. Part C* **2003**, *43*, 581.
- [6] a) L. Friebe, O. Nuyken, W. Obrecht, *Adv. Polym. Sci.* **2006**, *204*, 1; b) A. Fischbach, R. Anwander, *Adv. Polym. Sci.* **2006**, *204*, 155.
- [7] a) S. Kaita, Z. Hou, Y. Wakatsuki, *Macromolecules* **1999**, *32*, 9078; b) S. Kaita, Z. Hou, M. Nishiura, Y. Y. Doi, J. Kurazumi, A. C. Horiuchi, Y. Wakatsuki, *Macromol. Rapid Commun.* **2003**, *24*, 179; c) S. Kaita, Y. Doi, K. Kaneko, A. C. Horiuchi, Y. Wakatsuki, *Macromolecules* **2004**, *37*, 5860.
- [8] N. Ajellal, L. Furlan, C. M. Thomas, O. L. Casagrande Jr., J.-F. Carpentier, *Macromol. Rapid Commun.* **2006**, *27*, 338.
- [9] a) S. Maiwald, H. Weissenborn, H. Windisch, C. Sommer, G. Müller, R. Taube, *Macromol. Chem. Phys.* **1997**, *198*, 3305; b) S. Maiwald, C. Sommer, G. Müller, R. Taube, *Macromol. Chem. Phys.* **2001**, *202*, 1446; c) S. Maiwald, C. Sommer, G. Müller, R. Taube, *Macromol. Chem. Phys.* **2002**, *203*, 1029.
- [10] A. Fischbach, M. G. Klimpel, M. Widenmeyer, E. Herdtweck, W. Scherer, R. Anwander, *Angew. Chem.* **2004**, *116*, 2284; *Angew. Chem. Int. Ed.* **2004**, *43*, 2234.
- [11] L. Zhang, T. Suzuki, Y. Luo, M. Nishiura, Z. Hou, *Angew. Chem.* **2007**, *119*, 1941; *Angew. Chem. Int. Ed.* **2007**, *46*, 1909.
- [12] D. Barbier-Baudry, F. Bonnet, B. Domenichini, A. Dormond, M. Visseaux, *J. Organomet. Chem.* **2002**, *647*, 167.
- [13] F. Bonnet, M. Visseaux, A. Pereira, D. Barbier-Baudry, *Macromolecules* **2005**, *38*, 3162, and references therein.
- [14] For *trans*-1,4 polymerization of isoprene by NdCl₃ catalysts, see: a) J. H. Yang, M. Tsutsui, Z. Chen, D. E. Bergbreiter, *Macromolecules* **1982**, *15*, 230; b) Y. B. Monakov, Z. M. Sabirov, V. N. Urazbaev, V. P. Efimov, *Kinet. Catal.* **2001**, *42*, 310.
- [15] For *trans*-1,4 polymerization of butadiene by Ln allyl catalysts, see: a) S. Maiwald, H. Weissenborn, C. Sommer, G. Müller, R. Taube, *J. Organomet. Chem.* **2001**, *640*, 1, and references therein; b) D. Baudry-Barbier, N. Andre, A. Dormond, C. Pardes, P. Richard, M. Visseaux, C. J. Zhu, *Eur. J. Inorg. Chem.* **1998**, 1721.
- [16] For *trans*-1,4 polymerization of butadiene with Nd carboxylate/alk(aryl)oxide and magnesium alkyl components, see: a) D. K. Jenkins, *Polymer* **1985**, *26*, 147; b) J. Gromada, L. le Pichon, A. Montreux, F. Leising, J.-F. Carpentier, *J. Organomet. Chem.* **2003**, *683*, 44.
- [17] For a review, see: Z. Hou, Y. Luo, X. Li, *J. Organomet. Chem.* **2006**, *691*, 3114.
- [18] H. M. Dietrich, C. Zapilko, E. Herdtweck, R. Anwander, *Organometallics* **2005**, *24*, 5767.
- [19] a) A. D. Horton, *Organometallics* **1996**, *15*, 2675; b) A. D. Horton, J. de With, A. J. van der Linden, H. van de Weg, *Organometallics* **1996**, *15*, 2672.
- [20] a) The ion pair obtained from **2b** and **B** shows slightly different ¹H NMR chemical shifts for the [AlMe₄] moiety and AlMe₃, probably owing to interaction with [PhNMe₂]; b) The ¹H NMR spectrum of the [(C₅Me₅)Y(AlMe₄)] [B(C₆F₅)₄] (**3a**) shows almost identical signals and chemical shifts. The lifetime of the cationic complex in C₆D₆ at 25 °C, however, is limited and hampers further spectroscopic investigations.
- [21] For reactions of B(C₆F₅)₃ with AlR₃, see: a) J. S. Kim, L. M. Wojcinski II, S. Liu, J. C. Sworen, A. Sen, *J. Am. Chem. Soc.* **2000**, *122*, 5668; b) J. Klosin, G. R. Roof, E. Y.-X. Chen, *Organometallics* **2000**, *19*, 4684.
- [22] For reactions of [Ph₃C][B(C₆F₅)₄] with AlR₃, see: M. Bochmann, M. J. Sarsfield, *Organometallics* **1998**, *17*, 5908.
- [23] Compound **4** (C₆₆H₆₀Al₄F₃₀La₂, M_r = 1808.88) crystallizes from a hexane/chlorobenzene mixture in the triclinic space group P $\bar{1}$ with *a* = 12.0679(11), *b* = 13.0408(12), *c* = 13.2763(12) Å, α = 61.189(1), β = 66.538(1), γ = 89.390(2)°, *V* = 1636.1(3) Å³, and *d*_{calcd} = 1.836 g cm⁻³ for *Z* = 1. Data were collected at 103 K on a BRUKER-AXS 2K CCD system. The structure was solved by direct methods, and least-square refinement of the model based on 5750 (all data) and 4388 reflections (*I* > 2.0σ(*I*)) converged to a final *wR*₂ = 0.1924 and *R*₁ = 0.0903, respectively. CCDC 653206 contains the supplementary crystallographic data for this paper. These data can be obtained free of charge from The Cambridge Crystallographic Data Centre via www.ccdc.cam.ac.uk/data_request/cif.
- [24] For other examples of similar contact ion pairs, see: a) [(C₅H₄SiMe₃)₂Y{(μ-FC₆F₄)(μ-CH₃)(B(C₆F₅)_{2Organometallics **1998**, *17*, 1004; b) [(nacnac)Sc(CH₃)] [H₃CB(C₆F₅)₃] (nacnac = β-diketiminato); P. G. Hayes, W. E. Piers, R. McDonald, *J. Am. Chem. Soc.* **2002**, *124*, 2132.}
- [25] [(C₅Me₅)La(AlMe₄)₂] (**2b**): La–CH₃ av. 2.749 Å; [(C₅Me₅)₂La(AlMe₄)₂]: La–CH₃ av. 2.828 Å, H. M. Dietrich, E. Herdtweck, K. W. Törnroos, R. Anwander, unpublished results.
- [26] For an example of secondary La···F interactions in organometallic compounds, see: [(dme)₃Ln(SC₆F₅)₂][Hg₂(SC₆F₅)₄(μ₂-SC₆F₅)₂] (dme = 1,2-dimethoxyethane): 2.797(2) Å; S. Banerjee, T. J. Emge, J. G. Brennan, *Inorg. Chem.* **2004**, *43*, 6307.
- [27] M. Zimmermann, N. Å. Frøystein, A. Fischbach, P. Sirsch, H. M. Dietrich, K. W. Törnroos, E. Herdtweck, R. Anwander, *Chem. Eur. J.* **2007**, *13*, 8784.
- [28] B. Temme, G. Erker, J. Karl, H. Luftmann, R. Fröhlich, S. Kotila, *Angew. Chem.* **1995**, *107*, 1867; *Angew. Chem. Int. Ed. Engl.* **1995**, *34*, 1755.
- [29] Formation of BMe₃ could be proven by ¹H and ¹¹B NMR spectroscopy in C₆D₅Cl at 25 °C in an NMR tube equipped with a Young valve; signals at δ = 0.88 and 86.3 ppm, respectively, were observed.
- [30] P. G. Hayes, W. E. Piers, M. Parvez, *Organometallics* **2005**, *24*, 1173.
- [31] Compounds **2** did not show activity for the polymerization of isoprene without borate cocatalyst or with 1 equiv and 2 equiv of Me₂AlCl.
- [32] a) A. Peluso, R. Improta, A. Zambelli, *Organometallics* **2000**, *19*, 411; b) L. Friebe, O. Nuyken, H. Windisch, W. Obrecht, *Macromol. Chem. Phys.* **2002**, *203*, 1055; c) R. Taube, S. Maiwald, J. Sieler, *J. Organomet. Chem.* **2001**, *621*, 327; d) S. Kaita, N. Koga, Z. Hou, Y. Doi, Y. Wakatsuki, *Organometallics* **2003**, *22*, 3077; e) S. Tobisch, *Acc. Chem. Res.* **2002**, *35*, 96.

Kationische Halbsandwichkomplexe der Seltenerdmetalle für die lebende *trans*-1,4-Isoprenpolymerisation**

Melanie Zimmermann, Karl W. Törnroos und Reiner Anwander*

Professor William J. Evans zum 60. Geburtstag gewidmet

Die Natur erzeugt Polyterpene (Polymere des Isoprens) von außerordentlich hoher Stereoregularität, die sich durch sehr spezifische Eigenschaften auszeichnen.^[1] Naturkautschuk (NR, caoutchouc oder *cis*-1,4-Polyisopren [cPIP]; > 99% *cis*-Gehalt, $M_n = \text{ca. } 2 \times 10^6 \text{ g mol}^{-1}$) ist das wichtigste Polymer pflanzlichen Ursprungs und ist Ausgangsstoff zahlreicher Kautschukanwendungen. Unlängst wurde ein carbokationischer Polymerisationsmechanismus für die NR-Biosynthese postuliert.^[2] Guttapercha aus *Palaquium gutta* und anderen immergrünen Bäumen Ostasiens ist ein Isomer des NR, das eine all-*trans*-Konfiguration (> 99%) und erheblich niedrigere Molekulargewichte aufweist ($M_n = 1.4\text{--}1.7 \times 10^5 \text{ g mol}^{-1}$).^[1] Anders als NR ist es ein thermoplastisches, kristallines Polymer mit einem Schmelzpunkt (T_m) von 62 °C. Zwar wurde Guttapercha aus den meisten seiner Anwendungsgebiete von hoch entwickelten funktionellen Polymeren verdrängt, allerdings könnte die kontrollierte Vernetzung von synthetischem *trans*-1,4-Polyisopren oder seinen Mischungen (z. B. mit Naturkautschuk, Styrol-Butadien-Kautschuk, Butadienkautschuk) und die Herstellung von Block-Copolymeren (z. B. mit α -Olefinen) den Zugang zu neuen Hochleistungsmaterialien eröffnen.^[3]

Die Synthese von hoch stereoregulärem cPIP durch Ziegler-Katalysatoren ist ein etabliertes Verfahren.^[4,5] Katalysatormischungen, die Seltenerdmetallkomponenten wie Neodym enthalten, sind eine wichtige Klasse von Hochleistungskatalysatoren bei der industriellen, stereospezifischen 1,3-Dienpolymerisation (> 98% *cis*-1,4), auch wenn die Kontrolle der Molekulargewichte und Molekulargewichtsverteilungen noch immer Schwierigkeiten bereitet.^[6] Mithilfe von Lanthanoidocenen und Postmetallocenen konnten dagegen hoch stereoreguläre Polymere mit sehr engen Molekulargewichtsverteilungen erhalten werden.^[7–10] Die Mischung aus $[(C_5Me_5)_2Ln(AlMe_4)]/Al(iBu)_3/[Ph_3C][B(C_6F_5)_4]$ ($Ln = Sm, Gd$) lieferte *cis*-1,4-Polybutadien mit sehr hohem

cis-Anteil (bis zu 99.9%) und engen Molekulargewichtsverteilungen ($M_w/M_n = 1.20\text{--}1.23$); eine lebende Isoprenpolymerisation wurde jedoch nicht beobachtet.^[7] cPIP mit vergleichbaren Eigenschaften (95–99% *cis*-1,4; $M_w/M_n = 1.3\text{--}1.7$) konnte bei der Verwendung von Allyl-Nd-Komplexen in Gegenwart aktivierender Alkylaluminiumverbindungen erhalten werden,^[8,9] ebenso wie bei der Verwendung trägerfixierter Katalysatoren ($Et_2AlCl@Nd(AlMe_4)_3@MCM-48$).^[10] Kürzlich wurde von kationischen Alkylanthanoidinitiatoren $[(PNP^{Ph})Ln(CH_2SiMe_3)(thf)_2]^+$ ($PNP^{Ph} = \{[2-(Ph_2P)C_6H_4]_2N\}$, $Ln = Sc, Y, Lu$) berichtet, die sich durch hohe *cis*-1,4-Selektivität und eine lebende Polymerisation von Isopren und Butadien auszeichnen. Dies gelang ohne die Verwendung von Aluminiumadditiven (> 99% *cis*-1,4; $M_w/M_n = 1.05$).^[11] Die Herstellung von synthetischem Guttapercha oder Balatagummi gelingt mithilfe gemischter Organo-Ln/Mg-Initiatoren, darunter $[(CMe_2C_3H_4)_2Sm(C_3H_5)MgCl_2(OEt)_2LiCl(OEt_2)]$ (> 95% *trans*-1,4; $M_w/M_n = 1.32$)^[12] und der Halbsandwichkomplex $[(C_5Me_4nPr)Nd(BH_4)_2(thf)_2]/Mg(nBu)_2$ ($Mg/Nd = 0.9$; 98.5% *trans*-1,4, $M_w/M_n = 1.15$).^[13–16]

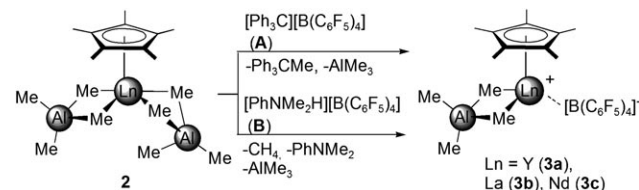
Die außergewöhnlichen katalytischen Eigenschaften der kationischen Monocyclopentadienylkomplexe $[(C_5Me_4(SiMe_3))Ln(CH_2SiMe_3)(thf)][B(C_6F_5)_4]$ von Hou et al.^[17] veranlassten uns nun, die entsprechende Kationisierung unserer Halbsandwich-Bis(tetramethylaluminat)-Komplexe $[(C_5Me_5)Ln(AlMe_4)_2]$ zu untersuchen. Wir berichten hier über die Reaktivität dieser Halbsandwichkomplexe gegen fluorierte Borat- und Boranaktivatoren und über ihre katalytischen Eigenschaften bei der Polymerisation von Isopren.

$[(C_5Me_5)Ln(AlMe_4)_2]$ ($Ln = Y$ (**2a**), La (**2b**), Nd (**2c**)) wurde mithilfe durch Alkaneliminierung aus $[Ln(AlMe_4)_3]$ (**1**) und $H(C_5Me_5)$ hergestellt.^[6b,18] Die NMR-spektroskopische Untersuchung der Reaktionen von **2** mit einem Äquivalent $[Ph_3C][B(C_6F_5)_4]$ (**A**) oder $[PhNMe_2H][B(C_6F_5)_4]$ (**B**) in C_6D_6 belegte das sofortige Verschwinden der Signale von **2** sowie die quantitative Bildung von Ph_3CMe und einem Äquivalent $AlMe_3$ bzw. von $PhNMe_2$ sowie je einem Äquivalent $AlMe_3$ und CH_4 (Schema 1). Neue Signale für die C_5Me_5 -Liganden waren leicht hochfeldverschoben, in Ein-

[*] M. Zimmermann, Prof. K. W. Törnroos, Prof. R. Anwander
Department of Chemistry
University of Bergen
Allégaten 41, 5007 Bergen (Norwegen)
Fax: (+47) 5558-9490
E-Mail: reiner.anwander@kj.uib.no

[**] Diese Arbeit wurde vom Norwegian Research Council (Projekt-Nr. 182547/I30) und dem Programm Nanoscience@UiB unterstützt. Ferner danken wir Till Diesing (bei Dr. Markus Klapper, MPI für Polymerforschung, Mainz) für GPC-Analysen.

Hintergrundinformationen (experimentelle und analytische Details) zu diesem Beitrag sind im WWW unter <http://www.angewandte.de> zu finden oder können beim Autor angefordert werden.

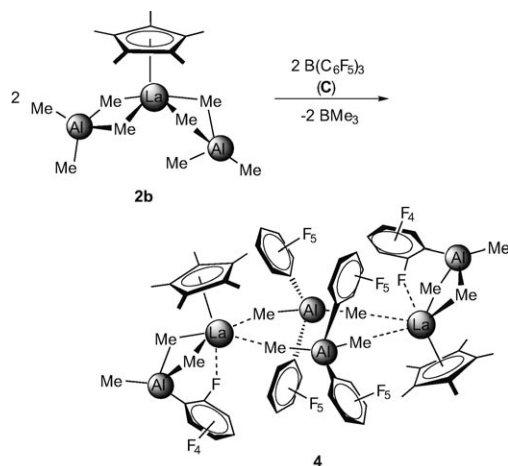


Schema 1. Kationisierung von **2** mit den Boratreagentien **A** und **B**.

klung mit einer stärkeren Koordination an das ausgeprägt elektronenarme Seltenerdmetallkation. Auch die Signale des verbleibenden $[\text{AlMe}_4]$ -Liganden waren hochfeldverschoben. Die Stabilität der kationischen Spezies **3** hängt signifikant von der Größe des Lanthanoidkations ab ($\text{La} \gg \text{Nd} > \text{Y}$).

$[(\text{C}_5\text{Me}_5)\text{La}(\text{AlMe}_4)][\text{B}(\text{C}_6\text{F}_5)_4]$ (**3b**), entstanden bei der Reaktion von **2b** mit **A**, löst sich in C_6D_6 oder $\text{C}_6\text{D}_5\text{Cl}$. Diese Lösungen sind mehrere Tage lang stabil, was eine genauere NMR-spektroskopische Untersuchung ermöglicht. Das ^{11}B -NMR-Spektrum von **3b** in C_6D_6 zeigt ein breites Signal bei $\delta = -16.2$ ppm, das in Kombination mit einem Abstand des *p*- und *m*-F-Signals von $\delta = 4.2$ ppm im ^{19}F -NMR-Spektrum ($\text{C}_6\text{D}_5\text{Cl}$) auf die Bildung eines Kontaktionenpaares hindeutet.^[19] Ein breites Singulett bei $\delta = -0.30$ ppm (12H) im ^1H -NMR-Spektrum kann eindeutig dem verbleibenden $[\text{AlMe}_4]$ -Liganden zugeordnet werden.^[20]

Die Umsetzung von $[(\text{C}_5\text{Me}_5)\text{La}(\text{AlMe}_4)_2]$ (**2b**) mit einem Äquivalent des Lewis-sauren $\text{B}(\text{C}_6\text{F}_5)_3$ (**C**) in $\text{C}_6\text{H}_5\text{Cl}$ bei Raumtemperatur führte zur sofortigen, quantitativen Bildung von $[\{[(\text{C}_5\text{Me}_5)\text{La}\{\mu\text{-}(\text{Me})_2\text{AlMe}(\text{C}_6\text{F}_5)\}][\text{Me}_2\text{Al}(\text{C}_6\text{F}_5)_2]\}_2]$ (**4**) als Produkt sehr schneller, sequenzieller $\text{CH}_3/\text{C}_6\text{F}_5$ -Austauschprozesse (Schema 2; **Vorsicht**: Wegen der Bildung von hitze- und schlagempfindlichem $[\text{Me}_2\text{Al}(\text{C}_6\text{F}_5)_2]^-$ sollte mit besonderer Vorsicht gearbeitet werden, speziell bei höheren Konzentrationen).^[21,22]



Schema 2. Synthese von **4**.

Bei Unterschichten einer Reaktionsmischung aus **2b** und **C** mit Hexan bildeten sich hellgelbe Einkristalle von **4**.^[23] Die Kristallstrukturanalyse ergab ein dimeres Kontaktionenpaar aus zwei La-haltigen kationischen Einheiten, die über zwei $[\text{Me}_2\text{Al}(\text{C}_6\text{F}_5)_2]^-$ -Ionen verbrückt sind (Abbildung 1). Relativ kurze Bindungen $\text{La}\cdots\text{C1}$ (2.78(1) Å) und $\text{La}\cdots\text{C2}'$ (2.79(1) Å) weisen auf eine starke Wechselwirkung des elektronenarmen Lanthankations und des Gegenions hin.^[24,25] (Alle Wasserstoffatome an den sp^3 -hybridisierten C1- und C2-Kohlenstoffatomen wurden lokalisiert und isotrop verfeinert.) Der Elektronenmangel zeigt sich des Weiteren an signifikant verkürzten $\text{La}\text{-C}(\text{C}_5\text{Me}_5)$ -Bindungen (durchschnittlich 2.66 Å gegenüber 2.78 Å in **2b**).

Ferner ermöglicht ein $\text{CH}_3/\text{C}_6\text{F}_5$ -Austausch am ehemaligen Tetramethylaluminatliganden einen nahen $\text{La}\cdots\text{F}$ -Kon-

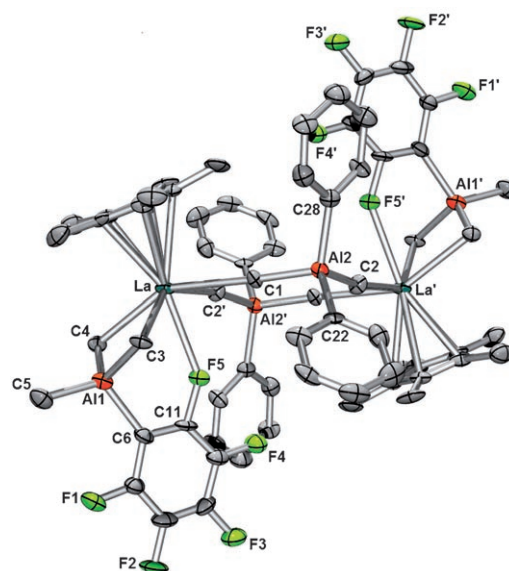


Abbildung 1. Molekülstruktur von **4** (die anisotropen Auslenkungsparameter entsprechen einer Aufenthaltswahrscheinlichkeit von 50%). Wasserstoffatome und Fluoratome an $\text{Al}(\text{C}_6\text{F}_5)_2$ sind nicht dargestellt. Ausgewählte Bindungslängen [Å] und -winkel [°]: $\text{La}\text{-C}(\text{C}_5\text{Me}_5)$ 2.63(1)–2.67(1), $\text{La}\cdots\text{C1}$ 2.78(1), $\text{La}\cdots\text{C2}'$ 2.79(1), $\text{La}\text{-C3}$ 2.62(1), $\text{La}\text{-C4}$ 2.65(1), $\text{La}\cdots\text{Al1}$ 3.16(1), $\text{Al1}\text{-C3}$ 1.99(1), $\text{Al1}\text{-C4}$ 1.98(1), $\text{Al1}\text{-C5}$ 1.88(1), $\text{Al1}\text{-C6}$ 1.95(1), $\text{Al2}\text{-C1}$ 1.96(1), $\text{Al2}\text{-C2}$ 1.95(1), $\text{Al2}\text{-C22}$ 1.95(1), $\text{Al2}\text{-C28}$ 1.96(1), $\text{La}\cdots\text{F5}$ 2.62(1); $\text{C1}\cdots\text{La}\cdots\text{C2}'$ 82.2(3), $\text{C3}\text{-La}\text{-C4}$ 76.8(4), $\text{La}\text{-C3}\text{-Al1}$ 85.1(4), $\text{La}\text{-C4}\text{-Al1}$ 84.5(4), $\text{C3}\text{-Al1}\text{-C5}$ 111.7(6), $\text{C3}\text{-Al1}\text{-C6}$ 101.2(5), $\text{La}\text{-C1}\text{-Al2}$ 169.3(6), $\text{La}\text{-C2}'\text{-Al2}'$ 176.8(5), $\text{La}\cdots\text{F5}\text{-C11}$ 139.8(7), $\text{C3}\text{-Al1}\text{-C4}$ 111.0(5), $\text{C1}\text{-Al2}\text{-C22}$ 108.9(5), $\text{C1}\text{-Al2}\text{-C28}$ 112.1(5), $\text{C2}\text{-Al2}\text{-C22}$ 109.6(5), $\text{C2}\text{-Al2}\text{-C28}$ 110.2(5), (C_5Me_5) (Zentroid)- $\text{La}\cdots\text{F5}$ 177.2(2) [Symmetriebedingung: $1-x, 1-y, 1-z$].

takt ($\text{La}\cdots\text{F5}$ 2.62(1) Å) in der Festkörperstruktur,^[26] der offensichtlich gegenüber einer $\{\text{La}(\mu\text{-}(\text{Me})_3\text{Al}(\text{C}_6\text{F}_5))\}$ -Koordination bevorzugt ist.^[27] Die $\text{La}\cdots\text{F}$ -Wechselwirkung führt zu einem nahezu linearen Bindungswinkel zwischen dem (C_5Me_5) -Zentroid, dem Lanthanzentrum und dem benachbarten Fluoratom ((C_5Me_5) (Zentroid)- $\text{La}\cdots\text{F5}$ 177.2(2)°) und zu einer erheblichen Verlängerung der C11-F5-Bindung auf 1.35(1) Å. (Die Längen von C-F-Bindungen mit nichtkoordinierendem Fluoratom betragen im Durchschnitt 1.30 Å.)

Die ^1H -, ^{19}F - und ^{27}Al -NMR-Spektren von **4** lassen auf eine Struktur in Lösung schließen, die in Einklang mit der Festkörperstruktur ist. Das ^{19}F -NMR-Spektrum weist bei 25°C zwei C_6F_5 -Signalsätze mit $\Delta\delta_{m,p} = 5.5$ und 4.1 ppm auf, die der $\{\text{Me}_2\text{Al}(\text{C}_6\text{F}_5)_2\}$ - und der $\{\text{AlMe}_3(\text{C}_6\text{F}_5)\}$ -Einheit zugeordnet werden können. Dem Fehlen von ^{19}F -Signalen bei hohem Feld zufolge scheint die $\text{La}\cdots\text{F5}$ -Wechselwirkung in Lösung jedoch weniger stark ausgeprägt zu sein.^[28] Einen weiteren Hinweis auf zwei Aluminium-haltige Einheiten liefert das ^{27}Al -NMR-Spektrum in Form zweier klar getrennter Signale bei $\delta = 142$ und 157 ppm (**2b**: $\delta = 166$ ppm).^[29] Der leichte Austausch von Alkyl- und C_6F_5 -Gruppen ist eine Reaktion, die in Katalysatorsystemen mit Methylaluminoxan-(MAO)/ AlR_3 - und $\text{M}(\text{C}_6\text{F}_5)_3$ -Aktivatoren ($\text{M} = \text{Al}, \text{B}$) beobachtet wurde und als unerwünschter Katalysator-Desaktivierungsweg gilt.^[21,22,30]

Dagegen zeigten die in situ aus **2** und einem Äquivalent **A**, **B** oder **C** gebildeten kationischen Spezies gute bis exzel-

lente Aktivitäten bei der Isoprenpolymerisation (Tabelle 1).^[31] Die Stereoregularität des hergestellten Polyisoprens ist in guter Übereinstimmung mit der Stabilität der kationischen Spezies (siehe oben) und hängt von der Größe des Seltenerdmetallkations und dem verwendeten Borreagens ab. Während die bisherigen Katalysatormischungen mit Tetramethylaluminat (z. B. $[\text{Ln}(\text{AlMe}_4)_3]$ (**1**)/ Et_2AlCl und $[(\text{C}_5\text{Me}_5)_2\text{Sm}(\text{AlMe}_4)]/\text{Al}(\text{iBu})_3/[\text{Ph}_3\text{C}][\text{B}(\text{C}_6\text{F}_5)_4]$,^[6,7,10] eine hohe *cis*-1,4-Selektivität ergaben, wurde mit den hier vorgestellten Katalysatorsystemen streng reguläres *trans*-1,4-PIP erhalten.^[12–14] Die *trans*-1,4-Selektivität erhöht sich maßgeblich mit größer werdendem Seltenerdmetallzentrum und durch die Verwendung von $\text{B}(\text{C}_6\text{F}_5)_3$ als Aktivator (Tabelle 1, Nr. 1–9). Mit der Katalysatormischung $[(\text{C}_5\text{Me}_5)\text{La}(\text{AlMe}_4)_2]/\text{B}(\text{C}_6\text{F}_5)_3$ wurde Polyisopren mit sehr hohem *trans*-1,4-Gehalt (99.5%) und sehr engen Molekulargewichtsverteilungen ($M_w/M_n=1.18$) erhalten (Tabelle 1, Nr. 9). Die Mischung lieferte damit ein Polymer mit dem bisher höchsten für einen homogenen Single-Site-Katalysator berichteten *trans*-1,4-Gehalt.^[12–14] Das ^{13}C -NMR-Spektrum enthält keine Signale, die auf *cis*-1,4-PIP-Einheiten hindeuten. Die Verwendung des isolierten kationischen Komplexes **4** unter denselben Reaktionsbedingungen lieferte *trans*-1,4-PIP mit nahezu gleichen Polymereigenschaften (Tabelle 1, Nr. 16), was die Vermutung stützt, dass es sich bei der definierten Verbindung **4** um die aktive Spezies der in situ hergestellten Katalysatormischung handelt.

In Einklang mit einem andersartigen Aktivierungsmechanismus führte die Verwendung von **A** und **B** als Aktivatoren für $[(\text{C}_5\text{Me}_5)\text{Ln}(\text{AlMe}_4)_2]$ zu einer sehr hohen Aktivität der lebenden Polymerisation. Die *trans*-1,4-Selektivität fiel jedoch niedriger aus als bei der Verwendung von **C** (bis zu

89.4%, Tabelle 1, Nr. 10). Wiederum wurden die höchste Zahl an *trans*-1,4-Verknüpfungen und sehr enge Molekulargewichtsverteilungen im Falle der kationischen Derivate der Lanthanvorstufe **2b** gefunden (Tabelle 1, Nr. 7 und 8).

2b wurde deshalb im Detail untersucht. Die Mischungen **2b/A** und **2b/B** führten binnen einer Stunde zur quantitativen Bildung von Polyisopren (Tabelle 1, Nr. 10 und 11). Die Aktivitäten liegen mit $68 \text{ kg mol}^{-1} \text{ h}^{-1}$ in beiden Fällen um einen Faktor 2 höher als diejenigen, die für analoge *trans*-spezifische Polymerisationen angegeben wurden.^[12–14] Wegen einer langen Induktionsperiode sind die Aktivitäten für **2b/C** relativ niedrig (Tabelle 1, Nr. 12). Die Polymerisationsrate erhöht sich jedoch langsam mit fortschreitender Reaktionszeit (Tabelle 1, Nr. 12, siehe auch die Hintergrundinformationen). Die erste Insertion eines Isoprenmonomers in die La-Me-Bindung des äußerst stabilen Kations **4** scheint kinetisch benachteiligt zu sein, was auch die niedrige Initiatoreffizienz (28%) erklärt. Theoretische Studien zu permethylierten Lanthanoidocenkatalysatoren deuten auf eine Abhängigkeit der Monomerkoordination vom Ausmaß der sterischen Hinderung am Metallzentrum hin. Folglich wird angenommen, dass der sterisch überfrachtete Komplex **4** eine einfache η^2 -Koordination des Diens gegenüber einer η^4 -Koordination bevorzugt, was in einer *trans*-spezifischen Polymerisation resultiert.^[32] In allen untersuchten Fällen nahm das Molekulargewicht des hergestellten Polymers linear mit dem Isoprenumsatz zu. Die Zugabe von weiteren 1000 Äquivalenten des Monomers zu einem abgeschlossenen Polymerisationsdurchlauf ergab PIP mit nahezu doppelt so hohem Molekulargewicht, unter Beibehaltung der hohen *trans*-1,4-Selektivität und der engen Molekulargewichtsverteilungen ($M_w/M_n=1.19$ – 1.23 , Tabelle 1, Nr. 13–15).

Die Kationisierung der Donorlösungsmittel-freien Halbsandwichkomplexe $[(\text{C}_5\text{Me}_5)\text{Ln}(\text{AlMe}_4)_2]$ durch fluorierte Borat- oder Boranokatalysatoren hat den Zugang zu neuartigen Initiatoren für die kontrollierte Isoprenpolymerisation eröffnet. Die systematische Untersuchung des Einflusses der Metallgröße und der Wechselwirkung mit dem Cokatalysator führte zu hochaktiven, *trans*-1,4-selektiven (99.5%) Katalysatoren für die lebende Isoprenpolymerisation. Die Isolierung und strukturelle Charakterisierung des kationischen Komplexes **4** gibt einen Einblick in den Aktivierungsmechanismus und liefert einen Einkomponentenkatalysator für die Synthese von Polyisopren mit sehr hohem *trans*-1,4-Gehalt. Unsere Befunde deuten auf einen stabilisierenden Effekt von Organoaluminiumreagentien auf kationische Halbsandwichkomplexe hin, der die Bildung eines poly-

Tabelle 1: Auswirkung der Ln-Größe und des Cokatalysators auf die Polymerisation von Isopren.^[a]

| Nr. | Präkat. | Cokat. ^[b] | t [h] | Ausb. [%] | Struktur ^[c] | | | $M_n^{[d]}(\times 10^5)$ | M_w/M_n | Eff. ^[e] |
|-------------------|----------------|-----------------------|---------|-----------|-------------------------|------------------|------|--------------------------|---------------------|---------------------|
| | | | | | <i>trans</i> -1,4- | <i>cis</i> -1,4- | 3,4- | | | |
| 1 | 2a (Y) | A | 24 | >99 | 20.6 | 60.5 | 18.9 | 0.2 | 8.95 | 3.98 |
| 2 | 2a (Y) | B | 24 | >99 | 28.7 | 43.5 | 27.8 | 0.6 | 1.59 | 1.06 |
| 3 | 2a (Y) | C | 24 | >99 | 93.6 | 1.9 | 4.5 | 0.9 | 1.78 | 0.82 |
| 4 | 2c (Nd) | A | 24 | >99 | 69.7 | 14.0 | 16.3 | 0.3 | 2.87 | 2.11 |
| 5 | 2c (Nd) | B | 24 | >99 | 79.9 | 6.9 | 13.2 | 0.4 | 1.16 | 1.73 |
| 6 | 2c (Nd) | C | 24 | >99 | 92.4 | 3.8 | 3.8 | 1.3 | 1.35 | 0.52 |
| 7 | 2b (La) | A | 24 | >99 | 87.0 | 3.5 | 9.5 | 0.7 | 1.28 | 1.98 |
| 8 | 2b (La) | B | 24 | >99 | 79.5 | 3.4 | 17.1 | 0.6 | 1.22 | 1.08 |
| 9 | 2b (La) | C | 24 | >99 | 99.5 | – | 0.5 | 2.4 | 1.18 | 0.28 |
| 10 | 2b (La) | A | 1 | >99 | 89.4 | 1.2 | 9.4 | 0.7 | 1.28 | 1.04 |
| 11 | 2b (La) | B | 1 | >99 | 87.5 | 2.9 | 9.6 | 0.7 | 1.23 | 1.04 |
| 12 | 2b (La) | C | 18 | >99 | 99.5 | – | 0.5 | 2.4 | 1.18 | 0.28 |
| 13 ^[f] | 2b (La) | A | 2 | >99 | 92.5 | 0.7 | 6.8 | 1.3 | 1.22 | 1.03 |
| 14 ^[f] | 2b (La) | B | 2 | >99 | 89.7 | 1.5 | 8.8 | 1.2 | 1.23 | 1.17 |
| 15 ^[g] | 2b (La) | C | 24 | >99 | 99.4 | – | 0.6 | 4.4 | 1.19 | 0.31 |
| 16 | 4 | – | 24 | >99 | 99.0 | 0.2 | 0.8 | 2.3 | 1.19 | 0.30 |
| 17 ^[h] | 2b (La) | C | 24 | >99 | 98.7 | – | 1.3 | n.b. ^[i] | n.b. ^[i] | – |

[a] Reaktionsbedingungen: 0.02 mmol Präkatalysator, $[\text{Ln}]/[\text{Cokat.}] = 1:1$, 8 mL Toluol, 20 mmol Isopren, 24 h, 40 °C. [b] Bildung des Katalysators binnen 20 min bei 40 °C. [c] Bestimmt durch ^1H - und ^{13}C -NMR-Spektroskopie in CDCl_3 . [d] Bestimmt durch Gelpermeationschromatographie (GPC) gegen Polystyrolstandards. [e] Initiatoreffizienz = $M_n(\text{ber.})/M_n(\text{gef.})$. [f] 12 mL Toluol; nach einstündiger Polymerisation von 20 mmol Isopren wurden weitere 20 mmol Isopren zugegeben, und die Reaktionsmischung wurde eine weitere Stunde gerührt. [g] 12 mL Toluol; nach der Polymerisation von 20 mmol Isopren innerhalb von 18 h wurden weitere 20 mmol Isopren zugegeben, und die Reaktionsmischung wurde weitere 6 h gerührt. [h] 8 mL Hexan. [i] Nicht bestimmt.

merisationsaktiven (fluorierten) Tetraalkylaluminatliganden umfasst.

Eingegangen am 2. August 2007,
veränderte Fassung am 5. September 2007
Online veröffentlicht am 13. Dezember 2007

Stichwörter: Aluminium · Isopren · Kationen · Lanthanoide · Polymerisationen

- [1] *Biopolymers, polyisoprenoids, Vol. 2* (Hrsg.: E. Koyama, A. Steinbüchel), Wiley-VCH, Weinheim, **2001**.
- [2] J. E. Puskas, E. Gautriaud, A. Deffieux, J. P. Kennedy, *Prog. Polym. Sci.* **2006**, *31*, 533.
- [3] J.-S. Song, B.-C. Huang, D.-S. Yu, *J. Appl. Polym. Sci.* **2001**, *82*, 81.
- [4] a) R. Taube, G. Sylvester in *Applied Homogeneous Catalysis with Organometallic Compounds* (Hrsg.: B. Cornils, W. A. Herrmann), Wiley-VCH, Weinheim, **2002**, S. 280–318; b) L. Porri, A. Giarrusso in *Comprehensive Polymer Science, Vol. 4* (Hrsg.: G. C. Eastmond, A. Ledwith, S. Russo, P. Sigwalt), Pergamon, Oxford, **1989**, S. 53–108.
- [5] S. K.-H. Thiele, D. R. Wilson, *J. Macromol. Sci., Part C* **2003**, *43*, 581.
- [6] a) L. Friebe, O. Nuyken, W. Obrecht, *Adv. Polym. Sci.* **2006**, *204*, 1; b) A. Fischbach, R. Anwender, *Adv. Polym. Sci.* **2006**, *204*, 155.
- [7] a) S. Kaita, Z. Hou, Y. Wakatsuki, *Macromolecules* **1999**, *32*, 9078; b) S. Kaita, Z. Hou, M. Nishiura, Y. Y. Doi, J. Kurazumi, A. C. Horiuchi, Y. Wakatsuki, *Macromol. Rapid Commun.* **2003**, *24*, 179; c) S. Kaita, Y. Doi, K. Kaneko, A. C. Horiuchi, Y. Wakatsuki, *Macromolecules* **2004**, *37*, 5860.
- [8] N. Ajellal, L. Furlan, C. M. Thomas, O. L. Casagrande Jr., J.-F. Carpentier, *Macromol. Rapid Commun.* **2006**, *27*, 338.
- [9] a) S. Maiwald, H. Weissenborn, H. Windisch, C. Sommer, G. Müller, R. Taube, *Macromol. Chem. Phys.* **1997**, *198*, 3305; b) S. Maiwald, C. Sommer, G. Müller, R. Taube, *Macromol. Chem. Phys.* **2001**, *202*, 1446; c) S. Maiwald, C. Sommer, G. Müller, R. Taube, *Macromol. Chem. Phys.* **2002**, *203*, 1029.
- [10] A. Fischbach, M. G. Klimpel, M. Widenmeyer, E. Herdtweck, W. Scherer, R. Anwender, *Angew. Chem.* **2004**, *116*, 2284; *Angew. Chem. Int. Ed.* **2004**, *43*, 2234.
- [11] L. Zhang, T. Suzuki, Y. Luo, M. Nishiura, Z. Hou, *Angew. Chem.* **2007**, *119*, 1941; *Angew. Chem. Int. Ed.* **2007**, *46*, 1909.
- [12] D. Barbier-Baudry, F. Bonnet, B. Domenichini, A. Dormond, M. Visseaux, *J. Organomet. Chem.* **2002**, *647*, 167.
- [13] F. Bonnet, M. Visseaux, A. Pereira, D. Barbier-Baudry, *Macromolecules* **2005**, *38*, 3162, zit. Lit.
- [14] *trans*-1,4-Polymerisation von Isopren mit NdCl_3 -Katalysatoren: a) J. H. Yang, M. Tsutsui, Z. Chen, D. E. Bergbreiter, *Macromolecules* **1982**, *15*, 230; b) Y. B. Monakov, Z. M. Sabirov, V. N. Urazbaev, V. P. Efimov, *Kinet. Catal.* **2001**, *42*, 310.
- [15] *trans*-1,4-Polymerisation von Butadien mit Allyl-Ln-Katalysatoren: a) S. Maiwald, H. Weissenborn, C. Sommer, G. Müller, R. Taube, *J. Organomet. Chem.* **2001**, *640*, 1, zit. Lit.; b) D. Baudry-Barbier, N. Andre, A. Dormond, C. Pardes, P. Richard, M. Visseaux, C. J. Zhu, *Eur. J. Inorg. Chem.* **1998**, 1721.
- [16] *trans*-1,4-Polymerisation von Butadien mit Carboxylat/Alkoxid-(Aryloxid)-Nd- und Alkylmagnesiumkomponenten: a) D. K. Jenkins, *Polymer* **1985**, *26*, 147; b) J. Gromada, L. le Pichon, A. Montreux, F. Leising, J.-F. Carpentier, *J. Organomet. Chem.* **2003**, *683*, 44.
- [17] Übersichtsartikel: Z. Hou, Y. Luo, X. Li, *J. Organomet. Chem.* **2006**, *691*, 3114.
- [18] H. M. Dietrich, C. Zapilko, E. Herdtweck, R. Anwender, *Organometallics* **2005**, *24*, 5767.
- [19] a) A. D. Horton, *Organometallics* **1996**, *15*, 2675; b) A. D. Horton, J. de With, A. J. van der Linden, H. van de Weg, *Organometallics* **1996**, *15*, 2672.
- [20] a) Das von **2b** und **B** gebildete Ionenpaar zeigt leicht veränderte chemische ^1H -Verschiebungen für die $[\text{AlMe}_4]$ -Einheit und AlMe_3 , vermutlich wegen einer Wechselwirkung mit $[\text{PhNMe}_2]$. b) Das ^1H -NMR-Spektrum von $[(\text{C}_5\text{Me}_5)\text{Y}(\text{AlMe}_4)][\text{B}(\text{C}_6\text{F}_5)_4]$ (**3a**) zeigt nahezu identische Signale und chemische Verschiebungen. Die Lebensdauer des kationischen Komplexes in C_6D_6 bei 25°C ist jedoch begrenzt, was weitere spektroskopische Untersuchungen erschwerte.
- [21] Reaktionen von $\text{B}(\text{C}_6\text{F}_5)_3$ mit AlR_3 : a) J. S. Kim, L. M. Wojcinski II, S. Liu, J. C. Sworen, A. Sen, *J. Am. Chem. Soc.* **2000**, *122*, 5668; b) J. Klosin, G. R. Roof, E. Y.-X. Chen, *Organometallics* **2000**, *19*, 4684.
- [22] Reaktionen von $[\text{Ph}_3\text{C}][\text{B}(\text{C}_6\text{F}_5)_4]$ mit AlR_3 : M. Bochmann, M. J. Sarsfield, *Organometallics* **1998**, *17*, 5908.
- [23] **4** ($\text{C}_{66}\text{H}_{60}\text{Al}_4\text{F}_{30}\text{La}_2$, $M_r = 1808.88$) kristallisiert aus einer Hexan/Chlorbenzol-Mischung in der triklinen Raumgruppe $P\bar{1}$ mit $a = 12.0679(11)$, $b = 13.0408(12)$, $c = 13.2763(12)$ Å, $\alpha = 61.189(1)$, $\beta = 66.538(1)$, $\gamma = 89.390(2)^\circ$, $V = 1636.1(3)$ Å³ und $d_{\text{ber.}} = 1.836$ g cm⁻³ für $Z = 1$. Die Daten wurden bei 103 K auf einem BRUKER-AXS-2K-CCD-Diffraktometer aufgenommen. Die Strukturlösung erfolgte durch Direkte Methoden und wurde nach der Methode der kleinsten Fehlerquadrate unter Einbeziehung von 5750 (vollständige Daten) und 4388 Reflexen ($I > 2.0\sigma(I)$) verfeinert; endgültige Werte: $wR2 = 0.1924$ und $R1 = 0.0903$. CCDC 653206 enthält die ausführlichen kristallographischen Daten zu dieser Veröffentlichung. Die Daten sind kostenlos beim Cambridge Crystallographic Data Centre über www.ccdc.cam.ac.uk/data_request/cif erhältlich.
- [24] Beispiele ähnlicher Kontaktionenpaare: a) $[(\text{C}_5\text{H}_4\text{SiMe}_3)_2\text{Y}\{\mu\text{-FC}_6\text{F}_4(\mu\text{-CH}_3)\text{B}(\text{C}_6\text{F}_5)_2\}]$, X. Song, M. Thornton-Pett, M. Bochmann, *Organometallics* **1998**, *17*, 1004; b) $\{[(\text{nacnac})\text{Sc}(\text{CH}_3)]\{\text{H}_3\text{CB}(\text{C}_6\text{F}_5)_3\}\}$ (nacnac = β -Diketiminato), P. G. Hayes, W. E. Piers, R. McDonald, *J. Am. Chem. Soc.* **2002**, *124*, 2132.
- [25] $[(\text{C}_5\text{Me}_5)\text{La}(\text{AlMe}_4)_2]$ (**2b**): La-CH₃ durchschnittlich 2.75 Å; $\{[(\text{C}_5\text{Me}_5)_2\text{La}(\text{AlMe}_4)_2]\}$: La-CH₃ durchschnittlich 2.83 Å, H. M. Dietrich, E. Herdtweck, K. W. Törnroos, R. Anwender, unveröffentlichte Ergebnisse.
- [26] Beispiel sekundärer La \cdots F-Wechselwirkungen in metallorganischen Verbindungen: $[(\text{dme})_3\text{Ln}(\text{SC}_6\text{F}_5)_2][\text{Hg}_2(\text{SC}_6\text{F}_5)_4(\mu_2\text{-SC}_6\text{F}_5)_2]$ (2.80(1) Å; dme = 1,2-Dimethoxyethan); S. Banerjee, T. J. Emge, J. G. Brennan, *Inorg. Chem.* **2004**, *43*, 6307.
- [27] M. Zimmermann, N. Å. Frøystein, A. Fischbach, P. Sirsch, H. M. Dietrich, K. W. Törnroos, E. Herdtweck, R. Anwender, *Chem. Eur. J.* **2007**, *13*, 8784.
- [28] B. Temme, G. Erker, J. Karl, H. Luftmann, R. Fröhlich, S. Kotila, *Angew. Chem.* **1995**, *107*, 1867; *Angew. Chem. Int. Ed. Engl.* **1995**, *34*, 1755.
- [29] Die Bildung von BMe_3 konnte durch ^1H - und ^{11}B -NMR-Spektroskopie in $\text{C}_6\text{D}_5\text{Cl}$ bei 25°C in einem Young-Teflonventil-NMR-Röhrchen nachgewiesen werden. Signale wurden bei $\delta = 0.88$ bzw. 86.3 ppm gefunden.
- [30] P. G. Hayes, W. E. Piers, M. Parvez, *Organometallics* **2005**, *24*, 1173.
- [31] Ohne Boratcokatalysator oder mit 1 Äquiv. und 2 Äquiv. Me_2AlCl zeigte **2** keine Aktivität bei der Isoprenpolymerisation.
- [32] a) A. Peluso, R. Improta, A. Zambelli, *Organometallics* **2000**, *19*, 411; b) L. Friebe, O. Nuyken, H. Windisch, W. Obrecht, *Macromol. Chem. Phys.* **2002**, *203*, 1055; c) R. Taube, S. Maiwald, J. Sieler, *J. Organomet. Chem.* **2001**, *621*, 327; d) S. Kaita, N. Koga, Z. Hou, Y. Doi, Y. Wakatsuki, *Organometallics* **2003**, *22*, 3077; e) S. Tobisch, *Acc. Chem. Res.* **2002**, *35*, 96.



Supporting Information

© Wiley-VCH 2007

69451 Weinheim, Germany

Living *trans*-1,4 Isoprene Polymerization by Cationic Single-Component Halflanthanidocene Complexes

Melanie Zimmermann, Karl W. Törnroos, and Reiner Anwander*

[*] Prof. Reiner Anwander, Melanie Zimmermann, and Prof. Karl W. Törnroos, Department of Chemistry, University of Bergen, Allégaten 41, 5007 Bergen, Norway, Fax.Nr.: +47 555 89490, E-mail: reiner.anwander@kj.uib.no

[**] Financial support from the Norwegian Research Council (Project No 171245/V30), the program Nanoscience@UiB, and the Fonds der Chemischen Industrie is gratefully acknowledged. We also thank Till Diesing (c/o Dr. Markus Klapper, MPI für Polymerforschung, Mainz (Germany)) for GPC analyses.

Experimental Details

General Procedures. All operations were performed with rigorous exclusion of air and water, using standard *Schlenk*, high-vacuum, and glovebox techniques (MBraun MBLab; <1 ppm O₂, <1 ppm H₂O). Hexane and toluene were purified by using *Grubbs* columns (MBraun SPS, solvent purification system) and stored in a glovebox. Monochlorobenzene was distilled from CaH₂ and degassed by the freeze-pump-thaw method. C₆D₆ was obtained from *Aldrich*, degassed, dried over Na for 24 h, and filtered. C₅HMe₄SiMe₃ and AlMe₃ were purchased from *Aldrich* and used as received. [Ph₃C][B(C₆F₅)₄], [PhNMe₂H][B(C₆F₅)₄], and [B(C₆F₅)₃] were purchased from *Boulder Scientific Company* and used without further purification. Homoleptic Ln(AlMe₄)₃ (**1**) (Ln = La, Nd, Y),^[27] and [(C₅Me₅)Ln(AlMe₄)₂] (**2**)^[18] were synthesized according to literature methods. Isoprene was dried over molecular sieves (3 Å) and distilled prior to use. The NMR spectra of air and moisture sensitive compounds were recorded by using *J. Young* valve NMR tubes at 25 °C on a *Bruker*-BIOSPIN-AV500 (5 mm BBO, ¹H: 500.13 Hz; ¹³C: 125.77 MHz). ¹H and ¹³C shifts are referenced to internal solvent resonances and reported in *parts per million* relative to TMS. ²⁷Al NMR spectra were recorded on the AV500 at 130.33 MHz. 2000 scans were averaged. The ²⁷Al chemical shifts are reported relative to an external reference: a solution of AlCl₃ in D₂O with a drop of concentrated HCl [Al(D₂O)₆³⁺]. ¹¹B NMR (161 MHz) spectra were referenced to an external standard of boron trifluoride diethyl etherate (0.0 ppm, C₆D₆). ¹⁹F NMR spectra (471 MHz) are referenced to external CFC₃. IR spectra were recorded on a *NICOLET Impact 410 FTIR* spectrometer as Nujol mulls sandwiched between CsI plates. Elemental analyses were performed on an *Elementar Vario EL III*. The molar masses (*M_w/M_n*) of the polymers were determined by size exclusion chromatography (SEC). Sample solutions (1.0 mg polymer per mL THF) were filtered through a 0.2 μm syringe filter prior to injection. SEC was operated with a pump supplied by *Waters* (type: Water510), and Ultrastyrigel[®] columns with pore sizes 500, 1 000, 10 000, and 100 000 Å were used. The signals were detected by a differential refractometer (*Waters* 410) and calibrated against polystyrene standards (*M_w/M_n* < 1.15). The flow rate was 1.0 mL min⁻¹. The microstructure of the polyisoprenes was examined via ¹H and ¹³C NMR experiments on the AV500 in CDCl₃ at room temperature, using TMS as internal standard.

Synthesis of [(C₅Me₅)La(AlMe₄)₂]⁺[B(C₆F₅)₄]⁻ (**3**) from (C₅Me₅)La(AlMe₄)₂ and [Ph₃C][B(C₆F₅)₄].

Preparation 1:

In a glovebox, (C₅Me₅)La(AlMe₄)₂ (**2b**) (15 mg, 0.03 mmol) and [Ph₃C][B(C₆F₅)₄] (30 mg, 0.03 mmol) were placed in a *J. Young* valve NMR tube and the tube was cooled to -30 °C. 0.5 mL of C₆D₆ (-10 °C) was added, the *J. Young* valve NMR tube sealed immediately, and the sample was slowly allowed to warm to 25 °C. ¹H NMR (500 MHz, C₆D₆, 25 °C): δ = 7.12-7.01 (m, 15 H, Ph), 2.04 (s, 3 H, CH₃), 1.74 (s, 15 H, CpCH₃), -0.39 (s br, 21 H, Al(CH₃)₄ and Al(CH₃)₃) ppm. ¹³C {¹H} NMR (126 MHz, C₆D₆, 25 °C): δ = 150.0 (C₆F₅), 149.6 (Ph), 148.1 (C₆F₅), 139.9, 138.3, 136.3 (C₆F₅), 130.1 (Ph), 126.2 (CpCH₃), 124.6 (Ph), 53.0 (Ph₃C), 30.7 (PhCCH₃), 10.9 (CpCH₃), 2.9 (Al(CH₃)₄), -7.2 (Al(CH₃)₃) ppm. ²⁷Al NMR (130 MHz, C₆D₆, 25 °C): δ = 162 (s br, Al(CH₃)₄ and Al(CH₃)₃) ppm. ¹¹B {¹H} NMR (161 MHz, C₆D₆, 25 °C): δ = -16.2 (s br) ppm.

Preparation 2:

In a glovebox, (C₅Me₅)La(AlMe₄)₂ (**2b**) (16 mg, 0.04 mmol) and [Ph₃C][B(C₆F₅)₄] (33 mg, 0.04 mmol) were placed in a *J. Young* valve NMR tube and the tube was cooled to -30 °C. 0.5 mL of C₆D₅Cl (-30 °C) was added, the *J. Young* valve NMR tube sealed immediately, and the sample was slowly allowed to warm to 25 °C. ¹H NMR (500 MHz, C₆D₅Cl, 25 °C): δ = 7.30-7.21 (m, 15 H, Ph), 2.18 (s, 3 H, CH₃), 2.00 (s, 15 H, CpCH₃), -0.17 (s br, 9 H, Al(CH₃)₃), -0.30 (s br, 12 H, Al(CH₃)₄) ppm. ¹⁹F NMR (471 MHz, C₆D₅Cl, 25 °C): δ = -130.7 (d, *o*-F), -159.9 (t, *p*-F), -164.1 (t, *m*-F) ppm.

Synthesis of $[(C_5Me_5)La(AlMe_4)]^+[B(C_6F_5)_4]^-$ (**3**) from $(C_5Me_5)La(AlMe_4)_2$ and $[PhNMe_2H][B(C_6F_5)_4]$.

Preparation 1:

In a glovebox, $(C_5Me_5)La(AlMe_4)_2$ (**2b**) (15 mg, 0.03 mmol) and $[PhNMe_2H][B(C_6F_5)_4]$ (27 mg, 0.03 mmol) were placed in a *J. Young* valve NMR tube and the tube was cooled to $-30\text{ }^\circ\text{C}$. 0.5 mL of C_6D_6 ($-10\text{ }^\circ\text{C}$) was added, the *J. Young* valve NMR tube sealed immediately, and the sample was slowly allowed to warm to $25\text{ }^\circ\text{C}$. Upon warming instant gas evolution was observed. ^1H NMR (500 MHz, C_6D_6 , $25\text{ }^\circ\text{C}$): $\delta = 7.01\text{--}6.85$ (m, 5 H, Ph), 2.31 (s, 3 H, NCH_3), 1.75 (s, 15 H, $CpCH_3$), 0.15 (s, CH_4), -0.41 (s, 9 H, $Al(CH_3)_3$), -0.66 (s br, 12 H, $Al(CH_3)_4$) ppm. ^{13}C $\{^1\text{H}\}$ NMR (126 MHz, C_6D_6 , $25\text{ }^\circ\text{C}$): $\delta = 150.0$, 148.1, 139.9, 138.3, 136.4 (C_6F_5), 129.5 (Ph), 126.2 ($CpCH_3$), 124.6, 120.3 (Ph), 45.5 ($PhN(CH_3)_2$), 11.0 ($CpCH_3$), 1.8 ($Al(CH_3)_4$), -7.2 ($Al(CH_3)_3$) ppm. ^{27}Al NMR (130 MHz, C_6D_6 , $25\text{ }^\circ\text{C}$): $\delta = 160$ (s br, $Al(CH_3)_4$ and $Al(CH_3)_3$) ppm. $^{11}\text{B}\{^1\text{H}\}$ NMR (161 MHz, C_6D_6 , $25\text{ }^\circ\text{C}$): $\delta = -16.2$ (s br) ppm.

Preparation 2:

In a glovebox, $(C_5Me_5)La(AlMe_4)_2$ (**2b**) (18 mg, 0.04 mmol) and $[PhNMe_2H][B(C_6F_5)_4]$ (33 mg, 0.04 mmol) were placed in a *J. Young* valve NMR tube and the tube was cooled to $-30\text{ }^\circ\text{C}$. 0.5 mL of C_6D_5Cl ($-30\text{ }^\circ\text{C}$) was added, the *J. Young* valve NMR tube sealed immediately, and the sample was slowly allowed to warm to $25\text{ }^\circ\text{C}$. Upon warming instant gas evolution was observed. ^1H NMR (500 MHz, C_6D_5Cl , $25\text{ }^\circ\text{C}$): $\delta = 7.31\text{--}7.16$ (m, 5 H, Ph), 2.73 (s, 3 H, NCH_3), 1.96 (s, 15 H, $CpCH_3$), -0.36 (s, 9 H, $Al(CH_3)_3$), -0.58 (s br, 12 H, $Al(CH_3)_4$) ppm. ^{19}F NMR (471 MHz, C_6D_5Cl , $25\text{ }^\circ\text{C}$): $\delta = -131.0$ (d, *o*-F), -160.3 (t, *p*-F), -164.4 (t, *m*-F) ppm.

Synthesis of $\{[(C_5Me_5)La[(\mu\text{-Me})_2AlMe(C_6F_5)]]^+[Me_2Al(C_6F_5)_2]_2\}_2$ (**4**).

Preparation 1:

In a glovebox, $(C_5Me_5)La(AlMe_4)_2$ (**2b**) (43 mg, 0.10 mmol) was dissolved in chlorobenzene (1 mL) and $B(C_6F_5)_3$ (50 mg, 0.10 mmol) dissolved in chlorobenzene (1 mL) was added slowly while the reaction mixture was shaken carefully (2 min). CAUTION: Due to the formation of thermal and shock sensitive $[Me_2Al(C_6F_5)_2]$, extra caution should be exercised when handling this mixture, especially in higher concentrations. The solution was layered with 1 mL of hexane and cooled to $-30\text{ }^\circ\text{C}$. Single crystals of **4** suitable for X-ray diffraction were obtained after 72 h.

Preparation 2:

In a glovebox, $(C_5Me_5)La(AlMe_4)_2$ (**2b**) (28 mg, 0.06 mmol) and $B(C_6F_5)_3$ (32 mg, 0.06 mmol) were placed in a *J. Young* valve NMR tube and the tube was cooled to $-30\text{ }^\circ\text{C}$. 0.5 mL of C_6D_6 ($-10\text{ }^\circ\text{C}$) was added, the *J. Young* valve NMR tube sealed immediately, and the sample was slowly allowed to warm to $25\text{ }^\circ\text{C}$. ^1H NMR (500 MHz, C_6D_6 , $25\text{ }^\circ\text{C}$): $\delta = 1.75$ (s, 30 H, $CpCH_3$), 0.72 (s, BMe_3), -0.04 (s br, 12 H, $(C_6F_5)_2Al(CH_3)_2$), -0.24 (s, 12 H, $Al(CH_3)_3$), -0.37 (s, 6 H, $Al(CH_3)_3$) ppm. ^{13}C $\{^1\text{H}\}$ NMR (126 MHz, C_6D_6 , $25\text{ }^\circ\text{C}$): $\delta = 155.6$, 151.0, 149.0, 143.1, 141.9, 139.4, 139.0, 138.6, 136.2, 130.5 (C_6F_5), 126.4 ($CpCH_3$), 14.9 ($B(CH_3)_3$), 10.9 ($CpCH_3$), 3.5 (s br, $Al(CH_3)_3$), -6.2 (s br, $(C_6F_5)_2Al(CH_3)_2$) ppm. ^{27}Al NMR (130 MHz, C_6D_6 , $25\text{ }^\circ\text{C}$): $\delta = 157$ (s br, $Al(CH_3)_3$), 142 (s br, $(C_6F_5)_2Al(CH_3)_2$) ppm.

Preparation 3:

In a glovebox, $(C_5Me_5)La(AlMe_4)_2$ (**2b**) (23 mg, 0.05 mmol) and $B(C_6F_5)_3$ (26 mg, 0.05 mmol) were placed in a *J. Young* valve NMR tube and the tube was cooled to $-30\text{ }^\circ\text{C}$. 0.5 mL of C_6D_5Cl ($-30\text{ }^\circ\text{C}$) was added, the *J. Young* valve NMR tube sealed immediately, and the sample was slowly allowed to warm to $25\text{ }^\circ\text{C}$. ^1H NMR (500 MHz, C_6D_5Cl , $25\text{ }^\circ\text{C}$): $\delta = 2.07$ (s, 30 H, $CpCH_3$), 0.88 (s, BMe_3), 0.12 (s br, 30 H, $(C_6F_5)_2Al(CH_3)_2$ and $Al(CH_3)_3$) ppm. ^{19}F NMR (471 MHz, C_6D_5Cl , $25\text{ }^\circ\text{C}$): $\delta = -120.8$ (s br, 8 F, *o*-F), -132.6 (d, 4 F, *o*-F), -153.7 (s br, 4 F, *p*-F), -159.2 (s br, 8 F, *m*-F), -159.5 (t, 2 F, *p*-F), -163.6 (t, 4 F, *m*-F) ppm. $^{11}\text{B}\{^1\text{H}\}$ NMR (161 MHz, C_6D_5Cl , $25\text{ }^\circ\text{C}$): $\delta = 86.3$ (s br, BMe_3) ppm.

Preparation 4:

In a glovebox, $(C_5Me_5)La(AlMe_4)_2$ (**2b**) (36 mg, 0.08 mmol) was dissolved in hexane (2 mL) and $B(C_6F_5)_3$ (41 mg, 0.08 mmol) dissolved in hexane (5 mL) was added slowly while the reaction mixture was shaken carefully (2 min). CAUTION: Due to the formation of thermal and shock sensitive $[Me_2Al(C_6F_5)_2]^-$, extra caution should be exercised when handling this mixture, especially in higher concentrations. Immediate formation of a white precipitate was observed. The solvent was carefully removed in vacuo to give **4** (143 mg, 0.79 mmol, 99%) as a powdery solid. Solid **4** can be stored under argon at $-30\text{ }^\circ\text{C}$ for two weeks without decomposition. Solutions of **4** in aromatic solvents are stable for min. 24 h. Elemental analysis (%) calcd for $C_{66}H_{60}F_{30}Al_4La_2$ (1808.901 g mol⁻¹): C 43.82; H 3.34; found: C 43.69; H 3.05.

Polymerization of Isoprene. A detailed polymerization procedure (run 27, Table 1) is described as a typical example. To a solution of **2b** (9 mg, 0.02 mmol) in toluene (8 mL) 1 equiv of $B(C_6F_5)_3$ (10 mg, 0.02 mmol) was added and the mixture aged at room temperature for 15 min. After the addition of isoprene (2.0 mL, 20 mmol) the polymerization was carried out at $40\text{ }^\circ\text{C}$ for 24 h. The polymerization mixture was poured onto a large quantity of acidified isopropanol containing 0.1% (w/w) 2,6-di-*tert*.butyl-4-methylphenol as a stabilizer. The polymer was washed with isopropanol and dried under vacuum at ambient temperature to constant weight. The polymer yield was determined gravimetrically.

Reaction of $\{(C_5Me_5)La[(\mu-Me)_2AlMe(C_6F_5)]\}^+[Me_2Al(C_6F_5)_2]^-$ (4**) with 10 equivalents of isoprene.** In a glovebox, $(C_5Me_5)La(AlMe_4)_2$ (**2b**) (9 mg, 0.02 mmol) and $B(C_6F_5)_3$ (10 mg, 0.02 mmol) were placed in a *J. Young* valve NMR tube and the tube was cooled to $-30\text{ }^\circ\text{C}$. 0.5 mL of C_6D_6 ($-10\text{ }^\circ\text{C}$) was added, followed by addition of 2 μL (1 eq) or 20 μL (10 eq) isoprene, respectively. The *J. Young* valve NMR tube was sealed immediately, and the sample was slowly allowed to warm to $25\text{ }^\circ\text{C}$. ^1H NMR spectra were measured hourly over a time period of 16 h and after 24 h.

^1H NMR spectra (500.13 MHz) of **4** with 10 eq of isoprene in C_6D_6 at $25\text{ }^\circ\text{C}$.

Monitoring the reaction of in situ prepared **4** with 10 eq of isoprene gave evidence for a long induction period (Figure S1). After 2 h only traces of oligomeric material could be observed, while polymerization rates increase with time according to the integral ratios of isoprene monomer (IP) and oligomeric isoprene (tPIP). Signals for (C_5Me_5) remain almost unchanged over time. A slight highfield shift and line broadening is observed for the methyl protons of the anionic moiety $[Me_2Al(C_6F_5)_2]^-$. Reasonably, the methyl signals of $\{La(\mu-Me)_2AlMe(C_6F_5)\}$ are most affected by the coordination/insertion of isoprene, as the monomer is assumed to insert into a La–Me bond of this moiety. The overall integral of $\{La(\mu-Me)_2AlMe(C_6F_5)\}$ methyl protons decreases but signals do not disappear completely (low initiation efficiency).

After 24 h catalyst decomposition can be recognized (Figure S1, 24 h).

Analogue experiments with in situ prepared **4** and 1 eq of isoprene revealed similar features as the ^1H NMR spectra depicted in Figure S1. They clearly showed the formation of metal-coordinated isoprene species as depicted in Figure S1, but further mechanistic details remain to be investigated.

In a polymerization experiment (following procedure “Polymerization of Isoprene”) with 20 mmol of isoprene, *trans*-PIP precipitate (high molecular weight) was obtained after ca. 8 h. When the polymerization was terminated after intervals of 1 h, 3 h, 6 h, 7 h only soluble low molecular weight PIP could be found.

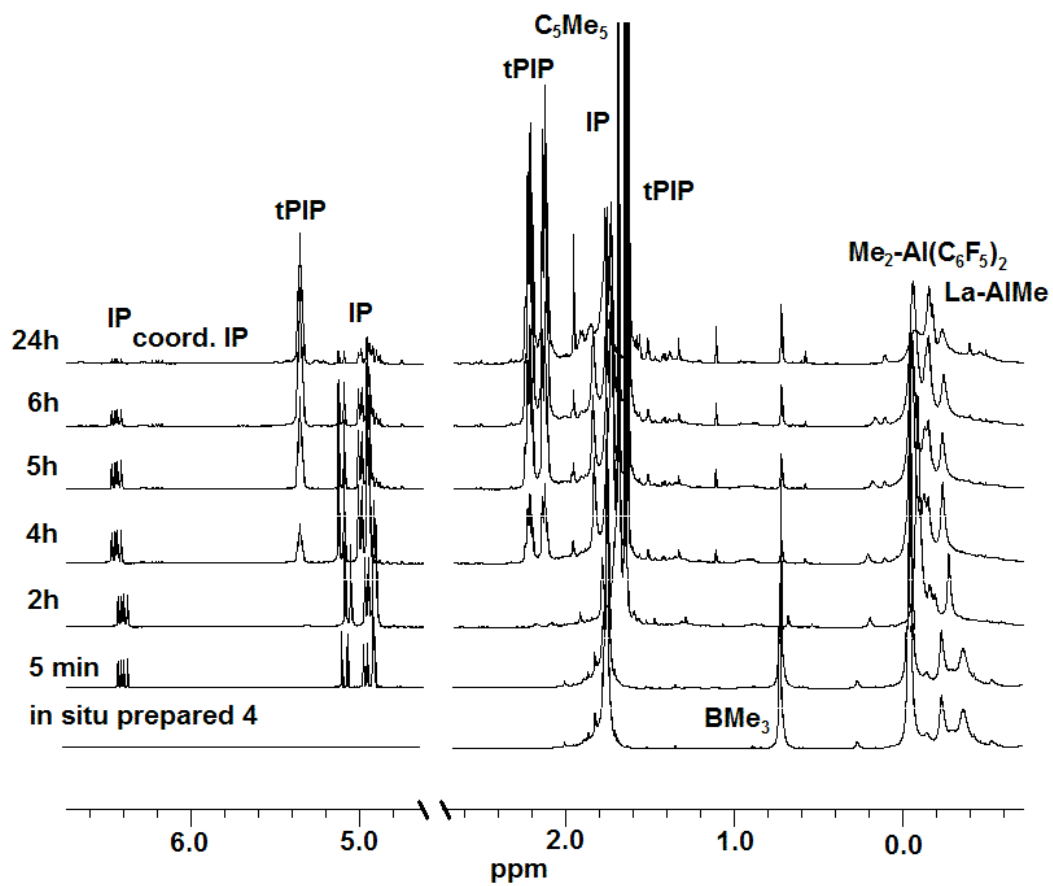


Figure S1. ^1H NMR spectra (500.13 MHz) of **4** with 10 equivalents of isoprene in C_6D_6 at 25°C .

Paper VII

Half-Sandwich Bis(tetramethylaluminate) Complexes of the Rare-Earth Metals: Synthesis, Structural Chemistry, and Performance in Isoprene Polymerization

Melanie Zimmermann,^[a] Karl W. Törnroos,^[a] Helmut Sitzmann,^[b] and Reiner Anwander*^[a]

Abstract: The protonolysis reaction of $[\text{Ln}(\text{AlMe}_4)_3]$ with various substituted cyclopentadienyl derivatives HCp^{R} gives access to a series of half-sandwich complexes $[\text{Ln}(\text{AlMe}_4)_2(\text{Cp}^{\text{R}})]$. Whereas bis(tetramethylaluminate) complexes with $[1,3-(\text{Me}_3\text{Si})_2\text{C}_5\text{H}_3]$ and $[\text{C}_5\text{Me}_4\text{SiMe}_3]$ ancillary ligands form easily at ambient temperature for the entire Ln^{III} cation size range ($\text{Ln} = \text{Lu}, \text{Y}, \text{Sm}, \text{Nd}, \text{La}$), exchange with the less reactive $[1,2,4-(\text{Me}_3\text{C})_3\text{C}_5\text{H}_3]$ was only obtained at elevated temperatures and for the larger metal centers Sm, Nd, and La. X-ray structure analyses of seven representative complexes of the type $[\text{Ln}(\text{AlMe}_4)_2(\text{Cp}^{\text{R}})]$ reveal a similar distinct $[\text{AlMe}_4]$ coordination (one η^2 , one bent η^2). Treatment with

Me_2AlCl leads to $[\text{AlMe}_4] \rightarrow [\text{Cl}]$ exchange and, depending on the Al/Ln ratio and the Cp^{R} ligand, varying amounts of partially and fully exchanged products $[\{\text{Ln}(\text{AlMe}_4)(\mu\text{-Cl})(\text{Cp}^{\text{R}})\}_2]$ and $[\{\text{Ln}(\mu\text{-Cl})_2(\text{Cp}^{\text{R}})\}_n]$, respectively, have been identified. Complexes $[\{\text{Y}(\text{AlMe}_4)(\mu\text{-Cl})(\text{C}_5\text{Me}_4\text{SiMe}_3)\}_2]$ and $[\{\text{Nd}(\text{AlMe}_4)(\mu\text{-Cl})\{1,2,4-(\text{Me}_3\text{C})_3\text{C}_5\text{H}_2\}\}_2]$ have been characterized by X-ray structure analysis. All of the chlorinated half-sandwich complexes are inactive in isoprene polymerization. However, activation of

the complexes $[\text{Ln}(\text{AlMe}_4)_2(\text{Cp}^{\text{R}})]$ with boron-containing cocatalysts, such as $[\text{Ph}_3\text{C}][\text{B}(\text{C}_6\text{F}_5)_4]$, $[\text{PhNMe}_2\text{H}][\text{B}(\text{C}_6\text{F}_5)_4]$, or $\text{B}(\text{C}_6\text{F}_5)_3$, produces initiators for the fabrication of *trans*-1,4-polyisoprene. The choice of rare-earth metal cation size, Cp^{R} ancillary ligand, and type of boron cocatalyst crucially affects the polymerization performance, including activity, catalyst efficiency, living character, and polymer stereoregularity. The highest stereoselectivities were observed for the precatalyst/cocatalyst systems $[\text{La}(\text{AlMe}_4)_2(\text{C}_5\text{Me}_4\text{SiMe}_3)]/\text{B}(\text{C}_6\text{F}_5)_3$ (*trans*-1,4 content: 95.6%, $M_w/M_n = 1.26$) and $[\text{La}(\text{AlMe}_4)_2(\text{C}_5\text{Me}_5)]/\text{B}(\text{C}_6\text{F}_5)_3$ (*trans*-1,4 content: 99.5%, $M_w/M_n = 1.18$).

Keywords: aluminum • boron • cyclopentadienyl ligands • isoprene • lanthanides • polymerization

Introduction

Bis(alkyl) complexes of the type $[\text{Ln}^{\text{III}}(\text{Do})(\text{L})\text{R}_2]$ bearing a monoanionic ancillary ligand (L^-) ($\text{R} = \text{CH}_2\text{SiMe}_3, \text{CH}_2\text{Ph}^{\text{R}}$; Do = neutral donor ligand) have proved to be extremely versatile catalyst precursors in organolanthanide-promoted polymerization reactions.^[1–5] In particular, Hou and Okuda noted a remarkable performance of these discrete com-

plexes in catalytic polymerizations of styrene and 1,3-diene following cationization with borate activators.^[1b, e, f, g, 2e, 4a] Pivotal structure–reactivity relationships revealed specific effects of the Ln^{III} cation size and the nature of the ancillary ligand (L^-) on the performance in polymerization, including activity, efficiency, living character, and polymer stereoregularity.^[1b, 2e, 4a, 6] For example, the cationic complex $[\text{Y}(\text{CH}_2\text{SiMe}_3)(\text{C}_5\text{Me}_4\text{SiMe}_3)(\text{thf})][\text{B}(\text{C}_6\text{F}_5)_4]$ has been reported to act as a highly efficient initiator for the syndiospecific polymerization of styrene (>99% *syndio*; $M_w/M_n = 1.39$),^[1b] while it showed only poor selectivity in the polymerization of isoprene (66% 3,4-; $M_w/M_n = 1.06$).^[6] On the other hand, complexes $[\text{Ln}(\text{CH}_2\text{SiMe}_3)(\text{PNP}^{\text{Ph}})(\text{thf})_2][\text{B}(\text{C}_6\text{F}_5)_4]$ ($\text{PNP}^{\text{Ph}} = [\{2-(\text{Ph}_2\text{P})\text{C}_6\text{H}_4\}_2\text{N}]$; $\text{Ln} = \text{Sc}, \text{Y}, \text{Lu}$) bearing an amido ancillary ligand afforded high *cis*-1,4 selectivity and “livingness” in the polymerization of isoprene in the absence of any aluminum additive (>99% *cis*-1,4; $M_w/M_n = 1.05$).^[4a]

[a] Dr. M. Zimmermann, Prof. Dr. K. W. Törnroos, Prof. Dr. R. Anwander
Department of Chemistry, University of Bergen
Allégaten 41, 5007 Bergen (Norway)
Fax: (+47) 5558-9490
E-mail: reiner.anwander@kj.uib.no

[b] Prof. Dr. H. Sitzmann
FB Chemie, Technische Universität Kaiserslautern
Erwin-Schrödinger-Straße 52, 67633 Kaiserslautern (Germany)

We have recently introduced half-sandwich bis(tetramethylaluminate) rare-earth metal complexes of the type $[\text{Ln}^{\text{III}}(\text{AlMe}_4)_2(\text{L})]$ ($\text{L} = \text{C}_5\text{Me}_5$) as alternative bis(hydrocarbyl) derivatives.^[7,8] The reactivity pattern of such alkylaluminate complexes is consistent with their formulation as “alkyls in disguise”, that is, $[\text{Ln}^{\text{III}}(\text{AlMe}_3)_2\text{Me}_2(\text{L})]$. Their most striking features are: a) availability for the entire Ln^{III} cation size range;^[9] b) accessibility by versatile synthesis protocols comprising both protonolysis and salt metathesis approaches;^[7,8,10] c) enhanced thermal stability (e.g., $[\text{Ln}(\text{AlMe}_4)_2(\text{C}_5\text{Me}_5)]$ may be sublimed) and hence suitability for storage;^[11] d) coordinational flexibility of the $[\text{AlMe}_4]$ ligands, as evidenced by $\eta^{1/2/3}$ coordination modes;^[9,12–14] e) an absence of coordinating donor molecules (Do);^[15] and f) the presence of AlMe_3 as an internal solvent scavenger.^[16] Moreover, our previous work highlighted the pivotal role of heterobimetallic $[\text{Ln}(\mu\text{-R})_n\text{Al}]$ moieties in the activation of rare-earth metal-based Ziegler-type catalysts.^[17–20] Based on these mechanistic insights and the favorable chemical and structural features of alkylaluminate ligands, we set out to develop a bis(tetramethylaluminate) postmetallocene library, considering carbocyclic (e.g., cyclopentadienyl),^[7,8] heterocyclic (e.g., phosphacyclopentadienyl),^[10] *N*-donor (e.g., amido),^[13,21] as well as *O*-donor (e.g., alkoxo) ancillary ligands **L** (Figure 1).^[20] The aim of creating this postmetallocene library is to gain a fundamental understanding of ancillary ligand and cocatalyst effects, and hence to elucidate the structure–reactivity relationships in non-metallocene polymerization catalysis.

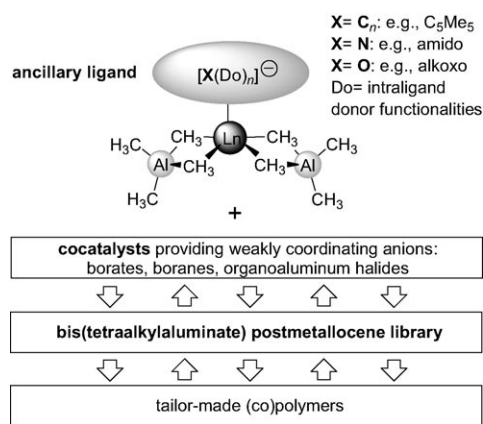


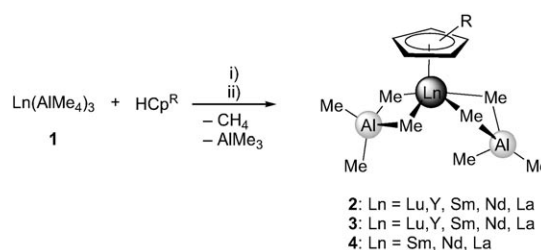
Figure 1. Rare-earth metal-based bis(tetraalkylaluminate) postmetallocene library.

Recently, we reported the remarkable potential of $[\text{Ln}(\text{AlMe}_4)_2(\text{C}_5\text{Me}_5)]$ to initiate the living *trans*-1,4 stereospecific polymerization of isoprene (*trans*-1,4 selectivity up to 99.5%), and hence the fabrication of synthetic gutta-percha.^[22] Herein, we present a more comprehensive account of the synthesis and structural chemistry of half-sandwich complexes $[\text{Ln}(\text{AlMe}_4)_2(\text{Cp}^{\text{R}})]$ containing various substituted cyclopentadienyl ancillary ligands.^[23] Special emphasis is placed on their catalytic performance in the polymeri-

zation of isoprene, considering precatalyst–cocatalyst interactions and structure–reactivity relationships.

Results and Discussion

Synthesis and structural chemistry of half-sandwich bis(tetramethylaluminate) complexes $[\text{Ln}(\text{AlMe}_4)_2(\text{Cp}^{\text{R}})]$: Protonolysis of homoleptic $[\text{Ln}(\text{AlMe}_4)_3]$ complexes ($\text{Ln} = \text{Lu}$ (**1a**), Y (**1b**), Sm (**1c**), Nd (**1d**), and La (**1e**))^[9] with one equivalent of substituted HCp^{R} ($\text{Cp}^{\text{R}} = [1,3-(\text{Me}_3\text{Si})_2\text{C}_5\text{H}_3]$ ^[24] and $[\text{C}_5\text{Me}_4\text{SiMe}_3]$) in hexane at ambient temperature yielded the corresponding bis(tetramethylaluminate) complexes $[\text{Ln}(\text{AlMe}_4)_2(\text{Cp}^{\text{R}})]$ (**2** and **3**) in quantitative yields (Scheme 1).^[25] Instant gas evolution evidenced the anticipated methane elimination reaction, and hence the immediate acid–base reaction of $[\text{Ln}(\text{AlMe}_4)_3]$ and the respective substituted cyclopentadiene. (CAUTION: volatiles containing trimethylaluminum react violently when exposed to air).



Scheme 1. Synthesis of $[\text{Ln}(\text{AlMe}_4)_2(\text{Cp}^{\text{R}})]$: i) hexane, 5 h, RT, ($\text{Ln} = \text{Lu}$, $\text{Cp}^{\text{R}} = [1,3-(\text{Me}_3\text{Si})_2\text{C}_5\text{H}_3]$ (**2a**); $\text{Ln} = \text{Y}$, $\text{Cp}^{\text{R}} = [1,3-(\text{Me}_3\text{Si})_2\text{C}_5\text{H}_3]$ (**2b**); $\text{Ln} = \text{Sm}$, $\text{Cp}^{\text{R}} = [1,3-(\text{Me}_3\text{Si})_2\text{C}_5\text{H}_3]$ (**2c**); $\text{Ln} = \text{Nd}$, $\text{Cp}^{\text{R}} = [1,3-(\text{Me}_3\text{Si})_2\text{C}_5\text{H}_3]$ (**2d**); $\text{Ln} = \text{La}$, $\text{Cp}^{\text{R}} = [1,3-(\text{Me}_3\text{Si})_2\text{C}_5\text{H}_3]$ (**2e**); $\text{Ln} = \text{Lu}$, $\text{Cp}^{\text{R}} = [\text{C}_5\text{Me}_4\text{SiMe}_3]$ (**3a**); $\text{Ln} = \text{Y}$, $\text{Cp}^{\text{R}} = [\text{C}_5\text{Me}_4\text{SiMe}_3]$ (**3b**); $\text{Ln} = \text{Sm}$, $\text{Cp}^{\text{R}} = [\text{C}_5\text{Me}_4\text{SiMe}_3]$ (**3c**); $\text{Ln} = \text{Nd}$, $\text{Cp}^{\text{R}} = [\text{C}_5\text{Me}_4\text{SiMe}_3]$ (**3d**); $\text{Ln} = \text{La}$, $\text{Cp}^{\text{R}} = [\text{C}_5\text{Me}_4\text{SiMe}_3]$ (**3e**)); ii) toluene, 24 h, 100 °C ($\text{Ln} = \text{Sm}$, $\text{Cp}^{\text{R}} = [1,2,4-(\text{Me}_3\text{C})_3\text{C}_5\text{H}_2]$ (**4c**); $\text{Ln} = \text{Nd}$, $\text{Cp}^{\text{R}} = [1,2,4-(\text{Me}_3\text{C})_3\text{C}_5\text{H}_2]$ (**4d**); $\text{Ln} = \text{La}$, $\text{Cp}^{\text{R}} = [1,2,4-(\text{Me}_3\text{C})_3\text{C}_5\text{H}_2]$ (**4e**)).

Attempts to prepare half-sandwich derivatives containing the sterically demanding and electronically deactivated $[1,2,4-(\text{Me}_3\text{C})_3\text{C}_5\text{H}_2]$ ligand by the same procedure were unsuccessful.^[26] However, heating $[\text{Ln}(\text{AlMe}_4)_3]$ ($\text{Ln} = \text{Sm}$ (**1c**), Nd (**1d**), La (**1e**)) with one equivalent of $[1,2,4-(\text{Me}_3\text{C})_3\text{C}_5\text{H}_2]$ in toluene at 100 °C for 24 h resulted in the formation of $[\text{Ln}(\text{AlMe}_4)_2[1,2,4-(\text{Me}_3\text{C})_3\text{C}_5\text{H}_2]]$ (**4**) in good yields (Scheme 1). Nevertheless, the availability of complexes **4** bearing such bulky cyclopentadienyl ligands seems to be limited to the large lanthanide metal centers ($\text{Ln} = \text{Sm}$, Nd , La). It is noteworthy that the formation of $[\text{Sm}(\text{AlMe}_4)_2[1,2,4-(\text{Me}_3\text{C})_3\text{C}_5\text{H}_2]]$ (**4c**) is accompanied by the precipitation of an insoluble purple solid. Characterization of this precipitate revealed it to be peralkylated divalent $[\text{SmAl}_2\text{Me}_8]_n$.^[27] Donor adduct formation in the presence of THF yielded $[\text{SmAl}_2\text{Me}_8(\text{thf})_2]$, further substantiating the reduction of the samarium metal center ($\text{Sm}^{\text{III}} \rightarrow \text{Sm}^{\text{II}}$).^[28] However, the observed reactivity has not been investigated further.

The ^1H NMR spectra of diamagnetic mono(cyclopentadienyl) complexes **2–4** ($\text{Ln}=\text{Lu}$, Y , La) show the expected sets of signals for the respective Cp^R ligands and only one narrow signal in the metal alkyl region, which can be assigned to the $[\text{Al}(\mu\text{-Me})_2\text{Me}_2]$ moieties, indicating a rapid exchange of bridging and terminal methyl groups. For compounds **2** and **3**, these resonances are slightly shifted to higher field compared to those of the homoleptic precursors,^[9] while a downfield shift is observed for compound **4e** (Table 1). A signal splitting of the ^1H methyl resonance in yttrium compounds **2b** ($^2J_{\text{YH}}=2.4$ Hz) and **3b** ($^2J_{\text{YH}}=2.0$ Hz) is clearly attributable to a two-bond $^1\text{H}\text{-}^{89}\text{Y}$ scalar coupling.

Good quality ^1H and ^{13}C NMR spectra could also be obtained for the paramagnetic compounds $[\text{Sm}(\text{AlMe}_4)_2(\text{Cp}^R)]$ (**2c**, **3c**, **4c**) and $[\text{Nd}(\text{AlMe}_4)_2(\text{Cp}^R)]$ (**2d**, **3d**, **4d**). The paramagnetic Ln^{III} metal centers influence the ^1H and ^{13}C NMR spectra differently, probably due to the varying relaxation behavior of their unpaired electron spins. Significant paramagnetic shifts and broadening effects for the ^1H and ^{13}C resonances are observed for complexes containing neodymi-

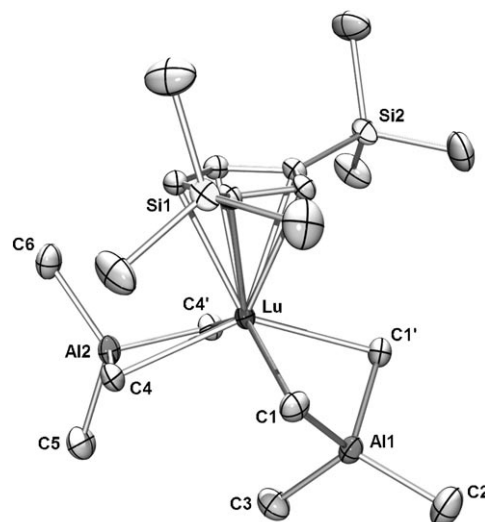


Figure 2. Molecular structure of $[\text{Lu}(\text{AlMe}_4)_2\{1,3\text{-(Me}_3\text{Si)}_2\text{C}_5\text{H}_3\}]$ (**2a**), representative of isostructural complexes **2**; atomic displacement parameters are set at the 50% level; hydrogen atoms have been omitted for clarity; symmetry code for (') is $x, 3/2-y, z$.

Table 1. ^1H NMR chemical shifts (ppm) of the $[\text{Al}(\text{CH}_3)_4]$ protons of tetramethylaluminate-containing complexes. Values are taken from ^1H NMR spectra of the respective compounds dissolved in $[\text{D}_6]$ benzene at 298 K.

| | Lu | Y | Sm | Nd | La |
|---|-------|-------|-------|-------|--------------|
| $[\text{Ln}(\text{AlMe}_4)_3]$ (1) ^[a] | -0.08 | -0.25 | -3.06 | 10.53 | -0.20 |
| $[\text{Ln}(\text{AlMe}_4)_2\{1,3\text{-(Me}_3\text{Si)}_2\text{C}_5\text{H}_3\}]$ (2) | -0.14 | -0.29 | -2.81 | 6.78 | -0.23 |
| $[\text{Ln}(\text{AlMe}_4)_2(\text{C}_5\text{Me}_4\text{SiMe}_3)]$ (3) | -0.14 | -0.31 | -3.14 | 5.25 | -0.25 |
| $[\text{Ln}(\text{AlMe}_4)_2\{1,2,4\text{-(Me}_3\text{C)}_3\text{C}_5\text{H}_2\}]$ (4) | - | - | -2.76 | 6.40 | -0.12 |
| $[\text{Ln}(\text{AlMe}_4)_2(\text{C}_5\text{Me}_5)]$ (5) ^[b] | -0.18 | -0.33 | -3.27 | 4.21 | -0.27 |
| $[\text{Ln}(\text{AlMe}_4)(\mu\text{-Cl})\{1,3\text{-(Me}_3\text{Si)}_2\text{C}_5\text{H}_3\}]_2$ (6) | - | -0.11 | - | - | - |
| $[\text{Ln}(\text{AlMe}_4)(\mu\text{-Cl})(\text{C}_5\text{Me}_4\text{SiMe}_3)]_2$ (8) | - | -0.20 | - | - | - |
| $[\text{Ln}(\text{AlMe}_4)(\mu\text{-Cl})\{1,2,4\text{-(Me}_3\text{C)}_3\text{C}_5\text{H}_2\}]_2$ (9) | - | - | - | 9.63 | - |
| $[\text{Ln}(\text{AlMe}_4)(\mu\text{-Cl})(\text{C}_5\text{Me}_5)]_2$ ^[c] | - | -0.15 | - | - | - |
| $[\text{La}(\text{AlMe}_4)(\text{C}_5\text{Me}_5)][\text{B}(\text{C}_6\text{F}_5)_4]$ ^[d] | - | - | - | - | -0.39 |
| $[[\text{La}(\text{C}_5\text{Me}_5)\{(\mu\text{-Me})_2\text{AlMe}(\text{C}_6\text{F}_5)\}][\text{Me}_2\text{Al}(\text{C}_6\text{F}_5)_2]]_2$ ^[d,e] | - | - | - | - | -0.24, -0.37 |

[a] Taken from ref. [9]. [b] Taken from refs. [7, 8, and 29]. [c] Taken from ref. [14]. [d] Taken from ref. [22]. [e] Chemical shifts for the bridging and terminal methyl groups of the $[(\mu\text{-Me})_2\text{AlMe}(\text{C}_6\text{F}_5)]$ moiety.

um, while such effects are less pronounced for the respective samarium compounds (Table 1).

Single crystals of $[\text{Ln}(\text{AlMe}_4)_2\{1,3\text{-(Me}_3\text{Si)}_2\text{C}_5\text{H}_3\}]$ ($\text{Ln}=\text{Lu}$ (**2a**), Y (**2b**), Nd (**2d**)), $[\text{Y}(\text{AlMe}_4)_2(\text{C}_5\text{Me}_4\text{SiMe}_3)]$ (**3b**), and $[\text{Ln}(\text{AlMe}_4)_2\{1,2,4\text{-(Me}_3\text{C)}_3\text{C}_5\text{H}_2\}]$ ($\text{Ln}=\text{Sm}$ (**4c**), Nd (**4d**), La (**4e**)) suitable for X-ray crystallographic structure determination were grown from saturated hexane solutions at -30°C . This series covers the differently substituted cyclopentadienyl ligands as well as a wide size range of Ln^{III} cations, thus allowing an insight into the ligand- and size-dependent characteristics of complexes $[\text{Ln}(\text{AlMe}_4)_2(\text{Cp}^R)]$ in the solid state. The X-ray crystallographic analyses revealed structural motifs as previously found for $[\text{Ln}(\text{AlMe}_4)_2(\text{C}_5\text{Me}_5)]$ ($\text{Ln}=\text{Lu}$ (**5a**), Y (**5b**), La (**5e**)), with one $[\text{AlMe}_4]$ ligand coordinating in the routinely observed planar η^2 fashion and the second one showing a bent η^2 -coordination (Figures 2 and 3).^[7,8,11]

All of the solid-state structures under investigation feature an additional short $\text{Ln}\cdots(\mu\text{-Me})$ contact ($\text{Ln}\cdots\text{C3}$, **2**; $\text{Ln}\cdots\text{C7}$, **3** and **4**). Due to enhanced steric unsaturation, this interaction becomes more distinct with increasing size of the lanthanide metal center, as is reflected in a gradual shortening of the (bond) distances $\text{Ln}\cdots\text{C3}$ (**2**, Table 2) and $\text{Ln}\cdots\text{C7}$ (**3** and **4**, Table 3), respectively.

This effect is, however, less pronounced for complexes **4**, as one might reasonably expect, due to effective stereoelectronic shielding by the bulky $[1,2,4\text{-(Me}_3\text{C)}_3\text{C}_5\text{H}_2]$ ligand. Interplanar angles $\text{LnC1C1}'\text{-Al1C1C1}'$ (**2**) and $\text{LnC5C6}\text{-Al2C5C6}$ (**3**, **4**) follow similar trends (**2a**: 128.5° , **2b**: 124.5° , **2d**: 117.7° ; **3b**: 121.0° ; **4c**: 126.8° , **4d**: 125.8° , **4e**: 124.0°). The $\text{Ln}\text{-C}(\mu\text{-Me})$ bond lengths increase with increasing Ln^{III} size, the bonds in the bent $[\text{AlMe}_4]$ ligand being significantly elongated compared to those in the planar tetramethylaluminate ligand of the same molecule (Tables 2 and 3). To minimize steric hindrance, the orientation of the trimethylsilyl substituents at the cyclopentadienyl ring in compounds $[\text{Ln}(\text{AlMe}_4)_2\{1,3\text{-(Me}_3\text{Si)}_2\text{C}_5\text{H}_3\}]$ (**2**) is nearly staggered with respect to the two aluminate ligands (Figure 2). Due to the increased steric crowding in complexes $[\text{Ln}(\text{AlMe}_4)_2\{1,2,4\text{-(Me}_3\text{C)}_3\text{C}_5\text{H}_2\}]$ (**4**), the mean metal–ring-carbon distances $\text{Ln}\text{-C}(1,2,4\text{-(Me}_3\text{C)}_3\text{C}_5\text{H}_2)$ are considerably elongated compared to those in $[\text{Ln}(\text{AlMe}_4)_2(\text{C}_5\text{Me}_5)]$ (**5**) (e.g., av. 2.807 Å in **4e** vs av. 2.777 Å in **5e**).^[8] Steric repulsion leads

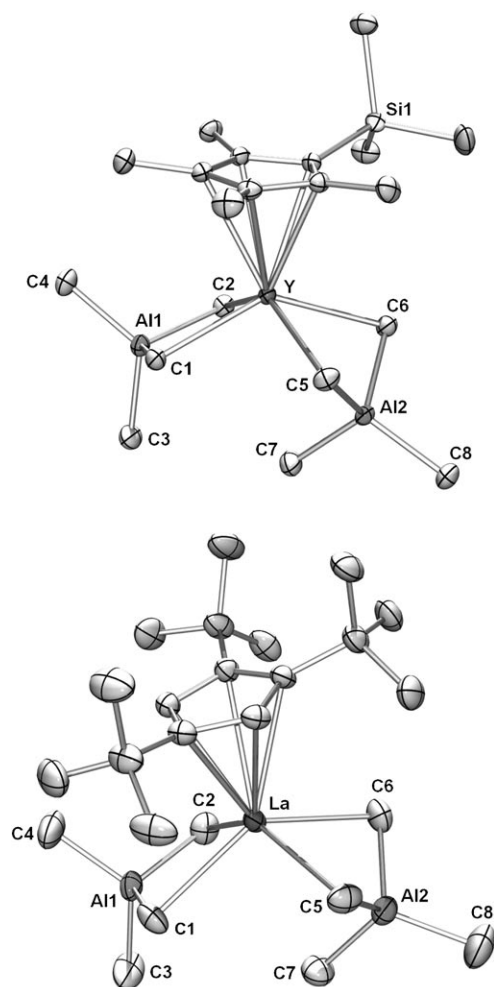


Figure 3. Molecular structures of $[Y(AlMe_4)_2(C_5Me_4SiMe_3)]$ (**3b**) (top) and $[La(AlMe_4)_2[1,2,4-(Me_3C)_3C_5H_2]]$ (**4e**) (bottom; representative of isostructural complexes **4**); atomic displacement parameters are set at the 50% level; hydrogen atoms have been omitted for clarity.

to the orientation of the *t*Bu groups in the apertures between the two aluminate ligands, resulting in a staggered conformation (Figure 3 (bottom)). Nevertheless, the 1H NMR spectra of **4** at ambient temperature show resonances of only two inequivalent *t*Bu groups due to ring rotation of the Cp^R rings about their pseudo C_5 axis.

Reactivity toward R_2AlCl : Mono(cyclopentadienyl) compounds $[Ln(AlMe_4)_2(Cp^R)]$ (**2–5**) feature a distinct pre-organized set of bridged, heterobimetallic Ln/Al moieties. Given the superb performance of Ln/Al heterobimetallic complexes such as $[Ln(AlMe_4)_3]$,^[18,19] $[LnAl_3Me_8(O_2CC_6H_2iPr_3-2,4,6)_4]$, and $[Ln(AlMe_3)_n(OR)_3]$ ($R = \text{neopentyl}, C_6H_3R'_2-2,6$ ($R' = tBu, iPr$)) as initiators for the *cis*-1,4 stereospecific polymerization of isoprene following activation with chloride donors such as Et_2AlCl or Ph_3CCl ,^[20] we investigated the catalytic potential of half-sandwich complexes $[Ln(AlMe_4)_2(Cp^R)]$. Accordingly, the initiating performance of $[Ln(AlMe_4)_2(Cp^R)]$ (**2–5**) in the polymerization of isoprene was examined in the presence of

Table 2. Selected structural parameters [\AA , $^\circ$] for complexes **2a**, **2b**, and **2d** ($C_g = \text{ring centroid}$). Symmetry code for (') depicts ($x, 3/2-y, z$).

| | 2a (Lu) | 2b (Y) | 2d (Nd) |
|--------------------------|-------------------|-------------------|-------------------|
| $Ln-C(Cp^R)$ | 2.580(2)–2.596(1) | 2.620(3)–2.641(2) | 2.713(2)–2.727(1) |
| $Ln-C_g$ | 2.29 | 2.34 | 2.44 |
| $Ln-C1/C1'$ | 2.563(1) | 2.624(2) | 2.731(2) |
| $Ln-C4/C4'$ | 2.517(1) | 2.560(2) | 2.645(2) |
| $Al1-C1/C1'$ | 2.069(1) | 2.062(2) | 2.057(2) |
| $Al1-C2$ | 1.959(2) | 1.949(3) | 1.957(2) |
| $Al1-C3$ | 1.974(2) | 1.983(3) | 2.012(2) |
| $Al2-C4/C4'$ | 2.082(2) | 2.085(2) | 2.084(2) |
| $Al2-C5$ | 1.971(2) | 1.969(3) | 1.973(2) |
| $Al2-C6$ | 1.971(2) | 1.964(3) | 1.971(2) |
| $Ln\cdots Al1$ | 2.9130(5) | 2.9133(9) | 2.9498(6) |
| $Ln\cdots Al2$ | 3.0292(5) | 3.078(1) | 3.1722(6) |
| $Ln\cdots C3$ | 3.492(2) | 3.302(3) | 3.088(2) |
| $C1-Ln-C1'$ | 79.98(5) | 78.2(1) | 74.52(7) |
| $C4-Ln-C4'$ | 84.45(5) | 83.3(1) | 80.53(6) |
| $Ln-C1-Al1$ | 77.13(4) | 75.8(1) | 74.57(5) |
| $Ln-C4-Al2$ | 81.80(4) | 82.31(7) | 83.35(5) |
| $C1-Al1-C1'$ | 105.50(7) | 106.8(1) | 106.95(9) |
| $C4-Al2-C4'$ | 108.73(6) | 109.4(1) | 110.25(8) |
| $C1'-Al1-C2$ | 106.55(5) | 108.0(1) | 111.35(6) |
| $C1'-Al1-C3$ | 108.09(5) | 106.06(9) | 104.56(6) |
| $C4'-Al2-C5$ | 105.73(5) | 105.89(9) | 106.05(6) |
| $C4-Al2-C6$ | 109.59(4) | 109.12(9) | 109.32(6) |
| $Al1\cdots Ln\cdots Al2$ | 114.58(1) | 117.47(3) | 123.36(2) |

one, two, and three equivalents of diethylaluminum chloride Et_2AlCl as a “weakly cationizing” cocatalyst.

Contrary to the reported high activities of binary catalyst mixtures containing the above-mentioned non-cyclopentadienyl Ln/Al heterobimetallic complexes and Et_2AlCl , mixtures of **2–5** and Et_2AlCl did not provide active catalysts for the polymerization of isoprene. Treatment of $[Ln(AlMe_4)_2(C_5Me_5)]$ (**5**) ($Ln = Y, Nd, La$) with varying amounts of Me_2AlCl has recently been reported to yield mixed tetramethylaluminate/chloride compounds.^[14] The extent of the $[AlMe_4] \rightarrow [Cl]$ exchange and the nuclearity of the resulting rare-earth metal complexes was found to be significantly affected by subtle changes in the rare-earth metal cation size. While alkyl/chloride interchange led to alkylated heterobimetallic half-sandwich $[La_6Al_4]$ and $[Nd_5Al]$ cluster compounds, chloro-bridged dimers $[Y_2Al_2]$ were obtained for the smaller yttrium metal center.

Addition of one equivalent of Me_2AlCl to solutions of half-sandwich complexes **2b**, **3b**, and **4d** in hexane yielded crystalline materials of the net composition $[Ln(AlMe_4)(Cl)(Cp^R)]$ ($Ln = Y, Cp^R = [1,3-(Me_3Si)_2C_5H_3]$ (**6**); $Ln = Y, Cp^R = (C_5Me_4SiMe_3)$ (**8**); and $Ln = Nd, Cp^R = [1,2,4-(Me_3C)_3C_5H_2]$ (**9**)) in low to moderate yields (Scheme 2).^[30] Molar ratios of $Me_2AlCl/2b > 1.0$ gave increasing amounts of an amorphous white solid material identified as $[YCl_2\{1,3-(Me_3Si)_2C_5H_3\}]_n$ (**7**) (Scheme 2).^[31]

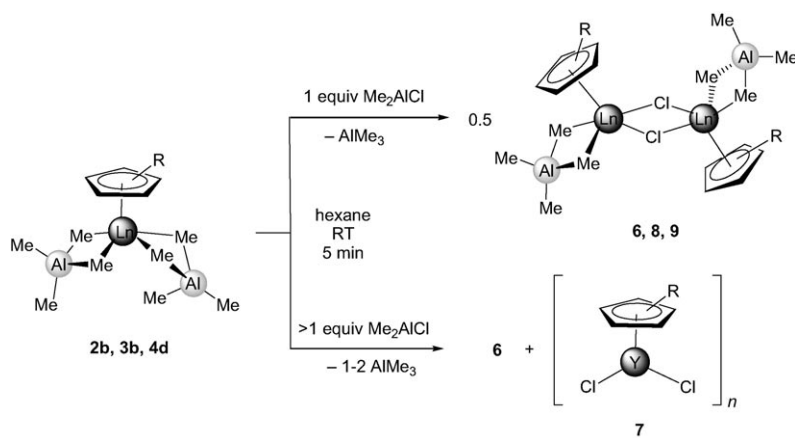
Complete $[AlMe_4] \rightarrow [Cl]$ exchange in **7** could be confirmed by 1H and ^{13}C NMR spectroscopy in $[D_6]benzene$, which showed only the signals of the Cp^R ligand. Examination of the hexane-soluble fractions, however, revealed mixtures of unreacted $[Y(AlMe_4)_2\{1,3-(Me_3Si)_2C_5H_3\}]$ (**2b**) and

Table 3. Selected structural parameters [\AA , $^\circ$] for complexes **3b**, **4c**, **4d**, and **4e** (C_g = ring centroid).

| | 3b (Y) | 4c (Sm) | 4d (Nd) | 4e (La) |
|------------------------|-------------------|-------------------|-------------------|-------------------|
| Ln–C(Cp ^R) | 2.610(3)–2.695(3) | 2.668(1)–2.748(1) | 2.694(2)–2.768(2) | 2.769(1)–2.838(1) |
| Ln–C _g | 2.35 | 2.42 | 2.45 | 2.53 |
| Ln–C1 | 2.530(3) | 2.603(1) | 2.626(2) | 2.694(1) |
| Ln–C2 | 2.520(3) | 2.618(1) | 2.652(2) | 2.716(1) |
| Ln–C5 | 2.680(3) | 2.722(2) | 2.748(2) | 2.797(1) |
| Ln–C6 | 2.669(3) | 2.672(2) | 2.732(2) | 2.790(2) |
| Al1–C1 | 2.063(3) | 2.069(2) | 2.067(2) | 2.069(2) |
| Al1–C2 | 2.081(3) | 2.070(2) | 2.067(3) | 2.061(2) |
| Al1–C3 | 1.983(4) | 1.970(2) | 1.960(3) | 1.961(2) |
| Al1–C4 | 1.976(4) | 1.969(2) | 1.973(2) | 1.975(2) |
| Al2–C5 | 2.054(3) | 2.069(2) | 2.059(2) | 2.065(2) |
| Al2–C6 | 2.061(3) | 2.075(2) | 2.070(3) | 2.067(2) |
| Al2–C7 | 1.982(4) | 1.988(2) | 1.994(3) | 2.000(2) |
| Al2–C8 | 1.952(4) | 1.954(2) | 1.956(2) | 1.959(2) |
| Ln...Al1 | 3.099(1) | 3.1664(4) | 3.1951(6) | 3.2652(4) |
| Ln...Al2 | 2.929(1) | 2.9855(4) | 3.0035(6) | 3.0494(4) |
| Ln...C7 | 3.297(4) | 3.377(2) | 3.326(3) | 3.293(2) |
| C1–Ln–C2 | 83.16(11) | 80.39(5) | 79.40(7) | 77.50(5) |
| C5–Ln–C6 | 76.31(10) | 77.43(5) | 76.30(7) | 74.54(5) |
| Ln–C1–Al1 | 84.20(11) | 84.51(5) | 84.93(6) | 85.49(4) |
| Ln–C2–Al1 | 84.09(11) | 84.12(5) | 84.27(8) | 85.05(5) |
| Ln–C5–Al2 | 75.16(10) | 75.73(4) | 75.84(6) | 76.03(4) |
| Ln–C6–Al2 | 75.32(10) | 76.81(5) | 76.03(7) | 76.15(7) |
| C1–Al1–C2 | 108.0(1) | 108.95(6) | 109.26(8) | 110.13(6) |
| C5–Al2–C6 | 106.8(1) | 108.97(6) | 110.12(9) | 109.95(6) |
| C1–Al1–C3 | 108.2(2) | 105.32(8) | 104.2(1) | 104.35(7) |
| C1–Al1–C4 | 109.2(2) | 110.97(8) | 111.4(1) | 110.84(8) |
| C5–Al2–C7 | 107.8(2) | 104.96(8) | 105.1(1) | 104.56(7) |
| C5–Al2–C8 | 109.9(2) | 110.36(7) | 110.2(1) | 111.19(8) |
| Al1...Ln...Al2 | 110.25(3) | 113.45(1) | 115.04(2) | 115.44(1) |

The average Y–C(μ -Me) bond length of 2.551 \AA in **8** appears slightly elongated compared to that of the η^2 -coordinated aluminate ligand of the respective precursor compound (av. 2.525 \AA (**3b**)) and is significantly longer than similar bonds in homoleptic $[\text{Y}(\text{AlMe}_4)_3]$ (av. 2.508 \AA (**1b**), Table 4).^[32] The solid-state structure of complex **9** revealed a slightly bent aluminate ligand (interplanar angle NdC1C2–Al1C1C2 26.1(14) $^\circ$, Nd...C3 4.075(3) \AA) and an average Nd–C(μ -Me) bond distance of 2.637 \AA (Table 4). For comparison, the Nd–C(μ -Me) aluminate bond lengths range from 2.639 \AA (η^2) to 2.740 \AA (bent η^2) in precursor compound **4d** and average 2.592 \AA in homoleptic $[\text{Nd}(\text{AlMe}_4)_3]$ (**1d**).^[32] The Ln–Cl bond distances (av. 2.693 \AA (**8**); av. 2.794 \AA (**9**)) are comparable to the corresponding bond lengths of the bridging chloro ligands in dimeric $[\{\text{Y}(\text{AlMe}_4)(\mu\text{-Cl})(\text{C}_5\text{Me}_5)_2\}_2]$ (av. 2.6752 \AA) and the $[\mu_2\text{-Cl}]$ bridges in the pentanuclear neodymium cluster $[\text{Nd}_5(\mu_4\text{-Cl})(\mu_3\text{-Cl})_2(\mu_2\text{-Cl})_6(\text{C}_5\text{Me}_5)_5\{\mu\text{-Me}\}_3\text{-AlMe}_4]$ (2.775 \AA).^[14]

Mixed tetramethylaluminate/chloride complexes **6**, **8**, and **9** are sparingly soluble in hydrocarbon solvents but readily dissolve in aromatic solvents. The ^1H NMR spectra of diamagnetic **6** and **8** in $[\text{D}_6]$ benzene feature sets of signals due to the respective Cp^R ligands and the $[\text{AlMe}_4]$ moiety, which are slightly shifted to lower field compared with those of the precursor compounds **2b** and **3b** (Table 1), albeit with the same



Scheme 2. Synthesis of $[\text{Ln}(\text{AlMe}_4)(\mu\text{-Cl})(\text{Cp}^{\text{R}})]_2$ (Ln = Y, Cp^R = [1,3-(Me₃Si)₂C₅H₃]₂ (**6**); Ln = Y, Cp^R = (C₅Me₄SiMe₃) (**8**); Ln = Nd, Cp^R = [1,2,4-(Me₃C)₃C₅H₂]₂ (**9**)) and $[\text{YCl}_2(\text{Cp}^{\text{R}})]_n$ (Cp^R = [1,3-(Me₃Si)₂C₅H₃], $n > 1$) (**7**).

$[\{\text{Y}(\text{AlMe}_4)(\mu\text{-Cl})\{1,3\text{-}(\text{Me}_3\text{Si})_2\text{C}_5\text{H}_3\}_2\}]_2$ (**6**), irrespective of the amount of Me₂AlCl used.

X-ray structure analyses of compounds **8** and **9** revealed dimeric complexes $[\{\text{Y}(\text{AlMe}_4)(\mu\text{-Cl})(\text{C}_5\text{Me}_4\text{SiMe}_3)_2\}]_2$ (Figure 4, top) and $[\{\text{Nd}(\text{AlMe}_4)(\mu\text{-Cl})\{1,2,4\text{-}(\text{Me}_3\text{C})_3\text{C}_5\text{H}_2\}_2\}]_2$ (Figure 4, bottom) with formally heptacoordinate lanthanide metal centers and a rare combination of homometal-bridging chloride ligands and η^2 -coordinated aluminate ligands.

two-bond ^1H - ^{89}Y scalar couplings of $^2J_{\text{YH}} = 2.4$ Hz (**6**) and $^2J_{\text{YH}} = 2.0$ Hz (**7**). The observed downfield shift is in accordance with a comparatively weakened coordination of the $[\text{AlMe}_4]$ ligands to the rare-earth metal center and is somewhat contrary to an anticipated cationization of complexes $[\text{Ln}(\text{AlMe}_4)_2(\text{Cp}^{\text{R}})]$ by dialkylaluminum chlorides (cationization of $[\text{Ln}(\text{AlMe}_4)_2(\text{Cp}^{\text{R}})]$ by borate or borane activators results in upfield shifts in accordance with a stronger ligand

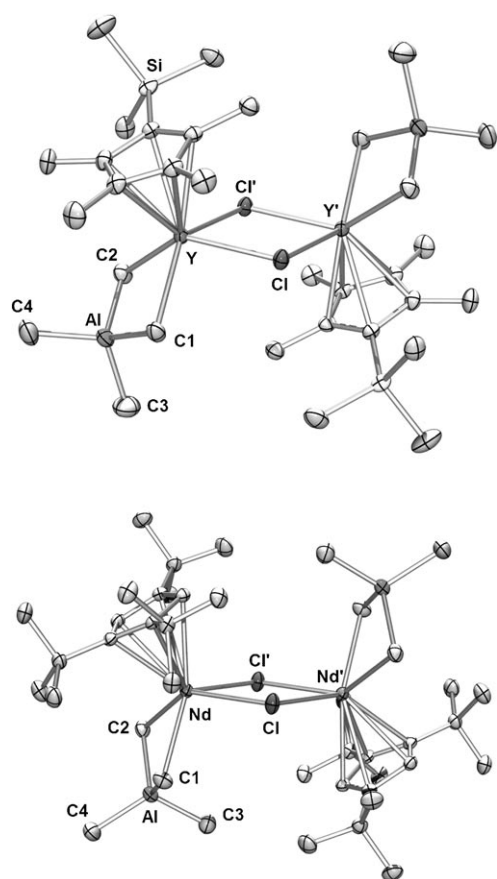


Figure 4. Molecular structures of **8** (top) and **9** (bottom) (atomic displacement parameters are set at the 50% level). Hydrogen atoms have been omitted for clarity. Symmetry code for (') depicts $(-x+1, -y, -z+1)$ for **8** and $(-x+1, -y+1, -z+2)$ for **9**.

Table 4. Selected structural parameters [\AA , $^\circ$] for complexes **8** and **9** (C_g = ring centroid). Symmetry code for (') is $(-x+1, -y, -z+1)$ for **8** and $(-x+1, -y+1, -z+2)$ for **9**.

| | 8 (Y) | 9 (Nd) |
|------------------------|---------------------|---------------------|
| Ln–C(Cp ^R) | 2.566(1)–2.645(1) | 2.690(2)–2.762(2) |
| Ln–C _g | 2.30 | 2.44 |
| Ln–C1 | 2.558(2) | 2.620(2) |
| Ln–C2 | 2.543(2) | 2.653(2) |
| Ln–Cl1/Cl1' | 2.6803(4)/2.7061(4) | 2.7807(6)/2.8077(6) |
| Al1–C1 | 2.074(2) | 2.078(2) |
| Al1–C2 | 2.073(2) | 2.067(2) |
| Al1–C3 | 1.968(2) | 1.970(3) |
| Al1–C4 | 1.969(2) | 1.967(3) |
| Ln...Al1 | 3.0992(5) | 3.1646(7) |
| Cl–Ln–C2 | 82.93(6) | 79.23(7) |
| Ln–C1–Al1 | 83.30(6) | 83.84(8) |
| Ln–C2–Al1 | 83.67(2) | 83.22(8) |
| Ln–Cl1–Ln' | 102.12(1) | 106.27(2) |
| Cl1–Al1–C2 | 109.06(7) | 108.42(10) |
| Cl1–Al1–C3 | 109.00(9) | 105.52(11) |
| Cl1–Al1–C4 | 105.46(9) | 107.55(12) |

coordination to the electron-deficient rare-earth metal cation, Table 1). Significant paramagnetic shifts and broadening effects were observed in the ^1H NMR spectrum of the neodymium complex **9**.

Contrary to the cluster formation observed for reactions of $[\text{Ln}(\text{AlMe}_4)_2(\text{C}_5\text{Me}_5)]$ (**5**) ($\text{Ln} = \text{Nd}, \text{La}$) with Me_2AlCl ,^[14] well-defined dimeric compounds $[\{\text{Ln}(\text{AlMe}_4)(\mu\text{-Cl})(\text{Cp}^{\text{R}})\}_2]$ were exclusively found for $\text{Cp}^{\text{R}} = [1,3\text{-}(\text{Me}_3\text{Si})_2\text{C}_5\text{H}_3]$, $[\text{C}_5\text{Me}_4\text{SiMe}_3]$, and $[1,2,4\text{-}(\text{Me}_3\text{C})_3\text{C}_5\text{H}_2]$, even for the large neodymium metal center in **9**. Such dinuclear compounds are formed in mixtures of **2–4** with Et_2AlCl as sterically and electronically saturated systems without catalytic activity toward isoprene polymerization.

Polymerization of isoprene: We recently reported new initiators for the controlled polymerization of isoprene based on half-sandwich complexes $[\text{Ln}(\text{AlMe}_4)_2(\text{C}_5\text{Me}_5)]$ (**5**) and fluorinated borate and borane reagents as cationizing agents.^[22] Remarkably, such mixtures yielded polyisoprene with a very high *trans*-1,4 content. Catalyst activities and selectivities showed a strong dependence on the size of the rare-earth metal cation and the nature of the boron cocatalyst. Half-sandwich complexes **2–4** were therefore employed as precatalysts in the polymerization of isoprene. The polymerization results are summarized in Table 5, along with data for catalysts based on $[\text{Ln}(\text{AlMe}_4)_2(\text{C}_5\text{Me}_5)]$ (**5**) taken from a previous study, which was performed under similar conditions (see Experimental Section).^[22]

Effect of the metal center: For a systematic investigation of the effect of the rare-earth metal on catalytic activities and catalyst selectivity, yttrium and lanthanum were selected representing one of the smaller and the largest rare-earth metal center for half-sandwich complexes **2** (Table 5, entries 1–6) and **3** (Table 5, entries 7–12). Due to the unavailability of complexes **4** for the smaller rare-earth metal centers, the neodymium and lanthanum derivatives **4d** and **4e** were chosen (Table 5, entries 13–18). All precatalysts under investigation showed extremely high activities upon cationization with $[\text{Ph}_3\text{C}][\text{B}(\text{C}_6\text{F}_5)_4]$ (**A**) or $[\text{PhNM}_2\text{H}][\text{B}(\text{C}_6\text{F}_5)_4]$ (**B**) as activators. No significant effect of the size of the metal cation on the catalytic activity was observed.

The activities obtained for catalyst systems activated by $\text{B}(\text{C}_6\text{F}_5)_3$ (**C**) were comparatively low, and were also only marginally affected by the Ln^{III} size. While the effect of the metal on the catalytic activity is less pronounced, the choice of metal center significantly affects the selectivity of the catalyst. In a previous study, we showed that the lanthanum half-sandwich complexes $[\text{La}(\text{AlMe}_4)_2(\text{C}_5\text{Me}_5)]$ (**5e**) greatly outperform their corresponding yttrium and neodymium congeners **5b** and **5d**, respectively (Table 5, runs 19–27).^[22] Similar effects have now been observed for complexes **2**, **3**, and **4**. The *trans*-selectivity increases remarkably with increasing size of the rare-earth metal cation ($\text{La} \gg \text{Y}$; Table 5, runs 4–6, 10–12, 16–18, 25–27).

Effect of the substituted cyclopentadienyl ancillary ligand: Quantitative polymer formation was observed in all experiments, irrespective of the substitution pattern on the cyclopentadienyl ancillary ligand (Cp^{R}). No effect of the steric bulk of the ligands on catalytic activity could be discerned.

Table 5. Effect of Ln size, Cp substituent, and cocatalyst on the polymerization of isoprene.

| Entry ^[a] | Precatalyst | Cocatalyst ^[b] | Yield [%] | Structure ^[c] | | | $M_n^{[d]}$ ($\times 10^5$) | M_w/M_n | Efficiency ^[e] [%] |
|----------------------|---|---------------------------|-----------|--------------------------|------------------|------|----------------------------------|-----------|----------------------------------|
| | | | | <i>trans</i> -1,4- | <i>cis</i> -1,4- | 3,4- | | | |
| 1 | [Y(AlMe ₄) ₂ {1,3-(Me ₃ Si) ₂ C ₅ H ₃ }] (2b) | A | >99 | 9.0 | 60.0 | 31.0 | 1.9 | 2.18 | 0.35 |
| 2 | [Y(AlMe ₄) ₂ {1,3-(Me ₃ Si) ₂ C ₅ H ₃ }] (2b) | B | >99 | 4.0 | 63.0 | 33.0 | 1.2 | 1.77 | 0.57 |
| 3 | [Y(AlMe ₄) ₂ {1,3-(Me ₃ Si) ₂ C ₅ H ₃ }] (2b) | C | >99 | 40.0 | 52.0 | 8.0 | 2.7 | 1.74 | 2.57 |
| 4 | [La(AlMe ₄) ₂ {1,3-(Me ₃ Si) ₂ C ₅ H ₃ }] (2e) | A | >99 | 80.3 | 14.5 | 5.2 | 0.6 | 1.28 | 1.12 |
| 5 | [La(AlMe ₄) ₂ {1,3-(Me ₃ Si) ₂ C ₅ H ₃ }] (2e) | B | >99 | 79.4 | 15.3 | 5.3 | 0.6 | 1.22 | 1.15 |
| 6 | [La(AlMe ₄) ₂ {1,3-(Me ₃ Si) ₂ C ₅ H ₃ }] (2e) | C | >99 | 89.3 | – | 10.7 | 3.3 | 1.52 | 0.21 |
| 7 | [Y(AlMe ₄) ₂ (C ₅ Me ₄ SiMe ₃)] (3b) | A | >99 | 26.4 | 38.1 | 35.5 | 0.1 | 20.41 | 5.59 |
| 8 | [Y(AlMe ₄) ₂ (C ₅ Me ₄ SiMe ₃)] (3b) | B | >99 | 34.6 | 38.3 | 27.1 | 0.3 | 1.74 | 2.11 |
| 9 | [Y(AlMe ₄) ₂ (C ₅ Me ₄ SiMe ₃)] (3b) | C | >99 | 80.8 | 3.4 | 15.8 | 0.5 | 1.73 | 1.42 |
| 10 | [La(AlMe ₄) ₂ (C ₅ Me ₄ SiMe ₃)] (3e) | A | >99 | 81.4 | 3.4 | 15.2 | 0.9 | 1.45 | 0.79 |
| 11 | [La(AlMe ₄) ₂ (C ₅ Me ₄ SiMe ₃)] (3e) | B | >99 | 87.7 | 10.5 | 1.8 | 0.6 | 1.20 | 1.20 |
| 12 | [La(AlMe ₄) ₂ (C ₅ Me ₄ SiMe ₃)] (3e) | C | >99 | 95.6 | 2.2 | 2.2 | 2.0 | 1.26 | 0.34 |
| 13 | [Nd(AlMe ₄) ₂ {1,2,4-(Me ₃ C) ₃ C ₅ H ₃ }] (4d) | A | >99 | 21.2 | 45.5 | 33.5 | 0.8 | 1.67 | 0.83 |
| 14 | [Nd(AlMe ₄) ₂ {1,2,4-(Me ₃ C) ₃ C ₅ H ₃ }] (4d) | B | >99 | 19.0 | 53.0 | 28.0 | 0.9 | 1.25 | 0.80 |
| 15 | [Nd(AlMe ₄) ₂ {1,2,4-(Me ₃ C) ₃ C ₅ H ₃ }] (4d) | C | >99 | 56.0 | 31.0 | 13.0 | 0.5 | 1.50 | 1.37 |
| 16 | [La(AlMe ₄) ₂ {1,2,4-(Me ₃ C) ₃ C ₅ H ₂ }] (4e) | A | >99 | 60.0 | 20.0 | 20.0 | 0.8 | 1.41 | 0.82 |
| 17 | [La(AlMe ₄) ₂ {1,2,4-(Me ₃ C) ₃ C ₅ H ₂ }] (4e) | B | >99 | 50.0 | 30.0 | 20.0 | 0.8 | 1.22 | 0.91 |
| 18 | [La(AlMe ₄) ₂ {1,2,4-(Me ₃ C) ₃ C ₅ H ₂ }] (4e) | C | >99 | 90.0 | 6.0 | 4.0 | 1.1 | 1.41 | 0.60 |
| 19 | [Y(AlMe ₄) ₂ (C ₅ Me ₅)] (5b) | A | >99 | 20.6 | 60.5 | 18.9 | 0.2 | 8.95 | 3.98 |
| 20 | [Y(AlMe ₄) ₂ (C ₅ Me ₅)] (5b) | B | >99 | 28.7 | 43.5 | 27.8 | 0.6 | 1.59 | 1.06 |
| 21 | [Y(AlMe ₄) ₂ (C ₅ Me ₅)] (5b) | C | >99 | 93.6 | 1.9 | 4.5 | 0.9 | 1.78 | 0.82 |
| 22 | [Nd(AlMe ₄) ₂ (C ₅ Me ₅)] (5d) | A | >99 | 69.7 | 14.0 | 16.3 | 0.3 | 2.87 | 2.11 |
| 23 | [Nd(AlMe ₄) ₂ (C ₅ Me ₅)] (5d) | B | >99 | 79.9 | 6.9 | 13.2 | 0.4 | 1.16 | 1.73 |
| 24 | [Nd(AlMe ₄) ₂ (C ₅ Me ₅)] (5d) | C | >99 | 92.4 | 3.8 | 3.8 | 1.3 | 1.35 | 0.52 |
| 25 | [La(AlMe ₄) ₂ (C ₅ Me ₅)] (5e) | A | >99 | 87.0 | 3.5 | 9.5 | 0.7 | 1.28 | 1.98 |
| 26 | [La(AlMe ₄) ₂ (C ₅ Me ₅)] (5e) | B | >99 | 79.5 | 3.4 | 17.1 | 0.6 | 1.22 | 1.08 |
| 27 | [La(AlMe ₄) ₂ (C ₅ Me ₅)] (5e) | C | >99 | 99.5 | – | 0.5 | 2.4 | 1.18 | 0.28 |

[a] Conditions: 0.02 mmol precatalyst, [Ln]/[cocat]=1:1, 8 mL toluene, 20 mmol isoprene, 24 h, 40 °C. [b] Cocatalyst: **A**=[Ph₃C][B(C₆F₅)₄], **B**=[PhNMe₂H][B(C₆F₅)₄], **C**=B(C₆F₅)₃; the catalyst was preformed for 20 min at 40 °C. [c] Determined by ¹H and ¹³C NMR spectroscopy in CDCl₃. [d] Determined by means of size-exclusion chromatography (SEC) against polystyrene standards. [e] Initiation efficiency = $M_n(\text{calculated})/M_n(\text{measured})$.

Little correlation between the degree of steric shielding and the observed stereospecificities was noted. Rather, the stereospecificity seems to be affected by the electronic properties of the Cp^R ligand and its propensity to undergo degradation reactions ([C₅Me₅] ≪ [C₅Me₄SiMe₃] < [1,2,4-(Me₃C)₃C₅H₂] ≪ [1,3-(Me₃Si)₂C₅H₃]). These findings are in good agreement with the stabilities of cationic species generated in mixtures [Ln(AlMe₄)₂(Cp^R)]/borate or [Ln(AlMe₄)₂(Cp^R)]/B(C₆F₅)₃ as monitored by ¹H NMR experiments. The cation stability significantly decreases in the series [C₅Me₅] ≫ [C₅Me₄SiMe₃] > [1,2,4-(Me₃C)₃C₅H₂] ≫ [1,3-(Me₃Si)₂C₅H₃], which is manifested in extensive ancillary ligand degradation for cationic complexes containing the latter two substituted cyclopentadienyl ligands.

Effect of the boron cocatalyst: As previously reported for [Ln(AlMe₄)₂(C₅Me₅)] (**5**),^[22] the reactions of [Ln(AlMe₄)₂(Cp^R)] (**2–4**) with one equivalent of [Ph₃C][B(C₆F₅)₄] (**A**) or [PhNMe₂H][B(C₆F₅)₄] (**B**) yield tight ion pairs [Ln(AlMe₄)₂(Cp^R)]⁺[B(C₆F₅)₄]⁻ (**9**). ¹H NMR spectroscopy clearly indicated instant disappearance of the signals of **2–4**. Upon reaction with [Ph₃C][B(C₆F₅)₄], quantitative formation of Ph₃CMe and one equivalent AlMe₃ was observed, while the reaction with [PhNMe₂H][B(C₆F₅)₄] was accompanied by quantitative formation of PhNMe₂ and one equivalent each of AlMe₃ and CH₄. New signals due to the respective Cp^R ligands appeared, with slight upfield shifts in accordance with

stronger coordination to the highly electron-deficient lanthanide cation. The use of [Ph₃C][B(C₆F₅)₄] and [PhNMe₂H][B(C₆F₅)₄] as activators for [(Cp^R)Ln(AlMe₄)₂] led to extremely high activity in the polymerization reactions. The activities of 68 kg mol⁻¹ h⁻¹ are twofold higher than those mentioned in the literature for similar *trans*-specific polymerizations.^[33–35] However, the *trans*-1,4 content in the resulting polyisoprene did not exceed 88%, even for catalyst systems based on the large lanthanum metal center (Table 5, runs 4/5, 10/11, 16/17, 25/26). In accordance with a different activation mechanism, the use of B(C₆F₅)₃ (**C**) as an activator for complexes [Ln(AlMe₄)₂(Cp^R)] resulted in the formation of a catalytically active species with a markedly different performance. Active species formed in mixtures of [Ln(AlMe₄)₂(Cp^R)]/B(C₆F₅)₃^[36] polymerized isoprene with comparatively low activities but with a high to very high *trans*-1,4 content and very narrow molecular weight distributions (Table 5). The highest *trans*-1,4 selectivities were observed with the large rare-earth metal center lanthanum, especially for precatalysts [La(AlMe₄)₂(C₅Me₄SiMe₃)] (**3e**; *trans*-1,4 content: 95.6%, $M_w/M_n=1.26$) and [La(AlMe₄)₂(C₅Me₅)] (**5e**; *trans*-1,4 content: 99.5%, $M_w/M_n=1.18$) (Table 5, runs 12 and 27; Figure 5).

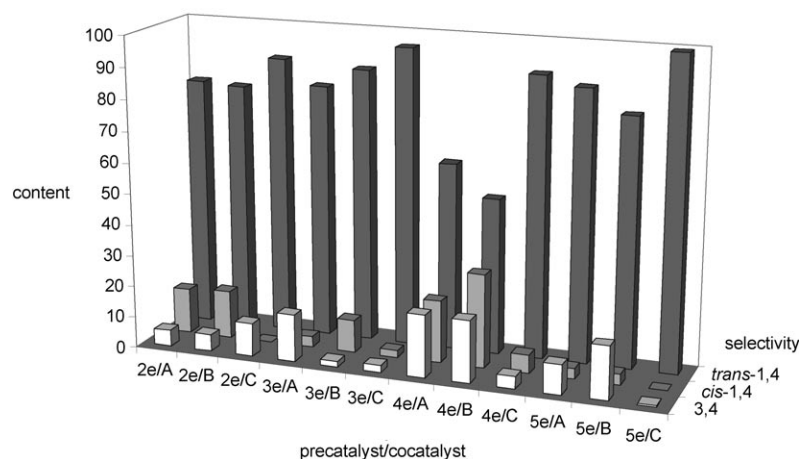


Figure 5. Representation of the *trans*-1,4-, *cis*-1,4-, and 3,4-contents of the polyisoprenes obtained from [La(AlMe₄)₂(Cp^R)] (**2e**, **3e**, **4e**, and **5e**) and cocatalysts **A**, **B**, and **C**.

Conclusion

The “aluminate route” offers a viable synthesis protocol for generating a series of donor-solvent-free half-sandwich complexes [Ln(AlMe₄)₂(Cp^R)] bearing cyclopentadienyl ligands with various stereoelectronic properties. X-ray structure analyses covering [Ln(AlMe₄)₂(Cp^R)] compounds with differently substituted cyclopentadienyl ligands, as well as a wide size range of Ln^{III} cations, have revealed similar structural motifs irrespective of the Cp^R ancillary ligand and the size of the rare-earth metal cation involved. All of the solid-state structures feature one η²-coordinating planar [AlMe₄] ligand, whereas the second such ligand shows a bent η²-coordination mode, allowing for an additional short Ln⋯(μ-Me) contact. These half-sandwich bis(tetramethylaluminate) complexes showed no catalytic activity in the polymerization of isoprene upon addition of one, two, or three equivalents of dialkylaluminum chloride reagents. Instead, mixtures of [Ln(AlMe₄)₂(Cp^R)]/Me₂AlCl yielded discrete dimeric mixed tetramethylaluminate/chloride complexes [(Ln(AlMe₄)(μ-Cl)(Cp^R))₂] and higher agglomerated fully exchanged derivatives [(Ln(μ-Cl)₂(Cp^R))_n]. However, catalytically active systems were obtained when fluorinated borate and borane reagents were applied as cocatalysts. Systematic investigations of the effects of metal cation size, the substituents on the cyclopentadiene ligand, and cocatalyst interactions (borate vs. borane) have revealed: a) good (for systems activated with B(C₆F₅)₃) to excellent catalytic activities for [Ln(AlMe₄)₂(Cp^R)] activated by borate cocatalysts [Ph₃C][B(C₆F₅)₄] or [PhNMe₂H][B(C₆F₅)₄], b) increased *trans*-1,4 selectivity with increasing size of the rare-earth metal cation (Y < Nd ≪ La), c) increased *trans*-1,4 selectivity with enhanced chemical “innocence” and stability of the Cp^R ligand ([1,3-(Me₃Si)₂C₅H₃] ≪ [1,2,4-(Me₃C)₃C₅H₂] < [C₅Me₄SiMe₃] ≪ [C₅Me₅]). The highest stereoselectivities were observed for the pre-catalyst/cocatalyst systems [La(AlMe₄)₂(C₅Me₄SiMe₃)]/B(C₆F₅)₃ (*trans*-1,4 content: 95.6%, *M_w/M_n*=1.26) and [La(AlMe₄)₂(C₅Me₅)]/B(C₆F₅)₃ (*trans*-1,4 content: 99.5%, *M_w/M_n*=1.18).

Experimental Section

General remarks: All operations were performed with rigorous exclusion of air and water, using standard Schlenk, high-vacuum, and glovebox techniques (MBraun MBLab; <1 ppm O₂, <1 ppm H₂O). Hexane and toluene were purified by using Grubbs columns (MBraun SPS, solvent purification system) and were stored in a glovebox. [D₆]Benzene was obtained from Aldrich, degassed, dried over Na for 24 h, and filtered. C₅HMe₄SiMe₃, AlMe₃, and Me₂AlCl were purchased from Aldrich and were used as received. [Ph₃C][B(C₆F₅)₄], [PhNMe₂H][B(C₆F₅)₄], and [B(C₆F₅)₃] were purchased from Boulder Scientific Company and were used without further purification. Homoleptic [Ln(AlMe₄)₃] (**1**) (Ln=Lu, Y, Sm, Nd, La),^[9] [1,3-(Me₃Si)₂C₅H₃],^[24] [1,2,4-

(Me₃C)₃C₅H₃],^[26] and [Ln(AlMe₄)₂(C₅Me₅)] (**5**) (Ln=Y, Nd, La)^[8] were synthesized according to literature methods. Isoprene was obtained from Aldrich, dried several times over activated 3 Å molecular sieves, and distilled prior to use. The NMR spectra of air- and moisture-sensitive compounds were recorded at 25 °C on a Bruker BIOSPIN AV500 (5 mm BBO, ¹H: 500.13 Hz; ¹³C: 125.77 MHz) or a Bruker BIOSPIN AV600 (5 mm cryo probe, ¹H: 600.13 MHz; ¹³C: 150.91 MHz) with samples in J. Young valve NMR tubes. ¹H and ¹³C shifts are referenced to internal solvent resonances and are reported in parts per million relative to TMS. IR spectra were recorded on a NICOLET Impact 410 FTIR spectrometer from samples in Nujol mulls sandwiched between CsI plates. Elemental analyses were performed on an Elementar Vario EL III. The molar masses (*M_w/M_n*) of the polymers were determined by size-exclusion chromatography (SEC). Sample solutions (1.0 mg polymer per mL THF) were filtered through a 0.2 μm syringe filter prior to injection. SEC was operated with a pump supplied by Waters (Waters 510), employing Ultrastaygel® columns with pore sizes of 500, 1000, 10000, and 100000 Å. Signals were detected by means of a differential refractometer (Waters 410) and calibrated against polystyrene standards (*M_w/M_n* < 1.15). The flow rate was 1.0 mL min⁻¹. The microstructure of the polyisoprenes was examined by means of ¹H and ¹³C NMR experiments on the AV500 spectrometer at ambient temperature, using [D]chloroform as solvent and TMS as internal standard.

General procedure for the preparation of [Ln(AlMe₄)₂-{1,3-(Me₃Si)₂C₅H₃}] (2**) and [Ln(AlMe₄)₂(C₅Me₄SiMe₃)] (**3**):** In a glovebox, [Ln(AlMe₄)₃] (**1**) was dissolved in hexane (2 mL), and then a solution of either [1,3-(Me₃Si)₂C₅H₃] (1 equiv) or (C₅HMe₄SiMe₃) (1 equiv) in hexane (2 mL) was added to the alkylaluminate solution under vigorous stirring. Upon the addition, instant gas formation was observed. After the reaction mixture had been stirred for a further 5 h at ambient temperature, the solvent was removed in vacuo to give **2** or **3** as crystalline solids. Crystallization from a solution in hexane at -35 °C gave high yields of single crystals of **2** or **3** suitable for X-ray diffraction analysis.

[Lu(AlMe₄)₂{1,3-(Me₃Si)₂C₅H₃}] (2a**):** Following the procedure described above, [Lu(AlMe₄)₃] (**1a**) (227 mg, 0.52 mmol) and [1,3-(Me₃Si)₂C₅H₃] (109 mg, 0.52 mmol) yielded **2a** (145 mg, 0.26 mmol, 50%) as colorless crystals. ¹H NMR (500 MHz, [D₆]benzene, 25 °C): δ = 6.53 (d, ³J = 1.5 Hz, 1H; CpH), 6.53 (s, 1H; CpH), 6.52 (d, ³J = 1.5 Hz, 1H; CpH), 0.17 (s, 18H; Si(CH₃)₃), -0.14 ppm (s, 24H; Al(CH₃)₄); ¹³C NMR (126 MHz, [D₆]benzene, 25 °C): δ = 125.7, 118.4, 114.8 (Cp), 1.5 (brs; Al(CH₃)₄), 0.2 ppm (Si(CH₃)₃); IR (Nujol): $\tilde{\nu}$ = 1463 (vs, Nujol), 1375 (vs, Nujol), 1318 (w), 1303 (w), 1251 (s), 1204 (m), 1194 (m), 1080 (s), 925 (s), 837 (s), 759 (m), 723 (s), 692 (m), 640 (w), 578 (m), 567 cm⁻¹ (w); elemental analysis calcd (%) for C₁₉H₄₅Al₂Si₂Lu (558.67): C 40.85, H 8.12; found: C 41.03, H 7.94.

Table 7. Crystallographic data for compounds **4c**, **4d**, **4e**, **8**, and **9**.

| | 4c | 4d | 4e | 8 | 9 |
|--|---|---|---|--|---|
| formula | C ₂₅ H ₅₃ Al ₂ Sm | C ₂₅ H ₅₃ Al ₂ Nd | C ₂₅ H ₅₃ Al ₂ La | C ₃₂ H ₆₆ Cl ₂ Al ₂ Si ₂ Y ₂ | C ₄₂ H ₈₂ Cl ₂ Al ₂ Nd ₂ |
| Fw | 557.98 | 551.87 | 546.54 | 809.70 | 1000.42 |
| color/habit | red/prism | blue/irregular prism | colorless/prism | colorless/prism | blue/needle |
| crystal dimensions [mm ³] | 0.48 × 0.25 × 0.22 | 0.62 × 0.42 × 0.30 | 0.48 × 0.45 × 0.35 | 0.25 × 0.15 × 0.05 | 0.32 × 0.06 × 0.03 |
| crystal system | triclinic | orthorhombic | orthorhombic | monoclinic | triclinic |
| space group | <i>P</i> $\bar{1}$ | <i>P</i> 2 ₁ 2 ₁ 2 ₁ | <i>P</i> 2 ₁ 2 ₁ 2 ₁ | <i>P</i> 2 ₁ / <i>c</i> | <i>P</i> $\bar{1}$ |
| <i>a</i> [Å] | 10.4475(3) | 9.9821(3) | 10.0116(3) | 12.2263(4) | 9.6135(4) |
| <i>b</i> [Å] | 11.5594(3) | 16.3710(5) | 16.4193(5) | 18.3134(6) | 11.6331(5) |
| <i>c</i> [Å] | 12.6169(3) | 18.4738(6) | 18.5254(5) | 9.5255(3) | 11.8715(5) |
| α [°] | 98.9720(4) | 90 | 90 | 90 | 70.350(1) |
| β [°] | 97.1495(4) | 90 | 90 | 96.228(1) | 75.971(1) |
| γ [°] | 96.1548(1) | 90 | 90 | 90 | 88.487(1) |
| <i>V</i> [Å ³] | 1480.84(7) | 3018.9(2) | 3045.3(2) | 2120.2(1) | 1210.83(9) |
| <i>Z</i> | 2 | 4 | 4 | 2 | 1 |
| <i>T</i> [K] | 123 | 123 | 123 | 123 | 123 |
| ρ_{calcd} [mgm ⁻³] | 1.251 | 1.214 | 1.192 | 1.268 | 1.372 |
| μ [mm ⁻¹] | 2.050 | 1.786 | 1.468 | 2.966 | 2.292 |
| <i>F</i> (000) | 582 | 1156 | 1144 | 848 | 514 |
| θ range [°] | 1.65/30.02 | 2.32/30.04 | 2.20/30.12 | 1.68/29.05 | 2.15/27.02 |
| index ranges | -14 ≤ <i>h</i> ≤ 14 -16 ≤ <i>k</i> ≤ 16 -17 ≤ <i>l</i> ≤ 17 | -14 ≤ <i>h</i> ≤ 14 -23 ≤ <i>k</i> ≤ 23 -26 ≤ <i>l</i> ≤ 26 | -14 ≤ <i>h</i> ≤ 14 -23 ≤ <i>k</i> ≤ 23 -26 ≤ <i>l</i> ≤ 26 | -16 ≤ <i>h</i> ≤ 16 -25 ≤ <i>k</i> ≤ 24 -13 ≤ <i>l</i> ≤ 12 | -12 ≤ <i>h</i> ≤ 12 -14 ≤ <i>k</i> ≤ 14 -15 ≤ <i>l</i> ≤ 15 |
| no. of reflns. integrated | 25046 | 51098 | 51756 | 33224 | 16676 |
| no. of indep. reflns./ <i>R</i> _{int} | 8638/0.0135 | 8806/0.0203 | 8960/0.0189 | 5652/0.0316 | 5294/0.0302 |
| no. of obsd. reflns (<i>I</i> > 2σ(<i>I</i>)) | 8366 | 8294 | 8729 | 4750 | 4767 |
| data/params/restraints | 8638/302/24 | 8806/302/24 | 8960/302/24 | 5652/208/12 | 5294/246/12 |
| <i>R</i> ₁ / <i>wR</i> ₂ (<i>I</i> > 2σ(<i>I</i>)) ^[a] | 0.0168/0.0442 | 0.0176/0.0410 | 0.0131/0.0338 | 0.0240/0.0559 | 0.0202/0.0437 |
| <i>R</i> ₁ / <i>wR</i> ₂ (all data) ^[a] | 0.0174/0.0446 | 0.0209/0.0430 | 0.0140/0.0343 | 0.0346/0.0603 | 0.0259/0.0457 |
| GOF (on <i>F</i> ²) ^[a] | 1.076 | 1.068 | 1.027 | 1.042 | 1.032 |
| largest diff. peak and hole [e Å ⁻³] | 3.018/-0.585 | 0.750/-0.456 | 0.524/-0.412 | 1.186/-0.608 | 0.473/-0.366 |

[a] $R_1 = \sum(|F_o| - |F_c|) / \sum |F_o|$; $wR_2 = \{\sum[w(F_o^2 - F_c^2)^2] / \sum[w(F_o^2)^2]\}^{1/2}$; GOF = $\{\sum[w(F_o^2 - F_c^2)^2] / (n - p)\}^{1/2}$.

with the C–Al bond axis. The isotropic displacement parameters for all methyl H-atoms were set at 1.5 times that of the pivot C-atom.

CCDC-653204, 653205, 679299, 679300, 679301, 679302, 679303, 679304, and 679305 contain the supplementary crystallographic data for this paper. These data can be obtained free of charge from the Cambridge Crystallographic Data Centre via www.ccdc.cam.ac.uk/data_request/cif.

Acknowledgements

Financial support from the Norwegian Research Council (Project No. 182547/130) and the program Nanoscience@UiB is gratefully acknowledged. We also thank Till Diesing (c/o Dr. Markus Klapper, MPI für Polymerforschung, Mainz (Germany)) for performing the GPC analyses.

- [1] a) K. C. Hultsch, T. P. Spaniol, J. Okuda, *Angew. Chem.* **1999**, *111*, 163; *Angew. Chem. Int. Ed.* **1999**, *38*, 227; b) Y. Luo, J. Baldamus, Z. Hou, *J. Am. Chem. Soc.* **2004**, *126*, 13910; c) X. Li, J. Baldamus, Z. Hou, *Angew. Chem.* **2005**, *117*, 984; *Angew. Chem. Int. Ed.* **2005**, *44*, 962; d) D. Cui, M. Nishiura, Z. Hou, *Macromolecules* **2005**, *38*, 4089; e) J. Hitzbleck, J. Okuda, *Z. Anorg. Allg. Chem.* **2006**, *632*, 1947; f) J. Hitzbleck, K. Beckerle, J. Okuda, T. Halbach, R. Mühlhaupt, *Macromol. Symp.* **2006**, *236*, 23; g) H. Zhang, Y. Luo, Z. Hou, *Macromolecules* **2008**, *41*, 1064.
- [2] a) S. Bambirra, D. van Leusen, A. Meetsma, B. Hessen, J. H. Teuben, *Chem. Commun.* **2003**, 522; b) S. Bambirra, M. W. Bouwkamp, A. Meetsma, B. Hessen, *J. Am. Chem. Soc.* **2004**, *126*, 9182; c) W. P. Kretschmer, A. Meetsma, B. Hessen, T. Schmalz, S. Qayyum, R. Kempe, *Chem. Eur. J.* **2006**, *12*, 8969; d) S. Bambirra, D. van Leusen, C. G. J. Tazelaar, A. Meetsma, B. Hessen, *Organometallics* **2007**, *26*, 1014; e) Y. Luo, M. Nishiura, Z. Hou, *J. Organomet. Chem.* **2007**, *692*, 536; f) Y. Yang, B. Liu, W. Gao, D. Cui, X. Chen, X. Jing, *Organometallics* **2007**, *26*, 4575; g) S. Li, W. Miao, T. Tang, W. Dong, X. Zhang, D. Cui, *Organometallics* **2008**, *27*, 718; h) A. Otero, J. Fernández-Baeza, A. Antinolo, A. Lara-Sánchez, E. Martínez-Caballero, J. Tejada, L. F. Sánchez-Barba, C. Alonso-Moreno, I. López-Solera, *Organometallics* **2008**, *27*, 976.
- [3] a) X. Liu, X. Shang, T. Tang, N. Hu, F. Pei, D. Cui, X. Chen, X. Jing, *Organometallics* **2007**, *26*, 2747; b) D. J. H. Emslie, W. E. Piers, M. Parvez, R. McDonald, *Organometallics* **2002**, *21*, 4226.
- [4] a) L. Zhang, T. Suzuki, Y. Luo, M. Nishiura, Z. Hou, *Angew. Chem.* **2007**, *119*, 1941; *Angew. Chem. Int. Ed.* **2007**, *46*, 1909; b) B. Liu, D. Cui, J. Ma, X. Chen, X. Jing, *Chem. Eur. J.* **2007**, *13*, 834.
- [5] a) X. Li, M. Nishiura, K. Mori, T. Mashiko, Z. Hou, *Chem. Commun.* **2007**, 4137; b) F. Jaroschik, T. Shima, X. Li, K. Mori, L. Ricard, X.-F. Le Goff, F. Nief, Z. Hou, *Organometallics* **2007**, *26*, 5654.
- [6] L. Zhang, Y. Luo, Z. Hou, *J. Am. Chem. Soc.* **2005**, *127*, 14562.
- [7] R. Anwander, M. G. Klimpel, H. M. Dietrich, D. J. Shorokhov, W. Scherer, *Chem. Commun.* **2003**, 1008.
- [8] H. M. Dietrich, C. Zapilko, E. Herdtweck, R. Anwander, *Organometallics* **2005**, *24*, 5767.
- [9] M. Zimmermann, N. Å. Frøystein, A. Fischbach, P. Sirsch, H. M. Dietrich, K. W. Törnroos, E. Herdtweck, R. Anwander, *Chem. Eur. J.* **2007**, *13*, 8784.
- [10] E. Le Roux, F. Nief, F. Jaroschik, K. W. Törnroos, R. Anwander, *Dalton Trans.* **2007**, 4866.
- [11] H. M. Dietrich, E. Herdtweck, K. W. Törnroos, R. Anwander, unpublished results.
- [12] W. T. Klooster, R. S. Lu, R. Anwander, W. J. Evans, T. E. Koetzle, R. Bau, *Angew. Chem.* **1998**, *110*, 1326; *Angew. Chem. Int. Ed.* **1998**, *37*, 1268.
- [13] M. Zimmermann, K. W. Törnroos, R. Anwander, *Angew. Chem.* **2007**, *119*, 3187; *Angew. Chem. Int. Ed.* **2007**, *46*, 3126.

- [14] H. M. Dietrich, O. Schuster, K. W. Törnroos, R. Anwänder, *Angew. Chem.* **2006**, *118*, 4977; *Angew. Chem. Int. Ed.* **2006**, *45*, 4858.
- [15] Catalyst deactivation is observed in the presence of excessive amounts of coordinating solvents. For examples, see: a) L. Friebe, O. Nuyken, W. Obrecht, *Adv. Polym. Sci.* **2006**, *204*, 1; b) P. G. Hayes, W. E. Piers, M. Parvez, *J. Am. Chem. Soc.* **2003**, *125*, 5622.
- [16] It is noteworthy that for a considerable number of binary catalysts $[\text{Ln}^{\text{III}}(\text{Do})(\text{L})\text{R}_2]/\text{borate}$ the presence of organoaluminum compounds such as $\text{Al}(\text{iBu})_3$ is required; for examples, see refs. [1e], [1f], [2a–c], [2f].
- [17] A. Fischbach, R. Anwänder, *Adv. Polym. Sci.* **2006**, *204*, 155.
- [18] A. Fischbach, M. G. Klimpel, M. Widenmeyer, E. Herdtweck, W. Scherer, R. Anwänder, *Angew. Chem.* **2004**, *116*, 2284; *Angew. Chem. Int. Ed.* **2004**, *43*, 2234.
- [19] C. Meermann, K. W. Törnroos, W. Nerdal, R. Anwänder, *Angew. Chem.* **2007**, *119*, 6628; *Angew. Chem. Int. Ed.* **2007**, *46*, 6508.
- [20] a) A. Fischbach, F. Perdih, P. Sirsch, W. Scherer, R. Anwänder, *Organometallics* **2002**, *21*, 4569; b) A. Fischbach, F. Perdih, E. Herdtweck, R. Anwänder, *Organometallics* **2006**, *25*, 1626; c) A. Fischbach, C. Meermann, G. Eickerling, W. Scherer, R. Anwänder, *Macromolecules* **2006**, *39*, 6811.
- [21] a) M. Zimmermann, K. W. Törnroos, R. Anwänder, *Organometallics* **2006**, *25*, 3593; b) M. Zimmermann, F. Estler, E. Herdtweck, K. W. Törnroos, R. Anwänder, *Organometallics* **2007**, *26*, 6029; c) M. Zimmermann, J. Takats, G. Kiel, K. W. Törnroos, R. Anwänder, *Chem. Commun.* **2008**, 612.
- [22] M. Zimmermann, K. W. Törnroos, R. Anwänder, *Angew. Chem.* **2008**, *120*, 787; *Angew. Chem. Int. Ed.* **2008**, *47*, 775.
- [23] The contents of this contribution have been presented at the XX. Tage der Seltenen Erden "Terrae Rarae 2007", Köln (Bonn-Röttgen), Germany, 29.11.–1.12.2007.
- [24] E. W. Abel, S. Moorhouse, *J. Organomet. Chem.* **1971**, *29*, 227.
- [25] After submission of this work, the synthesis of complexes **3** and the catalytic performance of mixtures **3**/ $[\text{Ph}_3\text{C}][\text{B}(\text{C}_6\text{F}_5)_4]/\text{Al}(\text{iBu})_3$ in the polymerization of butadiene was reported, see: D. Robert, T. P. Spaniol, J. Okuda, *Eur. J. Inorg. Chem.* **2008**, 2801.
- [26] a) E. V. Dehmlow, C. Bollmann, *Z. Naturforsch.* **1993**, *48b*, 457; b) H. Sitzmann, P. Zhou, G. Wolmershäuser, *Chem. Ber.* **1994**, *127*, 3.
- [27] a) M. G. Schrems, H. M. Dietrich, K. W. Törnroos, R. Anwänder, *Chem. Commun.* **2005**, 5922; b) H.-M. Sommerfeldt, C. Meermann, M. G. Schrems, K. W. Törnroos, N. Å. Frøystein, R. J. Miller, E.-W. Scheidt, W. Scherer, R. Anwänder, *Dalton Trans.* **2008**, 1899.
- [28] C. Ruspic, J. R. Moss, M. Schürmann, S. Harder, *Angew. Chem.* **2008**, *120*, 2151; *Angew. Chem. Int. Ed.* **2008**, *47*, 2121.
- [29] M. Zimmermann, K. W. Törnroos, R. Anwänder, unpublished results.
- [30] Alternative treatment with one equivalent of Ph_3CCl as chlorinating agent also yielded compounds **6**, **8**, and **9**.
- [31] For an example of a half-sandwich bis(chloride) rare-earth metal complex, see: M. D. Walter, D. Bentz, F. Weber, O. Schmitt, G. Wolmershäuser, H. Sitzmann, *New J. Chem.* **2007**, *31*, 305.
- [32] W. J. Evans, R. Anwänder, J. W. Ziller, *Organometallics* **1995**, *14*, 1107.
- [33] D. Barbier-Baudry, F. Bonnet, B. Domenichini, A. Dormond, M. Visseaux, *J. Organomet. Chem.* **2004**, *647*, 167.
- [34] a) F. Bonnet, M. Visseaux, A. Pereira, F. Bouyer, D. Barbier-Baudry, *Macromol. Rapid Commun.* **2004**, *25*, 873; b) F. Bonnet, M. Visseaux, D. Barbier-Baudry, E. Vigier, M. M. Kubicki, *Chem. Eur. J.* **2004**, *10*, 2428; c) F. Bonnet, M. Visseaux, A. Pereira, D. Barbier-Baudry, *Macromolecules* **2005**, *38*, 3162.
- [35] For *trans*-1,4 polymerization of isoprene by NdCl_3 catalysts, see: a) J. H. Yang, M. Tsutsui, Z. Chen, D. E. Bergbreiter, *Macromolecules* **1982**, *15*, 230; b) Y. B. Monakov, Z. M. Sabirov, V. N. Urazbaev, V. P. Efimov, *Kinet. Catal.* **2001**, *42*, 310.
- [36] The reaction of $[\text{La}(\text{AlMe}_4)_2(\text{C}_5\text{Me}_5)]$ and $\text{B}(\text{C}_6\text{F}_5)_3$ was shown to quantitatively produce the ion pair $[[\text{La}(\text{C}_5\text{Me}_5)\{\mu\text{-Me}\}_2\text{AlMe}(\text{C}_6\text{F}_5)]][\text{Me}_2\text{Al}(\text{C}_6\text{F}_5)_2]$ as the product of very fast sequential $\text{CH}_3/\text{C}_6\text{F}_5$ exchange processes. A similar initial activation scenario can be proposed for other half-sandwich bis(aluminate) complexes (see ref. [22]).
- [37] SMART, Ver. 5.054, **1999** and SAINT, Ver. 6.45a, Bruker AXS Inc., Madison, Wisconsin (USA), **2001**.
- [38] G. M. Sheldrick, *Acta Crystallographica*, *A64*, **2008**, 112.
- [39] SHELXTL, Ver. 6.14, Bruker AXS Inc., Madison, Wisconsin (USA), **2003**.
- [40] G. M. Sheldrick, SADABS, Ver. 2004/1, University of Göttingen (Germany), **2006**.

Received: March 16, 2008
Published online: July 4, 2008

Paper VIII

Structure–Reactivity Relationships of Amido-Pyridine-Supported Rare-Earth-Metal Alkyl Complexes

Melanie Zimmermann,[†] Karl W. Törnroos,[†] Robert M. Waymouth,^{*,‡} and Reiner Anwander^{*,†}

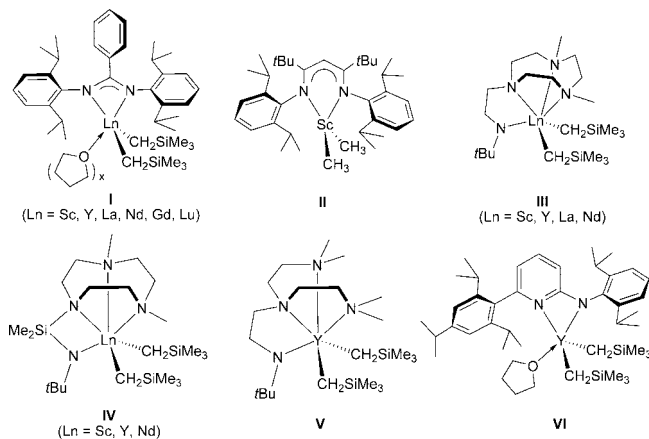
Department of Chemistry, University of Bergen, Allégaten 41, 5007 Bergen, Norway, and Chemistry Department, Stanford University, Stanford, California 94305

Received November 28, 2007

Treatment of rare-earth-metal dialkyl complexes with group 13 cocatalysts is a prominent approach to generate homogeneous catalysts active in olefin polymerization. Reaction of $\text{Ln}(\text{CH}_2\text{SiMe}_3)_3(\text{THF})_2$ with monovalent imino-amido-pyridine [2-((2,6-*i*Pr₂C₆H₃)N=CMe)-6-((2,6-*i*Pr₂C₆H₃)NHCMe₂)C₅H₃N] (**HL**₂) gives donor solvent-free discrete dialkyl compounds [**L**₂] $\text{Ln}(\text{CH}_2\text{SiMe}_3)_2$ ($\text{Ln} = \text{Sc}, \text{Y}, \text{Lu}$). In the solid state the scandium derivative is isostructural to the previously reported lutetium complex (Gordon et al.). Activation by borate cocatalysts $[\text{Ph}_3\text{C}][\text{B}(\text{C}_6\text{F}_5)_4]$ and $[\text{PhNMe}_2\text{H}][\text{B}(\text{C}_6\text{F}_5)_4]$ produces ion pairs that polymerize ethylene in moderate yields (activity: $\text{Sc} > \text{Lu}$). Cationization with *N*-[tris(pentafluorophenyl)borane]-3*H*-indole gives inactive species. ¹H/¹³C/¹¹B/¹⁹F NMR spectroscopy is applied to examine the interaction of the rare-earth-metal dialkyl complexes with the boron cocatalysts. In contrast to the monoalkyl diamido-pyridine compounds [**L**₁] $\text{Ln}(\text{CH}_2\text{SiMe}_3)(\text{THF})_x$ (**HL**₁ = [2,6-((2,6-*i*Pr₂C₆H₃)NHCMe₂)C₅H₃N]), the dialkyl imino-amido-pyridine complexes do not polymerize methyl methacrylate.

Much of the recent interest in organolanthanide chemistry is linked to the academic and industrial quest for novel types of olefin polymerization catalysts.¹ Improvement of the overall catalytic performance is by its very nature related to ancillary ligand design and the generation of highly electron deficient metal centers (*metal cationization*). While cyclopentadienyl and related carbocyclic ligand environments (e.g., indenyl) have yielded a number of isolable and active catalysts, the rich coordination chemistry of the lanthanides provides considerable opportunities for further ligand design and optimization.² Nitrogen (imines, amides) and oxygen donor ligands (alkoxides) have proven to be versatile components of polydentate ligands for lanthanide polymerization catalysts. *N*-type (amide, imine) ligands have been successfully employed for the synthesis of discrete organorare-earth-metal complexes; nevertheless the number of reported active catalyst systems remains limited.^{1b} Chart 1 depicts representative *N*-type (amide, imine) catalyst precursors for ethylene polymerization (Table 2).^{3–8} Typically, these complexes contain at least two alkyl ligands and only

Chart 1. Rare-Earth-Metal Bis(alkyl) Complexes with *N*-Type Ancillary Ligands, Active in Ethylene Polymerization upon Addition of Activators (cf., Table 2)



* To whom correspondence should be addressed. Fax: (+47) 5558-9490. E-mail: reiner.anwander@kj.uib.no.

[†] University of Bergen.

[‡] Stanford University.

(1) For reviews see: (a) Hou, Z.; Wakatsuki, Y. *Coord. Chem. Rev.* **2002**, *231*, 1. (b) Gromada, J.; Carpentier, J. F.; Mortreux, A. *Coord. Chem. Rev.* **2004**, *248*, 397. (c) Hyeon, J. Y.; Gottfriedsen, J.; Edelmann, F. T. *Coord. Chem. Rev.* **2005**, *249*, 2787. (d) Zeimentz, P. M.; Arndt, S.; Elvidge, B. R.; Okuda, J. *Chem. Rev.* **2006**, *106*, 2404, and references therein.

(2) For recent reviews see: (a) Piers, W. E.; Emslie, D. J. H. *Coord. Chem. Rev.* **2002**, *233–234*, 131. (b) Gibson, V. C.; Spitzmesser, S. K. *Chem. Rev.* **2003**, *103*, 283.

(3) (a) Bambirra, S.; Bouwkamp, M. W.; Meetsma, A.; Hessen, B. *J. Am. Chem. Soc.* **2004**, *126*, 9182. (b) Bambirra, S.; van Leusen, D.; Meetsma, A.; Hessen, B.; Teuben, J. H. *Chem. Commun.* **2003**, 522. (c) Bambirra, S.; Otten, E.; van Leusen, D.; Meetsma, A.; Hessen, B. *Z. Anorg. Allg. Chem.* **2006**, *632*, 1950. (d) Bambirra, S.; Meetsma, A.; Hessen, B. *Organometallics* **2006**, *25*, 3454.

(4) Hayes, P. G.; Piers, W. E.; McDonald, R. J. *Am. Chem. Soc.* **2002**, *124*, 2132.

(5) Bambirra, S.; van Leusen, D.; Meetsma, A.; Hessen, B.; Teuben, J. H. *Chem. Commun.* **2001**, 637.

become active for polymerization upon activation by organo-boron and/or organoaluminum cocatalysts.

Due to their successful application as ligands for group 4 chemistry,⁹ we investigated the coordination chemistry of the diamido-pyridine ligands of the [NNN]²⁻ type (**L**₁, Chart 2) for organorare-earth-metal chemistry.¹⁰ The influence of ligand modifications (aryl substituents, donor atoms) and the effect of

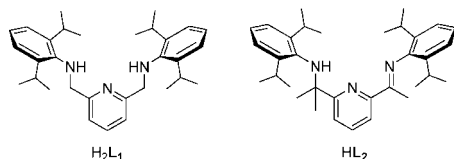
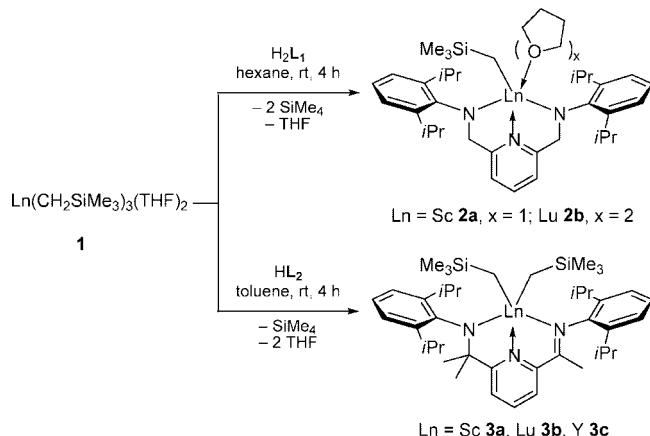
(6) Bambirra, S.; van Leusen, D.; Tazelaar, C. G. J.; Meetsma, A.; Hessen, B. *Organometallics* **2007**, *26*, 1014.

(7) Bambirra, S.; Boot, S. T.; van Leusen, D.; Meetsma, A.; Hessen, B. *Organometallics* **2004**, *23*, 1891.

(8) Kretschmer, W. P.; Meetsma, A.; Hessen, B.; Schmalz, T.; Qayyum, S.; Kempe, R. *Chem.–Eur. J.* **2006**, *12*, 8969.

(9) (a) Guérin, F.; McConville, D. H.; Payne, N. C. *Organometallics* **1996**, *15*, 5085. (b) Guérin, F.; McConville, D. H.; Vittal, J. J. *Organometallics* **1996**, *15*, 5586.

(10) Estler, F.; Eickerling, G.; Herdtweck, E.; Anwander, R. *Organometallics* **2003**, *22*, 1212.

Chart 2. Dianionic [NNN]²⁻ and Monoanionic [NNN]⁻ Ligand Precursors

Scheme 1. Synthesis of [L₁]Ln(CH₂SiMe₃)(THF)_x (2) and [L₂]Ln(CH₂SiMe₃)₂ (3) by Alkane Elimination


the lanthanide metal size revealed that the catalytic activity is sensitively balanced by steric and electronic factors.^{10,11} Monoanionic imino-amido-pyridine ligands (**L₂**, Chart 1) yield late transition metal catalysts active for ethylene polymerization¹² but also enabled the synthesis of discrete conformationally rigid lanthanide complexes.^{13,14} The [NNN]⁻ ligand **L₂**, a monoanionic analogue of its dianionic congener **L₁**, retains the characteristic features of the pyridine ligand backbone and the (aryl)substitution pattern at the amido/imino functionality, enabling a direct comparison of steric and electronic properties of lanthanide complexes derived from sterically similar monoanionic or dianionic ligand environments.

Herein, we describe structure–reactivity relationships of rare-earth-metal (Ln) alkyl complexes bearing diamido-pyridine (**L₁**) and imino-amido-pyridine ligands (**L₂**) and their performance as catalyst precursors for ethylene polymerization, giving special consideration to the impact of the Ln³⁺ size and the type of cocatalyst.

Results and Discussion

Synthesis and Characterization of [L₁]Ln(CH₂SiMe₃)(THF)_x and [L₂]Ln(CH₂SiMe₃)₂. Mono(alkyl)diamidopyridine complexes [L₁]Ln(CH₂SiMe₃)(THF)_x (Ln = Sc, x = 1 (**2a**); Lu, x = 2 (**2b**)) were prepared according to an alkane elimination reaction from H₂L₁ and Ln(CH₂SiMe₃)₃(THF)₂ in hexane as described previously (Scheme 1).¹⁰ The trialkyl Ln(CH₂SiMe₃)₃(THF)₂ (Ln = Sc (**1a**), Lu (**1b**), and Y (**1c**)) reacts similarly with light yellow [2-((2,6-*i*-Pr₂C₆H₃)N=CMe)-

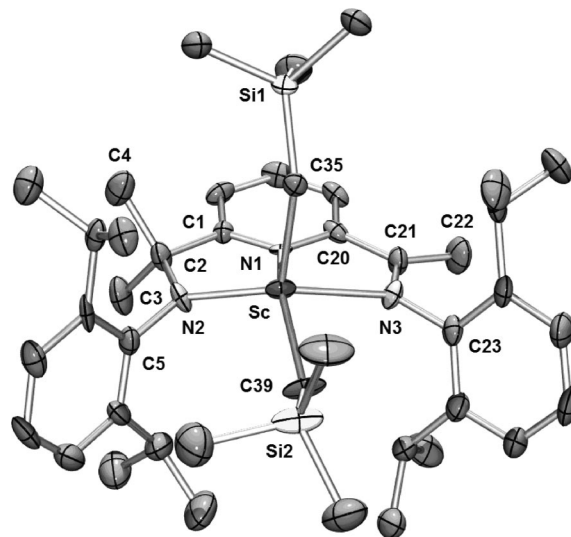


Figure 1. Molecular structure of **3a** (atomic displacement parameters set at the 50% level). Hydrogen atoms and solvent are omitted for clarity. Selected bond distances [Å] and angles [deg]: Sc–N1 2.245(9), Sc–N2 2.103(9), Sc–N3 2.436(9), Sc–C35 2.23(1), Sc–C39 2.25(1), N2–C2 1.48(2), N3–C21 1.31(2), C2–C3 1.52(2), C2–C4 1.56(2), C1–C2 1.51(2), C20–C21 1.49(2); N1–Sc–N2 72.3(3), N1–Sc–N3 67.6(3), N2–Sc–N3 134.1(3), N1–Sc–C35 103.4(3), N1–Sc–C39 145.3(4), C35–Sc–C39 107.6(5), N2–Sc–C35 111.5(4), N2–Sc–C39 109.4(5), N3–Sc–C35 99.0(4), N3–Sc–C39 92.1(4), C1–C2–N2 108.1(9), C20–C21–N3 116.1(10), C20–C21–C22 119.9(11), Sc–N2–C5 121.0(7), Sc–N3–C23 124.2(7).

6-((2,6-*i*-Pr₂C₆H₃)NHCMe₂)-C₃H₃N] (**HL₂**) with release of SiMe₄ and THF to form donor solvent-free compounds [L₂]Ln(CH₂SiMe₃)₂ (**3**) (Scheme 1, procedure described by Gordon).¹³ An instantaneous color change of the reaction mixture to dark red evidenced the coordination of the monoanionic imino-amido ligand to the lanthanide metal center. Upon removal of the solvent and the volatile reaction byproducts, dark red powdery complexes **3** were obtained with yields decreasing with increasing Ln³⁺ size (Ln = Sc, 92%; Lu, 52%; Y, 32%).

The IR spectra of complexes **3** show a strong absorption at 1582 cm⁻¹ attributed to the stretching vibration of a metal-coordinated imino group (**HL₂**: 1644 cm⁻¹). Similar shifts were observed in imino-amido pyridine complexes [L₂]Ln(AlMe₂)₂.¹⁴ Due to the insolubility in aliphatic solvents and low solubility in benzene, NMR spectroscopic investigations of compounds **3** were performed in chlorinated solvents. The ¹H NMR spectra of complexes **3** in CD₂Cl₂ at ambient temperature show a highly fluxional behavior even for the smallest metal center, scandium. Cooling to –50 °C, however, revealed ¹H and ¹³C NMR spectra in accordance with the solid state structure. Three singlets at 2.35 ppm (3 H), 1.64 ppm (3 H), and 1.10 ppm (3 H) (**3a**) are characteristic of the imino and amido functionalities of the pyridine ligand backbone (**3c**: 2.36, 1.71, and 1.33 ppm). The presence of four multiplets for the methine groups (ArCHMe₂) indicates a large rotational barrier for the aryl groups around the N–C_{ipso} bond at low temperature. As reported by Gordon¹³ for the lutetium derivative, the ¹H NMR spectrum of yttrium complex **3c** shows four distinct resonances for the α-CH₂ of the neosilylalkyl ligands. Surprisingly, the scandium complex **3a** revealed only two α-CH₂ resonances at low temperature. However, an X-ray structure analysis of the latter Sc compound **3a** (dark red single crystals were obtained from a saturated benzene solution at –30 °C) proved it to be isostructural to the previously reported lutetium derivative **3b** (Figure 1).¹³

(11) Zimmermann, M.; Estler, F.; Herdtweck, E.; Törnroos, K. W.; Anwander, R. *Organometallics* **2007**, *26*, 6029.

(12) Britovsek, G. J. P.; Gibson, V. C.; Mastroianni, S.; Oakes, D. C. H.; Redshaw, C.; Solan, G. A.; White, A. J. P.; Williams, D. J. *Eur. J. Inorg. Chem.* **2001**, 431.

(13) Cameron, T. M.; Gordon, J. C.; Michalczuk, R.; Scott, B. L. *Chem. Commun.* **2003**, 2282.

(14) Zimmermann, M.; Törnroos, K. W.; Anwander, R. *Angew. Chem., Int. Ed.* **2007**, *46*, 3126; *Angew. Chem.* **2007**, *119*, 3187.

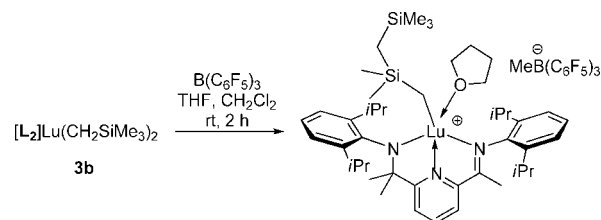
The geometry about the five-coordinate rare-earth-metal center is best described as distorted square pyramidal. The Sc atom is located 0.624(6) Å above the least-squares plane defined by the coordinating atoms N1, N2, N3, and C39, which is slightly less than in the corresponding lutetium compound **3b** (0.663 Å).¹³ In accordance with the smaller size of the scandium cation, all Sc–N bonds and the Sc–C35/C39 bonds are shortened compared to the lutetium derivative.^{10,13} In contrast, the geometry about the scandium metal center in [L₁]Sc(CH₂SiMe₃)(THF) (**2a**) was described as distorted trigonal bipyramidal with the pyridine nitrogen and the THF occupying the apical positions (N–Sc–O = 156.01(5)°).¹⁰ The N1–Sc–C39 angle as the widest angle in **3a**, however, measures only 145.3(5)°. Further, the ligand bite angle in bis(alkyl) **3a** is slightly smaller than the one found in the solid state structure of **2a** (134.1(3)° vs 137.04(6)°). The Sc–N(amido) (2.102(9) Å (**3a**); av 2.097 Å (**2a**)) and the Sc–C(alkyl) bond lengths (av 2.24(1) Å (**3a**); 2.248(2) Å (**2a**)) are comparable, while the Sc–N(pyridine) distance of 2.245(9) Å in **3a** appears slightly longer than that in **2a** (2.219(1) Å).

At ambient temperature complexes **3** undergo slow thermal decomposition. Monitoring the complex degradation by ¹H NMR spectroscopy revealed the protonated ligand precursor HL₂ and SiMe₄ as the only soluble decomposition products (Supporting Information Figure S1). Additionally the formation of a white rare-earth-metal-containing insoluble solid was observed. Pronounced thermal instability was found for the scandium (**3a**) (total decomposition after 24 h at 40 °C) and yttrium (**3c**) compounds (total decomposition after 4 days at 40 °C), while the lutetium derivative (**3b**) appeared to be more stable (decomposition after several weeks). Solids and solutions of **3** in toluene can be stored at –30 °C under argon for several weeks with only traces of decomposition. Decreasing thermal stability with increasing effective size of the metal cation had been found for complexes **2** (Sc > Lu > Y) and was assumed to reflect the “fit” of the ligand to the rare-earth-metal cation.¹⁰

Mechanistic details of the decomposition pathway, however, remain elusive. Further investigation of the white rare-earth-metal-containing solid was hampered by the insolubility in aliphatic, aromatic, and etheral solvents. Reasonable degradation pathways might include α-H or γ-H elimination from [Ln–CH₂SiMe₃] moieties, as previously proposed for the thermal decomposition of Ln(CH₂SiMe₃)₃(THF)_x.¹⁵ Alkyl migration to the ligand imino carbon atom—earlier found for the donor-induced cleavage of [L₂]La(AlMe₄)₂¹⁴ and for related salicylaldimine complexes¹⁶—was not observed.

Polymerization of Ethylene. The ethylene polymerization behavior of the mono(alkyl) diamido-pyridine complexes [L₁]Ln(CH₂SiMe₃)(THF)_x (Ln = Sc, x = 1 (**2a**); Lu, x = 2 (**2b**)) and the bis(alkyl) imino-amido-pyridine complexes [L₂]Ln(CH₂SiMe₃)₂ (Ln = Sc (**3a**), Lu (**3b**)) was investigated to assess the effect of the ancillary ligands (L₁ vs L₂), metal size, and the cocatalyst on the catalytic performance. In the absence of a cocatalyst neither mono(alkyl)s **2** nor bis(alkyl)s **3** displayed any activity.¹⁷ Interestingly, neutral complexes **2** had previously been found to initiate the polymerization of methyl methacrylate (MMA), but are inactive toward α-olefins.¹⁰

Scheme 2. Cationization of [L₂]Lu(CH₂SiMe₃)₂ with B(C₆F₅)₃ (the product was characterized by multinuclear NMR spectroscopy)¹³



Gordon et al. proved that the [NNN][–] ligand (L₂) is suitable to stabilize electron-deficient cationic lanthanide metal centers formed upon B(C₆F₅)₃ activation of [L₂]Lu(CH₂SiMe₃)₂ (Scheme 2).¹³

As Gordon et al. had prepared stable cationic Lu derivatives of the [NNN][–] ligand [L₂]Lu(CH₂SiMe₃)₂ (Scheme 2),¹³ we investigated the polymerization behavior of binary catalyst mixtures consisting of lanthanide bis(alkyl) complexes [L₂]Ln–(CH₂SiMe₃)₂ and [Ph₃C][B(C₆F₅)₄] (**A**), [PhNMe₂H][B(C₆F₅)₄] (**B**), or *N*-[tris(pentafluorophenyl)borane]-3*H*-indole (**C**), respectively. Each experiment was performed twice, and representative results are summarized in Table 1 (runs 1–4). Under similar polymerization conditions, the highest activities were observed for the Sc-based initiators (runs 1 and 3), while the lutetium catalysts exhibited slightly lower activity (runs 2 and 4). A similar impact of the lanthanide cation size on the catalytic performance has previously been reported for lanthanide catalysts based on neutral *fac*-κ³-coordinated [NNN]⁰-type donor ligands {(Me₃[9]aneN₃)Ln(CH₂SiMe₃)₃} and {[HC(Me₂pz)₃]Ln(CH₂SiMe₃)₃} (Sc > Y) as well as the recently reported [(6-amino-6-methyl-1,4-diazepine)Ln–(CH₂SiMe₃)₃] (Sc > Y).^{18,19}

For further comparison, the ethylene polymerization behavior of the most active rare-earth-metal catalysts based on amido/imino ancillary ligands (Chart 1) are listed in Table 2. The polymerization activities strongly depend on the ancillary ligand, the size of the rare-earth-metal center (Table 2, entries 1–3 and 8–11), polymerization temperatures (Table 2, entries 6, 7, and 14–16), and the cocatalyst/scavenger applied (Table 2, entries 4, 5, and 8–13).

We also observed a dependence of the polymerization activities of precatalysts **3** on the nature of the organoboron cocatalyst. The cocatalyst effect, **A** vs **B**, is more pronounced for initiators **3a**, featuring the smaller scandium center (Table 1, runs 1 and 3). Accordingly, catalyst mixtures containing [PhNMe₂H][B(C₆F₅)₄] produced species with higher activity (Table 1, run 3). The coordinating ability of the side-product PhNMe₂ has proven to influence the catalytic performance in several cases²⁰ and might as well interact with the active species formed by reaction of [L₂]Ln(CH₂SiMe₃)₂ (**3**) and [PhNMe₂H]–[B(C₆F₅)₄].

Resconi et al. developed the soluble *N*-[tris(pentafluorophenyl)borane]-3*H*-indole (**C**) as an activator for the polymerization

(15) (a) Schumann, H.; Müller, J. *J. Organomet. Chem.* **1978**, *146*, C5. (b) Schumann, H.; Freckmann, D. M. M.; Dechert, S. *Z. Anorg. Allg. Chem.* **2002**, *682*, 2422. (c) Ruffanov, K. A.; Freckmann, D. M. M.; Kroth, H.-J.; Schutte, S.; Schumann, H. *Z. Naturforsch. B: Chem. Sci.* **2005**, *60*, 533.

(16) (a) Emslie, D. J. H.; Piers, W. E.; Parvez, M.; McDonald, R. *Organometallics* **2002**, *21*, 4226. (b) Emslie, D. J. H.; Piers, W. E.; Parvez, M. *Dalton Trans.* **2003**, 2615.

(17) (a) Fryzuk, M. D.; Giesbrecht, G. R.; Rettig, S. J. *Organometallics* **1996**, *15*, 3329. (b) Fryzuk, M. D.; Giesbrecht, G. R.; Rettig, S. J. *Can. J. Chem.* **2000**, *78*, 1003.

(18) Lawrence, S. C.; Ward, B. D.; Dubberley, S. R.; Kozak, C. M.; Mountford, P. *Chem. Commun.* **2003**, 2880.

(19) Ge, S.; Bampirra, S.; Meetsma, A.; Hessen, B. *Chem. Commun.* **2006**, 3320.

(20) Pédeutour, J.-N.; Radhakrishnan, K.; Cramail, H.; Deffieux, A. *Macromol. Rapid Commun.* **2001**, *22*, 1095.

Table 1. Catalytic Ethylene Polymerization at 25 °C

| run ^a | precatalyst | cocatalyst ^b | polymer yield [g] | activity [kg/mol bar h] ^c | M_n^d | M_w^d | M_w/M_n |
|------------------|-------------|-------------------------|-------------------|--------------------------------------|---------|---------|-----------|
| 1 | 3a | A | 2.60 | 25 | 195 800 | 627 900 | 3.21 |
| 2 | 3b | A | 1.58 | 15 | 213 300 | 434 800 | 2.04 |
| 3 | 3a | B | 3.43 | 33 | 222 700 | 822 600 | 3.69 |
| 4 | 3b | B | 1.39 | 13 | 165 200 | 325 200 | 1.97 |
| 5 | 3a | C | | | | | |
| 6 | 3b | C | | | | | |

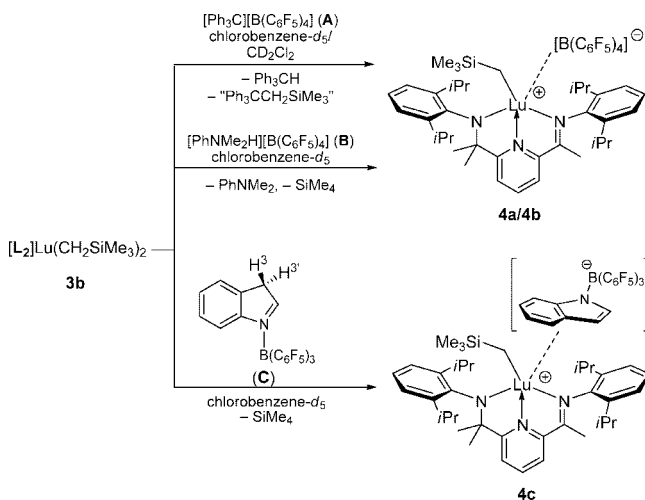
^a General polymerization procedure: 0.01 mmol of precatalyst, 50 mL of toluene, [cat]/[cocat] = 1:1 (mol/mol), ethylene 150 psi; 1 h, 25 °C. ^b Cocatalyst: **A** = [Ph₃C][B(C₆F₅)₄], **B** = [PhNMe₂H][B(C₆F₅)₄], **C** = *N*-[tris(pentafluorophenyl)borane]-3*H*-indole. ^c Given in kg polymer/(mol Ln atm h). ^d Determined by high-temperature gel permeation chromatography using polyethylene standards.

Table 2. Catalytic Ethylene Polymerization with Complexes Depicted in Chart 1

| entry | precatalyst ^a | cocatalyst (equiv) ^b | <i>T</i> [°C] | activity [kg/mol bar h] | M_w (× 10 ³) | M_w/M_n | ref |
|-------|--------------------------|--|---------------|-------------------------|----------------------------|-----------|-----|
| 1 | I (Ln = Sc) | B /TiBAO ^c (1/20) | 30 | 24 | 93 | 1.6 | 3a |
| 2 | I (Ln = Y) | B /TiBAO ^c (1/20) | 30 | 3006 | 1666 | 2.0 | 3a |
| 3 | I (Ln = La) | B /TiBAO ^c (1/20) | 30 | 14 | 470 | 2.5 | 3a |
| 4 | II | PMAO-IP ^d (20) | 50 | 1200 | 1866 | 2.0 | 4 |
| 5 | II | B(C ₆ F ₅) ₃ /PMAO-IP ^d (1.05/3.33) | 50 | 300 | 1051 | 1.7 | 4 |
| 6 | III (Ln = Y) | B (1) | 30 | 700 | 471 | 4.0 | 5 |
| 7 | III (Ln = Y) | B (1) | 80 | 1790 | 98 | 6.0 | 5 |
| 8 | IV (Ln = Sc) | A (1) | 50 | 75 | 690 | 2.2 | 6 |
| 9 | IV (Ln = Sc) | B (1) | 50 | 145 | 939 | 1.7 | 6 |
| 10 | IV (Ln = Y) | A (1) | 50 | 1343 | 127 | 6.6 | 6 |
| 11 | IV (Ln = Y) | B (1) | 50 | 1280 | 139 | 10.5 | 6 |
| 12 | V | A (1) | 50 | 20 | 55 | 2.2 | 7 |
| 13 | V | B (1) | 50 | | | | 7 |
| 14 | VI | [R ₂ N(CH ₃)H][B(C ₆ F ₅) ₄]/TiBAO ^c (1/20) | 30 | 40 | 68 | 43.0 | 8 |
| 15 | VI | [R ₂ N(CH ₃)H][B(C ₆ F ₅) ₄]/TiBAO ^c (1/20) | 80 | 1072 | 67 | 3.2 | 8 |
| 16 | VI | [R ₂ N(CH ₃)H][B(C ₆ F ₅) ₄]/TiBAO ^c (1/20) | 100 | 808 | 16 | 1.4 | 8 |

^a Precatalysts depicted in Chart 1. ^b Cocatalyst: **A** = [Ph₃C][B(C₆F₅)₄], **B** = [PhNMe₂H][B(C₆F₅)₄], **C** = TiBAO = tetraisobutylalumoxane. ^d PMAO-IP = AlMe₃-free methylalumoxane.

Scheme 3. Reaction of [L₂]Lu(CH₂SiMe₃)₂ (**3b**) with **A**, **B**, and **C**



of ethylene.²¹ Equimolar mixtures of dimethyl zirconocenes and *N*-[tris(pentafluorophenyl)borane]-3*H*-indole provided significantly higher catalytic activities than systems activated by methylalumoxane (MAO) or B(C₆F₅)₃/Al*i*Bu₃. *N*-[Tris(pentafluorophenyl)borane]-3*H*-indole, derived from the reaction of indole with B(C₆F₅)₃, contains a highly acidic sp³ carbon (indicated in Scheme 3), generated by a formal N→C hydrogen shift.²² This soluble proton source provides a convenient method for generating cationic alkyl metallocene precatalysts.²¹ However, treatment of [L₂]Ln(CH₂SiMe₃)₂ (**3**) with *N*-[tris(penta-

fluorophenyl)borane]-3*H*-indole (**C**) did not yield a catalytically active species (Table 1, runs 5 and 6). This distinct polymerization protocol implies a marked influence of the cocatalyst properties, especially the counterion's ability to stabilize and interact with the cationic lanthanide species.

In order to better understand the catalytic activity/inactivity of the catalyst–activator mixtures, we studied equimolar reactions of [L₂]Lu(CH₂SiMe₃)₂ (**3b**) with the borate activators [Ph₃C][B(C₆F₅)₄] (**A**), [PhNMe₂H][B(C₆F₅)₄] (**B**), and *N*-[tris(pentafluorophenyl)borane]-3*H*-indole (**C**) in more detail. Treatment of complex **3b** with 1 equiv of **A** in chlorobenzene-*d*₅ at 25 °C led to instant formation of a cationic lutetium alkyl species assignable to {[L₂]Lu(CH₂SiMe₃)₂}⁺{B(C₆F₅)₄}⁻ (**4a**) as monitored by ¹H, ¹¹B, and ¹⁹F NMR spectroscopy (Scheme 3, Figure 2B). The cation formation was accompanied by three organic side-products. While one species could clearly be identified as Ph₃CH (Ph₃CH: δ = 5.56 ppm), the ¹H NMR spectrum features two SiMe₃ resonances (0.01 and -0.30 ppm) and two methylene resonances (2.19 and 2.10 ppm) tentatively attributed to “Ph₃CCH₂SiMe₃” species. Similar organic byproducts have previously been observed by Mountford et al. when reacting [Ti(N*i*Bu)(Me₃9]aneN₃)(CH₂SiMe₃)₂ with [Ph₃C][B(C₆F₅)₄].²³ For comparison, the equimolar reaction of LiCH₂SiMe₃ and Ph₃CCl was monitored by ¹H NMR spectroscopy in chlorobenzene-*d*₅, revealing the formation of comparable organic products (Figure 2A).

Despite a detailed investigation of the organic side-products, the actual nature of the two “Ph₃CCH₂SiMe₃” species as well as mechanistic details leading to the formation of Ph₃CH remain unknown.²³ The analogous reaction of complex **3b** with 1 equiv of **A** in CD₂Cl₂ at 25 °C produced a complicated mixture of

(21) Guidotti, S.; Camurati, I.; Focante, F.; Angellini, L.; Moscardi, G.; Resconi, L.; Laerdini, R.; Nanni, D.; Mercandelli, P.; Sironi, A.; Beringhelli, T.; Maggioni, D. *J. Org. Chem.* **2003**, *68*, 5445.

(22) Bonazza, A.; Camurati, I.; Guidotti, S.; Mascellari, N.; Resconi, L. *Macromol. Chem. Phys.* **2004**, *205*, 319.

(23) Bolton, P. D.; Clot, E.; Adams, N.; Dubberley, S. R.; Cowley, A. R.; Mountford, P. *Organometallics* **2006**, *25*, 2806.

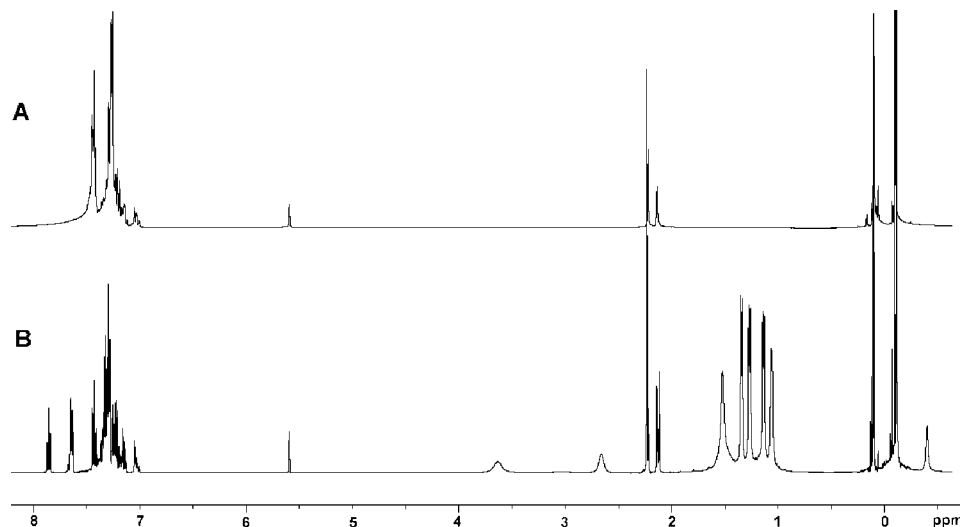


Figure 2. ^1H NMR spectra (400.13 MHz) of (A) the equimolar reaction of Ph_3CCl and $\text{LiCH}_2\text{SiMe}_3$ and (B) $\mathbf{3b}/[\text{Ph}_3\text{C}][\text{B}(\text{C}_6\text{F}_5)_4]$ in chlorobenzene- d_5 at 298 K.

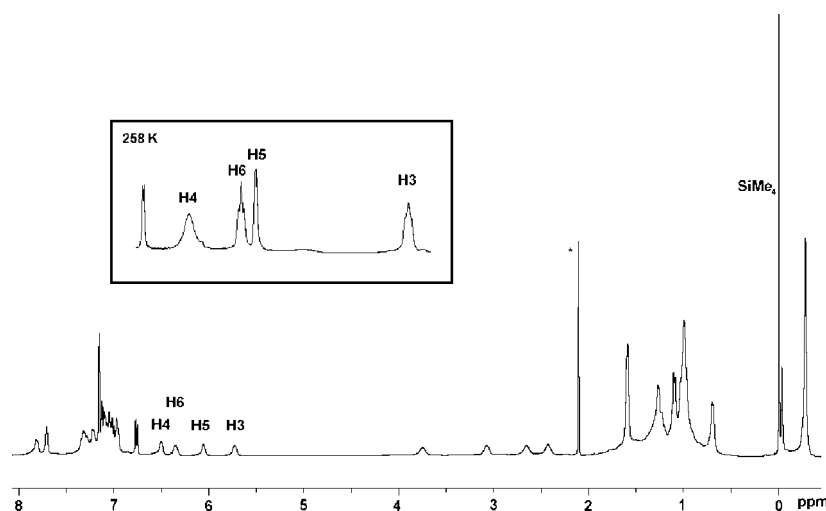


Figure 3. ^1H NMR spectrum (400.13 MHz) of $\mathbf{3b}/N$ -[tris(pentafluorophenyl)borane]- $3H$ -indole (**C**) in chlorobenzene- d_8 at 298 K (* = toluene residue).

Ph_3CH , “ $\text{Ph}_3\text{CCH}_2\text{SiMe}_3$ ”, and other silylated (aliphatic and olefinic) byproducts $[\text{R}_x\text{SiMe}_y]_n$ (Supporting Information; Figure S2).

^1H NMR investigations of the reaction of equimolar amounts of $[\text{L}_2]\text{Lu}(\text{CH}_2\text{SiMe}_3)_2$ (**3b**) and **B** in chlorobenzene- d_5 revealed the formation of an ion pair $\{[\text{L}_2]\text{Lu}(\text{CH}_2\text{SiMe}_3)\}\{\text{B}(\text{C}_6\text{F}_5)_4\}$ (**4b**), SiMe_4 , and PhNMe_2 (Figure S3, Supporting Information). ^{11}B and ^{19}F NMR spectra substantiate the presence of only one anionic species, the chemical shifts being similar to the ones observed for **4a**. The ^1H NMR spectrum, however, shows a highly fluxional behavior of the imino-amido-pyridine ancillary ligand at ambient temperature (Figure S3).

^1H NMR spectroscopic investigation of an equimolar $\mathbf{3b}/N$ -[tris(pentafluorophenyl)borane]- $3H$ -indole (**C**) mixture in chlorobenzene- d_5 at 25 °C showed the formation of a new species, which we tentatively assigned as $\{[\text{L}_2]\text{Lu}(\text{CH}_2\text{SiMe}_3)\}\{\text{B}(\text{indolyl})(\text{C}_6\text{F}_5)_3\}$ (**4c**, Scheme 3). The complete disappearance of the diagnostic indole H3/H3' signals at 2.48 ppm and the formation of SiMe_4 indicated the anticipated protonolysis of one $[\text{CH}_2\text{SiMe}_3]$ ligand by N -[tris(pentafluorophenyl)borane]- $3H$ -indole. Strikingly, the ^1H NMR spectrum features a set of relatively broad resonances between 5.63 and 6.43 ppm assignable to H3, H4, H5, and H6 of the indolyl counterion (Figure

3). These signals show a significant upfield shift compared to the ones found for the separated ion pair $[\text{Ind}_2\text{ZrMe}][\text{B}(\text{indolyl})(\text{C}_6\text{F}_5)_3]$ (6.37–7.14 ppm)²¹ and are in the range of π -coordinated indenyl moieties. These findings suggest a strong interaction of the indolyl π -system with the electron-deficient lutetium metal center. Few previous investigations document the coordination flexibility of indolyl ligands with respect to $\eta^6 \rightarrow \eta^5(\eta^3, \eta^1)$ shifts.²⁴ Further evidence of extensive steric constraint due to interaction with the counterion is given by the appearance of four multiplets for the methine groups (ArCHMe_2 ; $\delta = 3.65, 3.14, 2.66,$ and 2.53 ppm). This indicates a large rotational barrier for the aryl groups around the $\text{N}-\text{C}_{\text{ipso}}$ bond already at 25 °C, while resolution of these signals in $[\text{L}_2]\text{Lu}(\text{CH}_2\text{SiMe}_3)_2$ (**3b**) occurred only at low temperatures (*vide supra*). One single signal in the ^{11}B NMR spectrum corroborates the presence of only one boron-containing species, while the ^{19}F NMR spectrum shows a complicated pattern of 10 resonances, indicating conformational rigidity on the NMR

(24) (a) Evans, W. J.; Brady, J. C.; Ziller, J. W. *Inorg. Chem.* **2002**, *41*, 3340. (b) White, C.; Thompson, S. J.; Maitlis, P. M. *J. Chem. Soc., Dalton Trans.* **1977**, 1654. (c) Chen, S.; Carperos, V.; Noll, B.; Swope, R. J.; DuBois, M. R. *Organometallics* **1995**, *14*, 1221. (d) Chen, S.; Noll, B. C.; Peslherbe, L.; DuBois, M. R. *Organometallics* **1997**, *16*, 1089.

time scale. Each signal shows coupling with several other nuclei, suggesting additional intramolecular C–H...F “through-space” coupling.²⁵ Indeed, upon cooling to 258 K the indolyl signals in the ¹H NMR spectrum of **4c** shifted to higher field and the signal shape indicated coupling with fluorine (Figure 3).

Strong interaction with the counterion often results in a decreased catalytic activity and reduced molar mass of the polymer.^{20,25,26} These findings are in agreement with the observed inactivity of mixtures composed of [L₂]Ln(CH₂SiMe₃)₂ and *N*-[tris(pentafluorophenyl)borane]-3*H*-indole (**C**). Strong coordination of the anion competes with the coordination of ethylene at the active site and deactivates the “catalyst”.

All of the active catalyst mixtures produced linear polyethylene with molecular weights (*M_w*) ranging from 3.3 × 10⁵ to 8.2 × 10⁵. Significantly higher molecular weights were obtained for the Sc-based catalysts (Table 1, runs 1 and 3), while lower polydispersities (*M_w*/*M_n* = 1.97–2.04) could be achieved with the less active lutetium catalysts (Table 1, runs 2 and 4). Monomodal molecular weight distributions indicate the presence of a single active species.

In contrast to the bis(alkyl) imino-amido-pyridine precursors [L₂]Ln(CH₂SiMe₃)₂ (**3**), complexes [L₁]Ln(CH₂SiMe₃)(THF)_{*x*} (**2**) were inactive in the polymerization of ethylene. The dianionic nature of the diamido pyridine ancillary ligand (L₁) allows for only one further alkyl ligand being removed when adding the alkyl-abstracting borate/borane compounds. Most likely, the lack of an initiating alkyl group combined with high instability of the produced species (NMR experiments showed immediate decomposition) prevents the initiation of polymerization.

Polymerization Studies with Styrene and Methyl Methacrylate. Catalyst mixtures 3/[Ph₃C][B(C₆F₅)₄] were further investigated in the homopolymerization of styrene as well as copolymerization of ethylene and styrene. Attempted homopolymerization of styrene was carried out at 25 °C in 12 mL of toluene (21 μmol cat./21 μmol cocat./10.5 mmol styrene). No polymeric material could be obtained after 1.5 h. The copolymerization experiments were carried out in a 300 mL stainless steel reactor with a styrene solution in toluene at 25 °C. None of the cationic lanthanide complexes under investigation initiated the copolymerization of ethylene and styrene. Moreover, no homopolymerization of ethylene was observed even though these catalyst mixtures had shown catalytic activity in the absence of styrene. Monitoring the reaction of *in situ* formed cationic species **4a** with 1 equiv of styrene by ¹H and ¹³C NMR spectroscopy showed no evidence for an interaction between the cationic rare-earth-metal center and the olefinic bond. Due to extensive overlap of the aromatic signals, π-coordination of styrene to the electron-deficient lanthanide cation cannot be precluded and might inhibit further monomer coordination and catalytic activity. (See Supporting Information Figure S4.)

Motivated by the promising catalytic behavior of [L₁]Sc(CH₂SiMe₃)(THF) (**2a**) in the polymerization of methyl methacrylate (MMA)¹⁰ the initiating performance of corresponding neutral complexes [L₂]Ln(CH₂SiMe₃)₂ (**3**) as well as binary catalyst mixtures **3/A** and **3/B** has been investigated. However, under the same polymerization conditions only traces of polymeric product (PMMA) could be isolated from the reaction mixtures. Once again, these findings underline the pronounced

sensitivity of closely related compounds **2** and **3** to steric and electronic modifications.

Conclusions

A series of structurally related mono(alkyl) diamido-pyridine and bis(alkyl) imino-amido-pyridine lanthanide complexes have been synthesized, and their initiating performance in the polymerization of ethylene has been studied. While neutral alkyl complexes were inactive, cationic compounds bearing the imino-amido-pyridine ligand polymerized ethylene with moderate activities. The initiating performance is governed by the lanthanide metal size (Sc > Lu) and the nature of the cocatalyst. Routinely used borate cocatalysts [Ph₃C][B(C₆F₅)₄] and [PhNMe₂H][B(C₆F₅)₄] yielded polyethylene, while cationization with *N*-[tris(pentafluorophenyl)borane]-3*H*-indole gave inactive species, most likely due to π-coordination of the [B(indolyl)-(C₆F₅)₃] anion to the cationic lanthanide metal center. Generally, the activity/inactivity of the investigated catalysts in ethylene polymerization is sensitively influenced by the presence of species strongly coordinating to the electron-deficient cationic lanthanide metal center. The availability of an initiating alkyl group is essential to provide catalytic performance, as supported by the complete inactivity of cationic species derived from the dianionic diamido-pyridine ligand. In contrast, the homopolymerization of MMA is only initiated by the neutral mono(alkyl) diamido-pyridine complexes. Neither the neutral bis(alkyl) imino-amido-pyridine complexes nor their cationic variants gave positive polymerization protocols.

Experimental Section

General Considerations. All operations were performed with rigorous exclusion of air and water, using standard Schlenk, high-vacuum, and glovebox techniques (MBraun MBLab; <1 ppm O₂, <1 ppm H₂O). Hexane and toluene were purified by using Grubbs columns (MBraun SPS, solvent purification system) and stored in a glovebox. CD₂Cl₂ was obtained from Aldrich, vacuum transferred from calcium hydride, and degassed. [PhNMe₂H][B(C₆F₅)₄] and [Ph₃C][B(C₆F₅)₄] were purchased from Boulder Scientific Company and used without further purification. LnCl₃(THF)_{*x*},²⁷ LiCH₂-SiMe₃,²⁸ Ln(CH₂SiMe₃)₃(THF)₂,²⁹ 2-[(2,6-*i*Pr₂C₆H₃)N=CMe]-6-[(2,6-*i*Pr₂C₆H₃)NHCMe₂]C₅H₃N] (HL₂),³⁰ [L₁]Ln(CH₂SiMe₃)(THF)_{*x*} (**2**),¹⁰ [2-[(2,6-*i*Pr₂C₆H₃)N=CMe]-6-[(2,6-*i*Pr₂C₆H₃)NCMe₂]C₅H₃N][Lu(CH₂SiMe₃)₂ (**3b**),¹³ and *N*-[tris(pentafluorophenyl)borane]-3*H*-indole²¹ were prepared according to literature procedures. The NMR spectra of air- and moisture-sensitive compounds were recorded by using J. Young valve NMR tubes at 25 °C on a Varian UI 300 MHz, a Bruker-AVANCE-DMX400 (5 mm BB, ¹H: 400.13 MHz; ¹³C: 100.62 MHz), and a Bruker-BIOSPIN-AV500 (5 mm BBO, ¹H: 500.13 MHz; ¹³C: 125.77 MHz). ¹H and ¹³C shifts are referenced to internal solvent resonances and reported in parts per million relative to TMS. ¹¹B NMR (161 MHz) spectra were referenced to an external standard of boron trifluoride diethyl etherate (0.0 ppm, C₆D₆). ¹⁹F NMR spectra (471 MHz) are referenced to external CFCl₃. IR spectra were recorded on a Nicolet Impact 410 FTIR spectrometer as Nujol mulls sandwiched between CsI plates. Elemental analyses were performed on an Elementar Vario EL III.

(27) Anwander, R. *Top. Organomet. Chem.* **1999**, 2, 1.

(28) Hultsch, K. C. Ph.D. Thesis, Johannes Gutenberg-Universität Mainz, 1999.

(29) Lappert, M. F.; Pearce, R. *J. Chem. Soc., Chem. Commun.* **1973**, 126.

(30) Bruce, M.; Gibson, V. C.; Redshaw, C.; Solan, G. A.; White, A. J. P.; Williams, D. J. *Chem. Commun.* **1998**, 2523.

(25) Focante, F.; Camurati, I.; Resconi, L.; Guidotti, S.; Beringhelli, T.; D'Alfonso, G.; Donghi, D.; Maggioni, D.; Mercandelli, P.; Sironi, A. *Inorg. Chem.* **2006**, 45, 1683.

(26) Hayes, P. G.; Piers, W. E.; Parvez, M. J. *Am. Chem. Soc.* **2003**, 125, 5622.

equilibrated at 25 °C under constant ethylene pressure for at least 20 min. The catalyst (0.01 mmol) was dissolved in 20 mL of toluene, added into an injector, and injected into the reactor under ethylene pressure. Immediately prior to catalyst injection the ethylene line was disconnected and the pressure in the reactor was reduced by 60 psi to provide the pressure differential and allow the catalyst solution to flow into the reactor. The ethylene hose was reconnected immediately after catalyst injection. The reaction was run for 1 h at constant pressure and temperature; it was then quenched by injection of methanol (10 mL), and the reactor was slowly vented and opened. The polymer was precipitated in 400 mL of acidified methanol (5% HCl), filtered, washed with methanol, and dried under vacuum at 40 °C to a constant weight. Polymer molecular weights and molecular weight distributions were determined by the high-temperature gel permeation chromatography using polyethylene for GPC calibration. A Varian UI 300 spectrometer was used to perform ^{13}C NMR measurements. The polymer samples were prepared by dissolving 100–200 mg of polymer in 3 mL of

o-dichlorobenzene/10 vol % benzene- d_6 in a 10 mm NMR tube. The spectra were measured at 100 °C using acquisition times = 1 s, additional delays = 5 s, and gated proton decoupling.

Acknowledgment. Financial support from the Bayerische Forschungsförderung, the Norwegian Research Council, the Deutsche Forschungsgemeinschaft (SPP 1166), and the NSF (CHE-0611563) is gratefully acknowledged. We thank Lutz H. Gade and Rich Jordan for stimulating discussions.

Supporting Information Available: ^1H NMR spectra of the soluble decomposition products of **3a**, **3b**/[Ph $_3$ C][B(C $_6$ F $_5$) $_4$] in CD $_2$ Cl $_2$, **3b**/[PhNMe $_2$ H][B(C $_6$ F $_5$) $_4$] in chlorobenzene- d_5 , and **3b**/[Ph $_3$ C][B(C $_6$ F $_5$) $_4$] with 1 equiv of styrene, and a CIF file giving full crystallographic data for **3a**. This material is available free of charge via the Internet at <http://pubs.acs.org>.

OM701195X

Supporting Information

Structure-Reactivity Relationships of Amido- Pyridine Supported Rare-Earth Metal Alkyl Complexes

*Melanie Zimmermann,^a Karl. W. Törnroos,^a Robert M. Waymouth,^{*b}*

*and Reiner Anwander^{*a}*

^{a)} Department of Chemistry, University of Bergen, Allégaten 41, 5007 Bergen, Norway, and

^{b)} Chemistry Department, Stanford University, Stanford, California 94305, USA.

* To whom correspondence should be addressed: Fax: (+47) 5558-9490; e-mail

reiner.anwander@kj.uib.no.

RECEIVED DATE (to be automatically inserted after your manuscript is accepted if required according to the journal that you are submitting your paper to)

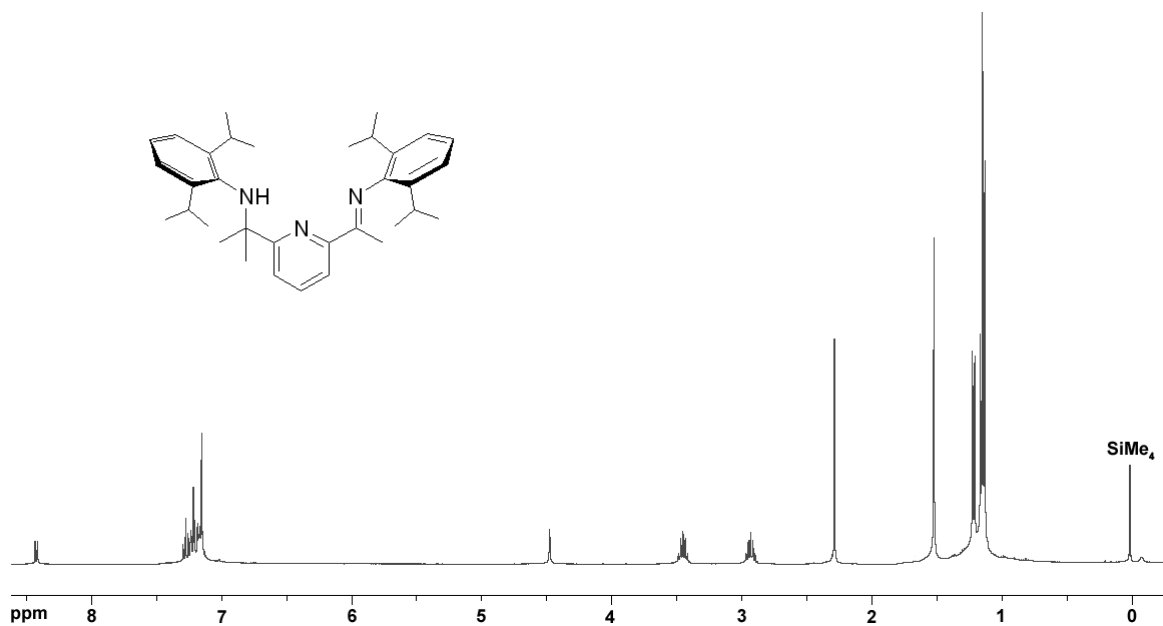


Figure S1. ^1H NMR spectrum (400.13 MHz) of the soluble decomposition products (HL_2 and SiMe_4) of **3a** in C_6D_6 at 298 K.

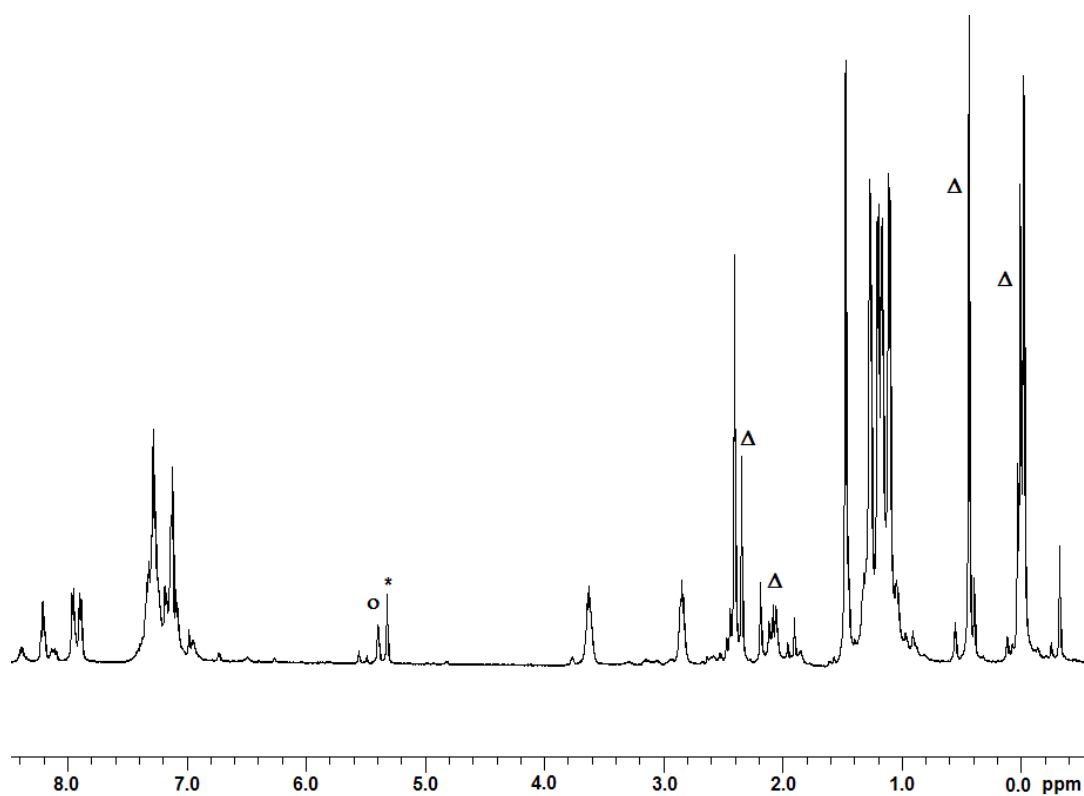


Figure S2. ^1H NMR spectrum (500.13 MHz) of **3b**/[Ph_3C][$\text{B}(\text{C}_6\text{F}_5)_4$] in CD_2Cl_2 at 298 K

(* = residual protons in CD_2Cl_2 ; O = Ph_3CH , Δ = $[\text{R}_x\text{SiMe}_y]_n$).

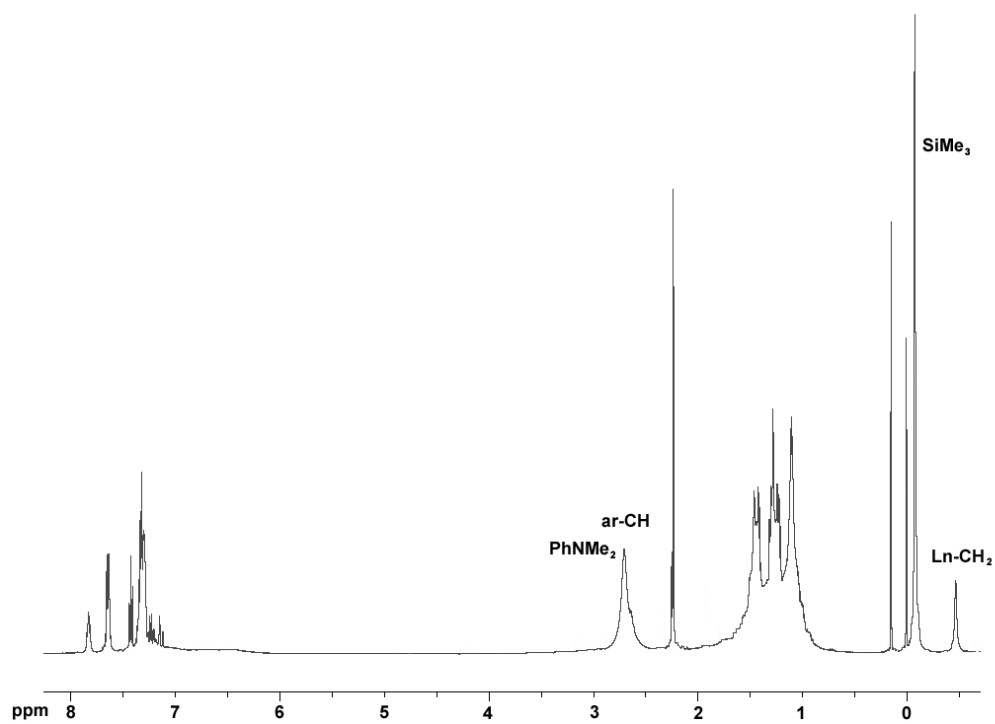


Figure S3. ^1H NMR spectrum (400.13 MHz) of **3b**/[PhNMe₂H][B(C₆F₅)₄] in chlorobenzene-*d*₅ at 298 K.

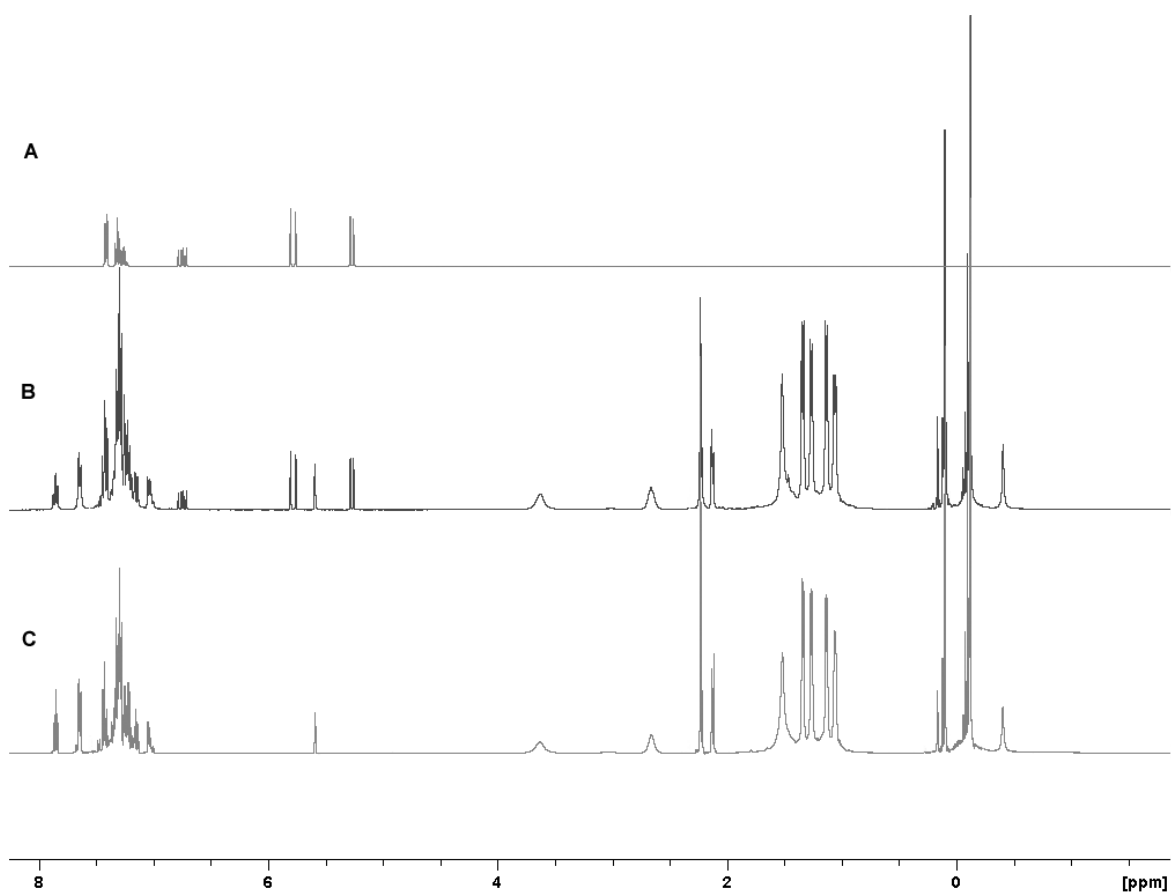


Figure S4. ^1H NMR spectra (400.13 MHz) of **A**) styrene, **B**) $\mathbf{3b}/[\text{Ph}_3\text{C}][\text{B}(\text{C}_6\text{F}_5)_4]$ with 1 eq of styrene, and **C**) $\mathbf{3b}/[\text{Ph}_3\text{C}][\text{B}(\text{C}_6\text{F}_5)_4]$ in chlorobenzene- d_5 at 298 K.

Appendix

Oral Presentations

“Postlanthanidocene complexes of the [NON]²⁻-type”

III. Euchem Conference on Nitrogen Ligands in Organometallic Chemistry and Homogeneous Catalysis, Camerino, Italy, September 8-12, **2004**.

“Postlanthanidocene complexes of the [NON]²⁻-type”

XVII. Tage der Seltenen Erden, Bayreuth, Germany, December 1-4, **2004**.

“Postlanthanidocene complexes of the [NON]²⁻-type”

229th ACS International Meeting, San Diego, USA, March 13-17, **2005**.

“Application of Ln(AlMe₄)₃ as precursors for postlanthanidocene chemistry”

XVIII. Tage der Seltenen Erden, Cologne, Germany, November 30 - December 2, **2005**.

“New Alkyl Precursors in Postlanthanidocene Chemistry”

XXII International Conference on Organometallic Chemistry, Zaragoza, Spain, July 23-28, **2006**.

“Alkyl migration and a new tetramethylaluminate coordination mode: Unusual reactivity of organolanthanide imino-amido-pyridine complexes”

XIX. Tage der Seltenen Erden, Oldenburg, Germany, November 29 - December 2, **2006**.

Poster Presentations

“Postlanthanidocene Complexes Supported by Functionalized Diamide Ligands”

XVI. Tage der Seltenen Erden, Berlin, Germany, December 4-6, **2003**.

“Postlanthanidocene complexes of the [NON]²⁻-type”

XVII. Tage der Seltenen Erden, Bayreuth, Germany, December 1-4, **2004**.

“Postlanthanidocene complexes of the [NON]²⁻-type”

Münchner Industrie-Tag, Munich, Germany, October 15, **2004**.

“Postlanthanidocene complexes of the [NON]²⁻-type”

14th International Symposium on Homogeneous Catalysis, Munich, Germany, July 5-9, **2004**.

“Dissociative versus associative alkyl exchange: An extended dynamic NMR spectroscopic study of Ln(AlMe₄)₃”

XIX. Tage der Seltenen Erden, Oldenburg, Germany, November 29 - December 2, **2006**.

“Tetramethylaluminate coordination modes in lanthanide complexes”

XIX. Tage der Seltenen Erden, Oldenburg, Germany, November 29 - December 2, **2006**.

Curriculum Vitae

Personal Details

Name: Zimmermann, Melanie
Date of Birth: November 16, 1977
Place of Birth: Freiburg im Breisgau
Nationality: German

Education

Sept. 1984 – July 1988: Grundschule Ebersberg

Sept. 1988 – June 1997: Theresia-Gerhardinger-Gymnasium am Anger München,
Specialization Music
Allgemeine Hochschulreife

Oct. 1997 – July 1998: Technische Universität München,
Study of Biology

Oct. 1998 – Nov. 2003: Study of Chemistry (Diplom), Technische Universität München

Oct. 2000: Diplomvorprüfung

Oct. 2000 – Nov. 2003: Main Studies Chemistry (Diplom), Technische Universität München
Main course: *"Process Technology and Catalysis"*

July 2001 - Oct. 2001: Technion Israel Institute of Technology, Haifa, Israel, Internship position, DAAD Fellowship

July 2002 - Oct. 2002: Norsk Hydro ASA, Porsgrunn, Norway, Internship position

April 2003: Diploma exam (Dipl.-Chem. Univ.)

May 2003 – Nov. 2003: Diploma thesis: *"Postlanthanidocene Complexes Supported by Functionalized Diamide Ligands"* (Priv.-Doz. Dr. R. Anwender)

Feb. 2004 – Oct. 2007: Promotion: *"Rare-Earth Metal Alkyls"* (Prof. Dr. R. Anwender)

Jan. 2005 - March 2005: Stanford University, Stanford, California, USA, research collaboration with Prof. R. M. Waymouth

